Investigating the effects of IGFs on immune responses in prostate cancer



Jinseon Kim

St. Hilda's College

University of Oxford

A thesis submitted for the degree of

Doctor of Philosophy

Trinity 2024

Acknowledgements

Dear Val,

It's been three months since your passing. It hasn't been easy, but knowing your dedication for WINGMEN trial has kept me going regardless. The WINGMEN trial team as well as the collaborators have been incredibly supportive, which speaks to your character, and I'm so happy to say both primary and secondary endpoints have been met (I still remember how stressed we were testing multiple IHC markers, but here we are!). I really wish you were here to see the results in person.

I honestly would not have been able to reach this milestone without your support. You've taught me how to be a logical yet creative scientist, importance of a good experimental design, and how to be passionate and hardworking whilst staying kind, humble, and considerate. I really appreciate your supervision, filled with advice and unwavering support, and I hope you know that you will always be my mentor at heart. Thank you so much for everything. This thesis is for you.

To my second supervisors Ian and Alastair: I can't put into words how grateful I am to have you as my supervisors. You really stepped up for me when I felt alone and gave me the support that I needed, and I can't thank you enough for it. Your insights and suggestions have been very helpful, and it's been a pleasure getting to know you more the last few months. Thank you for being there for me at my hardest times.

To my parents: Thank you so much for all your support, both financially and mentally, and encouraging me to spread my wings. Leaving here as the first female Dr. Kim in the family is a huge privilege, and all this would not have been possible without you. 엄마 아빠, 정말 사랑하고 감사합니다.

To Macaulay lab members, forever Val's Pals: The biggest reason I decided to do my PhD here was you all. I really appreciate your guidance and willingness to help at all times. You guys really made my time in the UK so much more enjoyable, and I'm looking forward to sharing more milestones and success with you all.

To my friends and sisters across the pond: Your visits, messages, and zoom calls, and all our trips together.. they really made this DPhil journey much more exciting. Thank you for constantly reminding me that distance doesn't matter and that the friendship/sisterhood is forever.

To my fiance and future husband Mark: I don't even know where to begin this one, because there's so much to be said. You've really been there for me since the beginning of my DPhil journey, and I honestly would not have done this without your support. Thank you for being my number 1, for listening to my rants when things don't work (which was.. about 90% of the time), for lending your shoulder whenever I needed to cry, for making me laugh even in the darkest times, and for constantly reminding me to have fun and enjoy the process. Leaving the program with you (and the ring) is such an exciting feeling, and I'm so excited to do life with you.

This work would not have been possible without support from Prostate Cancer UK and CRUK Oxford Centre. I also would like to give huge thanks to all my examiners who have provided valuable advice along this journey: Dr. Richard Bryant, Dr. Jelena Bezbradica Mirkovic, Dr. Simon Lord, Dr. Adam Sharp, and Dr. Monica Olcina del Molino.

List of Contributors

I declare that this thesis describes my own research work except for the following experiments, which were performed with the help of others:

David Ahern, Kennedy Mass spectometry facility	CyTOF sample run of WINGMEN samples (Chapter 2.18.2)
Dr. Alessandro Barberis, Macaulay Lab	Over-representation analysis in chapter 3.3.3 (Figure 3.17 and 3.18).
Molly Browne and Leticia Campo, Translational Histopathology Lab (THL)	Immunohistochemistry (IHC) for WINGMEN trial sample analysis (Chapter 2.6.4).
Dr. Fiona Hartley, Macaulay Lab	RNA sequencing data analysis of xentuzumab ± anti-PD-1 *in vivo* repeat experiment (Figure 3.29 and 3.30), WINGMEN trial sample RNA sequencing data analysis and CIBERSORTx (Figure 5.12 and 5.13).
Cameron Lang, Macaulay Lab	Generation of mCherry-tagged cell lines (Chapter 2.1.2), Human peripheral blood mononuclear cells (PBMCs) processing for *in vitro* experiments (Chapter 2.10.1), Processing and flow cytometry of tumours, spleen, and PBMCs from xentuzumab ± anti-PD-1 *in vivo* repeat experiment (Chapter 2.9.1, 2.9.2, and 2.9.3, Figure 3.28), WINGMEN sample processing analysis for CyTOF (Chapter 2.18.1 and 2.18.2, Figure 5.16).
Oxford Genomics Centre, Wellcome Centre for Human Genetics	3' RNA sequencing library preparation and sample run (Chapter 2.7.2)
Dr. Avigail Taylor, Macaulay Lab	GeneFEAST development and analysis in chapter 3.3.3 (Figure 3.19).
Dr. John Walsby-Tickle, James McCullagh Lab, Department of Chemistry	Metabolomics sample run and data analysis (Chapter **??**).
WINGMEN trial team, Oncology Clinical Trials Office	Trial sample and clinical dataset collection

Abstract

Prostate cancer is the second most common cancer in men. Insulin-like growth factor (IGF), a hormone necessary for normal cell growth, is correlated with prostate cancer progression and mortality and is known to have immunosuppressive actions in the tumour immune-microenvironment (TIME). The objective of the project was to investigate immune-modulatory impact of IGF signalling in prostate cancer *in vitro* and in patients. The first aim was to test the effects of IGF blockade in prostate cancer by exploring the effects of IGF blocking monoclonal antibody xentuzumab *in vitro* and *in vivo*, alone and in combination with anti-PD-1 immunotherapy. Xentuzumab treatment successfully inhibited IGF axis activation *in vitro* and changed T cell and macrophage effects and infiltration *in vivo*. Secondly, effects of IGFs on macrophage phenotype and phagocytic function were characterised *in vitro*. Xentuzumab treatment reduced tumour-promoting M2 macrophages, increased phagocytosis of cancer cells by pro-inflammatory M1 macrophages, and enhanced T cell activity. The last aim was to understand the impact of IGF blockade on localised prostate cancer TIME in the windows trial set-up (NCT05110495). In addition to successfully blocking IGF axis (primary endpoint) and confirming its safety and tolerability (secondary endpoint), xentuzumab treatment significantly increased CD8+ T cell infiltration and reduced serum IGF bioactivity, Ki67+ tumour proliferation, AR+ epithelium, and Treg subtypes. RNA sequencing of the tumours revealed inflammatory and senescence-associated secretory phenotype (SASP)-like signatures, suggesting cellular stress caused by the IGF axis blockade. In conclusion, IGF axis contributes to remodelling of prostate cancer TIME, with species-dependent changes in immune cell repertoire. Provided we learn more about the nature of this immune remodelling, this thesis presents therapeutic potential of xentuzumab to be used as an adjuvant therapy in combination with immune intervention.

Contents

List of Figures **vii**

List of Tables **viii**

List of Abbreviations **ix**

1 Introduction **1**

1.1 Prostate cancer 1

1.1.1 Treatment options 4

1.1.2 Molecular mechanisms 5

1.2 IGF-1 axis 7

1.2.1 Receptors and ligands 7

1.2.2 IGF-1R signalling pathways 8

1.2.2.1 PI3K/AKT pathway 9

1.2.2.2 MAPK pathway 10

1.2.2.3 JAK/STAT pathway 11

1.3 IGF axis and cancer 11

1.3.1 IGF axis and cancer risk 12

1.3.2 IGF axis and its effects on tumorigenesis 12

1.4 Anti-tumour immunity 16

1.4.1 Innate immune response to cancer 16

1.4.2 Adaptive immune response to cancer 17

1.5 Reported influence of IGFs on the immune response 20

1.5.1 Effects of IGFs on adaptive immunity 20

1.5.2 Effects of IGFs on innate immunity 21

1.6 Prostate cancer tumour microenvironment 22

1.7 Aims and hypothesis 23

2 Materials and Methods **25**

2.1 Cell lines 26

2.1.1 Cell lines and culture conditions . . . 26
2.1.2 mCherry-tagged cell lines . . . 28
2.1.3 Cryopreservation . . . 29
2.1.4 Cell seeding . . . 29
2.2 Cell treatments . . . 29
2.2.1 IGF-1 and xentuzumab treatment . . . 29
2.2.2 anti-CD47 treatment . . . 30
2.3 Western blot . . . 30
2.4 Viability assays . . . 31
2.4.1 2D viability assay . . . 31
2.4.2 2D clonogenic assay . . . 32
2.4.3 3D spheroid assay . . . 32
2.5 Mice . . . 33
2.5.1 Tumour cell preparation and injection for *in vivo* experiments . 33
2.5.2 Allograft model for IGF blockade . . . 34
2.5.3 Allograft model for IGF blockade and anti-PD1 (pilot, n=6) . . 34
2.5.4 Allograft model for IGF blockade and anti-PD1 (n=10) . . . 35
2.6 Immunohistochemistry (IHC) . . . 35
2.6.1 Formalin-Fixed, Paraffin-Embedded (FFPE) sections . . . 35
2.6.2 Immunohistochemical staining . . . 36
2.6.3 Haematoxylin and Eosin (H&E) staining . . . 38
2.6.4 WINGMEN trial IHC . . . 38
2.6.5 HALO Image Analysis . . . 39
2.7 3' RNA Sequencing . . . 40
2.7.1 RNA extraction from mouse tumour tissues and cell lines . . . 40
2.7.2 RNA Library Preparation and Sequencing . . . 40
2.7.3 Data Processing and Analysis . . . 40
2.8 Quantitative real-time polymerase chain reaction (qRT-PCR) . . . 41
2.8.1 Primer design . . . 41
2.8.2 Ribonucleic Acid (RNA) isolation . . . 44
2.8.3 Complementary DNA (cDNA) synthesis and qRT-PCR . . . 45

2.8.4 Relative quantification 46
2.9 Flow cytometry 46
2.9.1 Mouse tumour tissue processing 46
2.9.2 Mouse peripheral blood processing 46
2.9.3 Mouse spleen processing 47
2.9.4 Cell surface staining 47
2.9.5 Intracellular staining 49
2.9.6 Compensation 49
2.9.7 Data Acquisition and Analysis 50
2.10 Immune cell isolation 53
2.10.1 Human peripheral blood mononuclear cells (PBMCs) processing 53
2.10.2 PBMC-derived macrophage differentiation and polarisation . . . 54
2.10.3 T cell isolation 54
2.10.4 Bone marrow-derived macrophages (BMDMs) isolation and polarisation 54
2.11 Co-culture assay 55
2.11.1 Macrophages and cancer cell co-culture assay 55
2.11.2 Macrophages, T cells, and cancer cell co-culture assay 56
2.12 Cytokine array 56
2.13 *in vitro* Phagocytosis assay 58
2.14 Clinical samples 58
2.14.1 Research blood samples 58
2.14.2 Research tissue samples 60
2.15 Multiplex Immunofluorescence (mIF) 60
2.15.1 Antibody conjugation 60
2.15.2 Slide preparation 61
2.15.3 Data Analysis 63
2.16 RNA Sequencing of WINGMEN trial samples 63
2.16.1 RNA extraction from FFPE tissue sections 63
2.16.2 RNA Library Preparation and Sequencing 65
2.16.3 Data Processing and Analysis 66

2.17 phospho-IGF-1R enzyme-linked immunosorbent assay 66

2.18 PBMC immunoprofiling using Cytometry by Time-Of-Flight (CyTOF) 68

2.18.1 PBMC sample processing 68

2.18.2 CyTOF data acquisition and data analysis 68

2.19 Statistical Analysis 70

3 *In vitro* and *in vivo* effects of IGF blockade in prostate cancer 71

3.1 Introduction 71

3.2 *In vitro* effects of IGF blockade in prostate cancer 73

3.2.1 Assessing effects of IGF blockade in cell signalling 74

3.2.2 Investigating effects of IGF blockade on 2D viability and cell survival 74

3.2.3 Effects of IGF blockade on 3D growth of cells 77

3.3 Investigating IGF blockade in prostate cancer *in vivo* 79

3.3.1 Study design and tumour growth 79

3.3.2 Staining of IGF-1R-related markers and immune markers in tumours 79

3.3.3 Transcriptomic profiling of tumours 83

3.4 Effects of IGF blockade in response to PD-1 immunotherapy *in vivo* : pilot study 85

3.4.1 Assessment of tumour growth and morphology 85

3.4.2 Immunohistochemical analysis for markers of IGF-1R signalling and immune cells 85

3.4.3 Transcriptomic profiling of tumours 93

3.5 Investigating the effects of IGF axis and PD-1/PD-L1 axis blockade in prostate cancer: repeat experiment 104

3.5.1 Rationale and tumour growth 104

3.5.2 Immunohistochemical analysis of tumour tissues 107

3.5.3 Flow cytometric analysis of tumours 111

3.5.4 Transcriptomic profiling of tumours 113

3.6 Discussion 116

4 Effects of IGFs on macrophage phenotype and function in prostate cancer 126

4.1 Introduction 126

4.2 Effects of cancer cell co-culture on macrophage phenotype 130
4.2.1 Macrophage polarisation 130
4.2.2 Effects of IGF-1R signalling inhibition on human prostate cancer cell lines 133
4.2.3 Effects of co-culture on murine macrophage polarisation 136
4.2.4 Effects of co-culture on human macrophage polarisation 136
4.2.5 Cytokine array of co-culture conditioned medium 139
4.3 Effects of IGF axis manipulation on macrophage phenotype 141
4.3.1 Conditioned medium of xentuzumab-treated Myc-CaPs assessed by cytokine array 141
4.3.2 Effects of IGF axis manipulation on macrophage polarisation . . 143
4.4 CD47 and prostate cancer 146
4.4.1 CD47 expression in prostate cancer cells 146
4.4.2 Testing effects of anti-CD47 on IGF-1R signalling 149
4.5 Effects of IGF-1, anti-IGF and/or anti-CD47 on cancer cell phagocytosis 152
4.5.1 Testing conditions for phagocytosis assays 152
4.5.2 Assessing the effects of IGF-axis manipulation on phagocytosis . 155
4.5.3 Investigating the effects of xentuzumab on anti-CD47-induced phagocytosis 158
4.6 Investigating the effects of IGFs on macrophages regulating T cell effector functions 161
4.7 Discussion 168

5 WINGMEN Trial: clinical relevance 175
5.1 Introduction 175
5.2 WINGMEN trial design and baseline characteristics 177
5.2.1 WINGMEN trial design 177
5.2.2 Patient characteristics 179
5.2.3 Secondary endpoint: feasibility, safety, and tolerability of xentuzumab treatment in pre-operative setting 183
5.3 Investigating the changes in tissue markers following IGF blockade . . . 185
5.3.1 Primary endpoint: changes in IGF axis activation 185
5.3.2 Immunohistochemical staining of tissues 188
5.3.3 Multiplex immunofluorescence staining of tissues 191

5.3.4 Transcriptomic profiling of pre- and post-xentuzumab treated tumours 196
5.4 Analysis of blood samples following IGF blockade 199
5.4.1 Assessing circulating markers in pre- and post-xentuzumab treated serum 199
5.4.2 PBMC immunophenotyping by mass cytometry (CyTOF) . . . 201
5.5 Discussion 203

6 Conclusion **212**

7 Appendix **218**

List of Figures

1.1 **IGF-1R signalling pathway** 9

1.2 **IGF axis and hallmarks of cancer** 14

2.1 **Representative flow cytometry gating strategy** 51

2.2 **Representative compensation strategy** 52

2.3 **Representative flow cytometry gating of macrophages, T cells, and cancer cell co-culture assay** 57

3.1 **Response of murine prostate cancer cells to IGF neutralising antibody xentuzumab** 75

3.2 **Effects of IGF blockade on 2D growth and survival of murine prostate cancer cells** 76

3.3 **Effects of IGF blockade on 3D spheroid growth in murine prostate cancer cells** 78

3.4 **Investigating the effects of IGF blockade in vivo** 80

3.5 **IHC staining of IGF-1R and immune-related markers in murine Myc-CaP tumours** 81

3.6 **IHC staining results in murine Myc-CaP tumours** 82

3.7 **3' RNA sequencing analysis of xentuzumab vs control-treated tumours** 84

3.8 **Investigating the effects of IGF and PD-1 blockade in vivo** . . 86

3.9 **Effects of IGF-1 and PD-1 blockade pilot experiment on IGF-1R and T-cell markers in murine Myc-CaP tumours** 88

3.10 **Effects of IGF-1 and PD-1 blockade pilot experiment on expression of various markers in murine Myc-CaP tumours** . . . 89

3.11 **Haematoxylin and eosin (H&E) staining of the pilot experiment tumours** 90

3.12 **Immunohistochemical staining for macrophage markers in murine prostate tumours treated with xentuzumab** 91

3.13 **Effects of IGF and PD-1 blockade pilot experiment on macrophage marker expression in Myc-CaP allografts** 92

3.14 **RNA sequencing analysis of Myc-CaP tumours treated with xentuzumab compared to control: pilot experiment** 94

3.15 **RNA sequencing analysis of Myc-CaP tumours treated with xentuzumab + anti-PD-1 compared to xentuzumab: pilot experiment** 94

3.16 **RNA sequencing analysis of Myc-CaP tumours treated with xentuzumab and anti-PD-1 compared to control: pilot experiment** 95

3.17 **Pathway analysis of genes regulated by xentuzumab treatment on Myc-CaP tumours in the pilot experiment** 97

3.18 **Pathway analysis of genes regulated by xentuzumab + anti-PD-1 treatment on Myc-CaP tumours: pilot experiment** 98

3.19 **GeneFEAST analysis of significantly enriched pathways in xentuzumab + aPD1-treated tumours vs controls** 100

3.20 **Quantitative real-time PCR (qRT-PCR) validation of selected DEGs comparing Myc-CaP tumours treated with xentuzumab and anti-PD-1 compared to control** 101

3.21 **Quantitative real-time PCR (qRT-PCR) validation of selected DEGs comparing Myc-CaP tumours treated with xentuzumab compared to control** 103

3.22 **Quantitative real-time PCR (qRT-PCR) validation of selected DEGs comparing Myc-CaP tumours treated with xentuzumab + anti-PD-1 compared to xentuzumab** 103

3.23 **Investigating the effects of IGF and PD-1 blockade in vivo: repeat experiment** 105

3.24 **Haematoxylin and eosin (H&E) staining of the repeat experiment tumours** 106

3.25 **Effects of IGF-1 and PD-1 blockade repeat experiment on expression of IGF-1R and T-cell markers in Myc-CaP tumours** 108

3.26 **Immunohistochemical staining of IGF-1 and PD-1 blockade repeat experiment** 109

3.27 **Macrophage marker expression in Myc-CaP allografts with IGF and PD-1 blockade repeat experiment** 110

3.28 **Flow cytometric analysis of tumours, spleens, and PBMC of the mice treated with xentuzumab and/or anti-PD-1** 112

3.29 **RNA sequencing analysis of Myc-CaP tumours treated with xentuzumab compared to control: repeat experiment** 114

3.30 **RNA sequencing analysis of Myc-CaP tumours treated with xentuzumab and anti-PD-1 compared to control: repeat experiment** 115

4.1 **Functional interactions between IGF axis, IAP/CD47 and SHPS1/SIRPα in cis and trans** 129

4.2 **Murine macrophage polarisation** 131

4.3 **Human macrophage polarisation** . . . 132

4.4 **Response of human prostate cancer cells to IGF neutralising antibody xentuzumab** . . . 134

4.5 **Effects of IGF blockade on 2D growth of human prostate cancer cells** . . . 135

4.6 **Effects of co-culture on murine macrophage phenotype** . . . 137

4.7 **Effects of co-culture on human macrophage phenotype** . . . 138

4.8 **Comparing the conditioned media of BMDMs and of 24-72 hour co-culture with prostate cancer cells** . . . 140

4.9 **Comparing the conditioned media of Myc-CaPs treated with xentuzumab versus control** . . . 142

4.10 **Effects of IGF-1 alone or with xentuzumab on murine BMDM polarisation** . . . 144

4.11 **Effects of IGF-1 alone or with xentuzumab on murine J774 polarisation** . . . 144

4.12 **Effects of IGF-1 alone or with xentuzumab on human macrophage polarisation** . . . 145

4.13 **Effects of IGF-1 alone or with xentuzumab on CD47 expression in murine prostate cancer cells** . . . 147

4.14 **Effects of IGF-1 alone or with xentuzumab on CD47 expression in human prostate cancer cells** . . . 148

4.15 **Effects of IGF and CD47 blockade on IGF-1R signalling pathway on murine prostate cancer cells** . . . 150

4.16 **Effects of IGF and CD47 blockade on IGF-1R signalling pathway on human prostate cancer cells** . . . 151

4.17 **Investigating the phagocytosis of murine prostate cancer cells by J774 macrophages** . . . 153

4.18 **Investigating the phagocytosis of human prostate cancer cells by macrophages** . . . 154

4.19 **Effects of IGF axis manipulation on murine prostate cancer cells by J774 macrophages** . . . 156

4.20 **Effects of IGF axis manipulation on human prostate cancer cells by macrophages** . . . 157

4.21 **Effects of combined IGF and CD47 blockade on murine prostate cancer phagocytosis** . . . 159

4.22 **Effects of combined IGF and CD47 blockade on human prostate cancer phagocytosis** . . . 160

4.23 **Effects of IGF and xentuzumab-treated macrophages on T cell exhaustion** . . . 162

4.24 **Effects of IGF and xentuzumab-treated macrophages on T cell activation** . . . 164

4.25 **Effects of IGF and xentuzumab-treated macrophages on IFN-γ production** . . . 165

4.26 **Effects of IGF and xentuzumab-treated macrophages on T cell proliferation** . . . 167

5.1 **WINGMEN trial schematics** . . . 178

5.2 **Samples collected and analysed from the WINGMEN trial patients** . . . 178

5.3 **CONSORT diagram for WINGMEN study** . . . 180

5.4 **Testing phospho-IGF-1R and phospho-S6 antibodies on prostate cancer spheroids and tissues** . . . 186

5.5 **Primary endpoint markers at baseline (PRE) and after xentuzumab (POST)** . . . 187

5.6 **IGF-1R and Ki67 expression at baseline (PRE) and after xentuzumab (POST)** . . . 189

5.7 **RRM2 expression at baseline (PRE) and after xentuzumab (POST)** . . . 190

5.8 **Multiplex immunofluorescence imaging of WINGMEN patient samples** . . . 192

5.9 **CD31 expression at baseline (PRE) and after xentuzumab treatment (POST)** . . . 193

5.10 **Immune cell composition at baseline (PRE) and after xentuzumab treatment (POST)** . . . 194

5.11 **Immune cell infiltration at baseline (PRE) and after xentuzumab treatment (POST)** . . . 195

5.12 **Transcriptional profiling of tumours at baseline (PRE) and after xentuzumab treatment (POST)** . . . 197

5.13 **CIBERSORTx deconvolution analysis of RNA sequencing data of WINGMEN patients** . . . 198

5.14 **Effects of xentuzumab on circulating levels of PSA and insulin** 199

5.15 **Serum IGF bioactivity at baseline (PRE) and after xentuzumab treatment (POST)** . . . 200

5.16 **Immunophenotyping of PBMCs before (PRE) and after xentuzumab treatment (POST) using CyTOF** . . . 202

6.1 **Overview of chapter 3 findings** . . . 213

6.2 **Overview of chapter 4 findings** 214
6.3 **Overview of chapter 5 findings** 215

List of Tables

1.1 **Prostate cancer grade group system** 4

2.1 **List of cell lines** 27

2.2 **List of primary antibodies used for western blot** 31

2.3 **List of antibodies and antigen retrieval buffers used for immunohistochemistry** 37

2.4 **List of antibodies used for immunohistochemistry for WINGMEN trial samples** 39

2.5 **List of primers used for qRT-PCR** 42

2.6 **List of antibodies used for flow cytometry** 48

2.7 **List of antibodies used for flow cytometry of murine TIL, blood, and splenocytes** 49

2.8 **List of primary cells** 53

2.9 **List of antibodies used for multiplex IF** 62

2.10 **List of antibodies used for CyTOF** 69

5.1 **Treatment compliance and details of interventions** 181

5.2 **Baseline characteristics of WINGMEN patients** 182

5.3 **Feasibility of treatment in pre-operative setting** 184

5.4 **Safety and tolerability of xentuzumab administered in the pre-prostatectomy setting** 184

7.1 **List of buffers used for multiple assays** 219

7.2 **List of differentially expressed genes in mouse tumours treated with xentuzumab vs control** 220

7.3 **List of differentially expressed genes in mouse tumours treated with xentuzumab + anti-PD-1 vs control: pilot experiment** . . 223

7.4 **List of differentially expressed genes in mouse tumours treated with xentuzumab vs control: pilot experiment** 232

7.5 **List of differentially expressed genes in mouse tumours treated with xentuzumab + aPD1 vs xentuzumab: pilot experiment** . 234

7.6 **List of differentially expressed genes in mouse tumours treated with xentuzumab + anti-PD-1 vs control: repeat experiment** . 238

7.7 **List of differentially expressed genes in mouse tumours treated with xentuzumab vs control: repeat experiment** 242

7.8 **Eligibility criteria for entry into the study** 244

7.9 **Entry requirements for WINGMEN patients: Eastern Cooperative Oncology Group (ECOG) performance scale** 245

7.10 **Summary of changes in primary endpoint markers PRE/POST xentuzumab** 246

7.11 **Summary of changes in nuclear and non-nuclear staining of phospho-IGF-1R PRE/POST xentuzumab** 247

7.12 **Summary of changes in IGF-1R PRE/POST xentuzumab** . . . 248

7.13 **Summary of changes in nuclear and non-nuclear staining of IGF-1R PRE/POST xentuzumab** 249

7.14 **Summary of changes in Ki67 expression PRE/POST xentuzumab** 250

7.15 **Summary of changes in AR expression PRE/POST xentuzumab** 251

7.16 **List of differentially expressed genes in post-xentuzumab-treated in-theatre cores vs pre-treatment diagnostic biopsies of WINGMEN patients** 252

List of Abbreviations

18s . . . . . 18s ribosomal RNA
4E-BP1 . . . . Eukaryotic translation initiation factor 4E-binding protein 1
Adgre1 . . . . Adhesion G protein-coupled receptor E1
ADT . . . . . Androgen deprivation therapy
AE . . . . . Adverse event
AESI . . . . . Adverse events of special interest
AF . . . . . Alexa Fluor
AJCC . . . . . American Joint Committee on Cancer
AKT . . . . . Protein kinase B
ALS . . . . . Acid labile subunit
AMPK . . . . AMP-activated protein kinase
ANC . . . . . Absolute neutrophil count
Angpt4 . . . . Angiopoietin 4
ANOVA . . . . Analysis of variance
AP-1 . . . . . Activator protein-1
APCs . . . . . Antigen-presenting cells
AR . . . . . Androgen receptor
AR-V7 . . . . Androgen receptor-variant 7
ARG1 . . . . . Arginase-1
AS . . . . . Active surveillance
ATF2 . . . . . Activating transcription factor 2
Atg14 . . . . . Autophagy-related 14
BAD . . . . . Bcl-2 associated agonist of cell death
Bcl-2 . . . . . B-cell lymphoma-2
Bcl-xL . . . . . B-cell lymphoma-extra large
BMDMs . . . Bone marrow-derived macrophages
BMI . . . . . Body mass index
BPH . . . . . Benign prostatic hyperplasia
bpMRI . . . . Biparametric MRI

BRCA1 . . . . Breast cancer gene 1

BSA . . . . . Bovine serum albumin

CAFs . . . . . Cancer-associated fibroblasts

CANCAP . . Cambridge Neoadjuvant Carcinoma of the Prostate

CAR . . . . . Chimeric antigen receptors

CC3 . . . . . Cleaved caspase-3

Ccl2 . . . . . C-C motif chemokine ligand 2

Ccr2 . . . . . C-C motif chemokine receptor 2

CD . . . . . Cluster of Differentiation

CDK . . . . . Cyclin-dependent kinase

cDNA . . . . . Complementary DNA

CFSE . . . . . Carboxyfluorescein succinimidyl ester

CHG . . . . . Centre for Human Genetics

CNA . . . . . Copy number alterations

CONSORT . . Consolidated Standards of Reporting Trials

CREB . . . . . cAMP response element binding protein

CST . . . . . Cell Signalling Technology

C_T . . . . . Cycle Threshold

CTCAE . . . . Common terminology criteria for adverse events

CTLA-4 . . . . Cytotoxic T-lymphocyte associated protein 4

CTLs . . . . . Cytotoxic T lymphocytes

CXCL1 . . . . C-X-C motif chemokine ligand 1

CyTOF . . . . Cytometry by Time-Of-Flight

DAB 3,3-diaminobenzidine

DAMPs . . . . Damage-associated molecular patterns

DAPI . . . . . 4',6'-diamidino-2-phenylindole

DCE . . . . . Dynamic contrast-enhanced sequence

DCs . . . . . Dendritic cells

DDR . . . . . DNA damage repair

DEGs . . . . . Differentially expressed genes

DEPC . . . . . Diethyl pyrocarbonate

dH_2O . . . . . Deionised water

DHT . . . . . Dihydrotestosterone

DMEM . . . . Dulbecco's Modified Eagle Medium

DMSO . . . . . Dimethyl sulfoxide

DNA . . . . . Deoxyribonucleic acid

dNTP . . . . . Deoxyribonucleotide triphosphate

DPH6 . . . . . Diphthamine biosynthesis 6

DPX . . . . . Dibuthylphthalate polystyrene xylene

DRE . . . . . Digital rectal examination

DSB . . . . . DNA double strand breaks

DTT . . . . . Dithiothreitol

DWI . . . . . Diffusion-weighted sequence

ECOG . . . . . Eastern Cooperative Oncology Group

EDTA . . . . . Ethylenediaminetetraacetic acid

ELISA . . . . . Enzyme-linked immunosorbent assay

EMT . . . . . Epithelial-mesenchymal transition

ERG . . . . . ETS-related gene

ERK . . . . . Extracellular signal-regulated kinase

ETS . . . . . Erythroblast transformation specific

ETV . . . . . ETS variant transcription factor

FBS . . . . . Foetal bovine serum

FDA . . . . . Food and Drug Administration

FFPE . . . . . Formalin-fixed paraffin-embedded

FOS . . . . . c-Fos

FOXO . . . . . Class O of forkhead box

FoxP3 . . . . . Forkhead box P3

FSC . . . . . Forward scatter

GRB2 . . . . . Growth factor receptor-bound protein 2

GG . . . . . Grade group

GH . . . . . Growth hormone

GSK . . . . . Glycogen synthase kinase

GTP . . . . . Guanine trihosphate

H&E . . . . . Haematoxylin & eosin

H2-Aa . . . . . Histocompatibility 2, class II antigen A

Hb . . . . . Haemoglobin

HCC . . . . . Hepatocellular carcinoma

HPLC . . . . . High-performance liquid chromatography

HRP . . . . . Horseradish peroxidase

HSP . . . . . Heat shock protein

IAP . . . . . Integrin associated protein

ICOS . . . . . Inducible T-cell co-stimulatory molecule

IFN-γ . . . . . Interferon-gamma

Ig . . . . . Immunoglobulin

IGF . . . . . Insulin-like growth factor

IGF-1R . . . . Insulin-like growth factor-1 receptor

IGF-2R . . . . Insulin-like growth factor-2 receptor

IGFBPs . . . . Insulin-like growth factor-binding proteins

IHC . . . . . Immunohistochemistry

IL . . . . . Interleukin

IL-1RA . . . . Interleukin-1 receptor antagonist

ILCs . . . . . Innate lymphoid cells

ILTCs . . . . . Innate-like T cells

IMP . . . . . Investigational Medicinal Product

Insr . . . . . Insulin receptor

IP . . . . . Intraperitoneal injection

IR . . . . . Insulin receptor

IRS . . . . . Insulin receptor substrate

ITIMs . . . . . Immunoreceptor tyrosine-based inhibition motifs

iTregs . . . . . Induced regulatory T cells

IU . . . . . International unit

JAK . . . . . Januse kinase

JNK . . . . . c-Jun N-terminal kinase

LAG-3 . . . . . Lymphocyte-activation gene 3

LATITUDE . Abiraterone acetate plus prednisone in patients with newly diagnosed high-risk metastatic castration-sensitive prostate cancer

LHRH . . . . . Luteinising hormone-releasing hormone

Lgmn . . . . . Legumain

LPS . . . . . Lipopolysaccharide

M-CSF . . . . Macrophage colony-stimulating factor

mAbs . . . . . Monocloncal antibodies

MAIT . . . . . Mucosal-associated invariant T cells

MAPK . . . . Mitogen-activated protein kinase

mCRPC . . . . Metastatic castration-resistant prostate cancer

mCSPC . . . . Metastatic castration-sensitive prostate cancer

Mdm2 . . . . . Mouse double minute 2 homolog

MDSCs . . . . Myeloid-derived suppressor cells

MEK . . . . . MAPK/ERK kinase

MFI . . . . . Mean fluorescence intensity

MHC-I . . . . Major histocompatibility class I

mIF . . . . . Multiplex immunofluorescence

MIF . . . . . Macrophage inhibitory factor

MIP-1-α . . . Macrophage inflammatory protein-1-alpha

Mki67 . . . . . Marker of proliferation Ki-67

MMP . . . . . Matrix metallopeptidases

mpMRI . . . . Multiparametric MRI

Mrc1 . . . . . Mannose receptor C-type 1

MRI . . . . . Magnetic resonance imaging

mRNA . . . . Messenger ribonucleic acid

mTORC2 . . . Mammalian target of rapamycin complex 2

NBF . . . . . Neutral buffered formalin

NCBI . . . . . National Centre for Biotechnology Information

NK . . . . . Natural killer cells

NF-κB . . . . . Nuclear factor-kappa B

NKT . . . . . Natural killer T cells

Nos2 . . . . . Nitric oxide synthase 2

NR4A . . . . . Nuclear receptor subfamily 4A

NSCLC . . . . Non-small cell lung cancer

OCHRe . . . . Oxford Centre for Histopathology Research

ORB . . . . . Oxford Radcliffe Biobank

OS . . . . . Overall Survival

P/S . . . . . Penicillin-Streptomycin

PAMPs . . . . Pathogen-associated molecular patterns

PAPP-A . . . Pregnancy-associated plasma protein-A

PAR . . . . . Protease-activated receptor

PBMC . . . . Peripheral blood mononuclear cells

PBS . . . . . Phosphate buffered saline

PCA . . . . . Principal component analysis

PCK . . . . . Pan-cytokeratin

PCUK . . . . . Prostate Cancer UK

PD-1 . . . . . Programmed cell death protein-1

PD-L1 . . . . . Programmed death-ligand 1

Pdgfa . . . . . Platelet-derived growth factor subunit A

PDK . . . . . Phosphatidylinositol-dependent kinase

PDX . . . . . Patient-derived xenograft

Pf4 . . . . . Platelet factor 4

PFA . . . . . Paraformaldehye

PI3K . . . . . Phosphoinositide 3-kinase

PIN . . . . . Prostate intraepithelial neoplasia

PIP_2 . . . . . Phosphatidylinositol 4,5-bisphosphate

PIP_3 . . . . . Phosphatidylinositol 3,4,5-bisphosphate

PLS-DS . . . . Partial least squares-discriminant analysis

PRAS40 . . . Proline-rich Akt substrate of 40 kDa

PRIME . . . . Prostate Imaging Using MRI±Contrast Enhancement

ProMPT . . . Prostate Cancer: Mechanisms of Progression and Treatment

PROSPER . . Safety and Efficacy Study of Enzalutamide in Patients With Non-metastatic Castration-Resistant Prostate Cancer

ProtecT . . . . Prostate testing for cancer and Treatment

PSA . . . . . Prostate specific antigen

Psca . . . . . Prostate stem cell antigen

PTEN . . . . . Phosphatase and tensin homlog

Ptgds . . . . . Prostaglandin D2 synthase

Ptgs2 . . . . . Prostaglandin-endoperoxide synthase 2

qRT-PCR . . . Quantitative real-time polymerase chain reaction

RNA . . . . . Ribonucleic acid

ROI . . . . . Region of interest

RP . . . . . Radical prostatectomy

RPMI . . . . . Rowell Park Memorial Institute 1640 Medium

RRM2 . . . . . Ribonucleotide reductase regulatory subunit M2

RT . . . . . Room temperature

RTK . . . . . Receptor tyrosine kinase

S6K . . . . . Ribosomal protein S6 kinase

SAE . . . . . Serious adverse event

SASP . . . . . Senescence-associated secretory phenotype

SCBT . . . . . Santa Cruz Biotechnology

SDS . . . . . Sodium dodecyl sulfate

SDS-PAGE . . Sodium dodecyl sulphate-polyacrylamide gel electrophoresis

SEM . . . . . Standard error of the mean

Serpine2 . . . Serpin family E member 2

Shc . . . . . Src homology and collagen domain protein

SHP-1 . . . . . Src homology-2 domain-containing phosphatase-1

SHPS-1 . . . . Src homology 2 domain-containing protein tyrosine phosphatase substrate-1

SIRPα . . . . . Signal regulatory protein alpha

SOCS . . . . . Suppressors of cytokine signalling

SOS . . . . . Son of sevenless

SSC . . . . . Side scatter

STAMPEDE . Systemic Therapy in Advancing or Metastatic Prostate Cancer: Evaluation of Drug Efficacy

STAT . . . . . Signal transducer and activator of transcription

SUMOylation Addition of small ubiquitin-related modifiers

T2W . . . . . T2-weighted sequence

TAM . . . . . Tumour-associated macrophages

TAO . . . . . Thyroid-associated ophthalmopathy

TBS . . . . . Tris-buffered saline

TCR . . . . . T cell receptor

TE . . . . . Tris-EDTA

Tfh . . . . . Follicular helper T cells

TGF-β . . . . . Transforming growth factor-beta

Tgfb3 . . . . . Transforming growth factor-beta 3

Th . . . . . T helper

Th2 . . . . . Type 2 T helper

THL . . . . . Translational Histopathology Lab

TIGIT . . . . . T cell immunoreceptor with Ig and ITIM domains

TIL . . . . . Tumour-infiltrating lymphocyte

TIM-3 . . . . . T cell immunoglobulin and mucin-domain containing-3

TIME . . . . . Tumour immune microenvironment

TIMP1 . . . . Tissue inhibitor of metalloproteinase 1

TKI . . . . . Tyrosine kinase inhibitor

T_m . . . . . Melting temperature

TME . . . . . Tumour microenvironment

TMPRSS2 . . Transmembrane protease serine 2

TNF . . . . . Tumour necrosis factor

TNFα . . . . . Tumour necrosis factor alpha

TRAE . . . . . Treatment-related adverse event

Tregs . . . . . Regulatory T cells

TRUS . . . . . Transrectal ultrasound

TSC2 . . . . . Tuberous sclerosis complex 2

UV . . . . . Ultraviolet light

VEGFA . . . . Vascular endothelial growth factor A

Vim . . . . . Vimentin

VIP . . . . . Variable importance in projection

VST . . . . . Variance stabilising transformation

WBC . . . . . White blood count

WINGMEN . Windows trial of INsulin-like Growth factor neutralising antibody xentuzumab in MEN scheduled for radical prostatectomy

ZEB1 . . . . . Zinc finger E-box binding homeobox 1

1

Introduction

Contents

1.1 Prostate cancer 1
1.1.1 Treatment options 4
1.1.2 Molecular mechanisms 5
1.2 IGF-1 axis 7
1.2.1 Receptors and ligands 7
1.2.2 IGF-1R signalling pathways 8
1.3 IGF axis and cancer 11
1.3.1 IGF axis and cancer risk 12
1.3.2 IGF axis and its effects on tumorigenesis 12
1.4 Anti-tumour immunity 16
1.4.1 Innate immune response to cancer 16
1.4.2 Adaptive immune response to cancer 17
1.5 Reported influence of IGFs on the immune response . . . 20
1.5.1 Effects of IGFs on adaptive immunity 20
1.5.2 Effects of IGFs on innate immunity 21
1.6 Prostate cancer tumour microenvironment 22
1.7 Aims and hypothesis 23

1.1 Prostate cancer

Cancer is defined as a disease that involves uncontrolled proliferation of cells, with invasion of surrounding tissues. In general, cancer is identified by a series of hallmarks: sustaining proliferative signalling, evading growth suppressors, activating invasion and metastases, inducing angiogenesis, resisting cell death, enabling replicative immortality, tumour-promoting inflammation, avoiding immune destruction, genome instability and mutation, and deregulating cellular energetics (Hanahan et al., 2000; Hanahan et al., 2011). Recently, four new hallmarks have emerged, including nonmutational epigenetic reprogramming, unlocking phenotypic plasticity, senescent cells, and polymorphic

microbiomes (Hanahan, 2022). Prostate cancer is also characterised by some of these hallmarks (Datta et al., 2016).

Prostate cancer is the second most common cancer in men worldwide, with 1 in 8 men being diagnosed in their lifetime and more than 12,000 men dying from it in the UK (*Prostate cancer statistics, World Cancer Research Fund International* 2022; *About prostate cancer, Prostate Cancer UK* 2023; Bray et al., 2024). The risk factors include age, family history, race, and genetics, with additional factors such as diet and obesity (Bergengren et al., 2023; de Bono et al., 2020c). High serum levels of circulating insulin-like growth factors (IGFs) are also associated with increased risk of prostate cancer development (Travis et al., 2016; Price et al., 2012). Although prostate cancers are phenotypically heterogeneous, most prostate cancers are adenocarcinomas, where tumour-initiating cells originate from either basal or luminal epithelial cells due to genetic mutations (Goldstein et al., 2010; Chua et al., 2014). This leads to abnormal development of prostate epithelia, such as proliferative inflammatory atrophy (PIA) and prostate intraepithelial neoplasia (PIN), variously described as distinct forms or precursors to prostate adenocarcinoma (DeMarzo et al., 1999; DeMarzo et al., 2003; Anbarasan et al., 2024; Zhou, 2018). This can further develop into locally advanced prostate cancer, in which localised prostate cancers spread locally through adjacent structures into fat, muscle, bladder, or rectum, and then metastatic prostate cancer, where cancer cells spread to other organs such as lymph nodes and bone, and occasionally, lung, liver, and brain (Shen et al., 2010; Rebello et al., 2021).

Prostate cancers can be diagnosed by biopsies upon digital rectal examination (DRE), prostate specific antigen (PSA) test, and magnetic resonance imaging (MRI). DRE is an internal examination of a prostate to detect any nodules, induration, or asymmetry (Chodak et al., 1989; Schroder et al., 1998; Humphrey, 2007), but several studies suggest that DRE does not add significant benefit to diagnostics, recommending against it being a stand-alone screening test for prostate cancer (Naji et al., 2018; Krilaviciute et al., 2023). PSA is a protein produced by both normal and cancerous prostate tissue, and is often elevated in people with prostate cancer (Catalona et al., 1991; Balk

et al., 2003; Thompson et al., 2004). However, increased serum PSA levels can also occur in cases of benign prostatic hyperplasia (BPH) or prostatitis, as well as after cycling, sex, and vigorous exercise. The levels, therefore, have to be interpreted carefully (Nadler et al., 1995; Ilic et al., 2018), and there have been contradictory evidences on the benefits of PSA screening (Andriole et al., 2009; Martin et al., 2018). The European Randomised Study of Screening for Prostate Cancer showed that, although PSA screening reduced prostate cancer death by 20%, it was associated with high rate of overdiagnosis. Recently, multiparametric MRI (mpMRI), consisting of T2-weighted sequence (T2W), diffusion-weighted sequence (DWI), and dynamic contrast-enhanced sequence (DCE), has emerged as a promising diagnostic tool, capable of identifying 20% more clinically significant prostate cancers than tranrectal ultrasound (TRUS)-guided biopsy (Ahmed et al., 2017; Schoots et al., 2015; Stabile et al., 2020). Despite the benefits of mpMRI (de Rooij et al., 2014), some tumours are mpMRI-invisible, making it difficult to distinguish those clinically significant prostate cancers (Kim et al., 2020; Pachynski et al., 2021; Salami et al., 2019). Recently, Prostate Imaging using MRI±Contrast Enhancement (PRIME) study (NCT04571840) demonstrated biparametric MRI (bpMRI), which uses only T2W and DWI sequences, as an efficient and cost-effective way to screen men (Asif et al., 2023). At present, biopsy remains to be the most definitive way to diagnose prostate cancer (Ahdoot et al., 2020; Bryant et al., 2019). The TRANSFORM trial launched by Prostate Cancer UK (PCUK) will be the biggest prostate cancer screening trial in 20 years, with a mission to find the best prostate cancer screening method for men (Burki, 2024).

The Gleason scoring is used to grade prostate cancer, ranging from 1 to 5, based on the histological patterns of the cancer, where a higher grade denotes anaplastic, differentiated tissues (Gleason et al., 1974; Gleason, 1992). The Gleason score is determined by adding the most common grade of the cancers and the highest other grade in the sample. In 2016, grade group (GG) system was introduced as in Table 1.1 (Pierorazio et al., 2013; Epstein et al., 2016, Humphrey et al., 2016).

Table 1.1: Prostate cancer grade group system. The higher the grade group, more likely the cancer is to grow and spread.

Grade Group	Gleason Score
1	6 (3+3)
2	7 (3+4)
3	7 (4+3)
4	8 (3+5), (4+4), (5+3)
5	9 (4+5), (5+4) & 10 (5+5)

1.1.1 Treatment options

Treatment options for men with localised prostate cancer include active surveillance (AS), radical prostatectomy (RP), radiotherapy, and brachytherapy (D'Amico et al., 1998; Holmberg et al., 2002; Bill-Axelson et al., 2018). Prostate testing for cancer and Treatment (ProtecT) trial (NCT02044172) that compared effectiveness and cost-effectiveness of AS, RP, and radiotherapy for men with PSA-detected localised prostate cancer showed that there were no significant differences in prostate cancer-specific mortality among the three treatment options, but there were lower incidences of disease progression and metastasis in patients treated with RP or radiotherapy compared to AS (Lane et al., 2014; Hamdy et al., 2016; Hamdy et al., 2023). This, however, also highlighted side effects, such as significantly higher incidences of urinary continence and reduced sexual function in RP compared to radiotherapy or AS (Donovan et al., 2016). Recent publication after long-term follow-up of patients with GG1 prostate cancer under AS showed that the risk of cancer death or metastasis in these men were less than 1% (Tosoian et al., 2020).

More advanced prostate cancer requires hormone therapy to reduce testicular androgen levels, such as surgical castration by removing the testicles and androgen deprivation therapy (ADT), which involves treatment with luteinising hormone-releasing hormone (LHRH) agonist (Chodak, 1989; Schally et al., 2017; Westaby et al., 2022; Fujita et al., 2019). Although 80 - 90% of patients initially respond well to ADT, about 10 - 20% of those develop metastatic castration-resistant prostate cancer (mCRPC) (Harris et al.,

2009; Karantanos et al., 2013; Kirby et al., 2011; Vellky et al., 2020). This progression arises from point mutation or amplification of androgen receptor (*AR*) (Waltering et al., 2012; Taylor et al., 2010; Visakorpi et al., 1995; Lamb et al., 2014), changes in androgen biosynthesis and AR cofactors (Chang et al., 2013; LaTulippe et al., 2002; Agoulnik et al., 2005; Dasgupta et al., 2015), and constitutively active AR splice variants (Dehm et al., 2008; Antonarakis et al., 2016), AR-variant 7 (AR-V7) being the most abundant (Robinson et al., 2015; Sharp et al., 2019; Scher et al., 2018; Armstrong et al., 2019). Development of second-generation hormone therapy using anti-androgens, AR antagonists such as abiraterone, enzalutamide, and apalutamide helped improve the outcomes of patients with metastatic prostate cancer (de Bono et al., 2011; Scher et al., 2012; Davis et al., 2019; Smith et al., 2018a).

Recently, several trials have tested the benefits of combination of several treatment options for better survival of metastatic castration-sensitive prostate cancer (mCSPC) and mCRPC patients. Systemic Therapy in Advancing or Metastatic Prostate Cancer: Evaluation of Drug Efficacy (STAMPEDE) trial (NCT00268476) showed that adding chemotherapy, radiotherapy, or abiraterone to hormone therapy increases overall survival (OS) of prostate cancer patients (James et al., 2016; James et al., 2017; Attard et al., 2022; Parker et al., 2022). Abiraterone acetate plus prednisone in patients with newly diagnosed high-risk metastatic castration-sensitive prostate cancer (LATITUDE) trial (NCT01715285) revealed that adding abiraterone and prednisone to ADT increased OS of mCSPC patients (Fizazi et al., 2017). Safety and Efficacy Study of Enzalutamide in Patients With Nonmetastatic Castration-Resistant Prostate Cancer (PROSPER) trial (NCT02003924) showed that enzalutamide and ADT treatment results in longer median OS in patients with non-metastatic CRPC (Hussain et al., 2018; Sternberg et al., 2020).

1.1.2 Molecular mechanisms

The most prominent genetic alterations in localised prostate cancer are fusions of regions encoding erythroblast transformation specific (ETS) family of transcription factors with AR-regulated promoter regions (Tomlins et al., 2005; Carver et al., 2009).

The most prominent molecular subtype is the fusion of transmembrane protease serine 2 (TMPRSS2) and ETS-related gene (ERG), detected in almost 50% of prostate cancer biopsies in white men and less in African Americans and Asians (Tomlins et al., 2008; Perner et al., 2007; Magi-Galluzzi et al., 2011; Sedarsky et al., 2018). These gene fusions result in overexpression of ERG, ETS variant transcription factor (ETV)1, or ETV4 (Song et al., 2018; Tomlins et al., 2006; Tomlins et al., 2007; Tomlins et al., 2009), development of PIN in concurrent with phosphoinoside 3-kinase (PI3K) pathway activation, and prostate cancer development and progression in cooperation with phosphatase and tensin homolog (PTEN) loss (King et al., 2009; Carver et al., 2009; Wang et al., 2006; Berger et al., 2011). Functional loss of *PTEN* by deletion or mutation, which leads to PI3K-AKT signalling activation, occurs in primary tumours and is associated with adverse outcomes (Jamaspishvili et al., 2018; Chen et al., 2017b; Yang et al., 2018a; Gundem et al., 2015). Other key genetic alterations include mutations in genes such as *SPOP* and *FOXA1* (Abeshouse et al., 2015; Barbieri et al., 2012) and deoxyribonucleic acid (DNA) damage repair (DDR) genes such as *BRCA2* and *ATM* (Marshall et al., 2019; Fraser et al., 2017; Taylor et al., 2019).

Both *de novo* mCSPC and mCRPC have higher mutation burden and copy number alterations (CNAs) compared to localised prostate cancer (Stopsack et al., 2020; Mateo et al., 2020; Grist et al., 2022). They also have higher prevalence of PTEN deletion (Suzuki et al., 1998; Grasso et al., 2012; Jamaspishvili et al., 2018), DDR gene defects (Taylor et al., 2019; Pritchard et al., 2016; Abida et al., 2017; de Bono et al., 2020b), MYC overexpression (Gurel et al., 2008; Hubbard et al., 2016; Qiu et al., 2022), and PI3K pathway alterations (Carver et al., 2011; Pearson et al., 2018; Robinson et al., 2015). The most common mutation is genomic aberration of AR and regulators of AR transcription such as *FOXA1* as well as deletion of genes that inactivate AR signalling such as *ZBTB16* and *PLZF* (Hodgson et al., 2005; Mills, 2014; Hsieh et al., 2015).

AR, a transcription factor part of the steroid receptor superfamily, is the most studied oncogene in prostate cancer pathophysiology (Mangelsdorf et al., 1995; Tan et al., 2015). In unbinded state, AR is located in the cytoplasm, complexed to heat shock proteins

(HSPs) such as Hsp90 (Fang et al., 1996; Georget et al., 2002). Its ligands include androgens such as testosterone and its biologically active form dihydrotestosterone (DHT), which bind to and activate AR and drive its translocation into the nucleus (Simental et al., 1991; Cutress et al., 2008). In the nucleus, it binds to androgen response elements, acting as a transcription factor to regulate cell growth and survival (Shang et al., 2002; Shaffer et al., 2004).

1.2 IGF-1 axis

The IGF axis plays a critical role in normal cell growth and development by promoting cell proliferation and differentiation and inhibiting apoptosis. (Jones et al., 1995; Simpson et al., 2017). It is also involved in cancer development, including prostate cancer (Baserga et al., 2003; Matsushita et al., 2022). The IGF axis consists of ligands IGF-1, IGF-2, and insulin, receptors such as IGF-1 and IGF-2 receptors (IGF-1R and IGF-2R), insulin receptors (IR), and the IGF-1R/IR hybrid receptors, and a family of high-affinity IGF-binding proteins (IGFBPs) (Foulstone et al., 2005; LeRoith et al., 2003).

1.2.1 Receptors and ligands

The IGF axis is activated primarily by IGF-1 and IGF-2 ligands, single-chain polypeptides of 7 kDa. They are mainly produced in the liver with growth hormone (GH) as their key stimulator (endocrine mechanism) but can also be locally produced through autocrine or paracrine mechanism (Daughaday et al., 1989; Laron, 2001; Pollak et al., 2004; Bowers et al., 2015). IGF-1 binds to IGF-1R with the highest affinity, followed by IGF-2 and insulin, owing to their common structures (Meyts et al., 2002). IGF-2 also binds to IR-A, foetal isoform of IR, (Frasca et al., 1999; Frasca et al., 2008) and IGF-2R, a scavenger receptor with no tyrosine kinase activity (Moschos et al., 2002; Li et al., 2009).

IGF-1R is a heterotetrameric transmembrane receptor tyrosine kinase (RTK) made up of two extracellular α- and two transmembrane β-subunits that are linked by disulfide

bonds (Ullrich et al., 1986; Favelyukis et al., 2001). A polypeptide of 1,367 amino acids, IGF-1R is expressed in most cells and structurally similar to IR (Riedemann et al., 2006). As opposed to IR-A which binds to insulin and IGF-2 with equal affinity and is associated with cell growth and proliferation, IR-B, a classic IR isoform, only binds to insulin and regulates glucose uptake (Belfiore et al., 2017; Simpson et al., 2017). In addition, hybrid heterodimeric receptors of IGF-1R and IR isoforms bind both IGFs and insulin (Belfiore, 2007).

The six IGFBPs (IGFBP-1 to -6) bind to IGFs with high affinity and regulate their bioactivities (Baxter, 1993; Rechler et al., 1998). Most serum IGFs are bound to IGFBP-3 and acid labile subunit (ALS), forming a ternary complex that increases their half-life (Jones et al., 1995; Baxter, 2014). In addition, IGFBPs prevent potential interactions of IGFs with IR, regulate their transport to tissues, and modulate IGF-1R signalling by either restricting their access to IGF-1R or driving the pathway activation (Bach, 2018; Baxter, 2023; Conover et al., 2000). IGFBPs are also involved in IGF-independent actions that regulate cellular growth and differentiation (Baxter, 2014; Allard et al., 2018; Zhu et al., 2008b). IGFBPs are subject to proteolysis by proteases, such as serine proteases, metalloproteinases, and cathepsins, which cleave the IGFBP-IGF complex and free the IGFs to increase IGF-1R activation (Rajaram et al., 1997; Clay Bunn et al., 2003; Jones et al., 1995).

1.2.2 IGF-1R signalling pathways

Binding of IGFs to IGF-1R induces a conformational change and autophosphorylation of the tyrosine residues 1131, 1135, and 1136 in the kinase domain. Subsequent recruitment of the adaptor molecules, insulin receptor substrate (IRS) and Src homology and collagen domain protein (Shc), and janus kinase (JAK) activates PI3K, mitogen-activated protein kinase (MAPK)/extracellular signal-regulated kinase (ERK), and JAK/signal transducer and activator of transcription (STAT) pathways, respectively (Jansson et al., 1997; Li et al., 2009; Kooijman, 2006; Chitnis et al., 2008) (Figure 1.1).

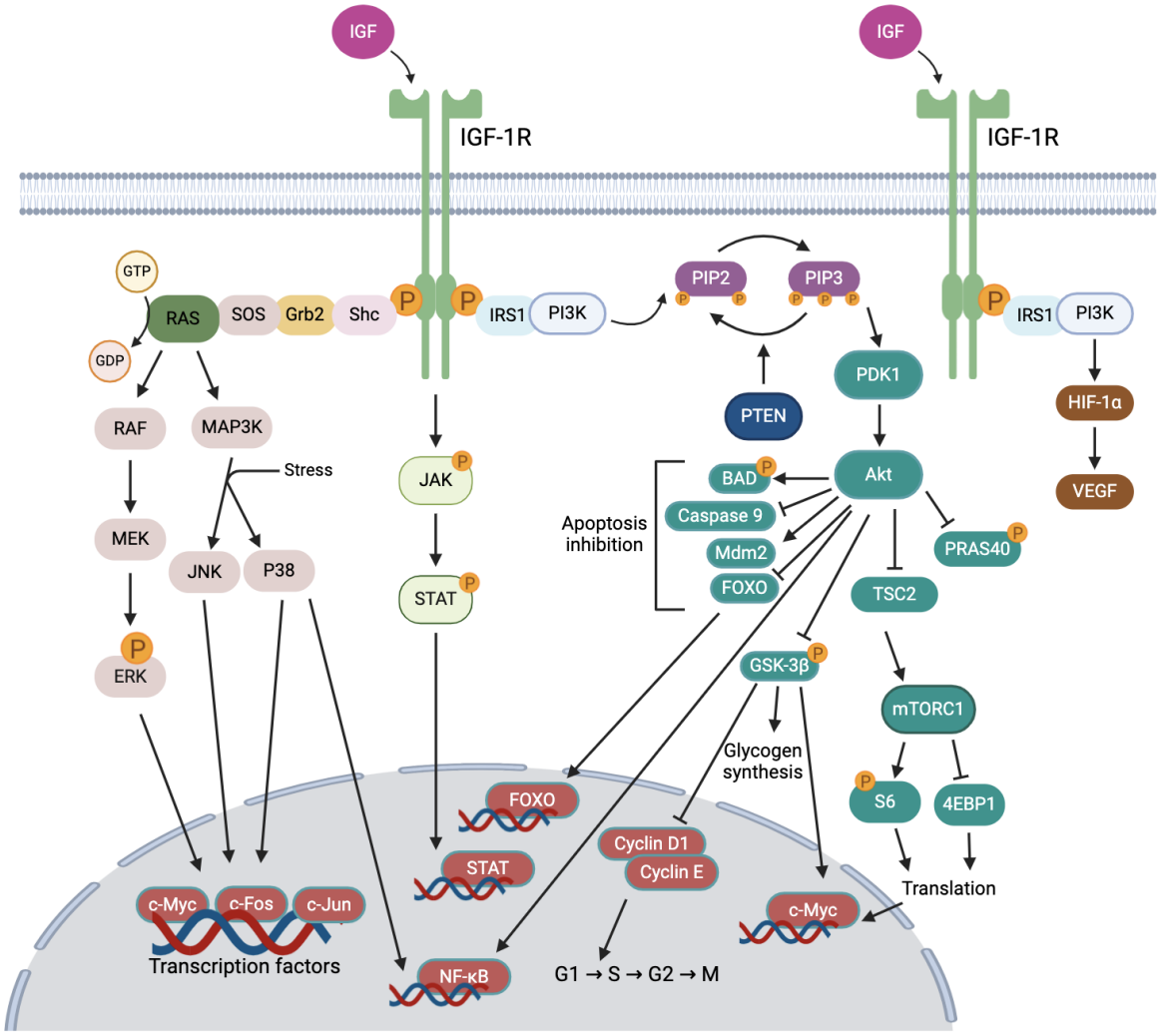


Figure 1.1: IGF-1R signalling pathway. Binding of IGFs to IGF-1R activates PI3K-AKT, MAPK, and JAK/STAT pathways, leading to downstream effects such as cell survival, growth and proliferation, and motility and invasion. Figure was created using BioRender with information from references cited in the text.

1.2.2.1 PI3K/AKT pathway

Recruitment of IRS-1 to its docking site binds and activates PI3K, which then phosphorylates phosphatidylinositol 4,5-bisphosphate (PIP_2) to phosphatidylinositol 3,4,5-bisphosphate (PIP_3). This activates protein kinase B (AKT) and phosphatidylinositol-dependent kinase (PDK)-1 (Li et al., 2009; Hennessy et al., 2005; Franke et al., 1997). AKT is then activated upon phosphorylation of threonine 308 by PDK-1 and of serine 473 by mammalian target of rapamycin complex 2 (mTORC2), which is activated by IGF-1R (Alessi et al., 1997; Sarbassov et al., 2005; Chitnis et al., 2008). AKT activation

can be inhibited by PTEN, which acts as a negative regulator of this pathway by dephosphorylating PIP_3 to PIP_2 (Stambolic et al., 1998).

Activated AKT then phosphorylates various targets to regulate cellular processes such as survival, growth, and proliferation (Manning et al., 2007; Hennessy et al., 2005). Upon AKT phosphorylation, BCL-2 associated agonist of cell death (BAD), instead of binding to and inhibiting the anti-apoptotic B-cell lymphoma-2 (Bcl-2) family proteins such as Bcl-2 and B-cell lymphoma-extra large (Bcl-xL), binds to the adaptor protein 14-3-3, inhibiting apoptosis and promoting cell survival (Kooijman, 2006; Datta et al., 1997). Activated AKT also regulates cell survival by phosphorylating caspase 9, mouse double minute 2 homolog (Mdm2), and class O of forkhead box (FOXO) transcription factors and inhibiting pro-apoptotic activity (Cardone et al., 1998; Ogawara et al., 2002; Brunet et al., 1999). AKT phosphorylates and inactivates glycogen synthase kinase (GSK)-3β, which not only increases glycogen synthesis but also regulates cyclin-dependent kinases (CDKs) and stimulates transcription factors such as *c-JUN* and *c-Myc* (Pearl et al., 2002; Diehl et al., 1998; Welcker et al., 2003; Yeh et al., 2004). In addition, AKT regulates translation by phosphorylating and inhibiting tuberous sclerosis complex 2 (TSC2) and proline-rich Akt substrate of 40 kDa (PRAS40) (Inoki et al., 2002; Sancak et al., 2007). This activates mTORC1, which phosphorylates eukaryotic translation initiation factor 4E-binding protein 1 (4E-BP1) and ribosomal protein S6 kinase (S6K), enhancing translation of messenger ribonucleic acid (mRNAs) that encodes for proteins involved in proliferation, such as c-Myc and cyclin D1 (Averous et al., 2008; Wendel et al., 2004; Mamane et al., 2006; Sabatini, 2006).

1.2.2.2 MAPK pathway

Docking of Shc to IGF-1R recruits growth factor receptor-bound protein 2 (GRB2), which in turn recruits son of sevenless (SOS) and aids in guanine triphosphate (GTP) loading of the RAS GTPase to activate RAS (Simanshu et al., 2017; Dhillon et al., 2007). This initiates a phosphorylation signalling cascade via RAF, MAPK/ERK kinase (MEK)1/2, and ERK1/2 (Stokoe et al., 1994; Seger et al., 1995). Activated ERK1/2 then translocates to the nucleus and activates various transcription factors involved

in proliferation and cell cycle progression, such as c-Myc, c-Fos, c-Jun, and cAMP response element binding protein (CREB) (Chitnis et al., 2008; Zhang et al., 2002; Yamamoto et al., 2006).

In response to cytokines and environmental stress such as DNA-damaging agents and ultraviolet light (UV) radiation, MAPK pathway can be activated via c-Jun N-terminal kinase (JNK) and p38 kinase (Weston et al., 2002; Davis, 2000). Activated JNK can phosphorylate transcription factors such as c-Jun, activating transcripton factor 2 (ATF2), and STAT3 (Davis, 2000; Dhillon et al., 2007). It also binds to and phosphorylates p53, leading to apoptosis (Fuchs et al., 1998; Wu, 2004). Activated p38 are involved in not only phosphorylation of transcription factors such as STAT1 and ATF2 but also pro-inflammatory cytokine production and regulation of nuclear factor-kappa B (NF-κB)-dependent transcription (Goh et al., 1999; Saha et al., 2007; Kumar et al., 2003).

1.2.2.3 JAK/STAT pathway

JAK/STAT pathway can also be induced by the IGF axis (Takahashi et al., 1999; Himpe et al., 2009; Hua et al., 2020; Werner, 2023). IGF-1R activation phosphorylates and activates JAK-1 and JAK-2, leading to recruitment and phosphorylation of STATs, especially STAT-1 and STAT-3, which then translocate to the nucleus and act as transcription factors (Gual et al., 1998; Zong et al., 2000; Himpe et al., 2009). Activated STAT-3 is involved in cytokine signalling, immune regulation, and cell growth and transformation (Zong et al., 2000; Yu et al., 2009a; Hu et al., 2021b). The family of suppressors of cytokine signalling (SOCS) act as a negative regulator of this pathway (Yadav et al., 2005; Zhou et al., 2018; Dey et al., 1998).

1.3 IGF axis and cancer

Several reports link the IGF axis with development of cancers, endocrine diseases such as thyroid eye disease, and skin diseases (Osher et al., 2019; Smith et al., 2018b; Gardner et al., 2022). In particular, IGF axis has been implicated in growth and metastasis

of various cancers such as prostate, breast, colon, lung, pancreas, ovarian, and skin (Sachdev et al., 2007; Pollak, 2012; Matsushita et al., 2022; Baserga et al., 2003).

1.3.1 IGF axis and cancer risk

Low-circulating serum IGFs can protect against cancer (Guevara-Aguirre et al., 2011; Steuerman et al., 2011). In mouse model, mice with liver-specific deletion of IGF-1 are resistant to tumour growth (Olivo-Marston et al., 2009; Wu et al., 2002). Similarly, patients with Laron dwarfism, characterised by low serum IGF-1 levels due to growth hormone receptor mutation, do not develop cancer (Laron, 2001; Laron et al., 2023).

High circulating levels of IGF-1 in serum are associated with increased risk of various cancers, including prostate, colorectal, and breast (Travis et al., 2016; Schmidt et al., 2014; Rinaldi et al., 2010; Christopoulos et al., 2015). Recent UK biobank study reported that high serum IGF-1 levels are associated with increased risk of multiple myeloma, malignant myeloma, and thyroid cancer (Knuppel et al., 2020). High serum IGF-1 levels are also associated with increased risk of prostate cancer mortality (Watts et al., 2021).

Studies on IGF-2 and IGFBP-3, which binds to circulating IGF-1, are varied. While some studies link high serum IGF-2 or IGFBP-3 with prostate cancer, postmenopausal breast cancer, and endometrial cancer risk, others report no correlation (Livingstone, 2013; Clayton et al., 2011; Roddam et al., 2008; Oh et al., 2004).

1.3.2 IGF axis and its effects on tumorigenesis

IGF-1R overexpression has been reported in prostate, breast, pancreatic, head and neck squamous cell, and lung cancers (Hellawell et al., 2002; Obr et al., 2018; Du et al., 2020; Dale et al., 2015; Alfaro-Arnedo et al., 2022), and our group has shown that high IGF-1R expression in prostate cancer is associated with risk of metastasis as well as recurrence post-radiotherapy (Aleksic et al., 2017). *IGF1R* gene has been reported as a negative regulator of tumour suppressors (Werner, 2012), and in turn, loss-of-function in tumour suppressor genes such as *TP53*, breast cancer gene 1 (*BRCA1*), Wilms tumour 1 (*WT1*), and von Hippel-Lindau (*vHL*) can result in IGF-1R upregulation (Ohlsson

et al., 1998; Maor et al., 2000; Werner et al., 1996; Yuen et al., 2007; Werner et al., 2016). Conversely, oncogenes and oncogenic fusion proteins such as *Myc*, EWSR1-WT1, and TMPRSS2-ERG can drive *IGF-1R* transcription (Sun et al., 2018; Finkeltov et al., 2002; Sharon et al., 2016; Werner et al., 2018).

Nuclear translocation of IGF-1R upon the addition of small ubiquitin-related modifiers (SUMOylation) can interact with ribonucleic acid (RNA) polymerase II to upregulate expression of JUN and FAM21 that mediate cancer cell migration and survival, as well as other transcription factors and nuclear proteins (Sehat et al., 2010; Aleksic et al., 2010; Sarfstein et al., 2012; Aleksic et al., 2018; Waraky et al., 2017; Rieger et al., 2020). It has been reported that nuclear IGF-1R, which is detected more frequently in malignant epithelium compared to benign, is associated with more aggressive prostate cancer (Aleksic et al., 2018; Mills et al., 2021) and increased resistance to chemotherapy (Codony-Servat et al., 2017; Hua et al., 2020).

Altered expression of the ligands can also drive IGF signalling in cancers (Samani et al., 2007). Secretion of IGF-1 or IGF-2 by stroma and cancer cells has been reported to promote cancer progression (Tape et al., 2016; Unger et al., 2017; Xu et al., 2017). Regulation of IGF-2 by a transcription factor GATA2 has been linked to aggressiveness in lethal prostate cancer (Vidal et al., 2015). In addition, IGFBP expression significantly correlates with tumour mutational burden, immune cell infiltration, and activation or suppression of various cancer-related pathways such as angiogenesis and epithelial-to-mesenchymal transition (EMT) (Liu et al., 2023b). Reduced IGFBP-3 levels are reported to be a predictor of advanced prostate cancer (Mehta et al., 2011 Chan et al., 2002; Shariat et al., 2002), while higher nuclear IGFBP-3 expression is a strong predictor of cancer recurrence (Seligson et al., 2013). Tumours have been reported to secrete IGFBP proteases, such as PSA in prostate cancer (Cohen et al., 1992; Cohen et al., 1994), which enhances IGF bioactivity in bone metastasis by cleaving IGFBP5 (Maeda et al., 2009). IGFBP5 has a diverse role in cancer progression, acting as both an oncogene and a tumour suppressor (Waters et al., 2022; Miyake et al., 2000). Recently, it has been reported to enhance glioblastoma stem-like cell invasion (Lin et al., 2023).

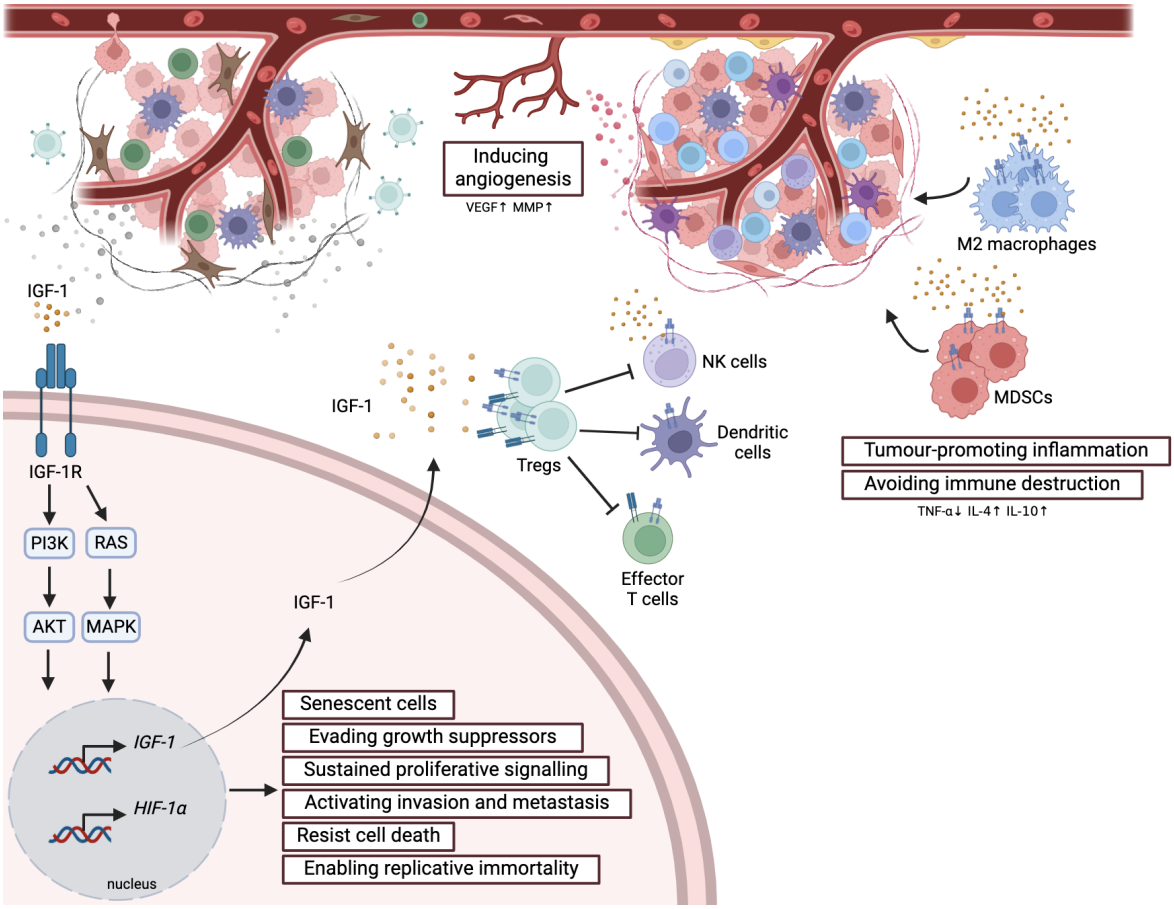


Figure 1.2: IGF axis and hallmarks of cancer. IGF axis contributes to multiple hallmarks of cancer, promoting cancer progression and immmunosuppression. Figure was created using BioRender with information from references cited in the text.

IGF axis promotes cancer progression by contributing to multiple hallmarks of cancer (Figure 1.2), which makes it more effective but complex therapeutic target (Shin et al., 2002; Hanahan et al., 2011). IGF-1 promotes cell cycle progression by upregulating cyclin D expression (Ren et al., 2009; Mawson et al., 2005). Recent papers from our lab reported that IGF blockade delays replication fork progression by downregulating ribonucleotide reductase regulatory subunit M2 (RRM2) and reducing deoxyribonucleotide triphosphate (dNTP) supply (Rieunier et al., 2021; Wu et al., 2021). IGF-1R inhibition evades DNA damage-induced apoptosis via translational regulation of p53-Mdm2 feedback loop (Xiong et al., 2007), and IGF-1R depletion impairs repair of radiation-induced DNA double strand breaks (DSBs) (Chitnis et al., 2014; Rochester et al., 2005; Turney et al., 2012; Ferte et al., 2013; Simpson et al., 2020). IGF axis also

contributes to cancer stem cell renewal and differentiation (Lee et al., 2022; Osuka et al., 2021; Cao et al., 2017; Liu et al., 2024). In addition, IGF-1R activation can promote EMT by increasing zinc finger E-box binding homeobox 1 (ZEB1) expression (Graham et al., 2008; Li et al., 2014) or by inactivating GSK-3β (Bachelder et al., 2005; Kim et al., 2007a; Zhou et al., 2004; Li et al., 2017). In addition, interleukin (IL)-6 induction by IGF-1R signalling activation has been reported to promote EMT (Rojas et al., 2011; Zheng et al., 2019). IGF axis can also promote angiogenesis by upregulating hypoxia-inducible factor 1α (HIF-1α) and growth factors such as vascular endothelial growth factor A (VEGFA) and matrix metallopeptidases (MMPs) (Fukuda et al., 2002; Lin et al., 2017; Bid et al., 2012; Liu et al., 2023a). IGF-1 is also implicated in cancer metastasis by promoting anchorage-independent growth and invasion (Rieunier et al., 2019; Sachdev et al., 2004; Sayeed et al., 2013; Sachdev et al., 2010).

In prostate cancer, IGF axis drives nuclear translocation of AR and AR-mediated transcription and enhances androgen signalling (Nickerson et al., 2001; Wu et al., 2006; Fan et al., 2007), and in turn, AR can elevate IGF axis signalling (Pandini et al., 2005; Kim et al., 2022). IGF-1R expression can also be regulated by TMPRSS2-ERG fusion, contributing to prostate cancer progression (Sharon et al., 2016; Mancarella et al., 2015; Mancarella et al., 2017; Barwick et al., 2010).

Due to the role of IGFs in cancer progression and survival, several therapies targeting IGF axis were attempted (Chapter 3.1). In particular, xentuzumab is an IGF blocking monoclonal antibody (mAb) that binds to IGF-1 and IGF-2 ligands and neutralises proliferative signalling of IGF-1R and IR-A without interfering with metabolic actions of IR-B (Friedbichler et al., 2014).

Despite advances in molecularly targeted therapies, prostate cancer is not curable apart from surgery or radiotherapy in localised prostate cancer. This lack of curative molecular interventions could partly be attributed to the nature of prostate cancer tumour immune-microenvironment (TIME) and the challenges in eliciting curative immune responses in patients.

1.4 Anti-tumour immunity

Evading immune destruction is one of the hallmarks of cancer (Hanahan et al., 2011). Cancer cells avoid immune surveillance by cancer immunoediting which consists of three phases: elimination, equilibrium, and escape (Schreiber et al., 2011; Dunn et al., 2002; Dunn et al., 2004; Chen et al., 2017a). Elimination phase involves innate and adaptive immune cells recognising and destroying the transformed cells. Those that survive this stage progresses to the equilibrium phase, where tumour cells are functionally dormant, while new immunosuppressive variants that resist immune recognition arise. Tumours that withstand this immune pressure undergo escape phase as clinically visible tumours, resulting in unrestrained growth and possible malignancy (Dunn et al., 2002; Mittal et al., 2014; O'Donnell et al., 2018).

Tumour surveillance involves both fast-acting innate immune system and antigen-dependent adaptive immune system (Gajewski et al., 2013; Demaria et al., 2019). These cells, along with non-immune cells such as cancer-associated fibroblasts (CAFs), endothelial cells, and vascular cells, comprise tumour microenvironment (TME) (de Visser et al., 2023; Mellman et al., 2023).

1.4.1 Innate immune response to cancer

Innate immune cells include myeloid lineage such as monocytes, macrophages, mast cells, myeloid-derived suppressor cells (MDSCs), dendritic cells (DCs), granulocytes such as neutrophils, eosinophils, and basophils, innate lymphoid cells (ILCs) such as natural killer (NK) cells, and innate-like T cells (ILTCs) such as natural killer T (NKT) and $\gamma\delta$ T cells (Demaria et al., 2019; Ruf et al., 2023). Complement system also acts as part of the innate immune system by acting as a first line of defense and promoting inflammation, thereby enhancing tumour growth and promoting metastasis (Afshar-Kharghan, 2017; Reis et al., 2018; Ricklin et al., 2010; Beach et al., 2023).

In cancer, innate immune cells can recognise any metabolic, hypoxic, and anatomical changes associated with tumour cells and either directly kill the tumour cells or trigger adaptive immune response (Buck et al., 2017; Yi et al., 2023). Macrophages

and granulocytes can phagocytose tumour cells by cellular engulfment and lysosomal degradation (Feng et al., 2019; Li et al., 2023b). Mast cells can bind to pathogens directly or associate with pathogen-associated molecular patterns (PAMPs) on their surface, thereby releasing inflammatory mediators that kill the pathogens (Krystel-Whittemore et al., 2016; Marshall, 2004; Varricchi et al., 2017). ILCs and ILTCs such as NK cells release cytotoxic granules such as perforins and granzymes to kill cancer cells (Prager et al., 2019; Bauer et al., 1999; Ruf et al., 2023). In turn, myeloid cells such as MDSCs and tumour-associated macrophages (TAMs) are emerging as new therapeutic targets, especially with their ability to negatively regulate adaptive immune cells (Veglia et al., 2021; Watanabe et al., 2008; Gabrilovich et al., 2009; Mantovani et al., 2017; Rodriguez-Garcia et al., 2021).

Adaptive immune system is activated by cross-priming, where antigen-presenting cells (APCs) such as DCs uptake tumour antigens and present them via major histocompatibility class I (MHC-I) and MHC-II molecules (cross presentation) (Chen et al., 2013a). This causes formation of immunological synapse between APCs and T cells, leading to priming and activation of naive cluster of differentiation (CD)8+ and CD4+ T cells, respectively (Iwasaki et al., 2010; Broz et al., 2014; Hildner et al., 2008; Grakoui et al., 1999; Dustin et al., 2016).

1.4.2 Adaptive immune response to cancer

T cells and B cells are major players of the adaptive immune system (Lam et al., 2024). CD4 T cells help CD8+ cytotoxic T lymphocytes (CTLs) by secreting IL-2 or by upregulating CD154, which binds to CD40 on DCs and stimulates secretion of tumoricidal cytokines as well as cytotoxic memory and effector functions of CD8+ CTLs (Borst et al., 2018; Smith et al., 2004; Janssen et al., 2003). In addition, anti-tumoral CD4+ T cells have been reported for their direct role in killing cancer cells (Corthay et al., 2005; Fauskanger et al., 2018; Kruse et al., 2023; Patterson et al., 2023; Bawden et al., 2024). Once activated by APCs, CD4+ T cells can differentiate into Th(T helper)1, Th2, Th17, follicular helper T (Tfh) cells and induced T regulatory cells (iTregs), depending on T cell receptor (TCR) affinity (Boyton et al., 2002). When

stimulated by IL-12, CD4+ T cells can be polarised to Th1 type and directly kill tumour cells by producing interferon-gamma (IFN-γ) and tumour necrosis factor alpha (TNFα) (Knutson et al., 2005). IL-4 induces Th2 differentiation, which induces humoral immunity (Zhou et al., 2009). IL-6 and transforming growth factor-beta (TGF-β) stimulates differentation of Th17, which produces pro-inflammatory cytokines IL-17, IL-21, and IL-22, and promotes inflammation and auto-immunity (Harrington et al., 2005; Dong, 2008; Martin-Orozco et al., 2009). Tfh cells help with activation and maturation of B cells and induce humoral immunity (Tay et al., 2021; Cui et al., 2021).

iTregs, induced by IL-2 and TGF-β, and regulatory T cells (Tregs) that originate from thymus express forkhead box P3 (FoxP3), which is required for their development and functions (Hori et al., 2003; Fontenot et al., 2003). Tregs are essential in maintaining self-tolerance and preventing autoimmune diseases, but in cancer, they contribute to immunosuppressive microenvironment (Vignali et al., 2008; Togashi et al., 2019). They secrete immunosuppressive cytokines such as IL-10, IL-35, and TGF-β (Owen et al., 2019; Knochelmann et al., 2018; Collison et al., 2007; Tay et al., 2023), mediate cytolysis of NK and CD8+ CTLs (Grossman et al., 2004; Gondek et al., 2005; Cao et al., 2007; Ren et al., 2007), and generate adenosine that suppresses T cell functions (Deaglio et al., 2007; Kobie et al., 2006; Zarek et al., 2008). Tregs can also reduce T cell activation by targeting DCs (Tadokoro et al., 2006; Tang et al., 2006; Liang et al., 2008; Wing et al., 2008).

A recent study suggests two stages of tumour-specific CD8+ T cell activation, whereby CD8+ T cells are initially activated in tumour-draining lymph nodes and migrate into tumours for further activation (Prokhnevska et al., 2023). There, CD8+ CTLs are activated upon binding of TCR to antigen/MHC-I of APCs. At the same time, its co-stimulatory receptor CD28 binds to CD80 (B7.1) or CD86 (B7.2) on APCs and activates downstream PI3K/AKT and NF-κB pathway, inducing T cell proliferation (Waldman et al., 2020; He et al., 2021). The immunological synapse that forms with MHC-I and TCR binding causes the CTLs to secrete lytic granules consisting of perforins, granzymes, cathepsin C, and granulysin (Peters et al., 1991; Basu et al., 2016). This,

in addition to expressing Fas ligand on the surface and activating death domains, can induce apoptosis in target cells either serially or simultaneously (Bossi et al., 1999; Stinchcombe et al., 2003; Wiedemann et al., 2006). In an environment with constant antigen stimulation, such as cancer, T cells can become exhausted, losing their effector functions and expressing immune-checkpoint receptors (Zajac et al., 1998; Wherry, 2011; Angelosanto et al., 2012). Exhausted T cells can contribute to immunosuppressive environment and ineffective immune checkpoint blockade (Li et al., 2019; McLane et al., 2019; Blank et al., 2019; Chow et al., 2022).

Immune checkpoints such as cytotoxic T-lymphocyte associated protein 4 (CTLA-4) and programmed cell death protein-1 (PD-1) are inhibitory receptors expressed on T cells that negatively regulate their immune responses. T cell activation upregulates CTLA-4 expression, which can bind CD80/86 with higher affinity than CD28 and prevent uncontrollable activation (Walunas et al., 1994; Schneider et al., 2006; Rowshanravan et al., 2018). PD-1 binds to programmed death-ligand 1 (PD-L1) and PD-L2 expressed by APCs and tumours, inhibiting T cell proliferation and regulating its fate (Ishida et al., 1992; Freeman et al., 2000; Latchman et al., 2001; Patsoukis et al., 2012). In turn, CTLA-4 and PD-1 can promote Treg proliferation and functions (Chen et al., 2013b). Due to these regulatory functions, PD-1 and CTLA-4 blocking antibodies have been used in immunotherapy (Leach et al., 1996; Iwai et al., 2002; Ribas et al., 2018). Some of the biomarkers for anti-PD-1 immunotherapy include high tumour mutational burden, high PD-L1 expression in tumours, and large numbers of tumour-infiltrating lymphocytes (TILs) such as CD8+ T cells and their IFN-γ production (Yi et al., 2018; Li et al., 2022b). Other checkpoints include T-cell immunoreceptor with Ig and ITIM domains (TIGIT), T cell immunoglobulin and mucin-domain containing-3 (TIM-3), inducible T-cell co-stimulatory molecule (ICOS), and lymphocyte-activation gene 3 (LAG-3) (Yu et al., 2009b; Wolf et al., 2020; Dong et al., 2001; Grebinoski et al., 2022).

B cells also play a key role in the adaptive immune system. Upon maturation in the bone marrow, they are activated by antigens presented by the follicular DCs in the secondary lymphoid organs (Batista et al., 2009; Laumont et al., 2022). The primed B

cells present antigens to Tfh cells and differentiate into memory B cells or plasma cells (Kwak et al., 2019; Akkaya et al., 2020). In response to re-exposure of antigens, plasma cells produce antibodies, and memory B cells rapidly get re-activated (Cyster et al., 2019; Kurosaki et al., 2015; Syeda et al., 2024).

1.5 Reported influence of IGFs on the immune response

IGF-1R is expressed by myeloid cells such as macrophages and dendritic cells, as well as lymphocytes (Spadaro et al., 2017; Somri-Gannam et al., 2020; Kooijman et al., 1992; Baudler et al., 2005). IGF axis has been reported to regulate anti-tumour immune responses in TME (Trojan et al., 1993; Pellegrino et al., 2024; Zhang et al., 2021; Ajona et al., 2020). Induction of JAK/STAT and NF-κB pathway by the IGF axis also contributes to immunosuppression by mediating activation of STAT transcription factors and regulating genes involved in immune and inflammatory responses, such as activation and differentiation of T cells and macrophage inflammatory responses (Zong et al., 2000; Gustin et al., 2004; Salminen et al., 2021).

1.5.1 Effects of IGFs on adaptive immunity

The first study to report immunosuppressive effects of IGFs was in rat glioblastoma model, where injection of tumour cells with antisense IGF-1 led to reduction in tumour growth and increase in CD8+ CTLs (Trojan et al., 1992; Trojan et al., 1993). Similar results were shown in melanoma and neuroblastoma models (Resnicoff et al., 1994; Liu et al., 1998). Conversely, IGF-1R overexpression led to CD8+ T cell inhibition in lung cancer (Zhao et al., 2020). IGF axis has been reported to induce proliferation and function of Tregs, which are associated with prostate cancer progression (Bilbao et al., 2014; Johannesson et al., 2014; Shapiro et al., 2023; Huang et al., 2022; Fridman et al., 2017; Rao et al., 2020). In addition, IGF-1 regulates Th17 and Treg balance in autoimmune diseases (DiToro et al., 2020), and increases IL-10 expression in T cells, which is required to suppress Th17 responses (Kooijman et al., 2004; Chaudhry et al., 2011). Recently, co-inhibition of IGF-1R and PD-1 in lung cancer model has

been reported to induce significant reduction of Tregs and increase in CD8+ T cell infiltration (Ajona et al., 2020). In addition, IGFs regulate B cell differentiation and proliferation (Landreth et al., 1992; Kimata et al., 1994; Jardieu et al., 1994; Dowery et al., 2021). IGF-1R is required for T cell-independent B cell responses (Baudler et al., 2005), and in patients with Graves' disease, an autoimmune disease affecting thyroid, B cells with overexpressed IGF-1R produce abnormal immunoglobulins (Ig) (Douglas et al., 2008).

1.5.2 Effects of IGFs on innate immunity

IGFs can influence innate immune cells and their immune responses. Monocytes and macrophages are important sources of IGF-1 (Tonkin et al., 2015; Spadaro et al., 2017; Nackiewicz et al., 2020; Yan et al., 2022; Lv et al., 2021; Shaw et al., 2015). IGF-1 stimulation of anti-inflammatory cytokine IL-10 in monocytes inhibits CD4+ T cell proliferation in colitis model (Ge et al., 2015). In pancreatic cancer, endogenous IGF-1 production by TAMs and myofibroblasts induces chemoresistance (Ireland et al., 2016), and IGF axis activation is correlated with increased macrophage infiltration in breast cancer (Ireland et al., 2018). Lung metastasis induction in IGF-1R deficient mouse model showed reduction in tumour burden as well as M2 macrophages (Alfaro-Arnedo et al., 2022). Combined inhibition of IGF-1R and CSF-1R in glioblastoma overcomes resistance and prolongs survival in glioblastoma (Quail et al., 2016). Both IGF-1 and IGF-2 drive polarisation of macrophages to anti-inflammatory M2 subtype (Spadaro et al., 2017; Barrett et al., 2015; Du et al., 2019), and IGF axis can induce anti-inflammatory neutrophils and regulate their functions (Nederlof et al., 2022; Himpe et al., 2008; Pineiro-Hermida et al., 2017). IGF axis has also been reported to modulate NK cell development and functions (Ni et al., 2013; Rahmoon et al., 2017; Auernhammer et al., 1996). In addition, IGFs can inhibit DC-mediated anti-tumour immune responses by suppressing its maturation and antigen-presenting capabilities (Huang et al., 2015; Somri-Gannam et al., 2020).

1.6 Prostate cancer tumour microenvironment

Prostate cancer is a genetically, phenotypically, and clinically heterogeneous disease (Haffner et al., 2021; Ge et al., 2022; Andreoiu et al., 2010; Roditi et al., 2022; Song et al., 2022). Several publications have reported that majority of primary as well as metastatic cancers show genetically, histologically and morphologically distinct tumour foci, presenting challenges in diagnosis and treatment strategies (Miller et al., 1994; Spratt et al., 2016; Boutros et al., 2015; Lovf et al., 2019; Gundem et al., 2015; Hong et al., 2015).

In addition, prostate cancer is considered "immune-cold" due to its immunosuppressive TME, characterised by low tumour mutational burden, high level of angiogenesis in the stroma, and infiltration by immunosuppressive cells such as TAMs, MDSCs, and Tregs (Hirz et al., 2023; Nonomura et al., 2011; Comito et al., 2014; Vitkin et al., 2019; Sfanos et al., 2008; Kwon et al., 2021; Kiniwa et al., 2007; Mitri et al., 2014; Calcinotto et al., 2018; Lopez-Bujanda et al., 2021; Bronte et al., 2005a). This explains prostate cancer resistance to immune checkpoint blockade (Sharma et al., 2017; Elia et al., 2018). Phase 3 clinical trials of anti-CTLA-4 antibody ipilimumab in mCRPC post-chemotherapy (Kwon et al., 2014) and chemotherapy-native (Beer et al., 2017) patients did not improve OS. Anti-PD-1 monotherapy using pembrolizumab showed limited clinical benefits in mCRPC patients (Antonarakis et al., 2020), and addition of anti-PD-1 antibody atezolizumab to enzalutamide did not improve OS of mCRPC patients (Powles et al., 2022). Anti-PD-1 Phase 2 trial combining ADT and anti-PD-1 antibody cemiplimab showed no significant PSA drop (Hawley et al., 2023a), despite inducing robust immune cell infiltration (Hawley et al., 2023b). Preliminary results of the CheckMate 650 trial, combining anti-CTLA-4 (ipilimumab) and anti-PD-1 antibody nivolumab on mCRPC patients, showed objective response rates of 25% and 10% in pre- and post-chemotherapy cohorts, respectively, and there were notable reduction in tumour size in several patients (Sharma et al., 2020; Sharma et al., 2023).

Lack of clinical benefits targeting T cells led to potential therapies targeting myeloid cells, which constitute up to 70% of immune subsets in prostate cancer tumour (Calcinotto

et al., 2018; Mitri et al., 2019; Chen et al., 2021). Several studies reported that immunosuppressive M2-like TAM infiltration of prostate cancer tumours led to prostate cancer invasion and worse outcomes (Erlandsson et al., 2019; Escamilla et al., 2015; Cioni et al., 2020; Maolake et al., 2017). Myeloid inflammatory cells have also been shown to drive immunosuppression in prostate cancer TME (Mitri et al., 2019; Garcia et al., 2014; Hossain et al., 2015). A recent study, upon testing various combinations of immunotherapies in a novel chimaeric mouse model, found combination of immune checkpoint blockade and MDSC-targeting therapy to be the most effective (Lu et al., 2017). An investigator-initiated clinical trial of CXCR2 inhibitor and enzalutamide on patients with mCRPC that is resistant to AR signalling inhibitors showed reduction of MDSC infiltration and durable anti-tumour activity in some patients (Guo et al., 2023).

1.7 Aims and hypothesis

IGF axis signalling plays an important role in cancer growth, proliferation, and survival (Hellawell et al., 2002; Knuppel et al., 2020). Despite the known immunosuppressive role of IGF axis, it is uncertain whether the IGF axis affects innate immunity including macrophage responses in prostate cancer TME.

To investigate the hypothesis that pharmacological inhibition of IGF signalling increases immune activity in prostate cancer, the following aims will be fulfilled:

1. To test the consequences of IGF blockade in prostate cancer *in vitro* and *in vivo*.

2. To investigate whether IGF blockade impacts the response to immunotherapy in a murine prostate cancer model.

3. To characterise the effects of IGFs on macrophage phenotype and function in prostate cancer *in vitro*.

4. To understand the effects of IGF blockade on localised prostate cancer TIME by analysing patient samples from Windows trial of INsulin-like Growth factor neutralising

antibody xentuzumab in MEN scheduled for radical prostatectomy (WINGMEN) trial (NCT05110495).

The overarching aim of this thesis is to investigate whether the IGF signalling contributes to immunosuppression in prostate cancer, and if so, whether IGF blockade offers the potential to overcome an immune-cold TME in prostate cancer *in vitro* and *in vivo*, and in patients.

2

Materials and Methods

Contents

2.1 Cell lines . . . 26
2.1.1 Cell lines and culture conditions . . . 26
2.1.2 mCherry-tagged cell lines . . . 28
2.1.3 Cryopreservation . . . 29
2.1.4 Cell seeding . . . 29
2.2 Cell treatments . . . 29
2.2.1 IGF-1 and xentuzumab treatment . . . 29
2.2.2 anti-CD47 treatment . . . 30
2.3 Western blot . . . 30
2.4 Viability assays . . . 31
2.4.1 2D viability assay . . . 31
2.4.2 2D clonogenic assay . . . 32
2.4.3 3D spheroid assay . . . 32
2.5 Mice . . . 33
2.5.1 Tumour cell preparation and injection for *in vivo* experiments 33
2.5.2 Allograft model for IGF blockade . . . 34
2.5.3 Allograft model for IGF blockade and anti-PD1 (pilot, n=6) . 34
2.5.4 Allograft model for IGF blockade and anti-PD1 (n=10) . . . 35
2.6 Immunohistochemistry (IHC) . . . 35
2.6.1 Formalin-Fixed, Paraffin-Embedded (FFPE) sections . . . 35
2.6.2 Immunohistochemical staining . . . 36
2.6.3 Haematoxylin and Eosin (H&E) staining . . . 38
2.6.4 WINGMEN trial IHC . . . 38
2.6.5 HALO Image Analysis . . . 39
2.7 3' RNA Sequencing . . . 40
2.7.1 RNA extraction from mouse tumour tissues and cell lines . . 40
2.7.2 RNA Library Preparation and Sequencing . . . 40
2.7.3 Data Processing and Analysis . . . 40
2.8 Quantitative real-time polymerase chain reaction (qRT-PCR) . . . 41
2.8.1 Primer design . . . 41
2.8.2 Ribonucleic Acid (RNA) isolation . . . 44
2.8.3 Complementary DNA (cDNA) synthesis and qRT-PCR . . . 45
2.8.4 Relative quantification . . . 46
2.9 Flow cytometry . . . 46
2.9.1 Mouse tumour tissue processing . . . 46

2.9.2 Mouse peripheral blood processing 46
2.9.3 Mouse spleen processing 47
2.9.4 Cell surface staining 47
2.9.5 Intracellular staining 49
2.9.6 Compensation 49
2.9.7 Data Acquisition and Analysis 50
2.10 Immune cell isolation 53
2.10.1 Human peripheral blood mononuclear cells (PBMCs) processing 53
2.10.2 PBMC-derived macrophage differentiation and polarisation . 54
2.10.3 T cell isolation 54
2.10.4 Bone marrow-derived macrophages (BMDMs) isolation and polarisation 54
2.11 Co-culture assay 55
2.11.1 Macrophages and cancer cell co-culture assay 55
2.11.2 Macrophages, T cells, and cancer cell co-culture assay 56
2.12 Cytokine array 56
2.13 *in vitro* Phagocytosis assay 58
2.14 Clinical samples 58
2.14.1 Research blood samples 58
2.14.2 Research tissue samples 60
2.15 Multiplex Immunofluorescence (mIF) 60
2.15.1 Antibody conjugation 60
2.15.2 Slide preparation 61
2.15.3 Data Analysis 63
2.16 RNA Sequencing of WINGMEN trial samples 63
2.16.1 RNA extraction from FFPE tissue sections 63
2.16.2 RNA Library Preparation and Sequencing 65
2.16.3 Data Processing and Analysis 66
2.17 phospho-IGF-1R enzyme-linked immunosorbent assay . . 66
2.18 PBMC immunoprofiling using Cytometry by Time-Of-Flight (CyTOF) 68
2.18.1 PBMC sample processing 68
2.18.2 CyTOF data acquisition and data analysis 68
2.19 Statistical Analysis 70

2.1 Cell lines

2.1.1 Cell lines and culture conditions

All cell lines used for this project and the culture media conditions are listed in Table 2.1. Mouse prostate cancer Myc-CaP (#CRL-3255) and PTEN-CaP8 (#CRL-3033), and mouse macrophage J774A.1 (#TIB-67) were purchased from ATCC. Human prostate cancers 22Rv1 and DU145 were obtained from Sir Walter Bodmer (Weatherall

Table 2.1: List of cell lines. Type of cell lines used, the culture media, and subculture time and ratio are summarised in the table.

Cell lines	Type	Species	Culture media	Subculture time (ratio)
Myc-CaP	PCa	Mouse (FVB)	DMEM + 10% FBS+ 1% P/S	4-5 days (1:20)
PTEN-CaP8	PCa	Mouse (C57Bl/6)	DMEM + 10% FBS+ 1% P/S	4-5 days (1:10)
DU145	PCa	Human	RPMI + 10% FBS+ 1% P/S	4-5 days (1:10)
22Rv1	PCa	Human	RPMI + 10% FBS+ 1% P/S	4-5 days (1:10)
J774A.1	Macrophage	Mouse (BALB/cN)	DMEM + 10% FBS+ 1% P/S	4-5 days (1:10)
HEK293T	Kidney	Human	DMEM + 10% FBS+ 1% P/S	4-5 days (1:10)

Abbreviations and Manufacturers: Prostate Cancer (PCa), Dulbecco's Modified Eagle Medium (DMEM, Gibco, #41966029), Roswell Park Memorial Institute 1640 Medium (RPMI, Gibco, #21875034), Foetal Bovine Serum (FBS, Gibco, #10500064), Penicillin-Streptomycin (P/S, Gibco, #15140122)

Institute of Molecular Medicine, University of Oxford, UK), and Cancer Research UK Laboratories, Clare Hall, Hertfordshire, UK, respectively. HEK293T cells for lentiviral transduction were from Eric O'Neill Lab, Department of Oncology, University of Oxford. All cells were cultured at 37°C in 5% CO_2. The cells were tested for mycoplasma regularly using the detection kit (Lonza, #LT07-418).

All cells were passaged when they were 70-80% confluent. Myc-CaP, PTEN-CaP8, DU145, and 22Rv1 cells were washed twice with sterile phosphate buffered saline (PBS, #P4417-100TAB), and disaggregated by incubating for 3 minutes at 37°C, 5% CO_2 in Trypsin 10X (Lonza, #BE02-007E) diluted 1:1 with sterile PBS. Then, the appropriate cell culture media (Table 2.1) was added to neutralise the trypsin, and the cells were reseeded in a new flask, either 1:10 or 1:20. J774A.1 cells were washed twice with sterile PBS, and 10 mL of fresh media were added to the flask. Cells were then scraped with a cell scraper (Corning, #3010) and reseeded either 1:5 or 1:10.

J774A.1 cells were polarised by treating with either 1 μg/mL lipopolysaccharide (LPS,

Sigma-Aldrich, #L2630-10MG) and 10 ng/mL IFN-γ (BioLegend, #575302) (classically activated, M1) or 20 ng/mL IL-4 (BioLegend, #574302) (alternatively activated, M2), for 48 hours.

2.1.2 mCherry-tagged cell lines

For co-culture and phagocytosis assays, all prostate cancer cell lines were lentivirally transduced with mCherry construct (Addgene, #36084) using HEK293T cells (ATCC, #CRL-11268) by Cameron Lang in our lab. The pLV-mCherry construct was a gift from Pntelis Tsoulfas (Department of Neurological Surgery, University of Miami, USA).

For lentiviral production, 1 million HEK293T cells were plated in a 25 cm^3 tissue culture plate and incubated overnight at 37°C, 5% CO_2. In 15 mL conical, 1 μg pLV-mChery plasmid, 750 ng psPAX2 packing plasmid (Addgene, #12260), and 250 ng pMD2.G envelope plasmid (Addgene, #12259) were added to 20 μL serum-free Dulbecco's Modified Eagle Medium (DMEM). This was added to a FuGENE mastermix that contains 6 μL FuGENE Transfection Reagent (Roche, #11814443001) and 74 μL serum-free DMEM, and mixed gently before incubating for 30 minutes at room temperature (RT). The mix was then added dropwise to HEK293T cells and left overnight at 37°C, 5% CO_2. The next day, cell media was replaced with 5 mL fresh DMEM + 10% foetal bovine serum (FBS)+ 1% penicillin-streptomycin (P/S) and incubated at 37°C, 5% CO_2. After 24 hours, cell media containing lentiviral particles were collected and transferred to a 15 mL conical and stored at 4°C.

For lentiviral transduction, 3 million Myc-CaP cells/well were plated in a 6-well plate and incubated overnight at 37°C, 5% CO_2. The next day, culture media was replaced with 1 mL DMEM + 10% FBS+ 1% P/S + 8 μg/mL polybrene (Sigma-Aldrich, #H9268) + 0.5 mL of lentiviral particles and incubated overnight at 37°C, 5% CO_2. After 24 hours, cell culture media was replaced by 1 mL DMEM + 10% FBS+ 1% P/S, and cells were expanded for at least 72 hours.

To select cells with similar expression patterns and transfection efficiencies, the cells were prepared for sorting (BD FACSAria Fusion) at the Weatherall Institute of Molecular

Medicine Flow Cytometry Facility. The disaggregated cells were washed once in PBS by centrifugation (1200 rpm, 5 minutes), resuspended in sorting buffer (Table 7.1) at a final concentration of 2 million cells/mL, and left on ice until sorting. The sorted cells were collected in the collection buffer (Table 7.1) in 15 mL tubes (Corning, #430766) and seeded in a 6-well plate (Corning, #3516). Once the plate was confluent, the cells were moved to bigger flasks and used for assays or cryopreserved for future use.

2.1.3 Cryopreservation

The dissociated cells were centrifuged at 1,200 rpm for 5 minutes and resuspended in banking media (Table 7.1), aliquoted into 1.2 mL cryogenic vials (Corning, #431486), and frozen at −80°C in a Mr. Frosty freezing container. The vials were taken out of Mr. Frosty the next day and stored in appropriate boxes for future use. For unbanking, the cells were thawed in a 37°C water bath and added to a flask with full media. The media was changed after 24 hours to remove dead cells and dimethyl sulfoxide (DMSO).

2.1.4 Cell seeding

All cell lines and primary cells were counted before seeding. Cells were mixed 1:1 with trypan blue solution, and 10 µL of the mix were added to the cell counting chamber slides (Invitrogen, #C10283) to count using the automated cell counter (Invitrogen Countess 3). After using the cell number to calculate the amount needed for the required seeding density, the cells were seeded in an appropriate media.

2.2 Cell treatments

2.2.1 IGF-1 and xentuzumab treatment

In most cases, cells were serum-starved with 0% FBS culture media and treated with 1 μM xentuzumab or solvent control (PBS) for 24 hours. For assays involving macrophages, human IgG1 lambda (Sigma-Aldrich, #I5029-1MG) was used as solvent control. Then, 50 nM IGF-1 (Sigma-Aldrich, #I1271-1MG) (Camblin et al., 2019; Wu et al., 2021; Rieunier et al., 2021) or solvent control (10 nM HCl) was added for 20 minutes before the cells were collected and used for downstream applications. For *in vitro* phagocytosis

and co-culture assays, cells were either serum-starved or in 10% FBS culture media and treated with 1 μM xentuzumab or IgG1 lambda for 2 hours before adding 50nM IGF-1 or 10 nM HCl for 4 - 72 hours.

2.2.2 anti-CD47 treatment

For phagocytosis assays, cancer cells were treated with 10 μg/mL anti-CD47 (BioXCell, #BE0283-1MG) or mouse IgG1 isotype control (BioXCell, #BE0083-1MG) for 30 mins to 24 hours. Then, treatments were removed and macrophages were added for 2 hours, before the cells were collected and stained for flow cytometry (Majeti et al., 2009; Feng et al., 2015).

2.3 Western blot

Cells seeded in a 10 cm dish were washed twice with ice-cold PBS, and with 1 mL of PBS left on the dish, the cells were scraped with a cell scraper (Corning, #3010) and put in a 1.5 mL Eppendorf tube. The cells were centrifuged for 30 minutes at maximum speed at 4°C, resuspended in 80 μL of lysis buffer containing 1% protease and phosphatase inhibitors (Table 7.1), and left on ice for 30 minutes. Protein concentration was quantified using Pierce BCA Protein Assay Kit (Thermo Scientific^{TM}, #23227) with POLARstar Omega Plate Reader. Then, equal amount of protein was prepared using 4x NuPAGE LDS Sample Buffer (Invitrogen, #NP0007) and 0.1 M dithiothreitol (DTT, Thermo Scientific^{TM}, #R0861). The samples were boiled at 95°C for 5 minutes and separated by sodium dodecyl sulphate-polyacrylamide gel electrophoresis (SDS-PAGE) on 7.5% Precast Protein Gel (Bio-Rad, #5671024). Then, proteins were transferred onto 0.2 μm nitrocellulose membrane using the transfer kit (Bio-Rad, #704271) with the Trans-Blot Turbo Transfer System (Bio-Rad, #1704150). The membrane was then blocked with Intercept Blocking Buffer (LI-COR, #927-70001) mixed 1:1 with PBS in a black 50 mL tube (Fisher Scientific, #15306558) for 1 hour at RT on a rocker. Afterwards, the membrane was incubated with diluted primary antibodies in the blocking buffer overnight at 4°C (Table 2.2).

Table 2.2: List of primary antibodies used for western blot. All antibodies were from Cell Signalling Technology (CST).

Target	Host	Cat no.	Dilution
Phospho-Y1135/1136 IGF-1R-β	Rabbit IgG	3024	1:500
IGF-1R-β	Rabbit IgG	3027	1:1000
Phospho-S473 AKT	Rabbit IgG	4060	1:1000
AKT	Rabbit IgG	9272	1:1000
Phospho-pT202/pY204 MAPK (ERK1/2)	Rabbit IgG	9101	1:1000
p44/42 MAPK (ERK1/2)	Mouse IgG	4696	1:1000
Phospho-T246 PRAS40	Rabbit IgG	2997	1:1000
PRAS40	Rabbit IgG	2610	1:1000
β-Tubulin	Mouse IgG	86298	1:1000

The next day, the membrane was washed three times with PBS-T (0.1% Tween in PBS) for 5 minutes on a rocker at RT and incubated with relevant IRDye secondary antibody (LI-COR, donkey-anti-rabbit: #926-68073, donkey-anti-mouse: #926-32212), diluted 1:10,000 in the blocking buffer, for 1 hour at RT. After the membrane was washed three times with PBS-T for 5 minutes on a rocker at RT, it was imaged using LI-COR Odyssey Imager. Fiji (imageJ) v1.54f software was used for protein quantification, and the results were graphed in GraphPad Prism 9.

2.4 Viability assays

2.4.1 2D viability assay

The cells were seeded in triplicates in a 96-well clear flat-bottom plate (Corning, #3595) at a density of 1,000 cells/80 μL/well. On the following day, various dosages of xentuzumab or PBS were prepared at 5 times the final concentration in 20 μL and added so that the final volume per well is 100 μL. After five days of culturing at 37°C with 5% CO_2, 20 μL of CellTiter-Blue reagent (Promega, #G8081) was added to each well and incubated for 2 hours at 37°C with 5% CO_2. Then, the fluorescence signal was measured at 560/590 nm with POLARstar Omega microplate reader (BMG Labtech).

The results were analysed in GraphPad Prism 9 as % viability of xentuzumab-treated cells compared to control.

2.4.2 2D clonogenic assay

The cells were seeded in a 6-well plate at a density of 500 cells/2 mL/well. The next day, the cells were treated with either xentuzumab or PBS at 5 times the final concentration in 500 μL so that the final volume per well is 2.5 mL. After incubating for 7 days at 37°C with 5% CO_2, the cells were washed with PBS and stained with Coomassie stain (Table 7.1), for 30 minutes at RT. The dishes were then gently washed with tap water, dipped in dH_2O, then left upside down to dry overnight. On the following day, the dishes were imaged and counted on the GelCount (Oxford Optronix). The results were analysed in GraphPad Prism 9 as % cell survival compared to control.

2.4.3 3D spheroid assay

The cells were seeded in 6 replicates at a density of 5,000 cells/160 μL/well in an ultra-low attachment 96-well plate (Corning, #7007) and centrifuged at 200 xg at RT for 10 minutes. After 3 days of incubation at 37°C with 5% CO_2, the spheroids were treated by adding xentuzumab or PBS at 5 times the final concentration in 40 μL for a final volume per well of 200 μL. The plate was then imaged daily at 1,200 dpi with GelCount for 8 days. All images were exported and analysed using Fiji (ImageJ) v1.54f software for spheroid size quantification.

Three of the six replicates per condition were used for 3D cell viability assay. The plates and the CellTiter-Glo 3D reagent (Promega, #G9683) were equilibrated to RT before the assay. With multichannel pipette, 100 μL of the medium was taken out from each well, taking care not to disturb the spheroids. Then, 100 μL of the CellTiter-Glo 3D reagent was added to each well. The plate was put in the POLARstar Omega Plate Reader (BMG Labtech) to mix for 300 seconds using the shake function, incubated at RT for an additional 25 minutes, and the luminescence was read. The results were analysed in GraphPad Prism 9 as % 3D cell viability compared to control.

The spheroids in the remaining three replicates per condition were collected in a 1.5 mL tube for western blot using wide bore pipette tips. The spheroids were washed with ice-cold PBS and directly lysed in 40 μL of 3x Laemmli sample buffer (Table 7.1). The samples were boiled at 95°C for 10 minutes and loaded into wells and run for western blot as in Chapter 2.3.

When spheroids were to be used as controls for IHC staining, the spheroids were collected in a 1.5 mL tube using wide bore pipette tips. Upon washing with ice-cold PBS and centrifuging at 1,200 rpm for 5 minutes, the cells were fixed in 10% NBF. The next day, the cells were moved to 70% ethanol for up to 2 weeks and paraffin-embedded as in Chapter 2.6.1.

2.5 Mice

Animal experiments were performed in accordance with United Kingdom Animals (Scientific Procedures) Act 1986 and ARRIVE guidelines (Kilkenny et al., 2010), under the Home Office-approved Project Licences of Professor Anderson Ryan (30-3395) and Dr. Eileen Parkes (PP7686743) at the University of Oxford. All experiments were conducted under PIL No. I38145687. Male 5-6-week-old immunocompetent FVB mice (Charles River Laboratories) were housed in groups of six or less in an individually ventilated cages in a pathogen-free facility, maintained at 22°C and 50% humidity with 12-hour light cycles. They had access to water and food ad libitum, and the animals were monitored daily and weighed twice per week. At the humane/experimental endpoint, the mice were euthanised by either pentobarbital injection or cervical dislocation.

2.5.1 Tumour cell preparation and injection for *in vivo* experiments

Disaggregated Myc-CaP cells were centrifuged at 1,200 rpm for 3 minutes and washed once with cold DMEM. Then, cells were counted, and injection mix was prepared so that 2 x 10^6 cells in DMEM were in 1:1 ratio with cold Matrigel (Corning, #354234). The mix was kept on ice for the duration of the experiment.

For tumour injection, mice were anaesthetised with 2% isoflurane in air/oxygen. The inoculation area of the mice was sterilised with 70% ethanol. Then, 100 µL of the mix was subcutaneously injected into the right flank of the mouse using an ice-cold insulin syringe (Unisharp, #UF30R-10) to establish a prostate cancer allograft. The mice were also ear-punched for identification at this time. Afterwards, the mice were put into a container with warm mat until they looked stable, and moved back to their cages. The mice were monitored the next day. Tumour volume was measured twice per week using a digital calliper and calculated as $(width \times length \times height)/2$.

2.5.2 Allograft model for IGF blockade

This experiment was conducted under the project license of Professor Anderson Ryan (30-3395). The mice were randomised into two treatment groups (n = 10 per group): 10 ml/kg PBS (control) or 100 mg/kg (10 ml per kg body weight) xentuzumab (Boehringer Ingelheim, BI836845) (Friedbichler et al., 2014). The group sizes were determined by G*Power software based on *in vitro* experiments that used xentuzumab on Myc-CaP cells. When the tumour size reached 80 - 100 mm^3, the mice were treated twice weekly via intraperitoneal injection (IP), until tumour size reached 400 mm^3. At this point or earlier if at a humane endpoint, the mice were euthanised by pentobarbital injection or cervical dislocation. Tumours were collected and fixed immediately in 10% neutral buffered formalin (NBF, Sigma-Aldrich, #HT501128-4L) for immunohistochemistry (IHC) or snap-frozen in 100% ethanol poured over dry ice for RNA extraction.

2.5.3 Allograft model for IGF blockade and anti-PD1 (pilot, n=6)

This experiment was conducted under the project license of Professor Anderson Ryan (30-3395). The mice were randomly assigned to four treatment groups (n = 6 per group): (a) 10 ml/kg PBS + 10 mg/kg isotype control (BioXCell, rat IgG2a, #BE0089), (b) 10 ml/kg PBS + 10 mg/kg anti-PD-1 (BioXCell, clone RMP1-14, #BE0146), (c) 100 mg/kg xentuzumab + 10 mg/kg isotype control, and (d) 100 mg/kg xentuzumab + 10 mg/kg anti-PD-1. G*Power software was used to determine the group size based

on the publication on a preclinical lung cancer model (Ajona et al., 2020). When the tumour size reached 80 - 100 mm^3, the mice were treated twice weekly via IP injection, where anti-PD-1 and isotype control were injected two hours before xentuzumab/PBS treatments. The mice were culled by pentobarbital injection and cervical dislocation once the tumour size reached 400 mm^3 (or before if humane endpoint was reached). Tumours were collected and fixed immediately in 10% NBF for IHC or snap-frozen for RNA extraction. Spleen was collected in PBS for flow cytometry.

2.5.4 Allograft model for IGF blockade and anti-PD1 (n=10)

This was conducted under the project license of Dr. Eileen Parkes (PP7686743). The treatment groups and conditions were the same as 2.5.3 except for the following: (a) the anti-PD-1/isotype control and xentuzumab/PBS treatments were given concurrently, mixed in the same syringe, to stay under the injection limit and to reduce stress for mice, (b) treatment groups increased to 8 - 9 mice per group to reduce variability, and (c) the tumour size limit was 1,000 mm^3. All groups had 9 mice except for the anti-PD-1 + PBS group, which had 8 mice. At the experimental endpoint or earlier if humane endpoint was reached, the mice were culled by pentobarbital injection followed by terminal cardiac puncture. Blood was collected in red-top serum tubes (Becton Dickinson, #365964) and spleen in PBS for flow cytometry. Tumours were collected in 10% NBF for IHC, snap-frozen for RNA extraction, or collected in PBS for flow cytometry.

2.6 Immunohistochemistry (IHC)

2.6.1 Formalin-Fixed, Paraffin-Embedded (FFPE) sections

Spheroid pellets (2.4.3) or tissues from *in vivo* experiments (2.5.2, 2.5.3, and 2.5.4) were fixed in 10% NBF for 24 hours at 4°C and moved to 70% ethanol for storage up to 14 days at 4°C. When ready for processing, tissues or pellets were moved to cassettes (Simport, #M490-2) and processed using the Epredia STP 120 Spin Tissue Processor (Thermo Fisher Scientific) with steps involving dehydration with increasing concentrations of ethanol, clearing with Citroclear (TCS Biosciences, #HC5005-5L) and

wax infiltration with Histoplast PE paraffin wax (Thermo Fisher Scientific, #12683026). Then, the tissues were embedded using Epredia HistoStar Embedding Workstation (Thermo Fisher Scientific). For embedding, tissues were moved to embedding base molds (Thermo Fisher Scientific, #11306820), paraffin wax was added to the molds, and the cassette lid was put on the top before cooling on the cold plate. The FFPE tissue blocks were then cut into 4 μm sections using a HistoCore microtome (Leica) and mounted onto SuperFrost Plus slides (VWR, #631-0108), which were dried overnight at 37°C.

2.6.2 Immunohistochemical staining

Slides were incubated at 37°C for up to 24 hours (minimum 15 minutes). For dewaxing, slides were put in two separate jars of Citroclear for 3 minutes each, and in decreasing concentrations of ethanol (3 minutes each in 100% ethanol, 100% ethanol, 70% ethanol, and 50% ethanol) for rehydration. The slides were then rinsed in tap water. Antigen retrieval was performed in either Tris-EDTA buffer (TE buffer, pH 9, Table 7.1) or 1X Citrate buffer (pH 6, Sigma-Aldrich, #C9999-1000ML) in an antigen decloaking chamber (Biocare Medical, #DC2002) at 125°C for 2 minutes and 80°C for 10 minutes (Table 2.3). Samples were cooled on ice for 30 minutes and washed three times in PBS for 5 minutes each on a shaker. The hydrophobic barrier PAP pen (Vector laboratories, #H-4000) was used to draw a barrier around the tissue, and the slides were pre-blocked in 3% H_2O_2 (Sigma-Aldrich, #H1009-500ML) for 20 minutes and washed three times in PBS for 5 minutes. Then, sections were blocked for 40 minutes with Dual Endogenous Enzyme-Blocking Reagent (Agilent, #S200389-2) and incubated overnight at 4°C with 50 μL of primary antibody in an antibody diluent (Abcam, #ab64211) at an appropriate dilution (Table 2.3). For IGF-1R staining, sections were blocked for 1 hour with 5% bovine serum albumin (BSA) in PBS and incubated overnight at 4°C with 50 - 100 μL of primary antibody in 5% BSA in PBS.

On the following day, the slides were washed in PBS for three times, 5 minutes each, and incubated with Envision+ HRP Rabbit secondary antibody solution (Agilent, #K400311-2) for 30 minutes at RT. For IGF-1R staining, the secondary antibody from

Table 2.3: List of antibodies and antigen retrieval buffers used for immunohistochemistry. Tris-EDTA buffer is pH 9, and citrate buffer is pH 6. All antibodies were against rabbit secondary. Abbreviations: inducible nitric oxide synthase (iNOS), cleaved caspase-3 (CC3).

Name	Provider	Cat no.	Buffer	Dilution
IGF-1R (phospho-Y1161)	Biorbyt	orb644426	TE	1:100
IGF-1R β	CST	9750	TE	1:50
Phospho-S235/26 S6	CST	2211	TE	1:40
CD68	Abcam	ab125212	Citrate	1:500
F4/80	CST	70076S	Citrate	1:100
iNOS	Abcam	ab15323	Citrate	1:200
CD163	Abcam	ab182422	Citrate	1:100
CD47	GeneTex	GTX53912	Citrate	1:100
CD4	Abcam	ab183685	Citrate	1:200
CD8α	CST	98941	TE	1:200
FoxP3	CST	12653	TE	1:200
PD1	Abcam	ab214421	TE	1:1000
CC3	CST	9661	TE	1:150
Ki67	CST	12202	Citrate	1:200
CD31 (PECAM-1)	CST	77699	TE	1:100

Menarini Diagnostics (#MP-531-M3R25) was used, where the slides were incubated with 1-3 drops of rabbit probe for 15 minutes, washed in PBS for 3 times, 5 minutes each, and incubated with rabbit horseradish peroxidase (HRP) polymer for 15 minutes. Sections were then washed in PBS for 5 minutes, three times, and visualised by incubating in 3,3-diaminobenzidine (DAB, DAB chromogen concentrate diluted 1:50 in DAB+ substrate buffer, Agilent, #K346811-2) for 3 - 7 minutes or unil the specimens turn brown. The slides were rinsed in tap water and counterstained with Gill's haematoxylin (Sigma-Aldrich, #GHS132-1L) for 30 seconds. Upon rinsing in tap water until it runs clear, the slides were dehydrated in increasing concentrations of ethanol (50%, 70%, 100%, 100%) and in two separate jars of xylene (Thermo Fisher Scientific, #10784001) for 3 minutes each. Then, slides were mounted onto coverslips (VWR, #631-0124) with dibutylphthalate polystyrene xylene (DPX, VWR, #RAYLLAMB/DPX) and scanned

with Aperio ScanScope CS slide scanner (Leica) at 20X magnification.

2.6.3 Haematoxylin and Eosin (H&E) staining

H&E staining of the murine tumour tissues was done using the H&E staining kit (abcam, #ab245880). Slides were incubated at 37°C for 15 minutes up to 24 hours and dewaxed as in Chapter 2.6.2. Upon hydrating the slides in dH_2O, the slides were added in Mayer's Haematoxylin for 5 minutes. The slides were then rinsed in two changes of dH_2O to remove any excess staining. Then, the slides were incubated in Bluing Reagent for 15 seconds and rinsed in two changes of dH_2O. The slides were dipped in in 100% ethanol, and upon blotting the excess off, the slides were added in Eosin Y solution for 3 minutes. The slides were rinsed and dehydrated in 4 changes of 100% ethanol and in two separate jars of xylene for 3 minutes each, before mounting onto coverslips with DPX.

2.6.4 WINGMEN trial IHC

Phospho-IGF-1R, phospho-S6, Ki67, and RRM2 IHC for the WINGMEN clinical trial samples were done by Leticia Campo and Molly Browne in Translational Histopathology Lab (THL), Department of Oncology, University of Oxford. The slides were baked for 30 minutes at 60°C and dewaxed with Bond Dewax solution (Leica Biosystems, #AR9222) for 30 seconds at 72°C, 30 seconds at 72°C, and 30 seconds at RT, before rehydrating with alcohol. Then, antigen retrieval was performed with Leica BOND RXm autostainer, using BOND Epitope Retrieval solution 2 (Leica Biosystems, #AR9640) for 20 minutes at 100°C followed by 12 minutes, RT. The slides were then washed with BOND Wash solution (Leica Biosystems, #AR9590) three times and blocked with 3% H_2O_2 for 5 minutes. After washing three times with BOND wash, the slides were incubated with primary antibodies in BOND primary antibody diluent (#AR9352) for 30 minutes at an appropriate dilution (Table 2.4). The slides were washed three times with BOND wash, incubated with rabbit anti-mouse IgG (Leica Biosystems, #DS9800) for 8 minutes, and washed three times with BOND wash. Upon incubating with anti-rabbit-poly-HRP-IgG (Leica Biosystems, #DS9800) for 8 minutes, the slides

Table 2.4: List of antibodies used for immunohistochemistry for WINGMEN trial samples. Immunohistochemistry (IHC) for WINGMEN trials was performed by Translational Histopathology Lab (THL), Department of Oncology, University of Oxford. Abbreviations: Santa Cruz Biotechnology (SCBT)

Name	Provider	Cat no.	Dilution
IGF-1R (phospho-Y1161)	Biorbyt	orb97626	1:200
S6 (phospho-Ser 235/236)	CST	2211	1:800
Ki67	Agilent	M7240	1:200
RRM2	SCBT	sc-376973	1:50

were washed twice with BOND wash and once with dH_2O. Then, the slides were incubated in DAB for 10 minutes for visualisation and washed three times with dH_2O. Upon counter-staining with haematoxylin, the slides were rinsed in water and mounted with coverslips using Aquatex (Sigma-Aldrich, #108562). Slides were scanned using the Vectra Polaris Automated Quantitative Pathology Imaging System (Akoya Biosciences).

Phospho-IGF-1R and phospho-S6 IHC, being primary endpoints of the clinical trial, were validated using IGF-1R null cell lines and everolimus-treated spheroids, respectively. All other markers were verified by the secondary only negative control, which would not have been appropriate for validation of the primary antibodies. All antibodies were stained on non-trial tissues and checked by the trial team, including the trial pathologist, before staining on the trial tissues.

IGF-1R IHC was done by Macaulay lab as in Chapter 2.6.2 with antibody dilution listed in Table 2.3.

2.6.5 HALO Image Analysis

The digital images were analysed using the HALO platform (Indica Labs, HALO v3.6.4134 and HALO AI v3.6.4134). The tumour was annotated using the magnetic pen tool. MiniNet AI classifier was used to distinguish between viable tumours, necrotic cells, fat, and glass in 5 µM/pixel resolution. Then, Multiplex IHC v3.2 module was used to analyse the staining of each markers in viable tumours. H-score was obtained

from the final analysis report generated by HALO, and the results were graphed in GraphPad Prism 10.

For WINGMEN trial tissue analysis (phospho-IGF-1R, phospho-S6, IGF-1R, Ki67, RRM2), the benign and tumour glands were annotated using the pen tool in QuPath, with training provided by Professor Clare Verrill in Nuffield Department of Surgical Sciences, University of Oxford. The annotations were saved in .json format and imported to HALO for analysis. Epithelium and stroma were classified using Object Phenotyper, and Multiplex IHC v3.4.9 module was used to analyse the staining of each marker in benign and tumour glands. Both classifer and analysis settings were created by Dr. Alistair Easton, Department of Oncology, University of Oxford. H-score, % positive cells, % positive nuclear stainings, and % positive non-nuclear stainings were obtained from the analysis report generated by HALO, and the results were graphed in GraphPad Prism 10.

2.7 3' RNA Sequencing

2.7.1 RNA extraction from mouse tumour tissues and cell lines

RNA from mouse tumour tissues as well as cell lines was isolated using the same methods as in 2.8.2. The RNA concentration was measured using Qubit 4 Fluorometer (Invitrogen), and A260/280 and A260/230 ratios were measured using NanoDrop One (Thermo Scientific). The RNA was stored at $-80°C$ until ready for shipment.

2.7.2 RNA Library Preparation and Sequencing

RNA library preparation and sequencing were performed at the Oxford Genomics Centre at the Centre for Human Genetics (CHG), University of Oxford. Briefly, cDNA was generated from total RNA using oligodT and random priming. The prepared libraries were quality-controlled and multiplexed and sequenced over NextSeq flow cell. Data was aligned to the reference and checked for quality.

2.7.3 Data Processing and Analysis

FASTQ files were quality-controlled using FastQC software (Andrews et al., 2012), and Cutadapt software was used to remove adapter and primer sequences (Martin, 2011). The two reads were then concatenated, and Salmon software was used to quantify the transcript expression (Patro et al., 2017). Differential expression analysis was performed using DESeq2 (Love et al., 2014) with sequencing depth normalisation by 'median of ratios' method. Pathways were generated from differentially expressed genes using clusterProfiler (Yu et al., 2012) by Dr. Alessandro Barberis and Dr Fiona Hartley in our lab. Developed by Dr. Avigail Taylor in our lab, GeneFEAST, gene-centric, python-based tool that summarises and visualises functional enrichment analysis results, was used to identify gene sets that drive multiple enrichments (https://github.com/avigailtaylor/GeneFEAST).

2.8 Quantitative real-time polymerase chain reaction (qRT-PCR)

2.8.1 Primer design

Primers were designed using National Centre for Biotechnology Information (NCBI) Primer-BLAST using the mRNA reference sequence accession numbers. Primer pairs were designed to have product size of 80 - 250 base pairs, melting temperatures (T_m) of 58 - 62°C with maximum 2°C difference, and less than 60% GC content. The lyophilised primers purchased from Integrated DNA Technologies (Table 2.5) were resuspended in nuclease-free water to make 100 μM stocks.

Table 2.5: List of primers used for qRT-PCR. The primer mix of 12.5 μM was made by mixing 50 μL forward and 50 μL reverse primers with 300 μL nuclease-free water.

Target	Sense	Sequence
Igf1r	Forward	ACAACTACTGCTCCAAAGACAAA
	Reverse	CAGTTTTAGGGCAAGCGCAG
Ccl2	Forward	CACTCACCTGCTGCTACTCA
	Reverse	GCTTGGTGACAAAAACTACAGC
Ccl9	Forward	CAGGCCGGGCATCATCTTTA
	Reverse	AGTAGCTGGCAGTTCACACC
Angpt4	Forward	CTGTGGAGGCACAGGTCCTAA
	Reverse	ATGTTGTGCTTCCAGTGCCT
Tgfbr2	Forward	ACGTTCCCAAGTCGGATGTG
	Reverse	GTTTCAGTGGATGGATGGTCCT
Igfbp7	Forward	AGCAACGGCATCACCTACC
	Reverse	CCCATATCAGAGACCCTTGCTC
Vegfa	Forward	ATTCAGCGGACTCACCAGC
	Reverse	ACCTCCTCAAACCGTTGGC
Psca	Forward	TGCTGCTCTGCAGTGCTATT
	Reverse	GAGTCCAATGGCCCGGATG
Vim	Forward	AGACCAGAGATGGACAGGTGA
	Reverse	TTGCGCTCCTGAAAAACTGC
Lyn	Forward	TTCCACCACGAGCGAGAAAT
	Reverse	GGAACTGGCCTTTGCTGTTT
Pf4	Forward	GTCCCGAAGAAAGCGATGGAG
	Reverse	ATTCTTCAGGGTGGCTATGAGCTG
Mmp14	Forward	ATTCCAATGATCCCTCCGCC
	Reverse	ACCCAGTGCTTATCTCCTTTGA
Mmp2	Forward	GCCCCCATGAAGCCTTGTTT
	Reverse	GGTCATAGTCCTCGGTGGTG
Pdgfa	Forward	TGGTACTGAATTTCGCCGCC
	Reverse	GGGGTATCTCGGCTTCCTCG
Lgmn	Forward	CTAGAGGTGGCTGCTCTGAGTC
	Reverse	CGTGTCCGCTACAGAAGACTGG
Serpine2	Forward	GCTAGTGCAGTGGTTGCACG
	Reverse	TTCCAACAAGGACAGCCCGT
Ptgs2	Forward	TGGGGGAAGAAATGTGCCAA
	Reverse	CAGCCATTTCCTTCTCTCCTGT
Ym1	Forward	AAGCTCTCCAGAAGCAATCCTG
	Reverse	ATCAGCTGGTAGGAAGATCCCAG

Target	Sense	Sequence
Il1b	Forward	TGCCACCTTTTGACAGTGATG
	Reverse	ATGTGCTGCTGCGAGATTTG
Il12a	Forward	TGCATCTGGCGTCTACACTG
	Reverse	GCCAAAAAGAGGAGGTAGCGT
Nos2	Forward	AGGGTCACAACTTTACAGGGAG
	Reverse	AAGCGTGAGGAGCCTCAGAA
Il10	Forward	ATTCCCTGGGTGAGAAGCTG
	Reverse	CACCTTGGTCTTGGAGCTTATT
Arg1	Forward	TTTCTCAAAAGGACAGCCTCG
	Reverse	CAGACCGTGGGTTCTTCACA
Mrc1	Forward	TTCAGCTATTGGACGCGAGG
	Reverse	GAATCTGACACCCAGCGGAA
Cd163	Forward	CTGAAATCCTCGGGGGTCAT
	Reverse	GCCTGGGCTCTTGTTCCATT
Adgre1	Forward	GACAAACACTTGGTGGTGTGA
	Reverse	GCCTGGGCTCTTGTTCCATT
Cd68	Forward	GTAGCCTAGCTGGTCTGAGC
	Reverse	ACGGCCTTTTTGTGAGGACA
Mki67	Forward	ATCATTGACCGCTCCTTTAGGT
	Reverse	TCTTTGAGCCATCTGAGGCA
Cd5l	Forward	GACGTCAACTGCTCAGGGAA
	Reverse	AGCCCACAGCCTGATGTAAC
H2Aa	Forward	GGAGCCGGTTCTGAAACACT
	Reverse	TCGCAGGCCTTGAATGATGA
Mmp12	Forward	AACCGTGTGCAATGCTTGTG
	Reverse	TGAGTTGTCCAGTTGCCCAG
Ccr2	Forward	TGCCATCATAAAGGAGCCATAC
	Reverse	TAGTCATACGGTGTGGTGGC
Tgfb3	Forward	AGACACAACCCATAGCACGG
	Reverse	CCTCAGCTGCACTTACACGA
Ccl4	Forward	GCAAGATTCGAAAAGGGCCA
	Reverse	ACTTTACTGCCCATCCAGCA
Ccl3	Forward	CCTACAGATGGAGCTGACACC
	Reverse	CTCTTACACTGTTCCTCACC
Cd47	Forward	AAATGGATAAGCGCGATGCC
	Reverse	TCAGTGTTGAAGGCCGTGC
18s	Forward	CCTGGATACCGCAGCTAGGA
	Reverse	GCGGCGCAATACGAATGCCCC

2.8.2 Ribonucleic Acid (RNA) isolation

RNA was isolated from fresh frozen tumours from in vivo experiments (Chapter 2.5.2, 2.5.3, and 2.5.4) or snap-frozen cell pellets using RNeasy plus mini kit (Qiagen, #74134) according to the manufacturer's protocol. In case of frozen tumour tissues, RNaseZap (Invitrogen, #AM9780) was sprayed on the lab benches, forceps, and scalpel before the tumours were cut and weighed so that less than 30 mg was used. The tissue was then quickly chopped up into smallest pieces possible and put in a clean Eppendorf tube. Depending on the weight of the total tumour tissues, either 350 μL (<20 mg tissue) or 600 μL (20 - 30 mg tissue) of Buffer RLT Plus was added. The tissues were then disrupted by pipetting up and down vigorously several times and homogenised by passing the lysate 5 times through 20-gauge needle (Terumo, #613-5391) fitted to a 1 mL syringe and centrifuged for 3 minutes at 14,000 rpm. In case of snap-frozen pelleted cells, 350 μL of Buffer RLT Plus was added to the pelleted cells, and the lysate was homogenized by pipetting up and down several times and vortexing for 30 seconds.

The homogenised lysate was transferred to a gDNA eliminator spin column placed in a 2 mL collection tube and centrifuged for 30 seconds at 10,000 rpm. Then, either 350 μL or 600 μL (depending on the amount of Buffer RLT Plus added in the lysing step) of 70% ethanol was added to the flow-through and mixed by pipetting. Up to 700 μL of the sample was moved to a RNeasy spin column placed into a 2 mL collection tube and centrifuged for 15 seconds at 10,000 rpm. Flow-through was discarded, the column was put back in the collection tube, and 700 μL of Buffer RW1 was added to the RNeasy spin column with centrifugation for 15 seconds at 10,000 rpm. Flow-through was discarded, and 500 μL of Buffer RPE was added to the column placed back on the collection tube before centrifuging for 15 seconds at 10,000 rpm. Flow-through was discarded, and the column was placed back on the collection tube before adding 500 μL Buffer RPE and centrifuging for 2 minutes at 10,000 rpm. Afterwards, the column was placed in a new 2 mL collection tube and centrifuged at 14,000 rpm for 1 minute. The column was then placed into a new 1.5 mL collection tube, and RNA was eluted by adding 30 μL of RNase-free water directly onto the column membrane and centrifuging

for 1 minute at 10,000 rpm. The RNA concentration and quality was measured using NanoDrop One (Thermo Scientific), and the RNA was stored at −80°C or immediately used for complementary DNA (cDNA) synthesis.

2.8.3 Complementary DNA (cDNA) synthesis and qRT-PCR

SuperScript III First-Strand Synthesis SuperMix (Invitrogen, #11752050) was used for cDNA synthesis of the purified RNA according to manufacturer's protocol. Up to 1 μg of the purified RNA, 10 μL of the RT Enzyme Mix, and 2 μL of the RT Enzyme Mix were added to a PCR tube (Invitrogen, #AM12230), and diethyl pyrocarbonate (DEPC)-treated water was added so that the final volume per tube was 20 μL. The contents were gently mixed, and the tube was moved to a thermal cycler (Applied Biosystems^{TM}) and incubated for 10 minutes at 25°C, 30 minutes at 50°C, and 5 minutes at 85°C, and chilled on ice. Then, 1 μL of E.coli RNase H was added to the tube before incubation at 37°C for 20 minutes. The cDNA concentration was measured using Qubit 4 Fluorometer (Invitrogen), and the cDNA was immediately used or stored at 4°C (short-term) or −20°C (long-term).

Quantitative real-time polymerase chain reaction (qRT-PCR) was performed using Luna Universal qPCR Master Mix (New England Biolabs, #M3003L). The 20 μL reaction mix was prepared by adding up to 100 ng of the synthesised cDNA, 1 μL of the primer mix, 10 μL of Luna Universal qPCR Master Mix, and nuclease-free water to make up the final volume. Each assay was run in triplicates with 18s as housekeeping gene, and the contents were added to a 96-well reaction plate (Applied Biosystems^{TM}, #4346907). The plate was sealed with transparent film (Thermo Scientific^{TM}, #AB-1170) and centrifuged at 3,000 rpm for 1 minute to remove bubbles. The assay was run on a QuantStudio^{TM}4 Real-Time PCR System (Applied Biosystems^{TM}) with initial denaturation step at 95°C for 60 seconds, 40 - 45 cycles of denaturation step at 95°C for 15 seconds and extension step at 60°C for 30 seconds, and melt curve step at $60 - 95$°C. Any new primers were checked for specificity using the melt curve step, where a single peak indicated a single product.

2.8.4 Relative quantification

The data was analysed using $2^{-\Delta\Delta C_T}$ method to quantify relative changes in gene expression. The mean cycle threshold (C_T) values were calculated from the technical replicates and used to calculate ΔC_T by subtracting C_T values of the housekeeping gene (18s) from that of the gene of interest. Then, $\Delta\Delta C_T$ was measured as the difference between ΔC_T of the experimental samples and the control samples (average of the biological replicates). Then, the fold gene expression was calculated as $2^{-\Delta\Delta CT}$. The results were graphed using GraphPad Prism 9.

2.9 Flow cytometry

2.9.1 Mouse tumour tissue processing

Processing of mouse tumours was done by Cameron Lang. Tumours collected from the *in vivo* experiment (Chapter 2.5.4) were weighed in a balance, and 0.1 - 1 g of tumour tissue per sample was added to mouse tissue processing buffer (Table 7.1) in a gentleMACS^{TM}C-tube (Miltenyi Biotech, #130-093-237). The tissues were then dissociated using the gentleMACS^{TM}Octo Dissociator (Miltenyi Biotech, #130-096-417) using gentleMACS program 37c-m-TDK-1. Then, non-cellular debris were removed by adding disaggregated cells into a 70 μm cell strainer (Merck, #CLS431750). Cells were then washed twice in PBS with centrifugation (500 x g, 5 minutes), and red blood cell lysis buffer (eBioscience^{TM}, #00-4300-54) was added for 3 minutes at RT. Upon washing the cells twice in 500 xg for 5 minutes, RT, and counting the cells, 1 million cells/well were added to 96-well plates and incubated with 1X cell stimulation cocktail (eBioscience^{TM}, #00-4975-93) in full Roswell Park Memorial Institute 1640 (RPMI) media for 4 hours in 37°C, 5% CO_2.

2.9.2 Mouse peripheral blood processing

Processing of mouse blood was done by Cameron Lang. Blood collected from the *in vivo* experiment (Chapter 2.5.4) was moved to a 15 mL conical, diluted 1:1 in ice-cold PBS, and mixed by inverting the tubes multiple times. Then, the blood was layered on

top of an equal volume of Ficoll-Paque PREMIUM 1.084 (Merck, #GE17-5446-02) in a new 15 mL conical and centrifuged at 400 xg for 40 minutes at RT. A clear buffy coat layer was carefully transferred to 1.5 mL Eppendorf tube, washed twice in 1 mL PBS at 350 xg for 4 minutes at RT, and counted before staining for flow cytometry.

2.9.3 Mouse spleen processing

Processing of mouse spleen was done by Cameron Lang. Spleens collected from the *in vivo* experiment (Chapter 2.5.4) were manually dissociated using 5 mL syringe in 6 cm dish containing 2 mL ice-cold sorting buffer (Table 7.1), and the cells were passed through a 70 μm cell strainer on a 50 mL conical. Residual cells were collected by washing the dish twice with 5 mL sorting buffer and passing the cells into the cell strainer. Cells were then centrifuged for 5 minutes at 350 xg, RT, and resuspended in 5 mL of red blood cell lysis buffer for 3 minutes at RT. Upon diluting in 15 mL PBS, cells were passed through a new 70 μm cell strainer before staining for flow cytometry.

2.9.4 Cell surface staining

For assays on ultra-low attachment 96-well plate, cells were washed twice in PBS by centrifugation (330 xg, 5 minutes) and moved to 1.5 mL Eppendorf tubes for staining. For assays on any other plates / flasks, cells were dissociated using either 2 mM PBS-EDTA or 20 mM PBS-EDTA buffer (Table 7.1) for 20 minutes at 37°C, 5% CO_2. The cells were then transferred to 1.5 mL Eppendorf tubes and washed twice in PBS by centrifugation (330 xg, 5 minutes).

For staining, cells were resuspended in 100 μL PBS containing master mix of Live-Dead stain and antibodies (Table 2.6) for 30 minutes at 4°C in dark before centrifuging once with PBS (330 xg, 5 minutes). Cells were then either further stained with intracellular markers and analysed immediately or fixed for later use. The cells were fixed using 4% paraformaldehyde (PFA, Fisher Scientific, #11400580) in PBS for 10 minutes at RT, washed once with PBS, and stored at 4°C in dark for no longer than 7 days.

Table 2.6: List of antibodies used for flow cytometry. All antibodies were diluted 1:100 in PBS.

Antigen	Species	Fluorophore	Supplier	Clone	Cat no.
Live-Dead	-	eFlour™506	eBioscience™	-	65-0866-18
CD45	Mouse Mouse	BV650 SuperBright™702	BioLegend eBioscience™	30-F11 30-F11	103151 67-0451-80
F4/80	Mouse	APC-eFlour™780	eBioscience™	BM8	47-4801-82
CD14	Human	PE	eBioscience™	61D3	12-0149-42
CD11b	Human Human Mouse Mouse	FITC Brilliant Violet 421 eFluor 450 Super Bright™702	eBioscience™	ICRF44 ICRF44 M1/70 M1/70	11-0118-41 404-0118-41 48-0112-80 67-0112-80
CD80	Human Mouse	Super Bright™702 FITC	eBioscience™	2D10.4 16-10A1	67-0809-41 11-0801-81
MHC Class II	Mouse	PE-Cyanine7	eBioscience™	M5/114.15.2	25-5321-80
CD206	Human Mouse	PE-Cyanine7 PE	eBioscience™	19.2 MR6F3	25-2069-41 12-2061-80
CD163	Mouse	PE-eFlour™610 APC	eBioscience™	TNKUPJ	61-1631-80 17-1631-80
CD47	Human Mouse	APC APC	eBioscience™	B6H12 miap301	17-0479-42 17-0471-82
CD4	Human	PE	BD Biosciences	RPA-T4	562425
CD8α	Human	APC-eFlour™780	eBioscience™	RPA-T8	47-0088-41
CD25	Human	PE-eFlour™610	eBioscience™	CD25-4E3	61-0257-41
CD69	Human	PE	eBioscience™	FN50	12-0699-41
CD366 (TIM3)	Human	APC	eBioscience™	F38-2E2	17-3109-41
IFN-γ	Human	PE-Cyanine7	eBioscience™	4S.B3	25-7319-41

For murine TILs, blood, and splenocytes staining from the *in vivo* experiment (Chapter 2.5.4), cells were washed with PBS in 1.5 mL Eppendorf tubes and incubated with anti-CD16/32 (BD Pharmingen™FC block, #553142) in 100 μL PBS for 15 minutes at 4°C. After washing twice in 1 mL PBS by centrifugation (350 x g, 5 minutes), cells were resuspended in 100 μL PBS containing master mix of Live-Dead stain and antibodies for 30 minutes at 4°C in dark (Table 2.7). Upon washing twice in 1 mL PBS (350

Table 2.7: List of antibodies used for flow cytometry of murine TIL, blood, and splenocytes. These antibodies were used for cells processed from tumours, blood, and spleen *in vivo* (Chapter 2.5.4). All antibodies were from eBioscience™.

Antigen	Amount used	Fluorophore	Clone	Cat no.
Live-Dead	1 μL	eFlour™506	-	65-0866-18
CD45	0.5 μg	Pacific Orange	30-F11	MCD4530
CD4	0.2 μg	APC-eFluor™780	GK1.5	47-0041-82
CD8a	0.2 μg	Alexa Fluor 700	53-6.7	56-0081-82
CD44	0.125 μg	PerCP-Cyanine5.5	IM7	45-0441-80
CD62L	0.015 μg	Super Bright 702	MEL-14	67-0621-82
FoxP3	0.4 μg	PE-Cyanine7	FJK-16s	25-5773-82
CD25	0.25 μg	PE-eFluor™610	PC61.5	61-0251-82
IFN-γ	0.3 μg	PerCP-Cyanine5.5	XMG1.2	45-7311-82
Granzyme B	0.2 μg	eFluor™450	NGZB	48-8898-80

xg, 5 minutes), cells were resuspended in 100 μL FACS buffer (Table 7.1) and either proceeded with intracellular staining or fixed and stored at 4°C in dark for no longer than 7 days.

2.9.5 Intracellular staining

Before collecting the cells, cells were treated with protein transport inhibitor cocktail (500x) (Invitrogen™, #00-4980-93) for 5 hours to inhibit intracellular trafficking and, thus, allow intracellular detection of cytokines. The cells were harvested and stained for cell surface markers as in Chapter 2.9.4. The cells were then fixed with 100 μL FoxP3 / Transcription Factor Staining Buffer Set (Invitrogen™, 00-5523-00) for 30 minutes at RT. The cells were washed once with PBS by centrifugation (300 xg, 5 minutes) and stained with intracellular markers (Table 2.6 and 2.7) for 30 minutes at RT. The cells were then washed once with PBS (300 xg, 5 minutes) and stored as in Chapter 2.9.4.

2.9.6 Compensation

Live-Dead antibody (Table 2.6 and 2.7) was compensated by adding 1 drop of ArC reactive beads (Invitrogen, #A10346) to 1 μL of the antibody for 20 minutes at RT.

Then, 500 μL of PBS and 1 drop of ArC negative beads were added to the tube. All other antibodies were compensated by adding 1 drop of compensation beads (Invitrogen, #01-2222-41) to 1 μL of antibodies for 20 minutes at room temperature before adding 500 μL of PBS.

2.9.7 Data Acquisition and Analysis

Flow cytometry data was acquired using Attune^{TM}NxT Flow Cytometer (Thermo Fisher Scientific). Each sample had 500 - 600 μL collected at a flow rate of 500 μL/min. Data was analysed using FlowJo v10.9 software (BD Biosciences). A typical gating strategy for all experiments is shown in Figure 2.1. When using more than one marker, compensation was done before data collection to correct for any spillover and to differentiate between distinct cell populations (Figure 2.2).

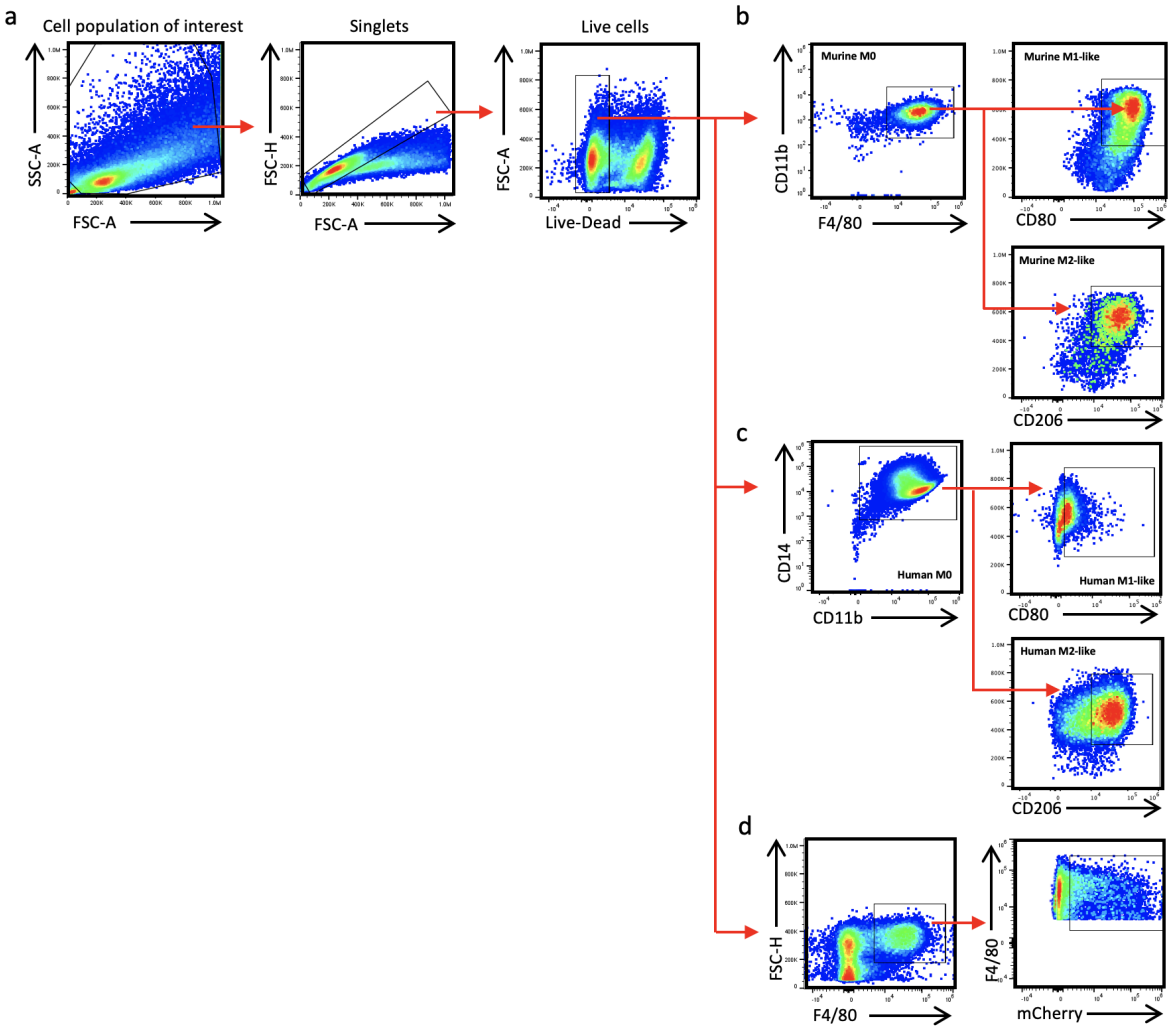


Figure 2.1: Representative flow cytometry gating strategy. a. For all experiments, debris and doublets were removed using forward scatter (FSC) and side scatter (SSC) gatings. After selecting for live cells using fixable viability dye, the cells were gated for either **b**. murine macrophages or **c**. human macrophages. M1-like and M2-like macrophages were gated using CD80 and CD206, respectively. **d**. For phagocytosis, F4/80+ (murine) or CD11b+ (human) macrophages were gated from the live cells, then mCherry+ tumour cells were gated from that macrophage population.

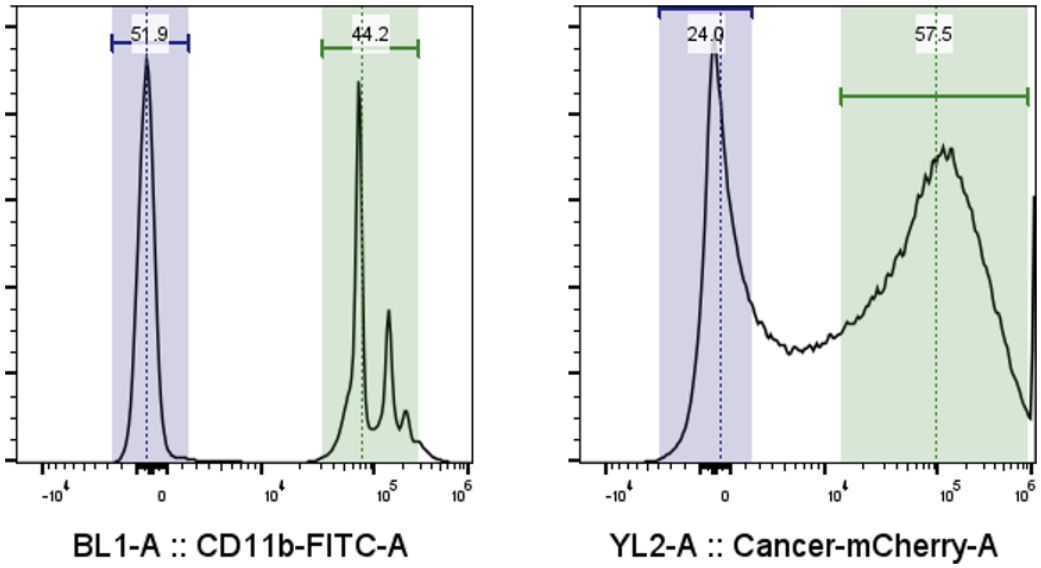


Figure 2.2: Representative compensation strategy. Compensation was done by identifying the positive (green) and negative (purple) populations.

2.10 Immune cell isolation

All isolated primary cells and the culture conditions are listed in Table 2.8.

Table 2.8: List of primary cells. Type of primary cells, the culture media, and culture time is listed in the table.

Primary cells	Culture media	Culture time
Human PBMC-derived macrophages	X-VIVO10 media + 2% FBS	6 days
Human PBMC-derived T cells	X-VIVO10 media + 2% FBS + 30 IU/mL IL-2	Ready to use
Mouse BMDMs	DMEM + 20ng/ml M-CSF + 10% FBS + 1% P/S	7 days (media supplemented on day 4)
Abbreviations and Manufacturers: Peripheral blood mononuclear cells (PBMC), Bone marrow-derived macrophages (BMDMs), X-VIVO10 media (Lonza, #BE04-380Q), Foetal Bovine Serum (FBS, Gibco, #10500064), Dulbecco's Modified Eagle Medium (DMEM, Gibco, #41966029), Macrophage colony-stimulating factor (M-CSF, Gibco, #PMC2044), Penicillin-Streptomycin (P/S, Gibco, #15140122), IU (International Unit), Interleukin-2 (IL-2, BD Biosciences, #554603)		

2.10.1 Human peripheral blood mononuclear cells (PBMCs) processing

Human NC24 leukocyte cones were obtained from consented healthy volunteers (NHS Blood and Transfusion Service, Oxford, UK) under the ethics of Dr. Kerry Fisher at the University of Oxford (REC 19/LO/1848, Protocol #ONC1NHSTblood1). The cones were processed for PBMC isolation by Cameron Lang.

For processing, 15 mL of Lymphoprep^{TM}(STEMCELL, #85450) was added through the central hole of the SepMate^{TM}-50 (IVD) insert (STEMCELL, #07801). Then, whole blood diluted to an equal volume of PBS + 2% FBS (STEMCELL, #07905) was carefully added to the top of the density gradient medium and centrifuged at 1,200 xg for 10 minutes at RT. The top layer containing mononuclear cells was collected and washed twice with PBS + 2% FBS. The cells were then counted before cryopreservation or for use in cell culture.

2.10.2 PBMC-derived macrophage differentiation and polarisation

Isolated monocytes were differentiated into PBMC-derived macrophages in a T75 ultra-low attachment flask (Corning, #3814) in the appropriate media (Table 2.8) for 6 days (undifferentiated, M0). On day 2, cells in suspension (T cells) were collected, and the flask was replaced with fresh media. On day 4, macrophages were treated with either 10 ng/mL lipopolysaccharide (Sigma-Aldrich, #L2630-10MG) and 25 ng/mL IFN-γ1b (Miltenyi Biotec, #130-096-873) (classically activated, M1-like) or 25 ng/mL IL-4 (Miltenyi Biotec, #130-095-373) and 25 ng/mL IL-6 (Miltenyi Biotec, #130-095-365) (alternatively activated, M2-like), for 48 hours.

For disaggregation, the cells were washed twice with PBS and left in 3 mL of 20 mM PBS-ethylenediaminetetraacetic acid (EDTA, Sigma-Aldrich, #03690-100mL) buffer (Table 7.1) for 25 minutes at 37°C in 5% CO_2. Then 7 mL of DMEM (10% FBS) was added, and the remaining adhered cells were scraped with a cell scraper for use in further experiments.

2.10.3 T cell isolation

T cells were isolated from PBMC suspension one day after PBMC was seeded (Chapter 2.10.2) and cultured in T25 flask (Corning, #430639) standing up in appropriate media (Table 2.8).

2.10.4 Bone marrow-derived macrophages (BMDMs) isolation and polarisation

The mouse was euthanised by cervical dislocation, and death was confirmed by noting its respiratory arrest. The mouse was then sterilised with 70% ethanol (diluted from 100% ethanol, Sigma-Aldrich, #32221-2.5L-M) before removing the skin of the legs and cutting the femur near the base of the lower limb. The feet and all muscles surrounding the femur and the tibia were removed before disconnecting the knee joint, leavng two femurs and two tibia for use. The epiphyses of femur and tibia were removed, and the ends of the bones were poked with a 1mL syringe (Terumo, #MDSS01SE)

with a 23-gauge needle (Terumo, #AN*2316R1) filled with PBS to wash the bone marrow into a 50 mL tube (Corning, #430291). After all marrows were flushed so that the remaining bone is opaque white, the bone marrow suspension was washed by centrifugation (Thermo Jouan C4i) at 200 xg, 5 minutes at 4°C. The cells were then resuspended in 1 mL of red blood cell lysis buffer (BD Biosciences, #555899) diluted 1:10 with deionised water (dH_2O) and incubated on ice for 3 minutes. Then, 10 mL of the DMEM supplemented with 10% FBS and 1% P/S were added to neutralise the buffer and washed at 200 xg, 5 minutes at 4°C. The pellet was resuspended in 1 mL of the relevant culture media (Table 2.8) and filtered through 100 µM cell strainer (Corning, #352360). Then the cell suspension was resuspended in culture media and differentiated into BMDMs in either a 12-well plate (Greiner, #665180) or a 10 cm dish (Corning, #430293) for 7 days. On day 4, half of the total volume of the media was freshly added. On day 6, macrophages were polarised by treating with either 1 μg/mL LPS and 10 ng/mL IFN-γ (classically activated, M1-like) or 20 ng/mL IL-4 (alternatively activated, M2-like), for 48 hours.

For disaggregation, the cells were washed twice with PBS, and either 500 μL/well (in a 12-well plate) or 3 mL (per 10 cm dish) of 20 mM PBS-EDTA was added for 20 minutes at 37°C in 5% CO_2. The remaining adherent cells were dislodged using a cell scraper and washed before using in further experiments.

2.11 Co-culture assay

2.11.1 Macrophages and cancer cell co-culture assay

mCherry-tagged cancer cells and macrophages (J774 cell line, BMDMs, or PBMC-derived) were seeded in triplicates in an ultra-low attachment 96-well plate at a density of 20,000 cells/well or in a 12-well plate at a density of 50,000 cells/well with or without treatments. After incubating at 37°C in 5% CO_2 for 24 - 72 hours, the cells were collected, stained, and prepared for flow cytometry as in Chapter 2.9.

2.11.2 Macrophages, T cells, and cancer cell co-culture assay

PBMC-derived macrophages were differentiated and polarised as in Chapter 2.10.2. Then, 20,000 M0, M1-like, or M2-like macrophages and 20,000 mCherry-tagged DU145 or 22Rv1 were co-cultured in an ultra-low attachment 96-well plate with appropriate treatments in triplicates and left for 48 hours. No treatments were added for the positive and negative control wells.

On the following day, T cells were thawed in an appropriate media (Table 2.8), and the next day, thawed T cells were stained with carboxyfluorescein succinimidyl ester (CFSE) using CellTrace™ CFSE Cell Proliferation Kit (Invitrogen™, #C34554) (Quah et al., 2010; Hilchey et al., 2007; Yamada-Hunter et al., 2024). Briefly, T cells were centrifuged in 15 ml conical at 1,200 rpm for 5 minutes. After removing the supernatants, 5 μL of CellTrace™ stock solution in 5 mL PBS was added to the cells, gently resuspended, and incubated at RT for 20 minutes, protected from light. Then, 25 μL of RPMI was added to the tube and incubated for 5 minutes at RT before centrifuging at 1,200 rpm for 5 minutes.

The plate containing macrophages and cancer cell co-culture was centrifuged at 1,200rpm, 5 minutes, to remove the media, and 40,000 T cells in RPMI were seeded to the co-culture with the following: 30 IU/mL of IL-2 (BD Biosciences, #554603) and 2 μL of T Cell TransAct™(Miltenyi Biotec, #130-111-160) containing CD3 and CD28 for experimental samples and positive controls, and 200 IU/mL of IL-2 for negative controls.

After 72 hours, the cells were collected, washed twice in PBS by centrifugation (330 xg, 5 minutes), and stained with Fixable Viability Dye, CD8, CD4, CD25, CD69, TIM-3, and IFNγ for flow cytometry, as in Chapter 2.9. Figure 2.3 illustrates the gating strategy for this assay.

2.12 Cytokine array

Proteome Profiler Mouse Cytokine Array Kit Panel A (R&D Systems, #ARY006) was used for the experiment according to the manufacturer's protocol. In each well of the

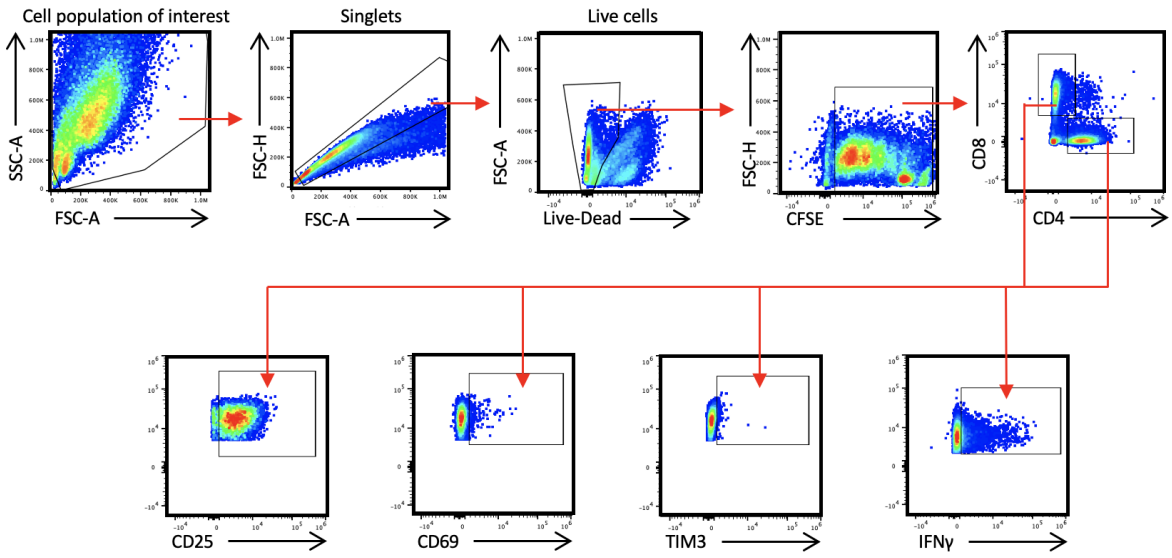


Figure 2.3: Representative flow cytometry gating of macrophages, T cells, and cancer cell co-culture assay. Debris and doublets were removed using forward scatter (FSC) and side scatter (SSC) gatings. Live cells were selected using fixable viability dye, and upon selecting for CFSE-stained T cells, the cells were gated for either CD4+ or CD8+. Each T cell types were then gated for CD25+, CD69+, TIM3+, and IFNγ.

4-well multi-dish, 2 mL of Array Buffer 6 was added, and the cytokine array membranes were placed in each well facing upward and incubated for one hour on a shaker.

For sample collection, 1 mL of cell culture supernatants were collected in Eppendorf tubes and centrifuged at 10,000 rpm for 5 minutes to remove cell debris. The supernatants were then added to 500 μL of Array buffer 4 in separate tubes. Then, 15 μL of the Detection Antibody Cocktail reconstituted in 100 μL of distilled water was added to each sample and mixed and incubated at RT for 1 hour. Array buffer 6 was aspirated from the wells, and the prepared sample/antibody mixtures were added to each well. The lid was placed on the dish and incubated overnight at 4°C on a rocker.

On the following day, the membranes were removed from the wells and washed three times with 20 mL of 1X wash buffer (25X Wash Buffer Concentrate diluted with distilled water) in individual plastic containers for 10 minutes each on a rocker. Then, 2 mL of Streptavidin-HRP diluted 1:10,000 in Array Buffer 6 was pipetted into each well of the 4-well multi-dish containing membranes, and the wells were covered with the lid. After incubating for 30 minutes at RT on a rocker, the membranes were washed three times

with 1X wash buffer for 10 minutes each on a rocker. The membranes were blotted onto paper towels to remove any excess wash buffer and placed on the plastic sheet protector. Then, 2 mL of Chemi Reagent 1 and Chemi Reagent 2 were mixed, and 1 mL of the mix was pipetted onto each membrane before covering the membrane with top sheet of the plastic sheet protector and incubating for 1 minute. The membranes were then imaged using LI-COR Odyssey Imager. The Protein Array Analyzer for ImageJ in Fiji (imageJ) v1.54f software was used for data analysis, and the results were graphed in GraphPad Prism 9.

2.13 *in vitro* Phagocytosis assay

mCherry-tagged cancer cells were seeded in triplicates in an ultra-low attachment 96-well plate at a density of 40,000 cells/150 μL/well with appropriate treatments and incubated at 37°C in 5% CO_2 for the treatment duration. Then, the plate was centrifuged (Thermo Scientific Heraeus Megafuge 40R) at 330 xg for 5 minutes to remove the media, and 20,000 polarised or unpolarised BMDMs, J774 macrophages, or PBMC-derived macrophages were seeded 150 μL/well in FBS-free DMEM with or without treatments and incubated for 2 hours at 37°C in 5% CO_2. Then, the plate was washed twice in PBS by centrifugation (330 xg, 5 minutes), and the cells were stained with Fixable Viability Dye and F4/80, CD80, and CD206 for murine macrophages, and CD11b, CD80, and CD206 for human macrophages as in Chapter 2.9. For analysis, cells were gated as in Figure 2.1d.

2.14 Clinical samples

All clinical samples for WINGMEN trial (NCT05110495) were collected under the ethics REC 21/SC/0170 and EudraCT 2018-000204-42.

2.14.1 Research blood samples

Insulin and PSA levels, as well as other clinical data were assayed in Haematology and Biochemistry Laboratory, John Radcliffe Hospital.

For serum samples, 6 mL of blood was collected in a 6 mL serum vacutainer (Midmeds, #P1541) and gently inverted 8 times. The blood was allowed to clot for 30 to 120 minutes at RT and centrifuged at 2,000 xg at RT for 10 minutes. Then, the separated serum was carefully transferred to a clean 15 ml conical, ensuring not to disturb the clot, aliquoted into cryovials, and frozen at −80°C in the Sample Handling Laboratory until ready for use. The pre-xentuzumab samples, collected on the day the first dose was given, and the post-xentuzumab samples, collected 1-3 days before RP, were used for phospho-IGF-1R enzyme-linked immunosorbent assay (ELISA) (Chapter 2.17).

For sodium heparin plasma samples, 10 mL of blood was collected in a 10 mL sodium heparin vacutainer (Midmeds, #P1524), gently inverted 8-10 times, and stored on wet ice to be processed within 30 minutes of collection. For plasma processing, the sample was centrifuged at 1,500 xg at 4°C for 15 minutes. Then, clear plasma was immediately transferred to a clean 15 ml conical, ensuring not to disturb the cell layer. The colour of the plasma was noted, as pink or red would indicate haemolysis. The plasma was aliquoted in 1 mL into cryovials and frozen at −80°C in the Sample Handling Lab. The pre-xentuzumab plasma, collected on the day the first dose was given, and post-xentuzumab plasma, colleted 1-3 days before RP, were used for metabolomics (Chapter **??**). For PBMC proessing, the remaining blood was transferred to 50 mL conical and incubated at RT, with gentle pipetting to break up any cellular aggregates formed when stored at 4°C. The sample was diluted with equal volume (about 5 mL) of PBS. Then, 7.5 mL of Ficoll-Paque PLUS (Cytiva, #17-1440-02) was added to a separate 50 mL conical, where 10 mL of dluted blood was added on top. The mix was centrifuged for 20 minutes at 800 xg, RT, in a horizontal rotor, with breaking speed set to low. The resulting blood was separated into 4 layers: upper layer of diluted plasma, second layer of white, fluffy PBMCs, third, cloudy layer of Ficoll Paque PLUS, and the bottom layer containing red blood cells. PBMC layer was carefully transferred to a new 50 mL conical, and ice-cold PBS was added so that the mix was 40 mL in total. Upon inverting the tubes few times, the mix was centrifuged at 500 xg for 10 minutes at 4°C. Supernatant was discarded, and the pellet was re-suspended in residual PBS by flicking. Then, 5 mL of ice-cold PBS was added to the tube, pipetted gently to mix, and 10 μL

of the mix was taken for cell count. Then, ice-cold PBS was added to the PBMCs up to 40 mL, and the tube was mixed by inversion and centrifuged at 500 xg for 10 minutes at 4°C. The supernatant was discarded, and upon re-centrifuging the tube at 500 xg for 1 minute at 4°C, residual supernatant was carefullly removed and re-suspended in residual PBS by flicking. Then, 2 mL of freezing medium containing 90% foetal calf serum and 10% DMSO was added to the tube. PBMCs were then mixed by pipetting and aliquoted to 1 mL per cryovial and stored in Mr. Frosty for minimum 4 hours at −80°C, before transferring to standard storage containers at −80°C until further use. PBMCs collected pre- and post-xentuzumab were used for PBMC immunoprofiling (Chapter 2.18).

2.14.2 Research tissue samples

Diagnostic prostate biopsies taken prior to trial entry were used as pre-treatment tissue. For post-treatment in-theatre cores, surgeons took 2 - 3 biopsy cores from the prostate as soon as the prostate was out, injecting ink into biopsy tracts to enable visualisation of biopsy sites. The cores were immediately fixed in formalin and taken to the Pathology Laboratory, John Radcliffe Hospital, for paraffin embedding. The tissue blocks were cut in 4 μm sections by Oxford Radcliffe Biobank (ORB)/Oxford Centre for Histopathology Research (OCHRe) for use in routine haematoxylin & eosin (H&E), primary endpoint and research endpoint IHC (Chapter 2.6.4), and RNA extraction for transcriptomics (Chapter 2.16).

2.15 Multiplex Immunofluorescence (mIF)

2.15.1 Antibody conjugation

Some of the antibodies used for multiplex immunofluorescence (mIF) were directly conjugated with fluorophores using the Alexa Fluor^{TM}Antibody Labelling kits (Thermo Fisher, #A20181 for Alexa Fluor^{TM}(AF)488, #A20187 for AF555, #A20186 for AF647) as per manufacturer's instructions. The antibodies were carrier (BSA/Azide) free and had stock solution of 1 mg/mL. Briefly, 1 mL of distilled water was added to the supplied sodium bicarbonate and vortexed until dissolved. Then 10 μL of the sodium

bicarbonate was added to the antibody, and the whole volume of the antibody stock solution was transfered to the vial containing reactive dye and vortexed. The solution was then incubated for 1 hour at RT in dark, with vortexing every 15 minutes. In the last 15 minutes of the incubation, spin column was prepared by adding 1 mL of the provided resin into the column and centrifuging at 1,100 xg for 3 minutes. After an hour of incubation, the antibody/dye mix was vortexed, pulse centrifuged and pipetted into the column, before centrifuging at 1,100 xg for 5 minutes. Then, collection tube was removed, and its concentration was measured using Nanodrop.

2.15.2 Slide preparation

Two consecutively cut slides were used to stain 17 markers, 11 in the first batch and 6 in the second batch. First, slides were baked in a 60°C oven overnight. The next day, slides were cleared using the Gemini Autostainer (Epredia, #A81500001) with the following protocol: wash twice in xylene for 5 minutes each, twice in 100% ethanol for 5 minutes each, twice in 95% ethanol for 5 minutes each, twice in 70% ethanol for 5 minutes each, twice in 50% ethanol for 5 minutes each, and twice in PBS for 5 minutes each, permeabilise in PBS with 0.3% Triton X100 for 10 minutes, and wash in PBS for 5 minutes. Then, antigen retrieval was done in the NxGen Decloaking Chamber (Biocare, #DC2012) for 20 minutes in citrate buffer (pH 6) and 20 minutes in 1X Tris-HCl buffer (pH 8.5; Sigma-Aldrich, #T6455-1000ML) once the pressure cooker reaches 110°C. The slides were left in Tris-HCl buffer to cool for 10 minutes in RT and washed 4 times in PBS, 5 minutes each, with gentle agitation. The slides were then blocked overnight in 10% donkey serum + 3% BSA in PBS.

The next day, the slides were washed once in PBS for 5 minutes, and incubated in 4',6'-diamidino-2-phenylindole (DAPI) for 15 minutes at RT with gentle agitation. Then, the slides were washed in PBS for 5 minutes, dipped in dH_2O, and coverslipped with mounting media (Table 7.1). The slides were imaged using CellDIVE platform (GE healthcare, IN Cell Analyzer 2500HS) at the Kennedy Institute of Rheumatology, University of Oxford. Scanplan and background imaging was done before the staining rounds to select regions of interest (ROIs).

After background imaging, the slides were de-coverslipped face-down in PBS, and blocked in 1:200 FcR blocking reagent (Miltenyi Biotec, #130-059-901) in 3% BSA in PBS (antibody diluent) for 20 minutes at RT. Then, slides were incubated overnight at 4°C with 100 μL of primary antibodies (Table 2.9) in antibody diluent, coverslipped with hydrophobic coverslip.

The next day, slides were washed twice in PBS-T for five minutes each and once in PBS for five minutes. The slides were dipped in dH_2O and coverslipped with mounting media. The staining round was imaged with different exposure times for each antibody (Table 2.9).

Table 2.9: List of antibodies used for multiplex IF. The isotype of all antibodies is IgG. * denotes antibodies conjugated using the conjugation kit. Abbreviations: Concentration (Conc.) Cell Signalling Technologies (CST), Pan-cytokeratin (PCK), Santa Cruz Biotechnology (SCBT), Vimentin (Vim), Androgen receptor (AR).

Round	Name	Conc.	Dye	Species	Supplier	Cat no.	Exposures
1	PD-1	10 μg/mL	488	Rabbit	Abcam	ab220300	500 ms
	CD68	10 μg/mL	555	Rabbit	Abcam	ab280860	200 ms
	CD45	10 μg/mL	647*	Rabbit	Abcam	ab282747	400 ms
2	PCK	5 μg/mL	488	Mouse	SCBT	sc-8018	600 ms
	FoxP3	10 μg/mL	555*	Rabbit	CST	74816SF	450 ms
	CD14	5 μg/mL	647*	Rabbit	Abcam	ab226121	300 ms
3	CD4	5 μg/mL	488	Rabbit	Abcam	ab196372	700 ms
	CD8	5 μg/mL	555*	Mouse	BioLegend	372902	550 ms
	CD163	10 μg/mL	647*	Mouse	Novus	NB110-40686	800 ms
4	Vim	10 μg/mL	555	Rabbit	Abcam	ab203428	50 ms
	AR	10 μg/mL	647	Rabbit	Abcam	ab194195	1000 ms
1	CD3	5 μg/mL	488*	Rabbit	Abcam	ab245731	300 ms
	CD19	5 μg/mL	555	Rabbit	Abcam	ab274888	450 ms
	TIM-3	10 μg/mL	647*	Rabbit	Abcam	ab242080	700 ms
2	CD47	5 μg/mL	488*	Mouse	Abcam	ab184675	700 ms
	PD-L1	5 μg/mL	555	Mouse	SCBT	sc-53319	500 ms
	CD31	10 μg/mL	647	Mouse	Novus	NBP2-34283	350 ms

Before subsequent rounds of staining, the slides were bleached. For bleaching, the slides were de-coverslipped in PBS, and dye inactivation solution (Table 7.1) was added to

the slides for 15 minutes at RT. The slides were washed with PBS for 1 minute, and incubated again with dye inactivation solution for 15 minutes. The slides were then washed three times for 5 minutes each and incubated in DAPI for 15 minutes at RT. Upon washing the slides in PBS for 5 minutes, the slides were dipped in dH_2O and coverslipped in mounting media before the bleaching round imaging.

Upon bleaching round imaging, the slides were incubated with primary antibody mix overnight. The steps of staining, staining round imaging, bleaching, and bleaching round imaging were repeated until the last staining round imaging.

2.15.3 Data Analysis

All images were analysed using the HALO platform. Random Forest classifier was used to classify the epithelium and the stroma with PCK staining. Then, HighPlex FL v4.2.14 analysis setting was used to set phenotypes for cells that require staining status for more than 1 markers and to quantify the % positive cells. Infiltration analysis algorithm, part of the Spatial analysis module, was used to identify spatial distribution and proximity of various immune cells relative to the epithelium. Ten bands of 15 μm width, ranging from 50 μm inside the epithelium to 100 μm outside the epithelium were selected for the annotated epithelium region, and the number of cells per mm^2 were determined for each band.

2.16 RNA Sequencing of WINGMEN trial samples

2.16.1 RNA extraction from FFPE tissue sections

The objective of RNA sequencing of trial samples was to identify and compare differentially expressed genes that arose from xentuzuamb treatment. Although using fresh frozen tissues would have yielded more RNAs with higher quality, pre-treatment samples of WINGMEN trial being diagnostic biopsies meant that FFPE sections had to be used for RNA sequencing (Figure 5.2). FFPE sections of 4 μm was cut by OCHRe in RNase-free conditions, and three adjacently cut sections were used per sample. RNA was extracted using the High Pure FFPET RNA Isolation Kit (Roche, #06650775001)

as per manufacturer's instructions. Briefly, slides were deparaffinised in Citroclear for 2 minutes. The tissue areas were then scraped with a scalpel (Fisher Scientific, #11758353) and carefully put into a 1.5 ml nuclease-free Eppendorf tube containing 800 μL xylene. The tube was vortexed several times, and 400 μL of absolute ethanol was added. The tube was vortexed briefly and centrifuged for 2 minutes at 16,000 xg before removing the supernatant. Then, 1 mL of absolute ethanol was added, and the tube was vortexed briefly and centrifuged for 2 minutes at 16,000 xg. Supernatants were discarded, and the tissue pellet was dried for 15 minutes at 56°C with the cap open.

To each tissue pellet, 100 μL of RNA Tissue Lysis Buffer (Vial 1), 16 μL of 10% SDS, and 40 μL of Proteinase K working solution were added. The tube was vortexed, spun down briefly, and incubated with shaking at 600 rpm for 30 minutes at 85°C. The tube was then cooled to 55°C after adding 80 μL of Proteinase K. The tube was vortexed for several seconds, spun down briefly, and incubated for 30 minutes at 55°C, with shaking at 600 rpm. Resulting tissue lysate was spun down briefly, and 325 μL of RNA Binding Buffer (Vial 3) and 325 μL of ethanol were added before vortexing and brief spin. Then, 900 μL of lysates were pipetted into a High Pure Filter Tube placed onto High Pure Collection Tube and centrifuged for 30 seconds at 6,000 xg. The High Pure Filter Tube was placed onto a new High Pure Collection Tube and centrifuged for 2 minutes at 16,000 xg to completely dry the filter fleece. The High Pure Filter Tube was placed onto a new High Pure Collection Tube, and 100 μL of DNase working solution (90 μL DNase Incubation buffer + 10 μL DNase I dissolved in Reagent Preparation Buffer) was added without touching the fleece before incubating for 15 minutes at RT. Then, 500 μL of Wash Buffer I working solution (Vial 4) was added, and the tube was centrifuged for 20 seconds at 6,000 xg. The flow through was discarded, and 500 μL of Wash buffer II working solution (Vial 5) was added before centrifuging for 20 seconds at 6,000 xg. After discarding the flow through, 500 μL of Wash buffer II working solution was added and centrifuged for 20 seconds at 6,000 xg. The flow through was discarded, and the tube was centrifuged for 2 minutes at 16,000 xg to completely dry the fleece. The High Pure Filter Tube was placed into a fresh 1.5 mL Eppendorf, and 25 μL of RNA Elution

Buffer (Vial 8) was added to the center of the tube. After 1 minute incubation at RT, the tube was centrifuged for 1 minute at 6,000 xg.

The RNA concentration was measured using Qubit 4 Fluorometer (Invitrogen), and A260/280 and A260/230 ratios were measured using NanoDrop One (Thermo Scientific). The RNA was stored at $-80°C$ until ready for shipment.

2.16.2 RNA Library Preparation and Sequencing

Initial RNA sample quality assessment, RNA exome library preparation, and sequencing were conducted at GENEWIZ (South Plainfield, NJ, USA) as follows.

The RNA was quality-controlled using the Agilent 4200 TapeStation (#G2991B). Library preparation was performed using the TruSeq RNA Exome kit (#20020189) manufactured by Illumina along with Illumina Truseq RNA Enrichment and Single Index kits, according to the manufacturer's guidelines.

Briefly, the RNA was fragmented enzymatically according to manufacturer's instructions and reverse transcribed into cDNA which was cleaned up and adenylated at the 3' ends. Adapters were ligated to the cDNA fragments, which were then enriched with limited cycle PCR and cleaned up. Once validated using Agilent 4200 TapeStation and quantified using Qubit 4.0 Fluorometer and Illumina Miseq Nano Reagent kit (#MS-102-2001), the adapter-ligated cDNA fragments were hybridized with biotinylated baits. The hybrid cDNAs were captured by streptavidin-coated binding bead, and after extensive washing, the captured cDNAs were amplified and indexed with Illumina indexing primers. Post-captured DNA libraries were validated using Agilent 4200 TapeStation and quantified using Qubit 4.0 Fluorometer.

Illumina reagents and kits for DNA library sequencing cluster generation and sequencing were used for enrichment cDNA sequencing. Post-captured libraries were multiplexed on a flow-cell and loaded on the Illumina NovaSeqX instrument according to the manufacturer's instructions. The samples were sequenced using a 2x150 paired-end (PE) configuration, and NovaSeq Control Software in the instrument was used for image

analysis and base calling. Raw sequencing data (.bcl files) generated from Illumina NovaSeq were converted into fastq files and de-multiplexed using Illumina's bcl2fastq software.

2.16.3 Data Processing and Analysis

Analysis of RNA sequencing data from the WINGMEN trial tissues was performed by Dr. Fiona Hartley in our lab. FastQC 0.11.9 was used to check the quality of RNA-seq data (Andrews et al., 2012), and adapters and low-quality bases were trimmed using Cutadapt (version 4.8) (Martin, 2011). Reads were aligned to the reference using STAR (version 2.7.8a) (Dobin et al., 2012), quantified using featureCounts from the Subread package (version 2.0.6) (Liao et al., 2013) and tabulated using pandas (version 1.5.2) in Python (version 3.11.0). Differential expression analysis was done using DESeq2 (version 1.38.3) (Love et al., 2014) with sequencing depth normalisation by 'median of ratios' method, and pathway enrichment analysis was performed using clusterProfiler (version 4.6.2) (Yu et al., 2012).

2.17 phospho-IGF-1R enzyme-linked immunosorbent assay

On day 1, DU145 were seeded into black 96-well clear bottom plate (Corning, #3603) with seeding density of 50,000 cells/well at 100 μL/well and incubated overnight at 37°C in 5% CO_2. Twenty wells were reserved for standards and six wells for cell controls (control, IGF-1 treatment, and IGF-1 + xentuzumab treatment), leaving the rest to be used to test serum samples.

The next day, cells were serum-starved by washing twice and adding 100 μL/well of serum-free RPMI and were incubated at 37°C in 5% CO_2. Xentuzumab-treated cell controls were prepared later in the day by adding 1 μM of xentuzumab to two of the wells and incubating overnight at 37°C in 5% CO_2.

On the next day, standards were prepared in duplicates by ten serial 3-fold dilutions starting from 500 nM of human IGF-1 (Sigma-Aldrich, #I3769-100ug) in serum-free

media. Serum samples were prepared by thawing 40 μL of serum from -80°C and mixing with 60 μL of serum-free RPMI. IGF-1 and IGF-1 + xentuzumab-treated cell controls were prepared by treating with 50 nM of IGF-1. Once standards and samples were prepared, medium was aspirated from the wells, and 100 μL of the samples (in triplicates), standards, and cell controls (in duplicates) were added to appropriate wells and incubated for 30 minutes at 37°C in 5% CO_2. Then, the standards and samples were aspirated, and the cells were fixed with 4% PFA in PBS for 20 minutes RT on a rocker. Afterwards, the cells were washed twice with wash buffer (0.1% Triton X-100 in Tris-buffered saline (TBS)) for 5 minutes and quenched by adding 1.2% H_2O_2 in wash buffer for 30 minutes at RT on a rocker. The wells were then washed once with wash buffer for 5 minutes and blocked with blocking solution (5% BSA in wash buffer) for 60 minutes at RT on rocker. Then, the blocking solution was aspirated, and 100 μL/well of phospho-IGF-IR-β (tyr1135/1136)/insulin receptor-β (tyr1150/1151) antibody (Cell Signalling Technology, #3024) at 1:1,000 dilution in blocking buffer was added. The plate was sealed with parafilm and incubated at 4°C on a rocker overnight.

On the following day, the wells were washed four times with wash buffer for 5 minutes each at RT, and HRP-linked anti-rabbit IgG antibody (Cell Signalling Technology, #7024) was added at 1:2,000 dilution in the blocking solution for 2 hours at RT on a rocker. The wells were then washed three times with wash buffer for 5 minutes each, and washed once with TBS for 5 minutes. After aspirating, 100 μL/well of tetramethylbenzidine (Thermo Scientific, #34028) equilibrated to RT was added 100 μL/well and incubated for 30 minutes on a rocker. The reaction was quenched by adding 100 μL/well of 2 M H_2SO_4, and the absorbance was measured at 450 nm on a POLARstar OMEGA plate reader. The results were graphed in dose response fit using GraphPad Prism 10.

2.18 PBMC immunoprofiling using Cytometry by Time-Of-Flight (CyTOF)

2.18.1 PBMC sample processing

PBMC sample processing was done by Cameron Lang. PBMCs were collected from Sample Handling Lab and thawed by warming at 37°C water bath for 5 minutes. Cells were then transferred to a 15 mL conical, diluted with 10 mL PBS containing 2% FBS and centrifuged at 500 xg for 5 minutes at RT.

The cells were incubated with Intercalator-103Rh (Fluidigm, #201103A) for 10 minutes at RT to exclude any dead cells, and stained with surface markers for 20 minutes at RT (Table 2.10). The cells were then fixed with FoxP3 Transcription Factor Staining Buffer Set for 30 minutes at RT, and stained with intracellular markers for 20 minutes at RT (Table 2.10). The cells were then washed with PBS and incubated with 0.125 nM Intercalator-191Ir diluted in Maxpar Fix and Perm Buffer (Fluidigm, #201067) overnight at 4°C.

2.18.2 CyTOF data acquisition and data analysis

Right before data acquisition, samples were washed twice with Maxpar cell staining buffer, and 500,000 cells/mL were resuspended in cell acquisition solution, containing EQ 4 Element beads (Fluidigm, #201078) in 1:10 dilution. The samples were run on a CyTOF Helios mass cytometer (Fluidigm, #400236) at an event rate of 300 events/sec. For pre-processing, samples were gated to exclude residual normalisation beads, debris, doublets, and dead cells. Data analysis was done manually using FlowJo v10.10.0 and using unsupervised clustering analysis by FlowSOM (version 4.1.0, Van Gassen et al., 2015) in R version 4.3.3 by Cameron Lang.

Table 2.10: List of antibodies used for CyTOF. All commercial antibodies were from Fluidigm and reactive to human.

Mass tag	Marker	Clone	Staining	Cat no.
116 Cd	CD45	HI30	Surface	3116001B
141 Pr	CD39		Surface	In-house
142 Nd	CD19	HIB19	Surface	3142001B
143 Nd	CD127	A019D5	Surface	3143012B
144 Nd	CD69	FN50	Surface	3144018B
145 Nd	CD4	RPA-T4	Surface	3145001B
146 Nd	IgD	IA6-2	Surface	3146005B
147 Sm	CD11c	Bu15	Surface	3147008B
148 Nd	CD16	3G8	Surface	3148004B
151 Eu	CD123	6H6	Surface	3151001B
152 Sm	CD66b	80H3	Surface	3152011B
153 Eu	TIGIT	MBSA43	Surface	3153019B
154 Sm	CD3	UCHT1	Surface	3154003B
155 Gd	CD36	5-271	Surface	3155012B
158 Gd	CCR4	205410	Surface	3158006A
159 Tb	CCR7	G043H7	Surface	3159003A
160 Gd	CD14	MSE2	Surface	3160006B
161 Dy	CTLA4	14D3	Cytoplasmic & surface	3161004B
162 Dy	FoxP3	259D/C7	Nuclear	3162024A
163 Dy	CD56	NCAM16.2	Surface	3163007B
164 Dy	CD161	HP-3G10	Surface	3164009B
165 Ho	CD45RO	UCHL1	Surface	3165011B
166 Er	CD141	M80	Surface	3166017B
167 Er	CD27	HIT2	Surface	3167001B
168 Er	CD8a	SK1	Surface	3168002B
169 Tm	CD25	2A3	Surface	3169003B
170 Er	CD45RA	HI100	Surface	3169008B
171 Yb	CD20	2H7	Surface	3171012B
172 Yb	Ki67	B56	Nuclear	3172024B

Mass tag	Marker	Clone	Staining	Cat no.
173 Yb	HLADR	L243	Surface	3174001B
174 Yb	PD1	EH12.2H7	Surface	3174020B
175 Lu	PDL1	29E.2A3	Surface	3175017B
176 Yb	CD57	HCD57	Surface	3176019B
194 Pt	Granzyme B	GB11	Cytoplasmic	3198002C
209 BI	CD11b	ICRF44	Surface	3209003B

2.19 Statistical Analysis

Statistical analyses were performed using GraphPad Prism 9 or 10. For preclinial studies, statistical significance between two treatment groups were measured using unpaired t-test, and differences in three or more treatment groups using one-way ANOVA or two-way ANOVA with multiple comparisons. For WINGMEN trial sample analyses, statistical significance between two treatment groups were assessed using paired t-test. P values of <0.05 were deemed statistically significant.

3

In vitro and *in vivo* effects of IGF blockade in prostate cancer

Contents

3.1 Introduction 71
3.2 *In vitro* effects of IGF blockade in prostate cancer 73
3.2.1 Assessing effects of IGF blockade in cell signalling 74
3.2.2 Investigating effects of IGF blockade on 2D viability and cell survival 74
3.2.3 Effects of IGF blockade on 3D growth of cells 77
3.3 Investigating IGF blockade in prostate cancer *in vivo* . . 79
3.3.1 Study design and tumour growth 79
3.3.2 Staining of IGF-1R-related markers and immune markers in tumours 79
3.3.3 Transcriptomic profiling of tumours 83
3.4 Effects of IGF blockade in response to PD-1 immunotherapy *in vivo* : pilot study 85
3.4.1 Assessment of tumour growth and morphology 85
3.4.2 Immunohistochemical analysis for markers of IGF-1R signalling and immune cells 85
3.4.3 Transcriptomic profiling of tumours 93
3.5 Investigating the effects of IGF axis and PD-1/PD-L1 axis blockade in prostate cancer: repeat experiment 104
3.5.1 Rationale and tumour growth 104
3.5.2 Immunohistochemical analysis of tumour tissues 107
3.5.3 Flow cytometric analysis of tumours 111
3.5.4 Transcriptomic profiling of tumours 113
3.6 Discussion 116

3.1 Introduction

Effects of IGFs on tumorigenesis, as described in Chapter 1.3.2, prompted therapies targeting IGF axis. IGF axis targeted therapies include anti-IGF-1R mAbs, IGF-1R

tyrosine kinase inhibitors (TKIs), and IGF-1/-2 blocking mAbs.

Anti-IGF-1R mAbs block IGF-1/2 binding to IGF-1R, inducing receptor internalisation and degradation (Cohen et al., 2005). Many IGF-1R targeting mAbs, such as ganitumab (Beltran et al., 2009; Fahrenholtz et al., 2013), figititumab (Cohen et al., 2005; Zhang et al., 2014), and R-1507 (Haluska et al., 2007; Kurzrock et al., 2010) were developed and showed promising preclinical results, but these agents can induce downregulation of IR and hybrid receptors leading to hyperglycaemia, or off-target effects on receptor activation (Sachdev et al., 2006; Cao et al., 2008; Osher et al., 2019). Several combination therapies with ganitumab were tried on patients with Ewing sarcoma, but phase II/III trials showed no clear clinical benefits (Beltran et al., 2011; Shulman et al., 2023; DuBois et al., 2023). One exception is tepromumab, which resulted in better clinical outcome for patients with thyroid-associated ophthalmopathy (TAO), and was approved by the US Food and Drug Administration (FDA) (Smith et al., 2017; Douglas et al., 2020; Fernando et al., 2021).

Small molecule TKIs inhibit RTKs, and although they were originally developed to target IGF-1R, its structural similarity with IR suggests that they can inhibit both (Ullrich et al., 1986; Wang et al., 2023). Despirate encouraging preclinical and phase I studies of linsitinib (Jones et al., 2015; Puzanov et al., 2015) and BMS-754807 (Carboni et al., 2009; Desai et al., 2010), further trials have been disappointing due to IR blockade that leads to hyperglycaemia and hyperinsulinemia (Garcia et al., 2013; Fassnacht et al., 2015; Macaulay et al., 2016; Oza et al., 2018). In contrast, AXL1717 and INSM-18 are non-ATP competitive TKIs that only inhibit IGF-1R, but clinical trials resulted in limited success (Ekman et al., 2016; Aiken et al., 2017; Bergqvist et al., 2017; Ryan et al., 2008; Friedlander et al., 2012).

IGF-1/-2 blocking mAbs target the IGF-1 and IGF-2 ligands, preventing the ligand-receptor interactions, in the form of IGF-ligand TRAPs and IGF neutralising antibodies. IGF-TRAP is an engineered molecule with IGF-1R extracellular domain fused to the Fc region of the human IgG_1 (Wang et al., 2015). Although IGF-TRAP shows promising anti-tumour effects in preclinical models of aggressive cancers, they have not been tested

in clinical trials yet (Vaniotis et al., 2018; Hashimoto et al., 2021; Chen et al., 2023c; Chen et al., 2020). Two IGF neutralising antibodies have been used in clinical trials. Dusigitumab, which binds IGF-2 with higher affinity, showed favorable preclinical and early phase trial results but was discontinued upon phase Ib/II trial that did not show clinical benefits (NCT01446159)(Gao et al., 2011; Haluska et al., 2014). Xentuzumab binds IGF-1 with higher affinity and cross-reacts with murine IGFs (Friedbichler et al., 2014; Mireuta et al., 2014; Rieunier et al., 2021). Although it showed favorable clinical benefits in early trials, no apparent clinical benefits in further trials led to discontinuation for most trials (de Bono et al., 2020a; Park et al., 2021; Schmid et al., 2023; Macaulay et al., 2023). The most recent and the first windows trial with xentuzumab as a single agent is the WINGMEN trial led by our group (NCT05110495) (Chapter 5).

Although several preclinical studies have been done to identify effcts of xentuzumab in colorectal, breast, and prostate cancers *in vitro* and *in vivo* (Rieunier et al., 2021; Weyer-Czernilofsky et al., 2020), the studies were done on human prostate cancers and in xenograft model, which does not take into account the immune microenvironment of cancers. To better understand and characterise the biology of IGF blockade, we tested how xentuzumab affects prostate cancer cells *in vitro* and *in vivo*, alone and in combination with anti-PD-1 immunotherapy in an allograft model. This would help elucidate effects of xentuzumab in prostate cancer as well as its consequences in TIME and generate comparable data types to WINGMEN clinical trial.

3.2 *In vitro* effects of IGF blockade in prostate cancer

Previous work from our group and others showed that IGF-1 activates IGF-1R and downstream signalling via AKT and ERK, increasing cellular proliferation and survival (Rochester et al., 2005, Ge et al., 2000). IGF neutralising antibody xentuzumab (Friedbichler et al., 2014) was tested to check whether blocking IGFs reduces IGF-1R phosphorylation and subsequent signalling pathway as well as cell growth and survival *in vitro*. Xentuzumab concentration was chosen based on information from

Boehringer Ingelheim that the steady state level of xentuzumab in patients treated at the recommended Phase 2 dose was ∼1.3 μM, which also concurs with concentrations used in previous publications *in vitro* (Weyer-Czernilofsky et al., 2020; Rieunier et al., 2021; Wu et al., 2021).

3.2.1 Assessing effects of IGF blockade in cell signalling

To assess the effects of IGF axis activation and inhibition on phosphorylation of proteins downstream of the IGF-1R *in vitro*, murine prostate cancer cells, PTEN-wildtype (WT) Myc-CaP and PTEN-null PTEN-CaP8, were treated with 50 nM IGF-1 and/or varying doses of xentuzumab as previously described (Chapter 2.2.1) and lysed before preparing for western blot (Figure 3.1). The dose of IGF-1 (380 ng/mL) was decided based on previous publications (Rieunier et al., 2021; Wu et al., 2021) and within the physiologic levels of IGF-1 in plasma (150 - 400 ng/mL).

Western blot analysis showed that IGF-1 induced significant IGF-1R and AKT activation, but xentuzumab treatment induced significant concentration-dependent inhibition of IGF-1R and AKT phosphorylation (Figure 3.1a). PTEN-CaP8 was less sensitive to the effect than Myc-CaP. ERK phosphorylation, however, was inhibited only in Myc-CaP but not in PTEN-CaP8 and was quantified in Figure 3.1b-c.

3.2.2 Investigating effects of IGF blockade on 2D viability and cell survival

To investigate whether IGF axis blockade affects viability of prostate cancer cells, 2D viability was assessed in murine prostate cancer cells treated with xentuzumab in serum-containing media.

Viability assay showed concentration-dependent inhibition of growth in Myc-CaP cells but not in PTEN-CaP8 cells (Figure 3.2a). In Myc-CaP, decrease in relative viability was comparable to the degree of IGF-1R inhibition in western blot (Figure 3.1b), where 10 nM xentuzumab treatment led to about 50% reduction in both IGF-1R phosphorylation and cell viability. In 2D, colony formation and survival was tested by

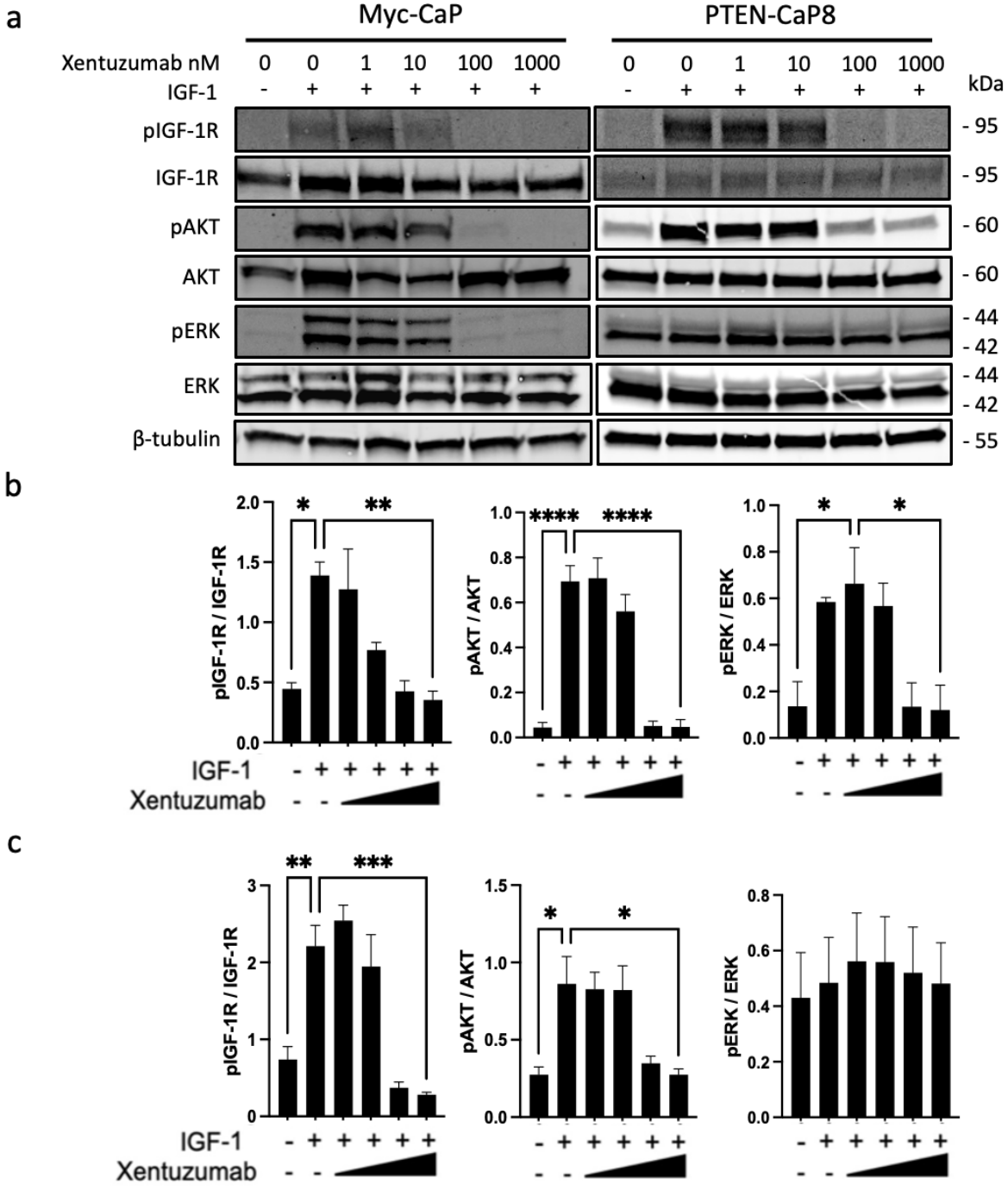


Figure 3.1: Response of murine prostate cancer cells to IGF neutralising antibody xentuzumab. Serum-starved Myc-CaP and PTEN-CaP8 cells were treated with PBS control or xentuzumab for 16 hours and with 50 nM IGF-1 for the final 20 minutes. **a**. The cells were lysed, and proteins involved in IGF-1R signalling pathway were measured using western blot (n=3 independent repeats per cell line) Phosphorylated IGF-1R, AKT, and ERK levels of **b**. Myc-CaP and **c**. PTEN-CaP8 were quantified after normalising to the loading control β-tubulin using Fiji ImageJ. (Graphs show mean ± SEM, *p<0.05, **p<0.01, ***p<0.001, ****p<0.0001, one-way ANOVA with multiple comparisons)

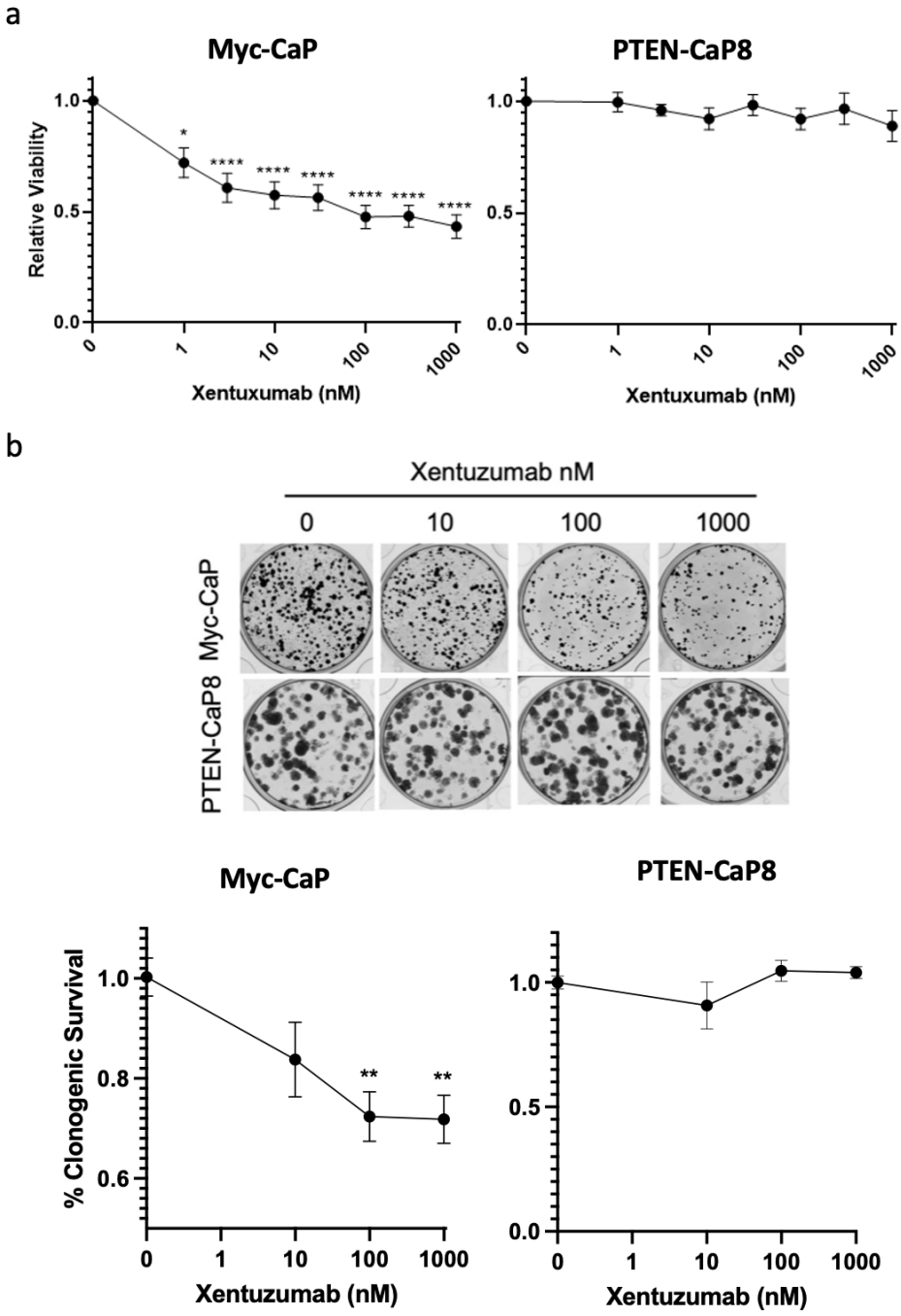


Figure 3.2: Effects of IGF blockade on 2D growth and survival of murine prostate cancer cells. a. Myc-CaP and PTEN-CaP8 cells were seeded in 96-well plates, treated with PBS control or 1 μM xentuzumab, and CellTiter Blue viability test was performed after 5 days (n=3 independent repeats per cell line). **b**. Myc-CaP and PTEN-CaP8 cells were seeded in 6-well plates and treated with PBS or xentuzumab. After 8-10 days, colonies of more than 50 cells were imaged and counted using GelCount. Upper: Representative images from n=3 independent assays in each cell line. Lower: pooled data. (Graphs show mean ± SEM, * $p<0.05$, ** $p<0.01$, *** $p<0.001$, **** $p<0.0001$, one-way ANOVA with multiple comparisons).

clonogenic assay, where it was significantly reduced upon 100 - 1,000 nM xentuzumab treatment in Myc-CaP, but there were no changes in PTEN-CaP8 (Figure 3.2b).

3.2.3 Effects of IGF blockade on 3D growth of cells

Effects of IGF axis inhibition on 3D growth was assessed using spheroid assay. This was important since 3D growth *in vitro* requires anchorage-independent growth, also required for *in vivo* tumorigenesis. The effects of IGF axis manipulation are reported to be more important for 3D than 2D growth (Resnicoff et al., 1994). Myc-CaP spheroid growth was suppressed upon xentuzumab treatment, evident from both spheroid size and viability, whereas PTEN-CaP8 spheroids were unaffected and showed lower spherogenic potential than Myc-CaP (Figure 3.3a-b). Relative 3D viability was also measured using CellTiterGlo 3D assay, which was significantly reduced in Myc-CaP (Figure 3.3c). Again, level of suppression mirrored western blot (Figure 3.1b) and 2D viability assay (Figure 3.2a), where 10 nM xentuzumab treatment resulted in about 50% reduction in 3D growth of Myc-CaP.

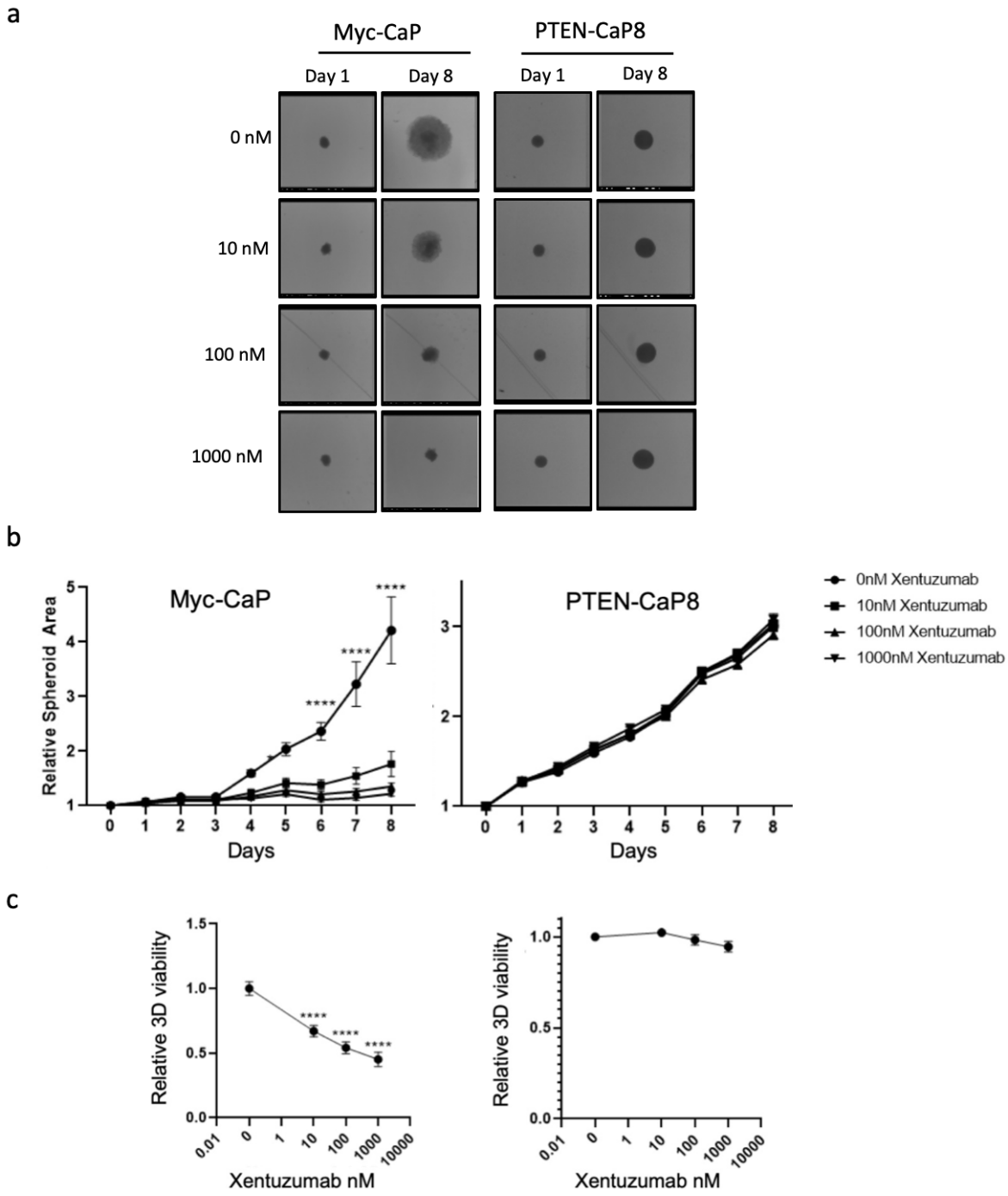


Figure 3.3: Effects of IGF blockade on 3D spheroid growth in murine prostate cancer cells. Cells were seeded in ultra-low attachment 96-well plates. After 3 days to allow spheroid formation, the spheroids were treated with either PBS or 1 μM xentuzumab, and the images were taken daily for 8 days using GelCount. **a**. Representative Myc-CaP and PTEN-CaP8 spheroid images for each condition on day 1 and 8 (n=3 independent assays/cell line). **b**. Graphs represent spheroid area relative to day 1, pooled from 3 assays. **c**. On day 8, CellTiterGlo 3D assay was performed (Graphs show mean ± SEM, **** $p<0.0001$, one-way ANOVA with multiple comparisons).

3.3 Investigating IGF blockade in prostate cancer *in vivo*

The *in vitro* assays showed that xentuzumab was ineffective in PTEN-null model. These results and the fact that PTEN mutation occurs in only 15% of primary cancers (Abeshouse et al., 2015) prompted us to focus on the PTEN-WT Myc-CaP model for the subsequent *in vivo* study.

3.3.1 Study design and tumour growth

To test the effects of IGF inhibition *in vivo*, 7 - 8 FVB mice were subcutaneously injected with syngeneic Myc-CaP cells and randomised into two treatment groups, PBS (control) or xentuzumab, as described in Chapter 2.5.2 (Figure 3.4a). Frequency of xentuzumab dose was advised by Boehringer Ingelheim (Friedbichler et al., 2014; Mireuta et al., 2014).

Although there were no significant tumour growth inhibition (Figure 3.4b), we aimed to investigate any tumour-intrinsic or immune effects of IGF blockade, so tumours were collected for IHC and bulk RNA sequencing at the endpoint of the study.

3.3.2 Staining of IGF-1R-related markers and immune markers in tumours

FFPE tumour sections were stained for IGF-axis markers, immune markers, and proliferation and vascular markers, focusing on T-cell infiltration as originally planned for the project (Figure 3.5). The scanned images were quantified by HALO platform, and the levels of staining were represented as % positive stainings of the markers.

To assess the degree of IGF blockade by xentuzumab, the tissues were stained with phospho-IGF-1R and further downstream marker phospho-S6 (Figure 1.1). Although AKT is closer to the receptor than S6 and may have been consistent with previous *in vitro* studies (Figure 3.1), the antibody could not be optimised to show a clear activation status. Xentuzumab inhibited IGF-1R phosphorylation but not phospho-S6 in Myc-CaP tumours. Of note, xentuzumab significantly suppressed CD4+ T cell infiltration,

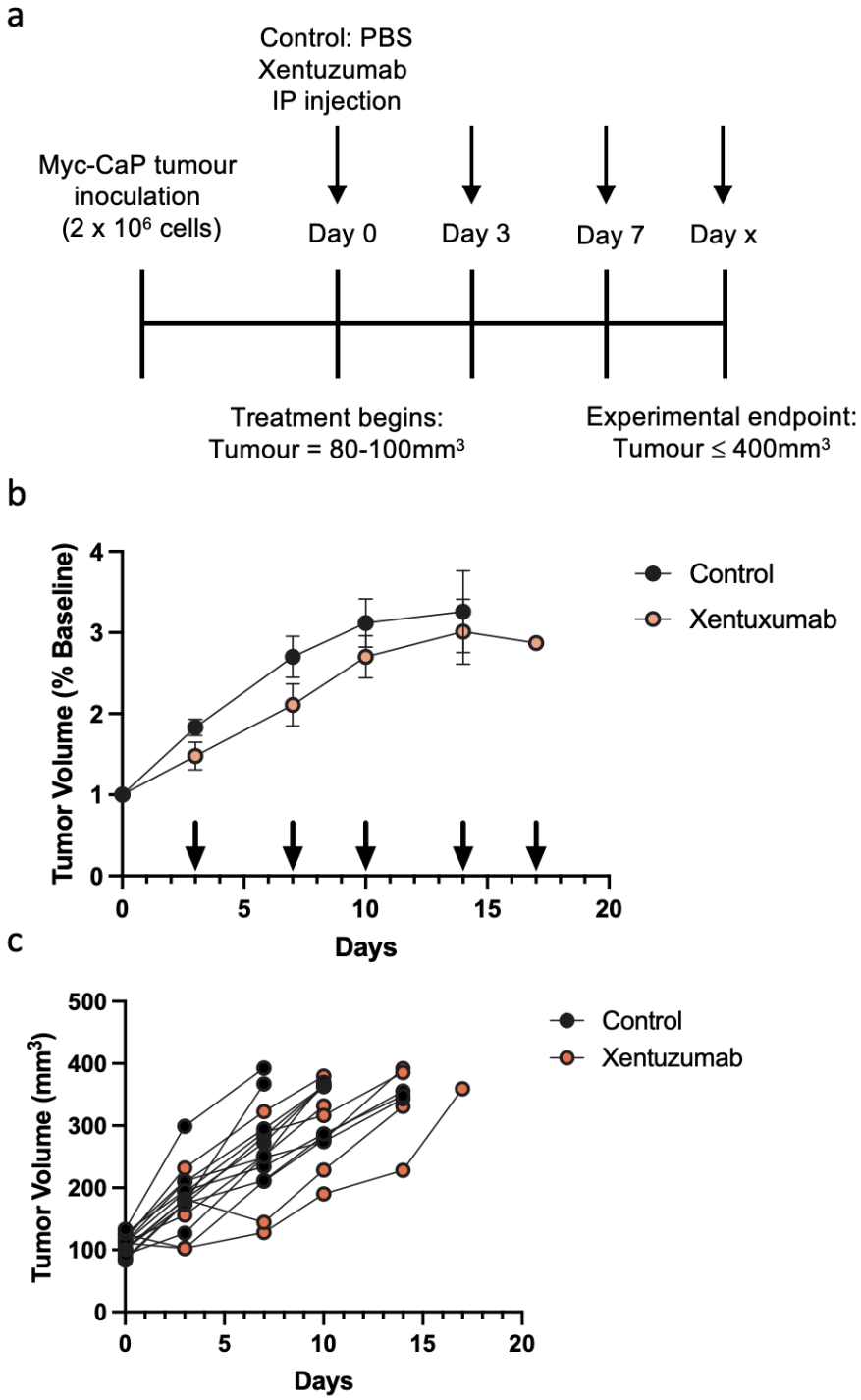


Figure 3.4: Investigating the effects of IGF blockade in vivo. a. Schematic of the experiment in which 2 million Myc-CaP cells were inoculated subcutaneously in the right flank of syngeneic FVB mice. Once tumour size reached 100 mm^3, animals were intraperitoneally injected with PBS (control) or xentuzumab (xent) twice weekly until tumour size reached 400 mm^3. Numbers of tumours collected at the endpoint per group were: control, n = 8 and xentuzumab, n = 7. **b**. % tumour growth over time. Graph represents mean ± SEM of independent mice that reached the endpoints, t-test. Arrows represent treatments given. **c**. Tumour volume of each mice during the experiment.

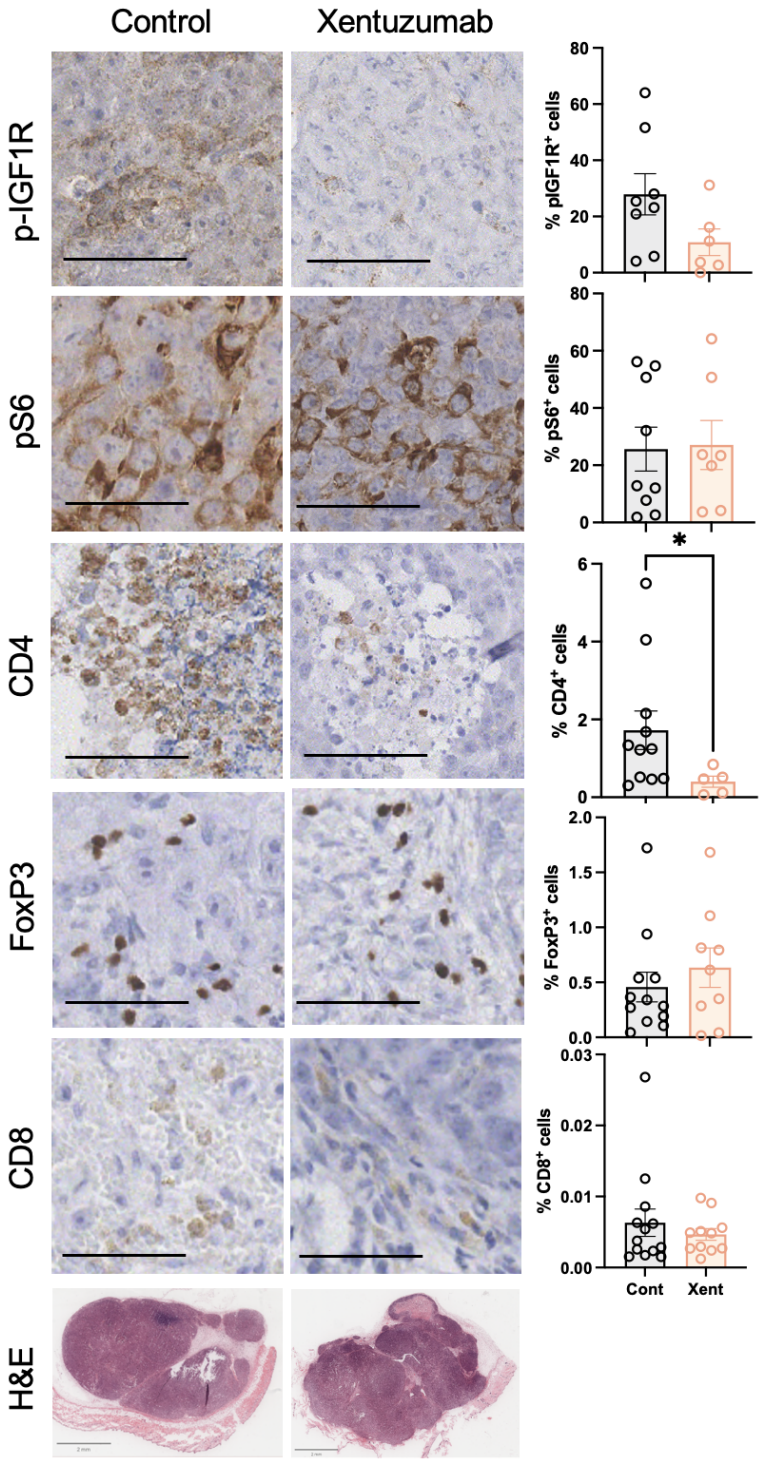


Figure 3.5: IHC staining of IGF-1R and immune-related markers in murine Myc-CaP tumours. At least 3 tumours/group were formalin-fixed and paraffin-embedded and cut into 4 μm sections. Levels of phospho-IGF1R, phospho-S6, CD4, FoxP3, and CD8 were detected by immunohistochemical staining. Images: representative IHC and haematoxylin and eosin (H&E) images, scale bar: 50 μm. H-scores were analysed by HALO software. Data are presented as mean ± SEM from at least three independent animals (*p<0.05, unpaired t-test).

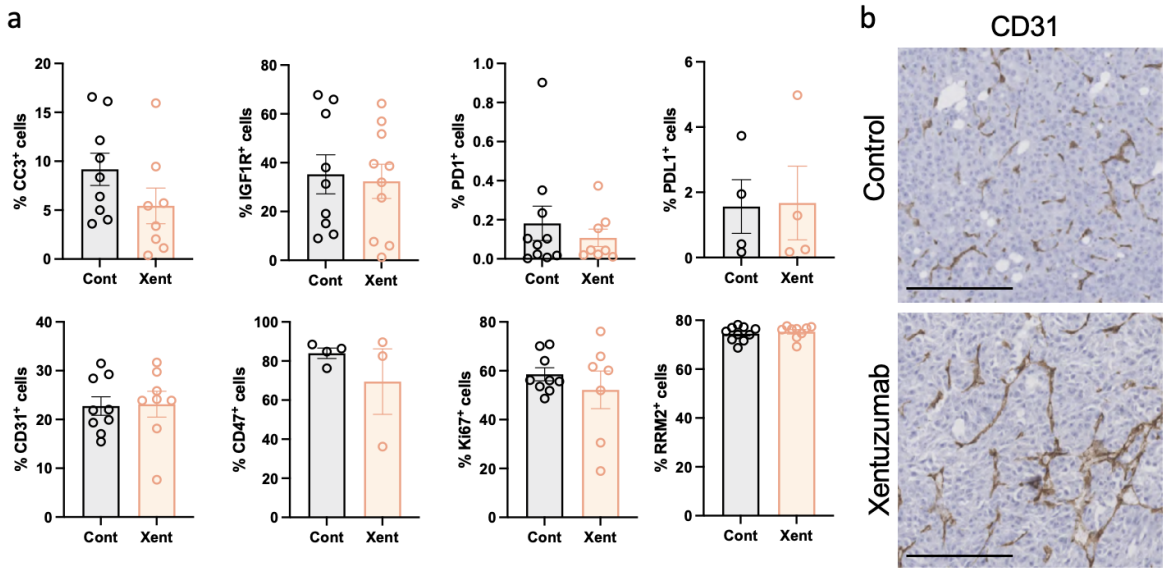


Figure 3.6: IHC staining results in murine Myc-CaP tumours. a. Graphs represent mean ± SEM quantification of IHC stainings using various markers that were not significantly different between the two groups. Each treatment group had tumours from at least 3 independent mice. **b**. CD31 expression was detected by immunohistochemical staining, scale bar: 100 μm.

and there was no difference in FoxP3 staining, suggesting that this could represent a reduction in conventional CD4+ helper T cells (Figure 3.5). There were no significant changes in markers of IGF-1R, proliferation (Ki67), apoptosis (cleaved caspase 3, CC3), vasculature (CD31), phagocytosis checkpoint (CD47), DNA replication (RRM2), and immune checkpoints PD-L1 and PD-1 (Figure 3.6a). Despite no difference in expression, xentuzumab-treated tumours showed more mature vascularisation, compared to punctate patterns in pre-treatment tumours (Figure 3.6b).

3.3.3 Transcriptomic profiling of tumours

RNA was extracted from snap frozen tumours and processed for 3' RNA sequencing at CHG, University of Oxford. Sequencing reads were analysed as in Chapter 2.7.3, and DESeq2 pipeline was used to identify differentially expressed genes (DEGs) in xentuzumab-treated Myc-CaP tumours versus (vs) controls. There were 40 upregulated and 46 downregulated DEGs (Figure 3.7a-b), with the full list in Table 7.2.

Of note and in contrast with protein markers, *Igf1r* and *Mki67*, which encodes proliferation marker Ki67, were downregulated by xentuzumab, and both genes were validated by qRT-PCR (Figure 3.7c-d). There were too few deregulated genes for meaningful pathway enrichment analysis.

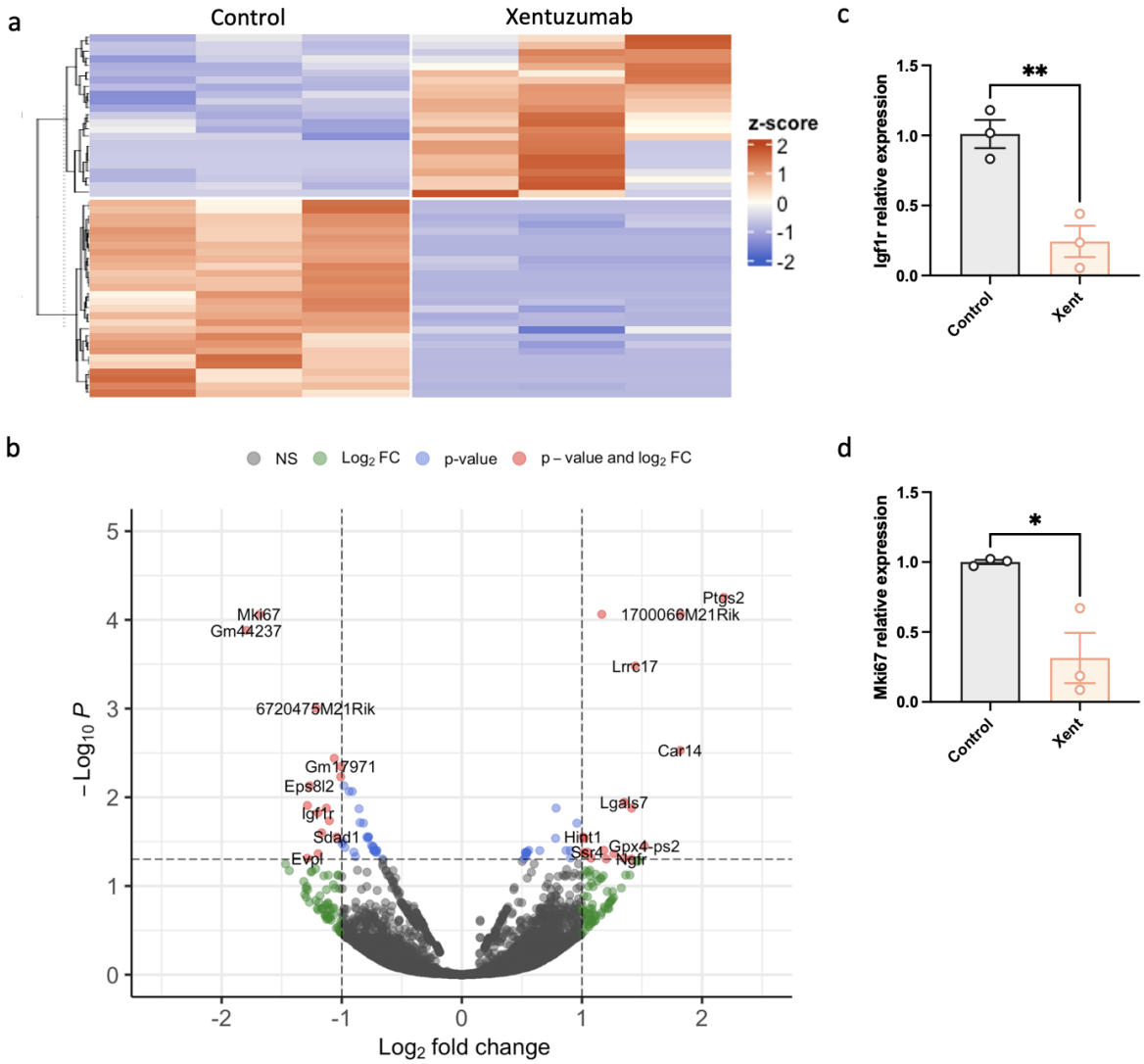


Figure 3.7: 3' RNA sequencing analysis of xentuzumab vs control-treated tumours. RNAs were extracted from fresh frozen tumours and sequenced using NextSeq platform. The reads were quality-checked and quantified, and differentially expressed genes (DEGs) were analysed using DESeq2 package on R studio. **a**. Heatmap of the deregulated genes in xentuzumab vs control-treated tumours using the Pheatmap package on R studio. **b**. Volcano plot of the DEGs (red) with adjusted p-value <0.05 and -log 10 adjusted p-value >1.3 using the EnhancedVolcano package on R studio. For validation, RNA was extracted from fresh frozen tumours, and **c**. Igf1r and **d**. Mki67 mRNA expression was measured using qRT-PCR (n=3 independent mice)

3.4 Effects of IGF blockade in response to PD-1 immunotherapy *in vivo* : pilot study

3.4.1 Assessment of tumour growth and morphology

In light of Ajona et al., 2020 that showed synergistic effects of IGF axis and PD-1 blockade in reducing non-small cell lung cancer tumour growth and boosting immune cell effects in the tumours *in vivo*, effects of combined inhibition of IGF-1 and PD-1 were tested in prostate cancer model. Myc-CaP cells were subcutaneously injected into 5-6 FVB mice and randomly treated with PBS and isotype control (Control), PBS and anti-PD1 (aPD1), Xentuzumab and isotype control (Xent), and xentuzumab and anti-PD1 (Xent+aPD1) as described in Chapter 2.5.3 (Figure 3.8a). Two treatments were given 2 hours apart on the same day with PBS/xentuzumab given before the IgG/anti-PD1, as suggested by Boehringer Ingelheim.

There was no tumour growth inhibition (Figure 3.8b), but the tumours of the control and the combination group looked and felt different, where tumours from the control group were firm whereas the combination-treated tumours were soft and bloody (Figure 3.8c). Combination-treated tumours also contained fluid sac that burst when the tumours were cut, which indicates that tumour growth difference may have been over-estimated. The tumours and spleen were collected for IHC and bulk RNA sequencing.

3.4.2 Immunohistochemical analysis for markers of IGF-1R signalling and immune cells

Immunohistochemical staining on the FFPE tumours showed insignificant reduction in IGF-1R phosphorylation upon xentuzumab treatment, which was further downregulated with combined IGF-1 and PD-1 blockade. S6 phosphorylation was increased with xentuzumab treatment, similar trend to previous in vivo experiment comparing IGF-treated tumours with control (Figure 3.5). There was no significant difference in CD4+ T cell or FoxP3+ Treg infiltration, but CD8+ T cell numbers were increased upon combined treatment of xentuzumab and anti-PD-1 (Figure 3.9). There were no significant changes in CC3 (apoptosis), IGF-1R, PD-1 and PD-L1 (immune checkpoints), CD31

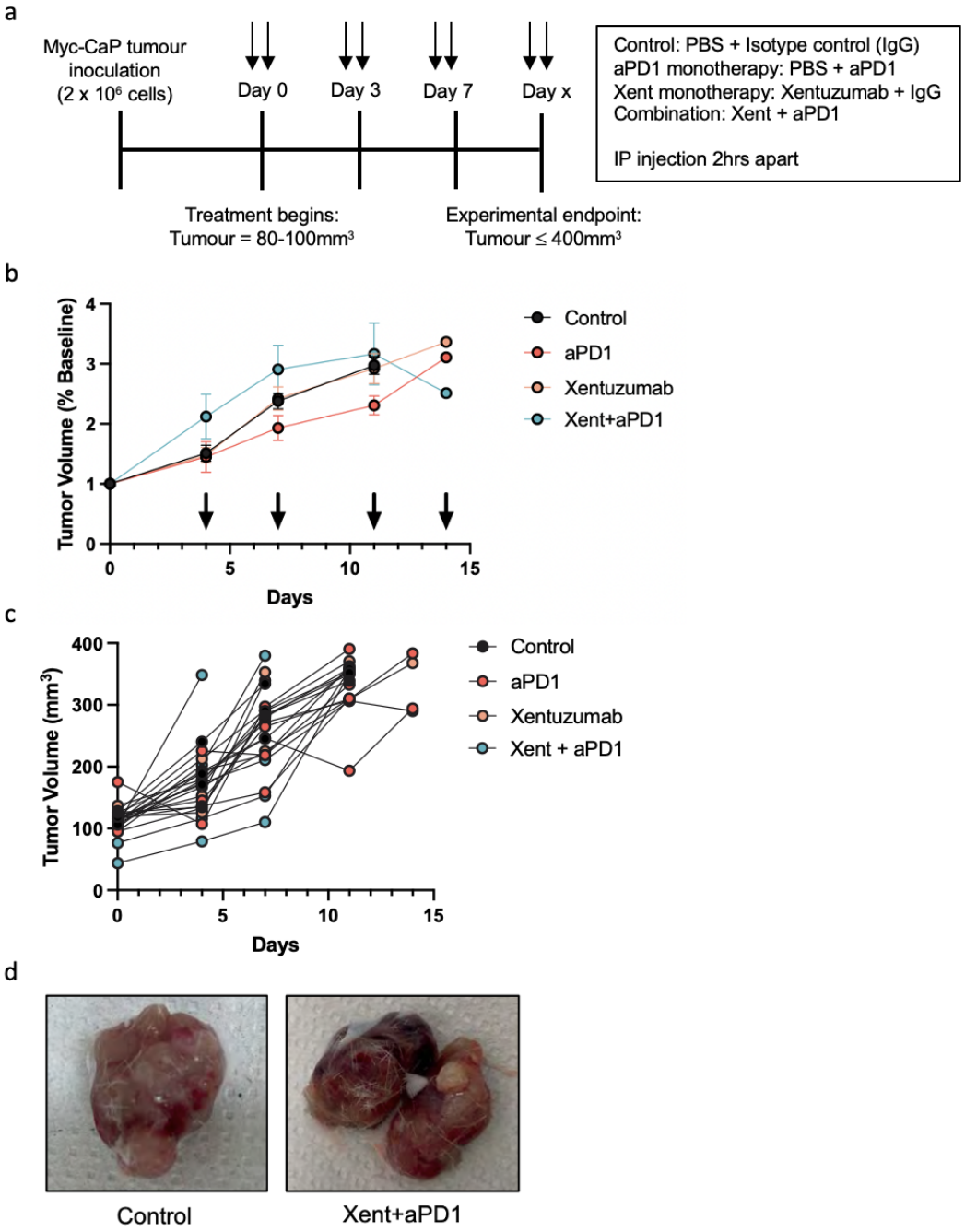


Figure 3.8: Investigating the effects of IGF and PD-1 blockade in vivo. a. Schematic of the experiment in which 2 million Myc-CaP cells were inoculated subcutaneously in the right flank of syngeneic FVB mice. Once tumour size reached 100 mm^3, animals were intraperitoneally injected with 100 mg/kg PBS + 10 mg/kg isotype matched IgG (control), 100 mg/kg PBS + 10 mg/kg anti-PD1 (aPD1), 100 mg/kg xentuzumab + 10 mg/kg IgG (xentuzumab), or 100 mg/kg xentuzumab + 10 mg/kg anti-PD1 (Xent+aPD1) twice weekly. Numbers of tumours collected at the endpoint per group were: control, n = 5, aPD1, n = 5, xentuzumab, n = 6, and Xent+aPD1, n = 6. **b**. % tumour growth over time. Graph represents mean ± SEM of independent mice that reached the endpoints, arrows represent treatments days. **c**. Tumour volume of each mice throughout the experiment. **d**. Images of the control and xent + aPD1-treated tumours.

(vasculature), CD47 (tumour cell phagocytosis), Ki67 (proliferation), and RRM2 (DNA damage) expression across all treatment groups (Figure 3.10).

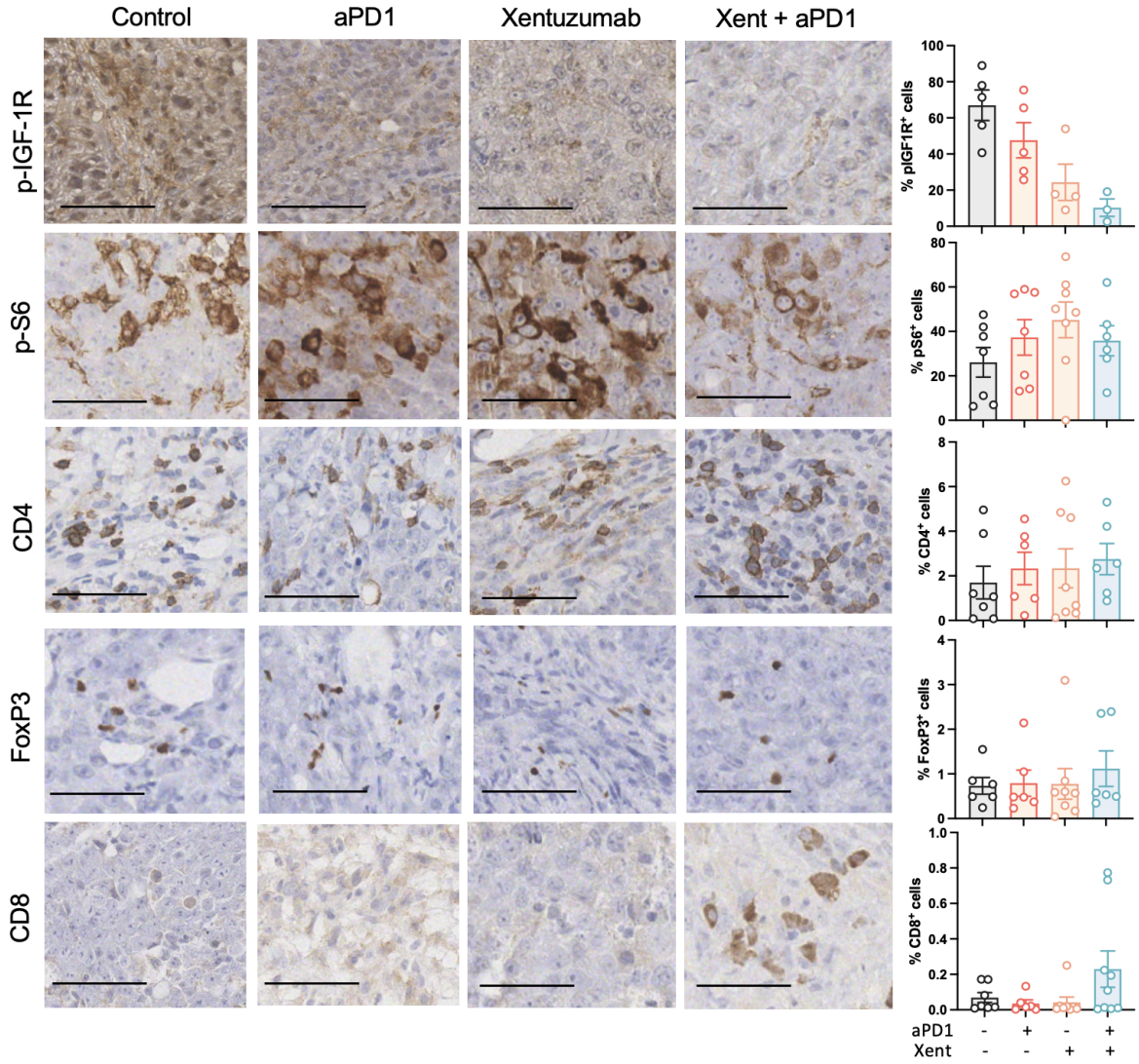


Figure 3.9: Effects of IGF-1 and PD-1 blockade pilot experiment on IGF-1R and T-cell markers in murine Myc-CaP tumours. At least 5 formalin-fixed and paraffin-embedded tumours/group were cut into 4 μm sections, and phospho-IGF1R, phospho-S6, CD4, FoxP3, and CD8 expressions were detected by immunohistochemistry (IHC) and analysed by HALO software. Images: representative IHC images, scale bar: 50 μm. Data are presented as the mean $\pm$ SEM from at least five independent animals (one-way ANOVA with multiple comparisons)

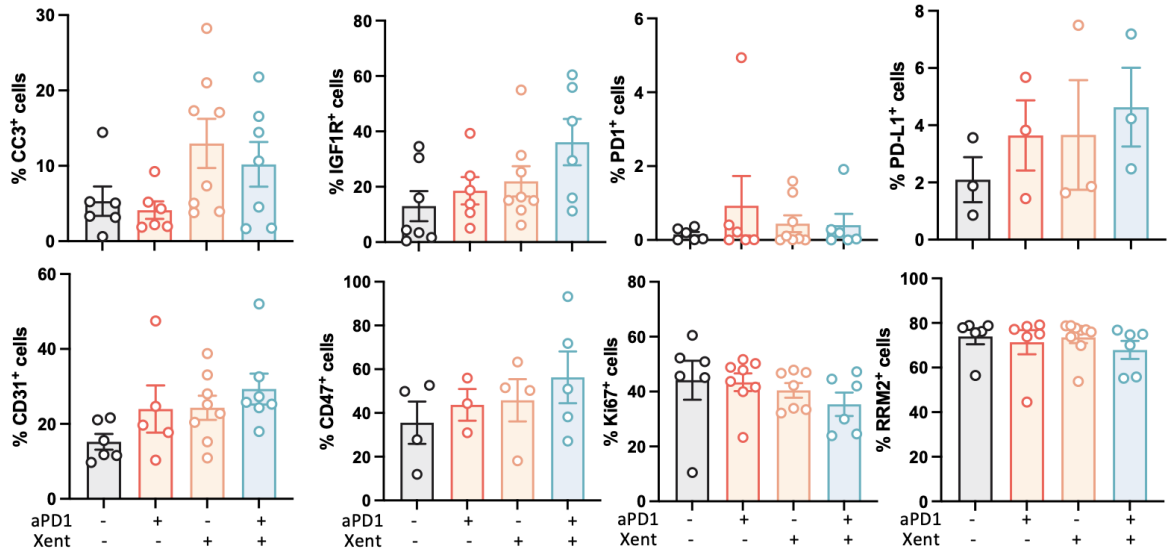


Figure 3.10: Effects of IGF-1 and PD-1 blockade pilot experiment on expression of various markers in murine Myc-CaP tumours. Boxplots showing CC3, IGF-1R, PD-1, PD-L1, CD31, CD47, Ki67, and RRM2 stainings detected by immunohistochemistry. All changes were not significant.

We then looked at the tissue morphology in detail using H&E staining. These tumours showed a higher percentage of necrosis in tumours treated with anti-PD-1 and xentuzumab, compared with any other groups (Figure 3.11), which may be the reason for different texure of the tumours in combination treatment vs control (Figure 3.8c). Programmed necrosis, also known as necroptosis, results in the swelling of organs and cells (Berghe et al., 2014), which may explain no difference in tumour volume. Although there were changes in T cell infiltration, the presence of necrosis is not typical of T cell-induced cell death (Snyder et al., 2019; Li et al., 2022a). This led us to focus on the innate immune population, specifically macrophages due to it being one of the most prevalent populations in prostate cancer TIME (Dai et al., 2017; Larionova et al., 2020; Siefert et al., 2021).

We then went back to previous *in vivo* experiment (Chapter 3.3) and stained the tumours with macrophage markers. There was no difference in myeloid-specific marker CD68, but pan-macrophage marker F4/80 was significantly increased in xentuzumab-treated tumours compared to control. Interestingly, both pro-inflammatory M1-like macrophage

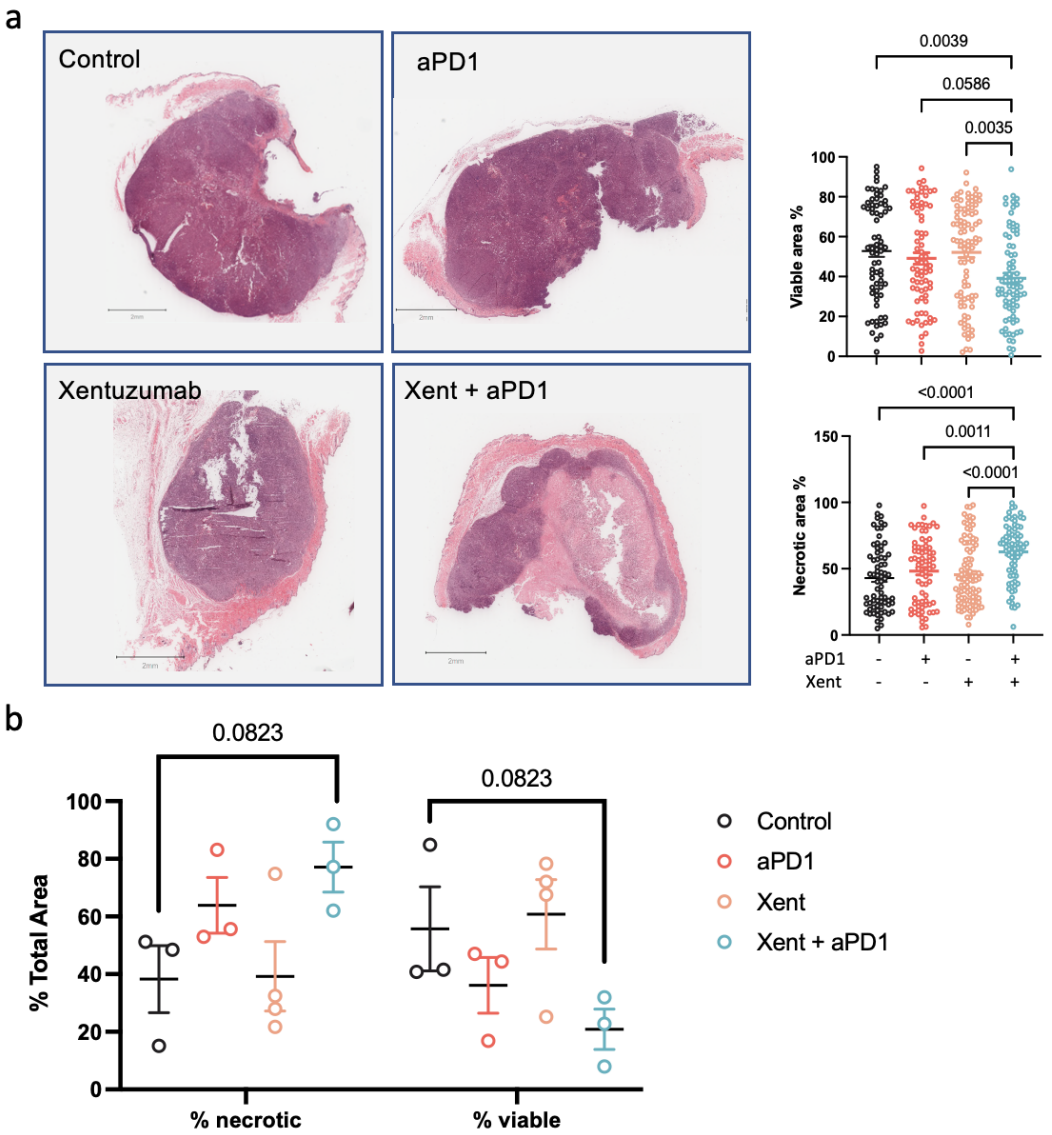


Figure 3.11: Haematoxylin and eosin (H&E) staining of the pilot experiment tumours. a. H&E staining of the tumours (scale bar = 2 mm) Graphs: the viable and necrotic area of all slides stained for immunohistohemistry were analysed for % viable and necrotic area on the HALO platform (n = 71-92 sections from 5-6 tumours per group), and the results were pooled and graphed (one-way ANOVA with multiple comparisons). **b**. The section with the biggest area was chosen per mouse, and its % viable and necrotic area were graphed. (*p<0.05, two-way ANOVA with multiple comparisons)

marker iNOS and anti-inflammatory M2-like marker CD163 were significantly decreased in xentuzumab-treated tumours (Figure 3.12).

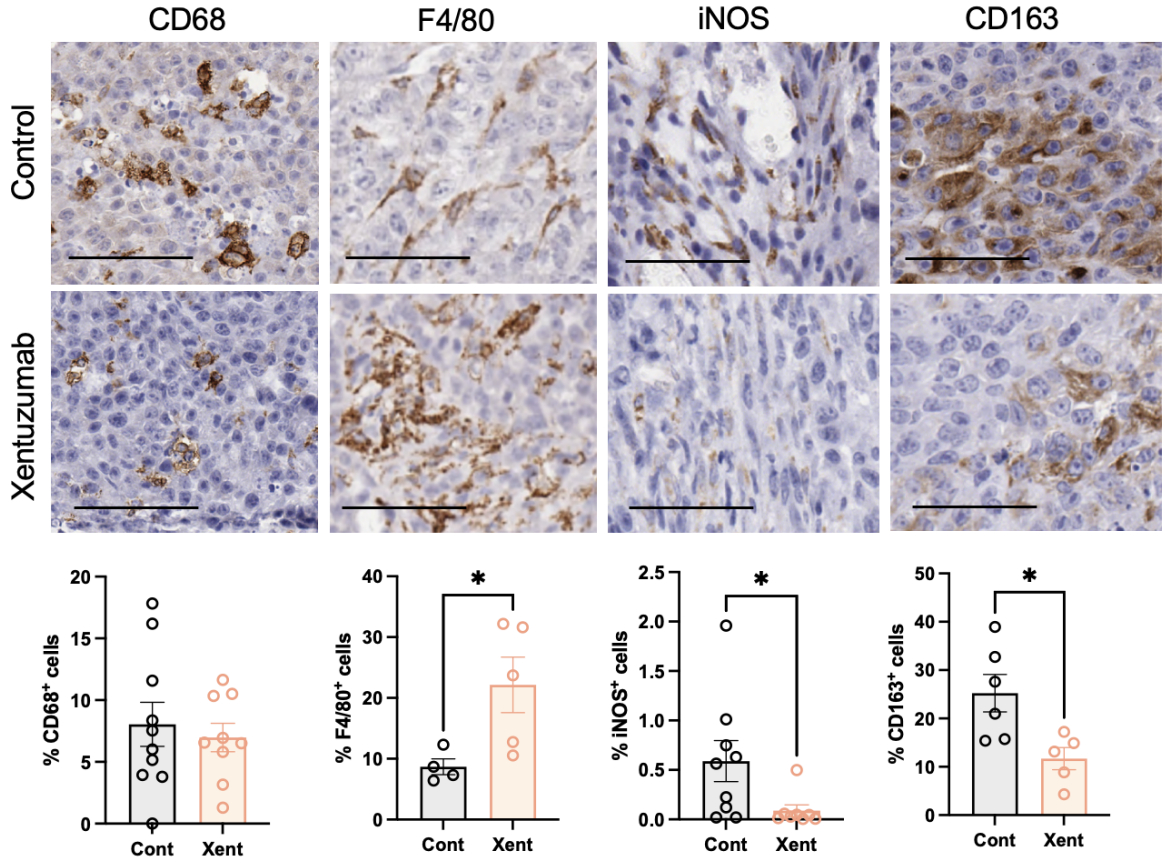


Figure 3.12: Immunohistochemical staining for macrophage markers in murine prostate tumours treated with xentuzumab. CD68, F4/80, iNOS, and CD163 expressions were determined by immunohistochemistry in mouse tumours treated with PBS control or xentzumab. Images: representative IHC images, scale bar: 50 μm. Data are presented as the mean ± SEM from at least three independent animals (*p<0.05, unpaired t-test).

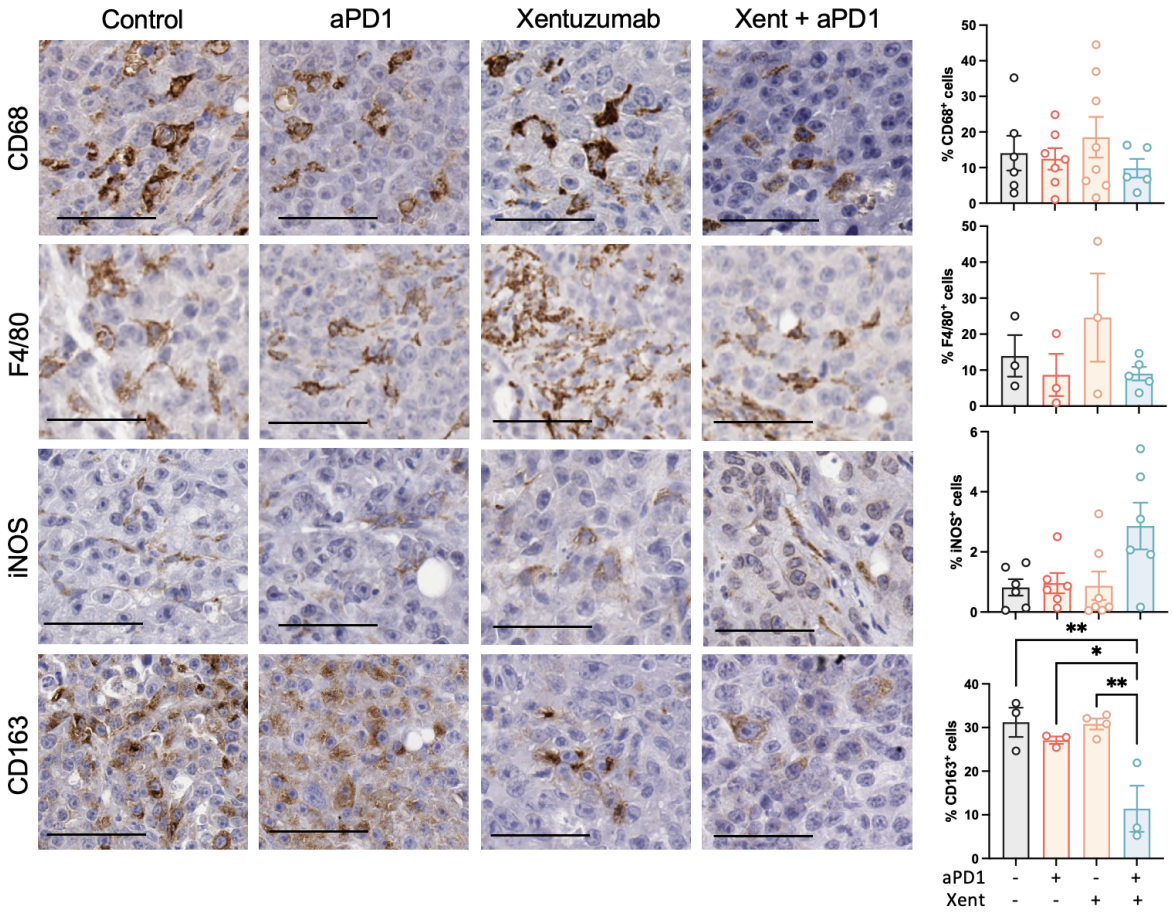


Figure 3.13: Effects of IGF and PD-1 blockade pilot experimenton macrophage marker expression in Myc-CaP allografts. Representative images of control and anti-PD1 and/or xentuzumab-treated tumours stained with CD68, F4/80, iNOS, and CD163, scale bar: 50 μm. Data are presented as the mean ± SEM from at least three independent animals (*p<0.05, **p<0.01, one-way ANOVA with multiple comparisons).

IHC for macrophage markers in anti-PD1 and/or xentuzumab-treated tumours showed no difference in CD68 positivity. There was an increasing trend of iNOS and significant decrease of CD163 in combination-treated tumours (Figure 3.13), suggesting more pro-inflammatory macrophages and less anti-inflammatory macrophages infiltration in the TIME.

These changes in macrophage population in both *in vivo* experiments, especially the decrease in CD163+ M2-like macrophages suggest that xentuzumab + anti-PD1 treatments could cause anti-tumour effects in prostate cancer TIME.

3.4.3 Transcriptomic profiling of tumours

For transcriptomic profiling, RNAs extracted from snap frozen tumours were processed for 3' RNA sequencing at the CHG, University of Oxford. Sequencing reads were analysed as in Chapter 3.3.3, and DEGs were identified pairwise using DESeq2 package. The comparisons made were combination treatment vs control, combination treatment vs xentuzumab, and xentuzumab treatment vs control, to better identify genes responsible for certain pathways.

Xentuzumab-treated vs control tumours resulted in 38 DEGs (Figure 3.14), with the full list in Appendix (Table 7.4). Analysis showed upregulation of matrix metallopeptidase 12 (Mmp12), insulin receptor (Insr), and Igfbp3 in xentuzumab-treated tumours. Cd74 and C-C motif chemokine receptor 2 (Ccr2) were significantly downregulated.

Combination vs xentuzumab-treated tumours resulted in 101 DEGs (Figure 3.15), with the full list in Appendix (Table 7.5). Histocompatibility 2, class II antigen A (H2-Aa), Ccr2, Cd74, and autophagy-related 14 (Atg14) were upregulated and Vegfa downregulated. The fact that Ccr2 and Cd74 were downregulated in xentuzumab vs control comparison suggests that these genes were affected by anti-PD-1 treatment.

When comparing combination treatment to control, one of the samples from the combination group was a clear outlier according to the principal component analysis (PCA) plot (Figure 3.16a). Removing the outlier resulted in a better clustered plot

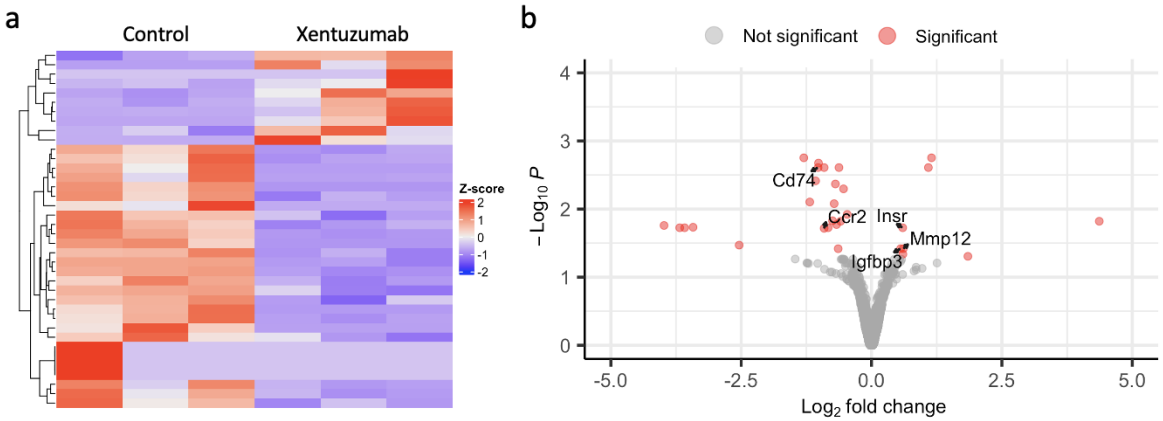


Figure 3.14: RNA sequencing analysis of Myc-CaP tumours treated with xentuzumab compared to control: pilot experiment. a. Heatmap showing normalised changes in the expression of all differentially expressed genes (DEGs) in xentuzumab vs control-treated groups. Z-scores are derived from variance stabilising formation (VST)-transformed counts. **b**. Volcano plot showing the DEGs (red) with adjusted p-value <0.05.

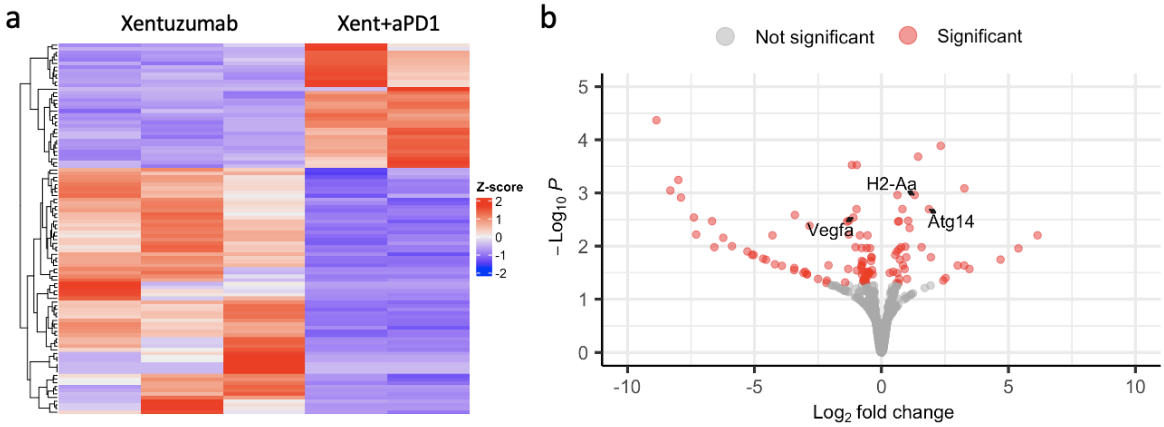


Figure 3.15: RNA sequencing analysis of Myc-CaP tumours treated with xentuzumab + anti-PD-1 compared to xentuzumab: pilot experiment. a. Heatmap showing normalised changes in the expression of all differentially expressed genes (DEGs) in xentuzumab + anti-PD-1 (Xent+aPD1) vs xentuzumab-treated groups. Z-scores are derived from variance stabilising formation (VST)-transformed counts. **b**. Volcano plot showing the DEGs (red) with adjusted p-value <0.05.

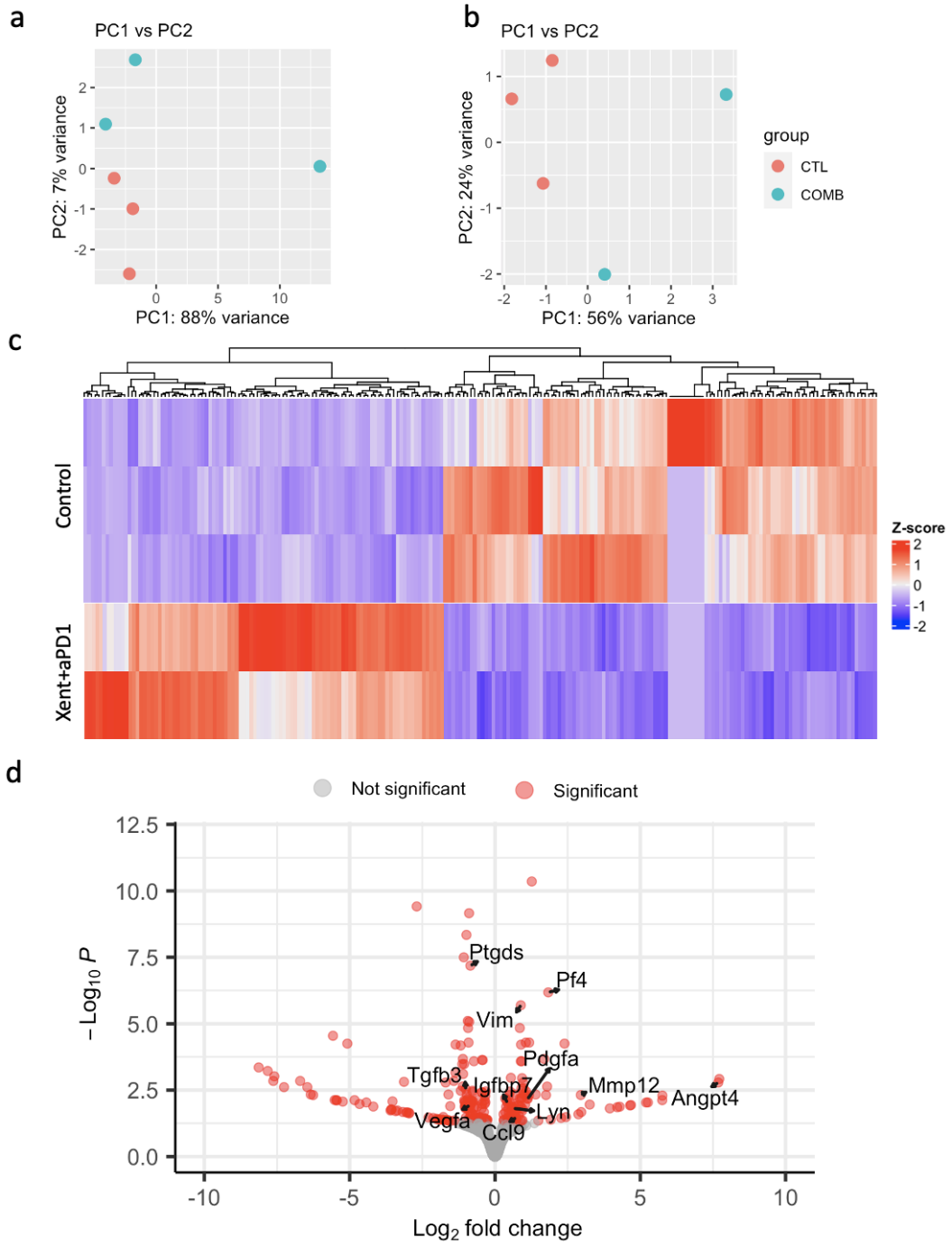


Figure 3.16: RNA sequencing analysis of Myc-CaP tumours treated with xentuzumab and anti-PD-1 compared to control: pilot experiment. a. PCA plot showing the clustering of tumours treated with xentuzumab + anti-PD-1 (blue, n=3) vs control (red, n=3). **b**. PCA plot after removing an outlier from the xentuzumab + anti-PD-1 treatment group. **c**. Heatmap showing normalised changes in the expression of all differentially expressed genes (DEGs) in combination vs control-treated groups. Z-scores are derived from variance stabilising formation (VST)-transformed counts. **d**. Volcano plot showing the DEGs (red) with adjusted p-value <0.05.

(Figure 3.16b), and further analysis identified 268 DEGs (Figure 3.16c), yielding the greatest number of DEGs among all comparisons (Table 7.3). The genes of interest were shown in volcano plot (Figure 3.16d), including upregulation of Igfbp7, Mmp12, and vimentin (Vim), and downregulation of Vegfa and transforming growth factor-beta 3 (Tgfb3). There were 6 overlapping genes between xentuzumab vs control and combination vs control, notably Mmp12 upregulation, suggesting that these genes are driven by xentuzumab. In addition, 7 genes, including Vegfa, overlapped when comparing combination vs xentuzumab and combination vs control, indicating its relation to PD-1 signalling.

Pathway enrichment analyses on these comparisons were performed using clusterProfiler package in R. Comparison of tumours treated with xentuzumab vs control yielded upregulation of pathways related to metabolism and downregulation of antigen processing and presentation-related pathways (Figure 3.17). Many immune pathways were enriched by both comparisons of xentuzumab + anti-PD-1-treated tumours versus control (Figure 3.18a) and tumours treated with xentuzumab + anti-PD-1 versus xentuzumab (Figure 3.18b), including response to transforming growth factor beta and regulation of myeloid leukocyte migration. We further analysed these pathways using GeneFEAST, developed by Dr. Avigail Taylor, that highlights DEGs driving enrichment of multiple pathways (Taylor et al., 2023).

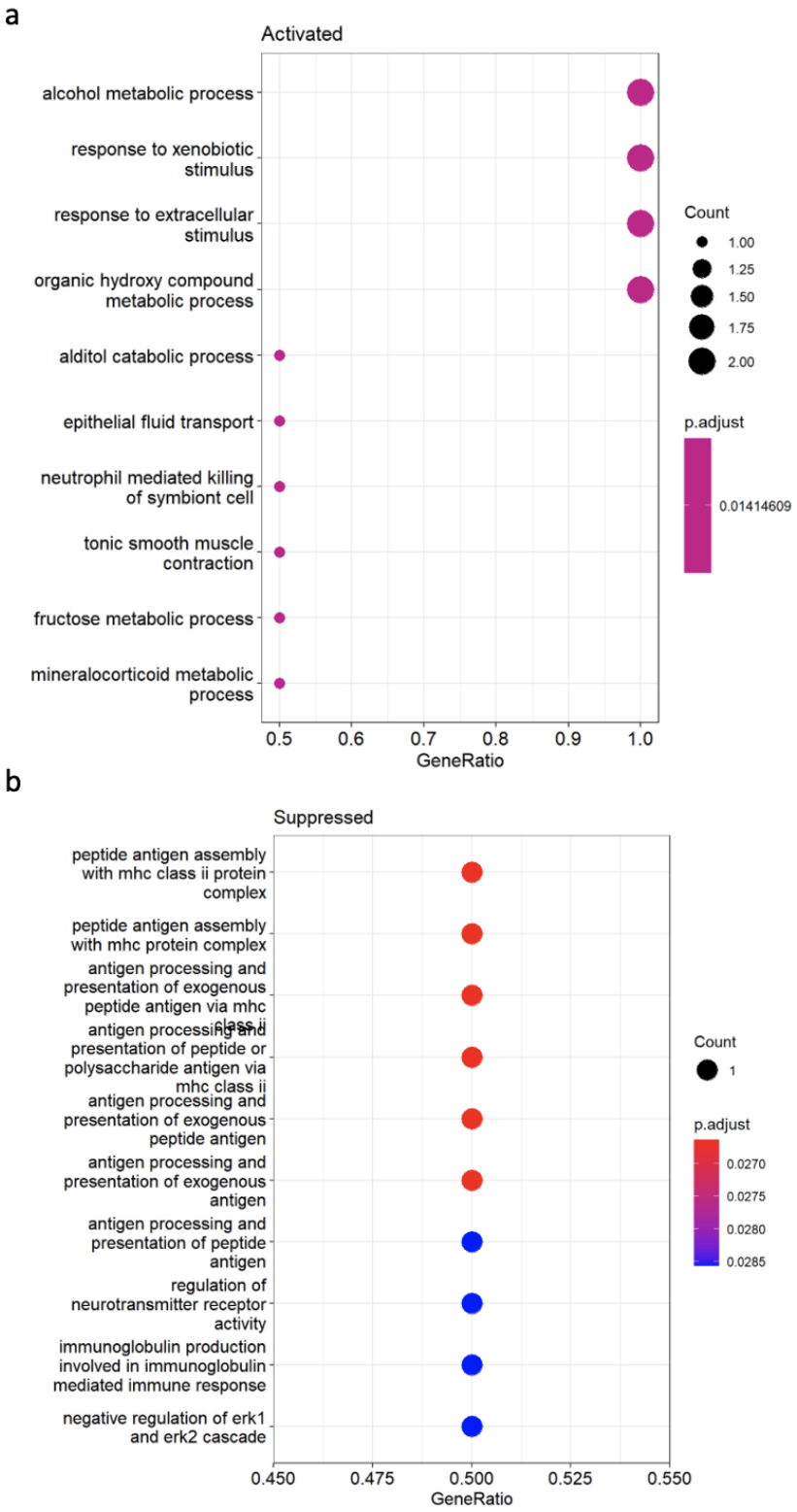


Figure 3.17: Pathway analysis of genes regulated by xentuzumab treatment on Myc-CaP tumours in the pilot experiment. a-b. Functional enrichment analysis of pathways upregulated (**a**) or downregulated (**b**) by xentuzumab treatment versus control. The analysis was done by Dr. Alessandro Barberis.

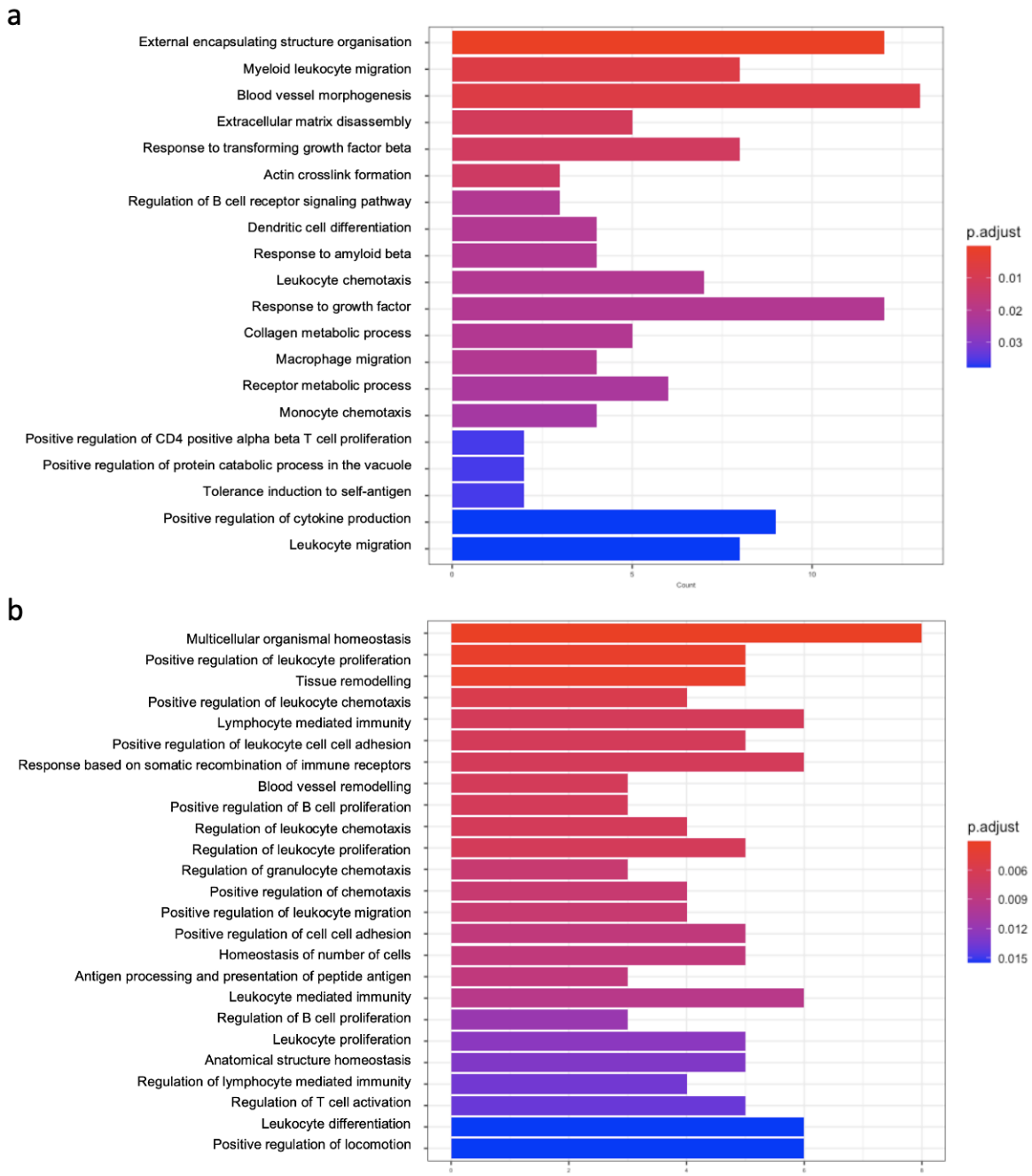


Figure 3.18: Pathway analysis of genes regulated by xentuzumab + anti-PD-1 treatment on Myc-CaP tumours: pilot experiment. a-b. Functional enrichment analysis of pathways upregulated by **a**. xentuzumab + anti-PD-1 treatment versus control, and **b**. xentuzumab + anti-PD-1 treatment versus xentuzumab single treatment. The analysis was done by Dr. Alessandro Barberis.

GeneFEAST analysis identified deregulation of EMT, consistent with reports that IGFs influence EMT in prostate cancer (Graham et al., 2008, Zhou et al., 2015), and myeloid leukocyte migration (Figure 3.19). This suggests that IGF blockade in combination with anti-PD-1 influences the myeloid component of innate immunity.

For validation by qRT-PCR, 17 DEGs from combination treatment vs control comparison that are related to EMT and myeloid/leukocyte cell migration were chosen, as well as 9 genes related to IGF axis and macrophage phenotype (Figure 3.20). Of note, five genes were validated as differentially expressed with significant differences. Platelet factor 4 (Pf4), C-C motif chemokine ligand 9 (CCl9), and Mmp12 expression was upregulated, and Tgfb3 and Lyn were downregulated in combination-treated tumours compared to control (Figure 3.20b-e).

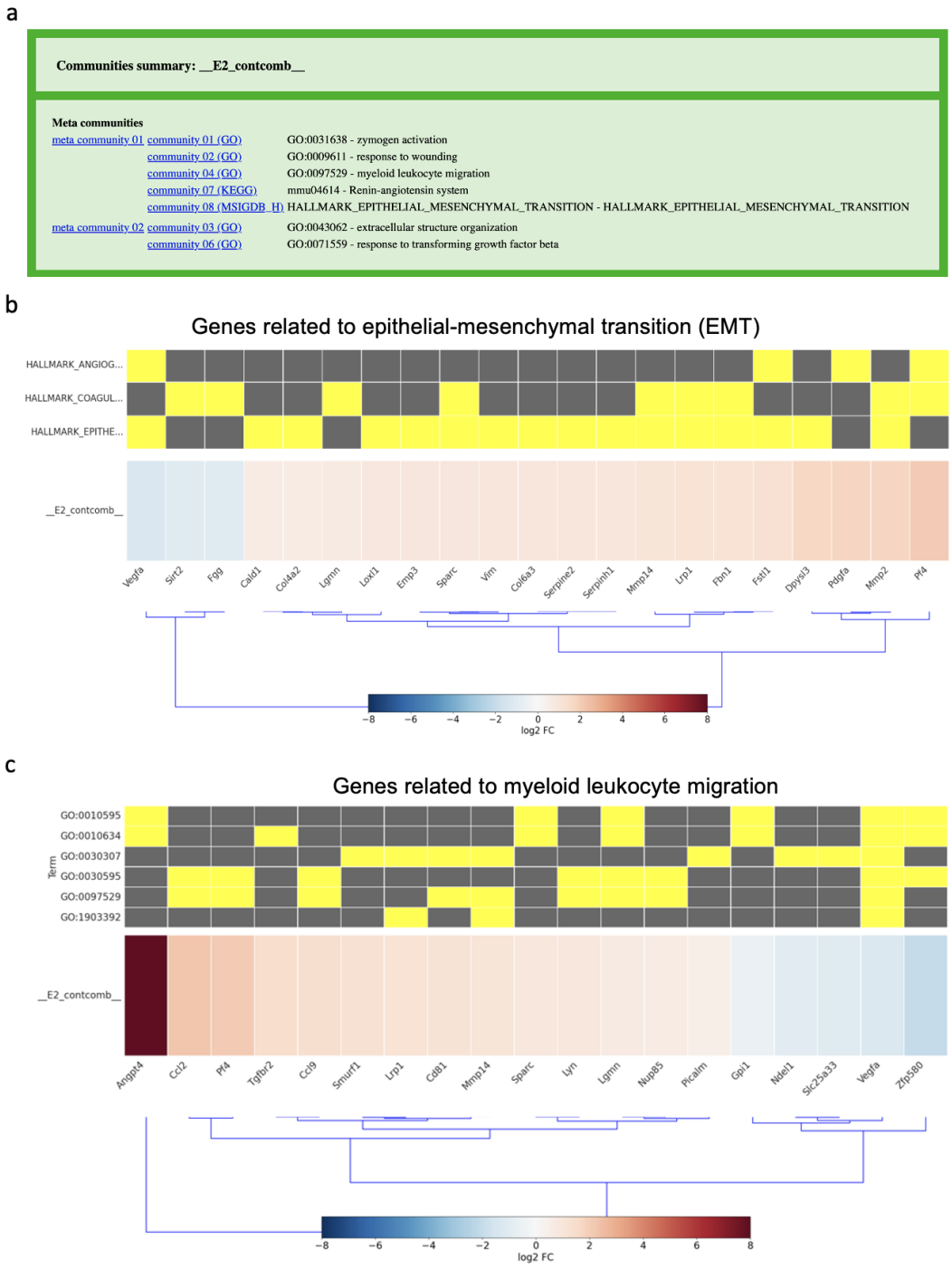


Figure 3.19: GeneFEAST analysis of significantly enriched pathways in xentuzumab + aPD1-treated tumours vs controls. a. Identified pathways are referred to as "communities", which are grouped into larger "meta communities". **b-c**. Split heatmaps showing the DEGs driving enrichment of **b**. EMT and **c**. myeloid leukocyte migration. Top heatmaps show genes annotated by a term (yellow). In the lower heatmaps, genes are coloured to show log2 fold changes in RNAseq (Figure 3.16). The analysis was performed with the help of Dr. Avigail Taylor.

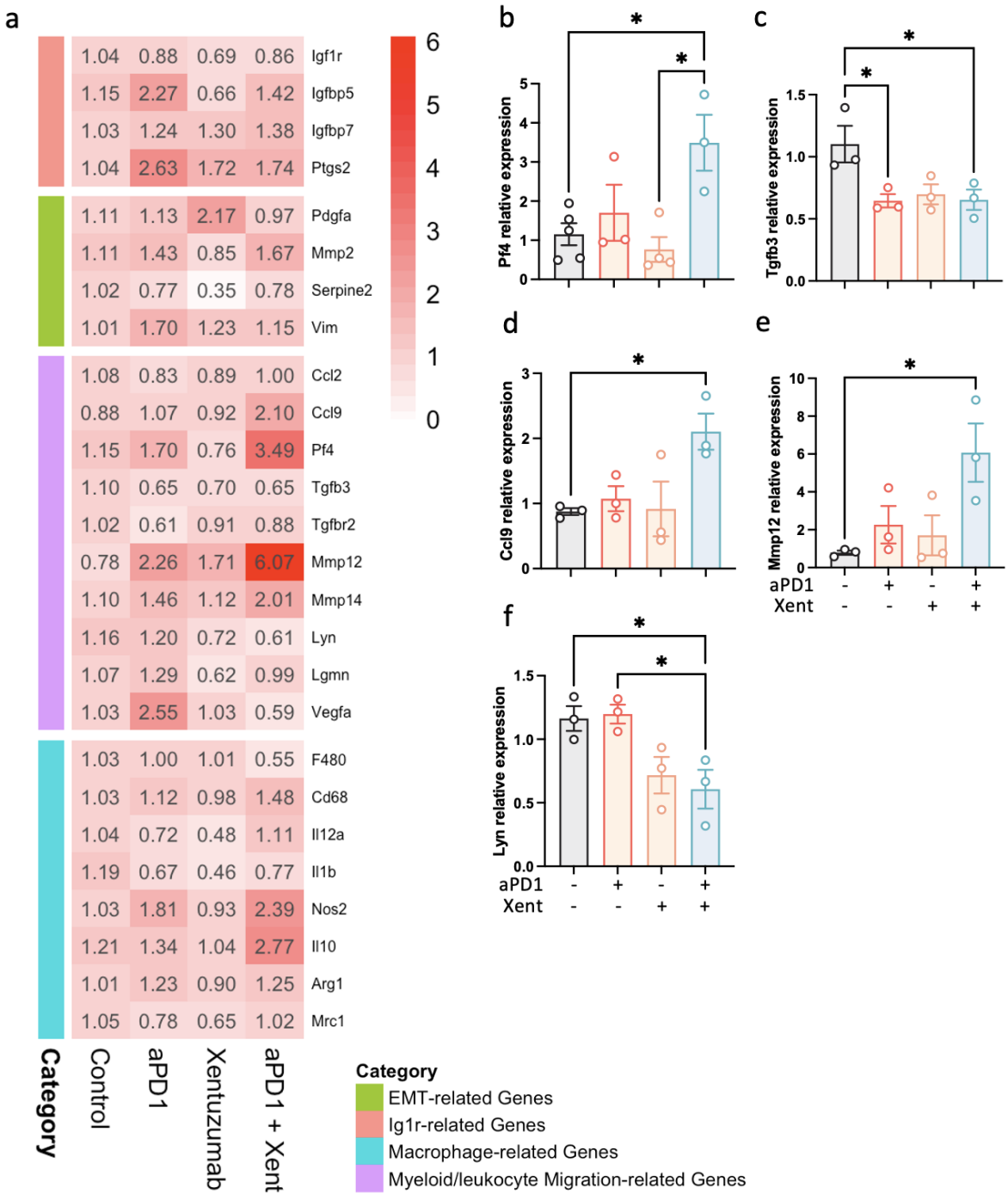


Figure 3.20: Quantitative real-time PCR (qRT-PCR) validation of selected DEGs comparing Myc-CaP tumours treated with xentuzumab and anti-PD-1 compared to control. a. Selected DEGs related to the IGF axis, EMT, myeloid cell migration, and macrophage phenotype were validated. RNAs were extracted from frozen tumours and processed for qRT-PCR. The numbers in the heat map represent relative expression after corrected for 18s expression. Five of the selected genes, **b**. platelet factor 4 (Pf4), **c**. transforming growth factor-beta 3 (Tgfb3), **d**. C-C motif chemokine lingand 9 (Ccl9), **e**. matrix metallopeptidase 12 (Mmp12), and **f**. Lyn, were validated with significance. Data are presented as the mean ± SEM from at least three independent animals (*p<0.05, **p<0.01).

Among the DEGs comparing xentuzumab treatment to control, Cd74 and Ccr2 were validated (Figure 3.21). Cd74 was significantly downregulated in not only xentuzumab-treated tumours but in all other treatment groups compared to control (Figure 3.21a). Ccr2 was significantly downregulated by xentuzumab treatment compared to control (Figure 3.21b).

Three DEGs that arose from combination treatment vs xentuzumab comparison were validated. H2-Aa was significantly downregulated by xentuzumab treatment compared to combination and control treatments, as was in PD1 treatment vs control, which suggests that this change could be both IGF and PD-1 dependent. (Figure 3.22a). Vegfa and Atg14 were significantly upregulated in xentuzumab treatment compared to combination (Figure 3.22b-c). Of note, Atg14 was significantly downregulated by combination treatment compared to control and either single agents.

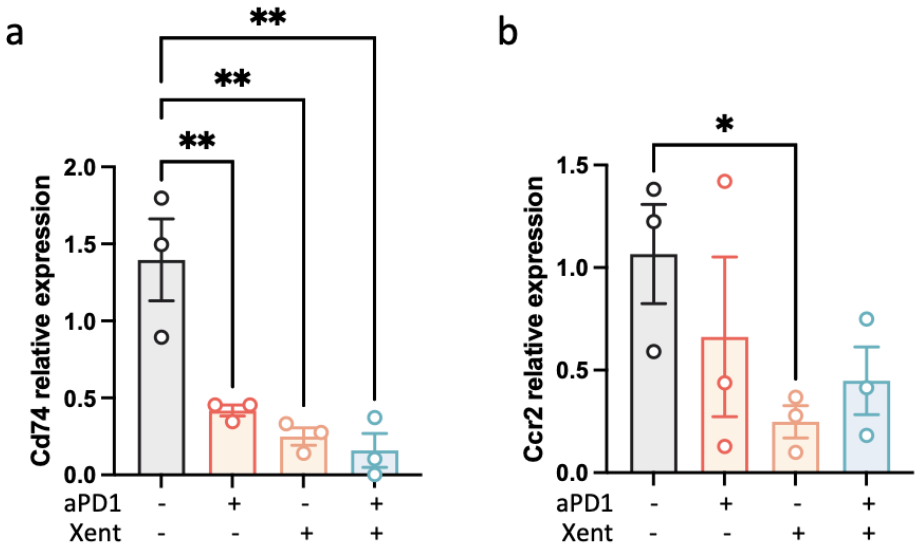


Figure 3.21: Quantitative real-time PCR (qRT-PCR) validation of selected DEGs comparing Myc-CaP tumours treated with xentuzumab compared to control. Among the DEGs comparing xentuzumab-treated tumours to control, **a**. Cd74 and **b**. Ccr2 were validated with significance by qRT-PCR. Data are presented as the mean ± SEM from at least three independent animals (*p<0.05, **p<0.01).

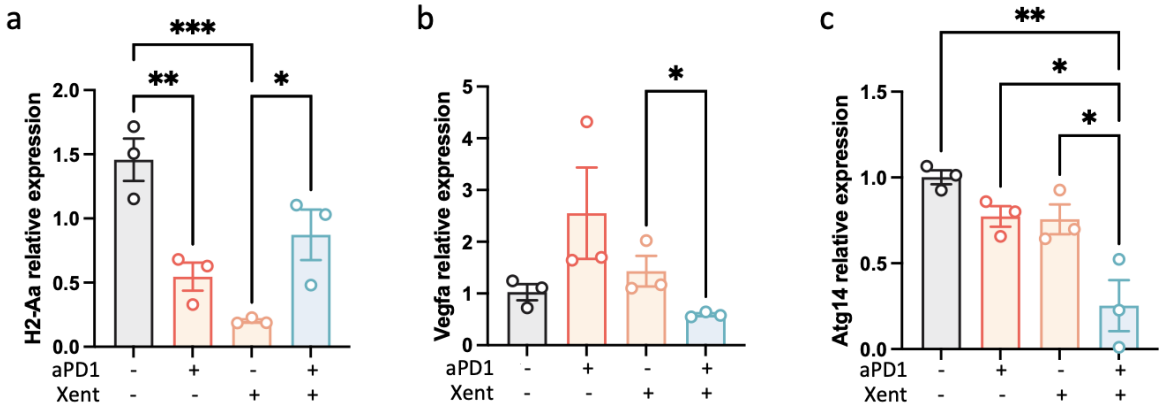


Figure 3.22: Quantitative real-time PCR (qRT-PCR) validation of selected DEGs comparing Myc-CaP tumours treated with xentuzumab + anti-PD-1 compared to xentuzumab. Among the DEGs comparing tumours treated with xentuzumab + anti-PD-1 compared to xentuzumab, **a**. H2-Aa, **b**. Vegfa, and **c**. Atg14 were validated by qRT-PCR. Data are presented as the mean ± SEM from at least three independent animals (*p<0.05, **p<0.01).

3.5 Investigating the effects of IGF axis and PD-1/PD-L1 axis blockade in prostate cancer: repeat experiment

3.5.1 Rationale and tumour growth

Following the pilot experiment with small group of mice that showed immune-modulatory actions of IGF and PD-1 axis in prostate cancer, we wanted to explore this combination further in a bigger scale to ensure more statistical power and to better observe long-term changes of each treatment condition. The design of the experiment was similar to the pilot study (Figure 3.8a), except the number of mice per group was increased to 10 mice per group, and tumour limit was increased to 1000 mm^3 compared to 400 mm^3 (Figure 3.23a). The increase in tumour limit meant a possibility of more injections for treatments, so to stay within the injection limit on the project license, we sought to combine anti-PD-1 and xentuzumab treatments in one syringe to treat for longer. Tolerability test was done on a small group of mice to ensure the solvent compatibility.

Again, there was no tumour growth inhibition (Figure 3.23b), but the tumours had the same features as in the pilot study (Figure 3.8c). Consistent with the pilot study (Figure 3.11), H&E staining confirmed significantly higher necrosis in combination-treated tumours, compared with any other group (Figure 3.24). The tumours, blood, and spleen were collected for IHC, bulk RNA sequencing, and flow cytometry, which was now possible with bigger tumours and more cell numbers.

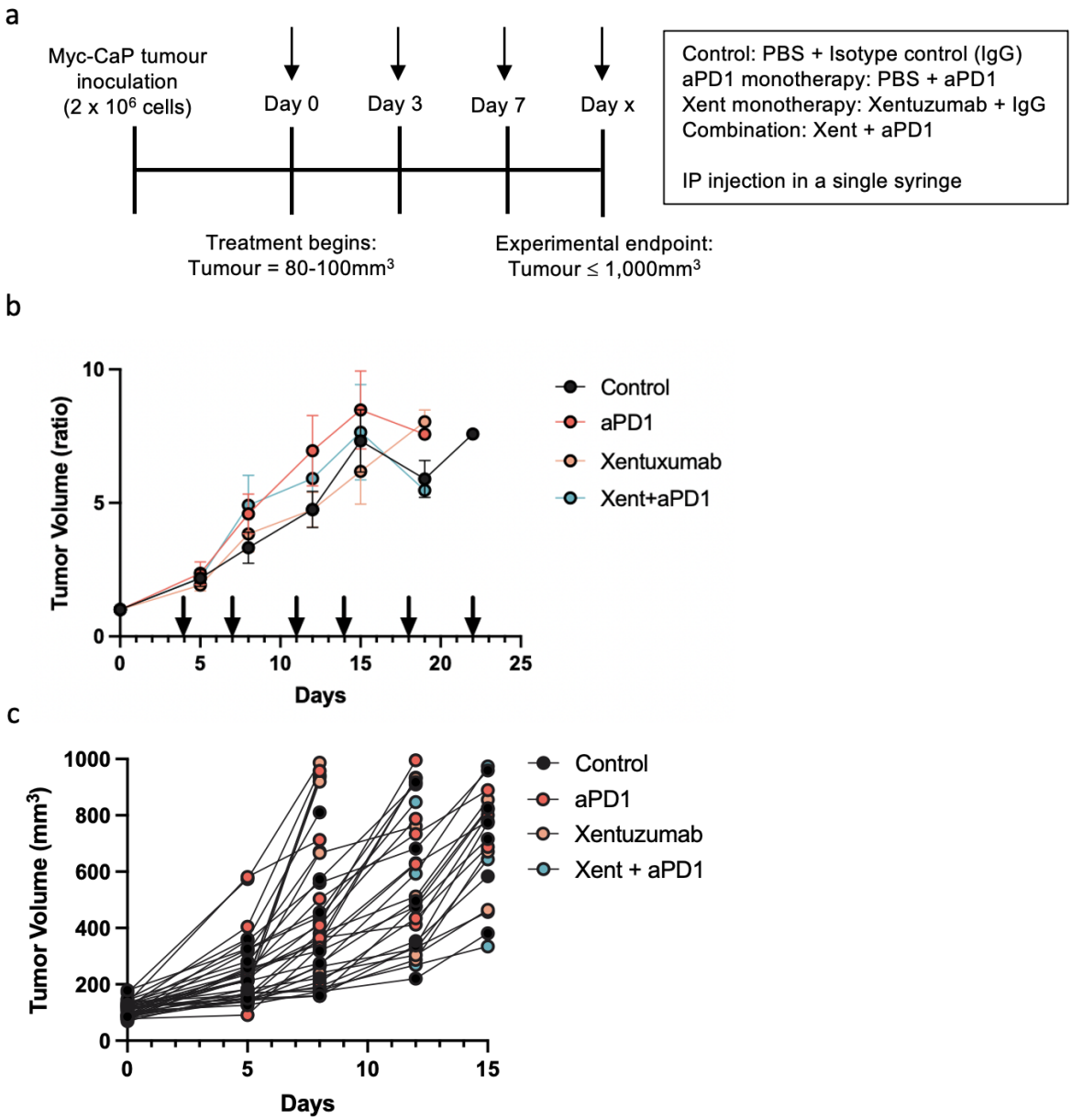


Figure 3.23: Investigating the effects of IGF and PD-1 blockade in vivo: repeat experiment. a. Schematic of the experiment in which 2 million Myc-CaP cells were inoculated subcutaneously in the right flank of syngeneic FVB mice. Once tumour size reached 100 mm^3, animals were intraperitoneally injected with 100 mg/kg PBS + 10 mg/kg isotype matched IgG (control), 100 mg/kg PBS + 10 mg/kg anti-PD1 (aPD1), 100 mg/kg xentuzumab + 10 mg/kg IgG (xentuzumab), or 100 mg/kg xentuzumab + 10 mg/kg anti-PD1 (Xent+aPD1) twice weekly. Numbers of tumours collected at the endpoint per group were: control, n = 8, aPD1, n = 8, xentuzumab, n = 9, and Xent+aPD1, n = 9. **b**. % tumour growth over time. Arrows represent treatment days.

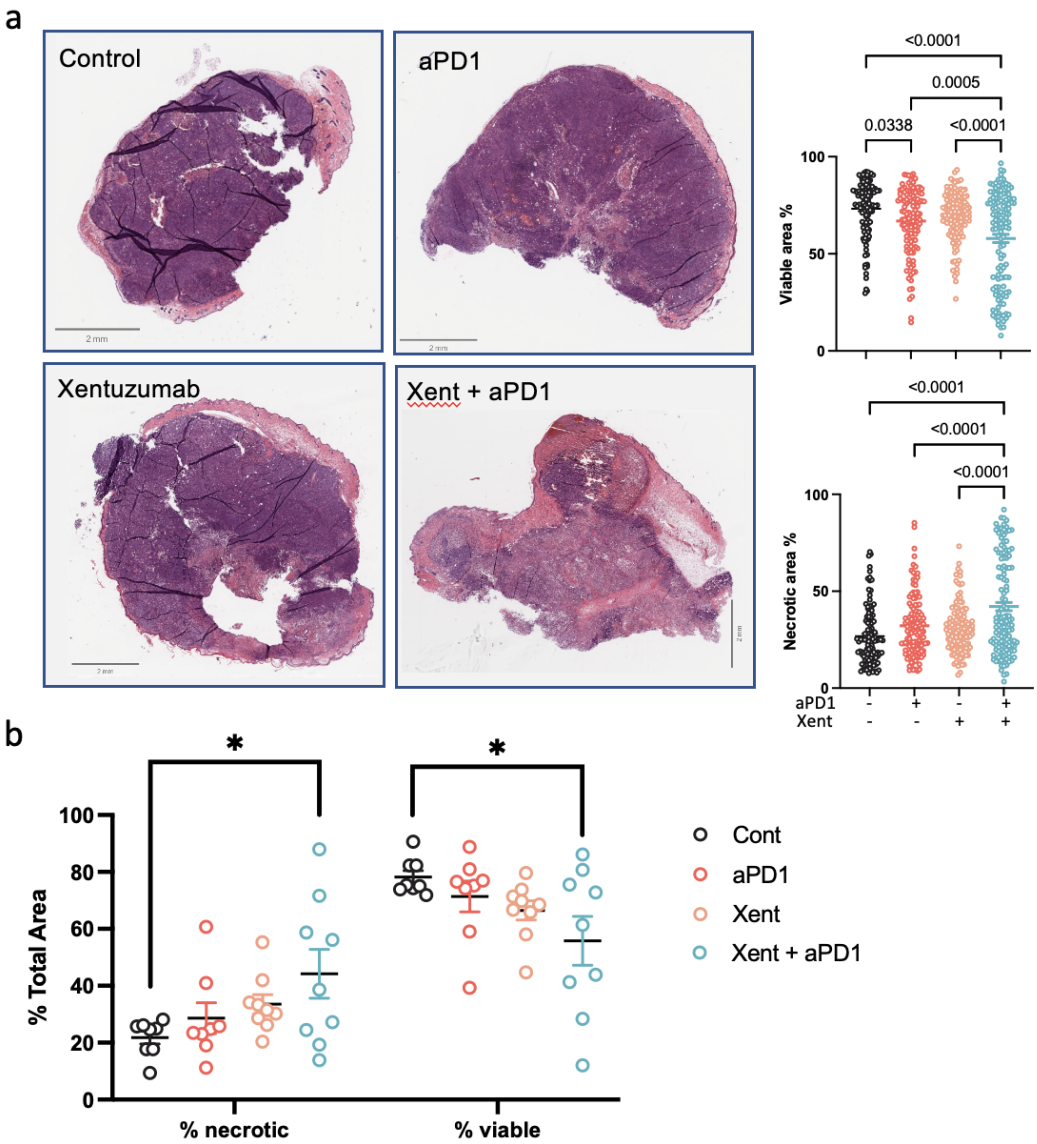


Figure 3.24: Haematoxylin and eosin (H&E) staining of the repeat experiment tumours. a. H&E staining of the tumours (scale bar = 2 mm) Graphs: the viable and necrotic area of all slides stained for immunochemistry were analysed for % viable and necrotic area on the HALO platform (n = 118-133 sections from 8-9 tumours per group), and the results were pooled and graphed (one-way ANOVA with multiple comparisons). **b**. The section with the biggest area was chosen per mouse, and its % viable and necrotic area were graphed. (*p<0.05, two-way ANOVA with multiple comparisons)

3.5.2 Immunohistochemical analysis of tumour tissues

Immunohistochemical staining showed reduction in IGF-1R phosphorylation upon xentuzumab treatment, but there were no changes in combination-treated tumours compared to control (Figure 3.25). S6 phosphorylation, however, was reduced in all treatments compared to control, though significant only in anti-PD-1 treatment compared to control. Apoptosis marker CC3 expression was significantly increased in anti-PD-1-treated tumours compared to control. There were no significant changes in CD4 and FoxP3 expression, and CD8 was barely detectable in all treatment groups, but PD-1 expression was reduced in all groups compared to control, significant in xentuzumab and combination treatment groups (Figure 3.25). There was no difference in IGF-1R, CD8, CD31, and Ki67 expression (Figure 3.26).

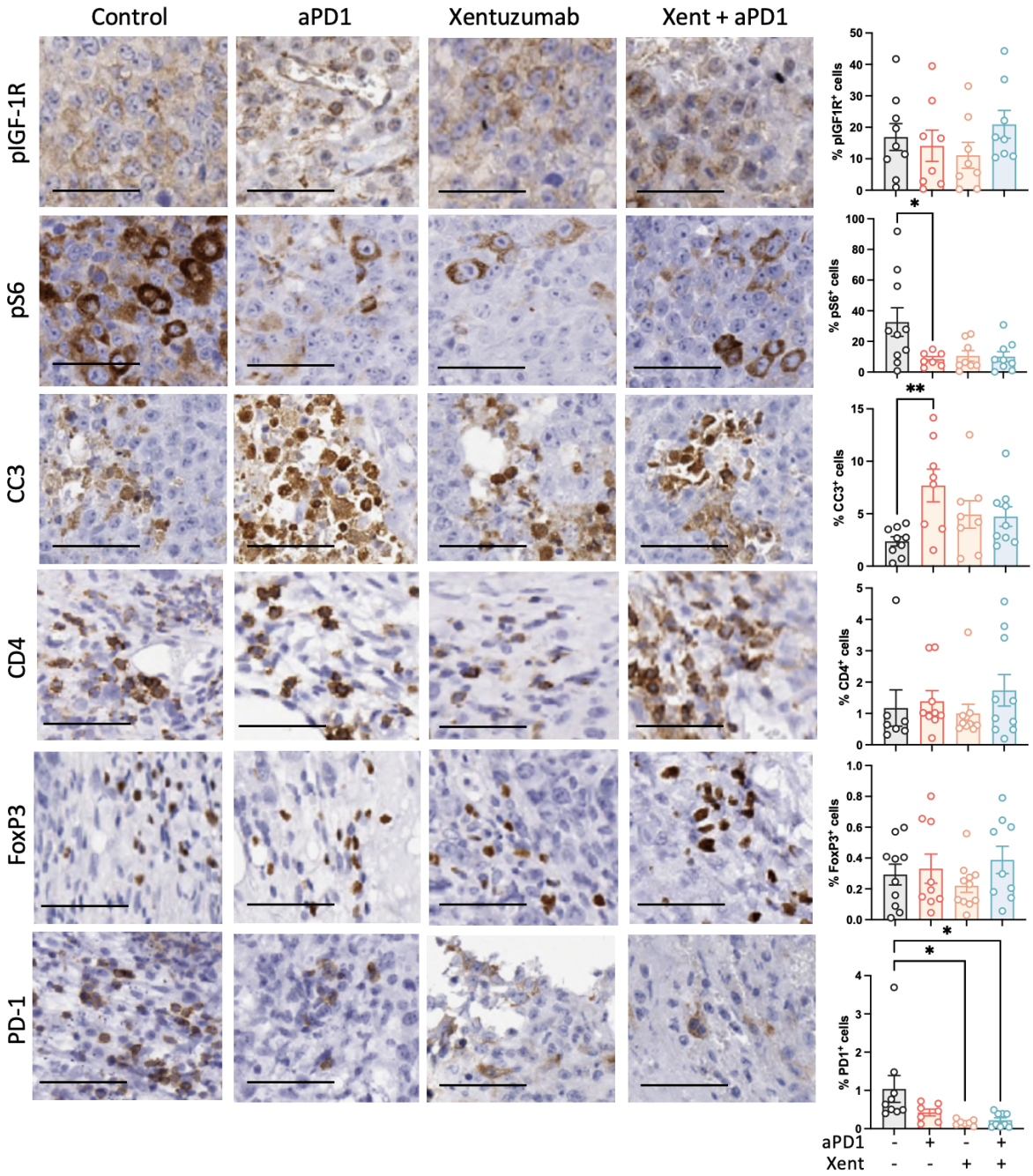


Figure 3.25: Effects of IGF-1 and PD-1 blockade repeat experiment on expression of IGF-1R and T-cell markers in Myc-CaP tumours. Formalin-fixed and paraffin-embedded tumours from each group (control, n = 8, aPD1, n = 8, xentuzumab, n = 9, and Xent+aPD1, n = 9) were cut into 4 μm sections, and phospho-IGF1R, phospho-S6, CC3, CD4, FoxP3, and PD-1 expression were detected by immunohistochemistry and analysed by HALO software. Images: representative IHC images, scale bar: 50 μm. Data are presented as the mean ± SEM from at least eight independent animals (one-way ANOVA with multiple comparisons).

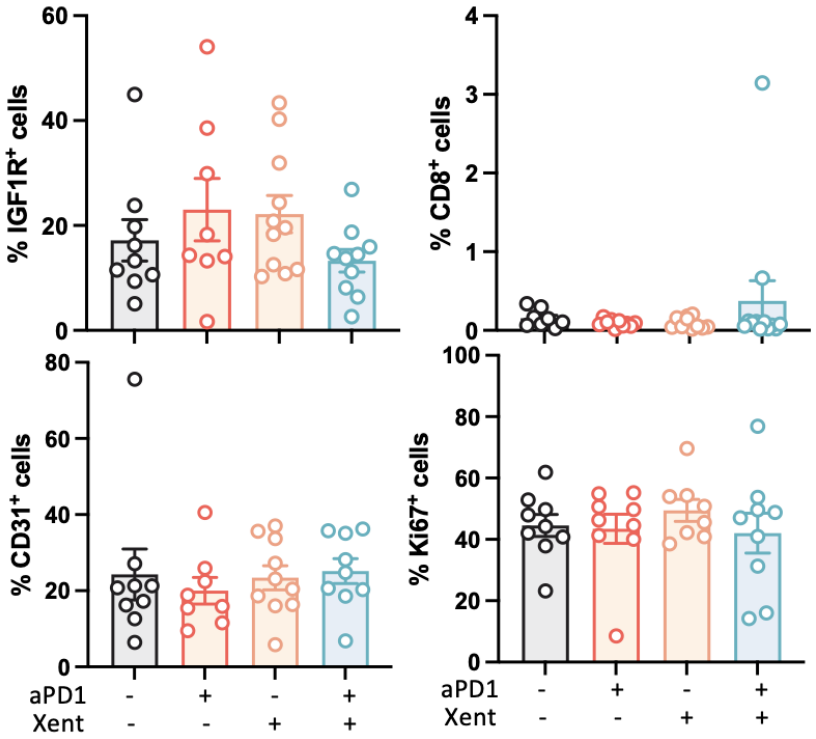


Figure 3.26: Immunohistochemical staining of IGF-1 and PD-1 blockade repeat experiment. Box plots show nonsignificant quantification of IGF-1R, CD8, CD31, and Ki67 expression detected by immunohistochemistry and analysed by HALO software.

Expressions of macrophage markers were visualised by IHC (Figure 3.27). There was no difference in myeloid marker CD68 expression, but total macrophage F4/80 and M1 macrophage marker iNOS were significantly increased upon combination treatment. There was no change in M2 macrophage marker CD163 in combination treatment compared to control, suggesting that the total macrophage increase can mainly be attributed to M1-like macrophages. CD163, however, was significantly increased in anti-PD1 treatment, compared to all other treatments. CD47, tumour cell marker which interacts with macrophage signal regulatory protein α (SIRPα) to inhibit phagocytosis, was significantly increased in combination treatment compared to control and xentuzumab treated tumours (Figure 3.27). These significant changes in macrophage population suggest consequences for TIME, consistent with the previous pilot experiment (Figure 3.13).

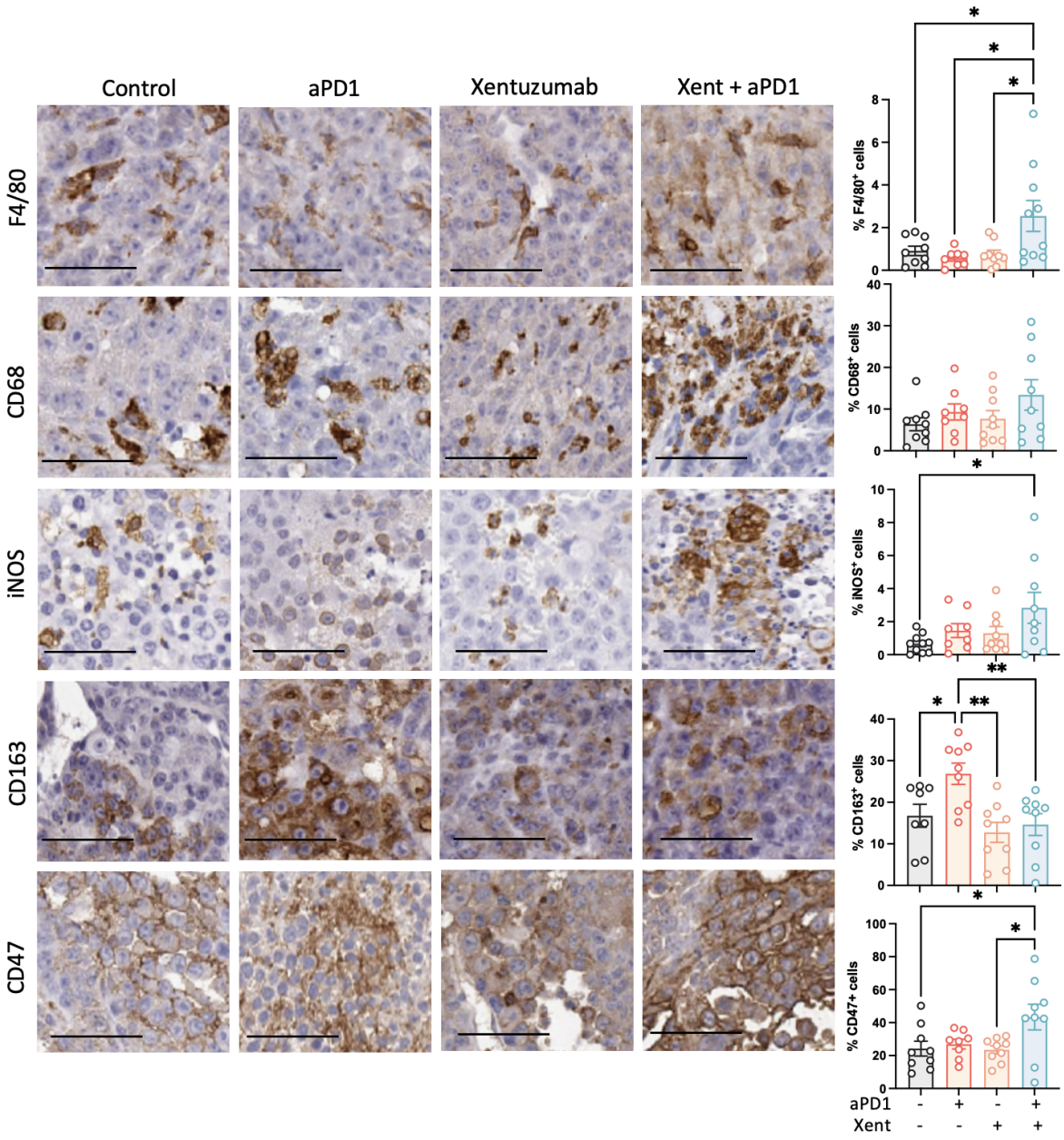


Figure 3.27: Macrophage marker expression in Myc-CaP allografts with IGF and PD-1 blockade repeat experiment. Representative images of control and anti-PD1 and/or xentuzumab-treated tumours stained with CD68, F4/80, iNOS, CD163, and CD47, scale bar: 50 μm. Data are presented as the mean ± SEM from at least three independent animals (*p<0.05, **p<0.01, one-way ANOVA with multiple comparisons).

3.5.3 Flow cytometric analysis of tumours

Tumour, spleen, and PBMCs were collected and prepared for flow cytometry. Quantification of TILs showed no change in either CD4 or CD8+ T cell population (Figure 3.28a), but xentuzumab reduced CD4+FoxP3+ Tregs (Figure 3.28b) as well as IFN-γ production of the Tregs (Figure 3.28c). Comparing all treatments, xentuzumab and anti-PD-1 combination treatment led to reduction in CD4+FoxP3+ Tregs, increase in CD8/Treg ratio, and increase in CD8+ T cells expressing granzyme B, all with significance (Figure 3.28d-f). In addition, xentuzumab caused significant expansion in effector memory CD4+ and CD8+ T cells in splenocytes (Figure 3.28g-h) as well as in PBMCs (Figure 3.28i-j). This suggests that IGF blockade influences T cell phenotype in tumours, spleens, and PBMCs and that xentuzumab and anti-PD-1 treatment has potential to enhance the T cell activity.

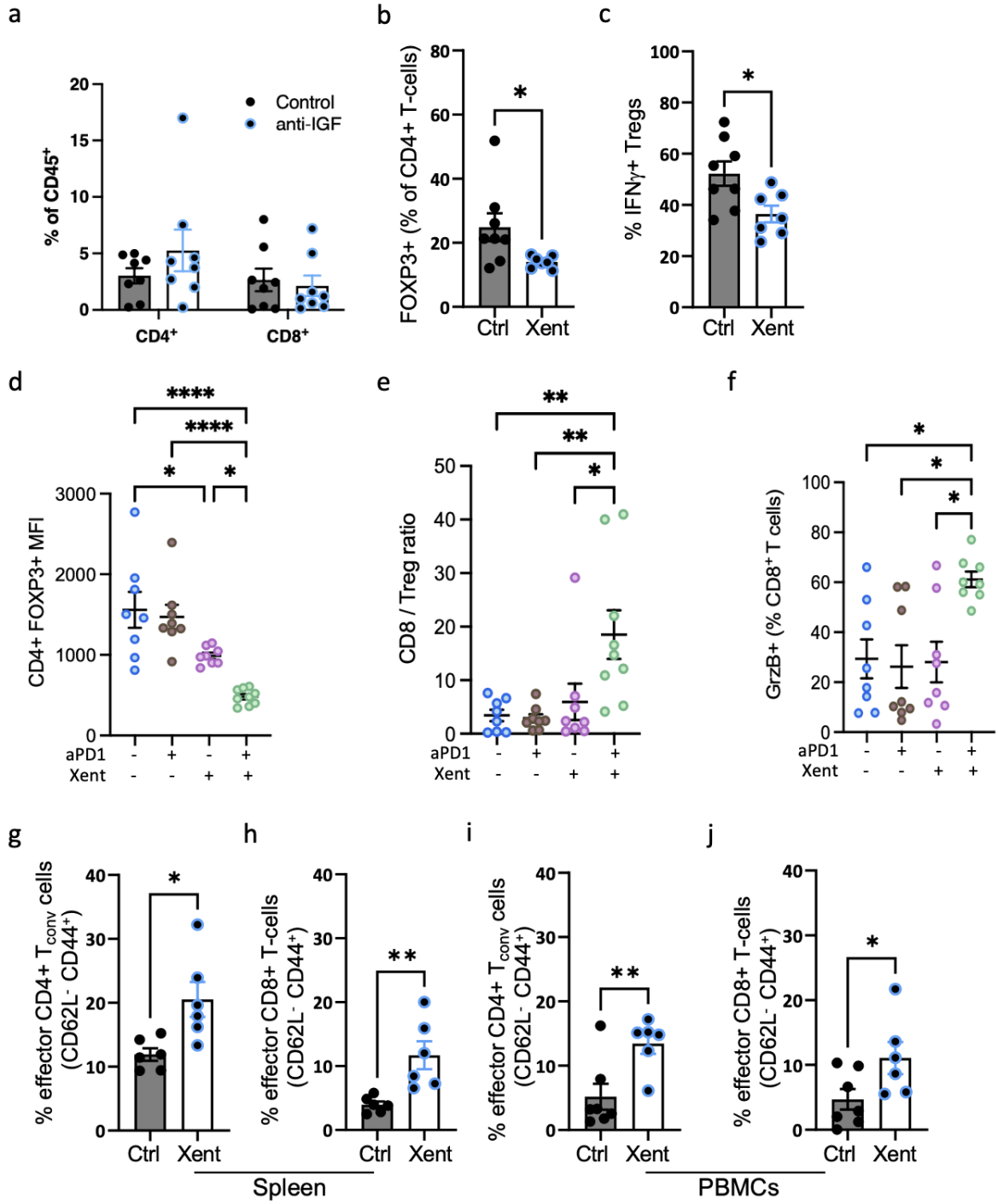


Figure 3.28: Flow cytometric analysis of tumours, spleens, and PBMC of the mice treated with xentuzumab and/or anti-PD-1. Cells from **a-f**. tumours, **g-h** spleens, and **i-j** PBMCs of the xentuzumab ± anti-PD-1 experiment were stained with Live/Dead, CD45, CD4, CD8, FoxP3,CD44, CD62L, CD25, IFN-γ, and Granzyme B in preparation for flow cytometry. These experiments were done by Cameron Lang in our lab. (*p<0.05, **p<0.01, ****p<0.0001, t-test or one-way ANOVA with multiple comparisons)

3.5.4 Transcriptomic profiling of tumours

Snap frozen tumours were cut and processed for RNA extraction, in preparation for 3' RNA sequencing at the CHG, University of Oxford. Sequencing reads were analysed, and DEGs were identified pairwise using DESeq2 package, as in Chapter 3.4.3. Unlike the pilot experiment, there were low number of DEGs, and data was not meaningful enough for further pathway enrichment analysis. None of the genes in either comparisons overlapped with the previous results (Figure 3.14, 3.15, and 3.16).

Xentuzumab vs control-treated tumours resulted in 59 DEGs (Table 7.7). Among DEGs, Il10ra was downregulated upon xentuzumab treatment (Figure 3.29). Among 120 genes identified in combination treatment compared to control, 25% of the genes were keratin-associated genes (Table 7.6). In addition, Il7r was downregulated upon combination treatment (Figure 3.30). We didn't take any of the genes forward for validation, because we failed to see anything relevant to IGF biology or any genes in connection with the previous experiment.

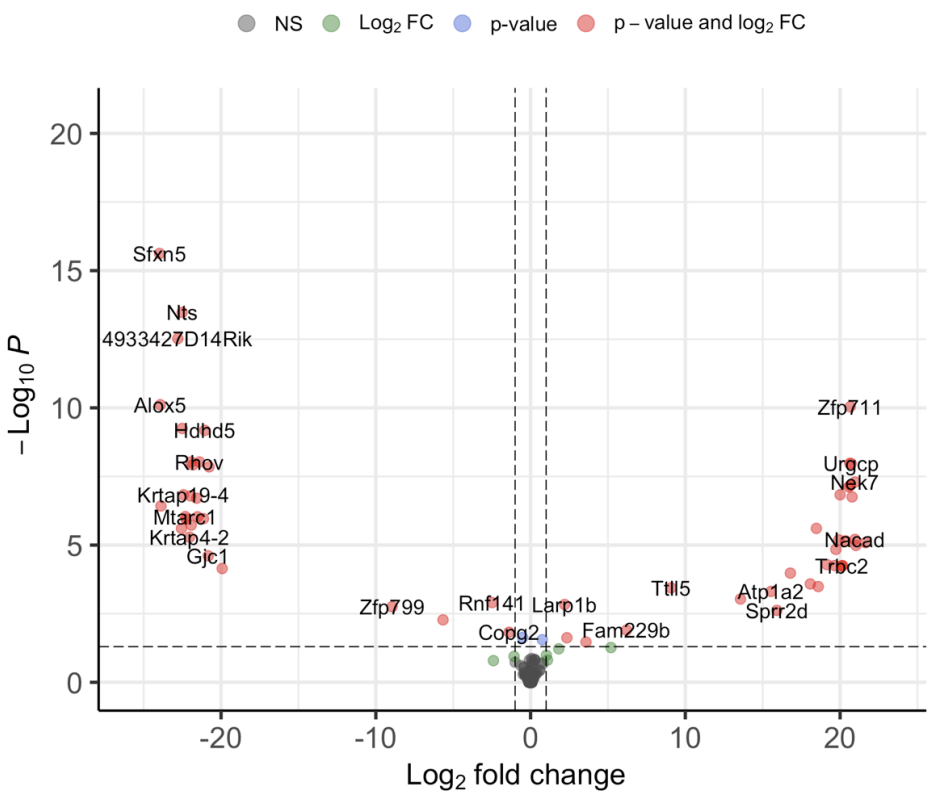


Figure 3.29: RNA sequencing analysis of Myc-CaP tumours treated with xentuzumab compared to control: repeat experiment. a. RNAs extracted from Myc-CaP allografts were quality-controlled using FastQC and quantified using Salmon. Volcano plot shows the DEGs (red) with adjusted p-value <0.05. This analysis was done by Dr. Alessandro Barberis and Dr. Fiona Hartley in our lab.

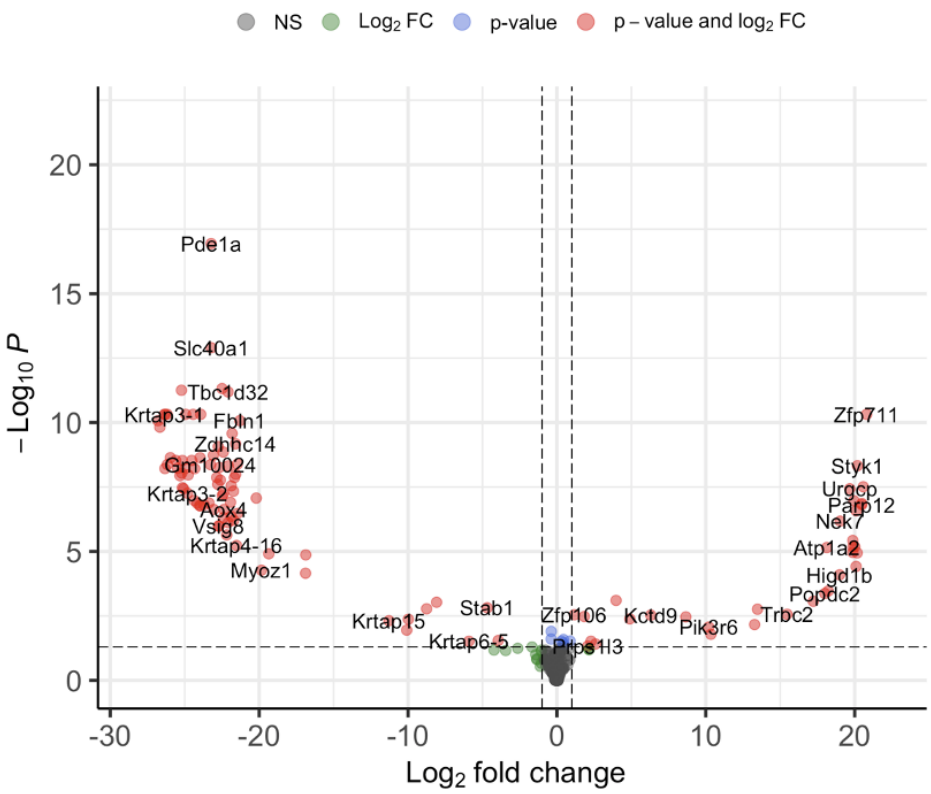


Figure 3.30: RNA sequencing analysis of Myc-CaP tumours treated with xentuzumab and anti-PD-1 compared to control: repeat experiment. a. RNAs extracted from Myc-CaP allografts were quality-controlled using FastQC and quantified using Salmon. Volcano plot shows the DEGs (red) with adjusted p-value <0.05. This analysis was done by Dr. Alessandro Barberis and Dr. Fiona Hartley in our lab.

3.6 Discussion

Xentuzumab successfully blocked phosphorylation of IGF-1R and downstream signalling proteins AKT and ERK in PTEN WT murine prostate cancers (Figure 3.1). This correlated with previous work from our group (Rieunier et al., 2021), that showed that xentuzumab blocked phosphorylation of IGF-1R and downstream signalling proteins. In murine PTEN-null PTEN-CaP8 cells, ERK phosphorylation was unaffected by xentuzumab. This could be due to reported crosstalk between PTEN and ERK, where PTEN is reported to inhibit ERK1/2, resulting in ERK activation upon PTEN loss (Chetram et al., 2012).

Xentuzumab blocked *in vitro* 2D growth and cell survival of PTEN WT prostate cancer cells but not PTEN-null cells (Figure 3.2). The latter was expected, since loss of PTEN activates downstream AKT signalling and promotes cell survival (Zhang et al., 2010). The results were also consistent with publications (Wu et al., 2021; Friedbichler et al., 2014) that showed decrease in viability of PTEN WT cancer cell lines treated with xentuzumab. In addition, xentuzumab significantly reduced 3D spheroid growth of Myc-CaP but not PTEN-CaP8 (Figure 3.3). A recent report showed that combination of xentuzumab and enzalutamide inhibited growth of castration-resistant LuCaP 96CR patient-derived xenograft (PDX) model, but xenograft growth inhibition was attenuated when PTEN was depleted (Weyer-Czernilofsky et al., 2020). This suggests that xentuzumab is unlikely to reduce tumorigenesis in PTEN-null prostate cancer tumours *in vivo*, though it could still cause IGF or immune-related responses.

The *in vivo* study was conducted only with Myc-CaP cells inoculated in syngeneic FVB mice (Figure 3.4a). This allograft model treated with either PBS (control) or xentuzumab did not result in any tumour growth reduction (Figure 3.4b), in contrast to the publications that showed xentuzumab's ability to reduce tumorigenesis in xenograft models of LuCaP 96CR prostate cancer and SK-CO-1 colorectal cancer models (Weyer-Czernilofsky et al., 2020; Rieunier et al., 2021). This suggests that additional effects on the TIME could be the cause of tumorigenesis despite IGF blockade. In future, further

experiments on PTEN WT human prostate cancer cells such as DU145 and 22Rv1 and subsequent *in vivo* experiment may show effects of xentuzumab on tumorigenesis of human prostate cancers. In addition, *in vitro* experiments with xentuzumab were conducted upon addition of IGF in serum-starved media to highlight the impact of IGFs on cancer cells, but the fact that there are other growth factors that influence the cancer cells *in vivo* could partly explain the discrepancy between the *in vitro* and *in vivo* experiments. It would be interesting to see if xentuzumab caused reduction in cancer cell growth and survival without prior serum starvation.

When the collected tumours were subject to IHC (Figure 3.5), it was clear that xentuzumab inhibited IGF-1R phosphorylation but not phospho-S6, possibly due to a negative feedback loop or compensation effect by other pathways (Zhang et al., 2015; Wan et al., 2007; Cao et al., 2008). There was a significant reduction in CD4+ T cells, which correlates with data from our group showing increase in CD4+ T cell infiltration in prostate cancer tissues of men with high serum IGF-1 (Nandakumar, 2022). IGF-1 administration has been known to promote immunosuppressive IL-10 secretion in CD4+ Th2 cells and increase the number of circulating CD4+ T cells in mice by inducing T cell proliferation and inhibiting apoptosis (Walsh et al., 2000), consistent with our data. IGF-1 is also reported to induce CD4+ Th17 cells (DiToro et al., 2020). Despite many studies that show IGF-1 stimulating Treg proliferation (Bilbao et al., 2014; Shapiro et al., 2023), there was no difference in FoxP3 infiltration upon xentuzumab treatment. For future work, mIF staining of multiple markers in a single section would be better at determining colocalisation of multiple T cell markers and, therefore, various functions and immune compartments of the tumour. In general, there was very low CD8 T cell infiltration in all tumours, supported by studies that reported lack of CD8 T cell infiltration in prostate cancer tissue (Ebelt et al., 2008). PD-1 and PD-L1 were downregulated by xentuzumab, though not significant (Figure 3.6a), which represents the reciprocal effect of IGF-1, upregulating PD-L1 in human prostate cancer cells *in vitro*. (Nandakumar, 2022). CD31, despite no changes in expression levels, showed more ribbon-like patterns and mature vascularisation upon xentuzumab treatment (Figure 3.6b), as opposed to short, punctate pattern in controls that represents neovasculature.

This is consistent with the reported role of IGFs in angiogenesis (Samani et al., 2007; Fukuda et al., 2002; Liu et al., 2023c).

The fact that we used a subcutaneous instead of an orthotopic model for the study could explain the insignificant immune changes seen by IHC. An orthotopic tumour model would have been better to clearly see the effects of xentuzumab in the tumour microenvironment (Stribbling et al., 2024; Zhang et al., 2019; Liu et al., 2021a). Although long term *in vivo* experiment could have yielded more complex and memory-focused adaptive immune responses, one of the purposes of the *in vivo* experiment was to generate comparable data types to WINGMEN trial, a short-term windows trial using xentuzumab (Figure 5.1).

Bulk RNA sequencing of RNAs extracted from the fresh frozen tumours identified 86 deregulated genes by xentuzumab (Figure 3.7a-b). Among the deregulated genes were *Igf1r* and *Mki67*, both significantly downregulated by xentuzumab compared to control and validated through qRT-PCR (Figure 3.7c-d). Previous studies from our lab showed IGF-1R upregulation in primary prostate cancers (Hellawell et al., 2002; Aleksic et al., 2017), suggesting that xentuzumab inhibits ability of IGF-1 to upregulate IGF-1R in malignant prostatic epithelium. Reduction in *Mki67*, which encodes for Ki67 cell proliferation marker, aligns with cell proliferation studies *in vitro* (Figure 3.2), and non-significant trends to xentuzumab-induced downregulation of Ki67 by IHC (Figure 3.6). This inconsistency could be explained by difference in RNA and protein level and sensitivity of the assays.

Several publications suggesting immunosuppressive effects of IGFs including Ajona et al., 2020 prompted the pilot experiment to test whether IGF blockade can sensitise prostate tumours to PD-1 targeting immunotherapy. Pilot experiment was done with 5-6 mice per group, tumour limit was 400 mm^3, and the two drugs were given 2 hours apart on the same day, whereas the repeat experiment consisted of 8-9 mice per group, tumour limit was 1,000 mm^3, and the two drugs were mixed and given in the same syringe. Although the repeat experiment was done to see the changes of and within the tumours in a larger scale, downside for treating the tumours longer with more injections

was that the tumours were more heterogeneous and it was very hard to find strong biological signals.

There was no difference in tumour growth, but the combination-treated tumours were softer, with blood and fluid sac bursting out when the tumours were cut (Figure 3.8c). This suggests that the tumour size difference may have been over-estimated compared to the actual size of the tumour mass. Injection of the luciferase-labelled cancer cells would have allowed for more accurate tumour growth measurement, though there is a risk of immune elimination caused by the reporters. There was a significant increase in necrosis in both pilot and the repeat experiment (Figure 3.11 and Figure 3.24). Bulk RNA sequencing of both pilot and the repeat experiment also supported this, where RIPK1-3 and MLKL, key mediators of necroptosis, were upregulated although not significant. Necrosis is not T-cell mediated, which is typically apoptotic (Martinez-Lostao et al., 2015; Voskoboinik et al., 2015; Jaime-Sanchez et al., 2020; Galluzzi et al., 2008). Instead, tumour necrosis is caused by metabolic stress such as hypoxia and by recruitment of innate immune cells such as macrophages and neutrophils (Mantovani et al., 2022; Yee et al., 2021; Liu et al., 2019b; Wallach et al., 2016). It has been reported to play both tumour promoting and suppressing roles; inflammatory pathway triggered by necrotic cells can promote anti-tumour immunity (Yatim et al., 2015; Snyder et al., 2019; Kearney et al., 2017), but others report that intracellular components released from necrotic cells as well as RIPK1 and RIPK3 can lead to tumour progression (Eil et al., 2016; Seifert et al., 2016; Karsch-Bluman et al., 2019). In prostate cancer, some link necrosis with poor prognosis and clinical outcomes (Acosta et al., 2018), but others suggest that promoting prostate cancer cell necroptosis can suppress cancer cell proliferation (Wu et al., 2024; Beretta et al., 2022).

This increase in necrosis could also be explained by immunogenic cell death, which induces damage-associated molecular patterns (DAMPs) and triggers macrophage recruitment (Gamrekelashvili et al., 2015; Kroemer et al., 2022). This also explains upregulation of macrophage migration in combination-treated, necrotic tumours (Figure 3.19).

The results from IHC and bulk RNA sequencing of the tumours were different between the pilot and the repeat experiment. As tumours were left to grow for longer in the repeat experiment, there may have been differences in TIME remodelling (Allen et al., 2020). In addition, whole tumours were used during the pilot experiment, whereas tumours were cut and distributed for various experiments in the repeat experiment, so tumours cut for IHC could have captured different TME than the tumours cut for bulk RNA sequencing.

In the pilot experiment, there was a decresing trend of IGF-1R phosphorylation in all groups compared to control but no difference in downstream S6 phosphorylation (Figure 3.9a), which could be explained by negative feedback loop (Zhang et al., 2015). In the repeat experiment, however, only xentuzumab-treated tumours had lower IGF-1R phosphorylation then control, though S6 phosphorylation were decreased in all treatment, significant in anti-PD-1-treated tumours compared to control (Figure 3.25). This suggests that either the way the drugs were given (separate versus mixed) or the difference in tumour size could have affected the treatment effect. In the repeat experiment, anti-PD-1 led to significant increase in intra-tumoral cell apoptosis. Although several studies using anti-PD-1 demonstrated increase in apoptosis by effector T cells (Haikala et al., 2019; Wang et al., 2022a), it cannot be certain death of which types of cells caused an increase in CC3. Similar trends of some of the T cell markers seen in anti-PD-1 and xentuzumab-treated tumours could be explained by crosstalk between IGFs and T cell stimulating pathways. IGF-1 regulates AKT, NF-κB, and ERK pathways, which are also downstream pathways of T-cell receptors and affected by anti-PD-1 treatment (Idelman et al., 2007; Kiernan et al., 2024; Patsoukis et al., 2012). Inhibition of these pathways by anti-PD-1 may have resulted in paracrine signaling from immune cells.

There were no significant differences in T cell markers CD4 and FoxP3 in both pilot and the repeat experiments, but in the pilot experiment, there was an increase in CD8 T cell infiltration in combination-treated tumours (Figure 3.9 and 3.25). Although not significant, the trend was consistent with published study in a lung cancer model,

which showed higher CD8+ T cell infiltration upon IGFs and PD-1 blockade (Ajona et al., 2020). In the repeat experiment, there was almost undetectable CD8 expression (Figure 3.26), which could be attributed to low CD8+ T cell numbers in prostate cancer TME (Vitkin et al., 2019; Ebelt et al., 2008). In the repeat experiment, there was a decrease in PD-1 in xentuzumab and combination-treated tumours compared to control (Figure 3.25). TILs with low PD-1 is associated with better clinical outcome in cancers (Mazzaschi et al., 2018).

Bulk RNA sequencing showed several immune-related pathways deregulated by co-inhibition of IGF-1 and PD-1/PD-L1 axis, such as myeloid leukocyte migration, response to TGF-β, and positive regulation of cytokine production (Figure 3.18). Further GeneFEAST analysis highlighted these pathways (Figure 3.19). EMT-related genes were deregulated by xentuzumab and anti-PD-1 treatment, which was expected with reports that suggest role of IGFs in promotion of EMT (Graham et al., 2008; Li et al., 2017).

For the first time, we found that co-inhibition of IGF and PD-1/PD-L1 axis leads to increase in genes associated with myeloid leukocyte migration (Figure 3.19c). Combination versus xentuzumab treatment also yielded upregulation of immune-related pathways, such as lymphocyte-mediated immunity and leukocyte proliferation, which is expected with reports of anti-PD-1 treatment affecting immune cell activities (Tumeh et al., 2014; Caushi et al., 2021). This was further validated by qRT-PCR (Figure 3.20). Pf4, a chemokine that induces differentiation of monocytes to macrophages (Scheuerer et al., 2000; Jian et al., 2017), was significantly upregulated by IGF-1R and PD-1 co-inhibition (Figure 3.20b). Tgfb3, an immunosuppressive cytokine that skews macrophages to be M2-like (Zhang et al., 2016a; Kelly et al., 2018), was significantly downregulated in anti-PD-1 and combination treatments compared to control (Figure 3.20c). Ccl9 is a macrophage inflammatory protein that recruits myeloid progenitors for tumour cell invasion (Kitamura et al., 2007; Yan et al., 2015), which was upregulated by combination treatment (Figure 3.20d). Mmp12, secreted by pro-inflammatory macrophages and reportedly contributes to tumour cell death (Houghton

et al., 2006; Dandachi et al., 2017; Aristorena et al., 2019), was increased in combination-treated tumours compared to controls (Figure 3.20e). Lyn, a Src-family kinase that regulates signalling in myeloid progenitor subtypes and mature myeloid cells (Scapini et al., 2009; Krebs et al., 2012; Zardan et al., 2014; Jiang et al., 2022), was downregulated by anti-PD-1 + xentuzumab treatment (Figure 3.20f).

Pathway enrichment analysis of xentuzumab treatment versus control comparison showed decrease in genes associated with antigen processing and MHC-II complex (Figure 3.17). In particular, Cd74, which encodes for receptors for macrophage inhibitory factor (MIF) and is overexpressed in prostate cancers (Meyer-Siegler et al., 2006; Li et al., 2024; Tuong et al., 2021), was significantly downregulated in all treatments compared to control (Figure 3.21a). Xentuzumab significantly reduced Ccr2 (Figure 3.21b), which promotes monocyte/macrophage recruitment and is associated with cancer progression (Sayed et al., 2022; Boniakowski et al., 2018; Willenborg et al., 2012; Fei et al., 2021; Lu et al., 2007; Tu et al., 2020; Fein et al., 2020). In addition, H2-Aa, murine MHC-II component, was significantly decreased in xentuzumab-treated tumours, compared to combination-treated and control tumours (Figure 3.22a). This was consistent with the enriched pathway analysis (Figure 3.17) as well as a report in TAO, where IGF-1 inhibitors including FDA-approved teprotumumab reduced MHC II expression in fibrocytes, suggesting that IGF blockade may reduce Th1 and Th17-polarised T cells (Fernando et al., 2021). Combination treatment further reduced angiogenesis marker Vegfa and autophagy marker Atg14 expression compared to xentuzumab (Figure 3.22b-c), suggesting that IGF-1 blockade has a potential to strengthen anti-metastatic effects of anti-PD-1.

Changes in macrophage-related genes as well as necrosis in these tumours led to IHC of macrophage markers. In the first *in vivo* experiment comparing xentuzumab-treated tumours with control, there were no difference in myeloid-marker CD68 but a significant increase in pan-macrophage marker F4/80 (Figure 3.12). Despite CD68 being a marker of macrophage activation, it also is a more general marker for mononuclear phagocytes, and F4/80 is a more accurate marker for mature murine macrophages (Lloyd et al.,

2008; Chistiakov et al., 2017). This also suggests that the interpretation of results may vary depending on which macrophage markers are used to determine macrophage subtypes via co-localisation of two markers. In xentuzumab-treated tumours, M1-like and M2-like macrophage numbers were significantly reduced (Figure 3.12). The decrease in M2 macrophages upon IGF blockade was consistent with a report that IGF signalling increases M2 macrophage activation (Spadaro et al., 2017).

In the pilot xentuzumab ± anti-PD-1 experiment, there was a significant decrease in M2 macrophage marker CD163 and an increasing trend of M1 macrophage marker iNOS in combination-treated tumours compared to control (Figure 3.13). In the repeat experiment, there was a significant increase in F4/80 and iNOS in combination-treated tumours compared to control, whereas CD163 expression was decreased in all treatments compared to anti-PD-1-treated tumours (Figure 3.27). This shift in macrophage polarisation is consistent with reports of anti-PD-1/PD-L1 therapy affecting macrophage maturation, function, and population (Gubin et al., 2018; Zhang et al., 2023a; Xiong et al., 2019; Gordon et al., 2017).

From the repeat experiment, tumours, spleens, and PBMCs collected from the mice were processed for flow cytometry (Figure 3.28). Although there were no differences in CD4+ and CD8+ T cells with either treatments, IGF blockade led to decrease in CD4+FoxP3+ Tregs as well as IFN-γ production of the Tregs (Figure 3.28a-c). This is consistent with previous studies that show Treg stimulation with IGF-1 treatment (Bilbao et al., 2014; Shapiro et al., 2023; Kiernan et al., 2024). Interestingly, anti-PD-1 treatment significantly reduced xentuzumab-driven decrease in Tregs, and the combination treatment significantly increased CD8+ T cell/Treg ratio with significantly higher granzyme B expression in CD8+ T cells compared to all treatments, (Figure 3.28d-f), consistent with published studies (Dyck et al., 2016; Ajona et al., 2020; Geels et al., 2024; Leung et al., 2023; Capasso et al., 2019). In addition, analysis of spleen and PBMCs of these mice showed significant increase in effector memory CD4+ and CD8+ T cells upon xentuzumab treatment (Figure 3.28g-j). These effector memory cells secrete high levels of IFN-γ and perforin and play an important role in anti-tumour response

(Sallusto et al., 1999; Han et al., 2020; Stemberger et al., 2007). Other studies of IGF blockade have shown both local and systemic immune changes in cancer (Moody et al., 2014; Bilbao et al., 2014), but this has not been shown with xentuzumab previously. These local (tumour) and systemic (spleen and PBMCs) immune changes suggest that, despite no tumour regression, IGF blockade as well as IGFs and PD-1 co-inhibition have a potential to enhance immune cell activation.

RNA sequencing of the repeat experiment, in contrast with the pilot experiment, did not show any significant pathways. Most of the deregulated genes were keratin-associated genes, which were downregulated upon combination treatment compared to control (Figure 3.30). This could be related to fibrosis and necrosis in the tumour tissues (Cao et al., 2016; Ku et al., 2016). In prostate cancer, keratins are expressed by basal and luminal cells (van Leenders et al., 2001; Verhagen et al., 1988), and studies suggest keratin as enriched in prostate cancer stem-like cells (Hu et al., 2021a; Trompetter et al., 2008). Keratinocytes, in addition to its role in hair formation, are regulated by growth factors, specifically TGF-β signalling (Wu et al., 2008; Takahashi et al., 2022; Hashimoto, 2000). Krtap genes have been reported to be associated with proliferation and migration of breast, head and neck, and oral cancer cells (Sack et al., 2018; Takahashi et al., 2022). In addition, IL-7r, highly expressed by conventional mature T cells and required for T cell survival (Belarif et al., 2018; Szabo et al., 2019; Schluns et al., 2000), was downregulated upon IGF-1 and PD-1 blockade (Figure 3.28). In prostate cancer, IL-7r and its ligand Il-7 are upregulated and promote prostate cancer invasion and migration (Qu et al., 2016; Seol et al., 2019).

Among 59 genes deregulated in xentuzumab-treated tumours compared to control, Il-10ra was significantly downregulated (Figure 3.29). IL-10ra is mainly expressed in macrophages, DCs, and lymphocytes (Llopiz et al., 2016; Saraiva et al., 2019), and its ligand IL-10 could act as both anti-inflammatory and immune-promoting cytokine (Carlini et al., 2023; Oft, 2014; Ouyang et al., 2019). The lack of meaningful results in the bulk RNA sequencing of the repeat experiment could be explained by large

heterogeneous tumours. As seen in flow cytometry (Figure 3.28), analysis of the tumours in single-cell or spatial resolution would have been more ideal.

In this chapter, pharmacological inhibition of IGF blockade via xentuzumab was used to investigate the effects of IGFs *in vitro* and *in vivo*. Several studies have been done using genetic manipulation with antisense IGF-1 cDNA or IGF-1R knockout cells (Trojan et al., 1993, Obr et al., 2022; Wang et al., 2019), and although we could have used siRNA or genetically modified cell lines of IGF-1R, we specifically wanted to explore the effects of xentuzumab (in relation to WINGMEN trial) and did not pursue this. Testing the specificity of xentuzumab with IGF-1 or IGF-1R knockout cell lines would have been beneficial, though previous studies report that xentuzumab is more responsive in cell lines that express high IGF-1 or IGF-1R mRNAs (Friedbichler et al., 2014).

Overall, preclinical *in vitro* work confirmed the ability of xentuzumab to block IGF-1R signalling and reduce cell viability *in vitro*. Although xentuzumab did not inhibit tumour growth *in vivo*, there were changes in the TIME suggested by reduction in *Igf1r* and *Mki67* at the RNA level and decrease in CD4 T cells at the protein level. Despite heterogeneity of tumours in the xentuzumab ± anti-PD-1 *in vivo* experiments, we were able to discover significant increase in necrosis as well as systemic immune changes involving T cells and macrophages. Although not effective for tumour growth control, this combination needs additional tumour controlling agent that are standard-of-care, such as those that target AR or are used for PARP inhibition.

4

Effects of IGFs on macrophage phenotype and function in prostate cancer

Contents

4.1 Introduction 126
4.2 Effects of cancer cell co-culture on macrophage phenotype 130
4.2.1 Macrophage polarisation 130
4.2.2 Effects of IGF-1R signalling inhibition on human prostate cancer cell lines 133
4.2.3 Effects of co-culture on murine macrophage polarisation . . . 136
4.2.4 Effects of co-culture on human macrophage polarisation . . . 136
4.2.5 Cytokine array of co-culture conditioned medium 139
4.3 Effects of IGF axis manipulation on macrophage phenotype 141
4.3.1 Conditioned medium of xentuzumab-treated Myc-CaPs assessed by cytokine array 141
4.3.2 Effects of IGF axis manipulation on macrophage polarisation 143
4.4 CD47 and prostate cancer 146
4.4.1 CD47 expression in prostate cancer cells 146
4.4.2 Testing effects of anti-CD47 on IGF-1R signalling 149
4.5 Effects of IGF-1, anti-IGF and/or anti-CD47 on cancer cell phagocytosis 152
4.5.1 Testing conditions for phagocytosis assays 152
4.5.2 Assessing the effects of IGF-axis manipulation on phagocytosis 155
4.5.3 Investigating the effects of xentuzumab on anti-CD47-induced phagocytosis 158
4.6 Investigating the effects of IGFs on macrophages regulating T cell effector functions 161
4.7 Discussion 168

4.1 Introduction

As previously discussed in Chapter 1.5.2, IGFs can affect innate immune cells and their immune responses to cancer (Spadaro et al., 2017; Ni et al., 2013; Huang et al.,

2015). Findings from previous chapter identified macrophages as one of the key immune regulators of IGF blockade in prostate cancer (Figure 3.12, 3.13, 3.19, and 3.27).

Macrophages can be polarised to different subtypes in response to cytokines and the innate and adaptive immune signals (Mills et al., 2000; Mantovani et al., 2002). IFN-γ produced by Th1 and NK cells and TNF produced by APCs can classically activate macrophages into M1 type. They express co-stimulatory molecules such as CD80 and CD86, secrete pro-inflammatory cytokines such as IL-6, IL-12, IL-1β, and TNFα, and have microcidal and tumoricidal functions (Chen et al., 2023b). They also express inducible nitric oxide synthase (iNOS), which uses L-arginine to produce nitric oxide that plays a critical role in host defense in inflammatory conditions (Palmieri et al., 2020; Sica et al., 2012; Bogdan et al., 2000; Lu et al., 2015). M2 macrophages can be alternatively activated by granulocytes and Th2 cells-induced IL-4, IL-10, and IL-13. These express CD163 and CD206, and are involved in tissue remodelling and repair, promote angiogenesis, and secrete anti-inflammatory cytokines such as IL-10, IL-1 receptor antagonist (IL-1RA), and TGF-β (Mosser et al., 2008; Mantovani et al., 2004; Wang et al., 2024). They express arginase 1 (ARG1), which hydrolyses L-arginine to L-ornithine, important for tissue damage repair (Rath et al., 2014; Mantovani et al., 2002). Macrophages are plastic and capable of shifting their phenotypes in response to environmental signals, contributing to disease resolution or progression (Mosser et al., 2008; Stout et al., 2005; Yaddanapudi et al., 2013). Recent studies have reported on plasticity of various macrophage subtypes and have begun to move away from the dichotomy of just M1 and M2 macrophages (Mantovani et al., 2022; Zhang et al., 2023b). For simplicity in this thesis, we referred to pro-inflammatory macrophages as 'M1' or 'M1-like' and all subtypes of anti-inflammatory M2 macrophages as 'M2' or 'M2-like'.

Specfically, macrophages are important for host defense and anti-microbial actions, and TAMs are a major part of the TME. They are crucial phagocytic cells that engulf microbes or other cells, initiating immune activities and maintaining tissue homeostasis (Mosser et al., 2008; Dooling et al., 2023; Chao et al., 2012; Kershaw

et al., 2013). A cell surface protein CD47, expressed by all cells including tumour cells, protects itself from phagocytosis by binding to SIRPα, present in macrophages and DCs (Majeti et al., 2009; Brown et al., 2001b). This interaction results in phosphorylation of immunoreceptor tyrosine-based inhibition motifs (ITIMs) on SIRPα's cytoplasmic tail and the recruitment of Src homology phosphatase-1 (SHP-1) and SHP-2 phosphatases. This is thought to block phagocytosis by preventing myosin-IIA accumulation at the phagocytic synapse (Timms et al., 1998, Kharitonenkov et al., 1997, Oldenborg et al., 2000, Osorio et al., 2023) and activating the "don't eat me" signal (Jaiswal et al., 2010; Willingham et al., 2012; Morrissey et al., 2020; Oldenborg et al., 2001).

There is a possible link between CD47, SIRPα, and IGF axis (Figure 4.1). In addition to the well-known CD47 and SIRPα interaction to regulate phagocytosis in trans, Clemmons lab reported that, integrin associated protein (IAP), also known as CD47, phosphorylates SHPS-1 and regulates further signalling effects of SRC homology 2 domain-containing protein tyrosine phosphatase substrate-1 (SHPS-1, SIRPα) in cis. IGFs binding to IGF-1R can also lead to phosphorylation of SIRPα and activate the downstream signalling pathway (Clemmons et al., 2005; Tahimic et al., 2013; Melo Garcia et al., 2021).

In addition, macrophages can regulate T cell functions in TME. Several reports suggest that macrophages can directly suppress T cell functions due to their Arg1 or iNOS expression that impacts T cell response (Doedens et al., 2010; Kusmartsev et al., 2005; Movahedi et al., 2010; Rodriguez et al., 2004; Bronte et al., 2005b). Macrophages can also indirectly regulate T cell recruitment and intratumoral localisation via CSF-CSF1R pathway, VEGFA expression, CCR2 inhibition, or CCL2/CCL5 nitration (Zhu et al., 2014; Mitchem et al., 2013; Shiao et al., 2015; Molon et al., 2011; Franciszkiewicz et al., 2012; Stockmann et al., 2008; Quaranta et al., 2018). In addition, macrophage's phagocytic clearance of DAMPs and subsequent pathways avoiding activation of cytosolic sensors can indirectly regulate T cell response (Roberts et al., 2017; Broz et al., 2014; Cunha et al., 2018; Han et al., 2016; Quail et al., 2016; Salmon et al., 2016; DeNardo et al., 2019). M1-like macrophages, in particular, have been reported

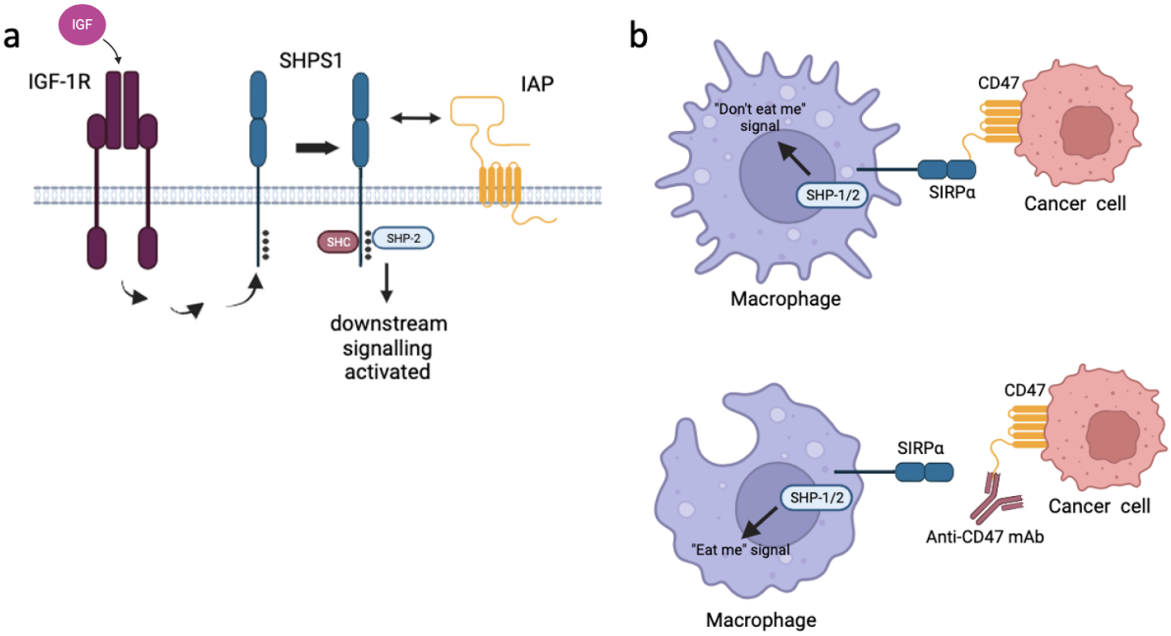


Figure 4.1: Functional interactions between IGF axis, IAP/CD47 and SHPS1/SIRPα in cis and trans. a. When IGF-1R is activated by IGF-1, phosphorylation of SRC homology 2 domain-containing protein tyrosine phosphatase substrate-1 (SHPS-1/SIRPα) recruits phosphatase SHP-2, activating MAPK and PI3K pathways. Integrin associated protein (IAP)/CD47 also associates with SHPS-1 phosphorylation, acting in cis to regulate IGF-1R phosphorylation. **b**. CD47 expressed by tumour cells interacts in trans with macrophage SIRPα to inhibit phagocytosis. Due to this function, CD47 is a key target for immunotherapy of cancer. Figure modified from references cited in the text and drawn in BioRender.

to restore anti-tumour immunity by promoting Th1 cell responses and improving T cell recruitment (Klug et al., 2013; Rolny et al., 2011; Johansson et al., 2012; Murray et al., 2011). Recent study showed that combination of anti-CD47 and chimeric antigen receptor (CAR)-T cells with engineered CD47 (so that they are not subject to clearance by macrophages) led to enhanced antitumour effects in osteosarcoma (Yamada-Hunter et al., 2024).

Several preclinical and clinical studies targeting macrophages have been published in various cancers such as ovarian, colon, and prostate cancers (Mantovani et al., 2002; Rodriguez-Garcia et al., 2021; Tian et al., 2022; Al-janabi et al., 2024; Kloosterman et al., 2023). The aim of this chapter was to identify how IGF affects phenotype and phagocytic function of macrophages in prostate cancer, as well as its consequences on T cell activity. The results of this chapter could shed light on a novel therapy targeting

macrophage functions in addition to IGF activity.

4.2 Effects of cancer cell co-culture on macrophage phenotype

Before assessing the effects of cancer cell co-culture on macrophage phenotype, I first optimised polarisation of murine J774 macrophages and BMDMs and human PBMC-derived macrophages.

4.2.1 Macrophage polarisation

Murine BMDMs and J774 cells were isolated and polarised as in Figure 4.2a. About 50% and 20% of unpolarised BMDMs expressed M1 marker CD80 and M2 marker CD206, respectively. Upon polarisation, almost all M1-polarised BMDMs expressed CD80, significantly higher percentage than unpolarised or M2-polarised BMDMs (Figure 4.2b), and 60% of M2-polarised BMDMs expressed CD206, significantly more than unpolarised or M1-polarised BMDMs (Figure 4.2c). Moreover, almost 100% of M1-polarised J774 macrophages expressed CD80, significantly higher than unpolarised J774 (30%) or M2-polarised J774 (30%) (Figure 4.2d). M2 polarisation of J774 macrophages resulted in about 70% expressing CD206, significantly more than unpolarised (30%) or M1-polarised (40%) J774 macrophages (Figure 4.2e). This suggests that J774 macrophages are more responsive to polarisation and a more sensitive model to assess the impact of IGF axis inhibition.

Human PBMC-derived macrophages were isolated and polarised as in Figure 4.3a. At baseline, about 18% of unpolarised macrophages expressed CD80, and 45% expressed CD206. Upon polarisation, 27% of the M1-polarised macrophages expressed CD80, significantly more than 15% of M2-polarised macrophages (Figure 4.3b). M2 polarisation led to almost 80% expressing CD206, significantly higher compared to 10% of M1-like macrophages that expressed CD206 (Figure 4.3c). Hereupon, macrophages were double-gated to represent M1-like and M2-like macrophages, as in Figure 2.1b and 2.1c.

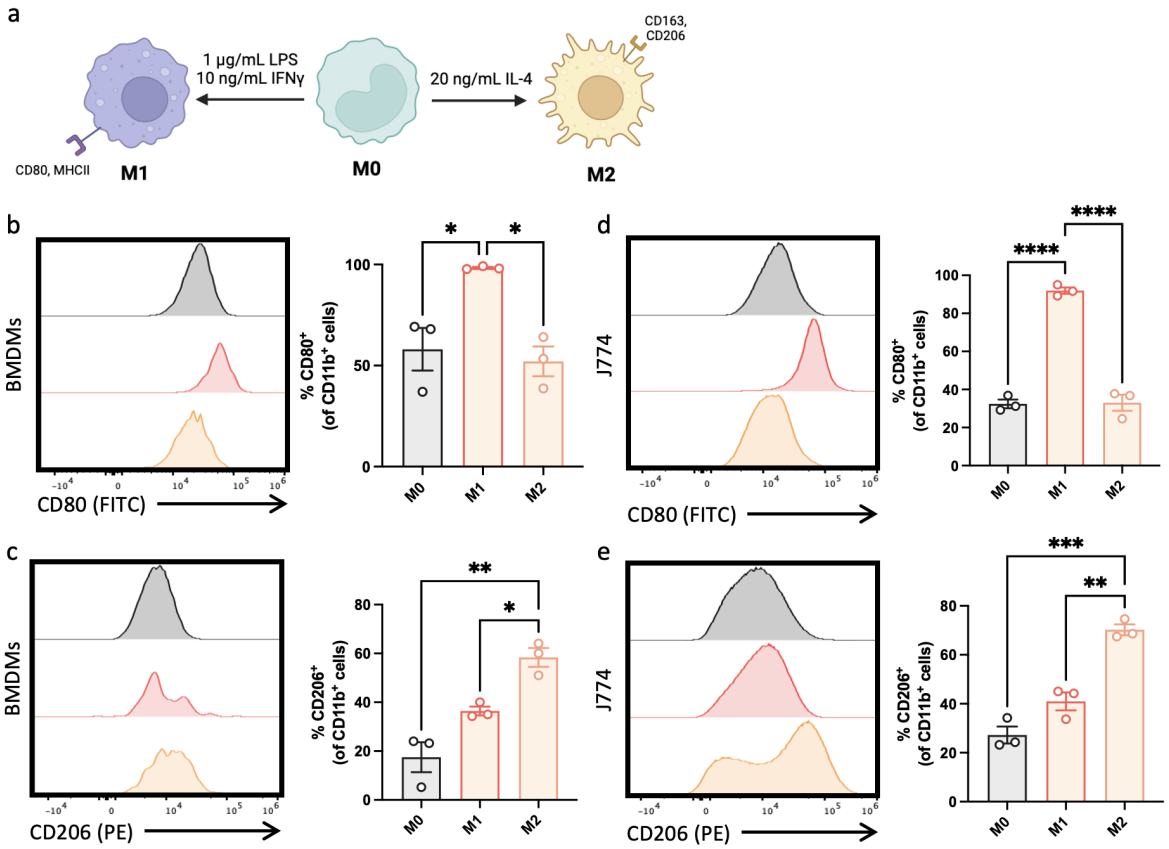


Figure 4.2: Murine macrophage polarisation. a. Unpolarised M0 BMDMs and J774 cell lines were seeded in ultra low-attachment T75 flask and polarised to M1 and M2 macrophages by adding 1 μg/mL LPS and 10 ng/mL IFNγ, and 20 ng/mL IL-4, respectively, for 48 hours. Polarised macrophages were dissociated and stained with Live/Dead, F4/80, CD80, and CD206 in preparation for flow cytometry. All F4/80+ BMDMs (**b-c**) and J774 macrophages (**d-e**) were gated for CD80 positivity to determine M1-like macrophage population (**b, d**) and for CD206 positivity to determine M2-like macrophage population (**c, e**). Data are presented as mean ± SEM from at least three independent experiments. (*p<0.05, **p<0.01, ***p<0.001, ****p<0.001, one-way ANOVA with multiple comparisons)

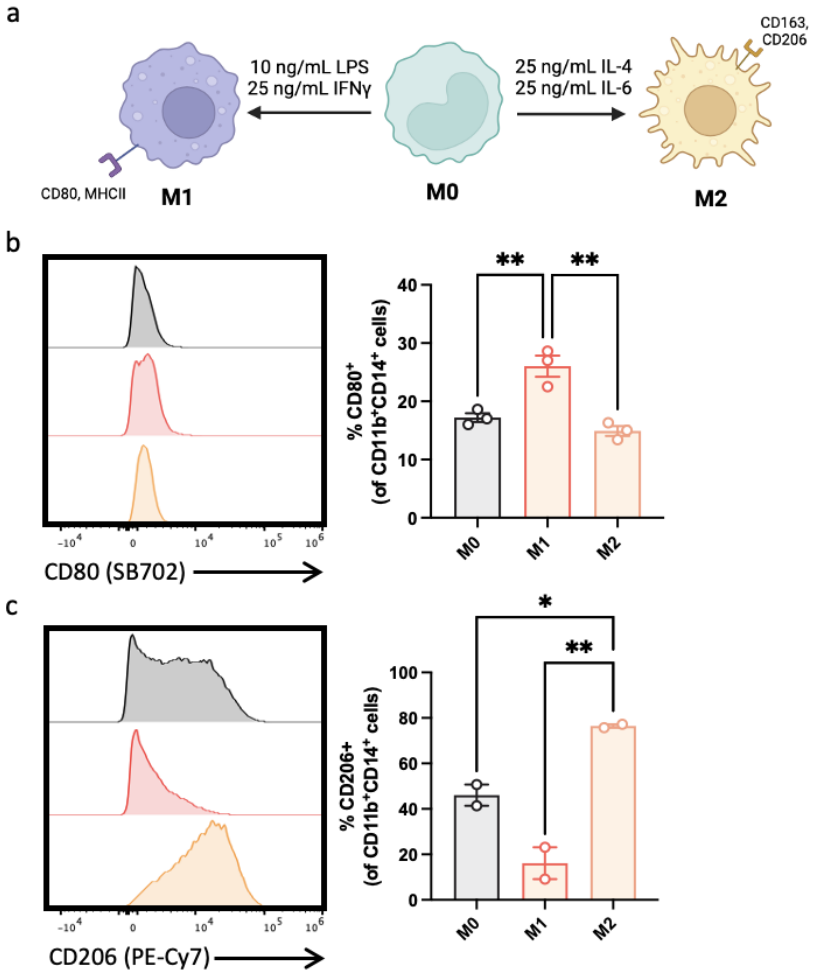


Figure 4.3: Human macrophage polarisation. a. Unpolarised M0 PBMC-derived macrophages were seeded in ultra low-attachment T75 flask and polarised to M1 and M2 macrophages by adding 10 ng/mL LPS and 25 ng/mL IFNγ, and 25 ng/mL IL-4 and 25 ng/mL IL-6, respectively, for 48 hours. Polarised macrophages were dissociated and stained with Live/Dead, CD14, CD11b, CD80, and CD206 in preparation for flow cytometry. All CD11b+CD14+ macrophages were gated for **b**. CD80 positivity to determine M1-like macrophage population and **c**. CD206 positivity to determine M2-like macrophage population. Data are presented as mean ± SEM from at least three independent experiments. (*p<0.05, **p<0.01, one-way ANOVA with multiple comparisons)

4.2.2 Effects of IGF-1R signalling inhibition on human prostate cancer cell lines

Before testing the effects of human cancer cell and macrophage co-culture on macrophage polarisation, western blot was performed to check the responses of the human prostate cancer cells to xentuzumab in terms of cell signalling and proliferation. As in Chapter 3.2.1, human prostate cancer cells were treated with IGF-1 and/or a single concentration of 1 μM xentuzumab and lysed for western blot.

Both DU145 and 22Rv1 showed significant decrease in IGF-1R phosphorylation, with 90% reduction upon xentuzumab treatment (Figure 4.4). There was no difference in ERK phosphorylation in 22Rv1, possibly due to negative feedback loop (Lito et al., 2012; Lake et al., 2016). Both cell lines also reduced in viability with xentuzumab treatment (Figure 4.5), consistent with the results with murine prostate cancer cell lines in Figure 3.1 and 3.2a. This confirms the ability of xentuzumab to block IGF-1R signalling and viability in human prostate cancer cells.

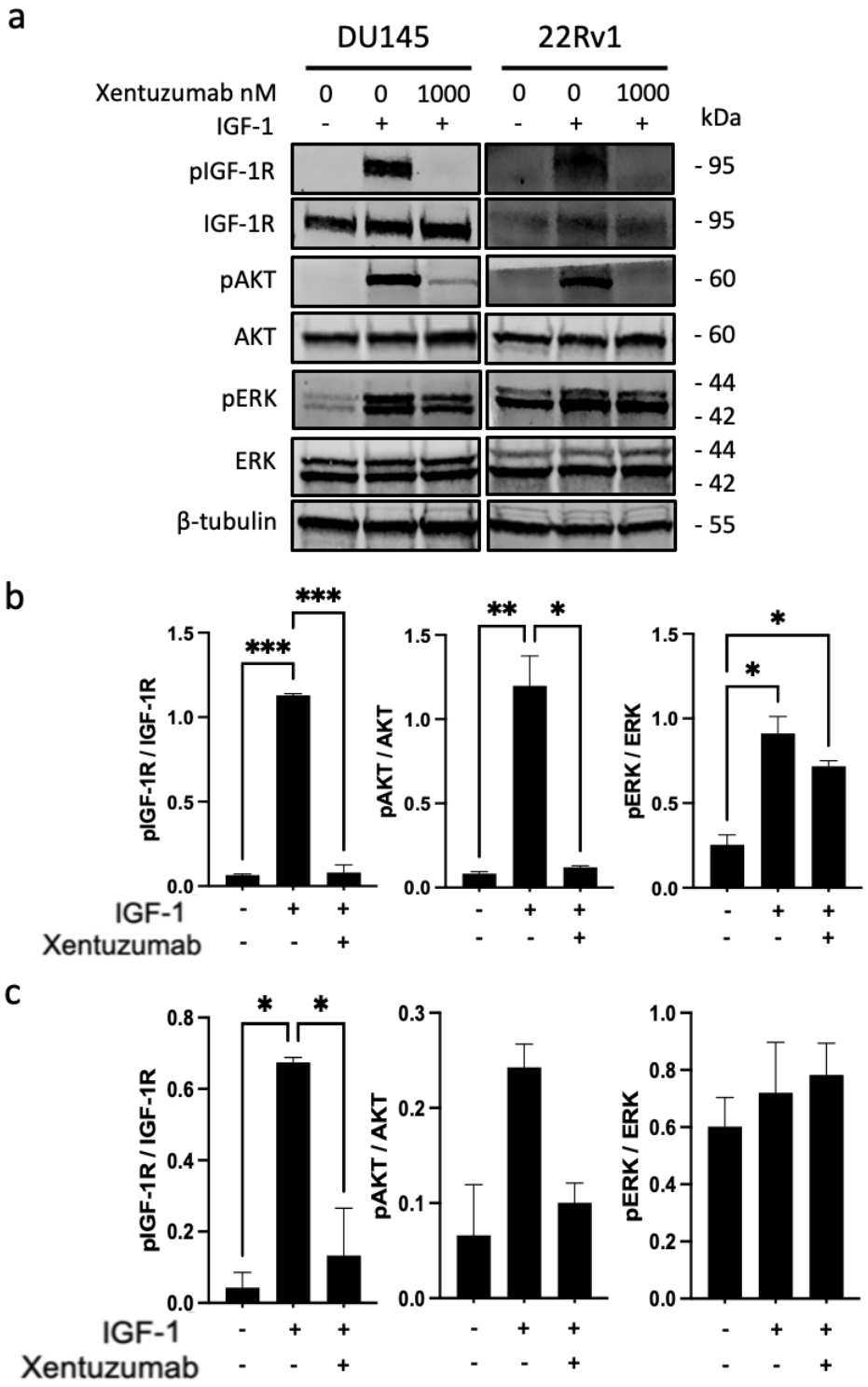


Figure 4.4: Response of human prostate cancer cells to IGF neutralising antibody xentuzumab. DU145 and 22Rv1 cells were serum-starved and treated with PBS control or xentuzumab for 16 hours and with 50 nM IGF-1 for the final 20 minutes. **a**. The proteins involved in IGF-1R signalling pathway were measured using western blot (n=3 independent repeats per cell line) Phosphorylated IGF-1R, AKT, and ERK levels of **b**. DU145 and **c**. 22Rv1 were quantified after normalising to the loading control β-tubulin using Fiji ImageJ. Graphs are presented as mean ± SEM. (*p<0.05, **p<0.01, ***p<0.001, one-way ANOVA with multiple comparisons)

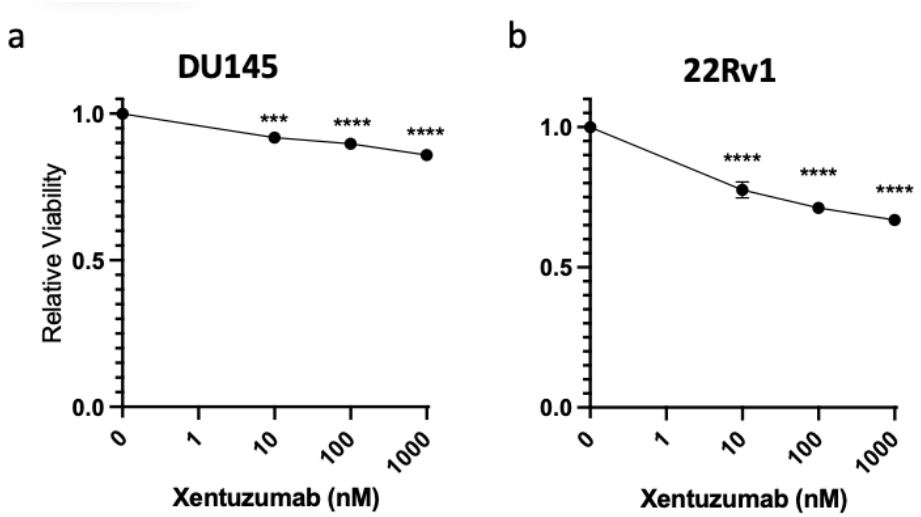


Figure 4.5: Effects of IGF blockade on 2D growth of human prostate cancer cells. a. DU145 and **b**. 22Rv1 cells treated with PBS control or 1 μM xentuzumab were seeded in 96-well plates, and CellTiter Blue viability test was performed after 5 days. Data are presented as the mean ± SEM from at least three independent repeats per cell line (***p<0.001, ****p<0.0001, one-way ANOVA with multiple comparisons)

4.2.3 Effects of co-culture on murine macrophage polarisation

To assess the effects macrophage and cancer cell co-culture have on macrophage phenotype, unpolarised J774 macrophage cell line was co-cultured with Myc-CaP and PTEN-CaP8. As seen in Figure 4.6a, Myc-CaP and J774 co-culture significantly increased CD206 expression in macrophages after 72 hours. When co-cultured with PTEN-CaP8 cell line, there was no difference in macrophage phenotype (Figure 4.6b), suggesting that the lack of PTEN in cancer cells may cause no changes in macrophage polarisation. The experiment was repeated with BMDMs, whose CD206 expression was also significantly increased upon 72-hour co-culture (Figure 4.6c). This shows that the presence of Myc-CaP increases macrophage polarisation towards M2-like phenotype.

4.2.4 Effects of co-culture on human macrophage polarisation

The effects of human macrophage and cancer cell co-culture on macrophage phenotype were assessed by co-culturing PBMC-derived macrophages with 22Rv1 and DU145 for 24 - 72 hours. The results were consistent with murine co-culture, with significantly higher CD206 expression with 72-hour co-culture in both human prostate cancer cell lines (Figure 4.7). CD80 expression was also significantly increased in 72-hour macrophage co-culture with 22Rv1, but not with DU145.

Together, these results demonstrate that both PTEN WT murine and human cancer cells and macrophage co-cultures for 72 hours increase CD206 expression in macrophages, driving them to be M2-like.

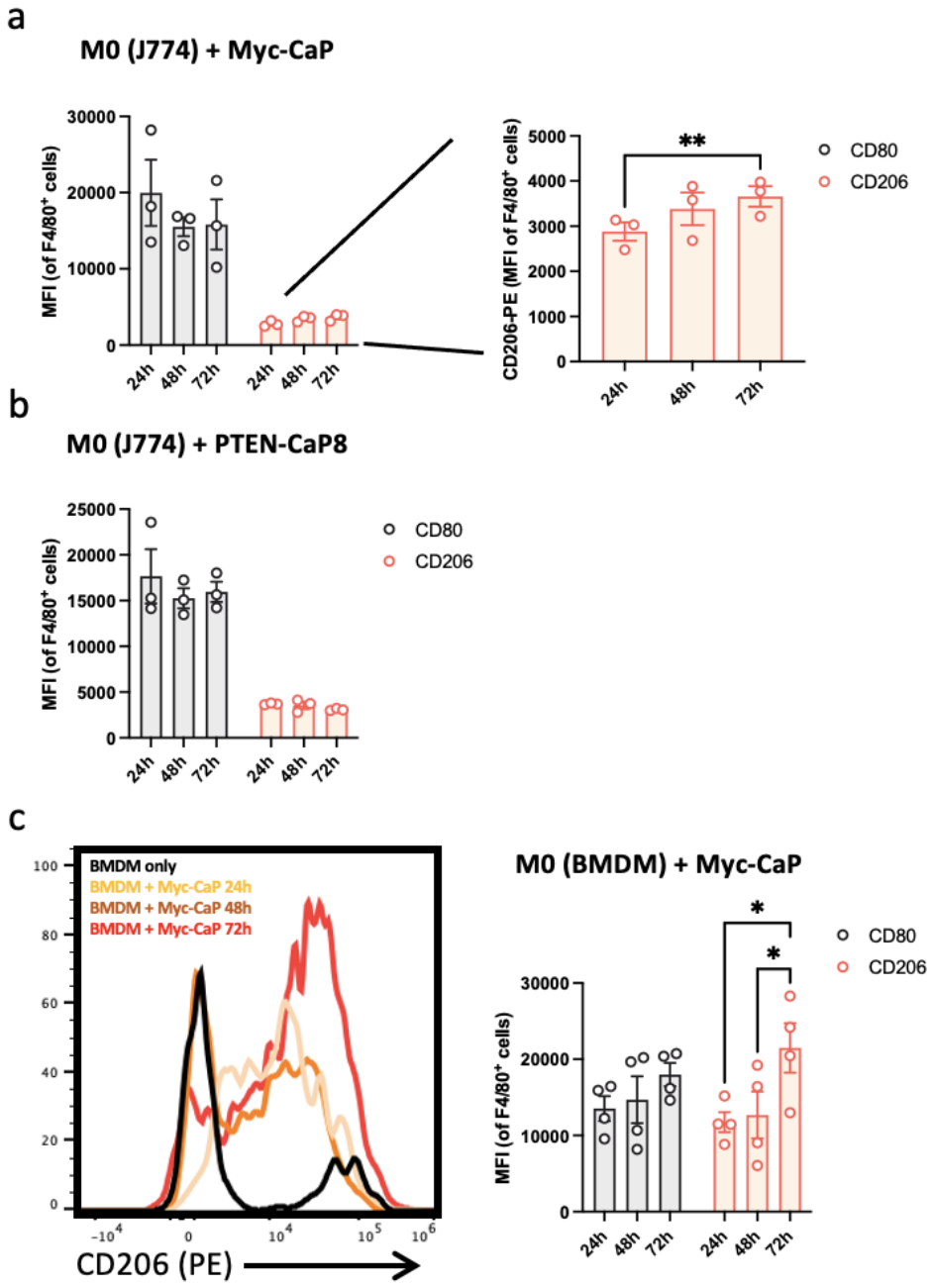


Figure 4.6: Effects of co-culture on murine macrophage phenotype. Unpolarised M0 macrophages and cancer cells were seeded in ultra-low adherent 96-well plates for 24, 48, and 72 hours. Cell surface expression of CD80 and CD206 was assessed by flow cytometry in co-cultures of **a**. murine J774 macrophages + Myc-CaP (right: magnified graph of CD206-PE MFI, **p<0.01, one-way ANOVA with multiple comparisons), **b**. murine J774 macrophages + PTEN-CaP8, and **c**. murine BMDM + Myc-CaP, Data represents the mean fluorescence intensity (MFI) of F4/80+ macrophages of at least threee repeats. Error bar shows mean ± SEM. (*p<0.05, two-way ANOVA with multiple comparisons)

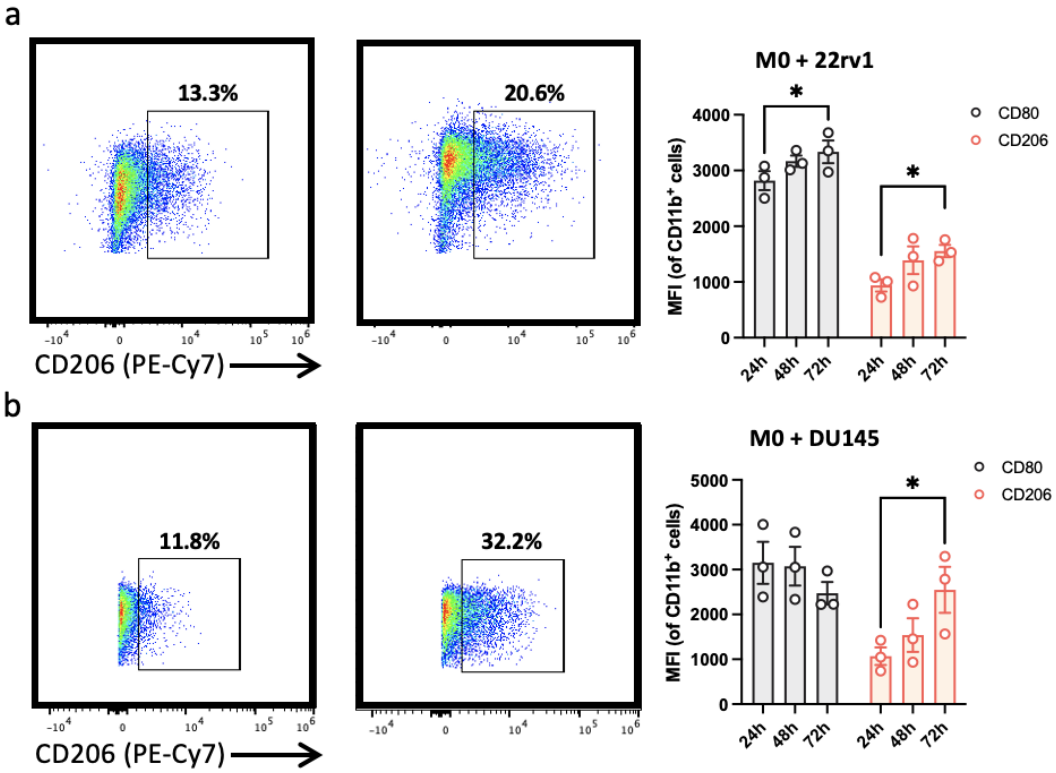


Figure 4.7: Effects of co-culture on human macrophage phenotype. Unpolarised M0 PBMC-derived macrophages and cancer cells were seeded in ultra-low adherent 96-well plates for 24, 48, and 72 hours. Cell surface expression of CD80 and CD206 was assessed by flow cytometry in co-cultures of macrophages and **a**. 22Rv1, and **b**. DU145. Data represents the mean fluorescence intensity (MFI) of CD11b+ macrophages of 3 repeats, with error bar showing mean ± SEM. (*$p<0.05$, two-way ANOVA with multiple comparisons)

4.2.5 Cytokine array of co-culture conditioned medium

To investigate whether macrophages and cancer cells secrete cytokines and whether this is affected by co-culture, we used a semi-quantitative approach (cytokine array) to assess levels in conditioned media of BMDMs and of 24, 48, and 72 hour co-culture with Myc-CaPs.

Of the 25 cytokines on the array known to affect macrophage polarisation, 8 were detectable: CXCL1, M-CSF, CCL2, CCL3, CXCL2, and IL-1RA were upregulated in 72 hour co-culture, and CXCL12 was downregulated (Figure 4.8). Tissue inhibitor of metalloproteinase 1 (TIMP-1) expression was high in all conditions. Of these, CXCL1, CCL2, and CCL3 were detectable at mutiple timepoints in co-culture and showed a temporal increase in expression. The strongest candidates as mediators of changes in macrophage polarisation were CXCL1, CCL3, and CXCL2, as they were not detectable in BMDM alone and were detectable at at least two co-culture timepoints.

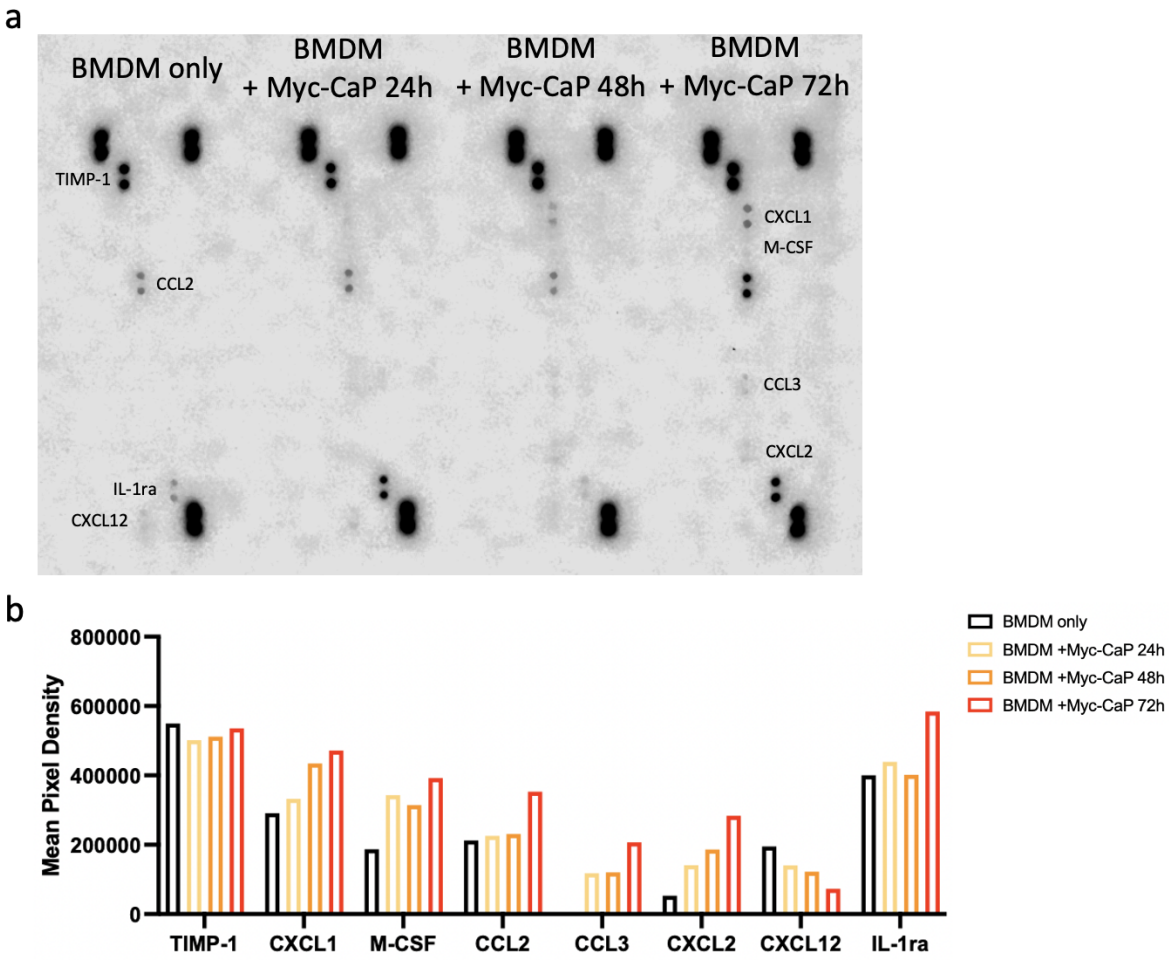


Figure 4.8: Comparing the conditioned media of BMDMs and of 24-72 hour co-culture with prostate cancer cells. a. Conditioned media from BMDM cultures and from BMDM and Myc-CaP co-culture of 24-72 hours were harvested and tested on cytokine arrays. **b**. The results were analysed using Protein Array Analyzer for ImageJ.

4.3 Effects of IGF axis manipulation on macrophage phenotype

4.3.1 Conditioned medium of xentuzumab-treated Myc-CaPs assessed by cytokine array

To assess whether Myc-CaPs secrete cytokines and chemokines that could affect macrophage polarisation and whether IGF blockade has any effects on it, conditioned media of Myc-CaP treated with either solvent control or xentuzumab were tested using the cytokine array.

The array detected 11 cytokines, of which CCL3 was downregulated upon xentuzumab treatment, with a minor reduction in CCL4, CXCL10, and TNFα (Figure 4.9a-b). Significant Ccl3 downregulation upon xentuzumab treatment was validated by qRT-PCR (Figure 4.9c).

Cytokines in Myc-CaP conditioned media (Figure 4.9) were also compared with BMDM+Myc-Cap co-culture media (Figure 4.8) to identify likely source of drivers for macrophage polarisation. CCL2 and IL-1RA were two cytokines that were not present in the blot with Myc-CaP conditioned media but were detectable in the blot with BMDM + Myc-CaP conditioned media, suggesting that BMDM may be the drivers of these cytokines.

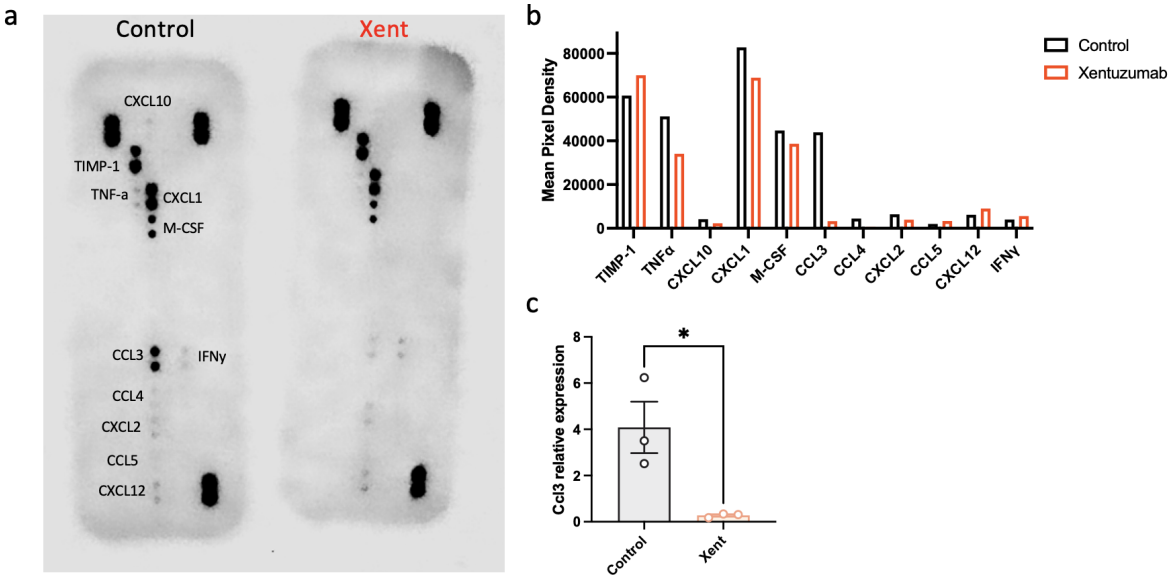


Figure 4.9: Comparing the conditioned media of Myc-CaPs treated with xentuzumab versus control. a-b. Conditioned media from Myc-CaP cultures were harvested after 24-hour treatment of solvent control or xentuzumab and tested using cytokine array. The results were analysed using Protein Array Analyzer for ImageJ. **c**. Ccl3 was validated using qRT-PCR on Myc-CaP cells treated with or without xentuzumab. Graph represents 3 repeats (*$p<0.05$, unpaired t-test).

4.3.2 Effects of IGF axis manipulation on macrophage polarisation

We then tested whether IGF axis manipulation affects macrophage phenotype by treating M0, M1, and M2-polarised macrophages with xentuzumab and/or IGF-1 and assessing the CD80 and CD206 expression of macrophages by flow cytometry. IGF-1 treatment was used only with J774 and not with BMDMs, due to low number of viable BMDMs per mouse.

There were no differences in CD80 and CD206 expression in unpolarised or M1-polarised BMDMs, but CD206 expression was significantly decreased in M2-polarised BMDMs upon xentuzumab treatment (Figure 4.10a-c). The results were consistent in M2-polarised J774 cells, with xentuzumab causing significant decrease in CD206 expression compared to control and IGF-treated conditions (Figure 4.11c). This suggests that xentuzumab causes significant reduction in CD206+ M2-like macrophages. Unpolarised J774s also had decreased CD80 expression with xentuzumab treatment (Figure 4.11a-c).

When the same experiments were repeated with human PBMC-derived macrophages, there were no difference in M2-polarised macrophage phenotype upon treatment with xentuzumab alone or with IGF-1. Unpolarised PBMC-derived macrophages had significantly increased CD80 expession upon IGF treatment (Figure 4.12).

These data demonstrate that IGF blockade reduces murine CD206+ immunosuppressive M2-like macrophages *in vitro*. Although there were no effects in PBMC-derived macrophages, this suggests effects of IGFs on immunosuppressive prostate cancer TIME.

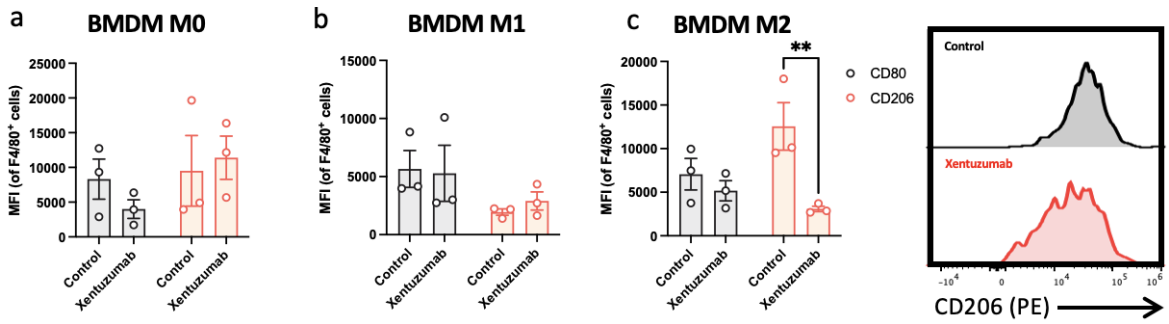


Figure 4.10: Effects of IGF-1 alone or with xentuzumab on murine BMDM polarisation. a. M0, **b**. M1, and **c**. M2-polarised BMDMs were treated with xentuzumab overnight. Cells were collected for flow cytometry to assess CD80 and CD206 expression. Data represents the mean fluorescence intensity (MFI) of F4/80+ macrophages of 3 repeats, with error bar showing mean ± SEM. (*p<0.05, **p<0.01, two-way ANOVA with multiple comparisons)

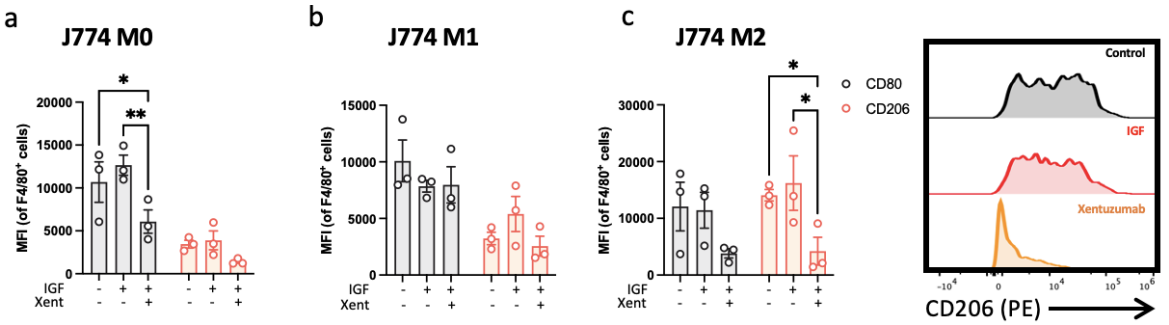


Figure 4.11: Effects of IGF-1 alone or with xentuzumab on murine J774 polarisation. a. M0, **b**. M1, and **c**. M2-polarised J774 cell lines were treated with xentuzumab alone or with IGF-1 overnight. Cells were collected for flow cytometry to assess CD80 and CD206 expression. Data represents the mean fluorescence intensity (MFI) of F4/80+ macrophages of 3 repeats, with error bar showing mean ± SEM. (*p<0.05, **p<0.01, two-way ANOVA with multiple comparisons)

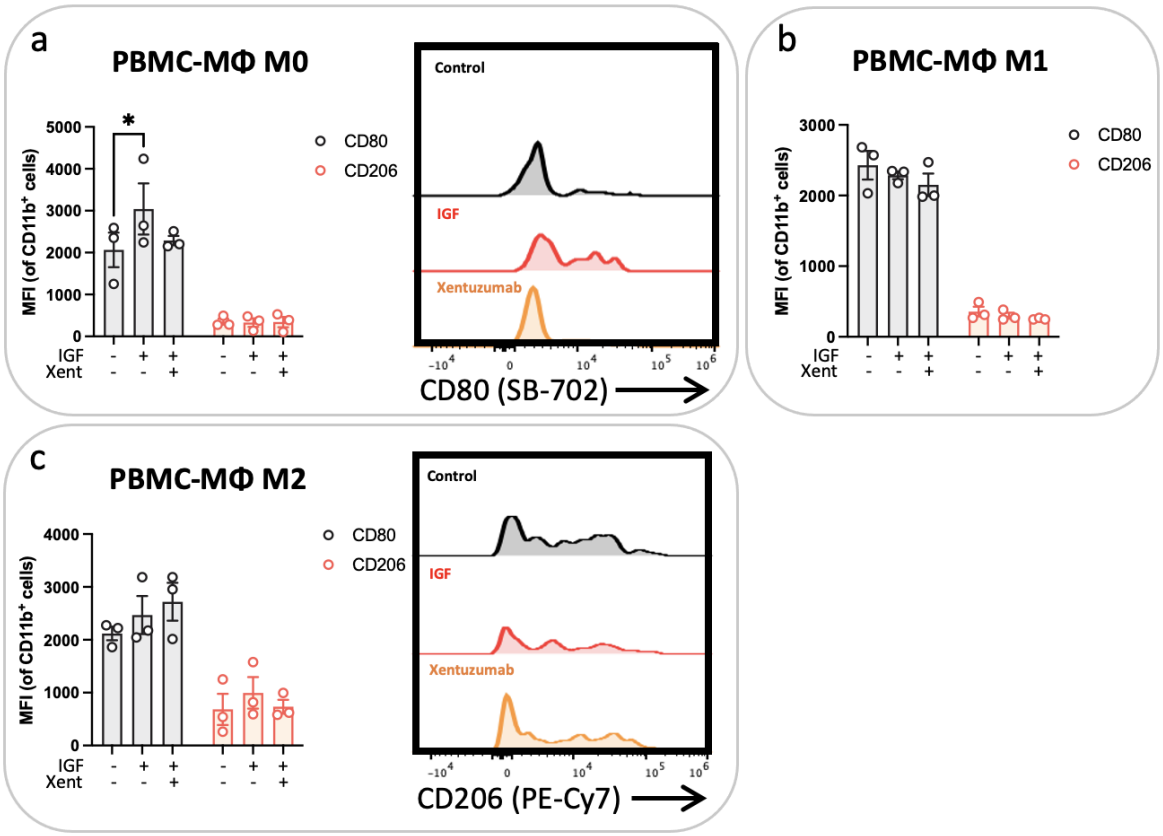


Figure 4.12: Effects of IGF-1 alone or with xentuzumab on human macrophage polarisation. a. M0, **b**. M1, and **c**. M2-polarised PBMC-derived macrophages were treated with xentuzumab alone or with IGF-1 overnight. Cells were collected for flow cytometry to assess CD80 and CD206 expression. Data represents the mean fluorescence intensity (MFI) of CD11b+ macrophages of 3 repeats, with error bar showing mean ± SEM. (*$p<0.05$, two-way ANOVA with multiple comparisons)

4.4 CD47 and prostate cancer

Having assessed the effects of IGFs on phenotype of mouse and human macrophages, we wanted to test the properties of the prostate cancer cells relevant to macrophage function, specifically phagocytosis, which is regulated by two cell surface proteins, CD47 and SIRPα.

4.4.1 CD47 expression in prostate cancer cells

To determine the effects IGFs have on CD47 expression in prostate cancer cells, murine and human prostate cancer cells were treated with xentuzumab alone or with IGF-1 for 4 or 24 hours, and CD47 expression was measured using flow cytometry.

There was a significant increase in CD47 expression upon 4-hour IGF-1 treatment but no difference with 4-hour xentuzumab treatment in Myc-CaP cells. However, CD47 expression was significantly increased upon 24-hour IGF-1 treatment, and this was prevented with xentuzumab treatment for 24 hours, with significance (Figure 4.13a). IGF-1 or xentuzumab did not change CD47 expression in PTEN-CaP8 (Figure 4.13b), DU145 (Figure 4.14a), and 22Rv1 (Figure 4.14b). This suggests that blocking IGFs decrease CD47 expression in murine PTEN WT cancer cells, which may make them more susceptible to phagocytosis.

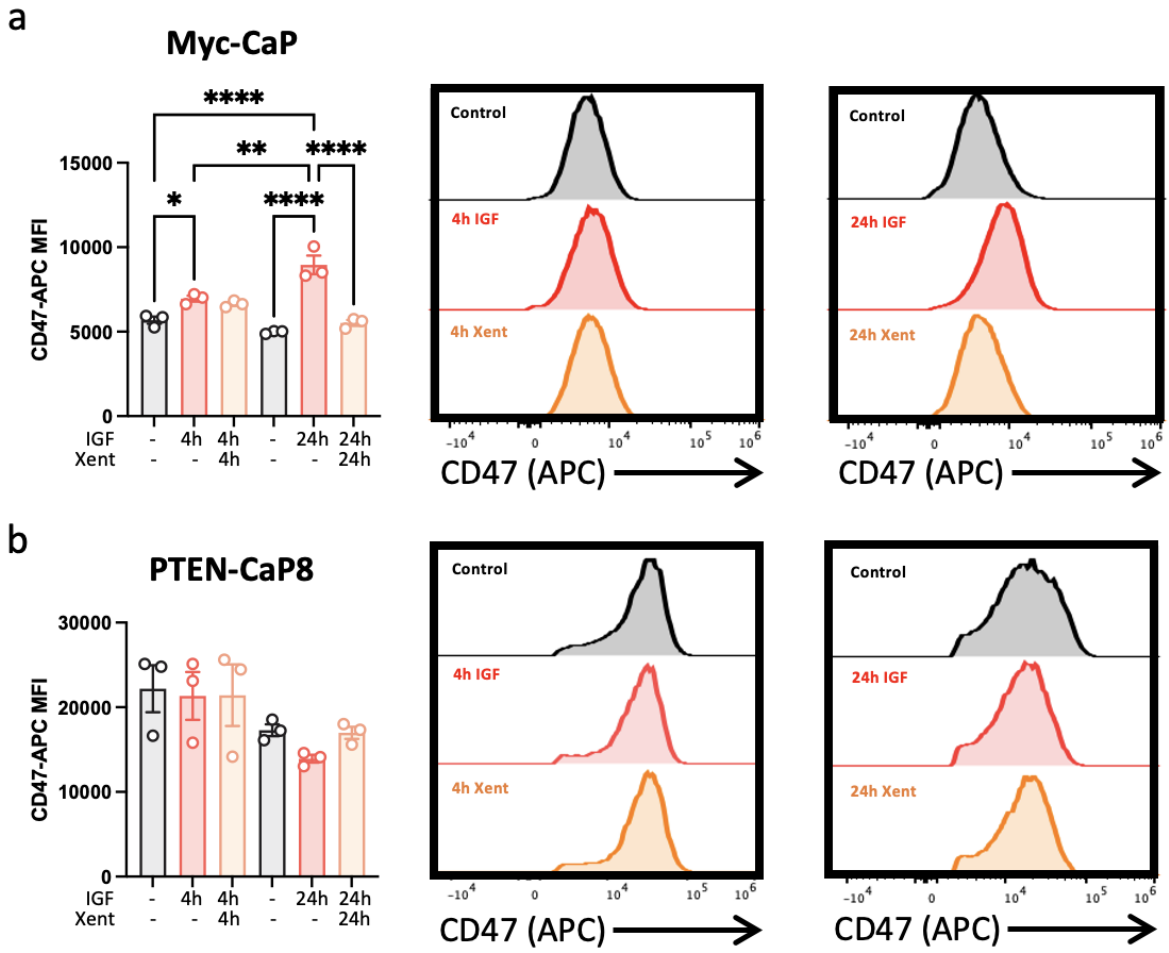


Figure 4.13: Effects of IGF-1 alone or with xentuzumab on CD47 expression in murine prostate cancer cells. Murine cancer cells **a**. Myc-CaP and **b**. PTEN-CaP8 were treated with IGF-1 alone or with xentuzumab for 4 and 24 hours, and cell surface expression of CD47 was assessed by flow cytometry. Data represents the mean fluorescence intensity (MFI) of CD47 of 3 repeats, with error bar showing mean ± SEM. (*p<0.05, **p<0.01, ****p<0.0001, one-way ANOVA with multiple comparisons)

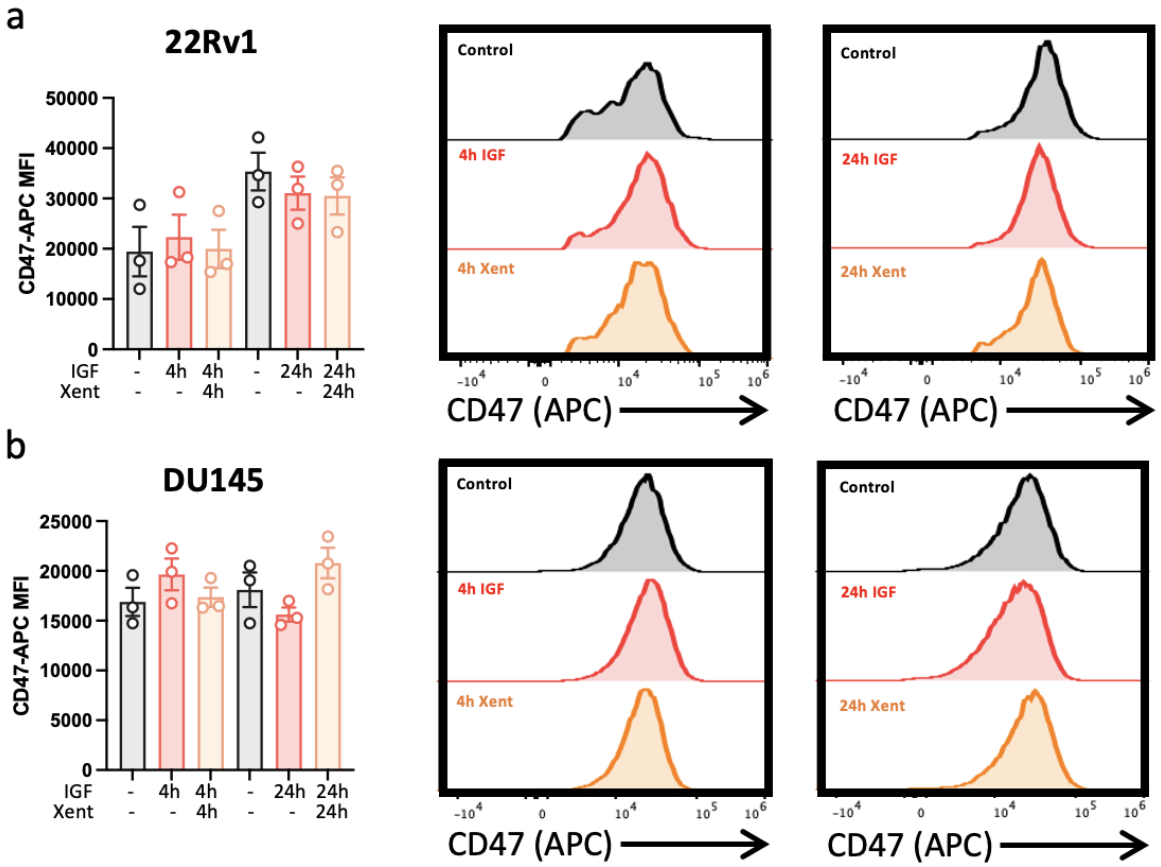


Figure 4.14: Effects of IGF-1 alone or with xentuzumab on CD47 expression in human prostate cancer cells. Human cancer cells **a**. 22Rv1 and **b**. DU145 were treated with IGF-1 alone or with xentuzumab for 4 and 24 hours, and cell surface expression of CD47 was assessed by flow cytometry. Data represents the mean fluorescence intensity (MFI) of CD47 of 3 repeats, with error bar showing mean ± SEM. (one-way ANOVA with multiple comparisons)

4.4.2 Testing effects of anti-CD47 on IGF-1R signalling

Based on publiations that show that CD47 can regulate IGF-1R signalling pathway in cis, illustrated in Figure 4.1 (Clemmons et al., 2005; Tahimic et al., 2013; Melo Garcia et al., 2021), we tested the effects of anti-CD47 on phosphorylation of proteins downstream of IGF-1R. Serum starved murine and human prostate cancer cells were treated with either PBS control, anti-CD47 and/or xentuzumab and lysed for western blot.

As expected, IGF-1R phosphorylation was not affected by anti-CD47. Anti-CD47 had no effect on ERK phosphorylation on murine PTEN-CaP8 (Figure 4.15) or either human prostate cancer cells (Figure 4.16).

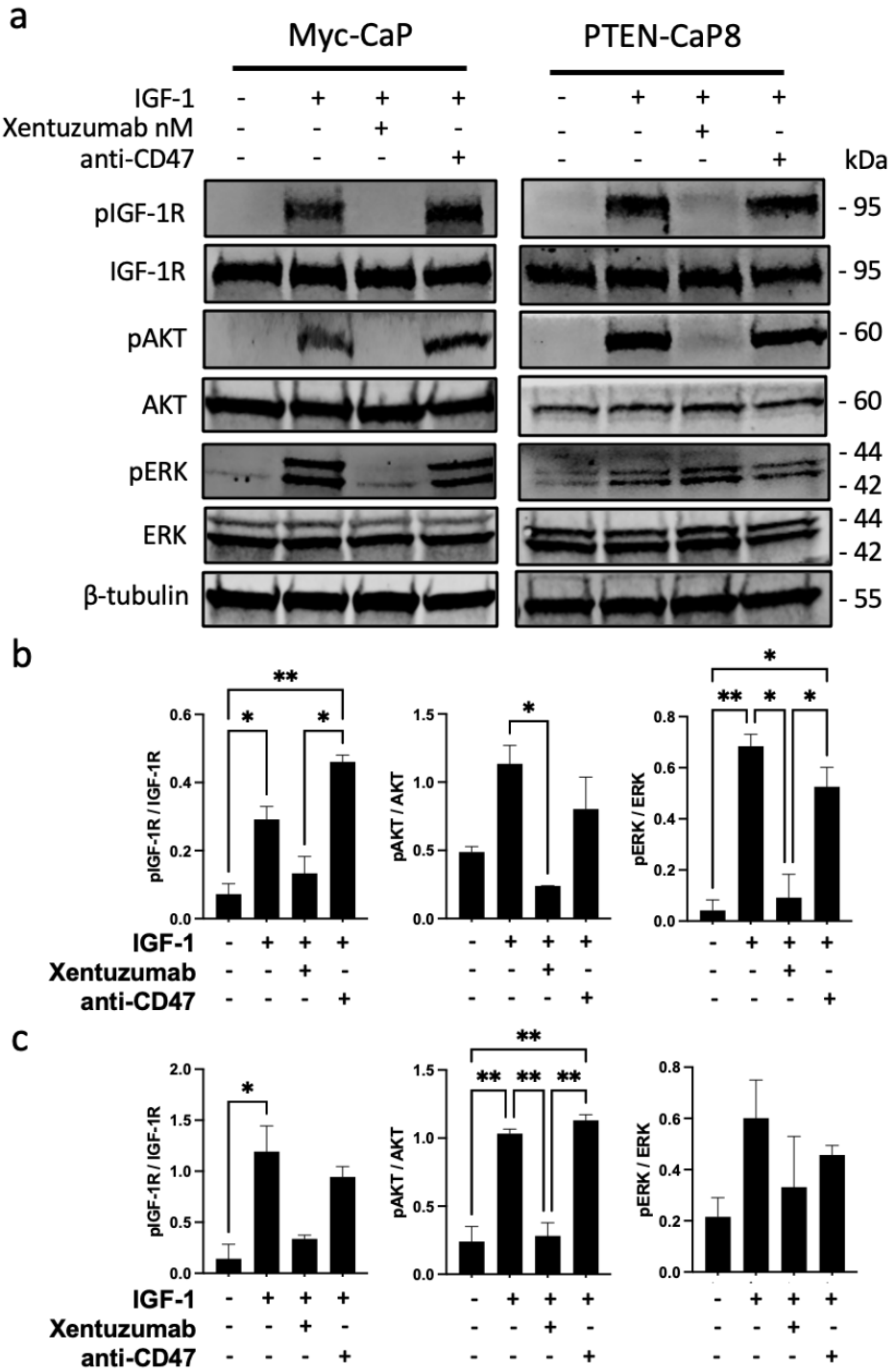


Figure 4.15: Effects of IGF and CD47 blockade on IGF-1R signalling pathway on murine prostate cancer cells. Serum-starved Myc-CaP and PTEN-CaP8 cells were treated with PBS control, anti-CD47 (MIAP410), or xentuzumab for 16 hours and with 50 nM IGF-1 for the final 20 minutes. **a**. The cells were lysed, and proteins involved in IGF-1R signalling pathway were measured using western blot. Phosphorylated IGF-1R, AKT, and ERK levels of **b**. Myc-CaP and **c**. PTEN-CaP8 were quantified after normalising to the loading control β-tubulin using Fiji ImageJ. Graph represents mean ± SEM with at least three independent repeats per cell line (*p<0.05, **p<0.01, one-way ANOVA with multiple comparisons)

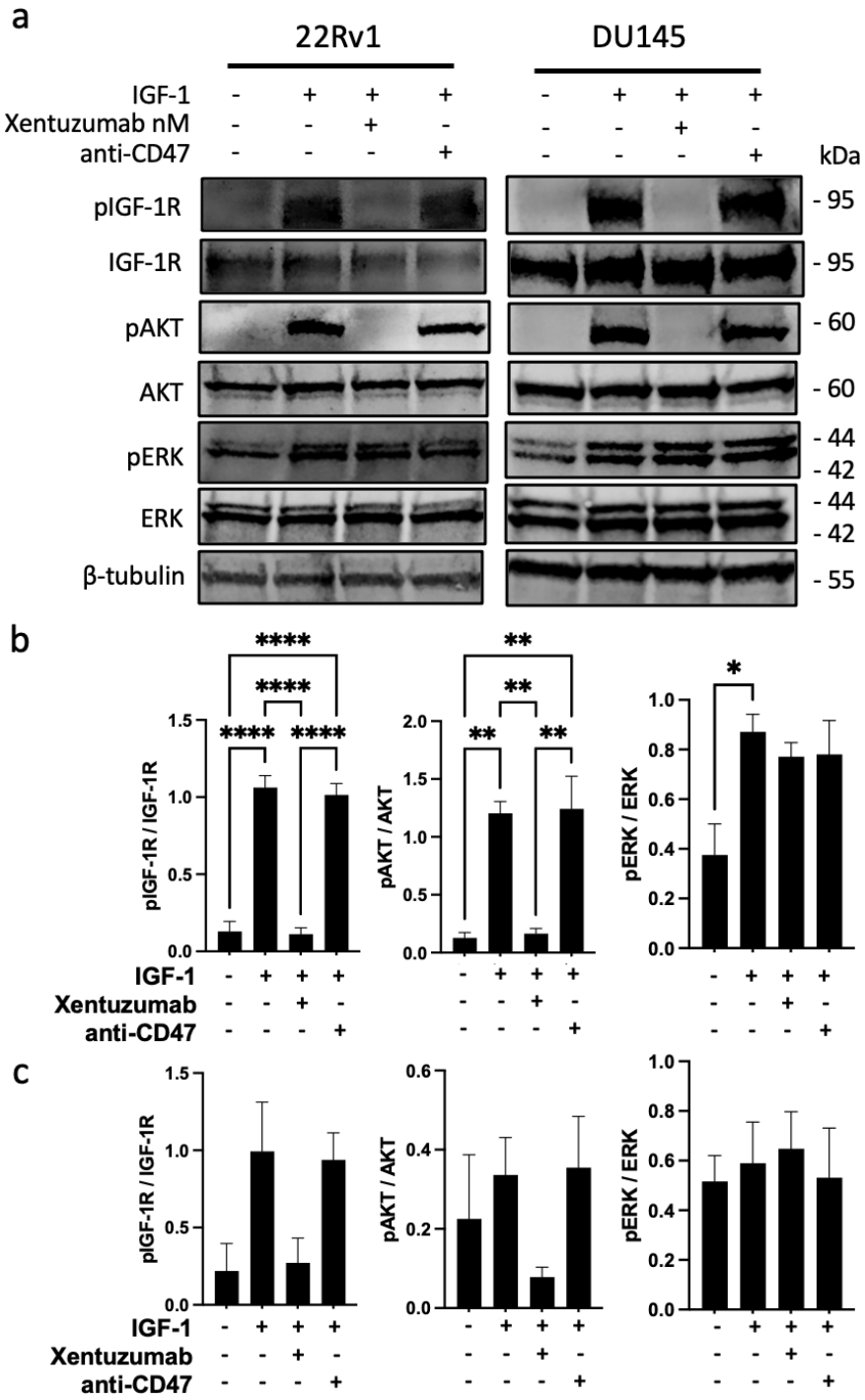


Figure 4.16: Effects of IGF and CD47 blockade on IGF-1R signalling pathway on human prostate cancer cells. Serum-starved 22Rv1 and DU145 cells were treated with PBS control, anti-CD47 (MIAP410), or xentuzumab for 16 hours and with 50 nM IGF-1 for the final 20 minutes. **a**. The cells were lysed, and proteins involved in IGF-1R signalling pathway were measured using western blot. Phosphorylated IGF-1R, AKT, and ERK levels of **b**. 22Rv1 and **c**. DU145 were quantified after normalising to the loading control β-tubulin using Fiji ImageJ. Graph represents mean ± SEM with at least three independent repeats per cell line (*p<0.05, **p<0.01, ****p<0.0001, one-way ANOVA with multiple comparisons)

4.5 Effects of IGF-1, anti-IGF and/or anti-CD47 on cancer cell phagocytosis

Having seen the effects of IGFs on CD47 expression, we next assessed whether IGF-1 affects phagocytosis of cancer cells by macrophages. Cancer cells labelled with mCherry and macrophages were co-cultured in ultra-low adherent 96-well plates with or without treatments for 2 hours and stained with various markers for flow cytometry (Chapter 2.11.1, Figure 2.1d).

4.5.1 Testing conditions for phagocytosis assays

We first tested phagocytosis conditions of mCherry-tagged murine and human prostate cancer cells with J774 and PBMC-derived macrophages, respectively. Positive control used was anti-CD47 (MIAP410), which is known to enable phagocytosis of tumour cells by macrophages (Majeti et al., 2009; Willingham et al., 2012), and negative control cytochalasin D, which inhibits actin polymerisation, blocking phagocytosis (Casella et al., 1981).

Both murine (Figure 4.17) and human (Figure 4.18) macrophages behaved as expected, with reduction in phagocytosis with cytochalasin D treatment and clear, significant increase upon anti-CD47 treatment. Anti-CD47 effect was stronger and more consistent than the cytochalasin D effect, possibly because cytochalasin D has broader impact on cell shape and trafficking and is not a phagocytosis-specific drug (Shoji et al., 2012; Loty et al., 1995; Brown et al., 2001a). This confirmed that anti-CD47 increases phagocytosis of prostate cancer cells by macrophages.

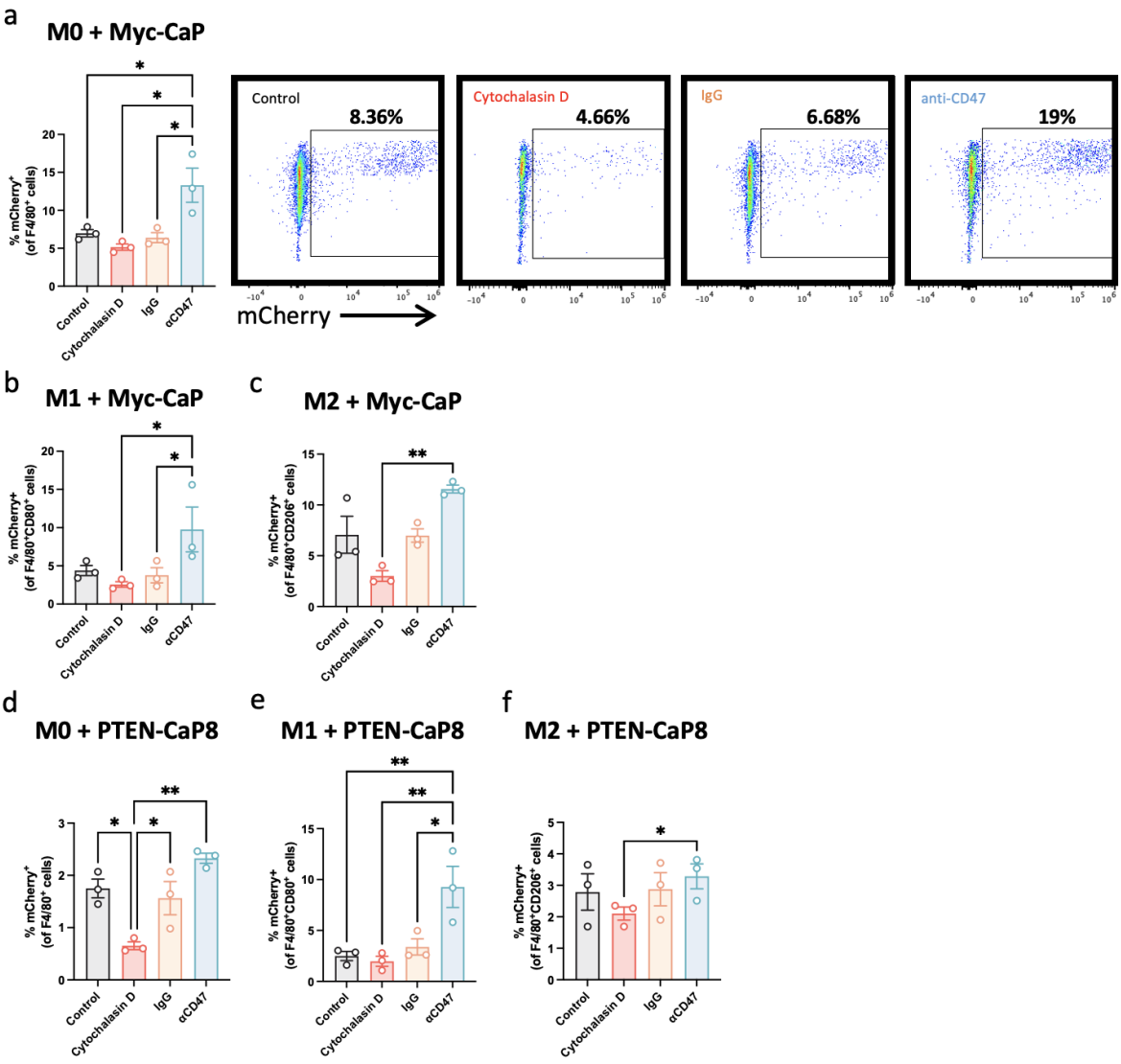


Figure 4.17: Investigating the phagocytosis of murine prostate cancer cells by J774 macrophages. mCherry-tagged Myc-CaP and PTEN-CaP8 were seeded 40,000 cells/well in an ultra low-adherent 96 well plates. Upon serum starvation, the cells were treated with solvent control (PBS), cytochalasin D, IgG isotype control, or anti-CD47 for 30 minutes. After removing the treatments, **a**. unpolarised M0, **b**. M1-like, and **c**. M2-like macrophages were added to Myc-CaPs, and **d**. unpolarised M0, **e**. M1-like, and **f**. M2-like macrophages were added to PTEN-CaP8 cells. After 2 hours, cells were stained with F4/80, CD80, and CD206, and % mCherry+ macrophages were quantified using flow cytometry. Graph represents mean ± SEM with at least three independent experiments. (*p<0.05, **p<0.01, one-way ANOVA with multiple comparisons)

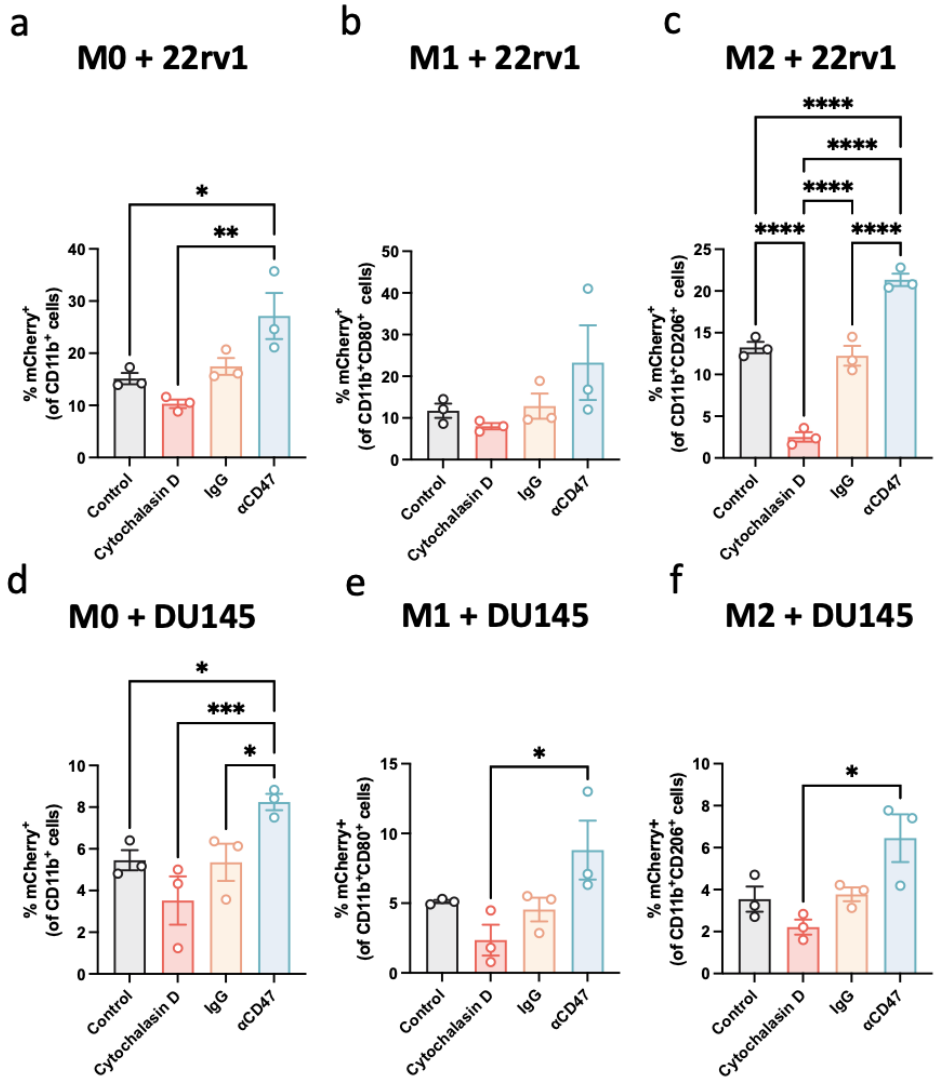


Figure 4.18: Investigating the phagocytosis of human prostate cancer cells by macrophages. mCherry-tagged 22Rv1 and DU145 were seeded 40,000 cells/well in an ultra low-adherent 96 well plates. Upon serum starvation, the cells were treated with solvent control (PBS), cytochalasin D, IgG isotype control, or anti-CD47 for 30 minutes. After removing the treatments, **a**. unpolarised M0, **b**. M1-like, and **c**. M2-like macrophages were added to wells containing 22Rv1 cells, and **d**. unpolarised M0, **e**. M1-like, and **f**. M2-like macrophages were added to wells containing DU145 cells. After 2 hours, cells were stained with CD11b, CD80, and CD206, and % mCherry+ macrophages were quantified using flow cytometry. Graph represents mean ± SEM with at least three independent experiments. (*p<0.05, **p<0.01, ***p<0.001, ****p<0.0001, one-way ANOVA with multiple comparisons)

4.5.2 Assessing the effects of IGF-axis manipulation on phagocytosis

We then assessed whether IGF axis manipulation would affect phagocytosis of murine and human cancer cells by macrophages. Prostate cancer cells were treated with IGF-1 alone or with xentuzumab for 24 hours before adding unpolarised or M1/M2-polarised macrophages for 2 hours, and phagocytosis activity was quantified using flow cytometry.

Overall, IGF-1 treatment in cancer cells reduced phagocytosis of macrophages compared to control, though only significant in M0 macrophage + Myc-CaP condition (Figure 4.19a). Myc-CaP and PTEN-CaP8 cells treated with xentuzumab were phagocytosed significantly more by M1-like and M2-like macrophages than those treated with IGF-1 (Figure 4.19). In addition, M1-like macrophages phagocytosed significantly more 22Rv1 and DU145 upon xentuzumab pre-treatment, but there were no changes in M0 or M2 phagocytosis (Figure 4.20).

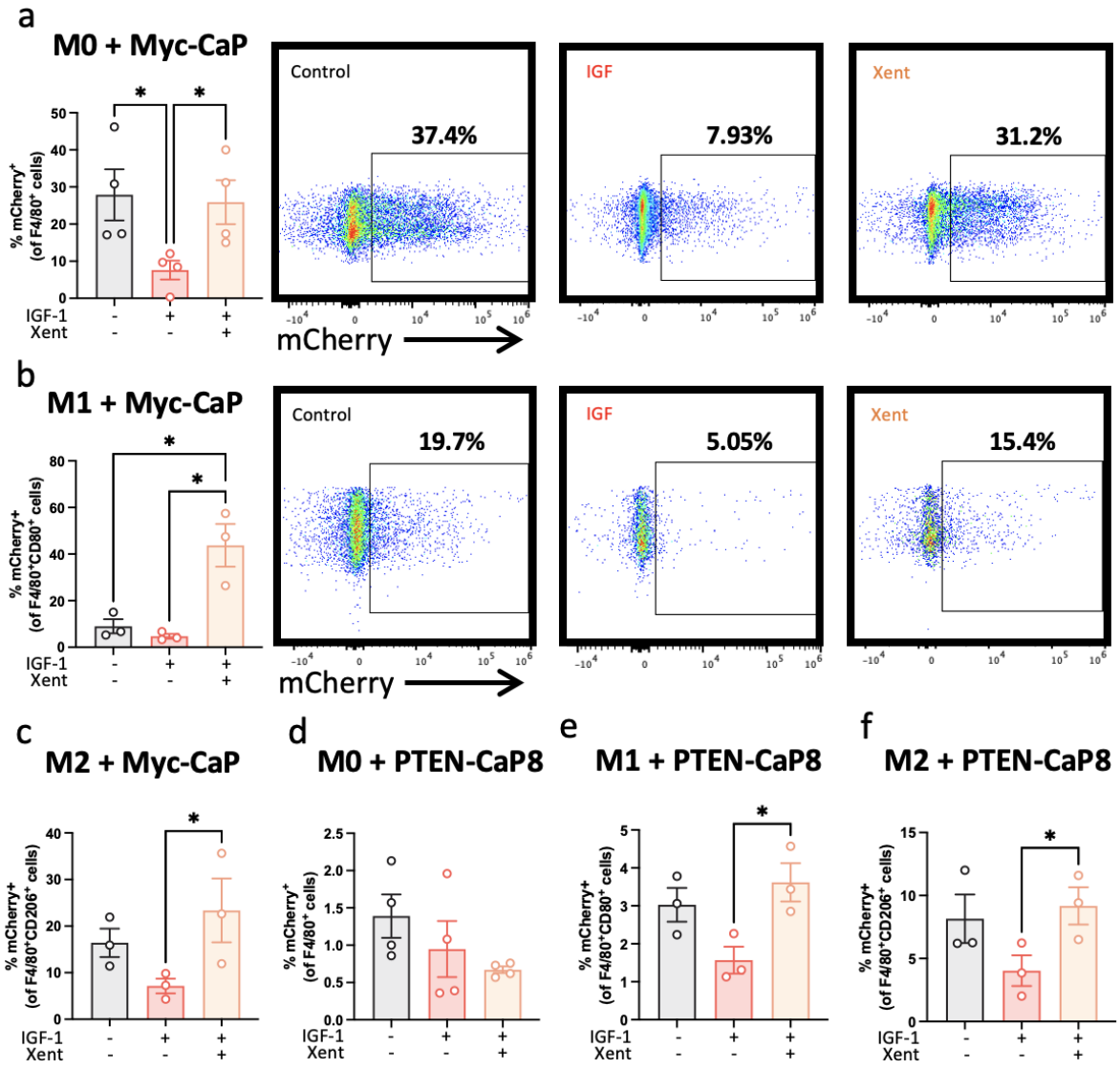


Figure 4.19: Effects of IGF axis manipulation on murine prostate cancer cells by J774 macrophages. mCherry-tagged Myc-CaP and PTEN-CaP8 were seeded 40,000 cells/well in an ultra low-adherent 96 well plates. Upon serum starvation, the cells were treated with IGF-1 alone or with xentuzumab for 24 hours. After removing the treatments, **a**. unpolarised M0, **b**. M1-like, and **c**. M2-like macrophages were added to Myc-CaPs, and **d**. unpolarised M0, **e**. M1-like, and **f**. M2-like macrophages were added to PTEN-CaP8 cells. After 2 hours, cells were stained with F4/80, CD80, and CD206, and % mCherry+ macrophages were quantified using flow cytometry. Graph represents mean ± SEM with at least three independent experiments. (*$p<0.05$, one-way ANOVA with multiple comparisons)

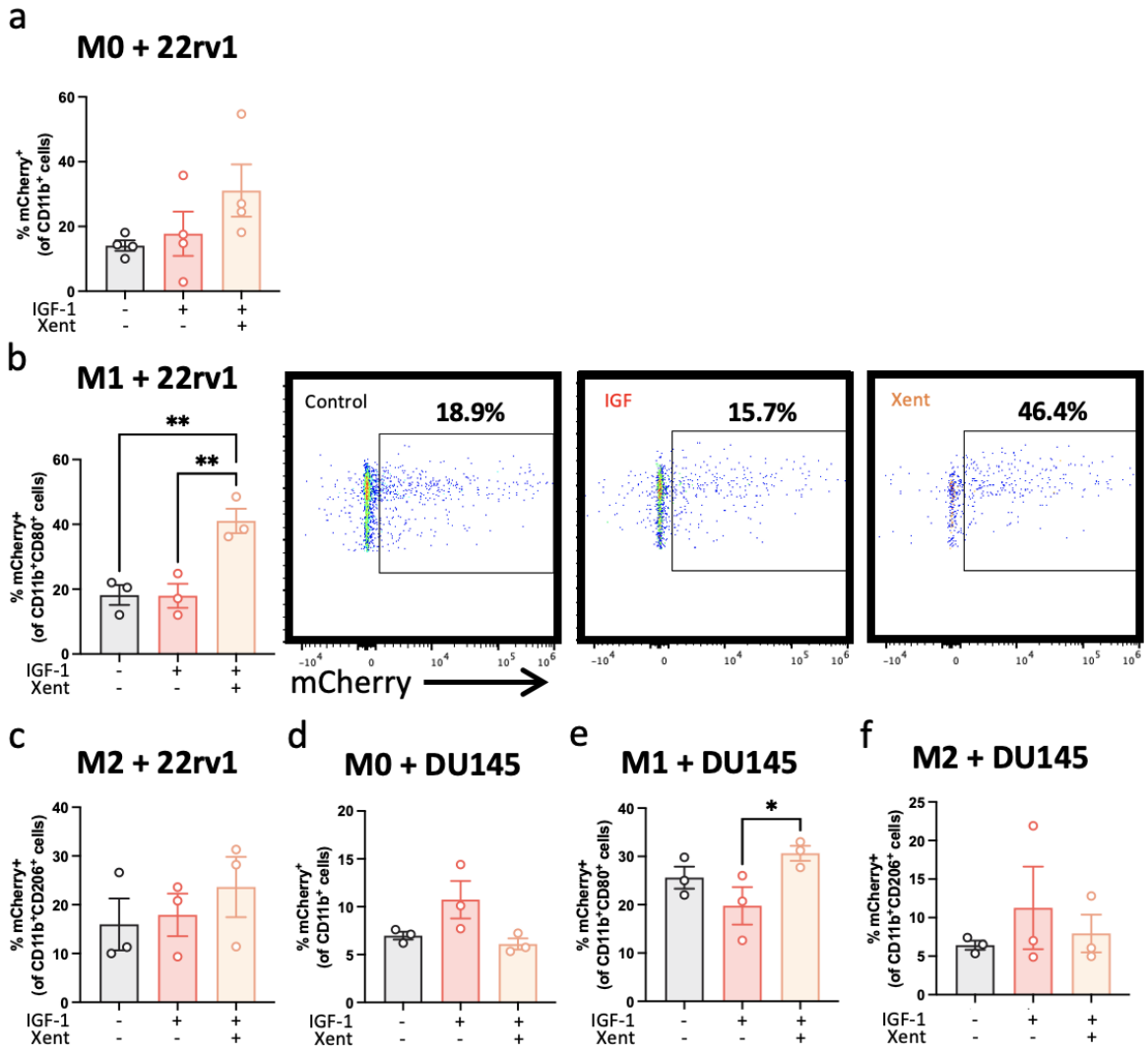


Figure 4.20: Effects of IGF axis manipulation on human prostate cancer cells by macrophages. mCherry-tagged 22Rv1 and DU145 were seeded 40,000 cells/well in an ultra low-adherent 96 well plates. Upon serum starvation, the cells were treated with IGF-1 alone or with xentuzumab for 24 hours. After removing the treatments, **a**. unpolarised M0, **b**. M1-like, and **c**. M2-like macrophages were added to 22Rv1, and **d**. unpolarised M0, **e**. M1-like, and **f**. M2-like macrophages were added to DU145. After 2 hours, cells were stained with CD11b, CD80, and CD206, and % mCherry+ macrophages were quantified using flow cytometry. Graph represents mean ± SEM with at least three independent experiments. (*p<0.05, **p<0.01, one-way ANOVA with multiple comparisons)

4.5.3 Investigating the effects of xentuzumab on anti-CD47-induced phagocytosis

Having confirmed effects of IGFs on phagocytosis, we investigated whether IGF blockade would further increase phagocytosis induced by anti-CD47. Murine and human mCherry-tagged cancer cells were treated with anti-CD47, xentuzumab, or both for 24 hours. Unpolarised or M1/M2-polarised macrophages were added to the cancer cells for 2 hours, and cells were stained for flow cytometry.

Anti-CD47 significantly increased phagocytosis of Myc-CaPs by all types of macrophages (Figure 4.21a-c). Although combination treatment increased M1-like and M2-like macrophage phagocytosis of Myc-CaPs and M1-like macrophage phagocytosis of PTEN-CaP8 compared to control, it did not enhance the effects of anti-CD47. In 22Rv1, however, combination treatment significantly increased M1-like macrophage phagocytosis of 22Rv1 (Figure 4.22b).

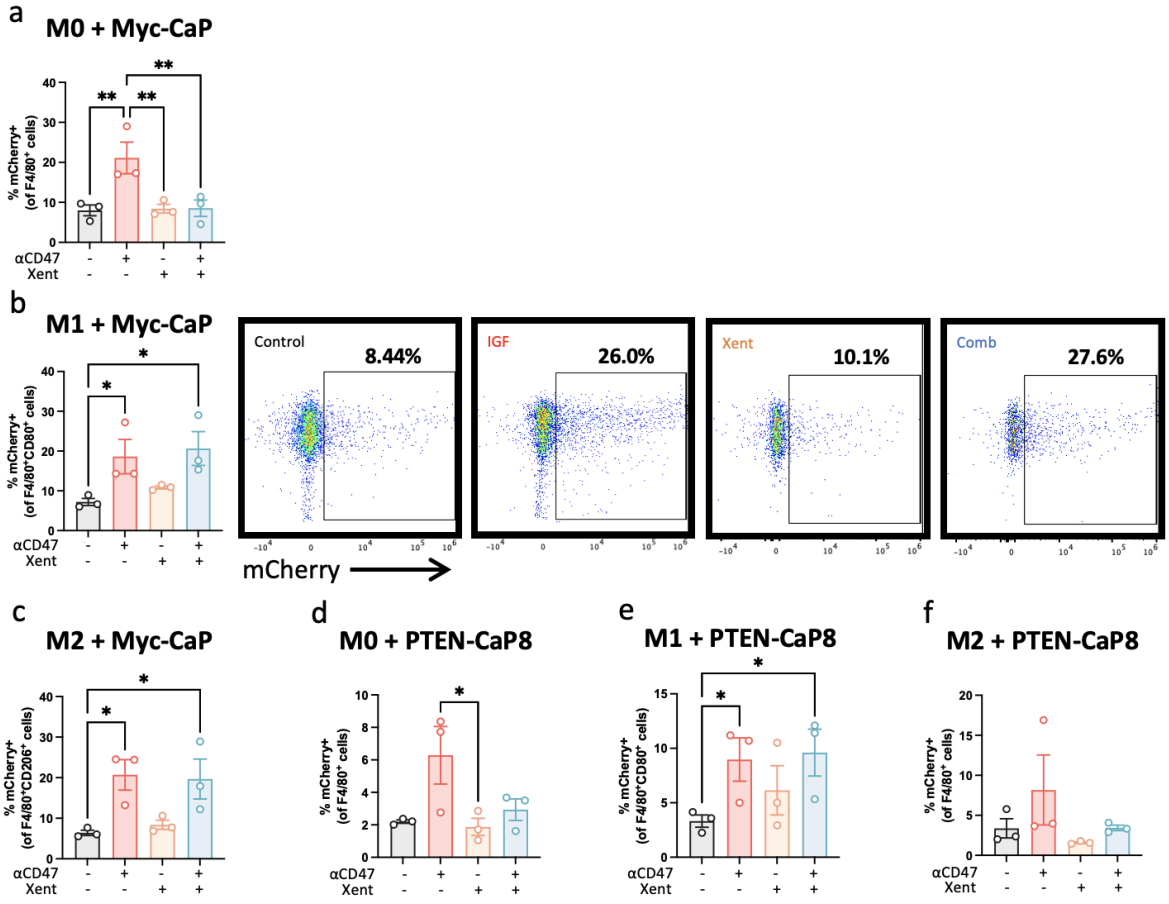


Figure 4.21: Effects of combined IGF and CD47 blockade on murine prostate cancer phagocytosis. mCherry-tagged Myc-CaP and PTEN-CaP8 were seeded 40,000 cells/well in an ultra low-adherent 96 well plates and treated with solvent control, xentuzumab, anti-CD47, or combination for 24 hours. After removing the treatments, **a**. unpolarised M0, **b**. M1-like, and **c**. M2-like macrophages were added to Myc-CaPs, and **d**. unpolarised M0, **e**. M1-like, and **f**. M2-like macrophages to PTEN-CaP8 cells. After 2 hours, cells were stained with F4/80, CD80, and CD206, and % mCherry+ macrophages were quantified using flow cytometry. Graph represents mean ± SEM with at least three independent experiments. (*$p<0.05$, one-way ANOVA with multiple comparisons)

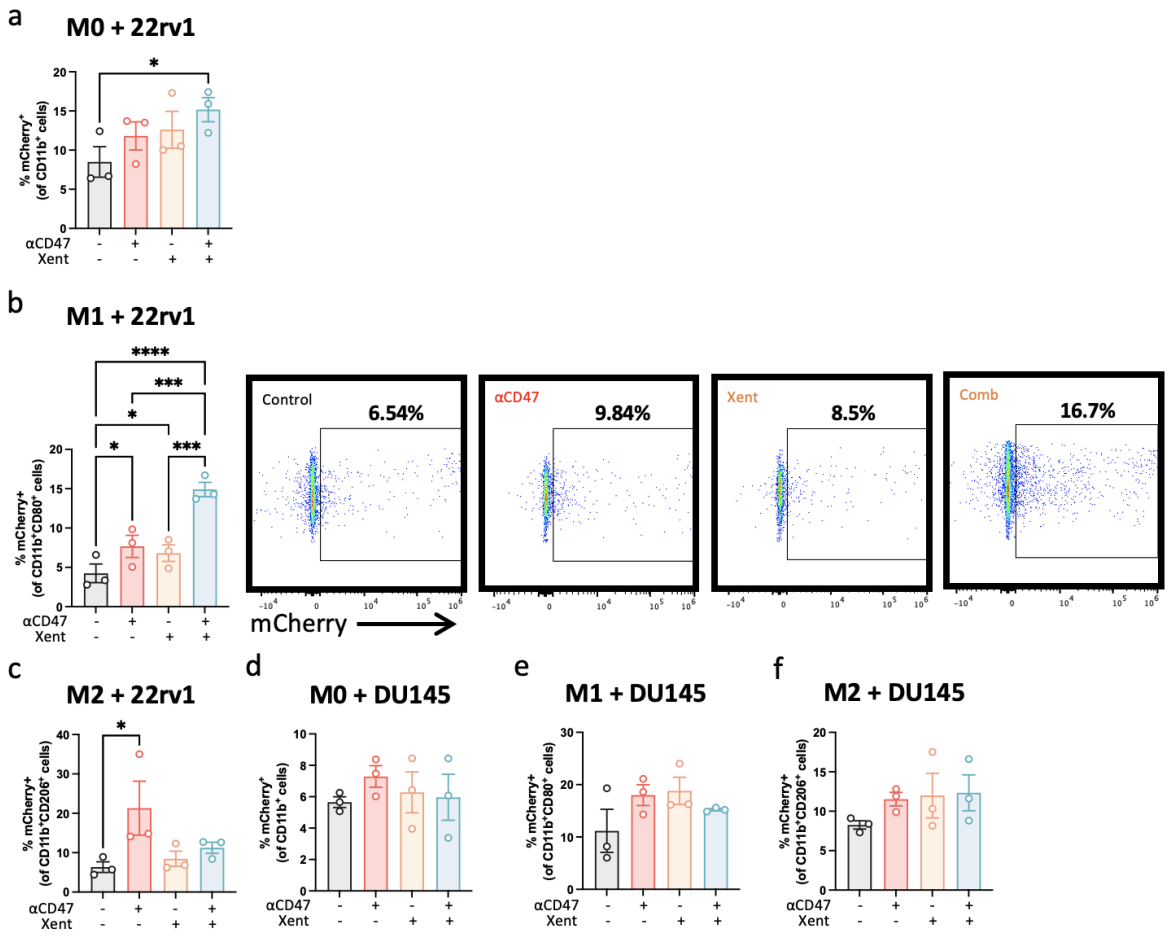


Figure 4.22: Effects of combined IGF and CD47 blockade on human prostate cancer phagocytosis. mCherry-tagged 22Rv1 and DU145 were seeded 40,000 cells/well in an ultra low-adherent 96 well plates and treated with solvent control, xentuzumab, anti-CD47, or combination for 24 hours. After removing the treatments, **a**. unpolarised M0, **b**. M1-like, and **c**. M2-like macrophages were added to 22Rv1, and **d**. unpolarised M0, **e**. M1-like, and **f**. M2-like macrophages to DU145 cells. After 2 hours, cells were stained with CD11b, CD80, and CD206, and % mCherry+ macrophages were quantified using flow cytometry. Graph represents mean ± SEM with at least three independent experiments. (*p<0.05, ***p<0.001, ****p<0.0001, one-way ANOVA with multiple comparisons)

4.6 Investigating the effects of IGFs on macrophages regulating T cell effector functions

Finally, we tested whether IGF effects on macrophage polarisation and phagocytosis have consequences for T cell functions. We co-cultured human prostate cancer cells and M0/M1/M2-polarised PBMC-derived macrophages with IGF-1 alone or with xentuzumab for 48 hours, before adding CFSE-stained T cells for 72 hours. T cells were then collected and stained for CD4, CD8, CD25, CD69, IFN-γ, and TIM-3 and analysed using flow cytometry (Figure 2.3).

CD8+ T cells exposed to 22Rv1 and M0/M1-polarised macrophages with xentuzumab treatment had significantly reduced exhaustion marker TIM-3 expression compared to those with IGF-1 treatment (Figure 4.23a), suggesting that IGF blockade causes T cells to become less exhausted. There were no changes in CD4+ T cells exposed to 22Rv1 and macrophage co-culture or in either T cell types exposed to DU145 and macrophage co-cultures (Figure 4.23b-d).

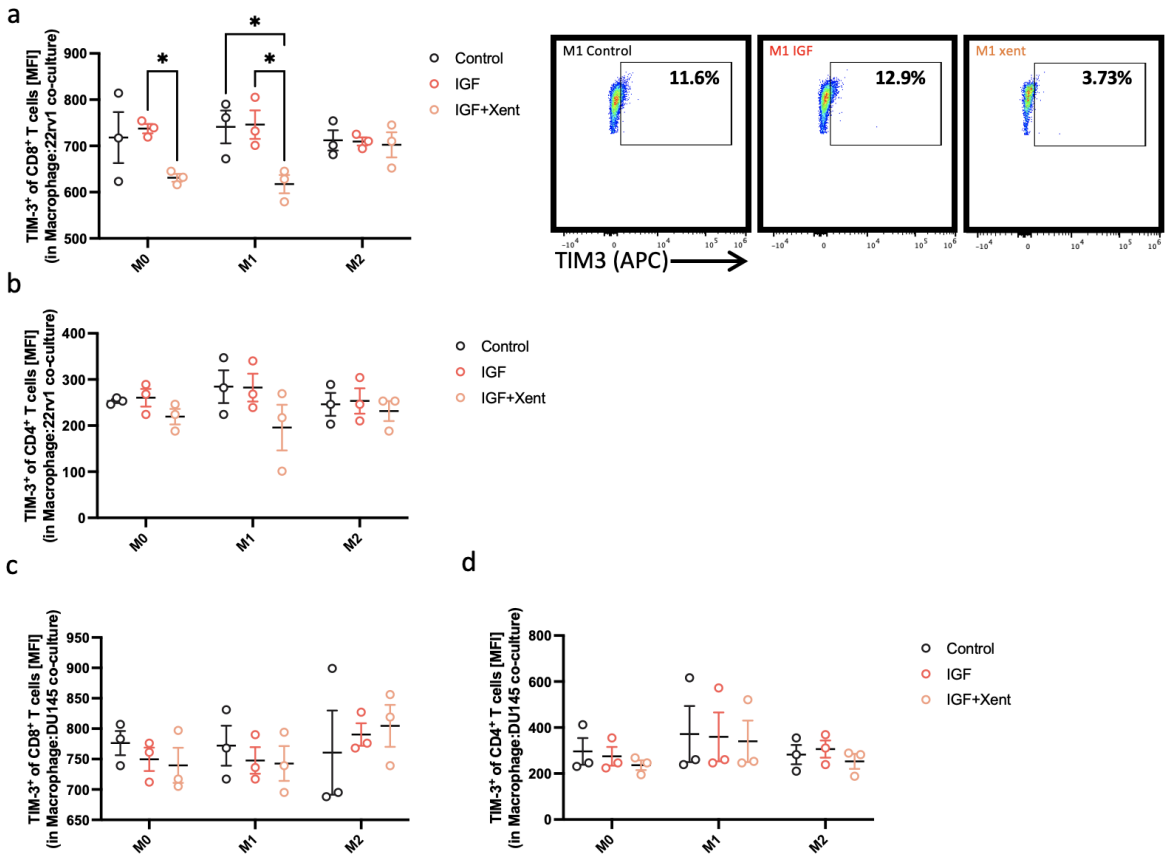


Figure 4.23: Effects of IGF and xentuzumab-treated macrophages on T cell exhaustion. 22Rv1 and DU145 were cocultured in an ultra low-adherent 96 well plates and treated with IGF-1 alone or with xentuzumab for 48 hours. After removing the treatments, CFSE-stained T cells were added for 72 hours. Collected T cells were stained with CD4, CD8, CD25, CD69, IFN-γ, and TIM-3, and quantified using flow cytometry. **a**. %CD8+TIM3+ T cells and **b**. %CD4+TIM3+ T cells exposed to macrophage:22Rv1 co-culture. **c**. %CD8+TIM3+ T cells, **d**. %CD4+TIM3+ T cells exposed to macrophage:DU145 co-culture. Graph represents mean ± SEM with at least three independent experiments. (*$p<0.05$, two-way ANOVA with multiple comparisons)

CD25, a marker for functional Tregs, is crucial in T cell proliferation (S et al., 1995; Sakaguchi, 2005; Bisikirska et al., 2005), and CD69 is an early activation marker that also plays a role in T helper cell differentiation (Testi et al., 1989; Yamashita et al., 1993; Shinoda et al., 2012; Cibrian et al., 2017). CD25+CD8+, CD25+CD4+, CD69+CD8+, and CD69+CD4+ T cells exposed to 22Rv1 and M0/M1 macrophage co-culture were reduced with xentuzumab treatment, though only significant in CD25+CD4+ T cells (Figure 4.24a-d). There were no difference when exposed to DU145 and macrophage co-culture (Figure 4.24e-h). In addition, there was a significant difference in IFN-γ production of CD8+ T cells exposed to xentuzumab-treated unpolarised macrophage and human prostate cancer co-culture (Figure 4.25a, c). There was no difference in IFN-γ production of CD4+ T cells upon IGF or xentuzumab treatments.

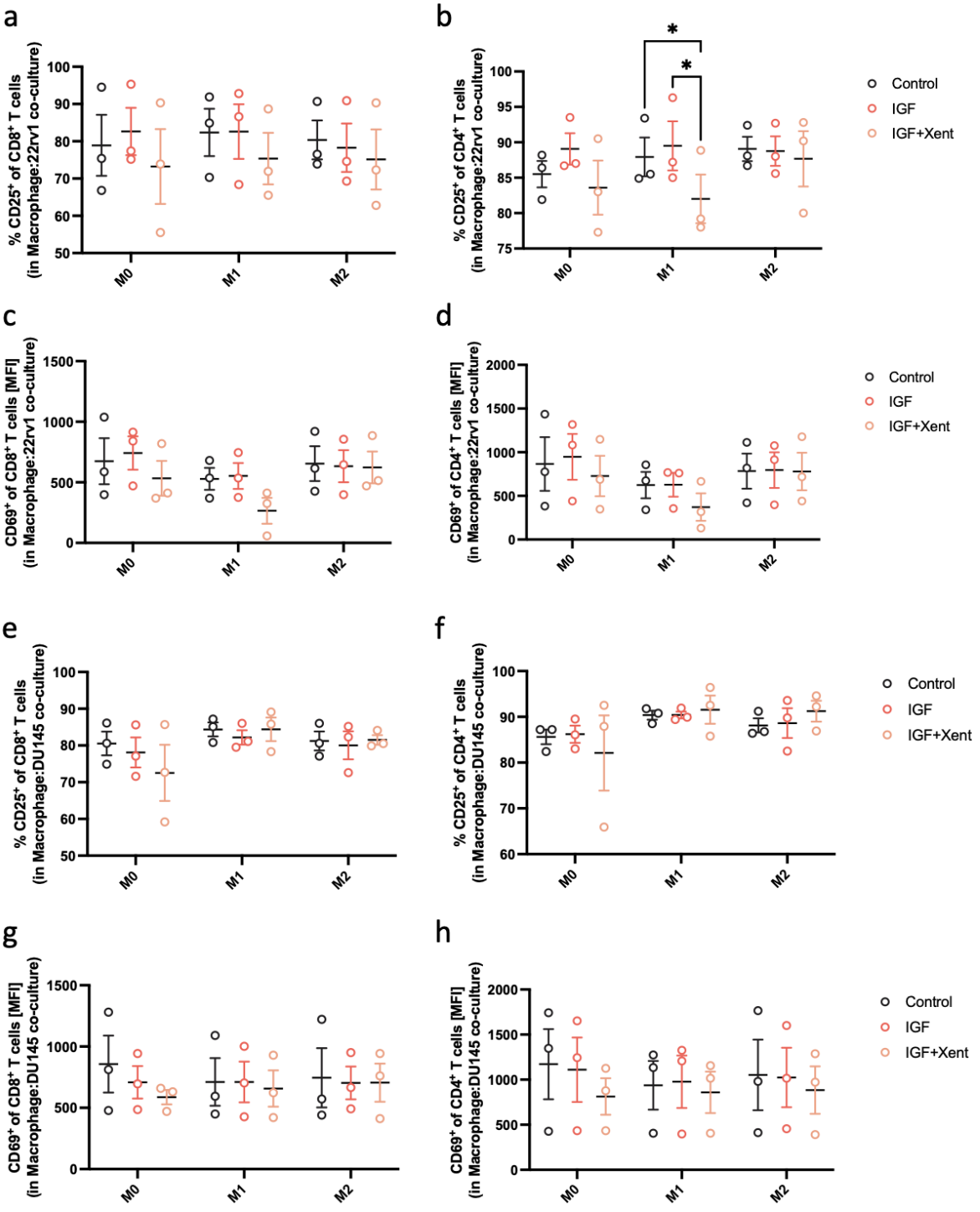


Figure 4.24: Effects of IGF and xentuzumab-treated macrophages on T cell activation. 22Rv1 and DU145 were cocultured in an ultra low-adherent 96 well plates and treated with IGF-1 alone or with xentuzumab for 48 hours. After removing the treatments, CFSE-stained T cells were added for 72 hours. Collected T cells were stained with CD4, CD8, CD25, CD69, IFN-γ, and TIM-3, and quantified using flow cytometry. **a**. %CD8+CD25+ T cells, **b**. %CD4+CD25+ T cells, **c**. %CD8+CD69+ T cells, and **d**. %CD4+CD69+ T cells exposed to macrophage:22Rv1 co-culture. **e**. %CD8+CD25+ T cells, **f**. %CD4+CD25+ T cells, **g**. %CD8+CD69+ T cells, and **h**. %CD4+CD69+ T cells exposed to macrophage:DU145 co-culture. Graph represents mean ± SEM with at least three independent experiments. (*$p<0.05$, two-way ANOVA with multiple comparisons)

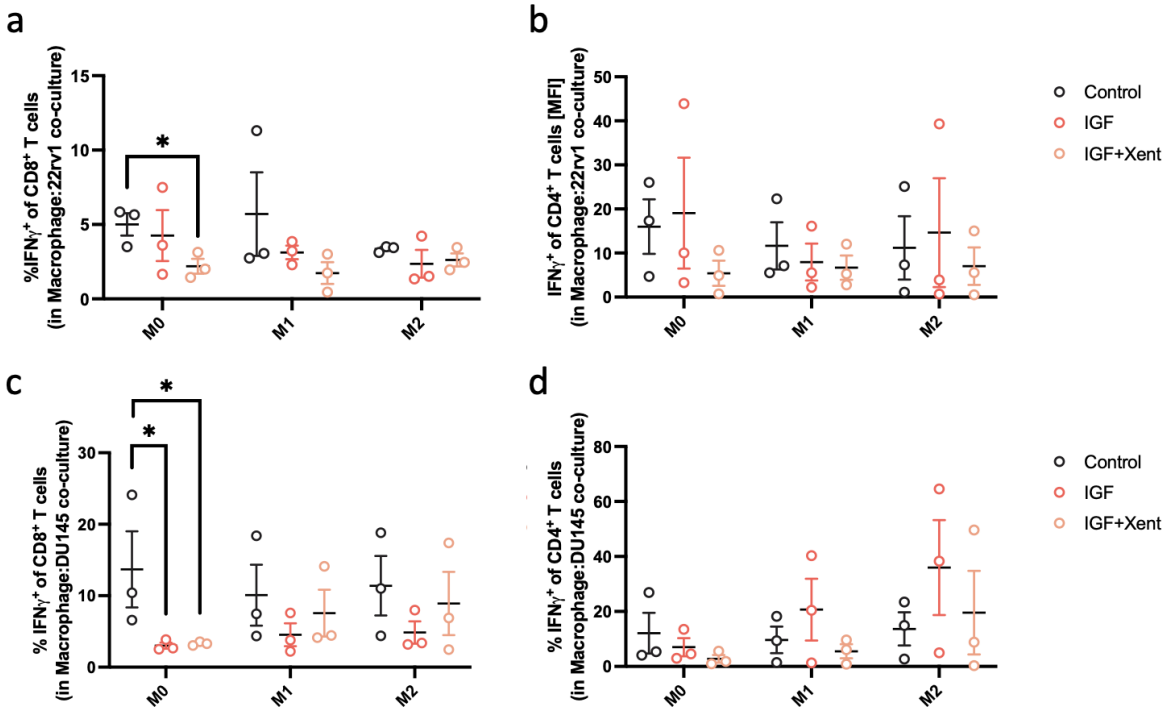


Figure 4.25: Effects of IGF and xentuzumab-treated macrophages on IFN-γ production. 22Rv1 and DU145 were cocultured in an ultra low-adherent 96 well plates and treated with IGF-1 alone or with xentuzumab for 48 hours. After removing the treatments, CFSE-stained T cells were added for 72 hours. Collected T cells were stained with CD4, CD8, CD25, CD69, IFN-γ, and TIM-3, and quantified using flow cytometry. IFNγ production of **a**. %CD8+ T cells and **b**. %CD4+ T cells exposed to macrophage:22Rv1 co-culture. IFNγ production of **c**. %CD8+ T cells and **d**. %CD4+ T cells exposed to macrophage:DU145 co-culture. Graph represents mean ± SEM with at least three independent experiments. (*$p<0.05$, two-way ANOVA with multiple comparisons)

CFSE staining of T cells was used to measure whether IGF-1 and/or xentuzumab affect their proliferation. Xentuzumab treatment on macrophage and 22Rv1 co-culture increased proliferation of CD8+ and CD4+ T cells, although only significant in CD8+ T cells (Figure 4.26a-b). There was no difference in proliferation of T cells exposed to macrophage and DU145 co-culture (Figure 4.26c-d).

These results show that IGF blockade causes significant increase of CD8+ T cell proliferation while reducing TIM-3 expression in macrophage:22Rv1 co-culture, suggesting the increase in activated CD8+ T cells. IGF blockade also significantly reduced CD25+CD4+ functional Treg proliferation and IFN-γ production of CD8+ T cells. This sheds light on anti-tumour effects of IGFs on T cell function.

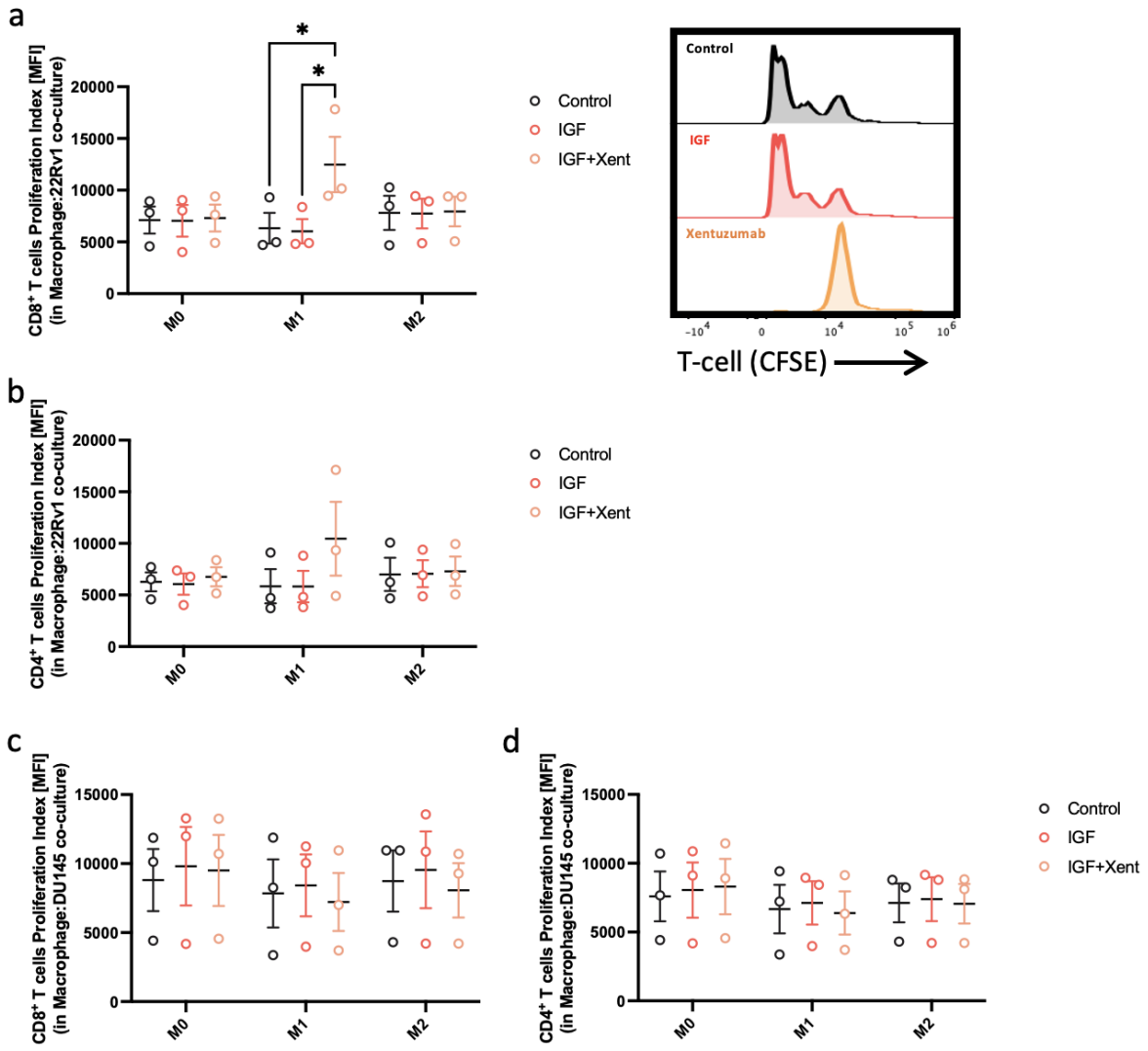


Figure 4.26: Effects of IGF and xentuzumab-treated macrophages on T cell proliferation. 22Rv1 and DU145 were cocultured in an ultra low-adherent 96 well plates and treated with IGF-1 alone or with xentuzumab for 48 hours. After removing the treatments, CFSE-stained T cells were added for 72 hours. Collected T cells were stained with CD4, CD8, CD25, CD69, IFN-γ, and TIM-3, and quantified using flow cytometry. CFSE staining was used to measure proliferation of **a**. %CD8+ T cells and **b**. %CD4+ T cells exposed to macrophage:22Rv1 co-culture, and **c**. %CD8+ T cells, **d**. %CD4+ T cells exposed to macrophage:DU145 co-culture. Graph represents mean ± SEM with at least three independent experiments. (*$p<0.05$, two-way ANOVA with multiple comparisons)

4.7 Discussion

Various cytokines and chemokines in the TIME can cause macrophages to polarise to two main subtypes, pro-inflammatory M1-like and anti-inflammatory M2-like macrophages (Gordon, 2003; Mantovani et al., 2004; Wang et al., 2013). First, We successfully polarised both mouse and human macrophages to different subtypes (Figure 4.2 and 4.3). In both mice and human, M1 and M2-polarised macrophages expressed significantly higher expression of CD80 and CD206, respectively, and more than 50% of the macrophages expressed the respective markers, consistent with previous studies (Shu et al., 2020; Vidyarthi et al., 2018; Christmann et al., 2011; Nordlohne et al., 2021). Although only 30% of the human PBMC-derived M1-polarised macrophages expressed M1 marker CD80 (Figure 4.3b), this is consistent with other reports that polarised PBMCs (Zhang et al., 2024; Khan et al., 2022).

Human prostate cancer cell lines DU145 and 22Rv1 were used in this study. Although these cell lines had to be chosen due to unforseen circumstances with lost liquid nitrogen storage, they are also known for their sensitivity to MAPK inhibition (Hagan et al., 2000; Segawa et al., 2001; BURKE et al., 2016; Ramamurthy et al., 2014). This may explain their senitivity to xentuzumab treatment (Figure 4.4 and 4.5).

Studies have reported that cancer cell and macrophage co-culture can induce a M2-like phenotype (Hagemann et al., 2006; Hollmen et al., 2015; Park et al., 2022), and range of secreted factors such as CXCL2, CXCL1, CCL2, and CCL3 were implicated in this (Mitri et al., 2019; Lindholm et al., 2015; Le et al., 2023; Su et al., 2019). Here, co-culturing murine or human macrophages with PTEN WT prostate cancer cells also resulted in a significant increase in CD206+ M2-like macrophages after 72 hours (Figure 4.6 and 4.7). Macrophages and 22Rv1 coculture also increased CD80+ M1-like macrophages after 72 hours (Figure 4.7a), which would support more active phagocytosis of macrophages when co-cultured with 22Rv1, compared to DU145 (Figure 4.18, 4.20, and 4.22; Huo et al., 2023).

Cytokine array experiments were performed to determine which factors secreted by cancer cells could affect macrophage polarisation in co-culture setting. CXCL1, M-CSF, CCL2, CCL3, CXCL2, and IL-1ra were identified as possible factors secreted by Myc-CaP or by BMDMs due to presence of Myc-CaPs (Figure 4.8). Previous studies showed that co-culture with monocyte lineage cells caused human prostate cancer cells to upregulate CCL2 (Lindholm et al., 2015), leading to CCL2-CCR2 activation, CCR2 and CCR4 upregulation, and increased prostate cancer cell invasion (Maolake et al., 2017). M-CSF has been reported to induce M2-like macrophage polarisation (Hamilton, 2008; Ushach et al., 2016). and reports show that M2-like macrophages produce IL-1ra (Mantovani et al., 2004; Fan et al., 2023). In addition, activation of CXCR2 by CXCL2 is known to polarise macrophages towards M2-like type (Mitri et al., 2019; Qin et al., 2023). There was a high expression of TIMP1, which controls MMPs and whose loss is associated with PTEN loss and prostate cancer cell invasion (Jackson et al., 2017; Guccini et al., 2021). For future work, an unbiased approach by bulk RNA sequencing would have been ideal to see if there are any transcriptional changes in cancer cells and macrophages cultured alone versus sorted from co-culture condition.

Taking this list, we also compared it to cytokines that were expressed by cancer cells in monoculture and could be influenced by IGF-1R inhibition (Figure 4.9). This was to determine whether xentuzumab affects production of cytokines or chemokines by Myc-CaPs and whether they play a role in macrophage polarisation. Quantification of the differences in signal using ImageJ revealed CCL4, CXCL1, CXCL10, M-CSF, CCL3, and TNF-α as cytokines that were present in Myc-CaP control media and suppressed by IGF blockade. CCL4, like CCL3, is part of MIP family and are involved in macrophage recruitment (Murdoch et al., 2004; Ruytinx et al., 2018). CXCL10 is known to regulate chemotaxis of macrophages, T cells, and NK cells and is associated with advanced cancer and poor prognosis (Wightman et al., 2015; Nagaya et al., 2020; Pandey et al., 2021). Pro-inflammatory cytokine TNFα is produced by M1-like macrophages and known for its anti-tumour activity (Muenchen et al., 2000; Mantovani et al., 2004; Tu et al., 2021; Han et al., 2022).

The cytokines that gave the strongest signal in the array and showed an increase in co-culture over time but were also detectable in media from cancer cell monoculture and suppressed by IGF-1R inhibition were CCL3 and CXCL1, representing one of the stronger cancer-cell specific factors that may impact polarisation. Studies on hepatocellular carcinoma (HCC), bladder cancer, and breast cancer showed correlation between CXCL1 and CD206+ macrophages (Wang et al., 2018; Zhao et al., 2023; Miyake et al., 2016). CCL3 has also been reported to play a significant role in M2 polarisation, where tumour-driven CCL3 binding to CCR1 programmed M2-like macrophage polarisation (Eum et al., 2020; Le et al., 2023). Since CCL3 is a key candidate driver of the M2-like phenotype and merits future in-depth study, one of the approaches that could be taken to further test this is to use CCL3 antagonists to confirm that CCL3 is required to mediate effects of IGF axis blockade on macrophage phenotype. Other approaches include mining spatial transcriptomic or proteomic data on prostate tissue to look for 'hotspots' of M2-like macrophages, CCL3+ cells, and IGF-1R+ cells.

From these two cytokine array experiments, blots with Myc-CaP conditioned-media and BMDM + Myc-CaP co-culture conditioned media were compared to identify CCL2 and IL-1ra as drivers for macrophage polarisation, consistent with several studies (Valeta-Magara et al., 2019; Su et al., 2019; Wang et al., 2022b; Yang et al., 2020a; Triozzi et al., 2010; Duan et al., 2021). As cytokine array is a semi-quantitative method and the signal is affcted by cell numbers, this comparison will need to be more controlled in the future. It would be informative to use a cytokine array to compare cytokines and chemokines in conditioned media of macrophages treated with and without xentuzumab.

Flow cytometry of murine M2-polarised macrophages treated with IGF-1 and xentuzumab had significantly decreased M2-marker CD206 (Figure **??**). This is consistent with the previous *in vivo* data where xentuzumab-treated tumours had significantly reduced M2-like macrophage population (Figure 3.12). This is also supported by Spadaro et al., 2017, which reports that M2-like macrophages secrete IGF-1 and require IGF-1R to sustain M2 macrophage activation and protection from helminth infection.

This suggests that IGF-dependent cancer signals via cytokines can induce M2-like polarisation that also results in activation of autocrine IGF signalling in the M2-like macrophage population. This type of cancer-associated paracrine signals leading to a microenvironmental change that promotes a self-sustaining autocrine niche are reported in other cancers (Ramirez-Castillejo et al., 2006; Meurette et al., 2018). The same effect was not seen in PBMC-derived M2-polarised macrophages (Figure 4.12), possibly due to difference in human and murine macrophages (Vijayan et al., 2019; Monnier et al., 2022). In addition, IGF-1 increased CD80+ expression in PBMC-derived macrophage, which is consistent with a study that showed pro-inflammatory effects of IGFs in PBMCs via MAPK pathway (Wolters et al., 2017). Several studies also consistently show regulation of macrophage polarisation by IGF-1R downstream pathways such as PI3K/AKT, ERK, and JAK/STAT (Bettencourt et al., 2017; Weichhart et al., 2015; Arranz et al., 2012; Zhou et al., 2022; Irey et al., 2019; Xia et al., 2023).

For the first time, we found that IGF-1 increases CD47 expression in murine PTEN WT Myc-CaP (Figure 4.13). This has been supported by a study in our lab where bulk RNA sequencing of Myc-CaPs in long-term IGF treatment showed significant upregulation of CD47 in high IGF-1 tumours (Nandakumar, 2022). The inconsistency in human PTEN WT prostate cancer cells (Figure 4.14) could be due to genetic variation among cell lines or species difference. Myc overexpression in Myc-CaP cells (Watson et al., 2005) could also have shown a clearer effect, as Myc oncogene has been found to upregulate CD47 in murine and human cancer cells (Casey et al., 2016). When looking at whether anti-CD47 can affect downstream signalling pathway of IGF-1R, there was no significant change in ERK phosphorylation by anti-CD47 treatment in two human prostate cancer cell lines (Figure 4.15 and 4.16). This is consistent with a previous publication that shows that IGF-1 did not induce significant increase in ERK phosphorylation upon anti-CD47 treatment on porcine aortic smooth muscle cells (Maile et al., 2003).

As seen in Figure 4.17 and 4.18, anti-CD47 increased phagocytosis of murine and human prostate cancer cells by unpolarised and M1/M2-polarised macrophages. Although

there are no previous studies using anti-CD47 in prostate cancer model, effects of anti-CD47 increasing phagocytosis of cancer cells were shown previously in glioblastoma, melanoma, leukemia, and ovarian cancer (Zhang et al., 2016b; von Roemeling et al., 2020; Al-Sudani et al., 2023; Willingham et al., 2012; Majeti et al., 2009). Increased phagocytosis by anti-CD47 was also seen in PTEN-null cells (Figure 4.17d-f), suggesting this phenomenon is mediated by different IGF-dependent effects from those required for cancer cell proliferation and survival.

As expected from an increase in CD47 expression in Myc-CaP with IGF-1 treatment, IGF-1 treatment reduced phagocytosis of Myc-CaP by unpolarised and M1/M2-polarised macrophages, which was reversed with xentuzumab-treatment (Figure 4.19a-c). This significant increase in phagocytosis with xentuzumab compared to IGF-1 treatment was seen in other prostate cancer cells (Figure 4.19d-f, Figure 4.20), suggesting that CD47 expression in cancer cells may not necessarily correlate with susceptibility to phagocytosis. In addition, effects of IGF-1 and xentuzumab on phagocytosis were the most striking in M1-like macrophage phagocytosis of prostate cancer cells. It was expected that M1-like macrophages phagocytose more than M2-like, as M1-like macrophages are reported to promote phagocytosis and remove dead cells (Atri et al., 2018; Kohno et al., 2021).

Although combination treatment of anti-CD47 and xentuzumab on murine cancer cells and M1-like macrophage co-culture showed siginificant increase in phagocytosis compared to control, the changes were not significant compared to anti-CD47 treatment alone (Figure 4.21). This could have been due to xentuzumab and anti-CD47 not synergising as well in murine models. However, there was a significant increase in phagocytosis of 22Rv1 cells by M1-like macrophages with the combination treatment (Figure 4.22b), suggesting that xentuzumab and anti-CD47 treatment could be a novel therapy targeting human macrophages in prostate cancer. Combination treatments of anti-CD47 and other drugs were tried in other cancers, such as Chao et al., 2010 that shows anti-CD47 and rituximab synergy in non-Hodgkin lymphoma and Theruvath et al., 2022, where anti-GD2 and anti-CD47 combination treatment significantly reduced

neuroblastoma tumour burden. In the future, an *in vivo* experiment of anti-CD47 and xentuzumab combination treatment on nude mice model with 22Rv1 tumours would be informative to assess this therapeutic potential.

The final experiment to test effects of IGFs on T cell functions showed that M1-like macrophage and 22Rv1 co-culture under xentuzumab treatment significantly increased overall T cell proliferation, while significantly decreasing CD4+CD25+ Treg proliferation and CD8+TIM3+ T cells (Figure 4.23, 4.24, and 4.26). TIM-3 is a co-inhibitory receptor in T cells, specifically expressed by exhausted T cells (Jones et al., 2008; Fourcade et al., 2010; Sakuishi et al., 2011; Wolf et al., 2020), suggesting that IGF inhibition reduced exhausted CD8+ T cell population. Many of these effects were not shown in T cells under M0/M2 macrophages and cancer cell co-culture settings, consistent with pro-inflammatory effects of M1-like macrophages (Mosser et al., 2008; Sica et al., 2012). The changes were not observed in T cells exposed to M1-like macrophage and DU145 coculture, in line with many of the pro-inflammatory effects shown by 22Rv1 only (Figure 4.7; Figure 4.20; and Figure 4.22). The only significant change occurred by both prostate cancer cell lines co-culture with M0 macrophages was significant reduction in IFN-γ production by CD8+ T cells upon xentuzumab treatment. IFN-γ is released by activated T cells (Bhat et al., 2017) and is known both for anti-tumour responses (Dighe et al., 1994; Kaplan et al., 1998) and for promoting immune evasion (Zaidi et al., 2011; Pai et al., 2019). Recent study on IFN-γ signalling on CD8+ T cell functions and differentiations showed that IFN-γ restricts stem-like T cell maintenance and proliferation (Mazet et al., 2023), suggesting possible anti-tumour responses by xentuzumab. One limitation was a concern with high variability among each tries, so it would have been better to collect and run all samples at once to remove batch effects and unwanted changes in experiment settings. More replicates would also have revealed clearer signal.

Throughout this chapter, there were discrepancies in the results where certain results varied depending on the cell lines used due to different characteristics of the cell lines. In particular, murine and human cell lines behaved differently, highlighting a need for a

better humanised *in vivo* model, or patients-derived organoids that better demonstrate translational capability of these findings. Despite these inconsistencies, this chapter, which stemmed from the findings on macrophage recruitment in previous chapter (Figure 3.12), provided more information and a reason to investigate macrophage infiltration and recruitment in clinical tissues (Chapter 5).

Overall, these *in vitro* work confirmed pro-inflammatory effects of xentuzumab by decreasing CD206+ M2-like macrophages, increasing phagocytosis of 22Rv1 by M1 macrophages, and reducing exhausted CD8+ T cells and CD25+ Tregs when exposed to 22Rv1, suggesting that IGF axis manipulation have a potential to influence macrophage phenotypes and phagocytic functions, and by doing so, enhance T cell functions. This is in line with published immunosuppressive effects of IGFs (Bilbao et al., 2014; Ajona et al., 2020) and sheds light on targeting macrophages for novel prostate cancer therapy.

5

WINGMEN Trial: clinical relevance

Contents

5.1 Introduction 175
5.2 WINGMEN trial design and baseline characteristics . . . 177
5.2.1 WINGMEN trial design 177
5.2.2 Patient characteristics 179
5.2.3 Secondary endpoint: feasibility, safety, and tolerability of xentuzumab treatment in pre-operative setting 183
5.3 Investigating the changes in tissue markers following IGF blockade 185
5.3.1 Primary endpoint: changes in IGF axis activation 185
5.3.2 Immunohistochemical staining of tissues 188
5.3.3 Multiplex immunofluorescence staining of tissues 191
5.3.4 Transcriptomic profiling of pre- and post-xentuzumab treated tumours 196
5.4 Analysis of blood samples following IGF blockade 199
5.4.1 Assessing circulating markers in pre- and post-xentuzumab treated serum 199
5.4.2 PBMC immunophenotyping by mass cytometry (CyTOF) . . 201
5.5 Discussion 203

5.1 Introduction

Researchers open clinical trials to assess how well the new medical approaches work in patients. There are two main types of trials: observational studies, which are based on monitoring people in different situations with no influence from researchers, and interventional trials, whereby researchers intercede during the study in forms of interventions or treatments (Ray et al., 2016; Thiese, 2014). One form of interventional trials is a window-of-opportunity (window) study, where patients receive novel treatment during the 'window' between diagnosis and cancer therapy, usually surgery (Aroldi

et al., 2020). This type of trial design enables understanding of the molecular and cellular mechanism of the treatment, especially in tumours that have not received any treatment previously (Marron et al., 2022).

There have been several window trials for prostate cancer therapy. For the Study of the Early Biological Effects of Testosterone Suppression in Prostate Cancer Using Neoadjuvant Degarelix Prior to Radical Prostatectomy (NCT01852864 and NCT00967889), degarelix was administered to 27 patients with high-risk prostate cancer 7 days before RP, and the study found reduced levels of intraprostatic androgens as well as proliferation marker Ki67 and deregulation of AR target gene expression (Shaw et al., 2016). Another window study used metformin, a drug typically used to treat type 2 diabetes but also affects AMP-activated protein kinase (AMPK) and mTOR activity (NCT00881725). Oral administration of metformin at increasing doses for 5 days over 4 - 12 week window before RP led to 65% reduction of Ki67 and phosphorylated 4E-BP1 (Joshua et al., 2014). In addition, oral prescription of fluvastatin between 4 - 12 weeks prior to RP (NCT01992042) led to 2.7-fold increase in tumour cell apoptosis in post-treatment tissues, measured by increase in CC3 (Longo et al., 2020). In Cambridge Neoadjuvant Carcinoma of the Prostate (CANCAP)02 (NCT02064608) and CANCAP03 (NCT02324998) studies, prostate cancer patients were treated with mTOR inhibitor vistusertib and PARP inhibitor olaparib ± degarelix, respectively, prior to RP. While CANCAP02 showed mTOR pathway inhibition with 4E-BP1 reduced in 100% of patients and p-S6 in 67% (Pacey et al., 2017; Pacey et al., 2018), CANCAP03 reported significant protease-activated receptor (PAR) inhibition upon olaparib and olaparib + degarelix treatment, as well as upregulation of homologous recombination deficiency gene signatures upon the combination treatment (Pacey et al., 2019; Dev et al., 2023; Reis et al., 2024).

In 2021, we carried out a Windows trial of INsulin-like Growth factor neutralising antibody Xentuzumab in MEN scheduled for radical prostatectomy (WINGMEN) trial (NCT05110495) to understand the consequences of IGFs on prostate cancer progression. The aim of this chapter and the trial is to test pre- and post-xentuzumab-treated tissues and blood samples with various molecular and cellular techniques to assess the

amount of pathway inhibition induced by xentuzumab (primary endpoint) as well as the feasibility of recruitment and safety of the drug (secondary endpoint), and to assess changes in tissue and circulating markers post-xentuzumab, including immune activities and transcriptomic and metabolic profile.

5.2 WINGMEN trial design and baseline characteristics

5.2.1 WINGMEN trial design

WINGMEN is an open-label, phase 0, window trial of IGF blocking monoclonal antibody xentuzumab (Figure 5.1). Men $\geq$ 18 years old with localised T1-T3a prostate cancer scheduled for radical prostatectomy were identified and approached. Patients consented and successfully screened for additional eligibility criteria (Table 7.8) were given weekly intravenous infusion of xentuzumab (1,000 mg) in a 4 - 6 week window before surgery. Patients whose surgery was delayed could receive up to 10 doses of xentuzumab, though the surgery had to happen within 6 days of their final xentuzumab dose. Blood and tissue samples were collected before the treatment began (pre-treatment samples; PRE) and after the last treatment and/or during surgery (post-treatment samples; POST) and analysed using various methods (Figure 5.2). For post-treatment tissue samples, cores were taken in theatre from the prostatectomy for rapid fixation to ensure comparability between the biopsy and prostatectomy and to avoid artefacts or loss of phosphorylation signals caused by slow fixation of large prostatectomy sample.

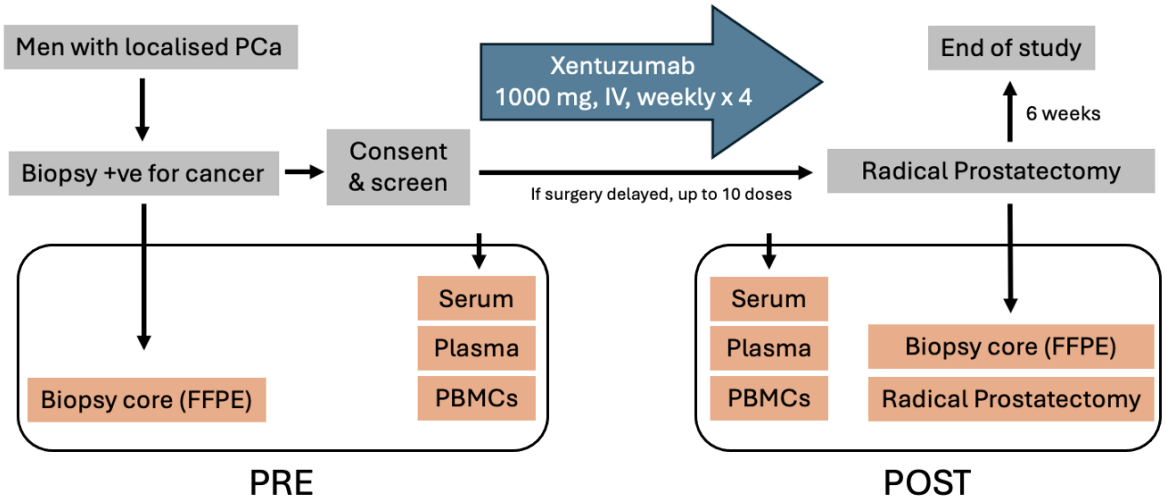


Figure 5.1: WINGMEN trial schematics. Flow chart summarising the WINGMEN trial design and the timepoints at which the samples were taken. Samples were collected before the treatment (PRE), and after treatment and/or during surgery (POST).

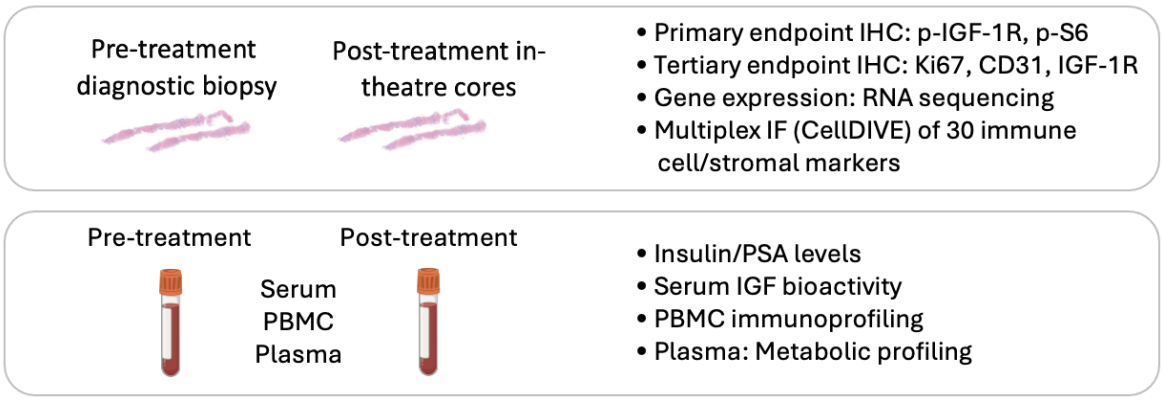


Figure 5.2: Samples collected and analysed from the WINGMEN trial patients. Pre-treatment diagnostic biopsies and post-treatment in-theatre cores of the removed prostate were compared using immunohistochemistry (including for primary endpoint), RNA sequencing, and multiplex immunonfluorescence. Blood samples collected during screening (PRE) and a day before surgery (POST) were analysed in various ways: serum to compare insulin/PSA levels and IGF bioactivity, PBMC for immune-profiling using mass cytometry, and plasma for metabolomics using mass cytometry.

5.2.2 Patient characteristics

Recruitment opened on 13th December 2021 with a target of 20 - 30 patients and was completed on the 31st January 2023. Among 72 patients approached for enrolment, 27 patients were recruited. All recruited patients received allocated investigational medicinal product (IMP) xentuzumab. At the end of the treatment, 26 patients had surgery after more than 4 doses of xentuzumab. One patient did not have surgery due to disease progression after treatment completion. This information is summarised in the Consolidated Standards of Reporting Trials (CONSORT) diagram (Figure 5.3) and Table 5.1.

Baseline characteristics of the WINGMEN patients are recorded in Table 5.2. Median age of the 27 patients was 66 years old, with Eastern Cooperative Oncology Group (ECOG) performance scale of 0 or 1. Median body mass index (BMI) of the patients was 27, in an overweight range, and the median PSA level was about 6 - 7. Median serum IGF-1 levels were reduced by 78% upon treatment. In addition, 74% of the patients had GG 2 and 3. Tumour stage was determined post-surgery by the RP sections, and 63% had pT2c or pT3a cancer, which is defined as cancer invading both sides of the prostate and cancer developing outside the prostate but not spread to the seminal vesicles, respectively.

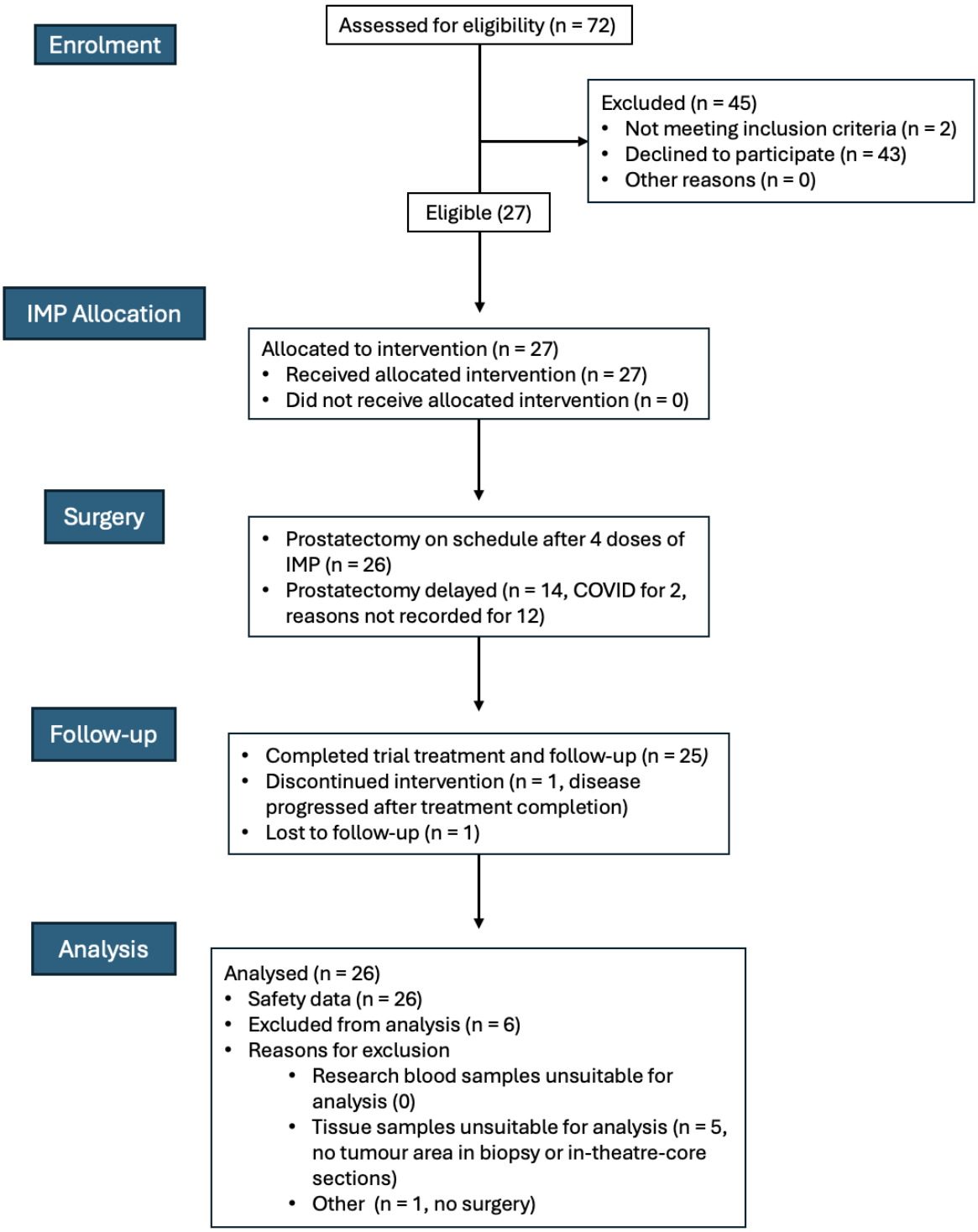


Figure 5.3: CONSORT diagram for WINGMEN study. Although reasons for surgery delay were not recorded, they are likely to be logistical/administrative reasons. Analysis section detailing samples excluded from analysis only refers to the primary endpoint, as different samples were excluded for various reasons relating to the study.

Table 5.1: Treatment compliance and details of interventions. Eligible patients were identified from outpatient clinic lists. Cycles given on schedule was defined as cycles that were given exactly 7 days apart from the last. Reasons for treatment delays (more than 7 days after from the previous dose) were not recorded, but IMP toxicity was not the reason for any delays. Patients excluded from analysis only refers to primary endpoint data. One patient (WN-01-10020), upon completion of treatment and POST-blood collection but before surgery, progressed on scan and went on to radiotherapy, so no tissue was collected from surgery and therefore was not analysed.

Patients screened (n)	72
Patients excluded (n)	45
Reasons for exclusion	
Inclusion criteria not met (n)	2
Patient declined (n)	43
Other (n)	0
Patients allocated to trial treatment (n)	27
Patients received treatment (n)	27
Patients who did not receive treatment (n)	0
Median xentuzumab cycles (range)	5 (4 - 9)
Cycles given on schedule (%)	75.00
Reason for treatment delays (more than 7 days after the previous dose)	Not recorded
Patient preference (n)	NA
Toxicity (n)	NA
Other (n)	NA
Early withdrawal (n)	0
Reason for withdrawal (n)	0
Patient preference (n)	NA
Toxicity (n)	NA
Other (n)	NA
Completed treatment and follow-up (n)	25
Lost to follow-up (n)	1
Patients whose data was analysed (n)	26
Patients excluded from analysis (n)	1
Reason for exclusion (n)	
Blood unsuitable for analysis (n)	0
Tissue unsuitable for analysis (n)	1 (no surgery)

Table 5.2: Baseline characteristics of WINGMEN patients. Detailed tumour stages, determined by TNM classification of American Joint Committee on Cancer (AJCC), were only recorded post-surgery.

Patients (n=27)	**Baseline**	**Post-treatment**
Median age, years (range)	66 (50-74)	66 (50 - 74)
ECOG performance status (%)		
0	92.6	7.4
1	92.6	7.4
BMI	27.43 (19.67 - 31.82)	27.09 (19.57 - 31.08)
Median PSA, ng/ml (range)	7 (2 - 24)	6 (2 - 27)
Median serum IGF-1, nmol/l (range)	18.05 (11 - 36)	4.05 (1.5 - 40)
Gleason score (n)	n = 26	n = 26
3+3	1	0
3+4	13	12
4+3	7	10
4+4	2	1
4+5	3	2
5+4	0	1
5+5	0	0
Grade group (n)	n = 27	n = 27
1	1	1
2	13	13
3	7	7
4	3	3
5	3	3
Tumour stage (n, AJCC TNM)	n = 27	n = 27
pT1		0
pT2a		5
pT2b		2
pT2c		8
pT3a		9
pT3b		2

5.2.3 Secondary endpoint: feasibility, safety, and tolerability of xentuzumab treatment in pre-operative setting

The secondary endpoint of the trial was to determine the feasibility of treatment in pre-operative setting and to assess the safety and tolerability of xentuzumab administration.

Feasibility of treatment before surgery was measured and tabulated in Table 5.3. Except for one patient (WN-01-10020) that progressed on scan and went on to radiotherapy, all patients had surgery on schedule upon 4+ doses of xentuzumab. There were 15 patients who had more than 4 doses of xentuzumab, 2 of which had COVID, and 1 that never had surgery due to disease progression, and the reason for delay for 12 patients was not recorded. Trial treatment, however, was not the reason for the delays.

Safety and tolerability of xentuzumab administered in pre-prostatectomy setting was assessed (Table 5.4). There were 24 adverse events reported by the patients in this trial, of which one of them had common terminology criteria for adverse events (CTCAE) grade of 3; patient WN-01-10016 had hypertension, which was deemed probably not caused by xentuzumab, and the condition improved for the patient. Of the 17 treatment-related adverse events (TRAE) that could have definitely, possibly, or probably be caused by xentuzumab, none of them had CTCAE grade of 3 or higher.

Table 5.3: Feasibility of treatment in pre-operative setting. This endpoint was determined by number of patients whose radical prostatectomy was performed on schedule after 4 doses of xentuzumab (Patients could receive up to 10 doses of xentuzumab if surgery is delayed).

Feasibility of treatment	**Patients (n = 27)**
Surgery performed on schedule (n)	26
Surgery delayed by trial treatment	0
Median delay, weeks (range)	NA
Surgery delayed by other factors	15
Median delay, weeks (range)	2 (2 - 9)

Table 5.4: Safety and tolerability of xentuzumab administered in the pre-prostatectomy setting. AE, adverse event; TRAE, treatment-related adverse events; SAE, serious adverse event; AESI, adverse events of special interest. CTCAEv5.0 was used to assess the grading.

Safety profile	**Patients (n = 27)**	
	Any Grade	**Grade 3, 4, or 5**
Any AE	24 (88.9%)	1 (3.7%)
Any TRAE	17 (70.8%)	0 (0%)
SAE	0 (0%)	0 (0%)
AESIs	0 (0%)	0 (0%)
Most common cause any AE		
Fatigue	10 (37.0%)	0 (0%)
Reduced appetite	0 (0%)	0 (0%)
Nausea	5 (18.5%)	0 (0%)
Vomiting	0 (0%)	0 (0%)
Diarrhoea	0 (0%)	0 (0%)
Constipation	2 (11.1%)	0 (0%)
Weight loss	0 (0%)	0 (0%)
Dry skin	1 (5.9%)	0 (0%)
Anaemia	1 (5.9%)	0 (0%)
Hypertension	2 (11.1%)	1 (3.7%)
Headaches	4 (14.8%)	0 (0%)

5.3 Investigating the changes in tissue markers following IGF blockade

5.3.1 Primary endpoint: changes in IGF axis activation

Primary endpoint of the WINGMEN trial was to assess the amount of IGF pathway inhibition by xentuzumab using IHC. Phospho-IGF-1R and downstream marker phospho-S6 were selected as the targets. In order to optimise the antibody staining, human prostate cancer spheroids cultured and treated by me (Figure 5.4a) as well as control prostate cancer tissues (Figure 5.4b) were stained by THL. For validation, diagnostic biopsies and in-theatre cores from RPs of non-trial patients were stained with phospho-IGF-1R (Figure 5.4c) and phospho-S6 antibodies (Figure 5.4d).

Upon successful validation with clear positive and negative control stainings (no primary), PRE-treatment diagnostic biopsies and POST-treatment in-theatre cores of WINGMEN patient tissues were sectioned by OCHRe and stained with phospho-IGF-1R (Figure 5.5a) and downstream phospho-S6 (Figure 5.5b) by THL. I then annotated tumour and benign areas, and % positively stained cells in tumour epithelium were quantified in HALO (Chapter 2.6.5). Among 22 patients with tumour area in both PRE and POST tissues, IGF-1R phosphorylation was reduced in 86% of the patients (Figure 5.5c). Since IGF-1R can be detected in both nucleus and cytoplasm, and nuclear IGF-1R is detectable in about 50% of radical prostatectomies and associated with advanced tumour stage (Aleksic et al., 2018), nuclear and cytoplasmic signals were detected and quantified separately. Reduction of IGF-1R activation in both nucleus and non-nuclear areas was also observed in 86% of the patients (Figure 5.5c). Reduction of downstream marker S6 activation was seen in 76% of the patients (Figure 5.5d). These results proved that the primary endpoint of the trial was met, where xentuzumab induced significant IGF axis pathway inhibition in tumours of prostate cancer patients.

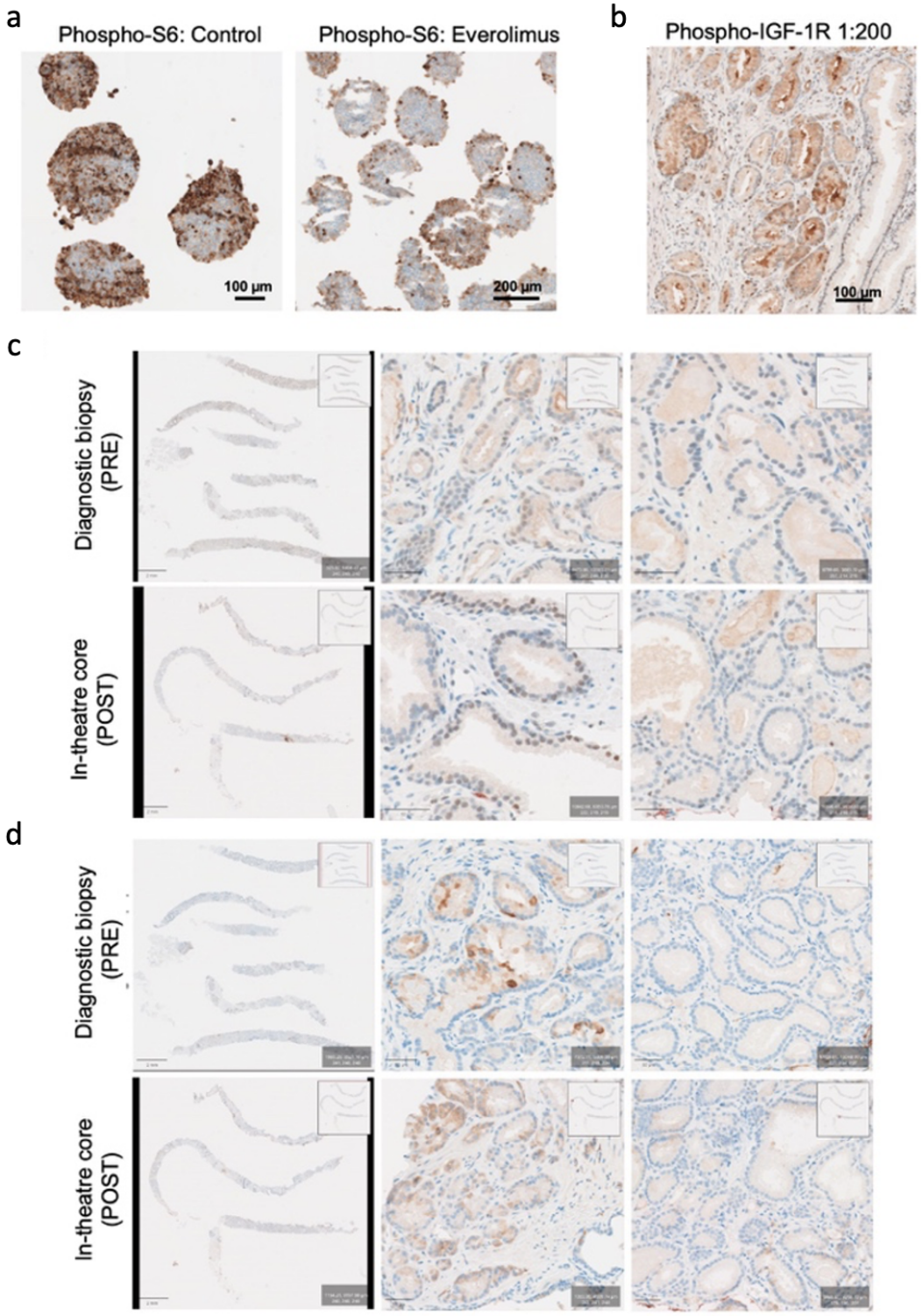


Figure 5.4: Testing phospho-IGF-1R and phospho-S6 antibodies on prostate cancer spheroids and tissues. a. IHC methods were optimised in the Translational Histopathology Lab using human prostate cancer spheroids cultured and treated in the Macaulay lab. Example shows effects of solvent (control) or everolimus on downstream marker phospho-S6 IHC. **b**. Sample prostate cancer stained with phospho-IGF-1R antibody (pY1161, 1:200, Biorbyt) during IHC optimisation. **c-d**. Testing stability of epitopes pY1161 IGF-1R (**c**, using Biorbyt antibody) and pS6 (**d**, pS235/236, 1:800, Cell Signaling Technology) in diagnostic and in-theatre biopsies of a non-trial patient.

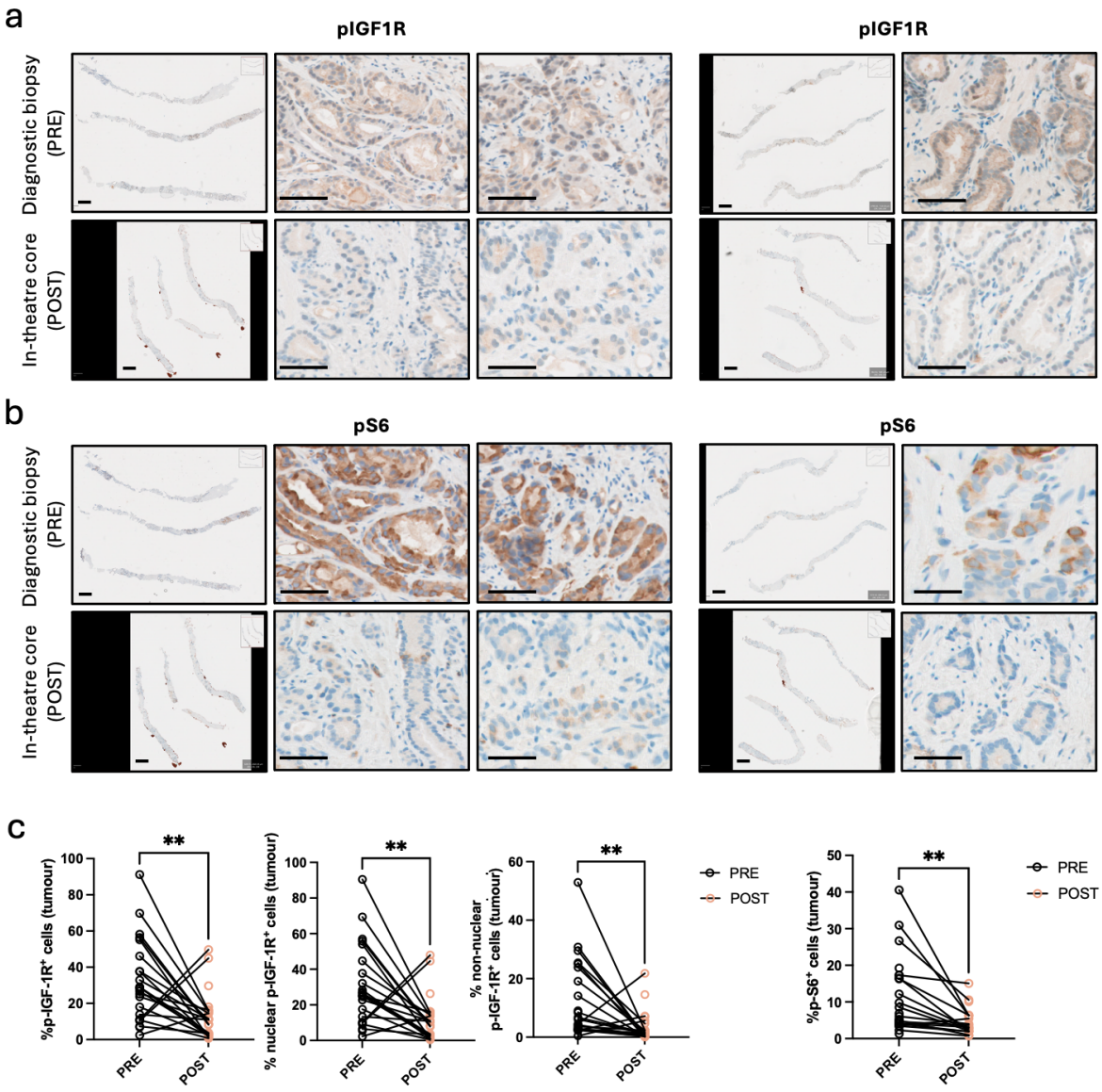


Figure 5.5: Primary endpoint markers at baseline (PRE) and after xentuzumab (POST). a-b Diagnostic biopsies (PRE; n = 27) and in-theatre cores (POST; n = 26) were stained by phospho-IGF-1R (**a**) and phospho-S6 (**b**) by Translational Histopathology Lab, Department of Oncology, University of Oxford. Left panel contains images of WN-01-10022 and right panel is of WN-01-10011. Scale bar: 2 μm for the whole section images, 50 μm for close-up images. **c-d** The stainings were analysed by me using HALO software and graphed using GraphPad Prism (version 10). **c**. Left: % p-IGF-1R+ tumour cells, Middle: % p-IGF-1R+ tumour cells with nuclear staining, and Right: % p-IGF-1R+ tumour cells with non-nuclear staining. **d**. % p-S6 tumour cells (**p<0.01, paired t-test).

5.3.2 Immunohistochemical staining of tissues

To add more information on the changes in the receptor expression as well as tumour cell proliferation following xentuzumab administration, total IGF-1R and Ki67 measures were assessed. In addition, RRM2 was chosen as an exploratory marker, having previously shown preclinically that IGF signalling regulates RRM2 (Rieunier et al., 2021).

IGF-1R staining done by me showed significant difference in total IGF-1R expression in tumour cells post-xentuzumab treatment, with 71% of the patients with reduced IGF-1R expression (Figure 5.6a-b) As in Figure 5.5c, nuclear and non-nuclear stainings were quantified, which showed no significant differences, with 50% of the patients showing changes in nuclear IGF-1R staining and 50% in non-nuclear IGF-1R staining (Figure 5.6b). The degree of changes in reduction of non-nuclear IGF-1R staining was smaller than that of nuclear IGF-1R staining, suggesting that changes in nuclear IGF-1R mainly drove the significant changes seen in total tumour cells. In addition, there was a significant decrease in cell proliferation marker Ki67 in xentuzumab-treated tissue (Figure 5.6c), with the reduction detected in 75% of the patients. RRM2 staining showed that 65% of the patients had reduced RRM2 upon xentuzumab treatment (Figure 5.7). This showed that IGF blockade significantly reduced tumour cell proliferation in prostate cancer patients.

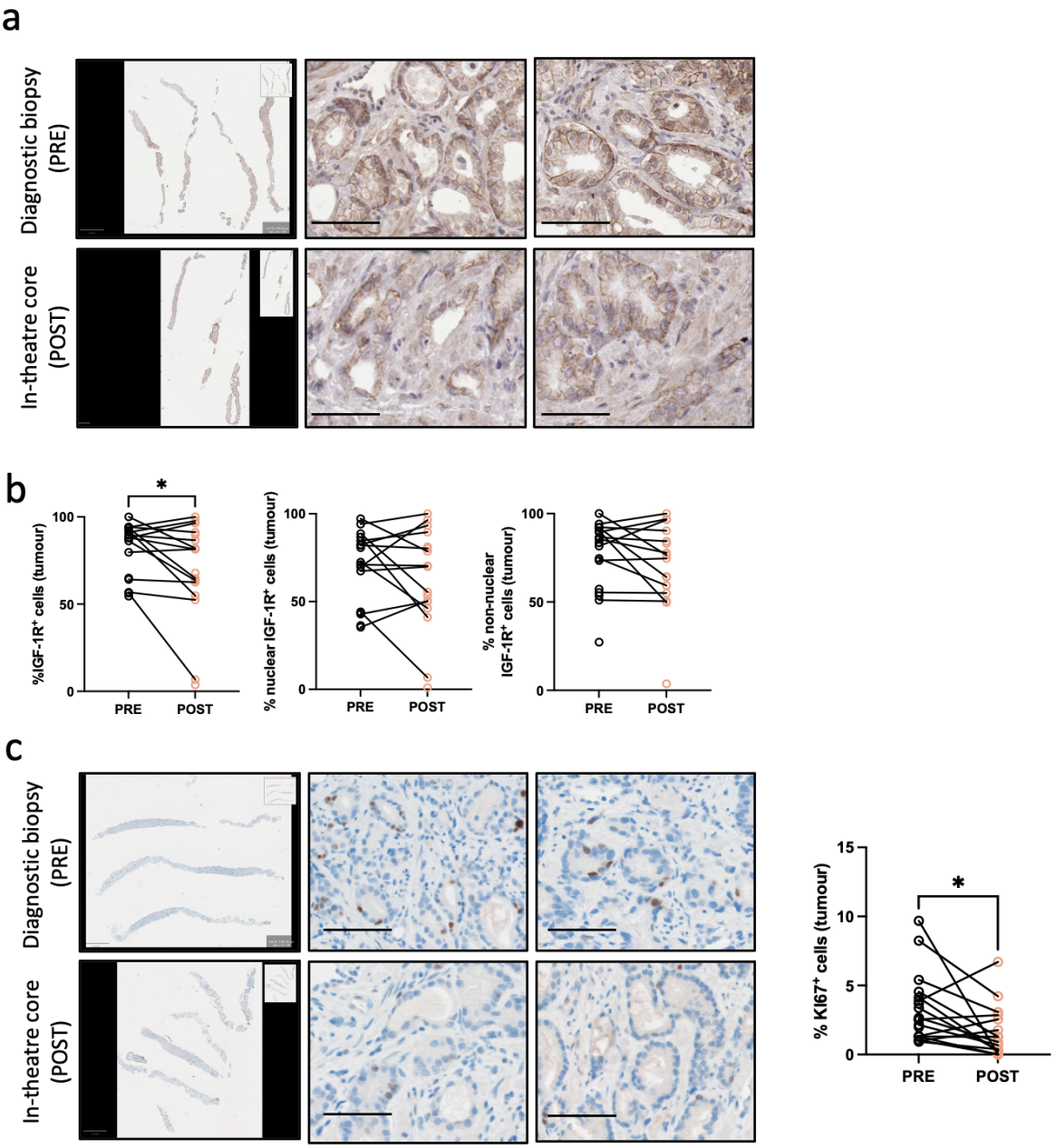


Figure 5.6: IGF-1R and Ki67 expression at baseline (PRE) and after xentuzumab (POST). Diagnostic biopsies (PRE; n = 27) and in-theatre cores (POST; n = 26) were stained with **a**. IGF-1R antibody (1:50, Cell Signalling Technology) with quantification (**b**, Left: % IGF-1R+ tumour cells, Middle: % IGF-1R tumour cells with nuclear staining, Right: % IGF-1R tumour cells with non-nuclear staining.) and **c**. Ki67 antibody (1:200, Cell Signalling Technology, stained by Translational Histopathology Lab, University of Oxford). The panels contain representative tissue stainings of WN-01-00008 (**a**) and WN-01-00004(**c**). Scale bar: 2 μm for the whole section, 50 μm for the close-up image. The stainings were analysed using HALO software and graphed using GraphPad Prism (version 10). *p<0.05, paired t-test.

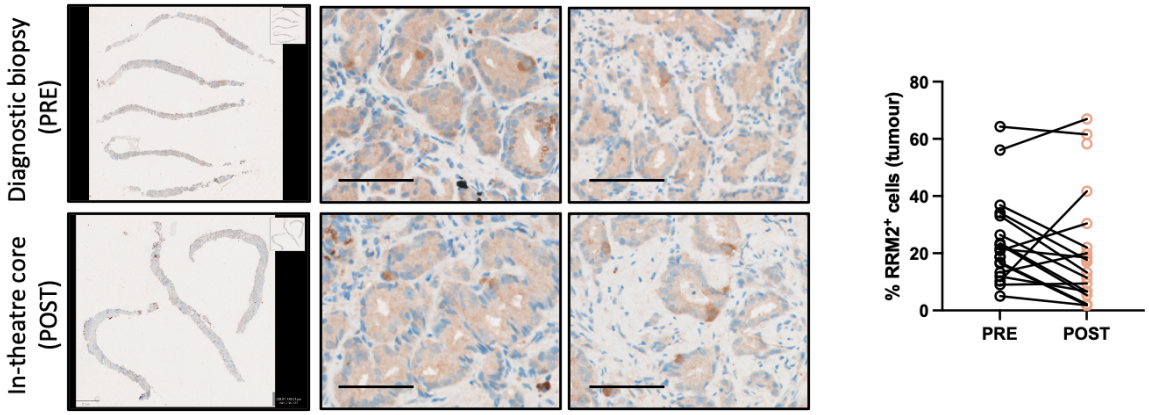


Figure 5.7: RRM2 expression at baseline (PRE) and after xentuzumab (POST). Diagnostic biopsy (PRE; n = 27) and in-theatre core (POST; n = 26) were stained with RRM2 antibody (1:50, Santa Cruz Technology) by Translational Histopathology Lab, University of Oxford. The images were analysed using HALO software and graphed using GraphPad Prism (version 10). Representative image of WN-01-00026, scale bar: 2 μm for the whole section, 50 μm for the close-up image. Paired t-test was used for statistical analysis

5.3.3 Multiplex immunofluorescence staining of tissues

To characterise the immune microenvironment of prostate cancer, pre-treatment diagnostic biopsies and post-treatment in-theatre cores were stained with 13 immune and structural markers and imaged using mIF platform CellDIVE, Kennedy Institute of Rheumatology, University of Oxford. Due to the fragility of small tissues and the brutal nature of repetitive cover-slipping and bleaching of the sections, two consecutively cut sections were used to stain for different markers as in Table 2.9. (Figure 5.8). Pan-cytokeratin (PCK), luminal cell marker, was selected as epithelial marker, vimentin as stromal marker, and CD31 as vasculature marker. AR was selected to determine androgen receptor expression in prostate cancer, and immune markers CD14, CD45, CD68, CD163, CD4, FOXP3, CD8, CD3, and TIM3 were used. The tissues were stained as in Chapter 2.15.

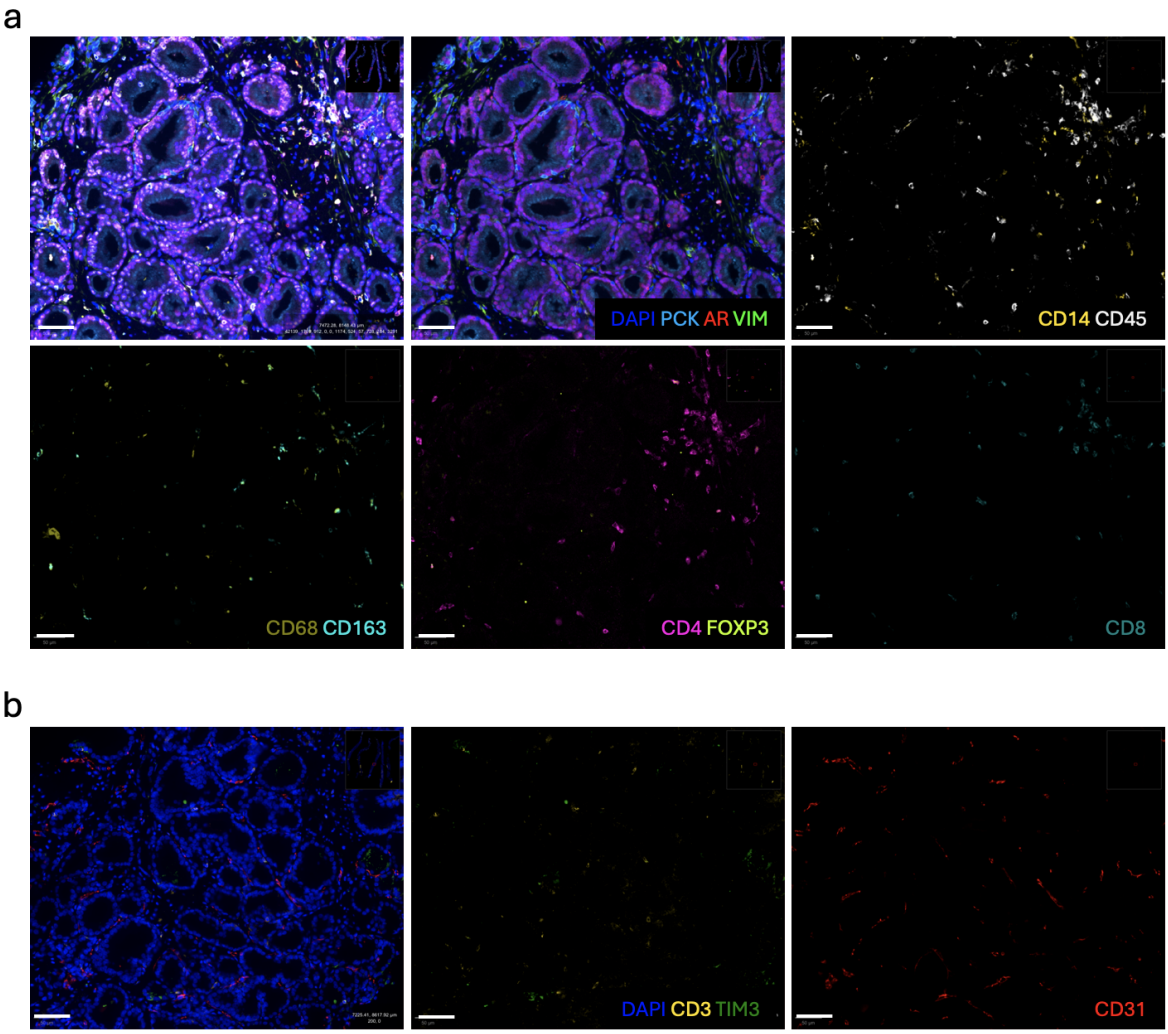


Figure 5.8: Multiplex immunofluorescence imaging of WINGMEN patient samples. Diagnostic biopsies (n = 27) and in-theatre cores (n = 26) were stained with 10 immune and structural markers and imaged using CellDIVE platform to show immune cell composition and distribution. Representative image is of tumour glands in the diagnostic biopsy of WN-01-00019. **a**. Markers used were: PCK, epithelium; AR, androgen receptor; Vimentin (Vim), stromal marker; CD14, monocytes; CD45, lymphocytes; CD68, tumour-associated macrophages; CD163, M2-like macrophages; CD4, helper T cell; FOXP3, regulatory T cells; and CD8, cytotoxic T cells. **b**. Markers used were CD3, total T cells; TIM3, T cell exhaustion marker; CD31: vasculature. Scale bar = 50 μm.

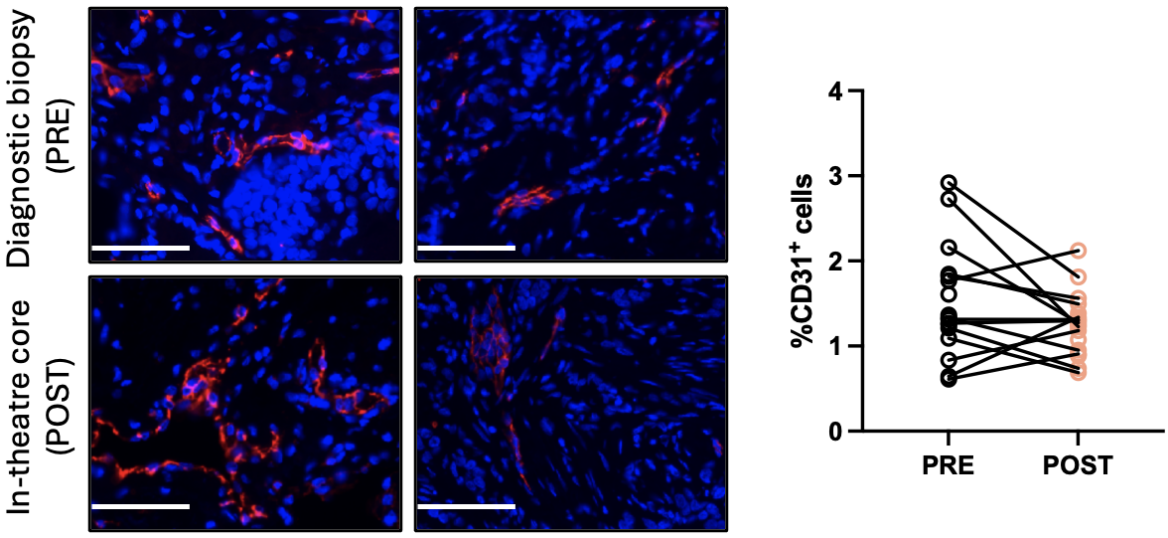


Figure 5.9: CD31 expression at baseline (PRE) and after xentuzumab treatment (POST). Diagnostic biopsies (PRE; n = 27) and in-theatre cores (POST; n = 26) were stained with CD31 antibody (10 ug/mL, Novus biologicals). The images were analysed using HALO software. The representative images are that of WN-01-00019. Scale bar = 50 μm. Paired t-test was used for statistical analysis

Vasculature marker CD31 was assessed as part of mIF. There was no significant difference in CD31 expression, but there seemed to be more punctate areas of CD31 staining in diagnostic biopsies compared to post-treatment tissue (Figure 5.9).

Multiplex IF allowed for visualisation of lymphoid aggregates as well as immune cell infiltration in tumour areas (Figure 5.10a). Further quantification revealed decreasing trend of total T cell (CD3+) population in xentuzumab-treated tissues, of which there was a significant reduction of CD3+TIM3+ exhausted T cell population and significant increase in CD8+ cytotoxic T cell population (Figure 5.10b). There were no significant changes in CD4+FOXP3- helper T cells and CD4+FOXP3+ Tregs. Monocyte population, including CD68+ macrophages and CD68+CD163- M1 and CD68+CD163+ M2 macrophage subtypes, was unchanged by xentuzumab treatment (Figure 5.10c). In addition, xentuzumab significantly reduced AR-expressing cells in 73% of the patients (Figure 5.10d).

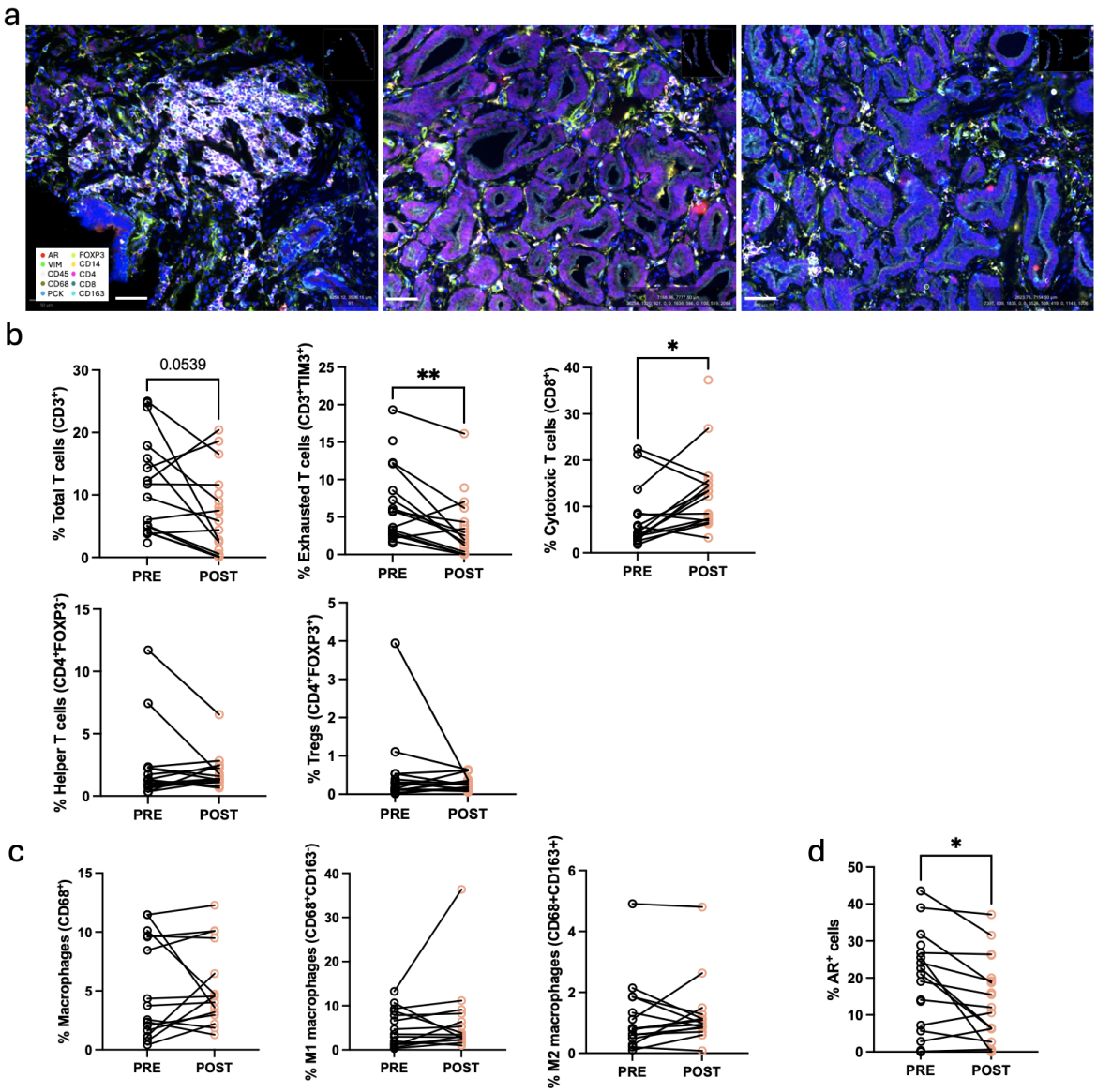


Figure 5.10: Immune cell composition at baseline (PRE) and after xentuzumab treatment (POST). a. Representative images of patient tissues, scale bar: 50um. Left: lymphoid structures in diagnostic biopsies (PRE; n = 27) of WN-01-10010. Middle: tumour areas and infiltrating immune cells in PRE tissues of WN-01-00002. Right: tumour areas and infiltrating immune cells in xentuzumab-treated (POST; n = 26) tissues of WN-01-00002. **b-d**. T cells (**b**), monocytes (**c**), and AR (**d**) expressions in pre- and post-xentuzumab treated tissues were quantified using HALO. *p<0.05, **p<0.01, paired t-test.

Infiltration analysis algorithm in HALO was used to determine the number of immune cells within and outside the epithelium. There was no significant difference in intraepithelial CD4+FOXP3- helper T cells and CD4+FOXP3+ Tregs, but xentuzumab significantly increased the number of CD8+ T cell infiltration into the epithelium (Figure 5.11a-c). In addition, CD68+CD163- M1 macrophage infiltration was significantly increased upon xentuzumab treatment within the epithelium but significantly decreased 10 - 100 μm outside the epitehlium (Figure 5.11d). There was no difference in intraepithelial CD68+CD163+ M2 macrophages (Figure 5.11e).

Overall, IGF blockade caused significant changes in T cell composition, AR expression, and immune cell infiltration in prostate cancer tissues, supporting immunosupressive actions of IGFs and reversing potential for xentuzumab.

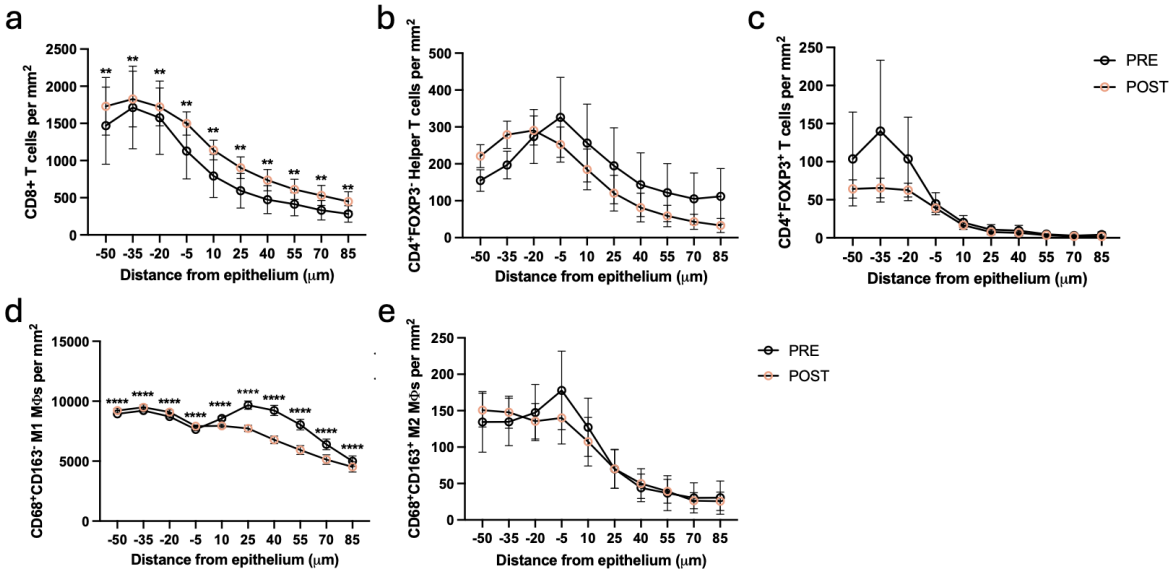


Figure 5.11: Immune cell infiltration at baseline (PRE) and after xentuzumab treatment (POST). Spatial analysis module in HALO was used to compare CD8+ T cells (**a**), CD4+FOXP3- helper T cells (**b**), CD4+FOXP3+ Tregs (**c**), CD68+CD206- M1 macrophages (**d**), and CD68+CD206+ M2 macrophages **e** infiltration into epithelium in pre- (n = 27) and post-xentuzumab (n = 26) treated tissues. **p<0.01, ****p<0.0001, two-way ANOVA.

5.3.4 Transcriptomic profiling of pre- and post-xentuzumab treated tumours

RNA was extracted from FFPE sections of pre-treatment diagnostic biopsies and post-treatment in-theatre cores and submitted for sequencing at GENEWIZ. Analysis was done as in Chapter 2.16.3.

PCA plot did not show clear separation between post-treated and pre-treated samples (Figure 5.12a). Further analysis identified 62 DEGs (Figure 5.12b-c), with a full list available in Table 7.16. There were separate clusters in the heatmap of DEGs, of which one cluster contained most of the PRE samples aside from three outliers. GSEA showed an enrichment of genes associated with immune pathways, senescence, and MAPK signalling (Figure 5.12d). In particular, IL-6, CXCR4, JUN, and ATF3 were upregulated upon xentuzumab treatment (Figure 5.12e).

Immune deconvolution digital cytometry CIBERSORTx (Newman et al., 2019) was used to estimate 22 immune cell type abundances using the RNA sequencing gene expression data (Figure 5.13a). There was a high variation of immune cells in each patient, which led to no clear segregation of samples in hieararchical clustering (Figure 5.13b). Interestingly, xentuzumab treatment led to significantly more gene signatures of activated mast cells (Figure 5.13c).

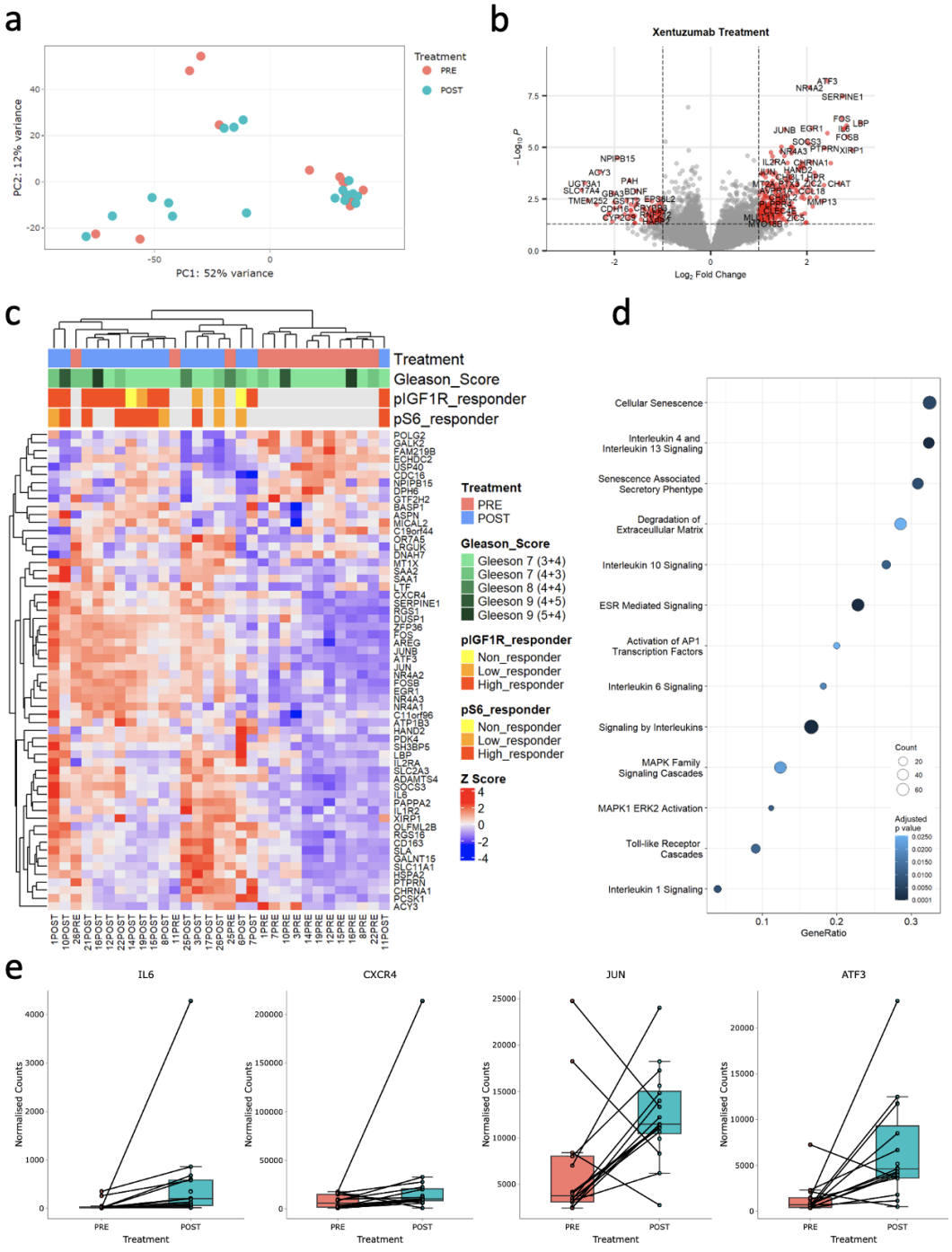


Figure 5.12: Transcriptional profiling of tumours at baseline (PRE) and after xentuzumab treatment (POST). **a**. Principal component analysis of the pre-treated biopsies (PRE) and post-xentuzumab-treated in-theatre cores (POST). **b** Volcano plot displaying differentially expressed genes (DEGs). **c**. Heatmap with hierarchical clustering of samples and significant DEGs. Patients were classified as: non-responders if they showed no decrease in pIGF1R or pS6 after treatment with Xentuzumab; low responders if they had a 0 - 60% decrease in the marker; and high responders if they had a >60% decrease in the marker. **d**. Selected significant pathways from GSEA using the Reactome database. **e**. Expression levels of a subset of DEGs. IL6 = Interleukin 6. CXCR4 = C-X-C chemokine receptor type 4. JUN = c-Jun. ATF3 = Activating Transcription Factor 3. Analysis was done by Dr. Fiona Hartley.

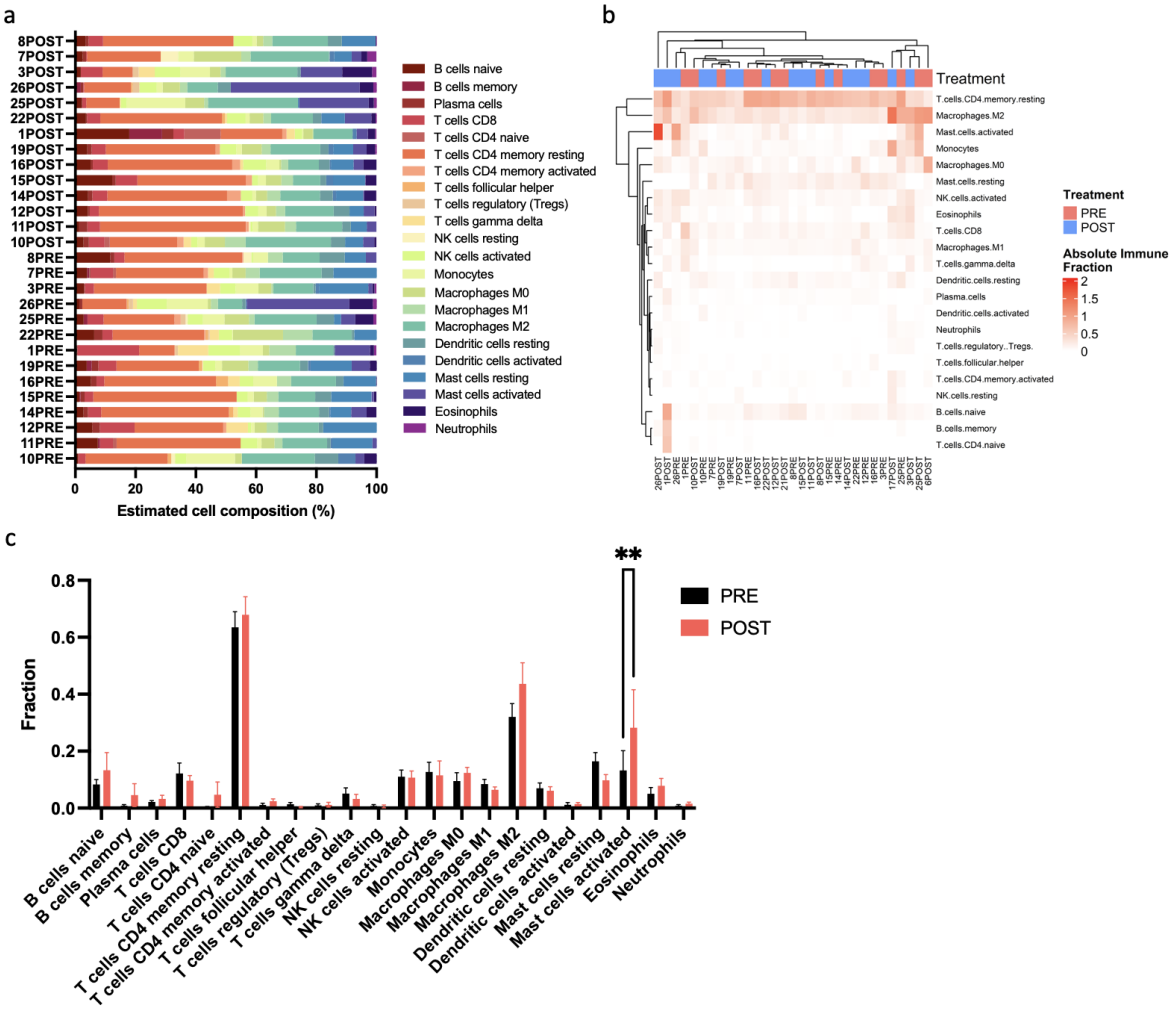


Figure 5.13: CIBERSORTx deconvolution analysis of RNA sequencing data of WINGMEN patients. a. Stacked bar plot showing the relative abundances of 22 immune cell types in each pre-treated biopsy (PRE; n = 27) and post-xentuzumab-treated in-theatre core (POST; n = 26) sample. **b** Heatmap illustrates the absolute abundances of the immune cell types with hierarchical clustering. **c**. Direct comparison of each immune cell types between PRE and POST. **p<0.01, two-way ANOVA with multiple comparisons. Analysis was done by Dr. Fiona Hartley.

5.4 Analysis of blood samples following IGF blockade

5.4.1 Assessing circulating markers in pre- and post-xentuzumab treated serum

PSA and insulin levels were measured before treatment (PRE) and a day before surgery (POST). There were no significant changes in PSA levels, but looking at individual patients, 8 patients had their PSA levels decrease by more than 20% (Figure 5.14a). There were no significant changes in insulin levels (Figure 5.14b).

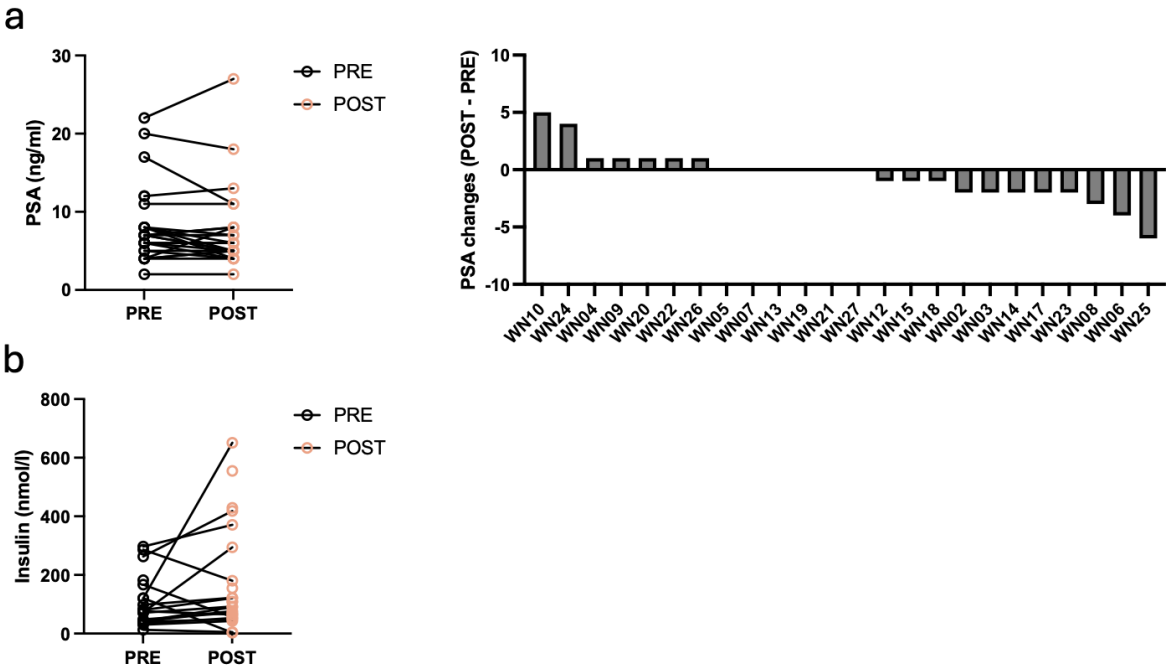


Figure 5.14: Effects of xentuzumab on circulating levels of PSA and insulin. Serum PSA (**a**) and insulin (**b**) levels of WINGMEN patients before (PRE) and after xentuzumab treatment (POST) were measured and compared. Right graph of **a** shows change in PSA values for each patient (POST - PSA).

Phospho-IGF-1R ELISA was used to assess IGF bioactivity in patient serum in three batches of 96-well plates due to lack of space in each plate. The control dilution curve was generated per plate using recombinant human IGF-1, which showed a good S-shaped curve with EC50 values in an expected range (Figure 5.15a). The ELISA results showed significant reduction in IGF bioactivity in xentuzumab-treated serum (Figure 5.15b-c).

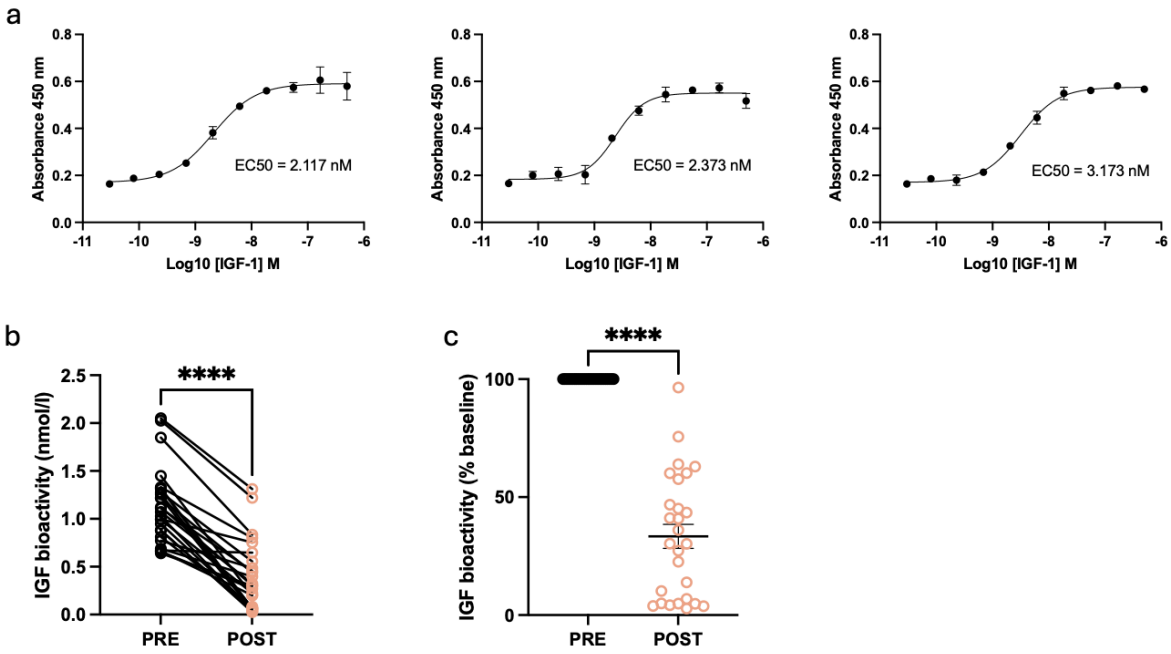


Figure 5.15: Serum IGF bioactivity at baseline (PRE) and after xentuzumab treatment (POST). Recombinant human IGF-1 (**a**) or serum (**b, c**) were added to triplicate wells of serum-starved prostate cancer cells (DU145). After 20 minutes at 37°C, cells were fixed for phospho-IGF-1R ELISA using phospho-Y1135/1136 IGF-1R monoclonal antibody (#3024, Cell Signalling Technology). The samples were analysed in three separate 96-well plates, while ensuring that the PRE/POST serum samples were analysed in the same batch. The results were expressed as **b**. IGF-1 nmol/l equivalents and **c**. % baseline (PRE) values (n = 27 patients, ****p<0.0001, paired t-test).

5.4.2 PBMC immunophenotyping by mass cytometry (CyTOF)

PBMCs were isolated from sodium heparin blood samples, thawed and stained with 36 metal-tagged antibodies (Table 2.10), and processed for immunoprofiling using cytometry by time-of-flight (CyTOF) at the Kennedy Institute of Rheumatology Mass Cytometry Facility. Data analysis was done by Cameron Lang (Chapter 2.18.2).

In the first instance, the data was analysed by manual gating using FlowJo to investigate the frequency of various CD45+ immune cell types in PBMCs. There was a significant increase in CD3+CD8+ cytotoxic T cells in xentuzumab-treated PBMCs and no changes in CD3+CD4+ helper T cells and CD4+CD127-CD25+ Tregs (Figure 5.16a-b). For more high dimensional analysis, unsupervised clustering algorithm FlowSOM was used (Van Gassen et al., 2015), which revealed various clusters of immune cells affected by the treatment (Figure 5.16c). Among the CD8+ T cell population, naive-central memory (CD45RA+, CD45RO+, CCR4+, CCR7+, TIGIT+, Granzyme-B+, CD127+, CD25+) and effector memory CD8+ T cells (CD45RO+, CD27+, CD57+, Granzyme-B+, CD127+, CD25+, CCR4+, CD20+), which can persist long-term in the absence of antigens, were significantly increased by xentuzumab treatment. Xentuzumab also significantly increased mucosal-associated invariant T (MAIT) and NKT cell population (CD161+, CD127+, CD45RO+, PD-1+, CD69+, CD27+, CD56+). In the CD4+ helper T cell population, xentuzumab significantly decreased naive CD4+ T cells (CD45RA+, CCR7+, CD27+, CD38+), which can differentiate into various subtypes. In addition, effector memory CD4+ T cells (CD45RO+, TIGIT+, PD-1+, Granzyme-B+, Ki67+, HLA-DR+, CD57+), which can enhance B and CD8+ T cell response and respond quicker to re-infection, were significantly increased by xentuzumab treatment. Lastly, two highly proliferative effector memory Treg populations (Ki67+ TIGIT+ FoxP3+ CD27+ HLA-DR+ CD39+ CD38+ PD-1+ CD25+ CTLA-4+ CD45RO+ Granzyme-B+ CD161+ CD69+ CD20+ CD57+ and Ki67+ HLA-DR+ CD38+ CD39+ TIGIT-PD-1+ CD45RO+ Granzyme-B+ CD27- CTLA-4+ CD161+ CD69+ CD57+) were significantly decreased by xentuzumab treatment, possibly reversing immunosuppression by Tregs.

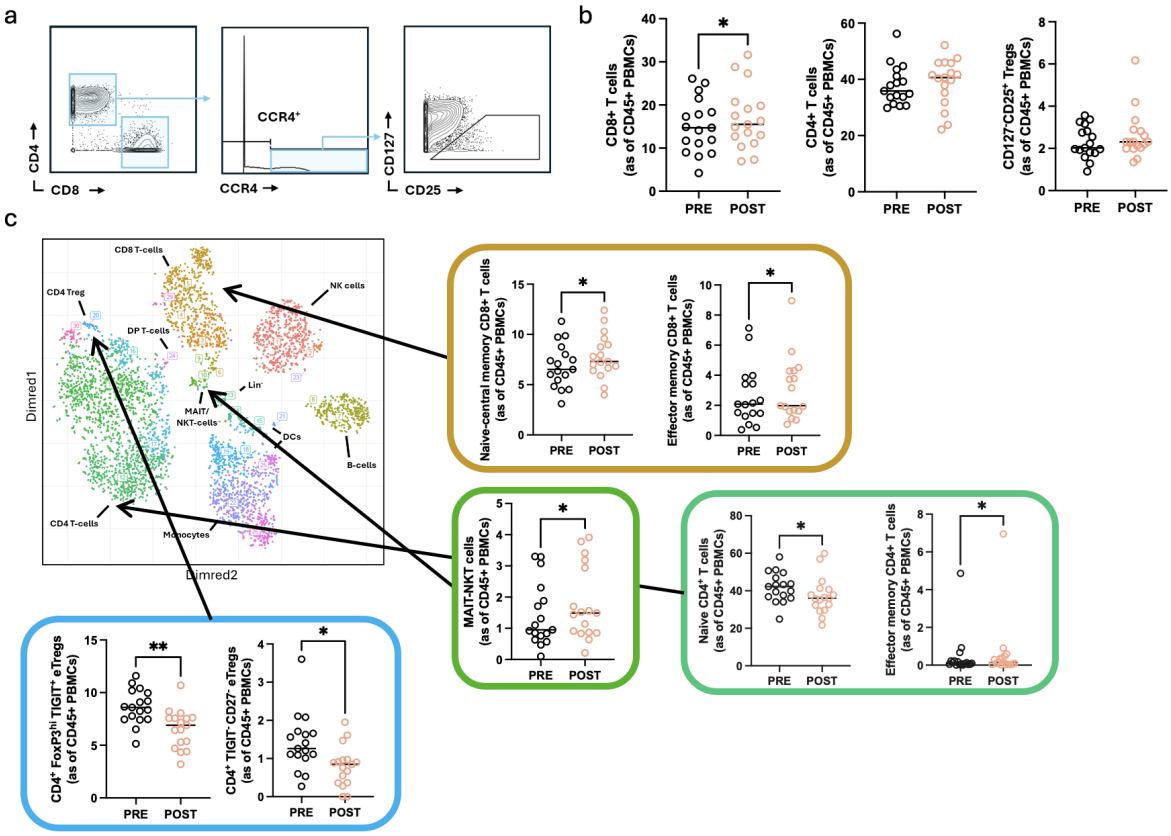


Figure 5.16: Immunophenotyping of PBMCs before (PRE) and after xentuzumab treatment (POST) using CyTOF. Thawed PBMCs were processed for analysis using cytometry by Time-Of-Flight (CyTOF). **a-b**. The data were gated to exclude residual normalisation beads, debris, dead cells, and doublet and manually analysed using FlowJo (version 10). Example in **a** shows manual gating strategy to identify CD8+, CD4+, and CD127-CD25+ Tregs, and **b** shows the proportions of individual cell types. To delve deeper into various subtypes of CD8+ T cells, CD4+ T cells, MAIT-NKT cells, and FoxP3+ regulatory T cells with different functions, unsupervised clustering analysis by FlowSOM was performed using FlowJo and **c** shows representative tSNE plot of CD45+ immune cell subsets and clusters of various cell types affected by xentuzumab treatment. n = 27 patients, *p<0.05, **p<0.01, Wilcoxon matched pairs signed rank test.

5.5 Discussion

This chapter outlined results from WINGMEN trial clinical dataset and various analysis of tissue and blood samples from the recruited patients. By administrating IGF blocking monoclonal antibody xentuzumab to localised prostate cancer patients due to have radical prostatectomy, the trial aimed to identify links between IGF axis and prostate cancer progression (Figure 5.1). Overall, 27 patients were recruited, with all receiving the allocated intervention. After receiving all allocated treatment and having the post-treatment blood collected, one patient (WN-01-00020) progressed on scan and went on to radiotherapy instead of surgery, resulting in no post-treatment tissue from this patient (Figure 5.3).

The primary endpoint of the trial was to assess the amount of IGF pathway inhibition induced by xentuzumab by performing phospho-IGF-1R and downstream phospho-S6 IHC on the pre-treatment diagnostic biopsies and post-xentuzumab-treated in-theatre cores. There was a significant reduction of IGF-1R and S6 activation upon xentuzumab treatment (Figure 5.5), suggesting that the IGF pathway was successfully inhibited by xentuzumab. There were three outlier patients (WN-01-00006, WN-01-10014, WN-01-10024) whose IGF-1R activation increased post-treatment and one patient (WN-01-00002) with increased S6 activation post-xentuzumab (Table 7.10 and Table 7.11). Previous report from our lab suggested that IGF-1R can be detected in both nucleus and membrane/cytoplasm, with more internalisation detected in tumours compared to benign glands (Aleksic et al., 2018). The results were consistent in that there was a higher percentage of positive nuclear IGF-1R phosphorlation compared to non-nuclear localisation in the tumours, and interestingly, xentuzumab reduced both nuclear and non-nuclear IGF-1R phosphorylation in tumours (Figure 5.5c). Several preclinical studies have shown reduction in IGF axis activity by xentuzumab via western blot or IHC in various cancer models (Rieunier et al., 2021; Weyer-Czernilofsky et al., 2020), but this is the first clinical study that shows clear reduction of IGF axis activity by xentuzumab in prostate cancer tissues.

The secondary endpoint of the trial was to assess the feasibility of treatment as well as the safety and tolerability of xentuzumab administered in the pre-operative setting. Feasibility of treatment was assessed by number of patients whose surgery was performed on schedule after 3 - 10 doses of xentuzumab. Among 27 recruited patients, 26 patients had surgery performed on schedule; one patient that did not have surgery was due to disease progression (Table 5.3). No surgery was delayed due to trial treatment. Although 15 patients had their surgeries after more than 4 doses of xentuzumab, their last doses were within 6 days of surgery, meeting the requirements. Among the 15 patients, reasons for delay for 2 patients was COVID infection, and although the reasons for delay for 13 patients were not recorded, it is likely due to backlog in surgery schedules. This suggests that it is feasible to treat patients with xentuzumab pre-prostatectomy.

Safety and tolerability of xentuzumab was assessed by adverse events recorded from study entry to the end of study visit. There were 24 adverse events recorded throughout the study, of which 17 were deemed treatment-related, but none was CTCAE grade 3 or higher (Table 5.4). This is consistent with previous clinical trials with xentuzumab, where the drug was deemed well-tolerated, and treatment-related adverse events were generally of CTCAE grade 1 or 2 (de Bono et al., 2020a; Hussain et al., 2018; Doi et al., 2022; Schmid et al., 2023; Macaulay et al., 2023). This suggests that xentuzumab is safe and well-tolerated to be given pre-prostatectomy.

Tertiary and exploratory endpoints aimed to assess changes in tissue and circulating markers. First, changes in PSA following xentuzumab administration in the pre-prostatectomy setting was assessed by measuring PSA levels in blood collected pre- and post-treatment (Figure 5.14a). Among the 24 patients with PSA levels in both timepoints recorded, 14 patients had no or minimal changes (<20%) in serum PSA. Patients WN-01-00010 and WN-01-00024 experienced increase in PSA upon xentuzumab treatment, and 8 patients had more than 20% reduction in PSA levels, with a notable PSA decrease for patients WN-01-10006 and WN-01-10025. In previous trial using IGF-1R blocking agents xentuzumab ± enzalutamide on CRPC patients with rising PSA levels, only one patient (4.2%) had a dramatic PSA response with addition of

xentuzumab, from PSA of 62.98 pre-xentuzumab to almost 0 after the treatment (Macaulay et al., 2023). Other trials with figititumab and cixutumumab on mCRPC patients did not significantly improve the PSA levels (de Bono et al., 2014; McHugh et al., 2020).

Second, changes in tissue markers upon xentuzumab administration in pre-operative setting were analysed using IHC, mIF, and bulk RNA sequencing. IGF-1R, KI67, and RRM2 expressions before and after xentuzumab treatment were assessed with IHC. In line with significant changes in IGF-1R phosphorylation, there was a significant reduction in total IGF-1R expression upon xentuzumab treatment (Figure 5.6a-b). There were four outliers (WN-01-10006, WN-01-10019, WN-01-10021, WN-01-10026), but % IGF-1R expression changes in these patients were less than 10% (Table 7.12). There was no difference in subcellular localisation, but the degree of changes in patients with reduced nuclear IGF-1R expression was higher than in non-nuclear IGF-1R expression, suggesting that nuclear IGF-1R changes drove the significance in total IGF-1R changes (Table 7.13). This was consistent with a study from our lab, which showed significant association between high circulating IGF-1 and increased IGF-1R in prostate tumour epithelium but not in benign epithelium (Aleksic et al., 2018). A tumour cell proliferation marker Ki67 was significantly decreased upon xentuzumab treatment (Figure 5.6c), driven by 75% of the patients (Table 7.14). In earlier preclinical study using xentuzumab on mice with Myc-CaP allografts, transcriptomics revealed significant reduction in *Igf1r* and *Mki67* (Figure 3.7), though there was no difference in protein level (Figure 3.6). Reduction in Ki67 is also consistent with studies that link IGF-1R deficiency with reduced Ki67 expression in preclinical solid cancers (Alfaro-Arnedo et al., 2022; Leiphrakpam et al., 2014), and in prostate cancer, Ki67 is reported to be a prognostic marker that is associated with prostate cancer risk and death (Hammarsten et al., 2019; Kammerer-Jacquet et al., 2019; Berney et al., 2009). Future work would be to do a correlation analysis of patients with reduced IGF-1R phosphorylation with those with Ki67 reduction. In addition, xentuzumab induced changes in RRM2 expression in 65% of the patients (Figure 5.7). This supports previous preclinical study from our lab which showed significant downregulation of RRM2 in colorectal cancer xenografts by

xentuzumab and IGF actions in mediating cell cycle progression and DNA replication (Rieunier et al., 2021; Wu et al., 2021). The fact that diagnostic biopsies used as pre-treatment samples are NHS materials was a limiting factor in the number of exploratory IHC markers chosen. It would have been beneficial to add more DNA damage-related markers such as CHK1 and BrdU.

Multiplex IF of 13-marker panel was used to visualise and quantify the effects of IGF blockade on prostate cancer TME including structural markers and tumour-infiltrating immune cells (Figure 5.8 and Figure 5.10a). There was no difference in CD31 expression (Figure 5.9), but CD31 in pre-xentuzumab tissues showed more short, punctate patterns, suggesting neovascularisation, as opposed to post-treatment tissues showing more ribbon-like, mature vascularisation. This was consistent with previous *in vivo* study of xentuzumab-treated tumours (Figure 3.6b). CD31 is a marker for angiogenesis and a prognostic marker for metastasis (Park et al., 2010; Zhang et al., 2018), and several studies have reported role of IGFs in angiogenesis (Samani et al., 2007; Liu et al., 2023c). In addition, AR expression was significantly reduced upon xentuzumab treatment (Figure 5.10d), mirrored in 73% of the patients (Table 7.15). This is consistent with previous reports that showed crosstalk between IGFs and AR (Culig et al., 1994; Kim et al., 2009; Zhu et al., 2008a; Orio et al., 2002; Wu et al., 2007). AR is an important oncogene in prostate cancer, and its overexpression or mutation can lead to cancer progression and therapeutic resistance (Tan et al., 2015; Watson et al., 2015). Although not significant, some of the AR-targeted genes identified in Shaw et al., 2016, *TMPRSS2* and *CAMKK2*, were downregulated upon xentuzumab treatment.

Results of mIF on WINGMEN tissues also demonstrated changes in prostate cancer TIME. In addition to a decreasing trend of CD3+ total T cells (p-value = 0.0539), there was a significant decrease in CD3+TIM3+ exhausted T cells upon xentuzumab treatment (Figure 5.10b). This was consistent with the *in vitro* study that showed decrease in TIM-3 expression in CD8+ cells exposed to macrophage:22Rv1 co-culture treated with xentuzumab (Figure 4.23). This novel finding in prostate cancer is consistent with a previous study that showed upregulation of IGF-1 signalling pathway in CD4+TIM3+

exhausted T cells in colorectal cancer patients via transcriptomics (Sasidharan Nair et al., 2020). In addition, xentuzumab treatment led to a significant increase in CD8+ T cell numbers and infiltration into prostate epithelium (Figure 5.10b and Figure 5.11a). Preclinical lung cancer model with combined inhibition of IGF-1R and PD-1 have shown significant increase in CD8+ T cells (Ajona et al., 2020), and we have demonstrated increase in CD8+/Treg ratio upon xentuzumab + anti-PD-1 treatment *in vivo* (Figure 3.28), but a significant increase with IGF blockade alone has not been shown previously. Despite several studies showing role of IGFs in Treg proliferation (DiToro et al., 2020; Shapiro et al., 2023) and our own *in vivo* study (Figure 3.28b-c) there was no difference in Treg population in post-xentuzumab tissues, possibly due to small number of Tregs present in the tissues and other factors affecting the TIME. Although my *in vitro* and *in vivo* results showed changes in macrophage phenotypes upon xentuzumab treatment (Figure 3.12, Figure 4.7 and Figure **??**), there was no significant change in macrophage phenotype in clinical tissues (Figure 5.10c), due to variations between patients. This was also not consistent with previous studies that show increase in M2 macrophages induced by IGF-1 (Spadaro et al., 2017; Ireland et al., 2018). However, there was significantly more CD68+CD206- M1 macrophages infiltrating the post-treatment prostate epithelium (Figure 5.11d), suggesting more macrophage phagocytosis of cells and pro-inflammatory actions within the epithelium (Atri et al., 2018, Kohno et al., 2021, Chen et al., 2023b).

RNA sequencing of the pre- and post-xentuzumab tumours showed significant upregulation of IL6, IL2RA, IL1R2, and CXCR4 in post-xentuzumab tumours (Figure 5.12b-c). These are crucial immune modulators in cancers, either causing immunosuppression or acting as pro-inflammatory cytokines (Orange et al., 2023; Hailemichael et al., 2022; Nguyen et al., 2020; Muhammad et al., 2023; Xia et al., 2024; Chen et al., 2022; Biasci et al., 2020; Shi et al., 2020; Guo et al., 2016). Xentuzumab also led to signficant upregulation of CD206, which is an anti-inflammatory M2 macrophage marker. This was not consistent with previous *in vitro* and *in vivo* studies (Figure 3.12, **??**, and 4.12). Transcription factors nuclear receptor subfamily 4A (NR4A)1-3 were upregulated with xentuzumab, suggesting xentuzumab as a regulator of genes that play a role in

immune cell differentiation (Liu et al., 2019a; Mahajan et al., 2015; Odagiu et al., 2020). In addition, several genes (FOS, JUN, FOSB, JUNB) which encode subunits of the Activator protein-1 (AP-1) transcription factor complex were significantly upregulated after treatment, with significantly higher activation of AP-1 transcription factors and enrichment of MAPK pathways (Figure 5.12b-e). These are stress response genes regulated by NF-κB (Fujioka et al., 2004; Ji et al., 2019; Liu et al., 2017). They also act as important immune regulators in cancers and inflammation (Atsaves et al., 2019; Song et al., 2023; Eferl et al., 2003), possibly relating to significant enrichment of genes related to immune pathways, such as IL-4, IL-13, IL-10, IL-6 and IL-1 signalling (Figure 5.12d). Consistent with high level of interleukins in the tissue, top pathways that were upregulated upon xentuzumab treatment included cellular senescence and senescence-associated secretory phenotype (SASP) (Kuilman et al., 2009; Coppe et al., 2008; Faget et al., 2019). This may also explain stronger and highly active transcription factor gene expressions across the samples (Chien et al., 2011; Schmitt et al., 2022) and could be linked to significant Ki67 downregulation in post-xentuzumab treated tumours (Figure 5.6c). This is also consistent with previous studies linking IGF-1 and IGFBPs that bind to IGFs with SASP (Saul et al., 2022; Kim et al., 2007b; Luo et al., 2019; Hou et al., 2020). These results indicate a short-term stress response imposed by important growth factor pathway inhibition, which may have driven compensation. SASPs can be both tumour-promoting and tumour-suppressing (Liu et al., 2007; Ruscetti et al., 2020; Xue et al., 2007; Chen et al., 2023a; Pernicova et al., 2011; Feng et al., 2023; Kallenbach et al., 2022; Haston et al., 2023; Dong et al., 2024). This suggests that SASP, with increase in CD8+ T cell infiltration and increased lymphoid aggregates, could potentially be beneficial to patients, though a longer timepoint would be necessary to see the effect.

The RNA sequencing dataset was used for immune deconvolution with CIBERSORTx. The results did not match what was seen in CellDIVE with increased CD8+ T cell expression, but there was a significant increase in mast cell population post-treatment (Figure 5.13). This may be related to the increase in interleukin signalling with xentuzumab treatment (Figure 5.12), as several studies have reported mast cell

production of interleukins and certain interleukins promoting increase in mast cell numbers as well as upregulation of mast cell-induced cytokines (Desai et al., 2016; Ma et al., 2013; Segura-Villalobos et al., 2022; McLeod et al., 2015; Hultner et al., 2000). In prostate cancer, mast cells can play a protumorigenic or anti-tumorigenic role depending on their localisation in the tumours, so it is unclear what this increase means for prostate cancer TIME (Pittoni et al., 2011; Fleischmann et al., 2009; Noto et al., 2021; Majorini et al., 2022; Pittoni et al., 2012; Teng et al., 2021; Johansson et al., 2010). One study reported that IGFs promote bone marrow-derived mast cell survival by PI3K pathway activation (Lessmann et al., 2006), which is inconsistent with the results, but is possible due to compensation by other pathways. Regardless, this finding may suggest novel relationship between IGFs and mast cells in prostate cancers. In the future, adding a mast cell marker in mIF of clinical tissues would validate this finding and allow for detection of mast cell localisation in the tumours.

Third, changes in circulating markers following xentuzumab administration before surgery was assessed using clinical dataset, phospho-IGF-1R ELISA, and mass cytometry. There were no significant differences in insulin levels, measured as part of routine blood collection pre- and post-treatment (Figure 5.14b). This is consistent with the fact that xentuzumab binds to the ligands IGF-1 and IGF-2 and not the receptor. It is reassuring that insulin levels were not affected by xentuzumab, as majority of the IGF-1R blocking reagents was discontinued due to increasing instances of hyperglycaemia. Serum IGF bioactivity was measured using phospho-IGF-1R ELISA, which showed significant reduction of IGF bioactivity in xentuzumab-treated serum (Figure 5.15). This was consistent with previous xentuzumab trials (de Bono et al., 2020a; Doi et al., 2022).

PBMC immunophenotyping of 36-marker panel using CyTOF showed changes in various T cell populations. There was a significant increase of CD8+ T cells in xentuzumab-treated PBMCs (Figure 5.16b). This was consistent with mIF analysis in xentuzumab-treated tumours (Figure 5.10b) and *in vivo* analysis (Figure 3.28), further supporting the idea that IGF blockade increases CD8+ T cell activity in prostate cancer tumours and blood. High-dimensional analysis showed significant increase in naive central memory

and effector memory CD8+ T cells (Figure 5.16c). CD45R0+ CCR7+ central memory CD8+ T cells, mainly in lymph nodes, mediate reactive memories and differentiate to effector cells upon antigen stimulation, and effector memory CD8+ T cells migrate to inflamed tissues to carry out effector funtions, containing perforins and producing IFN-γ, IL-4, and IL-5 (Johnson et al., 1975; Sallusto et al., 2004; Nolz et al., 2011; Cho et al., 1999; Harty et al., 2008). This is consistent with overall increase in CD8+ T cell population in blood and suggests that blocking IGFs increases memory CD8+ T cell population in all stages of differentiation. There were no significant changes in CD4+ helper T cells and Tregs (Figure 5.16b), again consistent with mIF analysis (Figure 5.10b). Unsupervised clustering, however, identified significant decrease in naive CD4+ T cells and significant increase in effector memory CD4+ T cells upon xentuzumab treatment (Figure 5.16c). Decrease in naive CD4+ T cells, which are activated and differentiated into various subtypes, is consistent with preclinical study that showed significant reduction in CD4+ T cells in tumours (Figure 3.5) and with previous clincial data from our group (Nandakumar, 2022). Effector memory CD4+ T cells are involved in protection from re-infection, autoimmunity, and chronic inflammation by migrating to inflammation sites and producing IFN-γ, IL-4, and IL-5 (Kunzli et al., 2023; Reinhardt et al., 2001; Pepper et al., 2011). Increase in effector memory CD4+ and CD8+ T cells in post-xentuzumab PBMCs were in line with preclinical results that showed significant increase in effector memory CD4+ and CD8+ T cells in xentuzumab-treated blood *in vivo* (Figure 3.28i-j).

Unsupervised clustering also identified significant reduction of two highly proliferative subtypes of Tregs in post-xentuzumab plasma (Figure 5.16c). Ki67+ TIGIT+ PD-1+ eTregs are known as activated Treg subset that can suppress Th1 and Th17 cells and have more suppressive functions than the TIGIT- eTregs (Joller et al., 2014; Yang et al., 2020b; Yang et al., 2018b). Decrease in either subtypes may be related to a previous study that showed ability of IGFs to increase Th17 cell proliferation (DiToro et al., 2020). This is also consistent with a preclinical study that showed reduction of CD4+FoxP3+ Tregs (Figure 3.28b). Lastly, MAIT-NKT population, which enhances anti-tumour immunity by activating CD8+ cytotoxic T cells and dendritic cells, was

significantly increased by xentuzumab (Figure 5.16c) (Petley et al., 2021; Li et al., 2023a; Liu et al., 2021b). This is supported by a previous study that showed significant increase in NKT cells linked with decrease in hepatic IGF-1 levels in amyotrophic lateral sclerosis model (Finkelstein et al., 2011).

Future work would be to integrate all the different datasets, including the analysis that has not been done yet with radical prostatectomy sections (PTEN IHC and tumour mutation profiling via DNA sequencing (Rao et al., 2020)). Overall, primary and secondary endpoints of the trial have been met, with significant inhibition of IGF pathways by xentuzumab and proven safety and tolerability of the drug given before prostatectomy. IGF blockade also significantly reduced serum IGF bioactivity as well as tumour cell proliferation and changed prostate cancer TIME, especially T cell profiles in both PBMCs and prostate epithelium. With RNA sequencing results that shows enrichment of pathways associated with senescence and SASPs, this suggests an importance in targeting the process that enables cells to survive stress, possibly a combination of IGF blockade and targeting of anti-tumourigenic markers such as STAT3 or IL-6.

6

Conclusion

The main aim of chapter 3 was to characterise the biology of IGF blockade by exploring the effects of xentuzumab *in vitro* and *in vivo*, alone and in combination with anti-PD-1 immunotherapy in an allograft model. *In vitro* analysis confirmed the ability of xentuzumab to block IGF-1R signalling and reduce cell viability as well as spheroid formation (Figure 3.1 - 3.3). Myc-CaP allograft model *in vivo* did not lead to reduction of tumour growth (Figure 3.4), but there were changes in tumour immune microenvironment, with reduction of *Igf1r* and *Mki67*, decrease in CD4 T cells, and reduction of immunosuppressive M2-like macrophages in xentuzumab-treated tumours (Figure 3.5 - 3.7, Figure 3.12). Potential of IGF blockade to enhance immunotherapy was observed in the same model (Figure 3.8 and 3.23). Despite heterogeneity of the tumours and no changes in tumour growth, combined therapy of xentuzumab and anti-PD-1 led to immune changes in prostate cancer TME. Significant increase in necrosis in combination-treated tumours (Figure 3.11 and 3.24) suggested involvement of innate immune cells (Mantovani et al., 2022), which was supported by IHC and RNA sequencing results showing changes in macrophage infiltration (Figure 3.13 and 3.27) and significant deregulation of genes related to myeloid leukocyte migration (Figure 3.16 and 3.18). Flow cytometry of the tumours, spleen, and PBMCs showed changes in T cell phenotypes by xentuzumab + anti-PD-1 treatment, including significant decrease in Tregs and increase in CD8+ T cells as well as its granzyme B production (Figure 3.28). Overall, IGF blockade affects phenotype of macrophage and TILs in tumours, and increases effector memory CD4+ and CD8+ T cells systematically in PBMCs and spleen. Xentuzumab and anti-PD-1 treatment has potential to enhance the T cell

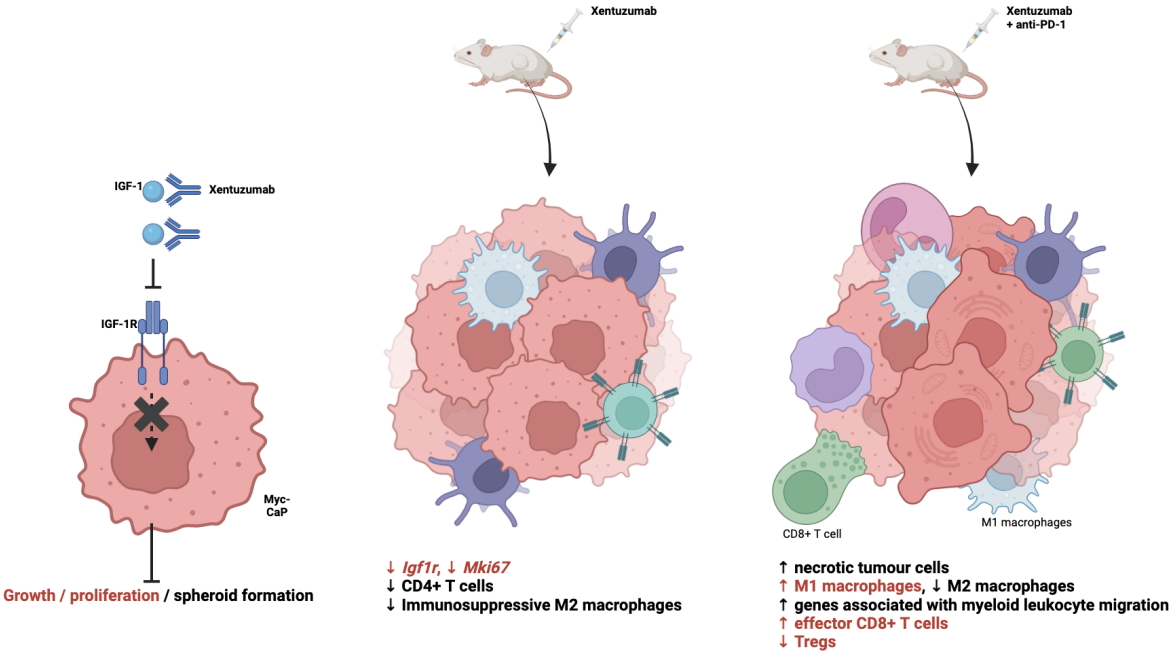


Figure 6.1: Overview of chapter 3 findings. Left: Xentuzumab treatment on Myc-CaP cells *in vitro* suppressed their growth, proliferation, and spherogenicity. Middle: Despite no tumour growth reduction, *in vivo* Myc-CaP allograft model suggested immune changes involving CD4+ T cells and immusuppressive M2-like macrophages. Right: Xentuzumab and anti-PD-1 combination treatment led to significant increase in necrosis, changes in macrophage population and migration, and enhanced T cell activity with reduced Tregs, and increased granzyme B-producing CD8+ T cells. Red text indicates changes observed in mouse, *in vitro* and in patients. Figure was created using BioRender.

activity, provided additional tumour-controlling standard-of-care agents be added to control the tumour growth (Figure 6.1).

As chapter 3 and previous related studies suggested potential impact of IGF blockade on macrophages in TME (Spadaro et al., 2017; Clemmons et al., 2005; Rodriguez-Garcia et al., 2021), the main focus of chapter 4 was the effects of xentuzumab on the macrophage phenotype and phagocytic functions as well as its influence on T cell activities. Xentuzumab significantly reduced murine immunosuppressive M2-like macrophages by reducing tumour-driven cytokines that drive M2 polarisation such as CCL3 and CXCL1 (Figure 4.6 - **??**). M1 macrophage phagocytosis of murine and human prostate cancer cells was significantly increased by xentuzumab, and in 22Rv1 and PBMC-derived M1 macrophage co-culture, xentuzumab significantly increased anti-CD47-driven phagocytosis of 22Rv1 (Figure 4.19 - 4.20 and Figure 4.22). In addition,

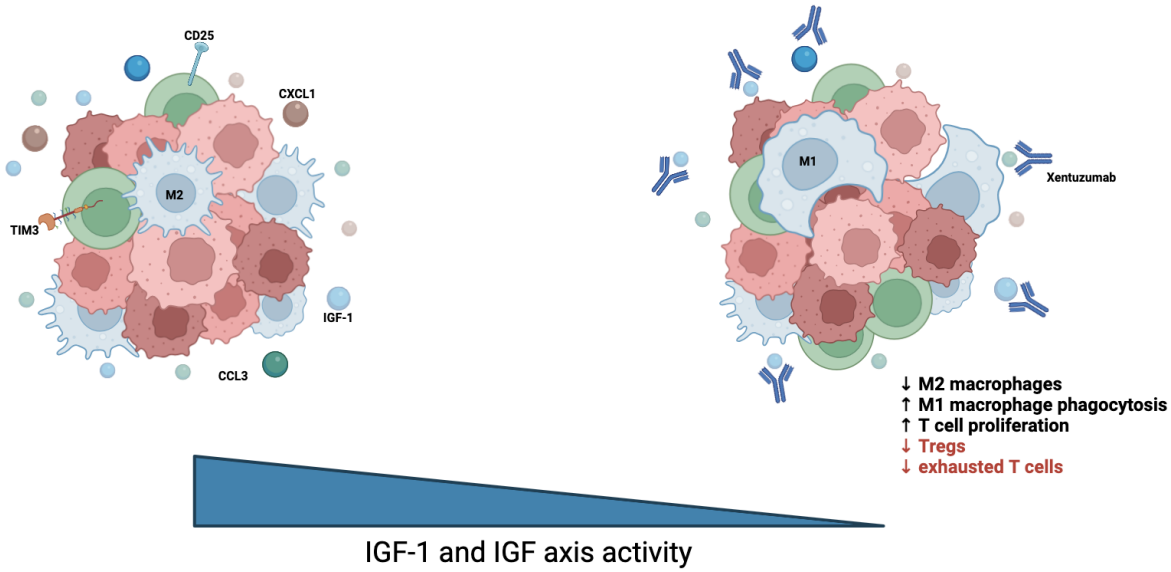


Figure 6.2: Overview of chapter 4 findings. Xentuzumab treatment *in vitro* significantly reduced M2 macrophages, while increasing M1 macrophage phagocytosis. In macrophage, cancer cell, and T cell co-culture, T cell proliferation was significantly increased while CD4+CD25+ Tregs and CD8+TIM3+ exhausted cytotoxic T cells were significnatly decreased, suggesting enhanced T cell activities. Red text indicates changes observed in mouse, *in vitro* and in patients. Figure was created using BioRender.

xentuzumab enhanced T cell functions in macrophages, T cells, and human prostate cancer cell co-culture conditions by significantly increasing overall T cell proliferation, while significantly decreasing CD4+CD25+ Tregs, CD8+TIM3+ exhausted cytotoxic T cells, and IFN-γ producing CD8+ T cells (Figure 4.23 - 4.26). Although several previous studies reported immunosuppressive effects of IGFs in other cancer or autoimmune models (Bilbao et al., 2014; Spadaro et al., 2017; Ajona et al., 2020), this is a novel finding in prostate cancer model (Figure 6.2). Future work would be to investigate whether anti-CD47 and xentuzumab combination treatment has therapeutic potential in prostate cancer by performing *in vivo* experiment on nude mice model with 22Rv1 tumours.

Chapter 5 covers WINGMEN clinical trial, a windows trial of xentuzumab, designed to understand the consequences of IGF activity on prostate cancer TIME and to assess immune and metabolic changes (Figure 5.1 - 5.2). Primary and secondary endpoints of the trial were met, with clear IGF pathway inhibition by xentuzumab (Figure 5.5) and confirmed safety and tolerability of xentuzumab given pre-prostatectomy (Table

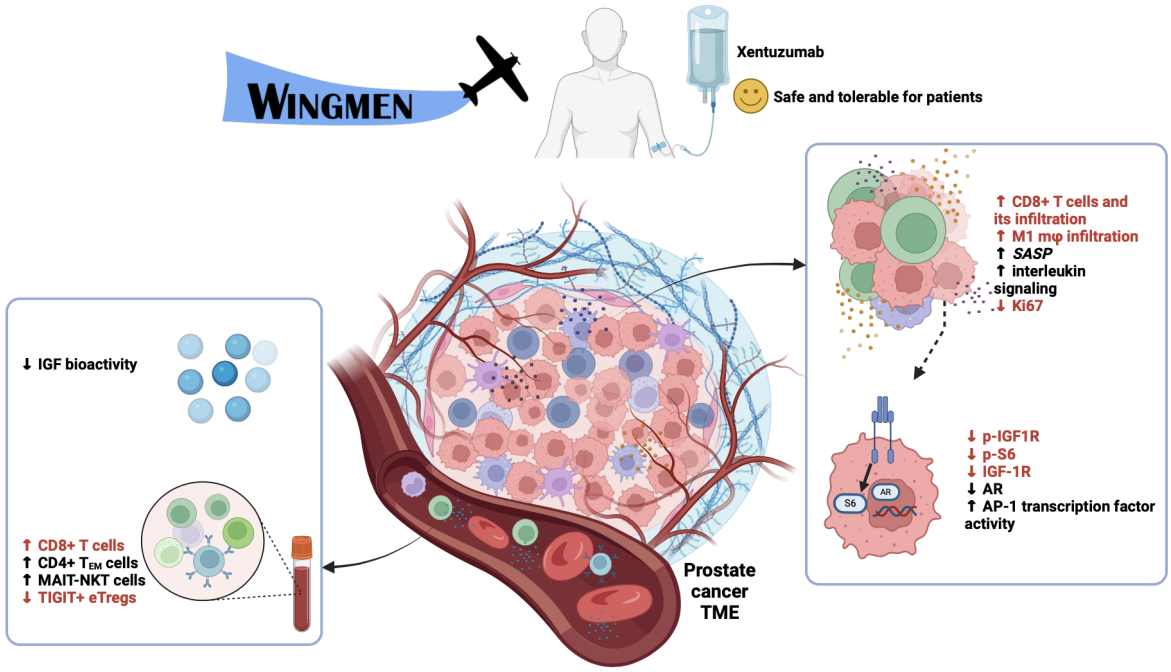


Figure 6.3: Overview of chapter 5 findings. WINGMEN trial tumour and blood sample analysis revealed systemic immune changes, while reducing IGF axis activity. Red text indicates changes observed in mouse, *in vitro* and in patients. Figure was created using BioRender.

5.3 - 5.4). Xentuzumab also significantly reduced IGF bioactivity in serum while not reducing insulin levels (Figure 5.15). In tumours, IGF-1R, Ki67, and AR expressions were significantly reduced by xentuzumab, important markers indicating prostate tumour cell proliferation (Figure 5.6 and Figure 5.10d). Xentuzumab also caused significant changes in prostate cancer TIME, with significant increase in CD8+ T cell expression and infiltration, while reducing CD3+TIM3+ exhausted T cells (Figure 5.10a-c and Figure 5.11a). In blood, xentuzumab significnatly increased CD8+ T cells, MAIT-NKT cells, and effector memory CD4+ T cells, while reducing proliferative Treg subtypes (Figure 5.16). RNA sequencing revealed significant increase in genes associated with senescence, interleukin signalling, and AP-1 transcription factors, suggesting increase in SASPs and stress from the pathway blockade (Figure 5.12). This strengthens the previous *in vitro* and *in vivo* studies that demonstrated immunosuppressive effects of IGFs (Figure 6.3). Despite a recent clinical study in mCRPC patient, which indicated that senescence-associated gene signatures could be the driver of disease progression (Guo et al., 2023), the fact that xentuzumab treatment also caused increase in CD8+ T

cell infiltration and lymphoid aggregates could indicate a positive prognosis for localised prostate cancer patients. This calls for importance in selecting another combinatory immune-modulating agent that could offset the cellular stress imposed by IGF blockade.

The main aim of the trial was to identify potential biomarkers in response to xentuzumab treatment. Future experiments, including prostate cancer gene mutation panel and PTEN IHC, on the RP sections from the trial, and further correlation analysis to integrate all datasets will be crucial to identify biomarkers of response or resistance. This will allow for selection of patients with localised prostate cancer that would benefit from xentuzumab treatment.

Overall, this thesis provided the first opportunity to see impacts of IGF blockade in immune microenvironment in both mouse and human. *In vitro* analysis revealed ability of xentuzumab to block IGF signalling and reduce cancer cell proliferation and survival and to cause changes in macrophage phenotype and phagocytic functions, as well as T cell functions. Although allograft *in vivo* model with xentuzumab and combination treatment with anti-PD-1 immunotherapy did not lead to any significant tumour growth inhibition, macrophage and T cell activities in tumours, spleen, and blood were positively altered. WINGMEN clinical trial revealed that immune response in prostate cancer patient samples can be a lot more complex than immune response *in vitro* and *in vivo*. Although xentuzumab significantly inhibited IGF axis activity and caused systemic immune changes in prostate cancer TME, no tumour growth inhibition was observed *in vivo*, and there were upregulation of genes related to SASPs and stress responses in clinical patients. This indicates that combination of xentuzumab with another immune-intervening agent would be required for more effective therapeutic responses that could reduce the stress caused by IGF blockade. Despite species differences, some constant effects of IGF blockade include inibition of IGF axis pathway, increased M1 macrophages and CD8+ T cell infiltration, and decrease in certain subtypes of Tregs and exhausted T cells. This indicates a need for a better humanised *in vivo* model, patients-derived organoids, or patient tissue grafts on mice (Issa et al., 2010) that better

demonstrate clinical effects of IGFs on T cell responses and the impact of targeting SASPs preclinically.

7

Appendix

Table 7.1: List of buffers used for multiple assays. The table explains the recipes of buffers used for multiple assays.

Buffer	Assays	Recipes
Banking media	Cryopreservation	10% dimethyl sulfoxide (DMSO, Sigma-Aldrich, #D2660-100ML), 40% culture media (Table 2.1), and 50% FBS (Gibco, #10500064),
Coomassie Stain	Clonogenic assay	0.1% Brilliant Blue R-250 (Bio-Rad, #1610436), 7% acetic acid, 50% methanol (Fisher Chemical, #M/3950/17)
3x Laemmli sample buffer	Western blot (3D spheroid assay)	30% glycerol, 15% β-mercaptoethanol (Sigma Aldrich, #M6250), 9% sodium dodecyl sulfate (SDS), 0.3 mg/ml Bromphenol blue, 150 mM Tris Cl, pH 6.8
Lysis buffer	Western blot	1% protease inhibitor cocktail (Roche, #11873580001), 1% phosphatase inhibitor cocktail 1 (Sigma-Aldrich, #P2850), 1% phosphatase cocktail inhibitor cocktail 2 (Sigma-Aldrich, #P5726) in RIPA buffer (Sigma-Aldrich, #R0278-50ML)
Sorting buffer	Cell sorting	2mM Ethylenediaminetetraacetic acid (EDTA, Sigma-Aldrich, #03690-100ML), 0.5% Bovine serum albumin (BSA, VWR, #421501J) in sterile PBS
Collection buffer	Cell sorting	50% foetal bovine serum (FBS, Gibco, #10500064) in sterile phosphate buffered saline (PBS)
TE buffer	IHC	1.21 g of Trizma base and 0.372 g of EDTA (Sigma-Aldrich, #03690-100ML) in 1 L distilled H_2O, pH 9
Mouse tissue processing buffer	Flow cytometry	100 μL Enzyme D, 50 μL Enzyme R, and 12.5 μL Enzyme A from gentaleMACS^{TM}Tumour Dissociation Kit, mouse (Miltenyi Biotech, #130-096-730) in 2.35 mL full RPMI culture media (Table 2.1)
FACS buffer	Flow cytometry	0.5% BSA and 2.5 mM EDTA in PBS
20 mM PBS-EDTA	Macrophage disaggregation	20mM EDTA (Sigma-Aldrich, #03690-100ML) in sterile PBS
2 mM PBS-EDTA	Cell disaggregation	2mM EDTA (Sigma-Aldrich, #03690-100ML) in sterile PBS
Mounting media	Multiplex IF	10 mL PBS, 90 mL glycerol, 4.0 g propyl gallate
Dye inactivation solution	Multiplex IF	20 mL $NaHCO_3$ + 70 mL millipore water, 10 mL 30 % H_2O_2 added right before use

Table 7.2: List of differentially expressed genes in mouse tumours treated with xentuzumab vs control. RNAs were extracted from harvested fresh frozen mouse tumours treated with xentuzumab vs PBS control and sequenced. Differential gene expression was analysed using the DESeq2 pipeline and genes with adjusted P-value < 0.05 were deemed significant.

Ensembl Gene ID	Symbol	Log2 Fold Change	Adjusted P-value
ENSMUSG00000107556	Gm44237	-1.79407851477308	0.00013168
ENSMUSG00000031004	Mki67	-1.68683373079128	0.00008653
ENSMUSG00000034282	Evpl	-1.28658311132509	0.04869296
ENSMUSG00000027634	Ndrg3	-1.28655739680739	0.01236663
ENSMUSG00000025504	Eps8l2	-1.26855294674902	0.00740831
ENSMUSG00000107009	6720475M21Rik	-1.21506079217869	0.00099177
ENSMUSG00000005533	Igf1r	-1.19825004256344	0.01497999
ENSMUSG00000062372	Otof	-1.19624987823453	0.04325097
ENSMUSG00000107390	Gm43323	-1.1678240816004	0.02516724
ENSMUSG00000018411	Mapt	-1.12804925557218	0.01325035
ENSMUSG00000104576	F830115B05Rik	-1.10371234545237	0.01837822
ENSMUSG00000107320	Gm42549	-1.06230546810092	0.00363127
ENSMUSG00000029415	Sdad1	-1.04030984096249	0.02796443
ENSMUSG00000116624	Gm49706	-1.00882909961158	0.0058793
ENSMUSG00000101122	Gm17971	-1.00600141562939	0.00449558
ENSMUSG00000054555	Adam12	-0.997145761015103	0.03339648
ENSMUSG00000018849	Wwc1	-0.993287140912296	0.03132422
ENSMUSG00000106739	Gm43499	-0.982094859575905	0.00740831
ENSMUSG00000112090	Gm48231	-0.973115957917983	0.03687555
ENSMUSG00000035247	Hectd1	-0.938845992322978	0.00859272
ENSMUSG00000019838	Slc16a10	-0.912674641941504	0.00859272
ENSMUSG00000106427	Gm42820	-0.899430230055668	0.04146525
ENSMUSG00000104569	Gm43054	-0.88504706743535	0.04671011
ENSMUSG00000111844	Gm47097	-0.855793638135625	0.01347446
ENSMUSG00000062077	Trim54	-0.847870506557317	0.01931975
ENSMUSG00000102133	Gm37106	-0.819506674513225	0.01958317
ENSMUSG00000020709	Adap2	-0.790637877473546	0.02796443

Ensembl Gene ID	Symbol	Log2 Fold Change	Adjusted P-value
ENSMUSG00000109314	Gm44699	-0.783669119828243	0.02900483
ENSMUSG00000031574	Star	-0.778070104201676	0.02796443
ENSMUSG00000055805	Fmnl1	-0.777256199874263	0.02796443
ENSMUSG00000105304	Gm43696	-0.752340362931285	0.03498963
ENSMUSG00000108042	B130021K23Rik	-0.741836559985846	0.03633566
ENSMUSG00000033396	Spg11	-0.737543609752534	0.0357703
ENSMUSG00000104524	Gm37333	-0.735267701125812	0.03981794
ENSMUSG00000032899	Styk1	-0.728233424800196	0.03981794
ENSMUSG00000106565	Gm43582	-0.727786492182394	0.03981794
ENSMUSG00000068551	Zfp467	-0.727032899251483	0.03981794
ENSMUSG00000107370	Gm43588	-0.718097362493561	0.04152067
ENSMUSG00000033147	Slc22a15	-0.712874875792275	0.04190251
ENSMUSG00000046295	Ankle1	-0.71033332659807	0.03981794
ENSMUSG00000106472	Gm43111	-0.70964827918836	0.03961798
ENSMUSG00000000861	Bcl11a	-0.660705450209529	0.04956481
ENSMUSG00000067616	Klk11	-0.367884785625282	0
ENSMUSG00000020461	Clhc1	-0.236808144844436	7e-8
ENSMUSG00000025431	Crisp1	-0.152121290923433	0.00000522
ENSMUSG00000031757	Mt4	-0.151989544047174	0.0000092
ENSMUSG00000050074	Spink8	1.02061810463001	0.02900483
ENSMUSG00000031278	Acsl4	1.20120153879782	0.04956481
ENSMUSG00000055555	Ct55	1.26737681890469	0.04325097
ENSMUSG00000053522	Lgals7	1.35151636509783	0.01138858
ENSMUSG00000110841	Gpx4-ps2	1.52043736510296	0.03532299
ENSMUSG00000032487	Ptgs2	2.18119805767573	0.00005568
ENSMUSG00000021214	Akr1c18	0.1524329734720533	2.8e-7
ENSMUSG00000067242	Lgi1	0.2412382765492058	1e-7
ENSMUSG00000057337	Chst3	0.2457289618142076	7e-8
ENSMUSG00000074155	Klk5	0.2575481501227094	3e-8
ENSMUSG00000068227	Il2rb	0.2773402381742886	1e-8
ENSMUSG00000033595	Lgi3	0.3503168809113292	0
ENSMUSG00000079487	Med12	0.5170558890634802	0.04956481

Ensembl Gene ID	Symbol	Log2 Fold Change	Adjusted P-value
ENSMUSG00000045475	Lce3c	0.5271212049637287	0.04190251
ENSMUSG00000032561	Acpp	0.5305034484670488	0.04603626
ENSMUSG00000057609	Lce1a1	0.5344536774470613	0.04190251
ENSMUSG00000001773	Folh1	0.5360467835779041	0.0439875
ENSMUSG00000096001	2610528A11Rik	0.5420816315035133	0.04143734
ENSMUSG00000048455	Sprr1b	0.5429635088418852	0.04152067
ENSMUSG00000020811	Wscd1	0.5574718377330086	0.03965922
ENSMUSG00000020891	Alox8	0.6484710860791093	0.03989812
ENSMUSG00000020585	Laptm4a	0.7801639414226496	0.02900483
ENSMUSG00000025351	Cd63	0.7844856751447294	0.01325035
ENSMUSG00000027133	Nop10	0.8670127213552788	0.03981794
ENSMUSG00000025289	Prdx4	0.9026233019267272	0.03981794
ENSMUSG00000020766	Galk1	0.9049337156554623	0.04844099
ENSMUSG00000024248	Cox7a2l	0.9574291549655727	0.01958317
ENSMUSG00000020267	Hint1	1.010135698723943	0.02796443
ENSMUSG00000090101	Snhg9	1.013618173380944	0.04190251
ENSMUSG00000002014	Ssr4	1.045109226485254	0.04146525
ENSMUSG00000026360	Rgs2	1.076471237448368	0.04869296
ENSMUSG00000054905	Stfa3	1.165203140893873	0.00008653
ENSMUSG00000042515	Pwwp3b	1.182666003312947	0.03961798
ENSMUSG00000100215	Gm8292	1.349557108845556	0.04869296
ENSMUSG00000000120	Ngfr	1.411846027156612	0.04956481
ENSMUSG00000115783	Bc1	1.414195536260413	0.01325035
ENSMUSG00000039883	Lrrc17	1.443759388503498	0.00033035
ENSMUSG00000038526	Car14	1.818652248431258	0.0029546
ENSMUSG00000038323	1700066M21Rik	1.820663373583311	0.00008653
ENSMUSG00000090485	Gm17416	2.155421075778372	0.00000163

Table 7.3: List of differentially expressed genes in mouse tumours treated with xentuzumab + anti-PD-1 vs control: pilot experiment. RNAs were extracted from harvested fresh frozen mouse tumours treated with xentuzumab and anti-PD-1 vs PBS control and sequenced. Differential gene expression was analysed using the DESeq2 pipeline and genes with adjusted P-value < 0.05 were deemed significant.

Ensembl Gene ID	Symbol	Log2 Fold Change	Adjusted P-value
ENSMUSG00000023041	Krt6b	-19.6552608739417	0.00008615
ENSMUSG00000102439	Flg	-19.4466615926929	0.00000022
ENSMUSG00000053797	Krt16	-19.291732918598	0.00012664
ENSMUSG00000063564	Col23a1	-19.2234197007223	0.00000066
ENSMUSG00000061527	Krt5	-19.1472536982623	0.00014372
ENSMUSG00000116819	Gm49586	-18.9964051005605	0.00000202
ENSMUSG00000075707	Dio3	-18.8291426416579	0.00000423
ENSMUSG00000071561	Cstdc5	-18.7873853198529	0.0002013
ENSMUSG00000027923	Lce1b	-18.7716570052024	0.00000506
ENSMUSG00000033508	Asprv1	-18.7709282329061	0.0002013
ENSMUSG00000043165	Lor	-18.652715941039	0.00021149
ENSMUSG00000035557	Krt17	-18.2483682813078	0.00025948
ENSMUSG00000050359	Sprr1a	-18.2390108302356	0.00025948
ENSMUSG00000060962	Dmkn	-18.2201033174498	0.00025948
ENSMUSG00000032013	Trim29	-18.1616932955955	0.00026425
ENSMUSG00000034362	Csta1	-17.833759587002	0.00033165
ENSMUSG00000053729	Spinkl	-8.1313281822738	0.00044376
ENSMUSG00000100627	A830008E24Rik	-7.8212635639281	0.00060238
ENSMUSG00000031757	Mt4	-7.62814960034888	0.00143063
ENSMUSG00000103898	Gm30238	-7.59235146022003	0.00095709
ENSMUSG00000105979	Gm43411	-7.26060326681742	0.00244044
ENSMUSG00000081058	H3c15	-6.70426137419869	0.00143063
ENSMUSG00000020256	Aldh1l2	-6.45740993712603	0.00244044
ENSMUSG00000097497	Gm26652	-6.34152090904239	0.00462758
ENSMUSG00000010529	Gm266	-6.25752528840172	0.00486783
ENSMUSG00000050914	Ankrd37	-5.57500809001747	0.00002848
ENSMUSG00000107994	D830050J10Rik	-5.51652235079341	0.00749199

Ensembl Gene ID	Symbol	Log2 Fold Change	Adjusted P-value
ENSMUSG00000114689	Gm9465	-5.46133721441662	0.00749199
ENSMUSG00000116813	4930579D07Rik	-5.44183468503375	0.00772277
ENSMUSG00000104916	Gm42830	-5.2387342915707	0.00857453
ENSMUSG00000044348	Slc25a53	-5.08145765426193	0.00005611
ENSMUSG00000026637	Traf5	-4.83313559060267	0.0075652
ENSMUSG00000026989	Dapl1	-4.66028177878971	0.01053898
ENSMUSG00000071648	Rom1	-4.4270715845677	0.0092359
ENSMUSG00000044139	Prss53	-4.18711441283078	0.01313692
ENSMUSG00000086714	0610009E02Rik	-3.59399027905024	0.01856468
ENSMUSG00000054598	9130230L23Rik	-3.57139706137577	0.01682581
ENSMUSG00000105453	Gm43702	-3.56010461729853	0.01719135
ENSMUSG00000103976	Gm37677	-3.52661399653186	0.00840904
ENSMUSG00000017412	Cacnb4	-3.41677218826389	0.0196409
ENSMUSG00000080797	Gm15760	-3.35849891259349	0.01856468
ENSMUSG00000111656	Gm47232	-3.17589172983005	0.02100289
ENSMUSG00000052105	Mtcl1	-3.1317620905558	0.00154283
ENSMUSG00000107000	Gm43481	-3.04931752136556	0.02199187
ENSMUSG00000085633	Bloc1s6os	-3.01946767437339	0.02199187
ENSMUSG00000060177	Klk1b22	-2.95524357918611	0.02380022
ENSMUSG00000056687	Gm11696	-2.95383544772743	0.02258286
ENSMUSG00000046213	Cym	-2.69388319704623	0
ENSMUSG00000100075	1700018L02Rik	-2.28591589900088	0.03389524
ENSMUSG00000107152	Gm43152	-2.1266474304073	0.03540388
ENSMUSG00000020847	Rph3al	-2.0074783652729	0.03814201
ENSMUSG00000020020	Usp44	-1.97074273733032	0.04035178
ENSMUSG00000113349	Gm48369	-1.91290891680451	0.04000711
ENSMUSG00000073177	Gm773	-1.87811288256011	0.04069715
ENSMUSG00000082515	Gm12902	-1.79396495493481	0.04106597
ENSMUSG00000116506	5730414N17Rik	-1.78890290216806	0.04171192
ENSMUSG00000110326	Gm45378	-1.78428216154395	0.04171192
ENSMUSG00000087445	Gm14286	-1.77859539732354	0.0325699
ENSMUSG00000033819	Ppp1r16a	-1.69745849621505	0.00164316

Ensembl Gene ID	Symbol	Log2 Fold Change	Adjusted P-value
ENSMUSG00000038637	Lrrc56	-1.68953394444114	0.04233128
ENSMUSG00000042564	Fam227a	-1.63044583947141	0.0434421
ENSMUSG00000041789	2700046A07Rik	-1.62347756516668	0.0434421
ENSMUSG00000035759	Bbs10	-1.61830466403475	0.0434421
ENSMUSG00000087626	Gm15050	-1.54096499129159	0.01266906
ENSMUSG00000031430	Vsig1	-1.53147383989357	0.04616276
ENSMUSG00000071847	Apcdd1	-1.41451457567539	0.00143063
ENSMUSG00000079467	Gm14966	-1.38398500804987	0.04360424
ENSMUSG00000014592	Camta1	-1.36122423294884	0.0007015
ENSMUSG00000096872	Scgb2a2	-1.35711531899803	0.00006104
ENSMUSG00000022749	Tbc1d23	-1.18053964508659	0.00006608
ENSMUSG00000071711	Mpst	-1.17832926649477	0.00335975
ENSMUSG00000066516	Klk1b21	-1.12768941531382	0.00033165
ENSMUSG00000113183	Gm47664	-1.10843309194762	0.00229269
ENSMUSG00000063177	Klk1b27	-1.10461892346496	0.00021134
ENSMUSG00000063713	Klk1b24	-1.09641746034731	0.00078222
ENSMUSG00000050074	Spink8	-1.07384538256154	0.00000003
ENSMUSG00000026943	Lcn12	-1.06084644118252	0.00033165
ENSMUSG00000015120	Ube2i	-1.06022777318557	0.00776748
ENSMUSG00000038773	Kdm3b	-1.04722670047964	0.00862406
ENSMUSG00000055633	Zfp580	-1.04235979573537	0.01310233
ENSMUSG00000086567	Gm2830	-1.02764522535898	0.00913636
ENSMUSG00000031802	Phxr4	-1.02239907551793	0.01154764
ENSMUSG00000063903	Klk1	-1.02238204729461	0.01532743
ENSMUSG00000021253	Tgfb3	-1.00833306563019	0.00289359
ENSMUSG00000103906	Tigd5	-1.00098842696152	0.03430943
ENSMUSG00000096740	Lbhd1	-0.992643088230505	0.01488975
ENSMUSG00000007038	Neu1	-0.982836913505868	0
ENSMUSG00000037904	Ankrd9	-0.972146729487853	0.00462758
ENSMUSG00000024654	Asrgl1	-0.943253881435266	0.0067352
ENSMUSG00000024036	Slc37a1	-0.938069323824089	0.01599338
ENSMUSG00000033860	Fgg	-0.936572424427469	0.00000785

Ensembl Gene ID	Symbol	Log2 Fold Change	Adjusted P-value
ENSMUSG00000060224	Pyroxd2	-0.927034211018409	0.00749199
ENSMUSG00000028982	Slc25a33	-0.926798107860698	0.00001454
ENSMUSG00000033022	Cdo1	-0.91037806834773	0.00005126
ENSMUSG00000025981	Coq10b	-0.907254613787509	0.03760886
ENSMUSG00000092274	Neat1	-0.892404428090271	0
ENSMUSG00000074207	Adh1	-0.889753178429095	0.00000849
ENSMUSG00000102142	Gm26930	-0.881227237847405	0.04233128
ENSMUSG00000023951	Vegfa	-0.869843877170213	0.01189278
ENSMUSG00000046947	Adck2	-0.859680777928173	0.01488975
ENSMUSG00000015090	Ptgds	-0.847715195616082	0.00000007
ENSMUSG00000027222	Pex16	-0.845888804642934	0.02472224
ENSMUSG00000039753	Fbxl5	-0.837952926987925	0.00776748
ENSMUSG00000060019	Gm10073	-0.830358953619266	0.0303454
ENSMUSG00000019883	Echdc1	-0.8240646761671	0.01053898
ENSMUSG00000015943	Bola1	-0.802640249359148	0.00776748
ENSMUSG00000045098	Kmt5b	-0.799453336732709	0.00857453
ENSMUSG00000055334	Snupn	-0.782523753418226	0.02420765
ENSMUSG00000021371	Mcur1	-0.776161796237608	0.00333816
ENSMUSG00000017764	Zswim1	-0.764946548762891	0.04035178
ENSMUSG00000018736	Ndel1	-0.758908689465694	0.00372731
ENSMUSG00000070953	Rabepk	-0.75655838413917	0.00840904
ENSMUSG00000019102	Aldh3a1	-0.739033928619055	0.03735688
ENSMUSG00000023044	Csad	-0.725585898546761	0.00025909
ENSMUSG00000015149	Sirt2	-0.720796078553706	0.01469026
ENSMUSG00000024039	Cbs	-0.689836718043841	0.03042656
ENSMUSG00000028255	Clca1	-0.682783198187732	0.04193063
ENSMUSG00000022545	Ercc4	-0.682156052729516	0.04069715
ENSMUSG00000034930	Rtkn	-0.677907506286819	0.04210101
ENSMUSG00000078576	Gm12886	-0.6736697895917	0.02781155
ENSMUSG00000024191	Bnip1	-0.664746857813897	0.04069715
ENSMUSG00000074629	4930518I15Rik	-0.655142401854256	0.0434421
ENSMUSG00000050846	Zfp623	-0.652531118012546	0.04558819

Ensembl Gene ID	Symbol	Log2 Fold Change	Adjusted P-value
ENSMUSG00000086290	Snhg12	-0.646395001150555	0.03735688
ENSMUSG00000005483	Dnajb1	-0.637914533607799	0.03553369
ENSMUSG00000026578	Ccdc181	-0.627144896883817	0.0434421
ENSMUSG00000032867	Fbxw8	-0.613289365026089	0.01304355
ENSMUSG00000046761	Fam83h	-0.581014382865075	0.04670827
ENSMUSG00000040562	Gstm2	-0.565187250878018	0.00745662
ENSMUSG00000000168	Dlat	-0.532349618217594	0.03272337
ENSMUSG00000028573	Fggy	-0.510071935268568	0.04210101
ENSMUSG00000005973	Rcn1	-0.500968410268384	0.03526223
ENSMUSG00000019254	Ppp1r12c	-0.481185104669473	0.04102255
ENSMUSG00000085396	Firre	-0.464134540216615	0.04193063
ENSMUSG00000021096	Ppm1a	-0.451242818915613	0.01520165
ENSMUSG00000042845	Wfdc12	-0.448129064803624	0.00023159
ENSMUSG00000036427	Gpi1	-0.446692337849357	0.00389664
ENSMUSG00000086841	2410006H16Rik	-0.446155224178598	0.00379828
ENSMUSG00000039367	Sec24c	-0.443680421276185	0.01053898
ENSMUSG00000038387	Rras	-0.439287647059107	0.04069715
ENSMUSG00000069080	Lcn11	-0.420533026540913	0.00023339
ENSMUSG00000032353	Tmed3	-0.397934484048555	0.04069715
ENSMUSG00000039960	Rhou	-0.378472392920068	0.02124014
ENSMUSG00000024537	Psmg2	-0.375988728342604	0.03526223
ENSMUSG00000038582	Pptc7	-0.356449452881537	0.03760886
ENSMUSG00000031029	Eif3f	-0.354702130362745	0.0075583
ENSMUSG00000029647	Pan3	-0.353140162659659	0.01053898
ENSMUSG00000032939	Nup93	-0.351775215976085	0.04210101
ENSMUSG00000055681	Cope	-0.350821613877055	0.04896484
ENSMUSG00000003031	Cdkn1b	-0.342597249962016	0.0434421
ENSMUSG00000008348	Ubc	-0.334001676823293	0.00527334
ENSMUSG00000022982	Sod1	-0.331383670963692	0.00913636
ENSMUSG00000042354	Gnl3	-0.329882953787797	0.04193063
ENSMUSG00000033831	Fgb	-0.318017930993886	0.00354351
ENSMUSG00000001576	Ergic1	-0.314885272491125	0.03965052

Ensembl Gene ID	Symbol	Log2 Fold Change	Adjusted P-value
ENSMUSG00000000738	Spg7	-0.308415577287403	0.04069715
ENSMUSG00000025967	Eef1b2	-0.302504768621818	0.04171192
ENSMUSG00000005667	Mthfd2	-0.290703040378633	0.04233128
ENSMUSG00000053332	Gas5	-0.277327101540392	0.04069715
ENSMUSG00000063882	Uqcrh	-0.259294395507215	0.04171192
ENSMUSG00000046841	Ckap4	0.292249289102792	0.02567736
ENSMUSG00000022708	Zbtb20	0.296402796468026	0.04193063
ENSMUSG00000068220	Lgals1	0.30894684448247	0.04360424
ENSMUSG00000073411	H2-D1	0.349983086646415	0.00657066
ENSMUSG00000039361	Picalm	0.358102214313025	0.02124014
ENSMUSG00000056394	Lig1	0.38315986227836	0.01332545
ENSMUSG00000021377	Dek	0.401696862494725	0.00776748
ENSMUSG00000036256	Igfbp7	0.42151795057337	0.00927924
ENSMUSG00000031503	Col4a2	0.425256307111645	0.03526223
ENSMUSG00000027199	Gatm	0.434760797247695	0.04924746
ENSMUSG00000045948	Mrps12	0.43688198015642	0.04924746
ENSMUSG00000046111	Cep295	0.452686161702105	0.04560453
ENSMUSG00000008373	Prpf31	0.458829892271896	0.04102255
ENSMUSG00000020739	Nup85	0.463801736470264	0.01482089
ENSMUSG00000029781	Fkbp9	0.481223266449395	0.02199187
ENSMUSG00000028228	Cpne3	0.490809455363624	0.00486783
ENSMUSG00000036905	C1qb	0.514752525162073	0.04193063
ENSMUSG00000021190	Lgmn	0.516401136266494	0.00927924
ENSMUSG00000063455	D630045J12Rik	0.520881173163932	0.03170048
ENSMUSG00000031367	Ap1s2	0.521857601952254	0.00359
ENSMUSG00000032334	Loxl1	0.528725038111132	0.03008227
ENSMUSG00000004891	Nes	0.545848296626372	0.04806317
ENSMUSG00000040212	Emp3	0.54664267652237	0.03773766
ENSMUSG00000040552	C3ar1	0.546873600712416	0.0434421
ENSMUSG00000029761	Cald1	0.547912776273175	0.00108884
ENSMUSG00000048126	Col6a3	0.574462065800526	0.04069715
ENSMUSG00000017760	Ctsa	0.57551791791742	0.01714012

Ensembl Gene ID	Symbol	Log2 Fold Change	Adjusted P-value
ENSMUSG00000026678	Rgs5	0.583959327779678	0.01332545
ENSMUSG00000034744	Nagk	0.593010548121732	0.04210101
ENSMUSG00000069516	Lyz2	0.59864474423033	0.04960094
ENSMUSG00000021277	Traf3	0.610697512695658	0.02100289
ENSMUSG00000050989	Selenon	0.618177638297877	0.0476631
ENSMUSG00000042228	Lyn	0.625563832209693	0.01532743
ENSMUSG00000029925	Tbxas1	0.62940369866277	0.04896484
ENSMUSG00000035268	Pkig	0.629759284953568	0.03318598
ENSMUSG00000022371	Col14a1	0.633708059384698	0.0434421
ENSMUSG00000032491	Nradd	0.638603385622364	0.0434421
ENSMUSG00000021982	Cdadc1	0.641198756907024	0.03915166
ENSMUSG00000055053	Nfic	0.649750221166858	0.01053898
ENSMUSG00000001119	Col6a1	0.656198336946689	0.04233128
ENSMUSG00000069662	Marcks	0.677406178622151	0.01803609
ENSMUSG00000036099	Vezt	0.677672204431518	0.03346836
ENSMUSG00000025538	Sumf2	0.677787046378031	0.02100289
ENSMUSG00000001270	Ckb	0.690410638092272	0.04069715
ENSMUSG00000018830	Myh11	0.691239922341549	0.04238513
ENSMUSG00000020777	Acox1	0.700780641034636	0.00463017
ENSMUSG00000035711	Dok3	0.701765160800635	0.04069715
ENSMUSG00000070436	Serpinh1	0.703483565632215	0.01304355
ENSMUSG00000038780	Smurf1	0.706221410378833	0.03430943
ENSMUSG00000045312	Lhfpl2	0.718272820701884	0.03991788
ENSMUSG00000000957	Mmp14	0.726010813935432	0.01856468
ENSMUSG00000019122	Ccl9	0.728237322084656	0.03430943
ENSMUSG00000038070	Cntln	0.729159624764434	0.04069715
ENSMUSG00000030772	Dkk3	0.732551222531092	0.03779234
ENSMUSG00000098188	Sowahc	0.818697302824862	0.02882378
ENSMUSG00000075602	Ly6a	0.823267857415299	0.01150018
ENSMUSG00000028339	Col15a1	0.848957608104146	0.00645021
ENSMUSG00000018593	Sparc	0.85394255284351	0.00001454
ENSMUSG00000024781	Lipa	0.886646920871149	0.01278636

Ensembl Gene ID	Symbol	Log2 Fold Change	Adjusted P-value
ENSMUSG00000024672	Ms4a7	0.888911516902249	0.00025909
ENSMUSG00000026728	Vim	0.889085025806103	0.00000202
ENSMUSG00000026249	Serpine2	0.896198615336206	0.00006133
ENSMUSG00000086533	Mypopos	0.897877568722317	0.04360424
ENSMUSG00000040249	Lrp1	0.899028137523888	0.00652334
ENSMUSG00000037706	Cd81	0.909665102656456	0.00270412
ENSMUSG00000006800	Sulf2	0.913882559737681	0.00025948
ENSMUSG00000044709	Gemin7	0.920596195103863	0.00608378
ENSMUSG00000056515	Rab31	0.931454816911126	0.00112065
ENSMUSG00000033467	Crlf2	0.936329275750802	0.01911338
ENSMUSG00000047735	Samd9l	0.943167772505267	0.01581877
ENSMUSG00000112843	Gm46224	0.943924513291234	0.0434421
ENSMUSG00000049866	Arl4c	0.968712499892792	0.00164316
ENSMUSG00000015340	Cybb	0.97966702845742	0.00456494
ENSMUSG00000027204	Fbn1	0.983816934308594	0.00265101
ENSMUSG00000031740	Mmp2	1.03394302978897	0.01113647
ENSMUSG00000032440	Tgfbr2	1.04594968744236	0.00484128
ENSMUSG00000038642	Ctss	1.05990584683164	0.00005126
ENSMUSG00000026817	Ak1	1.06459366019151	0.00354351
ENSMUSG00000024501	Dpysl3	1.11180675060417	0.00653631
ENSMUSG00000025856	Pdgfa	1.12692339928522	0.0067352
ENSMUSG00000026600	Soat1	1.1707840007359	0.00486075
ENSMUSG00000042254	Cilp	1.17730710393123	0.00005126
ENSMUSG00000021998	Lcp1	1.26530003393456	0
ENSMUSG00000035385	Ccl2	1.39894455005125	0.00462758
ENSMUSG00000078439	Smim24	1.48945420369122	0.04451378
ENSMUSG00000058099	Nfam1	1.69063187027357	0.00021149
ENSMUSG00000034685	Fam171a2	1.75592501532651	0.00486075
ENSMUSG00000032925	Itgbl1	1.79410082380497	0.00231609
ENSMUSG00000029373	Pf4	1.83391232400087	0.00000066
ENSMUSG00000095315	Gm10130	1.91720013329583	0.04102255
ENSMUSG00000115902	D730005E14Rik	2.27471736362581	0.03526223

Ensembl Gene ID	Symbol	Log2 Fold Change	Adjusted P-value
ENSMUSG00000061723	Tnnt3	2.3925393650603	0.00005611
ENSMUSG00000003418	St8sia6	2.44410013676956	0.03272337
ENSMUSG00000058571	Gpc6	2.8698129231485	0.02567736
ENSMUSG00000049723	Mmp12	2.9514475372046	0.00484128
ENSMUSG00000091387	Gcnt4	2.96589173376122	0.02124014
ENSMUSG00000018893	Mb	3.25896500800152	0.01105791
ENSMUSG00000026204	Ptprn	3.95189047297902	0.01544974
ENSMUSG00000027227	Sord	4.2063185797343	0.01393601
ENSMUSG00000044229	Nxpe4	4.28960379138207	0.01332545
ENSMUSG00000014164	Klhl3	4.64570518317045	0.01192504
ENSMUSG00000020788	Atp2a3	4.68072585439339	0.01150018
ENSMUSG00000069272	H2ac8	5.20023397606987	0.00927924
ENSMUSG00000116895	Gm3435	5.26258742843527	0.0092359
ENSMUSG00000045573	Penk	5.7546794582046	0.0075583
ENSMUSG00000063193	Cd300lb	5.76032959230854	0.00508299
ENSMUSG00000027460	Angpt4	7.68199333250445	0.00164316
ENSMUSG00000020811	Wscd1	7.71687093375146	0.0012044

Table 7.4: List of differentially expressed genes in mouse tumours treated with xentuzumab vs control: pilot experiment. RNAs were extracted from harvested fresh frozen mouse tumours treated with xentuzumab vs PBS control and sequenced. Differential gene expression was analysed using the DESeq2 pipeline and genes with adjusted P-value $<$ 0.05 were deemed significant.

Ensembl Gene ID	Symbol	Log2 Fold Change	Adjusted P-value
ENSMUSG00000114276	Gm47849	-20.6089172487458	0
ENSMUSG00000116819	Gm49586	-20.2862758776195	0
ENSMUSG00000027923	Lce1b	-20.0874150589505	0
ENSMUSG00000050359	Sprr1a	-19.9228202243813	0.00002836
ENSMUSG00000032013	Trim29	-19.8699417420485	0.00002836
ENSMUSG00000034362	Csta1	-19.6348762365525	0.00003567
ENSMUSG00000103898	Gm30238	-7.96626434931295	0.00093935
ENSMUSG00000065657	Gm25337	-7.31574474151348	0.00245681
ENSMUSG00000065100	Gm26132	-6.40430102971897	0.00504868
ENSMUSG00000105979	Gm43411	-6.00161057665242	0.0049328
ENSMUSG00000079467	Gm14966	-3.97930223108797	0.01740477
ENSMUSG00000061702	Tmem91	-3.67874083816085	0.01880194
ENSMUSG00000026989	Dapl1	-3.58465728597552	0.01880194
ENSMUSG00000010529	Gm266	-3.42280500769081	0.01848482
ENSMUSG00000054514	Atad3aos	-2.53902804458797	0.03387089
ENSMUSG00000025858	Get4	-1.29894261977489	0.00176643
ENSMUSG00000025723	Nmb	-1.18483687994398	0.00787179
ENSMUSG00000090086	AI480526	-1.07309007297015	0.00384813
ENSMUSG00000022598	Psca	-1.03377374629517	0
ENSMUSG00000024610	Cd74	-1.02547704277223	0.00245681
ENSMUSG00000040350	Trim7	-1.01749503357807	0.00211032
ENSMUSG00000049103	Ccr2	-0.909741779336707	0.01917643
ENSMUSG00000040562	Gstm2	-0.909121194239643	0.00245681
ENSMUSG00000030527	Crtc3	-0.832947085314656	0.01880194
ENSMUSG00000022749	Tbc1d23	-0.748512391940731	0.01484104
ENSMUSG00000074024	4632427E13Rik	-0.717237370266199	0.00832678
ENSMUSG00000050074	Spink8	-0.693037606622328	0.00428019

Ensembl Gene ID	Symbol	Log2 Fold Change	Adjusted P-value
ENSMUSG00000077704	Snord89	-0.672044900511331	0.01688018
ENSMUSG00000031864	Ints10	-0.640271974317598	0.03819173
ENSMUSG00000021288	Klc1	-0.624657423744344	0.00245681
ENSMUSG00000029816	Gpnmb	-0.593672719126878	0.01510274
ENSMUSG00000007038	Neu1	-0.537203170771267	0.00504868
ENSMUSG00000052911	Lamb2	-0.466740555538964	0.01197933
ENSMUSG00000020427	Igfbp3	0.557095577515821	0.03812108
ENSMUSG00000005534	Insr	0.597318217527435	0.01880194
ENSMUSG00000044042	Fmn1	0.601259787361164	0.04602315
ENSMUSG00000049723	Mmp12	0.608551815296719	0.03812108
ENSMUSG00000002797	Ggct	1.08971153008294	0.00245681
ENSMUSG00000028494	Plin2	1.14998921349356	0.00176643
ENSMUSG00000111065	Gm47676	1.84777066457204	0.04942393
ENSMUSG00000003418	St8sia6	4.36671132597754	0.01510274
ENSMUSG00000030873	Scnn1b	6.38029485655542	0.00384813
ENSMUSG00000027227	Sord	6.89149467764053	0.00384813
ENSMUSG00000050762	Prss27	19.090795341489	0.00007305

Table 7.5: List of differentially expressed genes in mouse tumours treated with xentuzumab + aPD1 vs xentuzumab: pilot experiment. RNAs were extracted from harvested fresh frozen mouse tumours treated with xentuzumab + anti-PD1 vs xentuzumab and sequenced. Differential gene expression was analysed using the DESeq2 pipeline and genes with adjusted P-value < 0.05 were deemed significant.

Ensembl Gene ID	Symbol	Log2 Fold Change	Adjusted P-value
ENSMUSG00000025431	Crisp1	-17.1368409795969	0.00004285
ENSMUSG00000117286	Gm1043	-14.3368350954999	0.00109306
ENSMUSG00000050762	Prss27	-14.288383458886	0.00109306
ENSMUSG00000032532	Cck	-8.86455944185451	0.00004285
ENSMUSG00000104554	Gm4610	-8.31490875412986	0.00089852
ENSMUSG00000107994	D830050J10Rik	-8.00099086013402	0.00056871
ENSMUSG00000054537	Tmprss11e	-7.89814010786857	0.00122046
ENSMUSG00000038296	Galnt18	-7.38785014032859	0.00289479
ENSMUSG00000029372	Ppbp	-7.29866884856873	0.00604788
ENSMUSG00000020256	Aldh1l2	-6.67223156565669	0.00339431
ENSMUSG00000050063	Klk6	-6.58449262395995	0.01048883
ENSMUSG00000060568	Fam78b	-6.23362317680302	0.0069745
ENSMUSG00000091514	Gm17484	-5.88730358889215	0.01002904
ENSMUSG00000027950	Chrnb2	-5.2802258573264	0.01261005
ENSMUSG00000104925	Gm43061	-5.09900429894211	0.01461281
ENSMUSG00000020738	Sumo2	-5.03452421885137	0.01465813
ENSMUSG00000028909	Ptpru	-4.66316174701353	0.01724854
ENSMUSG00000064023	Klk8	-4.5468068390672	0.01804508
ENSMUSG00000039419	Cntnap2	-4.29621566318704	0.00626675
ENSMUSG00000029228	Lnx1	-4.19604120327447	0.02196796
ENSMUSG00000108216	Gm44153	-3.92352371864184	0.02351782
ENSMUSG00000005983	1700037C18Rik	-3.44299017968266	0.02831734
ENSMUSG00000071648	Rom1	-3.43516436186827	0.025757
ENSMUSG00000045027	Prss22	-3.41302757383924	0.00259621
ENSMUSG00000106197	Gm42717	-3.07276981882039	0.03192298
ENSMUSG00000078495	Zfp984	-3.01056331317227	0.03027103
ENSMUSG00000117278	Gm36684	-2.93818779481249	0.03381445

Ensembl Gene ID	Symbol	Log2 Fold Change	Adjusted P-value
ENSMUSG00000114617	Gm48766	-2.93335400064043	0.03382337
ENSMUSG00000046213	Cym	-2.89885644912943	0
ENSMUSG00000087626	Gm15050	-2.83890552198964	0.00413777
ENSMUSG00000049670	Morn4	-2.49828867082129	0.0415472
ENSMUSG00000040836	Gpr161	-2.17028177066993	0.04943249
ENSMUSG00000085105	Gm12758	-2.15332629094156	0.04447438
ENSMUSG00000085929	Gm13421	-2.08856909138949	0.02295515
ENSMUSG00000074206	Adh6b	-1.43380075706114	0.04822981
ENSMUSG00000002797	Ggct	-1.3569928136208	0.00345958
ENSMUSG00000055305	Zfp93	-1.31190587110871	0.02689282
ENSMUSG00000063415	Cyp26b1	-1.29141324357009	0.00604788
ENSMUSG00000055334	Snupn	-1.27895510513361	0.00332493
ENSMUSG00000025176	Hoga1	-1.16709829832537	0.0002979
ENSMUSG00000023951	Vegfa	-1.10694184215546	0.00289479
ENSMUSG00000026437	Cdk18	-1.0216154846234	0.01048883
ENSMUSG00000006050	Sra1	-0.984637471113028	0.00201619
ENSMUSG00000033022	Cdo1	-0.976281830441855	0.0002979
ENSMUSG00000032348	Gsta4	-0.966985262832808	0.02873018
ENSMUSG00000038736	Nudcd1	-0.85259649486812	0.00626675
ENSMUSG00000024191	Bnip1	-0.788611809125005	0.02361174
ENSMUSG00000024654	Asrgl1	-0.781860296903674	0.02689282
ENSMUSG00000015149	Sirt2	-0.780465395384184	0.01086604
ENSMUSG00000046658	Zfp316	-0.777019171036777	0.01901751
ENSMUSG00000028645	Slc2a1	-0.776929725339202	0.02295515
ENSMUSG00000112096	A430103D13Rik	-0.773400257600396	0.03420191
ENSMUSG00000046679	C87436	-0.722490837241283	0.04534736
ENSMUSG00000036398	Ppp1r11	-0.717077960310854	0.01986181
ENSMUSG00000021671	Poc5	-0.70251678882421	0.04302648
ENSMUSG00000027175	Tcp11l1	-0.699438020205649	0.04343361
ENSMUSG00000028669	Pithd1	-0.677789967754564	0.03192298
ENSMUSG00000025921	Rdh10	-0.643831119733877	0.04943249
ENSMUSG00000039753	Fbxl5	-0.633151202346821	0.04361746

Ensembl Gene ID	Symbol	Log2 Fold Change	Adjusted P-value
ENSMUSG00000005483	Dnajb1	-0.62078956634455	0.03984489
ENSMUSG00000034936	Arl4d	-0.619494850762881	0.03382337
ENSMUSG00000017418	Arl5b	-0.605465383407895	0.04983332
ENSMUSG00000032867	Fbxw8	-0.584792811223678	0.01086604
ENSMUSG00000100801	Gm15459	-0.552508748586178	0.00626675
ENSMUSG00000028982	Slc25a33	-0.532642836790478	0.03027103
ENSMUSG00000029782	Tmem209	-0.532522319093283	0.0359424
ENSMUSG00000018736	Ndel1	-0.515801488930824	0.03027103
ENSMUSG00000058704	Memo1	-0.504796492233864	0.03192298
ENSMUSG00000033099	Nol12	-0.465050223555047	0.03192298
ENSMUSG00000036912	Piwil4	-0.450341312672432	0.01095746
ENSMUSG00000000628	Hk2	-0.410396091382981	0.01901751
ENSMUSG00000056851	Pcbp2	-0.400283668548912	0.01620872
ENSMUSG00000021149	Gtpbp4	-0.388657166781723	0.01620872
ENSMUSG00000032939	Nup93	-0.372220666008091	0.02831734
ENSMUSG00000022858	Tra2b	-0.34800531016288	0.03394167
ENSMUSG00000073411	H2-D1	0.321953649498936	0.03200323
ENSMUSG00000009905	Kdsr	0.459222114112751	0.0304605
ENSMUSG00000052911	Lamb2	0.53546550525229	0.01461281
ENSMUSG00000004056	Akt2	0.584116019062478	0.04972333
ENSMUSG00000048154	Kmt2d	0.606293554024697	0.01261005
ENSMUSG00000027199	Gatm	0.620745679625807	0.03200323
ENSMUSG00000021288	Klc1	0.62589658468561	0.00109306
ENSMUSG00000027198	Ext2	0.652122667410143	0.00345958
ENSMUSG00000026675	Hsd17b7	0.669277242166948	0.04983332
ENSMUSG00000024298	Zfp871	0.686511083465025	0.00339431
ENSMUSG00000020777	Acox1	0.693800338297172	0.01147529
ENSMUSG00000061119	Prcp	0.697704977927573	0.0415472
ENSMUSG00000049866	Arl4c	0.71903068478254	0.01793805
ENSMUSG00000022797	Tfrc	0.777811272510198	0.01048883
ENSMUSG00000040713	Creg1	0.823033106769673	0.00201619
ENSMUSG00000033624	Pdpr	0.844203089645619	0.02295515

Ensembl Gene ID	Symbol	Log2 Fold Change	Adjusted P-value
ENSMUSG00000021876	Rnase4	0.911322292809266	0.02689282
ENSMUSG00000041949	Tango6	0.936478055272334	0.01028024
ENSMUSG00000024140	Epas1	0.972906252722109	0.01620872
ENSMUSG00000049103	Ccr2	1.00214958661602	0.0415472
ENSMUSG00000024610	Cd74	1.05114735500222	0.00332493
ENSMUSG00000022488	Nckap1l	1.1063573001266	0.00456988
ENSMUSG00000036594	H2-Aa	1.30599519501039	0.00109306
ENSMUSG00000015340	Cybb	1.43905279821706	0.00020773
ENSMUSG00000078920	Ifi47	1.57864986011842	0.01048883
ENSMUSG00000037526	Atg14	1.86706173685107	0.00201619
ENSMUSG00000028978	Nos3	1.94380557125152	0.01620872
ENSMUSG00000050345	4930486L24Rik	2.33077361746187	0.00012966
ENSMUSG00000033196	Myh2	2.43250104851155	0.0443737
ENSMUSG00000114185	Gm47662	2.52351070864165	0.03984489
ENSMUSG00000046818	Ddit4l	2.99847681484213	0.02316455
ENSMUSG00000103423	Gm5845	3.25762928859714	0.02316455
ENSMUSG00000034685	Fam171a2	3.26205382798622	0.00081942
ENSMUSG00000087150	BC064078	3.46274187234297	0.02689282
ENSMUSG00000029330	Cds1	4.6870085331116	0.01793805
ENSMUSG00000041797	Abca9	5.39132096971153	0.01105056
ENSMUSG00000078780	Gm5150	6.14296134202296	0.00626675

Table 7.6: List of differentially expressed genes in mouse tumours treated with xentuzumab + anti-PD-1 vs control: repeat experiment. RNAs were extracted from harvested fresh frozen mouse tumours treated with xentuzumab and anti-PD-1 vs PBS control and sequenced. Differential gene expression was analysed using the DESeq2 pipeline and genes with adjusted P-value < 0.05 were deemed significant.

Ensembl Gene ID	Symbol	Log2 Fold Change	Adjusted P-value
ENSMUSG00000028166	Slc40a1	-23.2172399922501	0
ENSMUSG00000021504	Tbc1d32	-22.0925758175976	0
ENSMUSG00000091255	Gm10024	-23.2685615331805	0
ENSMUSG00000034053	Krtap3-1	-26.3600464851049	0
ENSMUSG00000047637	Krtap1-5	-25.6082145541444	0
ENSMUSG00000088277	Gm11938	-24.5281239988927	0
ENSMUSG00000052120	Krtap4-8	-23.9704396653155	0
ENSMUSG00000093237	Gm11567	-24.4330990359996	0
ENSMUSG00000062612	Krt35	-23.0841595748284	0
ENSMUSG00000029676	Fbln1	-21.2978860340276	0
ENSMUSG00000074794	Krtap19-1	-25.9662850221435	0
ENSMUSG00000074793	Krtap19-2	-26.3144841224313	0
ENSMUSG00000086505	Krtap19-9b	-26.8000812448851	0
ENSMUSG00000060353	Krtap16-3	-26.1720232442083	0
ENSMUSG00000086288	Krtap22-2	-26.6707291273029	0
ENSMUSG00000086312	Krtap21-1	-25.1604680582188	0
ENSMUSG00000052112	Krtap6-2	-25.2186389552376	0
ENSMUSG00000030879	Zdhhc14	-21.5906580860365	0
ENSMUSG00000043824	Psors1c2	-24.9425265973445	0
ENSMUSG00000020612	Kcng2	-22.0677650773731	0
ENSMUSG00000032945	Rbm20	-21.8181826797346	0
ENSMUSG00000027828	Pde1a	-23.2264792465342	0
ENSMUSG00000031556	Rhov	-21.4688816474825	0
ENSMUSG00000021611	Tchh	-26.1805138442484	0
ENSMUSG00000043914	Adamtsl1	-22.4092509449818	0
ENSMUSG00000029113	Rpusd3	-22.7474055543948	0
ENSMUSG00000002789	Alox5	-23.9295476478576	0

Ensembl Gene ID	Symbol	Log2 Fold Change	Adjusted P-value
ENSMUSG00000041299	Styk1	20.185181265285	0
ENSMUSG00000025015	Birc3	-22.4918652001159	0
ENSMUSG00000047331	Zfp711	20.8022518065411	0
ENSMUSG00000071495	Krtap9-3	-24.3332147464163	0.00000001
ENSMUSG00000064691	Krt33a	-25.4819567519435	0.00000001
ENSMUSG00000074284	Atp6v1c2	-21.5787135482249	0.00000001
ENSMUSG00000074796	Krtap19-3	-26.3310711481342	0.00000001
ENSMUSG00000074798	Krtap19-5	-25.2006479404522	0.00000001
ENSMUSG00000092207	1110025L11Rik	-24.9889940679062	0.00000001
ENSMUSG00000055360	Krtap11-1	-24.7694783505347	0.00000001
ENSMUSG00000006828	Gstp1	-25.3173396124288	0.00000001
ENSMUSG00000063618	Phldb3	-22.6688733678805	0.00000001
ENSMUSG00000024478	Crym	-22.8507470222964	0.00000001
ENSMUSG00000094608	Colca2	-21.6587104787308	0.00000001
ENSMUSG00000092344	Gm11559	-22.7793932889885	0.00000002
ENSMUSG00000154783	Fgd5	-22.6069352945172	0.00000002
ENSMUSG00000056079	Krtap4-1	-25.1536112733705	0.00000003
ENSMUSG00000042865	Gzmc	-21.874630953338	0.00000003
ENSMUSG00000044784	Mfsd8	20.5747228997306	0.00000003
ENSMUSG00000030849	Urgcp	19.6689665289983	0.00000004
ENSMUSG00000020836	Krt34	-25.078188410867	0.00000004
ENSMUSG00000024063	Flrt3	-21.7317187128873	0.00000005
ENSMUSG00000055424	Krtap3-2	-24.8113973841372	0.00000006
ENSMUSG00000021814	Il7r	-22.4064395246784	0.00000006
ENSMUSG00000074797	Krtap19-4	-22.4837747388732	0.00000007
ENSMUSG00000034892	Lcn6	-20.1939271624344	0.00000008
ENSMUSG00000062192	Krt31	-24.3621002178885	0.00000011
ENSMUSG00000095465	Gm21970	19.9468187169697	0.00000011
ENSMUSG00000032543	Fgf2	-21.9281300199891	0.00000012
ENSMUSG00000040558	Krtap1-3	-24.1724604957536	0.00000013
ENSMUSG00000032006	Vav3	-23.3771981246826	0.00000013
ENSMUSG00000064891	Spata33	20.4781109207521	0.00000014

Ensembl Gene ID	Symbol	Log2 Fold Change	Adjusted P-value
ENSMUSG00000042472	Parp12	20.4739741123517	0.00000015
ENSMUSG00000092012	Gm20716	-23.6952754287475	0.00000016
ENSMUSG00000064051	Krtap13-1	-23.9883874692391	0.00000017
ENSMUSG00000065206	Krtap14	-23.9679098652388	0.00000017
ENSMUSG00000023904	Aox4	-22.3653338535952	0.00000024
ENSMUSG00000071489	Krtap4-6	-23.0502578962655	0.00000024
ENSMUSG00000049602	Tctn3	20.1009719707566	0.00000026
ENSMUSG00000026602	Plxna4	-21.4553517776975	0.00000033
ENSMUSG00000020633	Mical1	-21.8808941709962	0.00000043
ENSMUSG00000078256	Gm11565	-22.3966238264408	0.00000049
ENSMUSG00000025170	Ap5b1	-21.7124265547758	0.00000062
ENSMUSG00000020663	Nek7	19.0203792726243	0.00000067
ENSMUSG00000023903	Wnk4	-22.0810031078889	0.00000076
ENSMUSG00000075297	Vsig8	-22.735611304349	0.00000102
ENSMUSG00000021854	Dynlt1b	-22.7021864983165	0.00000106
ENSMUSG00000056080	Krtap4-2	-22.178249622476	0.00000229
ENSMUSG00000027616	Ints6	19.8718870768876	0.00000375
ENSMUSG00000074776	Krtap4-16	-21.5202537638511	0.00000587
ENSMUSG00000027617	Card14	20.0079764426703	0.0000066
ENSMUSG00000039593	Hoxa1	19.8743741365628	0.00000671
ENSMUSG00000020800	Atp1a2	18.1228131559701	0.00000706
ENSMUSG00000051952	a	19.8723827744383	0.00001086
ENSMUSG00000026418	Agk	20.1692112447548	0.00001138
ENSMUSG00000043090	Mfap3l	-19.3547361938468	0.00001234
ENSMUSG00000029224	Csgalnact1	-16.8717314224966	0.00001356
ENSMUSG00000049069	Sprr2d	20.0950562638163	0.00003817
ENSMUSG00000027758	Myoz1	-19.8449233326691	0.00005345
ENSMUSG00000051532	Rasl12	-16.8864356324523	0.0000699
ENSMUSG00000042856	Higd1b	18.9840231332273	0.00008087
ENSMUSG00000079295	Gm379	18.2142383563991	0.00034417
ENSMUSG00000031051	Popdc2	17.9923093932306	0.00042811
ENSMUSG00000024995	Dnajb6	3.9723492794821	0.00079135

Ensembl Gene ID	Symbol	Log2 Fold Change	Adjusted P-value
ENSMUSG00000028409	Actn3	17.2202386369898	0.00085471
ENSMUSG00000030626	Pex26	-8.08460377337454	0.00093398
ENSMUSG00000015916	Stab1	-4.68185981275564	0.00153029
ENSMUSG00000078062	Zfp799	-8.75252808863114	0.00167376
ENSMUSG00000029101	Kcnk6	13.4716758288482	0.00174193
ENSMUSG00000090902	Trbc2	15.4591157773921	0.00272453
ENSMUSG00000029365	Zfp106	1.17330396382143	0.00285122
ENSMUSG00000031489	Kctd9	6.30419610489646	0.00295298
ENSMUSG00000042695	Thoc2	1.83338355974632	0.00332939
ENSMUSG00000041219	Mga	8.65871183047979	0.00344868
ENSMUSG00000031714	Casp9	4.89363382178051	0.00412554
ENSMUSG00000091318	Gm10228	-9.97929451503457	0.00426938
ENSMUSG00000088272	Krtap15	-11.2828840935926	0.00486596
ENSMUSG00000028684	Lonrf3	13.2757239758951	0.00684495
ENSMUSG00000037597	Pik3r6	10.1978912913048	0.0085301
ENSMUSG00000056839	Krtap8-1	-10.0896752161736	0.01124183
ENSMUSG00000032341	Cst3	-0.385623222616413	0.01261141
ENSMUSG00000025466	Igsf10	10.3426826111055	0.01629034
ENSMUSG00000030245	Fam117b	-0.391145413234637	0.02494778
ENSMUSG00000031342	Psmd1	0.438665994386068	0.02609443
ENSMUSG00000003923	Tlr7	-3.94389892053596	0.028495
ENSMUSG00000030143	Tm9sf4	0.88201915665826	0.02973918
ENSMUSG00000027639	Zxdc	2.28722483571284	0.03033571
ENSMUSG00000071491	Krtap6-5	-5.91304675845549	0.03042044
ENSMUSG00000028206	Slc6a6	0.31285031178119	0.03050681
ENSMUSG00000028750	Uso1	0.422186812014952	0.03476642
ENSMUSG00000027726	Zfp9	2.59691446633114	0.0387465
ENSMUSG00000026997	Gale	0.46846186742823	0.04180111
ENSMUSG00000043826	Prps1l3	2.07106435304559	0.0467667

Table 7.7: List of differentially expressed genes in mouse tumours treated with xentuzumab vs control: repeat experiment. RNAs were extracted from harvested fresh frozen mouse tumours treated with xentuzumab and anti-PD-1 vs PBS control and sequenced. Differential gene expression was analysed using the DESeq2 pipeline and genes with adjusted P-value < 0.05 were deemed significant.

Ensembl Gene ID	Symbol	Log2 Fold Change	Adjusted P-value
ENSMUSG00000020191	Nts	-22.5106857778133	0
ENSMUSG00000050150	4933427D14Rik	-22.7974605074569	0
ENSMUSG00000029200	Sfxn5	-23.9799235789648	0
ENSMUSG00000048778	Alox5	-23.9311606987351	0
ENSMUSG00000035226	Hdhd5	-21.0497384429799	0
ENSMUSG00000001918	Il10ra	-22.5140372902413	0
ENSMUSG00000054137	Zfp711	20.65150985886	0
ENSMUSG00000025310	Urgcp	20.7142169211894	0.00000001
ENSMUSG00000040791	Prss27	20.625874114879	0.00000001
ENSMUSG00000059828	Rhov	-21.4021266280164	0.00000001
ENSMUSG00000051030	Defb29	-21.936101122973	0.00000001
ENSMUSG00000023318	Pars2	-21.8173960926101	0.00000001
ENSMUSG00000052126	Zfp235	-20.7774340961428	0.00000001
ENSMUSG00000032603	Nek7	20.9627345246076	0.00000005
ENSMUSG00000035635	Kcnk6	20.6558479298657	0.00000007
ENSMUSG00000064856	Gm21970	20.5588865744732	0.00000008
ENSMUSG00000023874	Pik3r6	20.0001641692122	0.00000015
ENSMUSG00000074632	Krtap19-4	-22.4344876957972	0.00000015
ENSMUSG00000024079	Zfp780b	-21.9692953483255	0.00000016
ENSMUSG00000057181	Tctn3	20.7741640980871	0.00000018
ENSMUSG00000029654	Zfp11	-21.5783699705757	0.0000002
ENSMUSG00000063573	Krtap14	-23.884690466995	0.00000037
ENSMUSG00000064757	Mtarc1	-22.3168109786296	0.00000091
ENSMUSG00000060791	Tyw3	-21.5207342715158	0.00000093
ENSMUSG00000024066	H4c3	-21.1373251410652	0.00000109
ENSMUSG00000073743	Gm11565	-22.2664439318673	0.00000113
ENSMUSG00000041636	Wnk4	-21.9285176191919	0.00000186

Ensembl Gene ID	Symbol	Log2 Fold Change	Adjusted P-value
ENSMUSG00000029043	Dynlt1b	-22.5599303811602	0.00000246
ENSMUSG00000054092	Mfsd8	18.4681658641203	0.00000246
ENSMUSG00000074375	Krtap4-2	-22.037679339857	0.00000513
ENSMUSG00000036295	Nacad	20.9586185066641	0.00000621
ENSMUSG00000002703	Ints6	19.914902524524	0.00000642
ENSMUSG00000068443	Card14	20.3496021523513	0.00000699
ENSMUSG00000031831	Tmprss6	21.6432468799592	0.00000819
ENSMUSG00000063785	Dzip1	21.0213929263425	0.00001028
ENSMUSG00000032752	Hoxa1	19.7292252944873	0.00001431
ENSMUSG00000022225	Gjc1	-20.8309743606603	0.00002462
ENSMUSG00000015380	a	19.1453603699278	0.00005112
ENSMUSG00000023464	Higd1b	19.6476110665418	0.00005565
ENSMUSG00000034753	Popdc2	20.1657258539604	0.00005565
ENSMUSG00000031617	Trbc2	20.1181067359035	0.00005745
ENSMUSG00000074140	Gm379	20.0909252595323	0.00005825
ENSMUSG00000029922	Slc2a6	-19.9298086852328	0.0000713
ENSMUSG00000021113	Parp12	16.7880050849648	0.00010488
ENSMUSG00000030188	Agk	18.0750340144476	0.00025959
ENSMUSG00000056952	Lonrf3	18.5866554930672	0.00032339
ENSMUSG00000035579	Ttll5	9.07499310698855	0.00036101
ENSMUSG00000029926	Atp1a2	15.5351773559806	0.00048736
ENSMUSG00000055011	Styk1	13.562883327653	0.00092436
ENSMUSG00000054371	Rnf141	-2.48429097632767	0.00124056
ENSMUSG00000056765	Larp1b	2.2006996424609	0.00145631
ENSMUSG00000024524	Zfp799	-8.94691286459704	0.00176067
ENSMUSG00000066735	Sprr2d	15.9149012923319	0.00238766
ENSMUSG00000022116	Wdr83	-5.65844953302159	0.00529398
ENSMUSG00000030310	Fam229b	6.19676807803133	0.01252149
ENSMUSG00000051795	Copg2	-1.39356883654424	0.01491787
ENSMUSG00000021226	Rit1	-0.507827136344822	0.02305074
ENSMUSG00000042253	Clspn	2.34710277633743	0.02374584
ENSMUSG00000031066	Setd2	0.759029647131227	0.02797033

Table 7.8: Eligibility criteria for entry into the study. Patients that consented and met the following eligibility criteria were recruited to be part of the WINGMEN study.

Inclusion Criteria **A patient will be eligible if all of the following criteria apply:**	
1	Men with prostate adenocarcinoma confirmed on prostate biopsy and with sufficient cancer-containing biopsy tissue surplus to diagnostic need to provide ≥2 sections for primary endpoint analysis.
2	Scheduled for open or robotic radical prostatectomy.
3	Age ≥ 18 years.
4	Eastern Cooperative Oncology Group (ECOG) performance status 0 or 1. (Appendix 7.9)
5	The patient is willing and able to comply with the protocol scheduled follow-up visits and examinations for the duration of the study.
6	Participant is willing and able to give informed consent.
7	Participants whose partner is of child bearing potential must be willing to ensure that they or their partner use effective contraception during the trial and for 70 days thereafter.
8	Adequate haematologic, renal and hepatic function, defined as follows: Haemoglobin (Hb) ≥ 90g/L White Blood Count (WBC) > 2.5 x 10^9/L Absolute Neutrophil Count (ANC) ≥ 1.5 x 10^9/L Platelet Count ≥ 100 x 10^9/L Aspartate transaminase, alanine transaminase, and alkaline phosphatase ≤ 2.5 x upper limit of normal estimated glomerular filtration rate ≥ 30ml/min
Exclusion Criteria **A patient will not be eligible if any of the following applys:**	
1	Treated with systemic corticosteroids, insulin, metformin, other oral hypoglycaemic agent, or anti-androgens in the 28 days prior to first dose of study drug.
2	Diabetes mellitus.
3	Previous prostate radiotherapy.
4	Current or previous treatment with xentuzumab or other IGF or GH-modifying therapy.
5	Patients who are known to be serologically positive for Hepatitis B, Hepatitis C or HIV.
6	Treatment with any other investigational agent, or treatment in another interventional clinical trial within 28 days prior to enrolment.
7	Other psychological, social or medical condition, physical examination finding or a laboratory abnormality that the Investigator considers would make the patient a poor trial candidate or could interfere with protocol compliance or the interpretation of trial results.

Table 7.9: Entry requirements for WINGMEN patients: Eastern Cooperative Oncology Group (ECOG) performance scale. ECOG performance scale measures patient's level of functioning during care.

Activity Performance Description	Score
Fully active, able to carry out all or all pre-disease performance without restriction.	0
Restricted in physically strenuous activity but ambulatory and able to carry out work of a light or sedentary nature, e.g. light housework, office work.	1
Ambulatory and capable of all self-care, but unable to carry out any work activities. Up and about more than 50% of waking hours.	2
Capable of only limited self-care. Confined to bed or chair more than 50% of waking hours.	3
Completely disabled. Cannot carry out any self-care. Totally confined to bed or chair.	4

Table 7.10: Summary of changes in primary endpoint markers PRE/POST xentuzumab. Post-xentuzumab changes were expressed as % baseline (pre-treatment) values. Data points were missing when the biopsy or in-theatre cores did not contain any tumour areas.

	% Phospho-IGF-1R+ tumour cells			% Phospho-S6+ tumour cells		
Patient (WN-01-)	Pre-treatment	Post-treatment	Change (%)	Pre-treatment	Post-treatment	Change (%)
10001	37.850201	14.658903	-61.271268	4.031008	1.880878	-53.33976
10002	10.811448	0.734694	-93.204481	3.434222	5.498646	60.1132949
10003	25.233023	16.463875	-34.752665	2.256098	0.729661	-67.658275
10004	29.062113	3.67173	-87.365922	3.453991	1.999112	-42.121679
10005	27.998514			19.209375		
10006	2.494118	14.507772	481.679455	4.155417	3.1477	-24.250683
10007	32.86219	11.5625	-64.815187	1.321586		
10008	69.806709	15.578402	-77.683517	4.605812	3.635377	-21.069792
10009						
10010	91.176468	15.857112	-82.608328	9.762203	2.640169	-72.955193
10011	58.181248	8.447654	-85.480452	4.928797	0.987692	-79.96079
10012	26.725664	3.053435	-88.574896			
10013	37.5	2.290951	-93.890797	8.519046	2.1313	-74.98194
10014	11.134845	49.707813	346.416749	16.469151	2.040321	-87.611256
10015	46.099709	10.982659	-76.176294	17.320261		
10016	18.068104	2.34375	-87.028246	5.278422		
10017		18.066847			10.099622	
10018		29.708223				
10019	7.288826	3.438096	-52.830593	16.301352	2.926472	-82.047673
10020	6.887146	No surgery	NA	6.871831	No surgery	NA
10021	28.785358	1.848998	-93.576602	40.547142	6.24	-84.610506
10022	56.385117	8.179861	-85.492872	26.701164	10.571135	-60.40946
10023	55.178749	1.134127	-97.944631	12.140373	2.992226	-75.353097
10024	10.373796	44.984077	333.631787	30.944401	6.314602	-79.593717
10025		8.455506			2.833112	
10026	13.837074	10.985626	-20.607305	6.050522	3.967108	-34.433624
10027	23.743952	11.346154	-52.214551	17.329956	15.053763	-13.134442

Table 7.11: Summary of changes in nuclear and non-nuclear staining of phospho-IGF-1R PRE/POST xentuzumab. Post-xentuzumab changes were expressed as % baseline (pre-treatment) values. Data points were missing when the biopsy or in-theatre cores did not contain any tumour areas.

	% Phospho-IGF-1R+ nucleus			% Phospho-S6+ non-nuclear		
Patient (WN-01-)	Pre-treatment	Post-treatment	Change (%)	Pre-treatment	Post-treatment	Change (%)
10001	37.678673	14.499176	-61.518878	2.572899	1.365416	-46.930836
10002	9.105206	0.427002	-95.310353	4.238088	0.533752	-87.40583
10003	24.700399	16.173145	-34.522738	2.862849	1.205987	-57.874586
10004	26.630266	3.584308	-86.540472	14.145756	0.152989	-98.918481
10005	27.107315			9.023394		
10006	2.305882	13.73057	495.458484	0.470588	5.699482	1111.14053
10007	32.155476	10.9375	-65.985576	6.713781	1.5625	-76.726974
10008	69.375587	13.837177	-80.054688	25.422146	4.677225	-81.60177
10009						
10010	90.441177	15.519495	-82.840233	52.941177	2.352429	-95.556523
10011	56.993393	8.274368	-85.481882	30.844872	0.476534	-98.455062
10012	25.663717	3.053435	-88.102133	8.495575	0.763359	-91.014628
10013	25	2.284587	-90.861652	25	0.05091	-99.79636
10014	10.298595	47.99065	365.992206	4.481207	21.801672	386.513388
10015	44.721409	10.404624	-76.734579	19.149561	2.312139	-87.92589
10016	17.581654	0.78125	-95.556448	3.683113	2.34375	-36.364972
10017		16.169828			7.046071	
10018		26.259947			14.58886	
10019	6.488404	3.295848	-49.204026	2.389539	0.305966	-87.195606
10020	5.540402	No surgery	NA	3.307194	No surgery	NA
10021	28.369385	1.129943	-96.017034	2.49584	0.821777	-67.074131
10022	55.75666	7.821095	-85.972806	23.881348	1.722076	-92.789034
10023	54.143002	1.040397	-98.078428	29.568995	0.206205	-99.302631
10024	9.762824	44.612526	356.963334	2.291145	7.245223	216.22717
10025		8.148653			1.346744	
10026	13.352303	10.905772	-18.322914	2.697861	0.2966	-89.006105
10027	22.813547	10.961538	-51.951628	6.140677	1.153846	-81.209792

Table 7.12: Summary of changes in IGF-1R PRE/POST xentuzumab. Post-xentuzumab changes were expressed as % baseline (pre-treatment) values. Data points were missing when no sections were cut or the biopsy or in-theatre cores did not contain any tumour areas.

	% IGF-1R+ tumour cells		
Patient (WN-01-)	Pre-treatment	Post-treatment	Change (%)
10001	100	82.068962	-17.931038
10002	93.528015	64.769974	-30.748050
10003	94.230766	91.176468	-3.241295
10004	56.81382	52.403847	-7.762148
10005	64.957268		
10006	87.86982	96.428574	9.740265
10007	54.545456		
10008	92.2089	54.871796	-40.491865
10009			
10010		3.669725	
10011		67.796608	
10012	88.157898	81.481483	-7.573246
10013	86.231888	63.661972	-26.173514
10014	89.489952	86.629745	-3.196120
10015	56.25	6.666667	-88.148147
10016	64.155525	62.5	-2.580487
10017			
10018			
10019	91.184212	97.649734	7.090615
10020		No surgery	NA
10021	94.117645	100	6.250002
10022			
10023			
10024			
10025		89.61039	
10026	79.746834	81.506851	2.207005
10027	88.073395		

Table 7.13: Summary of changes in nuclear and non-nuclear staining of IGF-1R PRE/POST xentuzumab. Post-xentuzumab changes were expressed as % baseline (pre-treatment) values. Data points were missing when no sections were cut or the biopsy or in-theatre cores did not contain any tumour areas.

	% IGF-1R+ nucleus			% IGF-1R+ non-nuclear		
Patient (WN-01-)	Pre-treatment	Post-treatment	Change (%)	Pre-treatment	Post-treatment	Change (%)
10001	97.222221	78.620689	-19.133004	100	76.551727	-23.448273
10002	88.713493	55.447941	-37.49773	92.028412	64.043587	-30.408896
10003	84.615387	89.522057	5.798791	92.307693	90.257355	-2.221199
10004	35.412666	50.48077	42.550041	51.055664	50.48077	-1.126014
10005	43.589745			57.264957		
10006	69.822487	96.428574	38.105327	81.656807	96.428574	18.090061
10007	36.363636			27.272728		
10008	86.772263	41.025642	-52.720327	90.196915	49.743591	-44.850008
10009						
10010		0.917431			3.669725	
10011		53.389832			64.406776	
10012	71.052635	70.370369	-0.960226	85.526314	77.777779	-9.059825
10013	72.463768	46.197182	-36.247888	74.63768	59.295776	-20.555172
10014	82.019577	80.300636	-2.095769	86.553322	84.335442	-2.562443
10015	44.140625	6.666667	-84.896754	53.515625	54.234906	1.344057
10016	42.891857	50	16.572243	55.407047	55	-0.734648
10017						
10018						
10019	82.412277	93.328278	13.245600	89.517548	96.891586	8.23753
10020		No surgery	NA		No surgery	NA
10021	94.117645	100	6.250002	94.117645	100	6.250002
10022						
10023						
10024						
10025		81.168831			83.116882	
10026	67.40506	69.863014	3.646542	73.417725	74.657532	1.688702
10027	80.733948			83.486237		

Table 7.14: Summary of changes in Ki67 expression PRE/POST xentuzumab. Post-xentuzumab changes were expressed as % baseline (pre-treatment) values. Data points were missing when no sections were cut or the biopsy or in-theatre cores did not contain any tumour areas.

	% Ki67+ tumour cells		
Patient (WN-01-)	Pre-treatment	Post-treatment	Change (%)
10001			
10002	2.549919	2.853693	11.91308
10003	3.370786	0.315209	-90.648798
10004	5.400465	3.073055	-43.096474
10005	3.680501		
10006	1.05129	0	
10007	2.51046		
10008	2.145352	0.678189	-68.387984
10009			
10010	8.239096	4.21549	-48.835527
10011	0.981079	1.768551	80.26591
10012	9.67742	0	-100
10013	1.981132		
10014	1.336683	2.539083	89.954013
10015	1.305658	1.282051	-1.808053
10016	1.296296	0	-100
10017			
10018		0	
10019	0.929815	0.380494	-59.078526
10020		No surgery	NA
10021	4.131054	0.226757	-94.510916
10022	2.654867	0.906817	-65.843223
10023			
10024			
10025		0.137363	
10026	4.544589	1.293413	-71.539494
10027	3.885805	6.71141	72.716078

Table 7.15: Summary of changes in AR expression PRE/POST xentuzumab. Post-xentuzumab changes were expressed as % baseline (pre-treatment) values. Data points were missing when no sections were cut or the biopsy or in-theatre cores did not contain any tumour areas.

	% AR+ tumour cells		
Patient (WN-01-)	Pre-treatment	Post-treatment	Change (%)
10001		19.992945	
10002	19.078548	15.458635	-18.973734
10003	25.500713	0	-100
10004	24.103073	19.182468	-20.414845
10005	13.701606		
10006	31.796621	18.693853	-41.208051
10007	14.069516	12.001594	-14.697890
10008	2.830548	6.245626	120.650771
10009	22.615145	6.477026	-71.359785
10010	7.201585	10.564751	46.700358
10011	5.699131	2.700026	-52.62390
10012	0.007989	0.023529	194.517461
10013		0.423359	
10014	0.087133	0.663536	661.520893
10015	0.34955		
10016		15.994685	
10017			
10018			
10019	38.968971	37.136806	-4.701599
10020		No surgery	NA
10021	28.859718		
10022	26.775024	26.365826	-1.528282
10023			
10024			
10025		26.144396	
10026	43.528023	31.524294	-27.57701
10027	21.007946	6.360641	-69.722689

Table 7.16: List of differentially expressed genes in post-xentuzumab-treated in-theatre cores vs pre-treatment diagnostic biopsies of WINGMEN patients. RNAs were extracted from pre-treatment diagnostic biopsies and post-xentuzumab-treated in-theatre cores of WINGMEN patients and sequenced. Differential gene expression was analysed using the DESeq2 pipeline, and genes with adjusted P-value < 0.05 were deemed significant.

Ensembl Gene ID	Symbol	Log2 Fold Change	Adjusted P-value
ENSG00000196436	NPIPB15	-1.92838164543723	0.015123453
ENSG00000145736	GTF2H2	-0.940042131224773	0.00478162
ENSG00000118997	DNAH7	-0.713348101975114	0.01512345
ENSG00000155530	LRGUK	-0.646761876611815	0.04429095
ENSG00000105072	C19orf44	-0.588253633415043	0.04914294
ENSG00000134146	DPH6	-0.471552420789368	0.00118246
ENSG00000256525	POLG2	-0.461150965222658	0.01352469
ENSG00000156958	GALK2	-0.409493095479024	0.02110337
ENSG00000178761	FAM219B	-0.393072257836012	0.04606730
ENSG00000121310	ECHDC2	-0.377720015449424	0.02751410
ENSG00000112855	HARS2	-0.344213603965238	0.02110337
ENSG00000085982	USP40	-0.326904910766316	0.00929466
ENSG00000130177	CDC16	-0.292578036338371	0.02214389
ENSG00000135297	MTO1	-0.233006308400987	0.03963732
ENSG00000133816	MICAL2	0.382107230824399	0.04092035
ENSG00000069849	ATP1B3	0.760891693789509	0.01035642
ENSG00000131370	SH3BP5	0.896600400600691	0.01512345
ENSG00000155926	SLA	1.08702357838197	0.045967797
ENSG00000177606	JUN	1.16375488612678	0.039637323
ENSG00000176788	BASP1	1.22413236570665	0.049207498
ENSG00000126803	HSPA2	1.24561655885371	0.008883281
ENSG00000059804	SLC2A3	1.27971389825314	0.011372202
ENSG00000155659	VSIG4	1.29693203248109	0.046067307
ENSG00000134460	IL2RA	1.31268964524038	0.026939461
ENSG00000018280	SLC11A1	1.33342833428268	0.046067307
ENSG00000106819	ASPN	1.45804456862551	0.010492244
ENSG00000187193	MT1X	1.46548428034295	0.007120063

Ensembl Gene ID	Symbol	Log2 Fold Change	Adjusted P-value
ENSG00000187479	C11orf96	1.52508000214104	0.014278185
ENSG00000171223	JUNB	1.5318020820455	0.001871275
ENSG00000121966	CXCR4	1.58923715690974	0.022038559
ENSG00000131386	GALNT15	1.59599650329068	0.049091896
ENSG00000128016	ZFP36	1.66593441950205	0.006945913
ENSG00000143333	RGS16	1.67608204305365	0.013979345
ENSG00000177575	CD163	1.68999435864094	0.006860099
ENSG00000119508	NR4A3	1.72710269844402	0.009294662
ENSG00000164107	HAND2	1.81481188410308	0.044290957
ENSG00000120129	DUSP1	1.85246941893427	0.027514102
ENSG00000188269	OR7A5	1.86485652210789	0.034488495
ENSG00000116183	PAPPA2	1.89049635428909	0.022143898
ENSG00000175426	PCSK1	1.91890763128402	0.035534555
ENSG00000123358	NR4A1	1.92650486722314	0.027514102
ENSG00000184557	SOCS3	1.98702248280297	0.006160998
ENSG00000004799	PDK4	2.04129264642391	0.005734333
ENSG00000153234	NR4A2	2.04515409868874	0.000057140
ENSG00000138435	CHRNA1	2.0856099377587	0.027514102
ENSG00000120738	EGR1	2.09698605218171	0.001700229
ENSG00000012223	LTF	2.15317383205416	0.04596779
ENSG00000054356	PTPRN	2.35309359285522	0.00884193
ENSG00000090104	RGS1	2.41027517684637	0.00218813
ENSG00000162772	ATF3	2.41591186446103	0.00003938
ENSG00000115590	IL1R2	2.46357515303435	0.000000262
ENSG00000134339	SAA2	2.48876331384217	0.03362968
ENSG00000170345	FOS	2.72328006727078	0.00098534
ENSG00000106366	SERPINE1	2.72963707248017	0.00009809
ENSG00000173432	SAA1	2.75746445269548	0.00218813
ENSG00000136244	IL6	2.77682113607595	0.0021881
ENSG00000109321	AREG	2.81323675490805	0.00157817
ENSG00000125740	FOSB	2.83700743275654	0.0033815
ENSG00000168334	XIRP1	2.95170491524297	0.0088419

Ensembl Gene ID	Symbol	Log2 Fold Change	Adjusted P-value
ENSG00000158859	ADAMTS4	3.03934312841606	0.000000714
ENSG00000129988	LBP	3.12683435825681	0.00148790

Bibliography

Abeshouse, Adam et al. (Nov. 2015). "The Molecular Taxonomy of Primary Prostate Cancer". *Cell* 163 (4), pp. 1011–1025. DOI: 10.1016/J.CELL.2015.10.025/ATTACHMENT/3A81E1EE-9EEA-4C1F-99B2-012221338A58/MMC4.XLS.

Abida, Wassim, Joshua Armenia, Anuradha Gopalan, Ryan Brennan, Michael Walsh, David Barron, Daniel Danila, Dana Rathkopf, Michael Morris, Susan Slovin, Brigit McLaughlin, Kristen Curtis, David M. Hyman, Jeremy C. Durack, Stephen B. Solomon, Maria E. Arcila, Ahmet Zehir, Aijazuddin Syed, Jianjiong Gao, Debyani Chakravarty, Hebert Alberto Vargas, Mark E. Robson, Joseph Vijai, Kenneth Offit, Mark T.A. Donoghue, Adam A. Abeshouse, Ritika Kundra, Zachary J. Heins, Alexander V. Penson, Christopher Harris, Barry S. Taylor, Marc Ladanyi, Diana Mandelker, Liying Zhang, Victor E. Reuter, Philip W. Kantoff, David B. Solit, Michael F. Berger, Charles L. Sawyers, Nikolaus Schultz, and Howard I. Scher (2017). "Prospective Genomic Profiling of Prostate Cancer Across Disease States Reveals Germline and Somatic Alterations That May Affect Clinical Decision Making". *JCO Precision Oncology* 1, pp. 1–16. DOI: 10.1200/PO.17.00029. eprint: https://doi.org/10.1200/PO.17.00029.

About prostate cancer, Prostate Cancer UK (Aug. 2023).

Acosta, Andres M., Mohamed R.H. Al Rasheed, Garth H. Rauscher, Erica Vormittag, Khin Su Mon, Asma Sharif, Andre Kajdacsy-Balla, and Gayatry Mohapatra (2018). "Tumor necrosis in radical prostatectomies with high-grade prostate cancer is associated with multiple poor prognostic features and a high prevalence of residual disease". *Human Pathology* 75, pp. 1–9. DOI: 10.1016/j.humpath.2017.11.015.

Afshar-Kharghan, Vahid (Mar. 2017). "The role of the complement system in cancer". *The Journal of Clinical Investigation* 127.3, pp. 780–789. DOI: 10.1172/JCI90962.

Agoulnik, Irina U., Ajula Vaid, III Bingman William E., Halime Erdeme, Anna Frolov, Carolyn L. Smith, Gustavo Ayala, Michael M. Ittmann, and Nancy L. Weigel (Sept. 2005). "Role of SRC-1 in the Promotion of Prostate Cancer Cell Growth and Tumor Progression". *Cancer Research* 65.17, pp. 7959–7967. DOI: 10.1158/0008-5472.CAN-04-3541. eprint: https://aacrjournals.org/cancerres/article-pdf/65/17/7959/2536897/7959-7967.pdf.

Ahdoot, Michael, Andrew R. Wilbur, Sarah E. Reese, Amir H. Lebastchi, Sherif Mehralivand, Patrick T. Gomella, Jonathan Bloom, Sandeep Gurram, Minhaj Siddiqui, Paul Pinsky, Howard Parnes, W. Marston Linehan, Maria Merino, Peter L. Choyke, Joanna H. Shih, Baris Turkbey, Bradford J. Wood, and Peter A. Pinto (2020). "MRI-Targeted, Systematic, and Combined Biopsy for Prostate Cancer Diagnosis". *New England Journal of Medicine* 382.10, pp. 917–928. DOI: 10.1056/NEJMoa1910038. eprint: https://www.nejm.org/doi/pdf/10.1056/NEJMoa1910038.

Ahmed, Hashim U, Ahmed El-Shater Bosaily, Louise C Brown, Rhian Gabe, Richard Kaplan, Mahesh K Parmar, Yolanda Collaco-Moraes, Katie Ward, Richard G Hindley, Alex Freeman, Alex P Kirkham, Robert Oldroyd, Chris Parker, and Mark Emberton (Feb. 2017). "Diagnostic accuracy of multi-parametric MRI and TRUS biopsy in prostate cancer (PROMIS): a paired validating confirmatory study". *The Lancet* 389 (10071). doi: 10.1016/S0140-6736(16)32401-1, pp. 815–822. DOI: 10.1016/S0140-6736(16)32401-1.

Aiken, Robert, Magnus Axelson, Johan Harmenberg, Maria Klockare, Olle Larsson, Cecilia Wassberg, Robert Aiken, Magnus Axelson, Johan Harmenberg, Maria Klockare, Olle Larsson, and Cecilia Wassberg (Sept. 2017). "Phase I clinical trial of AXL1717 for treatment of relapsed malignant astrocytomas: analysis of dose and response". *Oncotarget* 8 (46), pp. 81501–81510. DOI: 10.18632/ONCOTARGET.20662.

Ajona, Daniel, Sergio Ortiz-Espinosa, Teresa Lozano, Francisco Exposito, Alfonso Calvo, Karmele Valencia, Miriam Redrado, Ana Remírez, Fernando Lecanda, Diego Alignani, Juan J. Lasarte, Irati Macaya, Yaiza Senent, Cristina Bértolo, Cristina Sainz, Ignacio Gil-Bazo, Iñaki Eguren-Santamaría, Jose M. Lopez-Picazo, Alvaro Gonzalez, Jose L. Perez-Gracia, Carlos E. de Andrea, Silvestre Vicent, Miguel F. Sanmamed, Luis M. Montuenga, and Ruben Pio (Jan. 2020). "Short-term starvation reduces IGF-1 levels to sensitize lung tumors to PD-1 immune checkpoint blockade". *Nature Cancer 2020 1:1* 1 (1), pp. 75–85. DOI: 10.1038/s43018-019-0007-9.

Akkaya, Munir, Kihyuck Kwak, and Susan K Pierce (2020). "B cell memory: building two walls of protection against pathogens". *Nature Reviews Immunology* 20 (4), pp. 229–238. DOI: 10.1038/s41577-019-0244-2.

Aleksic, Tamara, Meenali M. Chitnis, Olga V. Perestenko, Shan Gao, Peter H. Thomas, Gareth D. Turner, Andrew S. Protheroe, Mark Howarth, and Valentine M. Macaulay (Aug. 2010). "Type 1 Insulin-like Growth Factor Receptor Translocates to the Nucleus of Human Tumor Cells". *Cancer Research* 70.16, pp. 6412–6419. DOI: 10.1158/0008-5472.CAN-10-0052. eprint: https://aacrjournals.org/cancerres/article-pdf/70/16/6412/2635760/6412.pdf.

Aleksic, Tamara, Nicki Gray, Xiaoning Wu, Guillaume Rieunier, Eliot Osher, Jack Mills, Clare Verrill, Richard J. Bryant, Cheng Han, Kathryn Hutchinson, Adam G. Lambert, Rajeev Kumar, Freddie C. Hamdy, Ulrike Weyer-Czernilofsky, Michael P. Sanderson, Thomas Bogenrieder, Stephen Taylor, and Valentine M. Macaulay (July 2018). "Nuclear IGF1R Interacts with Regulatory Regions of Chromatin to Promote RNA Polymerase II Recruitment and Gene Expression Associated with Advanced Tumor Stage". *Cancer Research* 78.13, pp. 3497–3509. DOI: 10.1158/0008-5472.CAN-17-3498. eprint: https://aacrjournals.org/cancerres/article-pdf/78/13/3497/2766979/3497.pdf.

Aleksic, Tamara, Clare Verrill, Richard J Bryant, Cheng Han, Andrew Ross Worrall, Laurent Brureau, Stephane Larré, Geoff S Higgins, Fahad Fazal, Ahmad Sabbagh, Syed Haider, Francesca M Buffa, David Cole, and Valentine M Macaulay (2017). "IGF-1R associates with adverse outcomes after radical radiotherapy for prostate cancer". *British Journal of Cancer* 117 (11), pp. 1600–1606. DOI: 10.1038/bjc.2017.337.

Alessi, Dario R., Stephen R. James, C.Peter Downes, Andrew B. Holmes, Piers R.J. Gaffney, Colin B. Reese, and Philip Cohen (1997). "Characterization of a 3-phosphoinositide-dependent protein kinase which phosphorylates and activates protein kinase Ba". *Current Biology* 7.4, pp. 261–269. DOI: https://doi.org/10.1016/S0960-9822(06)00122-9.

Alfaro-Arnedo, Elvira, Iciar P. Lopez, Sergio Pineiro-Hermida, Marta Canalejo, Carolina Gotera, Jesus Javier Sola, Alejandra Roncero, German Peces-Barba, Carlos Ruiz-Martinez, and Jose G. Pichel (June 2022). "IGF1R acts as a cancer-promoting factor in the tumor microenvironment facilitating lung metastasis implantation and progression". *Oncogene* 41, pp. 3625–3639. DOI: 10.1038/s41388-022-02376-w.

Allard, John B. and Cunming Duan (2018). "IGF-Binding Proteins: Why Do They Exist and Why Are There So Many?" *Frontiers in Endocrinology* 9. DOI: 10.3389/fendo.2018.00117.

Allen, Breanna M, Kamir J Hiam, Cassandra E Burnett, Anthony Venida, Rachel DeBarge, Iliana Tenvooren, Diana M Marquez, Nam Woo Cho, Yaron Carmi, and Matthew H Spitzer (2020). "Systemic dysfunction and plasticity of the immune macroenvironment in cancer models". *Nature Medicine* 26 (7), pp. 1125–1134. DOI: 10.1038/s41591-020-0892-6.

Anbarasan, Thineskrishna, Mutie Raslan, Kanchan Ghosh, Philip Macklin, Claudia Mercader, Tom Leslie, Freddie C. Hamdy, Richard Colling, Lisa Browning, Ian Roberts, Clare Verrill, Richard J. Bryant, Francisco Lopez, and Alastair D. Lamb (2024). "Prostate cancer detection after atypical small acinar proliferation (ASAP): A 10-year single-centre cohort". *BJUI Compass* 5.9, pp. 834–836. DOI: https://doi.org/10.1002/bco2.407. eprint: https://bjui-journals.onlinelibrary.wiley.com/doi/pdf/10.1002/bco2.407.

Andreoiu, Matei and Liang Cheng (2010). "Multifocal prostate cancer: biologic, prognostic, and therapeutic implications". *Human Pathology* 41.6, pp. 781–793. DOI: https://doi.org/10.1016/j.humpath.2010.02.011.

Andrews, Simon, Felix Krueger, Anne Segonds-Pichon, Laura Biggins, Christel Krueger, and Steven Wingett (Jan. 2012). *FastQC*. Babraham Institute.

Andriole, Gerald L., E. David Crawford, Robert L. Grubb, Saundra S. Buys, David Chia, Timothy R. Church, Mona N. Fouad, Edward P. Gelmann, Paul A. Kvale, Douglas J. Reding, Joel L. Weissfeld, Lance A. Yokochi, Barbara O'Brien, Jonathan D. Clapp, Joshua M. Rathmell, Thomas L. Riley, Richard B. Hayes, Barnett S. Kramer, Grant Izmirlian, Anthony B. Miller, Paul F. Pinsky, Philip C. Prorok, John K. Gohagan, and Christine D. Berg (2009). "Mortality Results from a Randomized Prostate-Cancer Screening Trial". *New England Journal of Medicine* 360.13, pp. 1310–1319. DOI: 10.1056/NEJMoa0810696. eprint: https://www.nejm.org/doi/pdf/10.1056/NEJMoa0810696.

Angelosanto, Jill M., Shawn D. Blackburn, Alison Crawford, and E. John Wherry (2012). "Progressive Loss of Memory T Cell Potential and Commitment to Exhaustion during Chronic Viral Infection". *Journal of Virology* 86.15, pp. 8161–8170. DOI: 10.1128/jvi.00889-12. eprint: https://journals.asm.org/doi/pdf/10.1128/jvi.00889-12.

Antonarakis, E S, A J Armstrong, S M Dehm, and J Luo (2016). "Androgen receptor variant-driven prostate cancer: clinical implications and therapeutic targeting". *Prostate Cancer and Prostatic Diseases* 19 (3), pp. 231–241. DOI: 10.1038/pcan.2016.17.

Antonarakis, Emmanuel S., Josep M. Piulats, Marine Gross-Goupil, Jeffrey Goh, Kristiina Ojamaa, Christopher J. Hoimes, Ulka Vaishampayan, Ranaan Berger, Ahmet Sezer, Tuomo Alanko, Ronald de Wit, Chunde Li, Aurelius Omlin, Giuseppe Procopio, Satoshi Fukasawa, Ken-ichi Tabata, Se Hoon Park, Susan Feyerabend, Charles G. Drake, Haiyan Wu, Ping Qiu, Jeri Kim, Christian Poehlein, and Johann Sebastian de Bono (2020). "Pembrolizumab for Treatment-Refractory Metastatic Castration-Resistant Prostate Cancer: Multicohort, Open-Label Phase II KEYNOTE-199 Study". *Journal of Clinical Oncology* 38.5. PMID: 31774688, pp. 395–405. DOI: 10.1200/JCO.19.01638. eprint: https://doi.org/10.1200/JCO.19.01638.

Aristorena, Mikel, Eunate Gallardo-Vara, Matej Vicen, Mateo De Las Casas-Engel, Luisa Ojeda-Fernandez, Concepcion Nieto, Francisco J. Blanco, Ana C. Valbuena-Diez, Luisa M. Botella, Petr Nachtigal, Angel L. Corbi, Maria Colmenares, and Carmelo Bernabeu (June 2019). "MMP-12, Secreted by Pro-Inflammatory Macrophages, Targets Endoglin in Human Macrophages and Endothelial Cells". *International Journal of Molecular Sciences 2019, Vol. 20, Page 3107* 20 (12), p. 3107. DOI: 10.3390/IJMS20123107.

Armstrong, Andrew J., Susan Halabi, Jun Luo, David M. Nanus, Paraskevi Giannakakou, Russell Z. Szmulewitz, Daniel C. Danila, Patrick Healy, Monika Anand, Colin J. Rothwell, Julia Rasmussen, Blair Thornburg, William R. Berry, Rhonda S. Wilder, Changxue Lu, Yan Chen, John L. Silberstein, Gabor Kemeny, Giuseppe Galletti, Jason A. Somarelli, Santosh Gupta, Simon G. Gregory, Howard I. Scher, Ryan Dittamore, Scott T. Tagawa, Emmanuel S. Antonarakis, and Daniel J. George (2019). "Prospective Multicenter Validation of Androgen Receptor Splice Variant 7 and Hormone Therapy Resistance in High-Risk Castration-Resistant Prostate Cancer: The PROPHECY Study". *Journal of Clinical Oncology* 37.13. PMID: 30865549, pp. 1120–1129. DOI: 10.1200/JCO.18.01731. eprint: https://doi.org/10.1200/JCO.18.01731.

Aroldi, Francesca and Simon R Lord (2020). "Window of opportunity clinical trial designs to study cancer metabolism". *British Journal of Cancer* 122 (1), pp. 45–51. DOI: 10.1038/s41416-019-0621-4.

Arranz, Alicia, Christina Doxaki, Eleni Vergadi, Yeny Martinez de la Torre, Katerina Vaporidi, Eleni D. Lagoudaki, Eleftheria Ieronymaki, Ariadne Androulidaki, Maria Venihaki, Andrew N. Margioris, Efstathios N. Stathopoulos, Philip N. Tsichlis, and Christos Tsatsanis (2012). "Akt1 and Akt2 protein kinases differentially contribute to macrophage polarization". *Proceedings of the National Academy of Sciences* 109.24, pp. 9517–9522. DOI: 10.1073/pnas.1119038109. eprint: https://www.pnas.org/doi/pdf/10.1073/pnas.1119038109.

Asif, Aqua, Arjun Nathan, Alexander Ng, Pramit Khetrapal, Vinson Wai-Shun Chan, Francesco Giganti, Clare Allen, Alex Freeman, Shonit Punwani, Paula Lorgelly, Caroline S Clarke, Chris Brew-Graves, Nicola Muirhead, Mark Emberton, Ridhi Agarwal, Yemisi Takwoingi, Jonathan J Deeks, Caroline M Moore, and Veeru Kasivisvanathan (2023). "Comparing biparametric to multiparametric MRI in the diagnosis of clinically significant prostate cancer in biopsy-naive men (PRIME): a prospective, international, multicentre, non-inferiority within-patient, diagnostic yield trial protocol". *BMJ Open* 13.4. Ed. by, John Wilkinson, Marimo Rossiter, Réka Novotta, Philip Ryan, Alex Kirkham, Louise Dickinson, Tushar Narain, Hazel McBain, Antonette Andrews, Daniel Margolis, Valeria Panebianco, Antti Rannikko, Peter Albertsen, Lance Mynderse, Adam Froemming, Naoki Takahasi, Tristan Barrett, Raphaële Renard-Penna, Vibeke Løgager, Lars Boesen, Sangeet Ghai, Lars Budäus, Enrique Gómez Gómez, Jeremy Grummet, Tho Pham, Aiman Haider, Jing Yi Jessica Weng, Anders Bjartell, Wim Witjes, Christien Caris, and Joke Van Egmond. DOI: 10.1136/bmjopen-2022-070280. eprint: https://bmjopen.bmj.com/content/13/4/e070280.full.pdf.

Atri, Chiraz, Fatma Z. Guerfali, and Dhafer Laouini (2018). "Role of Human Macrophage Polarization in Inflammation during Infectious Diseases". *International Journal of Molecular Sciences* 19.6. DOI: 10.3390/ijms19061801.

Atsaves, Vasileios, Vasiliki Leventaki, George Z. Rassidakis, and Francois X. Claret (2019). "AP-1 Transcription Factors as Regulators of Immune Responses in Cancer". *Cancers* 11.7. DOI: 10.3390/cancers11071037.

Attard, Gerhardt et al. (Jan. 2022). "Abiraterone acetate and prednisolone with or without enzalutamide for high-risk non-metastatic prostate cancer: a meta-analysis of primary results from two randomised controlled phase 3 trials of the STAMPEDE platform protocol". *The Lancet* 399 (10323). doi: 10.1016/S0140-6736(21)02437-5, pp. 447–460. DOI: 10.1016/S0140-6736(21)02437-5.

Auernhammer, C J, H Feldmeier, R Nass, K Pachmann, and C J Strasburger (Dec. 1996). "Insulin-like growth factor I is an independent coregulatory modulator of natural killer

(NK) cell activity". *Endocrinology* 137.12, pp. 5332–5336. DOI: 10.1210/endo.137.12.8940354. eprint: https://academic.oup.com/endo/article-pdf/137/12/5332/10639298/endo5332.pdf.

Averous, J, B D Fonseca, and C G Proud (2008). "Regulation of cyclin D1 expression by mTORC1 signaling requires eukaryotic initiation factor 4E-binding protein 1". *Oncogene* 27 (8), pp. 1106–1113. DOI: 10.1038/sj.onc.1210715.

Bach, L A (2018). "40 YEARS OF IGF1: IGF-binding proteins". *Journal of Molecular Endocrinology* 61.1, pp. 11–28. DOI: 10.1530/JME-17-0254.

Bachelder, Robin E., Sang-Oh Yoon, Clara Franci, Antonio García de Herreros, and Arthur M. Mercurio (Jan. 2005). "Glycogen synthase kinase-3 is an endogenous inhibitor of Snail transcription : implications for the epithelial–mesenchymal transition ". *Journal of Cell Biology* 168.1, pp. 29–33. DOI: 10.1083/jcb.200409067. eprint: https://rupress.org/jcb/article-pdf/168/1/29/1532459/jcb168129.pdf.

Balk, Steven P., Yoo-Joung Ko, and Glenn J. Bubley (2003). "Biology of Prostate-Specific Antigen". *Journal of Clinical Oncology* 21.2. PMID: 12525533, pp. 383–391. DOI: 10.1200/JCO.2003.02.083. eprint: https://doi.org/10.1200/JCO.2003.02.083.

Barbieri, Christopher E, Sylvan C Baca, Michael S Lawrence, Francesca Demichelis, Mirjam Blattner, Jean-Philippe Theurillat, Thomas A White, Petar Stojanov, Eliezer Van Allen, Nicolas Stransky, Elizabeth Nickerson, Sung-Suk Chae, Gunther Boysen, Daniel Auclair, Robert C Onofrio, Kyung Park, Naoki Kitabayashi, Theresa Y MacDonald, Karen Sheikh, Terry Vuong, Candace Guiducci, Kristian Cibulskis, Andrey Sivachenko, Scott L Carter, Gordon Saksena, Douglas Voet, Wasay M Hussain, Alex H Ramos, Wendy Winckler, Michelle C Redman, Kristin Ardlie, Ashutosh K Tewari, Juan Miguel Mosquera, Niels Rupp, Peter J Wild, Holger Moch, Colm Morrissey, Peter S Nelson, Philip W Kantoff, Stacey B Gabriel, Todd R Golub, Matthew Meyerson, Eric S Lander, Gad Getz, Mark A Rubin, and Levi A Garraway (2012). "Exome sequencing identifies recurrent SPOP, FOXA1 and MED12 mutations in prostate cancer". *Nature Genetics* 44 (6), pp. 685–689. DOI: 10.1038/ng.2279.

Barrett, James P., Aedín M. Minogue, Aidan Falvey, and Marina A. Lynch (2015). "Involvement of IGF-1 and Akt in M1/M2 activation state in bone marrow-derived macrophages". *Experimental Cell Research* 335.2. Cell and Molecular Biology of the Synapse, pp. 258–268. DOI: https://doi.org/10.1016/j.yexcr.2015.05.015.

Barwick, B G, M Abramovitz, M Kodani, C S Moreno, R Nam, W Tang, M Bouzyk, A Seth, and B Leyland-Jones (2010). "Prostate cancer genes associated with TMPRSS2–ERG gene fusion and prognostic of biochemical recurrence in multiple cohorts". *British Journal of Cancer* 102 (3), pp. 570–576. DOI: 10.1038/sj.bjc.6605519.

Baserga, Renato, Francesca Peruzzi, and Krysztof Reiss (2003). "The IGF-1 receptor in cancer biology". *International Journal of Cancer* 107.6, pp. 873–877. DOI: https://doi.org/10.1002/ijc.11487. eprint: https://onlinelibrary.wiley.com/doi/pdf/10.1002/ijc.11487.

Basu, Roshni, Benjamin M Whitlock, Julien Husson, Audrey Le Floc'h, Weiyang Jin, Alon Oyler-Yaniv, Farokh Dotiwala, Gregory Giannone, Claire Hivroz, Nicolas Biais, Judy Lieberman, Lance C Kam, and Morgan Huse (Mar. 2016). "Cytotoxic T Cells Use Mechanical Force to Potentiate Target Cell Killing". *Cell* 165 (1). doi: 10.1016/j.cell.2016.01.021, pp. 100–110. DOI: 10.1016/j.cell.2016.01.021.

Batista, Facundo D and Naomi E Harwood (2009). "The who, how and where of antigen presentation to B cells". *Nature Reviews Immunology* 9 (1), pp. 15–27. DOI: 10.1038/nri2454.

Baudler, Stephanie, Julia Baumgartl, Brigitte Hampel, Thorsten Buch, Ari Waisman, Clifford M. Snapper, Wilhelm Krone, and Jens C. Bruning (May 2005). "Insulin-Like Growth Factor-1 Controls Type 2 T Cell-Independent B Cell Response". *The Journal of Immunology* 174.9, pp. 5516–5525. DOI: 10.4049/jimmunol.174.9.5516. eprint: https://journals.aai.org/jimmunol/article-pdf/174/9/5516/1201039/5516.pdf.

Bauer, Stefan, Veronika Groh, Jun Wu, Alexander Steinle, Joseph H. Phillips, Lewis L. Lanier, and Thomas Spies (1999). "Activation of NK Cells and T Cells by NKG2D, a Receptor for Stress-Inducible MICA". *Science* 285.5428, pp. 727–729. DOI: 10.1126/science.285.5428.727. eprint: https://www.science.org/doi/pdf/10.1126/science.285.5428.727.

Bawden, Emma G., Teagan Wagner, Jan Schroder, Maike Effern, Daniel Hinze, Lewis Newland, Grace H. Attrill, Ariane R. Lee, Sven Engel, David Freestone, Marcela de Lima Moreira, Elise Gressier, Nathan McBain, Annabell Bachem, Ashraful Haque, Ruining Dong, Angela L. Ferguson, Jarem J. Edwards, Peter M. Ferguson, Richard A. Scolyer, James S. Wilmott, Christopher M. Jewell, Andrew G. Brooks, David E. Gyorki, Umaimainthan Palendira, Sammy Bedoui, Jason Waithman, Katharina Hochheiser, Michael Holzel, and Thomas Gebhardt (2024). "CD4+T cell immunity against cutaneous melanoma encompasses multifaceted MHC II-dependent responses". *Science Immunology* 9.91, eadi9517. DOI: 10.1126/sciimmunol.adi9517. eprint: https://www.science.org/doi/pdf/10.1126/sciimmunol.adi9517.

Baxter, Robert C (Apr. 1993). "Circulating binding proteins for the insulinlike growth factors". *Trends in Endocrinology and Metabolism* 4 (3), pp. 91–96. DOI: 10.1016/1043-2760(93)90085-S.

– (Mar. 2023). "Signaling Pathways of the Insulin-like Growth Factor Binding Proteins". *Endocrine Reviews* 44.5, pp. 753–778. DOI: 10.1210/endrev/bnad008. eprint: https://academic.oup.com/edrv/article-pdf/44/5/753/51558873/bnad008.pdf.

– (2014). "IGF binding proteins in cancer: mechanistic and clinical insights". *Nature Reviews Cancer* 14.5, pp. 329–341. DOI: 10.1038/nrc3720.

Beach, Callum, David MacLean, Dominika Majorova, Stavros Melemenidis, Dhanya K. Nambiar, Ryan K. Kim, Gabriel N. Valbuena, Silvia Guglietta, Carsten Krieg, Mahnaz Darvish-Damavandi, Tatsuya Suwa, Alistair Easton, Lily V.S. Hillson, Ashley K. McCulloch, Ross K. McMahon, Kathryn Pennel, Joanne Edwards, Sean M. O'Cathail, Campbell S. Roxburgh, Enric Domingo, Eui Jung Moon, Dadi Jiang, Yanyan Jiang, Qingyang Zhang, Albert C. Koong, Trent M. Woodruff, Edward E. Graves, Tim Maughan, Simon J.A. Buczacki, Manuel Stucki, Quynh-Thu Le, Simon J. Leedham, Amato J. Giaccia, and Monica M. Olcina (Dec. 2023). "Improving radiotherapy in immunosuppressive microenvironments by targeting complement receptor C5aR1". *The Journal of Clinical Investigation* 133.23. DOI: 10.1172/JCI168277.

Beer, Tomasz M., Eugene D. Kwon, Charles G. Drake, Karim Fizazi, Christopher Logothetis, Gwenaelle Gravis, Vinod Ganju, Jonathan Polikoff, Fred Saad, Piotr Humanski, Josep M. Piulats, Pablo Gonzalez Mella, Siobhan S. Ng, Dirk Jaeger, Francis X. Parnis, Fabio A. Franke, Javier Puente, Roman Carvajal, Lisa Sengelov, M. Brent McHenry, Arvind Varma, Alfonsus J. van den Eertwegh, and Winald Gerritsen (2017). "Randomized, Double-Blind, Phase III Trial of Ipilimumab Versus Placebo in Asymptomatic or Minimally Symptomatic Patients With Metastatic Chemotherapy-Naive Castration-Resistant Prostate Cancer". *Journal of Clinical Oncology* 35.1. PMID: 28034081, pp. 40–47. DOI: 10.1200/JCO.2016.69.1584. eprint: https://doi.org/10.1200/JCO.2016.69.1584.

Belarif, Lyssia, Caroline Mary, Lola Jacquemont, Hoa Le Mai, Richard Danger, Jeremy Hervouet, David Minault, Virginie Thepenier, Veronique Nerriere-Daguin, Elisabeth Nguyen, Sabrina Pengam, Eric Largy, Arnaud Delobel, Bernard Martinet, Stephanie Le Bas-Bernardet, Sophie Brouard, Jean-Paul Soulillou, Nicolas Degauque, Gilles Blancho, Bernard Vanhove, and Nicolas Poirier (2018). "IL-7 receptor blockade blunts antigen-specific memory T cell responses and chronic inflammation in primates". *Nature Communications* 9 (1), p. 4483. DOI: 10.1038/s41467-018-06804-y.

Belfiore, Antonino, Roberta Malaguarnera, Veronica Vella, Michael C Lawrence, Laura Sciacca, Francesco Frasca, Andrea Morrione, and Riccardo Vigneri (June 2017). "Insulin Receptor Isoforms in Physiology and Disease: An Updated View". *Endocrine Reviews* 38.5, pp. 379–431. DOI: 10.1210/er.2017-00073.

Belfiore, Antonio (2007). "The Role of Insulin Receptor Isoforms and Hybrid Insulin/IGF-I Receptors in Human Cancer". *Current Pharmaceutical Design* 13.7, pp. 671–686. DOI: 10.2174/138161207780249173.

Beltran, Pedro J., Young-Ah Chung, Gordon Moody, Petia Mitchell, Elaina Cajulis, Steven Vonderfecht, Richard Kendall, Robert Radinsky, and Frank J. Calzone (2011). "Efficacy of Ganitumab (AMG 479), Alone and in Combination with Rapamycin, in Ewing's and Osteogenic Sarcoma Models". *Journal of Pharmacology and Experimental Therapeutics* 337.3, pp. 644–654. DOI: 10.1124/jpet.110.178400. eprint: https://jpet.aspetjournals.org/content/337/3/644.full.pdf.

Beltran, Pedro J., Petia Mitchell, Young-A Chung, Elaina Cajulis, John Lu, Brian Belmontes, Joanne Ho, Mei Mei Tsai, Min Zhu, Steven Vonderfecht, Renato Baserga, Richard Kendall, Robert Radinsky, and Frank J. Calzone (May 2009). "AMG 479, a fully human anti–insulin-like growth factor receptor type I monoclonal antibody, inhibits the growth and survival of pancreatic carcinoma cells". *Molecular Cancer Therapeutics* 8.5, pp. 1095–1105. DOI: 10.1158/1535-7163.MCT-08-1171. eprint: https://aacrjournals.org/mct/article-pdf/8/5/1095/1883655/1095.pdf.

Beretta, Giovanni Luca and Nadia Zaffaroni (2022). "Necroptosis and Prostate Cancer: Molecular Mechanisms and Therapeutic Potential". *Cells* 11.7. DOI: 10.3390/cells11071221.

Bergengren, Oskar, Kelly R. Pekala, Konstantina Matsoukas, Jonathan Fainberg, Sean F. Mungovan, Ola Bratt, Freddie Bray, Otis Brawley, Amy N. Luckenbaugh, Lorelei Mucci, Todd M. Morgan, and Sigrid V. Carlsson (2023). "2022 Update on Prostate Cancer Epidemiology and Risk Factors—A Systematic Review". *European Urology* 84.2, pp. 191–206. DOI: https://doi.org/10.1016/j.eururo.2023.04.021.

Berger, Michael F, Michael S Lawrence, Francesca Demichelis, Yotam Drier, Kristian Cibulskis, Andrey Y Sivachenko, Andrea Sboner, Raquel Esgueva, Dorothee Pflueger, Carrie Sougnez, Robert Onofrio, Scott L Carter, Kyung Park, Lukas Habegger, Lauren Ambrogio, Timothy Fennell, Melissa Parkin, Gordon Saksena, Douglas Voet, Alex H Ramos, Trevor J Pugh, Jane Wilkinson, Sheila Fisher, Wendy Winckler, Scott Mahan, Kristin Ardlie, Jennifer Baldwin, Jonathan W Simons, Naoki Kitabayashi, Theresa Y MacDonald, Philip W Kantoff, Lynda Chin, Stacey B Gabriel, Mark B Gerstein, Todd R Golub, Matthew Meyerson, Ashutosh Tewari, Eric S Lander, Gad Getz, Mark A Rubin, and Levi A Garraway (2011). "The genomic complexity of primary human prostate cancer". *Nature* 470 (7333), pp. 214–220. DOI: 10.1038/nature09744.

Berghe, Tom Vanden, Andreas Linkermann, Sandrine Jouan-Lanhouet, Henning Walczak, and Peter Vandenabeele (Jan. 2014). "Regulated necrosis: the expanding network of

non-apoptotic cell death pathways". *Nature Reviews Molecular Cell Biology 2014 15:2* 15 (2), pp. 135–147. DOI: 10.1038/nrm3737.

Bergqvist, Michael, Georg Holgersson, Igor Bondarenko, Elena Grechanaya, Alexey Maximovich, Gyorgy Andor, Maria Klockare, Marcus Thureson, Markus Jerling, and Johan Harmenberg (Mar. 2017). "Phase II randomized study of the IGF-1R pathway modulator AXL1717 compared to docetaxel in patients with previously treated, locally advanced or metastatic non-small cell lung cancer". *Acta Oncologica* 56 (3), pp. 441–447. DOI: 10.1080/0284186X.2016.1253866.

Berney, D M, A Gopalan, S Kudahetti, G Fisher, L Ambroisine, C S Foster, V Reuter, J Eastham, H Moller, M W Kattan, W Gerald, C Cooper, P Scardino, J Cuzick, and for The Trans-Atlantic Prostate Group (2009). "Ki-67 and outcome in clinically localised prostate cancer: analysis of conservatively treated prostate cancer patients from the Trans-Atlantic Prostate Group study". *British Journal of Cancer* 100 (6), pp. 888–893. DOI: 10.1038/sj.bjc.6604951.

Bettencourt, Ian A. and Jonathan D. Powell (Feb. 2017). "Targeting Metabolism as a Novel Therapeutic Approach to Autoimmunity, Inflammation, and Transplantation". *The Journal of Immunology* 198.3, pp. 999–1005. DOI: 10.4049/jimmunol.1601318. eprint: https://journals.aai.org/jimmunol/article-pdf/198/3/999/1428586/1601318.pdf.

Bhat, Purnima, Graham Leggatt, Nigel Waterhouse, and Ian H Frazer (2017). "Interferon-gamma derived from cytotoxic lymphocytes directly enhances their motility and cytotoxicity". *Cell Death and Disease* 8 (6), e2836–e2836. DOI: 10.1038/cddis.2017.67.

Biasci, Daniele, Martin Smoragiewicz, Claire M. Connell, Zhikai Wang, Ya Gao, James E. D. Thaventhiran, Bristi Basu, Lukasz Magiera, T. Isaac Johnson, Lisa Bax, Aarthi Gopinathan, Christopher Isherwood, Ferdia A. Gallagher, Maria Pawula, Irena Hudecova, Davina Gale, Nitzan Rosenfeld, Petros Barmpounakis, Elizabeta Cristina Popa, Rebecca Brais, Edmund Godfrey, Fraz Mir, Frances M. Richards, Douglas T. Fearon, Tobias Janowitz, and Duncan I. Jodrell (2020). "CXCR4 inhibition in human pancreatic and colorectal cancers induces an integrated immune response". *Proceedings of the National Academy of Sciences* 117.46, pp. 28960–28970. DOI: 10.1073/pnas.2013644117. eprint: https://www.pnas.org/doi/pdf/10.1073/pnas.2013644117.

Bid, Hemant K., Jun Zhan, Doris A. Phelps, Raushan T. Kurmasheva, and Peter J. Houghton (Mar. 2012). "Potent Inhibition of Angiogenesis by the IGF-1 Receptor-Targeting Antibody SCH717454 Is Reversed by IGF-2". *Molecular Cancer Therapeutics* 11.3, pp. 649–659. DOI: 10.1158/1535-7163.MCT-11-0575. eprint: https://aacrjournals.org/mct/article-pdf/11/3/649/2322815/649.pdf.

Bilbao, Daniel, Luisa Luciani, Bjarki Johannesson, Agnieszka Piszczek, and Nadia Rosenthal (Nov. 2014). "Insulin-like growth factor-1 stimulates regulatory T cells and suppresses autoimmune disease". *EMBO Molecular Medicine* 6 (11), pp. 1423–1435. DOI: 10.15252/EMMM.201303376/SUPPL_FILE/EMMM201303376.REVIEWER_COMMENTS.PDF.

Bill-Axelson, Anna, Lars Holmberg, Hans Garmo, Kimmo Taari, Christer Busch, Stig Nordling, Michael Häggman, Swen-Olof Andersson, Ove Andrén, Gunnar Steineck, Hans-Olov Adami, and Jan-Erik Johansson (2018). "Radical Prostatectomy or Watchful Waiting in Prostate Cancer — 29-Year Follow-up". *New England Journal of Medicine* 379.24, pp. 2319–2329. DOI: 10.1056/NEJMoa1807801. eprint: https://www.nejm.org/doi/pdf/10.1056/NEJMoa1807801.

Bisikirska, Brygida, John Colgan, Jeremy Luban, Jeffrey A. Bluestone, and Kevan C. Herold (Oct. 2005). "TCR stimulation with modified anti-CD3 mAb expands CD8+ T cell

population and induces CD8+CD25+ Tregs". *The Journal of Clinical Investigation* 115.10, pp. 2904–2913. DOI: 10.1172/JCI23961.

Blank, Christian U, W Nicholas Haining, Werner Held, Patrick G Hogan, Axel Kallies, Enrico Lugli, Rachel C Lynn, Mary Philip, Anjana Rao, Nicholas P Restifo, Andrea Schietinger, Ton N Schumacher, Pamela L Schwartzberg, Arlene H Sharpe, Daniel E Speiser, E John Wherry, Benjamin A Youngblood, and Dietmar Zehn (2019). "Defining 'T cell exhaustion'". *Nature Reviews Immunology* 19 (11), pp. 665–674. DOI: 10.1038/s41577-019-0221-9.

Bogdan, Christian, Martin Rollinghoff, and Andreas Diefenbach (2000). "The role of nitric oxide in innate immunity". *Immunological Reviews* 173.1, pp. 17–26. DOI: 10.1034/j.1600-065X.2000.917307.x.

Boniakowski, Anna E., Andrew S. Kimball, Amrita Joshi, Matt Schaller, Frank M. Davis, Aaron denDekker, Andrea T Obi, Bethany B. Moore, Steve L. Kunkel, and Katherine A. Gallagher (2018). "Murine macrophage chemokine receptor CCR2 plays a crucial role in macrophage recruitment and regulated inflammation in wound healing". *European Journal of Immunology* 48.9, pp. 1445–1455. DOI: https://doi.org/10.1002/eji.201747400. eprint: https://onlinelibrary.wiley.com/doi/pdf/10.1002/eji.201747400.

Borst, Jannie, Tomasz Ahrends, Nikolina Babala, Cornelis J. M. Melief, and Wolfgang Kastenmuller (2018). "CD4+ T cell help in cancer immunology and immunotherapy". *Nature Reviews Immunology* 18.10, pp. 635–647. DOI: 10.1038/s41577-018-0044-0.

Bossi, G. and G. M. Griffiths (1999). "Degranulation plays an essential part in regulating cell surface expression of Fas ligand in T cells and natural killer cells". *Nature Medicine* 5.1, pp. 90–96. DOI: 10.1038/4779.

Boutros, Paul C, Michael Fraser, Nicholas J Harding, Richard de Borja, Dominique Trudel, Emilie Lalonde, Alice Meng, Pablo H Hennings-Yeomans, Andrew McPherson, Veronica Y Sabelnykova, Amin Zia, Natalie S Fox, Julie Livingstone, Yu-Jia Shiah, Jianxin Wang, Timothy A Beck, Cherry L Have, Taryne Chong, Michelle Sam, Jeremy Johns, Lee Timms, Nicholas Buchner, Ada Wong, John D Watson, Trent T Simmons, Christine P'ng, Gaetano Zafarana, Francis Nguyen, Xuemei Luo, Kenneth C Chu, Stephenie D Prokopec, Jenna Sykes, Alan Dal Pra, Alejandro Berlin, Andrew Brown, Michelle A Chan-Seng-Yue, Fouad Yousif, Robert E Denroche, Lauren C Chong, Gregory M Chen, Esther Jung, Clement Fung, Maud H W Starmans, Hanbo Chen, Shaylan K Govind, James Hawley, Alister D'Costa, Melania Pintilie, Daryl Waggott, Faraz Hach, Philippe Lambin, Lakshmi B Muthuswamy, Colin Cooper, Rosalind Eeles, David Neal, Bernard Tetu, Cenk Sahinalp, Lincoln D Stein, Neil Fleshner, Sohrab P Shah, Colin C Collins, Thomas J Hudson, John D McPherson, Theodorus van der Kwast, and Robert G Bristow (2015). "Spatial genomic heterogeneity within localized, multifocal prostate cancer". *Nature Genetics* 47 (7), pp. 736–745. DOI: 10.1038/ng.3315.

Bowers, Laura W., Emily L. Rossi, Ciara H. O'Flanagan, Linda A. deGraffenried, and Stephen D. Hursting (2015). "The Role of the Insulin/IGF System in Cancer: Lessons Learned from Clinical Trials and the Energy Balance-Cancer Link". *Frontiers in Endocrinology* 6. DOI: 10.3389/fendo.2015.00077.

Boyton, Rosemary J and Daniel M Altmann (Nov. 2002). "Is selection for TCR affinity a factor in cytokine polarization?" *Trends in Immunology* 23 (11). doi: 10.1016/S1471-4906(02)02319-0, pp. 526–529. DOI: 10.1016/S1471-4906(02)02319-0.

Bray, Freddie, Mathieu Laversanne, Hyuna Sung, Jacques Ferlay, Rebecca L. Siegel, Isabelle Soerjomataram, and Ahmedin Jemal (2024). "Global cancer statistics 2022: GLOBOCAN estimates of incidence and mortality worldwide for 36 cancers in 185 countries". *CA: A Cancer Journal for Clinicians* 74.3, pp. 229–263. DOI: https://doi.org/10.3322/caac.21834. eprint: https://acsjournals.onlinelibrary.wiley.com/doi/pdf/10.3322/caac.21834.

Bronte, Vincenzo, Tihana Kasic, Giorgia Gri, Keti Gallana, Giovanna Borsellino, Ilaria Marigo, Luca Battistini, Massimo Iafrate, Tommaso Prayer-Galetti, Francesco Pagano, and Antonella Viola (Apr. 2005a). "Boosting antitumor responses of T lymphocytes infiltrating human prostate cancers ". *Journal of Experimental Medicine* 201.8, pp. 1257–1268. DOI: 10.1084/jem.20042028. eprint: https://rupress.org/jem/article-pdf/201/8/1257/1717453/jem20181257.pdf.

Bronte, Vincenzo and Paola Zanovello (2005b). "Regulation of immune responses by L-arginine metabolism". *Nature Reviews Immunology* 5 (8), pp. 641–654. DOI: 10.1038/nri1668.

Brown, Bruce K. and Wenxia Song (2001a). "The Actin Cytoskeleton is Required for the Trafficking of the B Cell Antigen Receptor to the Late Endosomes". *Traffic* 2.6, pp. 414–427. DOI: https://doi.org/10.1034/j.1600-0854.2001.002006414.x. eprint: https://onlinelibrary.wiley.com/doi/pdf/10.1034/j.1600-0854.2001.002006414.x.

Brown, Eric J and William A Frazier (Mar. 2001b). "Integrin-associated protein (CD47) and its ligands". *Trends in Cell Biology* 11 (3). doi: 10.1016/S0962-8924(00)01906-1, pp. 130–135. DOI: 10.1016/S0962-8924(00)01906-1.

Broz, Miranda L., Mikhail Binnewies, Bijan Boldajipour, Amanda E. Nelson, Joshua L. Pollack, David J. Erle, Andrea Barczak, Michael D. Rosenblum, Adil Daud, Diane L. Barber, Sebastian Amigorena, Laura J. van't Veer, Anne I. Sperling, Denise M. Wolf, and Matthew F. Krummel (Nov. 2014). "Dissecting the Tumor Myeloid Compartment Reveals Rare Activating Antigen-Presenting Cells Critical for T Cell Immunity". *Cancer Cell* 26 (5). doi: 10.1016/j.ccell.2014.09.007, pp. 638–652. DOI: 10.1016/j.ccell.2014.09.007.

Brunet, Anne, Azad Bonni, Michael J Zigmond, Michael Z Lin, Peter Juo, Linda S Hu, Michael J Anderson, Karen C Arden, John Blenis, and Michael E Greenberg (1999). "Akt Promotes Cell Survival by Phosphorylating and Inhibiting a Forkhead Transcription Factor". *Cell* 96.6, pp. 857–868. DOI: 10.1016/S0092-8674(00)80595-4.

Bryant, Richard J., Catherine P. Hobbs, Katie S. Eyre, Lucy C. Davies, Mark E. Sullivan, William Shields, Prasanna Sooriakumaran, Clare L. Verrill, Fergus V. Gleeson, Ruth E. Macpherson, Freddie C. Hamdy, and Simon F. Brewster (Mar. 2019). "Comparison of Prostate Biopsy with or without Prebiopsy Multiparametric Magnetic Resonance Imaging for Prostate Cancer Detection: An Observational Cohort Study". *The Journal of Urology* 201 (3), pp. 510–518. DOI: 10.1016/J.JURO.2018.09.049.

Buck, Michael D, Ryan T Sowell, Susan M Kaech, and Erika L Pearce (May 2017). "Metabolic Instruction of Immunity". *Cell* 169 (4). doi: 10.1016/j.cell.2017.04.004, pp. 570–586. DOI: 10.1016/j.cell.2017.04.004.

BURKE, AMY J., HUSNAIN ALI, ENDA O'CONNELL, FRANCIS J. SULLIVAN, and SHARON A. GLYNN (2016). "Sensitivity Profiles of Human Prostate Cancer Cell Lines to an 80 Kinase Inhibitor Panel". *Anticancer Research* 36.2, pp. 633–641. eprint: https://ar.iiarjournals.org/content/36/2/633.full.pdf.

Burki, Talha (2024). "Prostate Cancer UK launches the TRANSFORM trial". *The Lancet* 403.10438, p. 1738. DOI: https://doi.org/10.1016/S0140-6736(24)00912-7.

Calcinotto, Arianna, Clarissa Spataro, Elena Zagato, Diletta Di Mitri, Veronica Gil, Mateus Crespo, Gaston De Bernardis, Marco Losa, Michela Mirenda, Emiliano Pasquini, Andrea Rinaldi, Semini Sumanasuriya, Maryou B Lambros, Antje Neeb, Roberta Lucianò, Carlo A Bravi, Daniel Nava-Rodrigues, David Dolling, Tommaso Prayer-Galetti, Ana Ferreira, Alberto Briganti, Antonio Esposito, Simon Barry, Wei Yuan, Adam Sharp, Johann de Bono, and Andrea Alimonti (2018). "IL-23 secreted by myeloid cells drives castration-resistant prostate cancer". *Nature* 559 (7714), pp. 363–369. DOI: 10.1038/s41586-018-0266-0.

Camblin, Adam J, Gege Tan, Michael D Curley, Isabel Yannatos, Sergio Iadevaia, Victoria Rimkunas, Mari Mino-Kenudson, Troy Bloom, Birgit Schoeberl, Daryl C Drummond, Alexey A Lugovskoy, Chrystal U Louis, and Vasileios Askoxylakis (2019). "Dual targeting of IGF-1R and ErbB3 as a potential therapeutic regimen for ovarian cancer". *Scientific Reports* 9 (1), p. 16832. DOI: 10.1038/s41598-019-53322-y.

Cao, Liang, Yunkai Yu, Isaac Darko, Duane Currier, Linnia H. Mayeenuddin, Xiaolin Wan, Chand Khanna, and Lee J. Helman (Sept. 2008). "Addiction to Elevated Insulin-like Growth Factor I Receptor and Initial Modulation of the AKT Pathway Define the Responsiveness of Rhabdomyosarcoma to the Targeting Antibody". *Cancer Research* 68.19, pp. 8039–8048. DOI: 10.1158/0008-5472.CAN-08-1712. eprint: https://aacrjournals.org/cancerres/article-pdf/68/19/8039/2598588/8039.pdf.

Cao, Longxing, Haishuang Chang, Xiangyi Shi, Chao Peng, and Yongning He (2016). "Keratin mediates the recognition of apoptotic and necrotic cells through dendritic cell receptor DEC205/CD205". *Proceedings of the National Academy of Sciences* 113.47, pp. 13438–13443. DOI: 10.1073/pnas.1609331113. eprint: https://www.pnas.org/doi/pdf/10.1073/pnas.1609331113.

Cao, Xuefang, Sheng F Cai, Todd A Fehniger, Jiling Song, Lynne I Collins, David R Piwnica-Worms, and Timothy J Ley (Oct. 2007). "Granzyme B and Perforin Are Important for Regulatory T Cell-Mediated Suppression of Tumor Clearance". *Immunity* 27 (4). doi: 10.1016/j.immuni.2007.08.014, pp. 635–646. DOI: 10.1016/j.immuni.2007.08.014.

Cao, Zhongwei, Joseph M Scandura, Giorgio G Inghirami, Koji Shido, Bi-Sen Ding, and Shahin Rafii (Jan. 2017). "Molecular Checkpoint Decisions Made by Subverted Vascular Niche Transform Indolent Tumor Cells into Chemoresistant Cancer Stem Cells". *Cancer Cell* 31 (1). doi: 10.1016/j.ccell.2016.11.010, pp. 110–126. DOI: 10.1016/j.ccell.2016.11.010.

Capasso, A., J. Lang, T. M. Pitts, K. R. Jordan, C. H. Lieu, S. L. Davis, J. R. Diamond, S. Kopetz, J. Barbee, J. Peterson, B. M. Freed, B. W. Yacob, S. M. Bagby, W. A. Messersmith, J. E. Slansky, R. Pelanda, and S. G. Eckhardt (2019). "Characterization of immune responses to anti-PD-1 mono and combination immunotherapy in hematopoietic humanized mice implanted with tumor xenografts". *Journal for ImmunoTherapy of Cancer* 7.1. DOI: 10.1186/s40425-019-0518-z. eprint: https://jitc.bmj.com/content/7/1/37.full.pdf.

Carboni, Joan M., Mark Wittman, Zheng Yang, Francis Lee, Ann Greer, Warren Hurlburt, Stephen Hillerman, Carolyn Cao, Glenn H. Cantor, Janet Dell-John, Cliff Chen, Lorell Discenza, Krista Menard, Aixin Li, George Trainor, Dolatrai Vyas, Robert Kramer, Ricardo M. Attar, and Marco M. Gottardis (Dec. 2009). "BMS-754807, a small molecule inhibitor of insulin-like growth factor-1R/IR". *Molecular Cancer Therapeutics* 8.12,

pp. 3341–3349. DOI: 10.1158/1535-7163.MCT-09-0499. eprint: https://aacrjournals.org/mct/article-pdf/8/12/3341/1882364/3341.pdf.

Cardone, Michael H., Natalie Roy, Henning R. Stennicke, Guy S. Salvesen, Thomas F. Franke, Eric Stanbridge, Steven Frisch, and John C. Reed (1998). "Regulation of Cell Death Protease Caspase-9 by Phosphorylation". *Science* 282.5392, pp. 1318–1321. DOI: 10.1126/science.282.5392.1318. eprint: https://www.science.org/doi/pdf/10.1126/science.282.5392.1318.

Carlini, Valentina, Douglas M. Noonan, Eslam Abdalalem, Delia Goletti, Clementina Sansone, Luana Calabrone, and Adriana Albini (2023). "The multifaceted nature of IL-10: regulation, role in immunological homeostasis and its relevance to cancer, COVID-19 and post-COVID conditions". *Frontiers in Immunology* 14. DOI: 10.3389/fimmu.2023.1161067.

Carver, Brett S, Jennifer Tran, Zhenbang Chen, Arkaitz Carracedo-Perez, Andrea Alimonti, Caterina Nardella, Anuradha Gopalan, Peter T Scardino, Carlos Cordon-Cardo, William Gerald, and Pier Paolo Pandolfi (2009). "ETS rearrangements and prostate cancer initiation". *Nature* 457 (7231), E1–E1. DOI: 10.1038/nature07738.

Carver, Brett S., Caren Chapinski, John Wongvipat, Haley Hieronymus, Yu Chen, Sarat Chandarlapaty, Vivek K. Arora, Carl Le, Jason Koutcher, Howard Scher, Peter T. Scardino, Neal Rosen, and Charles L. Sawyers (May 2011). "Reciprocal Feedback Regulation of PI3K and Androgen Receptor Signaling in PTEN-Deficient Prostate Cancer". *Cancer Cell* 19 (5). doi: 10.1016/j.ccr.2011.04.008, pp. 575–586. DOI: 10.1016/j.ccr.2011.04.008.

Casella, James F, Michael D Flanagan, and Shin Lin (1981). "Cytochalasin D inhibits actin polymerization and induces depolymerization of actin filaments formed during platelet shape change". *Nature* 293 (5830), pp. 302–305. DOI: 10.1038/293302a0.

Casey, Stephanie C., Ling Tong, Yulin Li, Rachel Do, Susanne Walz, Kelly N. Fitzgerald, Arvin M. Gouw, Virginie Baylot, Ines Gütgemann, Martin Eilers, and Dean W. Felsher (2016). "MYC regulates the antitumor immune response through CD47 and PD-L1". *Science* 352.6282, pp. 227–231. DOI: 10.1126/science.aac9935. eprint: https://www.science.org/doi/pdf/10.1126/science.aac9935.

Catalona, William J., Deborah S. Smith, Timothy L. Ratliff, Kathy M. Dodds, Douglas E. Coplen, Jerry J.J. Yuan, John A. Petros, and Gerald L. Andriole (1991). "Measurement of Prostate-Specific Antigen in Serum as a Screening Test for Prostate Cancer". *New England Journal of Medicine* 324.17, pp. 1156–1161. DOI: 10.1056/NEJM199104253241702. eprint: https://www.nejm.org/doi/pdf/10.1056/NEJM199104253241702.

Caushi, Justina X, Jiajia Zhang, Zhicheng Ji, Ajay Vaghasia, Boyang Zhang, Emily Han-Chung Hsiue, Brian J Mog, Wenpin Hou, Sune Justesen, Richard Blosser, Ada Tam, Valsamo Anagnostou, Tricia R Cottrell, Haidan Guo, Hok Yee Chan, Dipika Singh, Sampriti Thapa, Arbor G Dykema, Poromendro Burman, Begum Choudhury, Luis Aparicio, Laurene S Cheung, Mara Lanis, Zineb Belcaid, Margueritta El Asmar, Peter B Illei, Rulin Wang, Jennifer Meyers, Kornel Schuebel, Anuj Gupta, Alyza Skaist, Sarah Wheelan, Jarushka Naidoo, Kristen A Marrone, Malcolm Brock, Jinny Ha, Errol L Bush, Bernard J Park, Matthew Bott, David R Jones, Joshua E Reuss, Victor E Velculescu, Jamie E Chaft, Kenneth W Kinzler, Shibin Zhou, Bert Vogelstein, Janis M Taube, Matthew D Hellmann, Julie R Brahmer, Taha Merghoub, Patrick M Forde, Srinivasan Yegnasubramanian, Hongkai Ji, Drew M Pardoll, and Kellie N Smith (2021). "Transcriptional programs of neoantigen-specific TIL in

anti-PD-1-treated lung cancers". *Nature* 596 (7870), pp. 126–132. DOI: 10.1038/s41586-021-03752-4.

Chan, June M., Meir J. Stampfer, Jing Ma, Peter Gann, J. Michael Gaziano, Michael Pollak, and Edward Giovannucci (July 2002). "Insulin-Like Growth Factor-I (IGF-I) and IGF Binding Protein-3 as Predictors of Advanced-Stage Prostate Cancer". *JNCI: Journal of the National Cancer Institute* 94.14, pp. 1099–1106. DOI: 10.1093/jnci/94.14.1099. eprint: https://academic.oup.com/jnci/article-pdf/94/14/1099/9849183/1099.pdf.

Chang, Kai-Hsiung, Rui Li, Barbara Kuri, Yair Lotan, Claus G. Roehrborn, Jiayan Liu, Robert Vessella, Peter S. Nelson, Payal Kapur, Xiaofeng Guo, Hamid Mirzaei, Richard J. Auchus, and Nima Sharifi (Aug. 2013). "A Gain-of-Function Mutation in DHT Synthesis in Castration-Resistant Prostate Cancer". *Cell* 154 (5). doi: 10.1016/j.cell.2013.07.029, pp. 1074–1084. DOI: 10.1016/j.cell.2013.07.029.

Chao, Mark P, Ravindra Majeti, and Irving L Weissman (2012). "Programmed cell removal: a new obstacle in the road to developing cancer". *Nature Reviews Cancer* 12 (1), pp. 58–67. DOI: 10.1038/nrc3171.

Chao, Mark P., Ash A. Alizadeh, Chad Tang, June H. Myklebust, Bindu Varghese, Saar Gill, Max Jan, Adriel C. Cha, Charles K. Chan, Brent T. Tan, Christopher Y. Park, Feifei Zhao, Holbrook E. Kohrt, Raquel Malumbres, Javier Briones, Randy D. Gascoyne, Izidore S. Lossos, Ronald Levy, Irving L. Weissman, and Ravindra Majeti (2010). "Anti-CD47 Antibody Synergizes with Rituximab to Promote Phagocytosis and Eradicate Non-Hodgkin Lymphoma". *Cell* 142.5, pp. 699–713. DOI: https://doi.org/10.1016/j.cell.2010.07.044.

Chaudhry, Ashutosh, Robert M. Samstein, Piper Treuting, Yuqiong Liang, Marina C. Pils, Jan-Michael Heinrich, Robert S. Jack, F. Thomas Wunderlich, Jens C. Bruning, Werner Muller, and Alexander Y. Rudensky (Apr. 2011). "Interleukin-10 Signaling in Regulatory T Cells Is Required for Suppression of Th17 Cell-Mediated Inflammation". *Immunity* 34 (4). doi: 10.1016/j.immuni.2011.03.018, pp. 566–578. DOI: 10.1016/j.immuni.2011.03.018.

Chen, Daniel S. and Ira Mellman (2013a). "Oncology Meets Immunology: The Cancer-Immunity Cycle". *Immunity* 39.1, pp. 1–10. DOI: https://doi.org/10.1016/j.immuni.2013.07.012.

– (Jan. 2017a). "Elements of cancer immunity and the cancer–immune set point". *Nature* 541 (7637), pp. 321–330. DOI: 10.1038/nature21349.

Chen, Hsuan-An, Yu-Jui Ho, Riccardo Mezzadra, Jose M. Adrover, Ryan Smolkin, Changyu Zhu, Katharina Woess, Nicholas Bernstein, Georgia Schmitt, Linda Fong, Wei Luan, Alexandra Wuest, Sha Tian, Xiang Li, Caroline Broderick, Ronald C. Hendrickson, Mikala Egeblad, Zhenghao Chen, Direna Alonso-Curbelo, and Scott W. Lowe (Feb. 2023a). "Senescence Rewires Microenvironment Sensing to Facilitate Antitumor Immunity". *Cancer Discovery* 13.2, pp. 432–453. DOI: 10.1158/2159-8290.CD-22-0528. eprint: https://aacrjournals.org/cancerdiscovery/article-pdf/13/2/432/3483973/432.pdf.

Chen, Lang and Deyin Guo (2017b). "The functions of tumor suppressor PTEN in innate and adaptive immunity". *Cellular and Molecular Immunology* 14 (7), pp. 581–589. DOI: 10.1038/cmi.2017.30.

Chen, Lieping and Dallas B Flies (2013b). "Molecular mechanisms of T cell co-stimulation and co-inhibition". *Nature Reviews Immunology* 13 (4), pp. 227–242. DOI: 10.1038/nri3405.

Chen, Lujun, Hao Huang, Xiao Zheng, Yuan Li, Junjun Chen, Bo Tan, Yingting Liu, Runzi Sun, Bin Xu, Min Yang, Bin Li, Changping Wu, Binfeng Lu, and Jingting Jiang (2022). "IL1R2 increases regulatory T cell population in the tumor microenvironment by enhancing MHC-II expression on cancer-associated fibroblasts". *Journal for ImmunoTherapy of Cancer* 10.9. DOI: 10.1136/jitc-2022-004585. eprint: https://jitc.bmj.com/content/10/9/e004585.full.pdf.

Chen, Shanze, Abdullah F U H Saeed, Quan Liu, Qiong Jiang, Haizhao Xu, Gary Guishan Xiao, Lang Rao, and Yanhong Duo (2023b). "Macrophages in immunoregulation and therapeutics". *Signal Transduction and Targeted Therapy* 8 (1), p. 207. DOI: 10.1038/s41392-023-01452-1.

Chen, Sujun, Guanghui Zhu, Yue Yang, Fubo Wang, Yu-Tian Xiao, Na Zhang, Xiaojie Bian, Yasheng Zhu, Yongwei Yu, Fei Liu, Keqin Dong, Javier Mariscal, Yin Liu, Fraser Soares, Helen Loo Yau, Bo Zhang, Weidong Chen, Chao Wang, Dai Chen, Qinghua Guo, Zhengfang Yi, Mingyao Liu, Michael Fraser, Daniel D De Carvalho, Paul C Boutros, Dolores Di Vizio, Zhou Jiang, Theodorus van der Kwast, Alejandro Berlin, Song Wu, Jianhua Wang, Housheng Hansen He, and Shancheng Ren (2021). "Single-cell analysis reveals transcriptomic remodellings in distinct cell types that contribute to human prostate cancer progression". *Nature Cell Biology* 23 (1), pp. 87–98. DOI: 10.1038/s41556-020-00613-6.

Chen, Yinhsuan Michely, Matthew Leibovitch, Michele Zeinieh, Nada Jabado, and Pnina Brodt (2023c). "Targeting the IGF-Axis in Cultured Pediatric High-Grade Glioma Cells Inhibits Cell Cycle Progression and Survival". *Pharmaceuticals* 16.2. DOI: 10.3390/ph16020297.

Chen, Yinhsuan Michely, Shu Qi, Stephanie Perrino, Masakazu Hashimoto, and Pnina Brodt (2020). "Targeting the IGF-Axis for Cancer Therapy: Development and Validation of an IGF-Trap as a Potential Drug". *Cells* 9.5. DOI: 10.3390/cells9051098.

Chetram, Mahandranauth A. and Cimona V. Hinton (Aug. 2012). "PTEN regulation of ERK1/2 signaling in cancer". *Journal of receptor and signal transduction research* 32 (4), p. 190. DOI: 10.3109/10799893.2012.695798.

Chien, Yuchen, Claudio Scuoppo, Xiaowo Wang, Xueping Fang, Brian Balgley, Jessica E. Bolden, Prem Premsrirut, Weijun Luo, Agustin Chicas, Cheng S. Lee, Scott C. Kogan, and Scott W. Lowe (Oct. 2011). "Control of the senescence-associated secretory phenotype by NF-kB promotes senescence and enhances chemosensitivity". *Genes and Development* 25 (20), pp. 2125–2136. DOI: 10.1101/GAD.17276711.

Chistiakov, Dimitry A, Murry C Killingsworth, Veronika A Myasoedova, Alexander N Orekhov, and Yuri V Bobryshev (2017). "CD68/macrosialin: not just a histochemical marker". *Laboratory Investigation* 97 (1), pp. 4–13. DOI: 10.1038/labinvest.2016.116.

Chitnis, M M, K A Lodhia, T Aleksic, S Gao, A S Protheroe, and V M Macaulay (2014). "IGF-1R inhibition enhances radiosensitivity and delays double-strand break repair by both non-homologous end-joining and homologous recombination". *Oncogene* 33 (45), pp. 5262–5273. DOI: 10.1038/onc.2013.460.

Chitnis, Meenali M., John S.P. Yuen, Andrew S. Protheroe, Michael Pollak, and Valentine M. Macaulay (Oct. 2008). "The Type 1 Insulin-Like Growth Factor Receptor Pathway". *Clinical Cancer Research* 14.20, pp. 6364–6370. DOI: 10.1158/1078-0432.CCR-07-4879. eprint: https://aacrjournals.org/clincancerres/article-pdf/14/20/6364/1977600/6364.pdf.

Cho, Bryan K., Changyu Wang, Satoshi Sugawa, Herman N. Eisen, and Jianzhu Chen (1999). "Functional differences between memory and naive CD8 T cells". *Proceedings of the National Academy of Sciences* 96.6, pp. 2976–2981. DOI: 10.1073/pnas.96.6.2976. eprint: https://www.pnas.org/doi/pdf/10.1073/pnas.96.6.2976.

Chodak, Gerald W (May 1989). "Luteinizing hormone-releasing hormone (LHRH) agonists for treatment of advanced prostatic carcinoma". *Urology* 33 (5). doi: 10.1016/0090-4295(89)90105-2, pp. 42–44. DOI: 10.1016/0090-4295(89)90105-2.

Chodak, Gerald W., Paul Keller, and Harry W. Schoenberg (1989). "Assessment of Screening for Prostate Cancer Using the Digital Rectal Examination". *The Journal of Urology* 141.5, pp. 1136–1138. DOI: https://doi.org/10.1016/S0022-5347(17)41192-X.

Chow, Andrew, Karlo Perica, Christopher A Klebanoff, and Jedd D Wolchok (2022). "Clinical implications of T cell exhaustion for cancer immunotherapy". *Nature Reviews Clinical Oncology* 19 (12), pp. 775–790. DOI: 10.1038/s41571-022-00689-z.

Christmann, Romy B., Everett Hayes, Sarah Pendergrass, Cristina Padilla, Giuseppina Farina, Alsya J. Affandi, Michael L. Whitfield, Harrison W. Farber, and Robert Lafyatis (2011). "Interferon and alternative activation of monocyte/macrophages in systemic sclerosis–associated pulmonary arterial hypertension". *Arthritis and Rheumatism* 63.6, pp. 1718–1728. DOI: https://doi.org/10.1002/art.30318. eprint: https://onlinelibrary.wiley.com/doi/pdf/10.1002/art.30318.

Christopoulos, Panagiotis F, Pavlos Msaouel, and Michael Koutsilieris (2015). "The role of the insulin-like growth factor-1 system in breast cancer". *Molecular Cancer* 14 (1), p. 43. DOI: 10.1186/s12943-015-0291-7.

Chua, Chee Wai, Maho Shibata, Ming Lei, Roxanne Toivanen, LaMont J Barlow, Sarah K. Bergren, Ketan K Badani, James M McKiernan, Mitchell C Benson, Hanina Hibshoosh, and Michael M Shen (2014). "Single luminal epithelial progenitors can generate prostate organoids in culture". *Nature Cell Biology* 16 (10), pp. 951–961. DOI: 10.1038/ncb3047.

Cibrian, Danay and Francisco Sanchez-Madrid (2017). "CD69: from activation marker to metabolic gatekeeper". *European Journal of Immunology* 47.6, pp. 946–953. DOI: https://doi.org/10.1002/eji.201646837. eprint: https://onlinelibrary.wiley.com/doi/pdf/10.1002/eji.201646837.

Cioni, Bianca, Anniek Zaalberg, Judy R. van Beijnum, Monique H. M. Melis, Johan van Burgsteden, Mauro J. Muraro, Erik Hooijberg, Dennis Peters, Ingrid Hofland, Yoni Lubeck, Jeroen de Jong, Joyce Sanders, Judith Vivié, Henk G. van der Poel, Jan Paul de Boer, Arjan W. Griffioen, Wilbert Zwart, and Andries M. Bergman (2020). "Androgen receptor signalling in macrophages promotes TREM-1-mediated prostate cancer cell line migration and invasion". *Nature Communications* 11.1, p. 4498. DOI: 10.1038/s41467-020-18313-y.

Clay Bunn, R. and John L. Fowlkes (2003). "Insulin-like growth factor binding protein proteolysis". *Trends in Endocrinology and Metabolism* 14.4, pp. 176–181. DOI: 10.1016/S1043-2760(03)00049-3.

Clayton, Peter E, Indraneel Banerjee, Philip G Murray, and Andrew G Renehan (2011). "Growth hormone, the insulin-like growth factor axis, insulin and cancer risk". *Nature Reviews Endocrinology* 7 (1), pp. 11–24. DOI: 10.1038/nrendo.2010.171.

Clemmons, D. R. and L. A. Maile (Jan. 2005). "Interaction between Insulin-Like Growth Factor-I Receptor and aVB3 Integrin Linked Signaling Pathways: Cellular Responses to Changes in Multiple Signaling Inputs". *Molecular Endocrinology* 19.1, pp. 1–11. DOI:

10.1210/me.2004-0376. eprint:
https://academic.oup.com/mend/article-pdf/19/1/1/10716870/mend0001.pdf.

Codony-Servat, Jordi, Miriam Cuatrecasas, Elena Asensio, Carla Montironi, Anna Martinez-Cardus, Mercedes Marín-Aguilera, Carlos Horndler, Eva Martinez-Balibrea, Michele Rubini, Pedro Jares, Oscar Reig, Ivan Victoria, Lydia Gaba, Marta Martin-Richard, Vicente Alonso, Pilar Escudero, Carlos Fernandez-Martos, Jaime Feliu, Jose Carlos Mendez, Miguel Mendez, Javier Gallego, Antonieta Salud, Federico Rojo, Antoni Castells, Aleix Prat, Rafael Rosell, Xabier Garcia-Albeniz, Jordi Camps, and Joan Maurel (2017). "Nuclear IGF-1R predicts chemotherapy and targeted therapy resistance in metastatic colorectal cancer". *British Journal of Cancer* 117, pp. 1777–1786. DOI: 10.1038/bjc.2017.279.

Cohen, Bruce D., Deborah A. Baker, Catherine Soderstrom, George Tkalcevic, Ann Marie Rossi, Penny E. Miller, Mark W. Tengowski, Faye Wang, Antonio Gualberto, Jean S. Beebe, and James D. Moyer (2005). "Combination Therapy Enhances the Inhibition of Tumor Growth with the Fully Human Anti–Type 1 Insulin-Like Growth Factor Receptor Monoclonal Antibody CP-751 871". *Clinical Cancer Research* 11.5, pp. 2063–2073. DOI: 10.1158/1078-0432.CCR-04-1070. eprint:
https://aacrjournals.org/clincancerres/article-pdf/11/5/2063/1962670/2063-2073.pdf.

Cohen, P, H C Graves, D M Peehl, M Kamarei, L C Giudice, and R G Rosenfeld (Oct. 1992). "Prostate-specific antigen (PSA) is an insulin-like growth factor binding protein-3 protease found in seminal plasma". *The Journal of Clinical Endocrinology and Metabolism* 75.4, pp. 1046–1053. DOI: 10.1210/jcem.75.4.1383255. eprint:
https://academic.oup.com/jcem/article-pdf/75/4/1046/10501722/jcem1046.pdf.

Cohen, P., D. M. Peehl, H. C.B. Craves, and R. C. Rosenfeld (Sept. 1994). "Biological effects of prostate specific antigen as an insulin-like growth factor binding protein-3 protease". *Journal of Endocrinology* 142 (3), pp. 407–415. DOI: 10.1677/JOE.0.1420407.

Collison, Lauren W, Creg J Workman, Timothy T Kuo, Kelli Boyd, Yao Wang, Kate M Vignali, Richard Cross, David Sehy, Richard S Blumberg, and Dario A A Vignali (2007). "The inhibitory cytokine IL-35 contributes to regulatory T-cell function". *Nature* 450 (7169), pp. 566–569. DOI: 10.1038/nature06306.

Comito, G., E. Giannoni, C P Segura, P. Barcellos-de-Souza, M R Raspollini, G. Baroni, M. Lanciotti, S. Serni, and P. Chiarugi (2014). "Cancer-associated fibroblasts and M2-polarized macrophages synergize during prostate carcinoma progression". *Oncogene* 33.19, pp. 2423–2431. DOI: 10.1038/onc.2013.191.

Conover, C. A., L. K. Bale, S. K. Durham, and D. R. Powell (Sept. 2000). "Insulin-Like Growth Factor (IGF) Binding Protein-3 Potentiation of IGF Action Is Mediated through the Phosphatidylinositol-3-Kinase Pathway and Is Associated with Alteration in Protein Kinase B/AKT Sensitivity". *Endocrinology* 141.9, pp. 3098–3103. DOI: 10.1210/endo.141.9.7660. eprint: https://academic.oup.com/endo/article-pdf/141/9/3098/10360884/endo3098.pdf.

Coppe, Jean-Philippe, Christopher K Patil, Francis Rodier, Yu Sun, Denise P Munoz, Joshua Goldstein, Peter S Nelson, Pierre-Yves Desprez, and Judith Campisi (Dec. 2008). "Senescence-Associated Secretory Phenotypes Reveal Cell-Nonautonomous Functions of Oncogenic RAS and the p53 Tumor Suppressor". *PLOS Biology* 6.12, pp. 1–1. DOI: 10.1371/journal.pbio.0060301.

Corthay, Alexandre, Dag K Skovseth, Katrin U Lundin, Egil Rosjo, Hilde Omholt, Peter O Hofgaard, Guttorm Haraldsen, and Bjarne Bogen (Mar. 2005). "Primary

Antitumor Immune Response Mediated by CD4+ T Cells". *Immunity* 22 (3). doi: 10.1016/j.immuni.2005.02.003, pp. 371–383. DOI: 10.1016/j.immuni.2005.02.003.

Cui, Can, Jiawei Wang, Eric Fagerberg, Ping-Min Chen, Kelli A Connolly, Martina Damo, Julie F Cheung, Tianyang Mao, Adnan S Askari, Shuting Chen, Brittany Fitzgerald, Gena G Foster, Stephanie C Eisenbarth, Hongyu Zhao, Joseph Craft, and Nikhil S Joshi (Dec. 2021). "Neoantigen-driven B cell and CD4 T follicular helper cell collaboration promotes anti-tumor CD8 T cell responses". *Cell* 184 (25), 6101–6118.e13. DOI: 10.1016/j.cell.2021.11.007.

Culig, Zoran, Alfred Hobisch, Marcus V Cronauer, Christian Radmayr, Jan Trapman, Anton Hittmair, Georg Bartsch, and Helmut Klocker (Oct. 1994). "Androgen Receptor Activation in Prostatic Tumor Cell Lines by Insulin-like Growth Factor-I, Keratinocyte Growth Factor, and Epidermal Growth Factor1". *Cancer Research* 54 (20), pp. 5474–5478.

Cunha, Larissa D, Mao Yang, Robert Carter, Clifford Guy, Lacie Harris, Jeremy C Crawford, Giovanni Quarato, Emilio Boada-Romero, Halime Kalkavan, Michael D L Johnson, Sivaraman Natarajan, Meghan E Turnis, David Finkelstein, Joseph T Opferman, Charles Gawad, and Douglas R Green (Oct. 2018). "LC3-Associated Phagocytosis in Myeloid Cells Promotes Tumor Immune Tolerance". *Cell* 175 (2). doi: 10.1016/j.cell.2018.08.061, 429–441.e16. DOI: 10.1016/j.cell.2018.08.061.

Cutress, Mark L., Hayley C. Whitaker, Ian G. Mills, Murray Stewart, and David E. Neal (Apr. 2008). "Structural basis for the nuclear import of the human androgen receptor". *Journal of Cell Science* 121.7, pp. 957–968. DOI: 10.1242/jcs.022103. eprint: https://journals.biologists.com/jcs/article-pdf/121/7/957/1501956/957.pdf.

Cyster, Jason G and Christopher D C Allen (Apr. 2019). "B Cell Responses: Cell Interaction Dynamics and Decisions". *Cell* 177 (3). doi: 10.1016/j.cell.2019.03.016, pp. 524–540. DOI: 10.1016/j.cell.2019.03.016.

D'Amico, Anthony V., Richard Whittington, S. Bruce Malkowicz, Delray Schultz, Kenneth Blank, Gregory A. Broderick, John E. Tomaszewski, Andrew A. Renshaw, Irving Kaplan, Clair J. Beard, and Alan Wein (Sept. 1998). "Biochemical Outcome After Radical Prostatectomy, External Beam Radiation Therapy, or Interstitial Radiation Therapy for Clinically Localized Prostate Cancer". *JAMA* 280.11, pp. 969–974. DOI: 10.1001/jama.280.11.969. eprint: https://jamanetwork.com/journals/jama/articlepdf/187980/joc80111.pdf.

Dai, Jinlu, Yi Lu, Hernan Roca, Jill M. Keller, Jian Zhang, Laurie K. McCauley, and Evan T. Keller (2017). "Immune mediators in the tumor microenvironment of prostate cancer". *Chinese Journal of Cancer* 36 (1), p. 29. DOI: 10.1186/S40880-017-0198-3.

Dale, Oliver T., Tamara Aleksic, Ketan A. Shah, Cheng Han, Hisham Mehanna, Davy C.M. Rapozo, Jon D.H. Sheard, Paul Goodyear, Navdeep S. Upile, Max Robinson, Terence M. Jones, Stuart Winter, and Valentine M. Macaulay (Apr. 2015). "IGF-1R expression is associated with HPV-negative status and adverse survival in head and neck squamous cell cancer". *Carcinogenesis* 36.6, pp. 648–655. DOI: 10.1093/carcin/bgv053. eprint: https://academic.oup.com/carcin/article-pdf/36/6/648/776156/bgv053.pdf.

Dandachi, Nadine, Neil J. Kelly, John P. Wood, Christine L. Burton, Josiah E. Radder, Adriana S. Leme, Alyssa D. Gregory, and Steven D. Shapiro (Aug. 2017). "Macrophage elastase induces TRAIL-mediated tumor cell death through its carboxy-terminal domain". *American Journal of Respiratory and Critical Care Medicine* 196 (3), pp. 353–363. DOI: 10.1164/RCCM.201606-1150OC/SUPPL_FILE/DISCLOSURES.PDF.

Dasgupta, Subhamoy, Nagireddy Putluri, Weiwen Long, Bin Zhang, Jianghua Wang, Akash K. Kaushik, James M. Arnold, Salil K. Bhowmik, Erin Stashi, Christine A. Brennan, Kimal Rajapakshe, Cristian Coarfa, Nicholas Mitsiades, Michael M. Ittmann, Arul M. Chinnaiyan, Arun Sreekumar, and Bert W. O'Malley (Mar. 2015). "Coactivator SRC-2–dependent metabolic reprogramming mediates prostate cancer survival and metastasis". *The Journal of Clinical Investigation* 125.3, pp. 1174–1188. DOI: 10.1172/JCI76029.

Datta, Dipamoy, Md. Aftabuddin, Dinesh Kumar Gupta, Sanghamitra Raha, and Prosenjit Sen (2016). "Human Prostate Cancer Hallmarks Map". *Scientific Reports* 6 (1), p. 30691. DOI: 10.1038/srep30691.

Datta, Sandeep Robert, Henryk Dudek, Xu Tao, Shane Masters, Haian Fu, Yukiko Gotoh, and Michael E Greenberg (1997). "Akt Phosphorylation of BAD Couples Survival Signals to the Cell-Intrinsic Death Machinery". *Cell* 91.2, pp. 231–241. DOI: 10.1016/S0092-8674(00)80405-5.

Daughaday, William H. and Peter Rotwein (Feb. 1989). "Insulin-Like Growth Factors I and II. Peptide, Messenger Ribonucleic Acid and Gene Structures, Serum, and Tissue Concentrations". *Endocrine Reviews* 10.1, pp. 68–91. DOI: 10.1210/edrv-10-1-68. eprint: https://academic.oup.com/edrv/article-pdf/10/1/68/9081539/edrv0068.pdf.

Davis, Ian D., Andrew J. Martin, Martin R. Stockler, Stephen Begbie, Kim N. Chi, Simon Chowdhury, Xanthi Coskinas, Mark Frydenberg, Wendy E. Hague, Lisa G. Horvath, Anthony M. Joshua, Nicola J. Lawrence, Gavin Marx, John McCaffrey, Ray McDermott, Margaret McJannett, Scott A. North, Francis Parnis, Wendy Parulekar, David W. Pook, M. Neil Reaume, Shahneen K. Sandhu, Alvin Tan, T. Hsiang Tan, Alastair Thomson, Emily Tu, Francisco Vera-Badillo, Scott G. Williams, Sonia Yip, Alison Y. Zhang, Robert R. Zielinski, and Christopher J. Sweeney (2019). "Enzalutamide with Standard First-Line Therapy in Metastatic Prostate Cancer". *New England Journal of Medicine* 381.2, pp. 121–131. DOI: 10.1056/NEJMoa1903835. eprint: https://www.nejm.org/doi/pdf/10.1056/NEJMoa1903835.

Davis, Roger J (Oct. 2000). "Signal Transduction by the JNK Group of MAP Kinases". *Cell* 103 (2), pp. 239–252. DOI: 10.1016/S0092-8674(00)00116-1.

Deaglio, Silvia, Karen M. Dwyer, Wenda Gao, David Friedman, Anny Usheva, Anna Erat, Jiang-Fan Chen, Keiichii Enjyoji, Joel Linden, Mohamed Oukka, Vijay K. Kuchroo, Terry B. Strom, and Simon C. Robson (May 2007). "Adenosine generation catalyzed by CD39 and CD73 expressed on regulatory T cells mediates immune suppression ". *Journal of Experimental Medicine* 204.6, pp. 1257–1265. DOI: 10.1084/jem.20062512. eprint: https://rupress.org/jem/article-pdf/204/6/1257/1725727/jem_20062512.pdf.

De Bono, Johann, Chia Chi Lin, Li Tzong Chen, Jesus Corral, Vasiliki Michalarea, Karim Rihawi, Michael Ong, Jih Hsiang Lee, Chih Hung Hsu, James Chih Hsin Yang, Her Shyong Shiah, Chia Jui Yen, Alan Anthoney, Maria Jove, Susanne Buschke, René Fuertig, Ulrike Schmid, Rainer Georg Goeldner, Natalja Strelkowa, Dennis Chin Lun Huang, Thomas Bogenrieder, Chris Twelves, and Ann Lii Cheng (Mar. 2020a). "Two first-in-human studies of xentuzumab, a humanised insulin-like growth factor (IGF)-neutralising antibody, in patients with advanced solid tumours". *British Journal of Cancer* 122, pp. 1324–1332. DOI: 10.1038/s41416-020-0774-1.

De Bono, Johann, Joaquin Mateo, Karim Fizazi, Fred Saad, Neal Shore, Shahneen Sandhu, Kim N. Chi, Oliver Sartor, Neeraj Agarwal, David Olmos, Antoine Thiery-Vuillemin, Przemyslaw Twardowski, Niven Mehra, Carsten Goessl, Jinyu Kang, Joseph Burgents, Wenting Wu, Alexander Kohlmann, Carrie A. Adelman, and Maha Hussain (2020b).

"Olaparib for Metastatic Castration-Resistant Prostate Cancer". *New England Journal of Medicine* 382.22, pp. 2091–2102. DOI: 10.1056/NEJMoa1911440. eprint: https://www.nejm.org/doi/pdf/10.1056/NEJMoa1911440.

De Bono, Johann S, Christina Guo, Bora Gurel, Angelo M De Marzo, Karen S Sfanos, Ram S Mani, Jesus Gil, Charles G Drake, and Andrea Alimonti (2020c). "Prostate carcinogenesis: inflammatory storms". *Nature Reviews Cancer* 20.8, pp. 455–469. DOI: 10.1038/s41568-020-0267-9.

De Bono, Johann S., Christopher J. Logothetis, Arturo Molina, Karim Fizazi, Scott North, Luis Chu, Kim N. Chi, Robert J. Jones, Oscar B. Goodman, Fred Saad, John N. Staffurth, Paul Mainwaring, Stephen Harland, Thomas W. Flaig, Thomas E. Hutson, Tina Cheng, Helen Patterson, John D. Hainsworth, Charles J. Ryan, Cora N. Sternberg, Susan L. Ellard, Aude Fléchon, Mansoor Saleh, Mark Scholz, Eleni Efstathiou, Andrea Zivi, Diletta Bianchini, Yohann Loriot, Nicole Chieffo, Thian Kheoh, Christopher M. Haqq, and Howard I. Scher (2011). "Abiraterone and Increased Survival in Metastatic Prostate Cancer". *New England Journal of Medicine* 364.21, pp. 1995–2005. DOI: 10.1056/NEJMoa1014618. eprint: https://www.nejm.org/doi/pdf/10.1056/NEJMoa1014618.

De Bono, Johann S., Josep M. Piulats, Hardev S. Pandha, Daniel P. Petrylak, Fred Saad, Luis Miguel A. Aparicio, Shahneen K. Sandhu, Peter Fong, Silke Gillessen, Gary R. Hudes, Tao Wang, Judith Scranton, and Michael N. Pollak (Mar. 2014). "Phase II Randomized Study of Figitumumab plus Docetaxel and Docetaxel Alone with Crossover for Metastatic Castration-Resistant Prostate Cancer". *Clinical Cancer Research* 20.7, pp. 1925–1934. DOI: 10.1158/1078-0432.CCR-13-1869. eprint: https://aacrjournals.org/clincancerres/article-pdf/20/7/1925/2024906/1925.pdf.

Dehm, Scott M., Lucy J. Schmidt, Hannelore V. Heemers, Robert L. Vessella, and Donald J. Tindall (July 2008). "Splicing of a Novel Androgen Receptor Exon Generates a Constitutively Active Androgen Receptor that Mediates Prostate Cancer Therapy Resistance". *Cancer Research* 68.13, pp. 5469–5477. DOI: 10.1158/0008-5472.CAN-08-0594. eprint: https://aacrjournals.org/cancerres/article-pdf/68/13/5469/2596500/5469.pdf.

Demaria, Olivier, Stephanie Cornen, Marc Daeron, Yannis Morel, Ruslan Medzhitov, and Eric Vivier (Oct. 2019). "Harnessing innate immunity in cancer therapy". *Nature* 574 (7776), pp. 45–56. DOI: 10.1038/s41586-019-1593-5.

DeMarzo, Angelo M, William G Nelson, William B Isaacs, and Johnathan I Epstein (2003). "Pathological and molecular aspects of prostate cancer". *The Lancet* 361.9361, pp. 955–964. DOI: 10.1016/S0140-6736(03)12779-1.

DeMarzo, Angelo M., Valerie L. Marchi, Jonathan I. Epstein, and William G. Nelson (Dec. 1999). "Proliferative inflammatory atrophy of the prostate: Implications for prostatic carcinogenesis". *American Journal of Pathology* 155.6, pp. 1985–1992. DOI: 10.1016/S0002-9440(10)65517-4.

DeNardo, David G and Brian Ruffell (2019). "Macrophages as regulators of tumour immunity and immunotherapy". *Nature Reviews Immunology* 19 (6), pp. 369–382. DOI: 10.1038/s41577-019-0127-6.

De Rooij, Maarten, Esther H. J. Hamoen, Jurgen J. Futterer, Jelle O. Barentsz, and Maroeska M. Rovers (2014). "Accuracy of Multiparametric MRI for Prostate Cancer Detection: A Meta-Analysis". *American Journal of Roentgenology* 202.2. PMID: 24450675, pp. 343–351. DOI: 10.2214/AJR.13.11046. eprint: https://doi.org/10.2214/AJR.13.11046.

Desai, Avanti, Mi-Yeon Jung, Ana Olivera, Alasdair M Gilfillan, Calman Prussin, Arnold S Kirshenbaum, Michael A Beaven, and Dean D Metcalfe (June 2016). "IL-6 promotes an increase in human mast cell numbers and reactivity through suppression of suppressor of cytokine signaling 3". *Journal of Allergy and Clinical Immunology* 137 (6). doi: 10.1016/j.jaci.2015.09.059, pp. 1863–1871. DOI: 10.1016/j.jaci.2015.09.059.

Desai, J., B. J. Solomon, I.D. Davis, L.R. Lipton, R. Hicks, A. M. Scott, J. Park, P. L. Clemens, T. A. Gestone, and F. G. Finckenstein (2010). "Phase I dose-escalation study of daily BMS-754807, an oral, dual IGF-1R, insulin receptor inhibitor in subjects with solid tumors". *Journal of Clinical Oncology* 28, p. 3104.

Dev, Harveer, Mark Linch, Howard Kynaston, Greg Shaw, Krishna Narahari, Tatiana Hernández, Anne Warren, Alopa Malaviya, Vincent Gnanapragasam, Elizabeth Harrington, Niedzica Camacho, Silvia Glont, Massimo Sqautrito, Joshua Armenia, Luiza Moore, Robert Hanson, Toby Milne-Clarke, Shubha Anand, Charlie Massie, Nimish Shah, and Simon Pacey (June 2023). "Abstract B061: Updated analysis of "CANCAP03" – A study into the pharmacodynamic biomarker effects of olaparib (PARP inhibitor) ± degarelix (GnRH antagonist) given prior to radical prostatectomy". *Cancer Research* 83. DOI: 10.1158/1538-7445.PRCA2023-B061.

De Visser, Karin E. and Johanna A. Joyce (2023). "The evolving tumor microenvironment: From cancer initiation to metastatic outgrowth". *Cancer Cell* 41.3, pp. 374–403. DOI: https://doi.org/10.1016/j.ccell.2023.02.016.

Dey, Bhakta R, Susan L Spence, Peter Nissley, and Richard W Furlanetto (Sept. 1998). "Interaction of Human Suppressor of Cytokine Signaling (SOCS)-2 with the Insulin-like Growth Factor-I Receptor". *Journal of Biological Chemistry* 273 (37), pp. 24095–24101. DOI: 10.1074/jbc.273.37.24095.

Dhillon, A S, S Hagan, O Rath, and W Kolch (2007). "MAP kinase signalling pathways in cancer". *Oncogene* 26 (22), pp. 3279–3290. DOI: 10.1038/sj.onc.1210421.

Diehl, J. Alan, Mangeng Cheng, Martine F. Roussel, and Charles J. Sherr (Nov. 1998). "Glycogen synthase kinase-3B regulates cyclin D1 proteolysis and subcellular localization". *Genes and Development* 12 (22), pp. 3499–3511. DOI: 10.1101/GAD.12.22.3499.

Dighe, Anand S., Elizabeth Richards, Lloyd J. Old, and Robert D. Schreiber (Sept. 1994). "Enhanced in vivo growth and resistance to rejection of tumor cells expressing dominant negative IFN gamma receptors". *Immunity* 1 (6), pp. 447–456. DOI: 10.1016/1074-7613(94)90087-6.

DiToro, Daniel, Stacey N. Harbour, Jennifer K. Bando, Gloria Benavides, Steven Witte, Vincent A. Laufer, Carson Moseley, Jeffery R. Singer, Blake Frey, Henrietta Turner, Jens Bruning, Victor Darley-Usmar, Min Gao, Cheryl Conover, Robin D. Hatton, Stuart Frank, Marco Colonna, and Casey T. Weaver (Apr. 2020). "Insulin-Like Growth Factors Are Key Regulators of T Helper 17 Regulatory T Cell Balance in Autoimmunity". *Immunity* 52 (4), 650–667.e10. DOI: 10.1016/J.IMMUNI.2020.03.013/ATTACHMENT/75C08CCF-73CB-4E9A-944C-0D38D315729F/MMC1.PDF.

Dobin, Alexander, Carrie A. Davis, Felix Schlesinger, Jorg Drenkow, Chris Zaleski, Sonali Jha, Philippe Batut, Mark Chaisson, and Thomas R. Gingeras (Oct. 2012). "STAR: ultrafast universal RNA-seq aligner". *Bioinformatics* 29.1, pp. 15–21. DOI: 10.1093/bioinformatics/bts635. eprint: https://academic.oup.com/bioinformatics/article-pdf/29/1/15/49060422/bioinformatics_29_1_15.pdf.

Doedens, Andrew L., Christian Stockmann, Mark P. Rubinstein, Debbie Liao, Na Zhang, David G. DeNardo, Lisa M. Coussens, Michael Karin, Ananda W. Goldrath, and Randall S. Johnson (Sept. 2010). "Macrophage Expression of Hypoxia-Inducible Factor-1a Suppresses T-Cell Function and Promotes Tumor Progression". *Cancer Research* 70.19, pp. 7465–7475. DOI: 10.1158/0008-5472.CAN-10-1439. eprint: https://aacrjournals.org/cancerres/article-pdf/70/19/7465/2640444/7465.pdf.

Doi, Toshihiko, Yasutoshi Kuboki, Yoichi Naito, Masahiro Ishida, Tetsuya Tanaka, and Yoshito Takeuchi (2022). "A phase 1 trial of xentuzumab, an IGF-neutralizing antibody, in Japanese patients with advanced solid tumors". *Cancer Science* 113.3, pp. 1010–1017. DOI: https://doi.org/10.1111/cas.15231. eprint: https://onlinelibrary.wiley.com/doi/pdf/10.1111/cas.15231.

Dong, Chen (2008). "TH17 cells in development: an updated view of their molecular identity and genetic programming". *Nature Reviews Immunology* 8 (5), pp. 337–348. DOI: 10.1038/nri2295.

Dong, Chen, Amy E Juedes, Ulla-Angela Temann, Sujan Shresta, James P Allison, Nancy H Ruddle, and Richard A Flavell (2001). "ICOS co-stimulatory receptor is essential for T-cell activation and function". *Nature* 409 (6816), pp. 97–101. DOI: 10.1038/35051100.

Dong, Zening, Yahan Luo, Zhangchen Yuan, Yu Tian, Tianqiang Jin, and Feng Xu (2024). "Cellular senescence and SASP in tumor progression and therapeutic opportunities". *Molecular Cancer* 23 (1), p. 181. DOI: 10.1186/s12943-024-02096-7.

Donovan, Jenny L., Freddie C. Hamdy, J. Athene Lane, Malcolm Mason, Chris Metcalfe, Eleanor Walsh, Jane M. Blazeby, Tim J. Peters, Peter Holding, Susan Bonnington, Teresa Lennon, Lynne Bradshaw, Deborah Cooper, Phillipa Herbert, Joanne Howson, Amanda Jones, Norma Lyons, Elizabeth Salter, Pauline Thompson, Sarah Tidball, Jan Blaikie, Catherine Gray, Prasad Bollina, James Catto, Andrew Doble, Alan Doherty, David Gillatt, Roger Kockelbergh, Howard Kynaston, Alan Paul, Philip Powell, Stephen Prescott, Derek J. Rosario, Edward Rowe, Michael Davis, Emma L. Turner, Richard M. Martin, and David E. Neal (2016). "Patient-Reported Outcomes after Monitoring, Surgery, or Radiotherapy for Prostate Cancer". *New England Journal of Medicine* 375.15, pp. 1425–1437. DOI: 10.1056/NEJMoa1606221. eprint: https://www.nejm.org/doi/pdf/10.1056/NEJMoa1606221.

Dooling, Lawrence J, Jason C Andrechak, Brandon H Hayes, Siddhant Kadu, William Zhang, Ruby Pan, Manasvita Vashisth, Jerome Irianto, Cory M Alvey, Leyuan Ma, and Dennis E Discher (2023). "Cooperative phagocytosis of solid tumours by macrophages triggers durable anti-tumour responses". *Nature Biomedical Engineering* 7 (9), pp. 1081–1096. DOI: 10.1038/s41551-023-01031-3.

Douglas, Raymond S., George J. Kahaly, Amy Patel, Saba Sile, Elizabeth H.Z. Thompson, Renee Perdok, James C. Fleming, Brian T. Fowler, Claudio Marcocci, Michele Marinò, Alessandro Antonelli, Roger Dailey, Gerald J. Harris, Anja Eckstein, Jade Schiffman, Rosa Tang, Christine Nelson, Mario Salvi, Sara Wester, Jeffrey W. Sherman, Thomas Vescio, Robert J. Holt, and Terry J. Smith (2020). "Teprotumumab for the Treatment of Active Thyroid Eye Disease". *New England Journal of Medicine* 382.4, pp. 341–352. DOI: 10.1056/NEJMoa1910434. eprint: https://www.nejm.org/doi/pdf/10.1056/NEJMoa1910434.

Douglas, Raymond S., Vibharavi Naik, Catherine J. Hwang, Nikoo F. Afifiyan, Andrew G. Gianoukakis, Daniel Sand, Shweta Kamat, and Terry J. Smith (Oct. 2008). "B Cells from Patients with Graves' Disease Aberrantly Express the IGF-1 Receptor:

Implications for Disease Pathogenesis". *The Journal of Immunology* 181.8, pp. 5768–5774. DOI: 10.4049/jimmunol.181.8.5768. eprint: https://journals.aai.org/jimmunol/article-pdf/181/8/5768/1264744/zim02008005768.pdf.

Dowery, Reem, David Benhamou, Eli Benchetrit, Ofer Harel, Alex Nevelsky, Simona Zisman-Rozen, Yolanda Braun-Moscovici, Alexandra Balbir-Gurman, Irit Avivi, Arik Shechter, Daniela Berdnik, Tony Wyss-Coray, and Doron Melamed (Nov. 2021). "Peripheral B cells repress B-cell regeneration in aging through a TNF-a/IGFBP-1/IGF-1 immune-endocrine axis". *Blood* 138.19, pp. 1817–1829. DOI: 10.1182/blood.2021012428. eprint: https://ashpublications.org/blood/article-pdf/138/19/1817/1834659/bloodbld2021012428.pdf.

Du, Chunxia, Annacarolina da Silva, Vicente Morales-Oyarvide, Andressa Dias Costa, Margaret M. Kozak, Richard F. Dunne, Douglas A. Rubinson, Kimberly Perez, Yohei Masugi, Tsuyoshi Hamada, Lauren K. Brais, Chen Yuan, Ana Babic, Matthew D. Ducar, Aaron R. Thorner, Andrew Aguirre, Matthew H. Kulke, Kimmie Ng, Thomas E. Clancy, Jennifer J. Findeis-Hosey, Daniel T. Chang, Jason L. Hornick, Charles S. Fuchs, Shuji Ogino, Albert C. Koong, Aram F. Hezel, Brian M. Wolpin, and Jonathan A. Nowak (Aug. 2020). "Insulin-Like Growth Factor-1 Receptor Expression and Disease Recurrence and Survival in Patients with Resected Pancreatic Ductal Adenocarcinoma". *Cancer Epidemiology, Biomarkers and Prevention* 29.8, pp. 1586–1595. DOI: 10.1158/1055-9965.EPI-19-1315. eprint: https://aacrjournals.org/cebp/article-pdf/29/8/1586/1945709/1586.pdf.

Du, Liming, Liangyu Lin, Qing Li, Keli Liu, Yin Huang, Xuefeng Wang, Kai Cao, Xiaodong Chen, Wei Cao, Fengying Li, Changshun Shao, Ying Wang, and Yufang Shi (June 2019). "IGF-2 Preprograms Maturing Macrophages to Acquire Oxidative Phosphorylation-Dependent Anti-inflammatory Properties". *Cell Metabolism* 29 (6). doi: 10.1016/j.cmet.2019.01.006, 1363–1375.e8. DOI: 10.1016/j.cmet.2019.01.006.

Duan, Zhaojun and Yunping Luo (2021). "Targeting macrophages in cancer immunotherapy". *Signal Transduction and Targeted Therapy* 6 (1), p. 127. DOI: 10.1038/s41392-021-00506-6.

DuBois, Steven G., Mark D. Krailo, Julia Glade-Bender, Allen Buxton, Nadia Laack, R. Lor Randall, Helen X. Chen, Nita L. Seibel, Matthew Boron, Stephanie Terezakis, Christine Hill-Kayser, Andrea Hayes, Joel M. Reid, Lisa Teot, Dinesh Rakheja, Richard Womer, Carola Arndt, Stephen L. Lessnick, Brian D. Crompton, E. Anders Kolb, Heike Daldrup-Link, Eric Eutsler, Damon R. Reed, Katherine A. Janeway, and Richard G. Gorlick (2023). "Randomized Phase III Trial of Ganitumab With Interval-Compressed Chemotherapy for Patients With Newly Diagnosed Metastatic Ewing Sarcoma: A Report From the Children's Oncology Group". *Journal of Clinical Oncology* 41.11. PMID: 36669140, pp. 2098–2107. DOI: 10.1200/JCO.22.01815. eprint: https://doi.org/10.1200/JCO.22.01815.

Dunn, Gavin P., Allen T. Bruce, Hiroaki Ikeda, Lloyd J. Old, and Robert D. Schreiber (2002). "Cancer immunoediting: from immunosurveillance to tumor escape". *Nature Immunology* 3 (11), pp. 991–998. DOI: 10.1038/ni1102-991.

Dunn, Gavin P., Lloyd J. Old, and Robert D. Schreiber (2004). "The Immunobiology of Cancer Immunosurveillance and Immunoediting". *Immunity* 21.2, pp. 137–148. DOI: https://doi.org/10.1016/j.immuni.2004.07.017.

Dustin, Michael L. and Kaushik Choudhuri (2016). "Signaling and Polarized Communication Across the T Cell Immunological Synapse". *Annual Review of Cell and Developmental*

Biology 32.Volume 32, 2016, pp. 303–325. DOI: https://doi.org/10.1146/annurev-cellbio-100814-125330.

Dyck, Lydia, Mieszko M Wilk, Mathilde Raverdeau, Alicja Misiak, Louis Boon, and Kingston H G Mills (2016). "Anti-PD-1 inhibits Foxp3+ Treg cell conversion and unleashes intratumoural effector T cells thereby enhancing the efficacy of a cancer vaccine in a mouse model". *Cancer Immunology, Immunotherapy* 65 (12), pp. 1491–1498. DOI: 10.1007/s00262-016-1906-6.

Ebelt, Kathleen, Gregor Babaryka, Ainhoa M. Figel, Heike Pohla, Alexander Buchner, Christian G. Stief, Wolfgang Eisenmenger, Thomas Kirchner, Dolores J. Schendel, and Elfriede Noessner (Jan. 2008). "Dominance of CD4+ lymphocytic infiltrates with disturbed effector cell characteristics in the tumor microenvironment of prostate carcinoma". *The Prostate* 68 (1), pp. 1–10. DOI: 10.1002/PROS.20661.

Eferl, Robert and Erwin F Wagner (2003). "AP-1: a double-edged sword in tumorigenesis". *Nature Reviews Cancer* 3 (11), pp. 859–868. DOI: 10.1038/nrc1209.

Eil, Robert, Suman K Vodnala, David Clever, Christopher A Klebanoff, Madhusudhanan Sukumar, Jenny H Pan, Douglas C Palmer, Alena Gros, Tori N Yamamoto, Shashank J Patel, Geoffrey C Guittard, Zhiya Yu, Valentina Carbonaro, Klaus Okkenhaug, David S Schrump, W Marston Linehan, Rahul Roychoudhuri, and Nicholas P Restifo (2016). "Ionic immune suppression within the tumour microenvironment limits T cell effector function". *Nature* 537 (7621), pp. 539–543. DOI: 10.1038/nature19364.

Ekman, Simon, Johan Harmenberg, Jan-Erik Frodin, Stefan Bergstrom, Cecilia Wassberg, Staffan Eksborg, Olle Larsson, Magnus Axelson, Markus Jerling, Lars Abrahmsen, Asa Hedlund, Carina Alvfors, Birgitta Stahl, and Michael Bergqvist (2016). "A novel oral insulin-like growth factor-1 receptor pathway modulator and its implications for patients with non-small cell lung carcinoma - A phase I clinical trial". *Acta Oncologica* 55.2, pp. 140–148. DOI: 10.3109/0284186X.2015.1049290. eprint: https://doi.org/10.3109/0284186X.2015.1049290.

Elia, Angela Rita, Sara Caputo, and Matteo Bellone (2018). "Immune Checkpoint-Mediated Interactions Between Cancer and Immune Cells in Prostate Adenocarcinoma and Melanoma". *Frontiers in Immunology* 9. DOI: 10.3389/fimmu.2018.01786.

Epstein, Jonathan I., Michael J. Zelefsky, Daniel D. Sjoberg, Joel B. Nelson, Lars Egevad, Cristina Magi-Galluzzi, Andrew J. Vickers, Anil V. Parwani, Victor E. Reuter, Samson W. Fine, James A. Eastham, Peter Wiklund, Misop Han, Chandana A. Reddy, Jay P. Ciezki, Tommy Nyberg, and Eric A. Klein (2016). "A Contemporary Prostate Cancer Grading System: A Validated Alternative to the Gleason Score". *European Urology* 69.3, pp. 428–435. DOI: https://doi.org/10.1016/j.eururo.2015.06.046.

Erlandsson, Ann, Jessica Carlsson, Marie Lundholm, Anna Fält, Sven-Olof Andersson, Ove Andrén, and Sabina Davidsson (2019). "M2 macrophages and regulatory T cells in lethal prostate cancer". *The Prostate* 79.4, pp. 363–369. DOI: https://doi.org/10.1002/pros.23742. eprint: https://onlinelibrary.wiley.com/doi/pdf/10.1002/pros.23742.

Escamilla, Jemima, Shiruyeh Schokrpur, Connie Liu, Saul J. Priceman, Diana Moughon, Ziyue Jiang, Frederic Pouliot, Clara Magyar, James L. Sung, Jingying Xu, Gang Deng, Brian L. West, Gideon Bollag, Yves Fradet, Louis Lacombe, Michael E. Jung, Jiaoti Huang, and Lily Wu (Mar. 2015). "CSF1 Receptor Targeting in Prostate Cancer Reverses Macrophage-Mediated Resistance to Androgen Blockade Therapy". *Cancer Research* 75.6, pp. 950–962. DOI: 10.1158/0008-5472.CAN-14-0992.

Eum, Hye Hyeon, Minsuk Kwon, Daeun Ryu, Areum Jo, Woosung Chung, Nayoung Kim, Yourae Hong, Dae-Soon Son, Seung Tae Kim, Jeeyun Lee, Hae-Ock Lee, and Woong-Yang Park (2020). "Tumor-promoting macrophages prevail in malignant ascites of advanced gastric cancer". *Experimental and Molecular Medicine* 52 (12), pp. 1976–1988. DOI: 10.1038/s12276-020-00538-y.

Faget, Douglas V, Qihao Ren, and Sheila A Stewart (2019). "Unmasking senescence: context-dependent effects of SASP in cancer". *Nature Reviews Cancer* 19 (8), pp. 439–453. DOI: 10.1038/s41568-019-0156-2.

Fahrenholtz, Cale D., Pedro J. Beltran, and Kerry L. Burnstein (2013). "Targeting IGF-IR with Ganitumab Inhibits Tumorigenesis and Increases Durability of Response to Androgen-Deprivation Therapy in VCaP Prostate Cancer Xenografts". *Molecular Cancer Therapeutics* 12.4, pp. 394–404. DOI: 10.1158/1535-7163.MCT-12-0648. eprint: https://aacrjournals.org/mct/article-pdf/12/4/394/2325548/394.pdf.

Fan, Yu-Ching, Yu-Cin Fong, Chun-Tse Kuo, Chia-Wei Li, Wei-Yu Chen, Jian-Da Lin, Florian Bürtin, Michael Linnebacher, Quoc Thang Bui, Kuan-Der Lee, and Yuan-Chin Tsai (2023). "Tumor-derived interleukin-1 receptor antagonist exhibits immunosuppressive functions and promotes pancreatic cancer". *Cell and Bioscience* 13 (1), p. 147. DOI: 10.1186/s13578-023-01090-8.

Fan, WuQiang, Toshihiko Yanase, Hidetaka Morinaga, Taijiro Okabe, Masatoshi Nomura, Hiroaki Daitoku, Akiyoshi Fukamizu, Shigeaki Kato, Ryoichi Takayanagi, and Hajime Nawata (Mar. 2007). "Insulin-like Growth Factor 1/Insulin Signaling Activates Androgen Signaling through Direct Interactions of Foxo1 with Androgen Receptor". *Journal of Biological Chemistry* 282 (10). doi: 10.1074/jbc.M610447200, pp. 7329–7338. DOI: 10.1074/jbc.M610447200.

Fang, Yifang, Albert E. Fliss, Diane M. Robins, and Avrom J. Caplan (1996). "Hsp90 Regulates Androgen Receptor Hormone Binding Affinity in Vivo". *Journal of Biological Chemistry* 271.45, pp. 28697–28702. DOI: https://doi.org/10.1074/jbc.271.45.28697.

Fassnacht, Martin, Alfredo Berruti, Eric Baudin, Michael J Demeure, Jill Gilbert, Harm Haak, Matthias Kroiss, David I Quinn, Elizabeth Hesseltine, Cristina L Ronchi, Massimo Terzolo, Toni K Choueiri, Srinivasu Poondru, Tanya Fleege, Ramona Rorig, Jihong Chen, Andrew W Stephens, Francis Worden, and Gary D Hammer (Apr. 2015). "Linsitinib (OSI-906) versus placebo for patients with locally advanced or metastatic adrenocortical carcinoma: a double-blind, randomised, phase 3 study". *The Lancet Oncology* 16 (4). doi: 10.1016/S1470-2045(15)70081-1, pp. 426–435. DOI: 10.1016/S1470-2045(15)70081-1.

Fauskanger, Marte, Ole Audun Werner Haabeth, Frode Miltzow Skjeldal, Bjarne Bogen, and Anders Aune Tveita (2018). "Tumor Killing by CD4+ T Cells Is Mediated via Induction of Inducible Nitric Oxide Synthase-Dependent Macrophage Cytotoxicity". *Frontiers in Immunology* 9. DOI: 10.3389/fimmu.2018.01684.

Favelyukis, Svetlana, Jeffrey H Till, Stevan R Hubbard, and W Todd Miller (2001). "Structure and autoregulation of the insulin-like growth factor 1 receptor kinase". *Nature Structural Biology* 8 (12), pp. 1058–1063. DOI: 10.1038/nsb721.

Fei, Liyang, Xiaochen Ren, Haijia Yu, and Yifan Zhan (2021). "Targeting the CCL2/CCR2 Axis in Cancer Immunotherapy: One Stone, Three Birds?" *Frontiers in Immunology* 12. DOI: 10.3389/fimmu.2021.771210.

Fein, Miriam R., Xue-Yan He, Ana S. Almeida, Emilis Bruzas, Arnaud Pommier, Ran Yan, Anais Eberhardt, Douglas T. Fearon, Linda Van Aelst, John Erby Wilkinson, Camila O. dos Santos, and Mikala Egeblad (July 2020). "Cancer cell CCR2 orchestrates

suppression of the adaptive immune response". *Journal of Experimental Medicine* 217.10, e20181551. DOI: 10.1084/jem.20181551. eprint: https://rupress.org/jem/article-pdf/217/10/e20181551/1816165/jem_20181551.pdf.

Feng, Dechao, Jie Wang, Dengxiong Li, Ruicheng Wu, Wuran Wei, and Chi Zhang (2023). "Senescence-associated secretory phenotype constructed detrimental and beneficial subtypes and prognostic index for prostate cancer patients undergoing radical prostatectomy". *Discover Oncology* 14 (1), p. 155. DOI: 10.1007/s12672-023-00777-1.

Feng, Mingye, James Y. Chen, Rachel Weissman-Tsukamoto, Jens-Peter Volkmer, Po Yi Ho, Kelly M. McKenna, Samuel Cheshier, Michael Zhang, Nan Guo, Phung Gip, Siddhartha S. Mitra, and Irving L. Weissman (2015). "Macrophages eat cancer cells using their own calreticulin as a guide: Roles of TLR and Btk". *Proceedings of the National Academy of Sciences* 112.7, pp. 2145–2150. DOI: 10.1073/pnas.1424907112. eprint: https://www.pnas.org/doi/pdf/10.1073/pnas.1424907112.

Feng, Mingye, Wen Jiang, Betty Y S Kim, Cheng Cheng Zhang, Yang-Xin Fu, and Irving L Weissman (2019). "Phagocytosis checkpoints as new targets for cancer immunotherapy". *Nature Reviews Cancer* 19 (10), pp. 568–586. DOI: 10.1038/s41568-019-0183-z.

Fernando, Roshini, Oshadi Caldera, and Terry J. Smith (2021). "Therapeutic IGF-I receptor inhibition alters fibrocyte immune phenotype in thyroid-associated ophthalmopathy". *Proceedings of the National Academy of Sciences* 118.52, e2114244118. DOI: 10.1073/pnas.2114244118. eprint: https://www.pnas.org/doi/pdf/10.1073/pnas.2114244118.

Ferte, Charles, Yohann Loriot, Celine Clemenson, Frederic Commo, Andrea Gombos, Jean-Emmanuel Bibault, Ingrid Fumagalli, Saad Hamama, Nathalie Auger, Benoit Lahon, Cyrus Chargari, Julien Calderaro, Jean-Charles Soria, and Eric Deutsch (July 2013). "IGF-1R Targeting Increases the Antitumor Effects of DNA-Damaging Agents in SCLC Model: An Opportunity to Increase the Efficacy of Standard Therapy". *Molecular Cancer Therapeutics* 12.7, pp. 1213–1222. DOI: 10.1158/1535-7163.MCT-12-1067. eprint: https://aacrjournals.org/mct/article-pdf/12/7/1213/2326105/1213.pdf.

Finkelstein, Arseny, Gilad Kunis, Akop Seksenyan, Ayal Ronen, Tamara Berkutzki, David Azoulay, Maya Koronyo-Hamaoui, and Michal Schwartz (Aug. 2011). "Abnormal Changes in NKT Cells, the IGF-1 Axis, and Liver Pathology in an Animal Model of ALS". *PLOS ONE* 6.8, pp. 1–12. DOI: 10.1371/journal.pone.0022374.

Finkeltov, Ina, Scott Kuhn, Tova Glaser, Gila Idelman, John J Wright, Charles T Roberts, and Haim Werner (2002). "Transcriptional regulation of IGF-I receptor gene expression by novel isoforms of the EWS-WT1 fusion protein". *Oncogene* 21 (12), pp. 1890–1898. DOI: 10.1038/sj.onc.1205042.

Fizazi, Karim, NamPhuong Tran, Luis Fein, Nobuaki Matsubara, Alfredo Rodriguez-Antolin, Boris Y. Alekseev, Mustafa Özgüroğlu, Dingwei Ye, Susan Feyerabend, Andrew Protheroe, Peter De Porre, Thian Kheoh, Youn C. Park, Mary B. Todd, and Kim N. Chi (2017). "Abiraterone plus Prednisone in Metastatic, Castration-Sensitive Prostate Cancer". *New England Journal of Medicine* 377.4, pp. 352–360. DOI: 10.1056/NEJMoa1704174. eprint: https://www.nejm.org/doi/pdf/10.1056/NEJMoa1704174.

Fleischmann, Achim, Thorsten Schlomm, Jens Köllermann, Nikolina Sekulic, Hartwig Huland, Martina Mirlacher, Guido Sauter, Ronald Simon, and Andreas Erbersdobler (2009). "Immunological microenvironment in prostate cancer: High mast cell densities are associated with favorable tumor characteristics and good prognosis".

The Prostate 69.9, pp. 976–981. DOI: https://doi.org/10.1002/pros.20948. eprint: https://onlinelibrary.wiley.com/doi/pdf/10.1002/pros.20948.

Fontenot, Jason D, Marc A Gavin, and Alexander Y Rudensky (2003). "Foxp3 programs the development and function of CD4+CD25+ regulatory T cells". *Nature Immunology* 4 (4), pp. 330–336. DOI: 10.1038/ni904.

Foulstone, E, S Prince, O Zaccheo, JL Burns, J Harper, C Jacobs, D Church, and AB Hassan (2005). "Insulin-like growth factor ligands, receptors, and binding proteins in cancer". *The Journal of Pathology* 205.2, pp. 145–153. DOI: https://doi.org/10.1002/path.1712. eprint: https://pathsocjournals.onlinelibrary.wiley.com/doi/pdf/10.1002/path.1712.

Fourcade, Julien, Zhaojun Sun, Mourad Benallaoua, Philippe Guillaume, Immanuel F. Luescher, Cindy Sander, John M. Kirkwood, Vijay Kuchroo, and Hassane M. Zarour (Sept. 2010). "Upregulation of Tim-3 and PD-1 expression is associated with tumor antigen–specific CD8+ T cell dysfunction in melanoma patients". *Journal of Experimental Medicine* 207.10, pp. 2175–2186. DOI: 10.1084/jem.20100637. eprint: https://rupress.org/jem/article-pdf/207/10/2175/1736223/jem_20100637.pdf.

Franciszkiewicz, Katarzyna, Alexandre Boissonnas, Marie Boutet, Christophe Combadière, and Fathia Mami-Chouaib (Dec. 2012). "Role of Chemokines and Chemokine Receptors in Shaping the Effector Phase of the Antitumor Immune Response". *Cancer Research* 72.24, pp. 6325–6332. DOI: 10.1158/0008-5472.CAN-12-2027. eprint: https://aacrjournals.org/cancerres/article-pdf/72/24/6325/2675041/6325.pdf.

Franke, Thomas F, David R Kaplan, and Lewis C Cantley (1997). "PI3K: Downstream AKTion Blocks Apoptosis". *Cell* 88.4, pp. 435–437. DOI: https://doi.org/10.1016/S0092-8674(00)81883-8.

Frasca, F., G. Pandini, P. Scalia, L. Sciacca, R. Mineo, A. Costantino, I. D. Goldfine, A. Belfiore, and R. Vigneri (1999). "Insulin Receptor Isoform A, a Newly Recognized, High-Affinity Insulin-Like Growth Factor II Receptor in Fetal and Cancer Cells". *Molecular and Cellular Biology* 19.5, pp. 3278–3288. DOI: 10.1128/MCB.19.5.3278. eprint: https://doi.org/10.1128/MCB.19.5.3278.

Frasca, Francesco, Giuseppe Pandini, Laura Sciacca, Vincenzo Pezzino, Sebastiano Squatrito, Antonio Belfiore, and Riccardo Vigneri (2008). "The role of insulin receptors and IGF-I receptors in cancer and other diseases". *Archives of Physiology and Biochemistry* 114.1, pp. 23–37. DOI: 10.1080/13813450801969715. eprint: https://doi.org/10.1080/13813450801969715.

Fraser, Michael, Veronica Y Sabelnykova, Takafumi N Yamaguchi, Lawrence E Heisler, Julie Livingstone, Vincent Huang, Yu-Jia Shiah, Fouad Yousif, Xihui Lin, Andre P Masella, Natalie S Fox, Michael Xie, Stephenie D Prokopec, Alejandro Berlin, Emilie Lalonde, Musaddeque Ahmed, Dominique Trudel, Xuemei Luo, Timothy A Beck, Alice Meng, Junyan Zhang, Alister D'Costa, Robert E Denroche, Haiying Kong, Shadrielle Melijah G Espiritu, Melvin L K Chua, Ada Wong, Taryne Chong, Michelle Sam, Jeremy Johns, Lee Timms, Nicholas B Buchner, Michele Orain, Valerie Picard, Helene Hovington, Alexander Murison, Ken Kron, Nicholas J Harding, Christine P'ng, Kathleen E Houlahan, Kenneth C Chu, Bryan Lo, Francis Nguyen, Constance H Li, Ren X Sun, Richard de Borja, Christopher I Cooper, Julia F Hopkins, Shaylan K Govind, Clement Fung, Daryl Waggott, Jeffrey Green, Syed Haider, Michelle A Chan-Seng-Yue, Esther Jung, Zhiyuan Wang, Alain Bergeron, Alan Dal Pra, Louis Lacombe, Colin C Collins, Cenk Sahinalp, Mathieu Lupien, Neil E Fleshner, Housheng H He, Yves Fradet, Bernard Tetu, Theodorus van der Kwast, John D McPherson,

Robert G Bristow, and Paul C Boutros (2017). "Genomic hallmarks of localized, non-indolent prostate cancer". *Nature* 541 (7637), pp. 359–364. DOI: 10.1038/nature20788.

Freeman, Gordon J., Andrew J. Long, Yoshiko Iwai, Karen Bourque, Tatyana Chernova, Hiroyuki Nishimura, Lori J. Fitz, Nelly Malenkovich, Taku Okazaki, Michael C. Byrne, Heidi F. Horton, Lynette Fouser, Laura Carter, Vincent Ling, Michael R. Bowman, Beatriz M. Carreno, Mary Collins, Clive R. Wood, and Tasuku Honjo (Oct. 2000). "Engagement of the Pd-1 Immunoinhibitory Receptor by a Novel B7 Family Member Leads to Negative Regulation of Lymphocyte Activation". *Journal of Experimental Medicine* 192.7, pp. 1027–1034. DOI: 10.1084/jem.192.7.1027. eprint: https://rupress.org/jem/article-pdf/192/7/1027/1699884/001387.pdf.

Fridman, Wolf H, Laurence Zitvogel, Catherine Sautes–Fridman, and Guido Kroemer (2017). "The immune contexture in cancer prognosis and treatment". *Nature Reviews Clinical Oncology* 14 (12), pp. 717–734. DOI: 10.1038/nrclinonc.2017.101.

Friedbichler, Katrin, Marco H. Hofmann, Monika Kroez, Elinborg Ostermann, Herbert R. Lamche, Christian Koessl, Eric Borges, Michael N. Pollak, Geunther Adolf, and Paul J. Adam (Feb. 2014). "Pharmacodynamic and Antineoplastic Activity of BI 836845, a Fully Human IGF Ligand-Neutralizing Antibody, and Mechanistic Rationale for Combination with Rapamycin". *Molecular Cancer Therapeutics* 13 (2), pp. 399–409. DOI: 10.1158/1535-7163.MCT-13-0598/85425/AM/PHARMACODYNAMIC-AND-ANTINEOPLASTIC-ACTIVITY-OF-BI.

Friedlander, Terence W., Vivian K. Weinberg, Yong Huang, Joanna T. Mi, Carl G. Formaker, Eric J. Small, Andrea L. Harzstark, Amy M. Lin, Lawrence Fong, and Charles J. Ryan (Jan. 2012). "A phase II study of insulin-like growth factor receptor inhibition with nordihydroguaiaretic acid in men with non-metastatic hormone-sensitive prostate cancer". *Oncology Reports* 27 (1), pp. 3–9. DOI: 10.3892/OR.2011.1487/HTML.

Fuchs, Serge Y., Victor Adler, Matthew R. Pincus, and Ze'ev Ronai (1998). "MEKK1/JNK signaling stabilizes and activates p53". *Proceedings of the National Academy of Sciences* 95.18, pp. 10541–10546. DOI: 10.1073/pnas.95.18.10541. eprint: https://www.pnas.org/doi/pdf/10.1073/pnas.95.18.10541.

Fujioka, Shuichi, Jiangong Niu, Christian Schmidt, Guido M. Sclabas, Bailu Peng, Tadashi Uwagawa, Zhongkui Li, Douglas B. Evans, James L. Abbruzzese, and Paul J. Chiao (2004). "NF-kB and AP-1 Connection: Mechanism of NF-kB-Dependent Regulation of AP-1 Activity". *Molecular and Cellular Biology* 24.17. PMID: 15314185, pp. 7806–7819. DOI: 10.1128/MCB.24.17.7806-7819.2004. eprint: https://doi.org/10.1128/MCB.24.17.7806-7819.2004.

Fujita, Kazutoshi and Norio Nonomura (Sept. 2019). "Role of Androgen Receptor in Prostate Cancer: A Review". *World J Mens Health* 37 (3), pp. 288–295.

Fukuda, Ryo, Kiichi Hirota, Fan Fan, Young Do Jung, Lee M Ellis, and Gregg L Semenza (Oct. 2002). "Insulin-like Growth Factor 1 Induces Hypoxia-inducible Factor 1-mediated Vascular Endothelial Growth Factor Expression, Which is Dependent on MAP Kinase and Phosphatidylinositol 3-Kinase Signaling in Colon Cancer Cells". *Journal of Biological Chemistry* 277 (41). doi: 10.1074/jbc.M203781200, pp. 38205–38211. DOI: 10.1074/jbc.M203781200.

Gabrilovich, Dmitry I and Srinivas Nagaraj (2009). "Myeloid-derived suppressor cells as regulators of the immune system". *Nature Reviews Immunology* 9 (3), pp. 162–174. DOI: 10.1038/nri2506.

Gajewski, Thomas F., Hans Schreiber, and Yang Xin Fu (Sept. 2013). "Innate and adaptive immune cells in the tumor microenvironment". *Nature Immunology* 14 (10), pp. 1014–1022. DOI: 10.1038/ni.2703.

Galluzzi, Lorenzo and Guido Kroemer (Dec. 2008). "Necroptosis: A Specialized Pathway of Programmed Necrosis". *Cell* 135 (7). doi: 10.1016/j.cell.2008.12.004, pp. 1161–1163. DOI: 10.1016/j.cell.2008.12.004.

Gamrekelashvili, Jaba, Tim F Greten, and Firouzeh Korangy (2015). "Immunogenicity of necrotic cell death". *Cellular and Molecular Life Sciences* 72 (2), pp. 273–283. DOI: 10.1007/s00018-014-1741-x.

Gao, Jin, Jon W. Chesebrough, Susan A. Cartlidge, Sally-Ann Ricketts, Leonard Incognito, Margaret Veldman-Jones, David C. Blakey, Mohammad Tabrizi, Bahija Jallal, Pamela A. Trail, Steven Coats, Klaus Bosslet, and Yong S. Chang (Feb. 2011). "Dual IGF-I/II–Neutralizing Antibody MEDI-573 Potently Inhibits IGF Signaling and Tumor Growth". *Cancer Research* 71.3, pp. 1029–1040. DOI: 10.1158/0008-5472.CAN-10-2274. eprint: https://aacrjournals.org/cancerres/article-pdf/71/3/1029/2663142/1029.pdf.

Garcia, Alejandro J., Marcus Ruscetti, Teresita L. Arenzana, Linh M. Tran, Daniella Bianci-Frias, Elysia Sybert, Saul J. Priceman, Lily Wu, Peter S. Nelson, Stephen T. Smale, and Hong Wu (2014). "Pten Null Prostate Epithelium Promotes Localized Myeloid-Derived Suppressor Cell Expansion and Immune Suppression during Tumor Initiation and Progression". *Molecular and Cellular Biology* 34.11, pp. 2017–2028. DOI: 10.1128/MCB.00090-14.

Garcia, Jorge A, Paul Elson, Matthew M Cooney, Allison Janine Tyler, Victoria Rezash, Ernest C Borden, and Robert Dreicer (May 2013). "Inhibition of the IGF pathway in metastatic castrate resistant prostate cancer (CRPC) Results from a phase II study of OSI-906 (linsitinib)." *Journal of Clinical Oncology* 31. DOI: 10.1200/jco.2013.31.15_suppl.e16022.

Gardner, Eugene J., Katherine A. Kentistou, Stasa Stankovic, Samuel Lockhart, Eleanor Wheeler, Felix R. Day, Nicola D. Kerrison, Nicholas J. Wareham, Claudia Langenberg, Stephen O'Rahilly, Ken K. Ong, and John R.B. Perry (2022). "Damaging missense variants in IGF1R implicate a role for IGF-1 resistance in the etiology of type 2 diabetes". *Cell Genomics* 2.12, p. 100208. DOI: https://doi.org/10.1016/j.xgen.2022.100208.

Ge, Nie-Lin and Stuart Rudikoff (2000). "Insulin-like growth factor I is a dual effector of multiple myeloma cell growth". *Blood* 96.8, pp. 2856–2861. DOI: https://doi.org/10.1182/blood.V96.8.2856.

Ge, Rong-Ti, Li-Hua Mo, Ruijin Wu, Jiang-Qi Liu, Huan-Ping Zhang, Zhigang Liu, Zhanju Liu, and Ping-Chang Yang (2015). "Insulin-like growth factor-1 endues monocytes with immune suppressive ability to inhibit inflammation in the intestine". *Scientific Reports* 5 (1), p. 7735. DOI: 10.1038/srep07735.

Ge, Rongbin, Zongwei Wang, and Liang Cheng (2022). "Tumor microenvironment heterogeneity an important mediator of prostate cancer progression and therapeutic resistance". *npj Precision Oncology* 6 (1), p. 31. DOI: 10.1038/s41698-022-00272-w.

Geels, Shannon N, Alexander Moshensky, Rachel S Sousa, Claire Murat, Matias A Bustos, Benjamin L Walker, Rima Singh, Stacey N Harbour, Giselle Gutierrez, Michael Hwang, Thorsten R Mempel, Casey T Weaver, Qing Nie, Dave S B Hoon, Anand K Ganesan, Shivashankar Othy, and Francesco Marangoni (June 2024). "Interruption of the intratumor

CD8+ T cell:Treg crosstalk improves the efficacy of PD-1 immunotherapy". *Cancer Cell* 42 (6). doi: 10.1016/j.ccell.2024.05.013, 1051–1066.e7. DOI: 10.1016/j.ccell.2024.05.013.

Georget, Virginie, Beatrice Terouanne, Jean-Claude Nicholas, and Charles Sultan (Oct. 2002). "Mechanism of Antiandrogen Action: Key Role of Hsp90 in Conformational Change and Transcriptional Activity of the Androgen Receptor". *Biochemistry* 41 (39), pp. 11824–11831. DOI: 10.1021/bi0259150.

Gleason, Donald F. (1992). "Histologic grading of prostate cancer: A perspective". *Human Pathology* 23.3. The Pathobiology of Prostate Cancer-Part 1, pp. 273–279. DOI: https://doi.org/10.1016/0046-8177(92)90108-F.

Gleason, Donald F., George T. Mellinger, and The Veterans Administration Cooperative Urological Research Group (1974). "Prediction of Prognosis for Prostatic Adenocarcinoma by Combined Histological Grading and Clinical Staging". *The Journal of Urology* 111 (1), pp. 58–64. DOI: 10.1016/S0022-5347(17)59889-4.

Goh, Kee Chuan, S.Jaharul Haque, and Bryan R.G. Williams (1999). "p38 MAP kinase is required for STAT1 serine phosphorylation and transcriptional activation induced by interferons". *The EMBO Journal* 18.20, pp. 5601–5608. DOI: https://doi.org/10.1093/emboj/18.20.5601. eprint: https://www.embopress.org/doi/pdf/10.1093/emboj/18.20.5601.

Goldstein, Andrew S., Jiaoti Huang, Changyong Guo, Isla P. Garraway, and Owen N. Witte (2010). "Identification of a Cell of Origin for Human Prostate Cancer". *Science* 329.5991, pp. 568–571. DOI: 10.1126/science.1189992. eprint: https://www.science.org/doi/pdf/10.1126/science.1189992.

Gondek, David C., Li-Fan Lu, Sergio A. Quezada, Shimon Sakaguchi, and Randolph J. Noelle (Feb. 2005). "Cutting Edge: Contact-Mediated Suppression by CD4+CD25+ Regulatory Cells Involves a Granzyme B-Dependent, Perforin-Independent Mechanism". *The Journal of Immunology* 174.4, pp. 1783–1786. DOI: 10.4049/jimmunol.174.4.1783. eprint: https://journals.aai.org/jimmunol/article-pdf/174/4/1783/1196612/1783.pdf.

Gordon, Siamon (2003). "Alternative activation of macrophages". *Nature Reviews Immunology* 3 (1), pp. 23–35. DOI: 10.1038/nri978.

Gordon, Sydney R, Roy L Maute, Ben W Dulken, Gregor Hutter, Benson M George, Melissa N McCracken, Rohit Gupta, Jonathan M Tsai, Rahul Sinha, Daniel Corey, Aaron M Ring, Andrew J Connolly, and Irving L Weissman (2017). "PD-1 expression by tumour-associated macrophages inhibits phagocytosis and tumour immunity". *Nature* 545 (7655), pp. 495–499. DOI: 10.1038/nature22396.

Graham, Tisheeka R., Haiyen E. Zhau, Valerie A. Odero-Marah, Adeboye O. Osunkoya, K. Sean Kimbro, Mourad Tighiouart, Tongrui Liu, Jonathan W. Simons, and Ruth M. O'Regan (Apr. 2008). "Insulin-like Growth Factor-I–Dependent Up-regulation of ZEB1 Drives Epithelial-to-Mesenchymal Transition in Human Prostate Cancer Cells". *Cancer Research* 68 (7), pp. 2479–2488. DOI: 10.1158/0008-5472.CAN-07-2559.

Grakoui, Arash, Shannon K. Bromley, Cenk Sumen, Mark M. Davis, Andrey S. Shaw, Paul M. Allen, and Michael L. Dustin (1999). "The Immunological Synapse: A Molecular Machine Controlling T Cell Activation". *Science* 285.5425, pp. 221–227. DOI: 10.1126/science.285.5425.221. eprint: https://www.science.org/doi/pdf/10.1126/science.285.5425.221.

Grasso, Catherine S, Yi-Mi Wu, Dan R Robinson, Xuhong Cao, Saravana M Dhanasekaran, Amjad P Khan, Michael J Quist, Xiaojun Jing, Robert J Lonigro, J Chad Brenner, Irfan A Asangani, Bushra Ateeq, Sang Y Chun, Javed Siddiqui, Lee Sam, Matt Anstett,

Rohit Mehra, John R Prensner, Nallasivam Palanisamy, Gregory A Ryslik, Fabio Vandin, Benjamin J Raphael, Lakshmi P Kunju, Daniel R Rhodes, Kenneth J Pienta, Arul M Chinnaiyan, and Scott A Tomlins (2012). "The mutational landscape of lethal castration-resistant prostate cancer". *Nature* 487 (7406), pp. 239–243. DOI: 10.1038/nature11125.

Grebinoski, Stephanie, Qianxia Zhang, Anthony R Cillo, Sasikanth Manne, Hanxi Xiao, Erin A Brunazzi, Tracy Tabib, Carly Cardello, Christine G Lian, George F Murphy, Robert Lafyatis, E John Wherry, Jishnu Das, Creg J Workman, and Dario A A Vignali (2022). "Autoreactive CD8+ T cells are restrained by an exhaustion-like program that is maintained by LAG3". *Nature Immunology* 23 (6), pp. 868–877. DOI: 10.1038/s41590-022-01210-5.

Grist, Emily, Stefanie Friedrich, Christopher Brawley, Larissa Mendes, Marina Parry, Adnan Ali, Aine Haran, Alex Hoyle, Claire Gilson, Sharanpreet Lall, Leila Zakka, Carla Bautista, Alex Landless, Karolina Nowakowska, Anna Wingate, Daniel Wetterskog, A M Mahedi Hasan, Nafisah B Akato, Malissa Richmond, Sofeya Ishaq, Nik Matthews, Anis A Hamid, Christopher J Sweeney, Matthew R Sydes, Daniel M Berney, Stefano Lise, Mahesh K B Parmar, Noel W Clarke, Nicholas D James, Paolo Cremaschi, Louise C Brown, Gerhardt Attard, and STAMPEDE investigators (2022). "Accumulation of copy number alterations and clinical progression across advanced prostate cancer". *Genome Medicine* 14 (1), p. 102. DOI: 10.1186/s13073-022-01080-4.

Grossman, William J., James W. Verbsky, Benjamin L. Tollefsen, Claudia Kemper, John P. Atkinson, and Timothy J. Ley (Nov. 2004). "Differential expression of granzymes A and B in human cytotoxic lymphocyte subsets and T regulatory cells". *Blood* 104.9, pp. 2840–2848. DOI: 10.1182/blood-2004-03-0859. eprint: https://ashpublications.org/blood/article-pdf/104/9/2840/1703244/zh802104002840.pdf.

Gual, Philippe, Véronique Baron, Valerie Lequoy, and Emmanuel Van Obberghen (Mar. 1998). "Interaction of Janus Kinases JAK-1 and JAK-2 with the Insulin Receptor and the Insulin-Like Growth Factor-1 Receptor". *Endocrinology* 139.3, pp. 884–893. DOI: 10.1210/endo.139.3.5829. eprint: https://academic.oup.com/endo/article-pdf/139/3/884/10349805/endo0884.pdf.

Gubin, Matthew M, Ekaterina Esaulova, Jeffrey P Ward, Olga N Malkova, Daniele Runci, Pamela Wong, Takuro Noguchi, Cora D Arthur, Wei Meng, Elise Alspach, Ruan F V Medrano, Catrina Fronick, Michael Fehlings, Evan W Newell, Robert S Fulton, Kathleen C F Sheehan, Stephen T Oh, Robert D Schreiber, and Maxim N Artyomov (Nov. 2018). "High-Dimensional Analysis Delineates Myeloid and Lymphoid Compartment Remodeling during Successful Immune-Checkpoint Cancer Therapy". *Cell* 175 (4). doi: 10.1016/j.cell.2018.09.030, 1014–1030.e19. DOI: 10.1016/j.cell.2018.09.030.

Guccini, Ilaria, Ajinkya Revandkar, Mariantonietta D'Ambrosio, Manuel Colucci, Emiliano Pasquini, Simone Mosole, Martina Troiani, Daniela Brina, Raheleh Sheibani-Tezerji, Angela Rita Elia, Andrea Rinaldi, Nicolò Pernigoni, Jan Hendrik Rüschoff, Susanne Dettwiler, Angelo M. De Marzo, Emmanuel S. Antonarakis, Costanza Borrelli, Andreas E. Moor, Ramon Garcia-Escudero, Abdullah Alajati, Giuseppe Attanasio, Marco Losa, Holger Moch, Peter Wild, Gerda Egger, and Andrea Alimonti (2021). "Senescence Reprogramming by TIMP1 Deficiency Promotes Prostate Cancer Metastasis". *Cancer Cell* 39.1, 68–82.e9. DOI: https://doi.org/10.1016/j.ccell.2020.10.012.

Guevara-Aguirre, Jaime, Priya Balasubramanian, Marco Guevara-Aguirre, Min Wei, Federica Madia, Chia-Wei Cheng, David Hwang, Alejandro Martin-Montalvo, Jannette Saavedra, Sue Ingles, Rafael de Cabo, Pinchas Cohen, and Valter D. Longo (2011). "Growth Hormone Receptor Deficiency Is Associated with a Major Reduction in Pro-Aging Signaling, Cancer, and Diabetes in Humans". *Science Translational Medicine* 3.70, 70ra13–70ra13. DOI: 10.1126/scitranslmed.3001845. eprint: https://www.science.org/doi/pdf/10.1126/scitranslmed.3001845.

Gundem, Gunes, Peter Van Loo, Barbara Kremeyer, Ludmil B. Alexandrov, Jose M. C. Tubio, Elli Papaemmanuil, Daniel S. Brewer, Heini M. L. Kallio, Gunilla Högnäs, Matti Annala, Kati Kivinummi, Victoria Goody, Calli Latimer, Sarah O'Meara, Kevin J. Dawson, William Isaacs, Michael R. Emmert-Buck, Matti Nykter, Christopher Foster, Zsofia Kote-Jarai, Douglas Easton, Hayley C. Whitaker, David E. Neal, Colin S. Cooper, Rosalind A. Eeles, Tapio Visakorpi, Peter J. Campbell, Ultan McDermott, David C. Wedge, G. Steven Bova, and ICGC Prostate UK Group (2015). "The evolutionary history of lethal metastatic prostate cancer". *Nature* 520.7547, pp. 353–357. DOI: 10.1038/nature14347.

Guo, Christina, Adam Sharp, Bora Gurel, Mateus Crespo, Ines Figueiredo, Suneil Jain, Ursula Vogl, Jan Rekowski, Mahtab Rouhifard, Lewis Gallagher, Wei Yuan, Suzanne Carreira, Khobe Chandran, Alec Paschalis, Ilaria Colombo, Anastasios Stathis, Claudia Bertan, George Seed, Jane Goodall, Florence Raynaud, Ruth Ruddle, Karen E Swales, Jason Malia, Denisa Bogdan, Crescens Tiu, Reece Caldwell, Caterina Aversa, Ana Ferreira, Antje Neeb, Nina Tunariu, Daniel Westaby, Juliet Carmichael, Maria Dolores Fenor de la Maza, Christina Yap, Ruth Matthews, Hannah Badham, Toby Prout, Alison Turner, Mona Parmar, Holly Tovey, Ruth Riisnaes, Penny Flohr, Jesus Gil, David Waugh, Shaun Decordova, Anna Schlag, Bianca Cali, Andrea Alimonti, and Johann S de Bono (2023). "Targeting myeloid chemotaxis to reverse prostate cancer therapy resistance". *Nature* 623 (7989), pp. 1053–1061. DOI: 10.1038/s41586-023-06696-z.

Guo, F, Y Wang, J Liu, S C Mok, F Xue, and W Zhang (2016). "CXCL12/CXCR4: a symbiotic bridge linking cancer cells and their stromal neighbors in oncogenic communication networks". *Oncogene* 35 (7), pp. 816–826. DOI: 10.1038/onc.2015.139.

Gurel, Bora, Tsuyoshi Iwata, Cheryl M Koh, Robert B Jenkins, Fusheng Lan, Chi Van Dang, Jessica L Hicks, James Morgan, Toby C Cornish, Siobhan Sutcliffe, William B Isaacs, Jun Luo, and Angelo M De Marzo (Sept. 2008). "Nuclear MYC protein overexpression is an early alteration in human prostate carcinogenesis". *Modern Pathology* 21 (9). doi: 10.1038/modpathol.2008.111, pp. 1156–1167. DOI: 10.1038/modpathol.2008.111.

Gustin, Jason A, Osman N Ozes, Hakan Akca, Roxana Pincheira, Lindsey D Mayo, Qiutang Li, Javier Rivera Guzman, Chandrashekhar K Korgaonkar, and David B Donner (Jan. 2004). "Cell Type-specific Expression of the IkB Kinases Determines the Significance of Phosphatidylinositol 3-Kinase/Akt Signaling to NFkB Activation". *Journal of Biological Chemistry* 279 (3). doi: 10.1074/jbc.M306976200, pp. 1615–1620. DOI: 10.1074/jbc.M306976200.

Haffner, Michael C, Wilbert Zwart, Martine P Roudier, Lawrence D True, William G Nelson, Jonathan I Epstein, Angelo M De Marzo, Peter S Nelson, and Srinivasan Yegnasubramanian (2021). "Genomic and phenotypic heterogeneity in prostate cancer". *Nature Reviews Urology* 18 (2), pp. 79–92. DOI: 10.1038/s41585-020-00400-w.

Hagan, Michael, Li Wang, John R. Hanley, Jong Sung Park, and Paul Dent (Apr. 2000). "Ionizing Radiation-Induced Mitogen-Activated Protein (MAP) Kinase Activation in

DU145 Prostate Carcinoma Cells: MAP Kinase Inhibition Enhances Radiation-Induced Cell Killing and G2/M-Phase Arrest". *Radiation Research* 153 (4), pp. 371–383. DOI: 10.1667/0033-7587(2000)153.

Hagemann, Thorsten, Julia Wilson, Frances Burke, Hagen Kulbe, Ninfeng Fiona Li, Annette Plüddemann, Kellie Charles, Siamon Gordon, and Frances R. Balkwill (Apr. 2006). "Ovarian Cancer Cells Polarize Macrophages Toward A Tumor-Associated Phenotype1". *The Journal of Immunology* 176.8, pp. 5023–5032. DOI: 10.4049/jimmunol.176.8.5023. eprint: https://journals.aai.org/jimmunol/article-pdf/176/8/5023/1219476/5023.pdf.

Haikala, Heidi M, Johanna M Anttila, Elsa Marques, Tiina Raatikainen, Mette Ilander, Henna Hakanen, Hanna Ala-Hongisto, Mariel Savelius, Diego Balboa, Bjoern Von Eyss, Vilja Eskelinen, Pauliina Munne, Anni I Nieminen, Timo Otonkoski, Julia Schuler, Teemu D Laajala, Tero Aittokallio, Harri Sihto, Johanna Mattson, Paivi Heikkila, Marjut Leidenius, Heikki Joensuu, Satu Mustjoki, Panu Kovanen, Martin Eilers, Joel D Leverson, and Juha Klefström (2019). "Pharmacological reactivation of MYC-dependent apoptosis induces susceptibility to anti-PD-1 immunotherapy". *Nature Communications* 10 (1), p. 620. DOI: 10.1038/s41467-019-08541-2.

Hailemichael, Yared, Daniel H Johnson, Noha Abdel-Wahab, Wai Chin Foo, Salah-Eddine Bentebibel, May Daher, Cara Haymaker, Khalida Wani, Chantal Saberian, Dai Ogata, Sang T Kim, Roza Nurieva, Alexander J Lazar, Hamzah Abu-Sbeih, Faisal Fa'ak, Antony Mathew, Yinghong Wang, Adewunmi Falohun, Van Trinh, Chrystia Zobniw, Christine Spillson, Jared K Burks, Muhammad Awiwi, Khaled Elsayes, Luisa Solis Soto, Brenda D Melendez, Michael A Davies, Jennifer Wargo, Jonathan Curry, Cassian Yee, Gregory Lizee, Shalini Singh, Padmanee Sharma, James P Allison, Patrick Hwu, Suhendan Ekmekcioglu, and Adi Diab (May 2022). "Interleukin-6 blockade abrogates immunotherapy toxicity and promotes tumor immunity". *Cancer Cell* 40 (5). doi: 10.1016/j.ccell.2022.04.004, pp. 509–523. DOI: 10.1016/j.ccell.2022.04.004.

Haluska, Paul, Michael Menefee, Elizabeth R. Plimack, Jonathan Rosenberg, Donald Northfelt, Theresa LaVallee, Li Shi, Xiang-Qing Yu, Patricia Burke, Jaiqi Huang, Jaye Viner, Jennifer McDevitt, and Patricia LoRusso (Sept. 2014). "Phase I Dose-Escalation Study of MEDI-573, a Bispecific, Antiligand Monoclonal Antibody against IGFI and IGFII, in Patients with Advanced Solid Tumors". *Clinical Cancer Research* 20.18, pp. 4747–4757. DOI: 10.1158/1078-0432.CCR-14-0114. eprint: https://aacrjournals.org/clincancerres/article-pdf/20/18/4747/2021459/4747.pdf.

Haluska, Paul, Heather M. Shaw, Gretchen N. Batzel, Donghua Yin, Julian R. Molina, L. Rhoda Molife, Timothy A. Yap, M. Luisa Roberts, Amarnath Sharma, Antonio Gualberto, Alex A. Adjei, and Johann S. de Bono (Oct. 2007). "Phase I Dose Escalation Study of the Anti–Insulin-Like Growth Factor-I Receptor Monoclonal Antibody CP-751,871 in Patients with Refractory Solid Tumors". *Clinical Cancer Research* 13.19, pp. 5834–5840. DOI: 10.1158/1078-0432.CCR-07-1118. eprint: https://aacrjournals.org/clincancerres/article-pdf/13/19/5834/1970506/5834.pdf.

Hamdy, Freddie C., Jenny L. Donovan, J. Athene Lane, Malcolm Mason, Chris Metcalfe, Peter Holding, Michael Davis, Tim J. Peters, Emma L. Turner, Richard M. Martin, Jon Oxley, Mary Robinson, John Staffurth, Eleanor Walsh, Prasad Bollina, James Catto, Andrew Doble, Alan Doherty, David Gillatt, Roger Kockelbergh, Howard Kynaston, Alan Paul, Philip Powell, Stephen Prescott, Derek J. Rosario, Edward Rowe, and David E. Neal (2016). "10-Year Outcomes after Monitoring, Surgery, or Radiotherapy for Localized Prostate Cancer". *New England Journal of Medicine* 375.15, pp. 1415–1424. DOI:

10.1056/NEJMoa1606220. eprint: https://www.nejm.org/doi/pdf/10.1056/NEJMoa1606220.

Hamdy, Freddie C., Jenny L. Donovan, J. Athene Lane, Chris Metcalfe, Michael Davis, Emma L. Turner, Richard M. Martin, Grace J. Young, Eleanor I. Walsh, Richard J. Bryant, Prasad Bollina, Andrew Doble, Alan Doherty, David Gillatt, Vincent Gnanapragasam, Owen Hughes, Roger Kockelbergh, Howard Kynaston, Alan Paul, Edgar Paez, Philip Powell, Derek J. Rosario, Edward Rowe, Malcolm Mason, James W.F. Catto, Tim J. Peters, Jon Oxley, Naomi J. Williams, John Staffurth, and David E. Neal (2023). "Fifteen-Year Outcomes after Monitoring, Surgery, or Radiotherapy for Prostate Cancer". *New England Journal of Medicine* 388.17, pp. 1547–1558. DOI: 10.1056/NEJMoa2214122. eprint: https://www.nejm.org/doi/pdf/10.1056/NEJMoa2214122.

Hamilton, John A (2008). "Colony-stimulating factors in inflammation and autoimmunity". *Nature Reviews Immunology* 8 (7), pp. 533–544. DOI: 10.1038/nri2356.

Hammarsten, Peter, Andreas Josefsson, Elin Thysell, Marie Lundholm, Christina Hägglöf, Diego Iglesias-Gato, Amilcar Flores-Morales, Pär Stattin, Lars Egevad, Torvald Granfors, Pernilla Wikström, and Anders Bergh (2019). "Immunoreactivity for prostate specific antigen and Ki67 differentiates subgroups of prostate cancer related to outcome". *Modern Pathology* 32 (9), pp. 1310–1319. DOI: 10.1038/s41379-019-0260-6.

Han, Chenglin, Yuxuan Deng, Wenchao Xu, Zhuo Liu, Tao Wang, Shaogang Wang, Jihong Liu, and Xiaming Liu (2022). "The Roles of Tumor-Associated Macrophages in Prostate Cancer". *Journal of Oncology* 2022. Ed. by Eshan Khan, p. 8580043. DOI: 10.1155/2022/8580043.

Han, Claudia Z, Ignacio J Juncadella, Jason M Kinchen, Monica W Buckley, Alexander L Klibanov, Kelly Dryden, Suna Onengut-Gumuscu, Uta Erdbrügger, Stephen D Turner, Yun M Shim, Kenneth S Tung, and Kodi S Ravichandran (2016). "Macrophages redirect phagocytosis by non-professional phagocytes and influence inflammation". *Nature* 539 (7630), pp. 570–574. DOI: 10.1038/nature20141.

Han, Jichang, Nikhil Khatwani, Tyler G. Searles, Mary Jo Turk, and Christina V. Angeles (2020). "Memory CD8+ T cell responses to cancer". *Seminars in Immunology* 49. SI: Anti-tumor immunity, p. 101435. DOI: https://doi.org/10.1016/j.smim.2020.101435.

Hanahan, Douglas (Jan. 2022). "Hallmarks of Cancer: New Dimensions". *Cancer Discovery* 12.1, pp. 31–46. DOI: 10.1158/2159-8290.CD-21-1059. eprint: https://aacrjournals.org/cancerdiscovery/article-pdf/12/1/31/3052722/31.pdf.

Hanahan, Douglas and Robert A Weinberg (Jan. 2000). "The Hallmarks of Cancer". *Cell* 100 (1). doi: 10.1016/S0092-8674(00)81683-9, pp. 57–70. DOI: 10.1016/S0092-8674(00)81683-9.

– (Mar. 2011). "Hallmarks of Cancer: The Next Generation". *Cell* 144 (5). doi: 10.1016/j.cell.2011.02.013, pp. 646–674. DOI: 10.1016/j.cell.2011.02.013.

Harrington, Laurie E, Robin D Hatton, Paul R Mangan, Henrietta Turner, Theresa L Murphy, Kenneth M Murphy, and Casey T Weaver (2005). "Interleukin 17-producing CD4+ effector T cells develop via a lineage distinct from the T helper type 1 and 2 lineages". *Nature Immunology* 6 (11), pp. 1123–1132. DOI: 10.1038/ni1254.

Harris, William P, Elahe A Mostaghel, Peter S Nelson, and Bruce Montgomery (2009). "Androgen deprivation therapy: progress in understanding mechanisms of resistance and optimizing androgen depletion". *Nature Clinical Practice Urology* 6 (2), pp. 76–85. DOI: 10.1038/ncpuro1296.

Harty, John T and Vladimir P Badovinac (2008). "Shaping and reshaping CD8+ T-cell memory". *Nature Reviews Immunology* 8 (2), pp. 107–119. DOI: 10.1038/nri2251.

Hashimoto, Koji (Dec. 2000). "Regulation of keratinocyte function by growth factors". *Journal of Dermatological Science* 24. doi: 10.1016/S0923-1811(00)00141-9, pp. 46–50. DOI: 10.1016/S0923-1811(00)00141-9.

Hashimoto, Masakazu, John David Konda, Stephanie Perrino, Maria Celia Fernandez, Andrew M. Lowy, and Pnina Brodt (Dec. 2021). "Targeting the IGF-Axis Potentiates Immunotherapy for Pancreatic Ductal Adenocarcinoma Liver Metastases by Altering the Immunosuppressive Microenvironment". *Molecular Cancer Therapeutics* 20.12, pp. 2469–2482. DOI: 10.1158/1535-7163.MCT-20-0144. eprint: https://aacrjournals.org/mct/article-pdf/20/12/2469/3016793/2469.pdf.

Haston, Scott, Estela Gonzalez-Gualda, Samir Morsli, Jianfeng Ge, Virinder Reen, Alexander Calderwood, Ilias Moutsopoulos, Leonidas Panousopoulos, Polina Deletic, Gabriela Carreno, Romain Guiho, Saba Manshaei, Jose Mario Gonzalez-Meljem, Hui Yuan Lim, Daniel J Simpson, Jodie Birch, Husayn A Pallikonda, Tamir Chandra, David Macias, Gary J Doherty, Doris M Rassl, Robert C Rintoul, Massimo Signore, Irina Mohorianu, Arne N Akbar, Jesus Gil, Daniel Munoz-Espin, and Juan Pedro Martinez-Barbera (July 2023). "Clearance of senescent macrophages ameliorates tumorigenesis in KRAS-driven lung cancer". *Cancer Cell* 41 (7). doi: 10.1016/j.ccell.2023.05.004, 1242–1260.e6. DOI: 10.1016/j.ccell.2023.05.004.

Hawley, Jessica E., Matthew Dallos, Emerson A. Lim, Karie Runcie, Jianhua Hu, Israel Lowy, Charles G. Drake, and Mark N. Stein (May 2023a). "The PRIME-CUT study: A single-arm phase 2 study of ADT with PD-1 blockade and docetaxel in men with metastatic hormone-sensitive prostate cancer". *Journal of Clinical Oncology* 41, p. 17098.

Hawley, Jessica E., Aleksandar Z. Obradovic, Matthew C. Dallos, Emerson A. Lim, Karie Runcie, Casey R. Ager, James McKiernan, Christopher B. Anderson, Guarionex J. Decastro, Joshua Weintraub, Renu Virk, Israel Lowy, Jianhua Hu, Matthew G. Chaimowitz, Xinzheng V. Guo, Ya Zhang, Michael C. Haffner, Jeremy Worley, Mark N. Stein, Andrea Califano, and Charles G. Drake (2023b). "Anti-PD-1 immunotherapy with androgen deprivation therapy induces robust immune infiltration in metastatic castration-sensitive prostate cancer". *Cancer Cell* 41.11, pp. 1972–1988. DOI: 10.1016/j.ccell.2023.10.006.

He, Yan, Miao Miao Sun, Guo Geng Zhang, Jing Yang, Kui Sheng Chen, Wen Wen Xu, and Bin Li (2021). "Targeting PI3K/Akt signal transduction for cancer therapy". *Signal Transduction and Targeted Therapy* 6 (1), p. 425. DOI: 10.1038/s41392-021-00828-5.

Hellawell, Giles O, Gareth D H Turner, David R Davies, Richard Poulsom, Simon F Brewster, and Valentine M Macaulay (May 2002). "Expression of the Type 1 Insulin-like Growth Factor Receptor Is Up-Regulated in Primary Prostate Cancer and Commonly Persists in Metastatic Disease". *Cancer Research* 62 (10), pp. 2942–2950.

Hennessy, Bryan T., Debra L. Smith, Prahlad T. Ram, Yiling Lu, and Gordon B. Mills (2005). "Exploiting the PI3K/AKT Pathway for Cancer Drug Discovery". *Nature Reviews Drug Discovery* 4.12, pp. 988–1004. DOI: 10.1038/nrd1902.

Hilchey, Shannon P. and Steven H. Bernstein (2007). "Use of CFSE to Monitor Ex Vivo Regulatory T-cell Suppression of CD4+ and CD8+ T-cell Proliferation within Unseparated Mononuclear Cells from Malignant and Non-Malignant Human Lymph Node Biopsies". *Immunological Investigations* 36.5-6, pp. 629–648. DOI: 10.1080/08820130701674463. eprint: https://doi.org/10.1080/08820130701674463.

Hildner, Kai, Brian T. Edelson, Whitney E. Purtha, Mark Diamond, Hirokazu Matsushita, Masako Kohyama, Boris Calderon, Barbara U. Schraml, Emil R. Unanue, Michael S. Diamond, Robert D. Schreiber, Theresa L. Murphy, and Kenneth M. Murphy

(2008). "Batf3 Deficiency Reveals a Critical Role for CD8a+ Dendritic Cells in Cytotoxic T Cell Immunity". *Science* 322.5904, pp. 1097–1100. DOI: 10.1126/science.1164206. eprint: https://www.science.org/doi/pdf/10.1126/science.1164206.

Himpe, Eddy, Celine Degaillier, Astrid Coppens, and Ron Kooijman (2008). "Insulin-like growth factor-1 delays Fas-mediated apoptosis in human neutrophils through the phosphatidylinositol-3 kinase pathway". *Journal of Endocrinology* 199.1, pp. 69–80. DOI: 10.1677/JOE-08-0028.

Himpe, Eddy and Ron Kooijman (2009). "Insulin-like growth factor-I receptor signal transduction and the Janus Kinase/Signal Transducer and Activator of Transcription (JAK-STAT) pathway". *BioFactors* 35.1, pp. 76–81. DOI: https://doi.org/10.1002/biof.20. eprint: https://iubmb.onlinelibrary.wiley.com/doi/pdf/10.1002/biof.20.

Hirz, Taghreed, Shenglin Mei, Hirak Sarkar, Youmna Kfoury, Shulin Wu, Bronte M Verhoeven, Alexander O Subtelny, Dimitar V Zlatev, Matthew W Wszolek, Keyan Salari, Evan Murray, Fei Chen, Evan Z Macosko, Chin-Lee Wu, David T Scadden, Douglas M Dahl, Ninib Baryawno, Philip J Saylor, Peter V Kharchenko, and David B Sykes (2023). "Dissecting the immune suppressive human prostate tumor microenvironment via integrated single-cell and spatial transcriptomic analyses". *Nature Communications* 14 (1), p. 663. DOI: 10.1038/s41467-023-36325-2.

Hodgson, Myles C., Inna Astapova, Shinta Cheng, Larissa J. Lee, Manon C. Verhoeven, Eunis Choi, Steven P. Balk, and Anthony N. Hollenberg (2005). "The Androgen Receptor Recruits Nuclear Receptor CoRepressor (N-CoR) in the Presence of Mifepristone via Its N and C Termini Revealing a Novel Molecular Mechanism for Androgen Receptor Antagonists". *Journal of Biological Chemistry* 280.8, pp. 6511–6519. DOI: 10.1074/jbc.M408972200.

Hollmen, Maija, Filip Roudnicky, Sinem Karaman, and Michael Detmar (2015). "Characterization of macrophage - cancer cell crosstalk in estrogen receptor positive and triple-negative breast cancer". *Scientific Reports* 5, p. 9188.

Holmberg, Lars, Anna Bill-Axelson, Fred Helgesen, Jaakko O. Salo, Per Folmerz, Michael Häggman, Swen-Olof Andersson, Anders Spångberg, Christer Busch, Steg Nordling, Juni Palmgren, Hans-Olov Adami, Jan-Erik Johansson, and Bo Johan Norlén (2002). "A Randomized Trial Comparing Radical Prostatectomy with Watchful Waiting in Early Prostate Cancer". *New England Journal of Medicine* 347.11, pp. 781–789. DOI: 10.1056/NEJMoa012794. eprint: https://www.nejm.org/doi/pdf/10.1056/NEJMoa012794.

Hong, Matthew K H, Geoff Macintyre, David C Wedge, Peter Van Loo, Keval Patel, Sebastian Lunke, Ludmil B Alexandrov, Clare Sloggett, Marek Cmero, Francesco Marass, Dana Tsui, Stefano Mangiola, Andrew Lonie, Haroon Naeem, Nikhil Sapre, Pramit M Phal, Natalie Kurganovs, Xiaowen Chin, Michael Kerger, Anne Y Warren, David Neal, Vincent Gnanapragasam, Nitzan Rosenfeld, John S Pedersen, Andrew Ryan, Izhak Haviv, Anthony J Costello, Niall M Corcoran, and Christopher M Hovens (2015). "Tracking the origins and drivers of subclonal metastatic expansion in prostate cancer". *Nature Communications* 6 (1), p. 6605. DOI: 10.1038/ncomms7605.

Hori, Shohei, Takashi Nomura, and Shimon Sakaguchi (2003). "Control of Regulatory T Cell Development by the Transcription Factor Foxp3". *Science* 299.5609, pp. 1057–1061. DOI: 10.1126/science.1079490. eprint: https://www.science.org/doi/pdf/10.1126/science.1079490.

Hossain, Dewan M. S., Sumanta K. Pal, Dayson Moreira, Priyanka Duttagupta, Qifang Zhang, Haejung Won, Jeremy Jones, Massimo D'Apuzzo, Stephen Forman, and Marcin Kortylewski (Aug. 2015). "TLR9-Targeted STAT3 Silencing Abrogates Immunosuppressive Activity of Myeloid-Derived Suppressor Cells from Prostate Cancer Patients". *Clinical Cancer Research* 21.16, pp. 3771–3782. DOI: 10.1158/1078-0432.CCR-14-3145. eprint: https://aacrjournals.org/clincancerres/article-pdf/21/16/3771/2027210/3771.pdf.

Hou, Xuwei, Zhaohui Li, Yusuke Higashi, Patrice Delafontaine, and Sergiy Sukhanov (2020). "Insulin-Like Growth Factor I Prevents Cellular Aging via Activation of Mitophagy". *Journal of Aging Research* 2020.1, p. 4939310. DOI: https://doi.org/10.1155/2020/4939310. eprint: https://onlinelibrary.wiley.com/doi/pdf/10.1155/2020/4939310.

Houghton, A. Mc Garry, Jay L. Grisolano, Mary L. Baumann, Dale K. Kobayashi, R. Dean Hautamaki, Leslie C. Nehring, Lynn A. Cornelius, and Steven D. Shapiro (June 2006). "Macrophage Elastase (Matrix Metalloproteinase-12) Suppresses Growth of Lung Metastases". *Cancer Research* 66 (12), pp. 6149–6155. DOI: 10.1158/0008-5472.CAN-04-0297.

Hsieh, Chen-Lin, Ginevra Botta, Shuai Gao, Tiantian Li, Eliezer M. Van Allen, Daniel J. Treacy, Changmeng Cai, Housheng Hansen He, Christopher J. Sweeney, Myles Brown, Steven P. Balk, Peter S. Nelson, Levi A. Garraway, and Philip W. Kantoff (May 2015). "PLZF, a Tumor Suppressor Genetically Lost in Metastatic Castration-Resistant Prostate Cancer, Is a Mediator of Resistance to Androgen Deprivation Therapy". *Cancer Research* 75.10, pp. 1944–1948. DOI: 10.1158/0008-5472.CAN-14-3602. eprint: https://aacrjournals.org/cancerres/article-pdf/75/10/1944/2716912/1944.pdf.

Hu, Wen-Yang, Dan-Ping Hu, Lishi Xie, Larisa Nonn, Ranli Lu, Michael Abern, Toshihiro Shioda, and Gail S. Prins (2021a). "Keratin Profiling by Single-Cell RNA-Sequencing Identifies Human Prostate Stem Cell Lineage Hierarchy and Cancer Stem-Like Cells". *International Journal of Molecular Sciences* 22.15. DOI: 10.3390/ijms22158109.

Hu, Xiaoyi, Jing li, Maorong Fu, Xia Zhao, and Wei Wang (2021b). "The JAK/STAT signaling pathway: from bench to clinic". *Signal Transduction and Targeted Therapy* 6.1, p. 402. DOI: 10.1038/s41392-021-00791-1.

Hua, Hui, Qingbin Kong, Jie Yin, Jin Zhang, and Yangfu Jiang (2020). "Insulin-like growth factor receptor signaling in tumorigenesis and drug resistance: a challenge for cancer therapy". *Journal of Hematology and Oncology* 13 (1), p. 64. DOI: 10.1186/s13045-020-00904-3.

Huang, Ching-Ting, Ming-Cheng Chang, Yu-Li Chen, Tsung-Ching Chen, Chi-An Chen, and Wen-Fang Cheng (2015). "Insulin-like growth factors inhibit dendritic cell-mediated anti-tumor immunity through regulating ERK1/2 phosphorylation and p38 dephosphorylation". *Cancer Letters* 359.1, pp. 117–126. DOI: https://doi.org/10.1016/j.canlet.2015.01.007.

Huang, Yabing, Ling Huang, Jiling Zhu, Yin Wu, Jinzhi Shi, and Kai Dai (Feb. 2022). "Differential expression of insulin-like growth factor type 1 receptor identifies heterogeneous intrahepatic regulatory T subsets in mouse hepatocellular carcinoma". *Clinical and Experimental Immunology* 208.1, pp. 47–59. DOI: 10.1093/cei/uxac011. eprint: https://academic.oup.com/cei/article-pdf/208/1/47/43703960/uxac011.pdf.

Hubbard, Gretchen K., Laura N. Mutton, May Khalili, Ryan P. McMullin, Jessica L. Hicks, Daniella Bianchi-Frias, Lucas A. Horn, Ibrahim Kulac, Michael S. Moubarek, Peter S. Nelson, Srinivasan Yegnasubramanian, Angelo M. De Marzo, and Charles J. Bieberich (Jan. 2016). "Combined MYC Activation and Pten Loss Are Sufficient to Create Genomic Instability and Lethal Metastatic Prostate Cancer". *Cancer Research* 76.2, pp. 283–292. DOI: 10.1158/0008-5472.CAN-14-3280. eprint: https://aacrjournals.org/cancerres/article-pdf/76/2/283/2739174/283.pdf.

Hultner, Lothar, Stephan Kolsch, Michael Stassen, Uwe Kaspers, Jean-Pierre Kremer, Reinhard Mailhammer, Jochen Moeller, Hannelore Broszeit, and Edgar Schmitt (June 2000). "In Activated Mast Cells, IL-1 Up-Regulates the Production of Several Th2-Related Cytokines Including IL-9". *The Journal of Immunology* 164.11, pp. 5556–5563. DOI: 10.4049/jimmunol.164.11.5556. eprint: https://journals.aai.org/jimmunol/article-pdf/164/11/5556/1313459/5556.pdf.

Humphrey, P A (2007). "Diagnosis of adenocarcinoma in prostate needle biopsy tissue". *Journal of Clinical Pathology* 60.1, pp. 35–42. DOI: 10.1136/jcp.2005.036442. eprint: https://jcp.bmj.com/content/60/1/35.full.pdf.

Humphrey, Peter A., Holger Moch, Antonio L. Cubilla, Thomas M. Ulbright, and Victor E. Reuter (2016). "The 2016 WHO Classification of Tumours of the Urinary System and Male Genital Organs—Part B: Prostate and Bladder Tumours". *European Urology* 70.1, pp. 106–119. DOI: https://doi.org/10.1016/j.eururo.2016.02.028.

Huo, Yi, Han Zhang, Longqi Sa, Wenjing Zheng, Yang He, Haohan Lyu, Mengjie Sun, Lingling Zhang, Lequn Shan, Angang Yang, and Tao Wang (2023). "M1 polarization enhances the antitumor activity of chimeric antigen receptor macrophages in solid tumors". *Journal of Translational Medicine* 21 (1), p. 225. DOI: 10.1186/s12967-023-04061-2.

Hussain, Maha, Karim Fizazi, Fred Saad, Per Rathenborg, Neal Shore, Ubirajara Ferreira, Petro Ivashchenko, Eren Demirhan, Katharina Modelska, De Phung, Andrew Krivoshik, and Cora N. Sternberg (2018). "Enzalutamide in Men with Nonmetastatic, Castration-Resistant Prostate Cancer". *New England Journal of Medicine* 378.26, pp. 2465–2474. DOI: 10.1056/NEJMoa1800536. eprint: https://www.nejm.org/doi/pdf/10.1056/NEJMoa1800536.

Idelman, Gila, Gabriella Rustici, Adriana DeSiervi, Quentin Li, Idalia Montano, Cynthia Haggerty, Dennis Taub, and Kevin Gardner (May 2007). "The role of the IGF system in T-lymphocyte activation". *Cancer Research* 67, p. 4392.

Ilic, Dragan, Mia Djulbegovic, Jae Hung Jung, Eu Chang Hwang, Qi Zhou, Anne Cleves, Thomas Agoritsas, and Philipp Dahm (2018). "Prostate cancer screening with prostate-specific antigen (PSA) test: a systematic review and meta-analysis". *BMJ* 362. DOI: 10.1136/bmj.k3519. eprint: https://www.bmj.com/content/362/bmj.k3519.full.pdf.

Inoki, Ken, Yong Li, Tianquan Zhu, Jun Wu, and Kun-Liang Guan (2002). "TSC2 is phosphorylated and inhibited by Akt and suppresses mTOR signalling". *Nature Cell Biology* 4 (9), pp. 648–657. DOI: 10.1038/ncb839.

Ireland, Lucy, Almudena Santos, Muhammad S. Ahmed, Carolyn Rainer, Sebastian R. Nielsen, Valeria Quaranta, Ulrike Weyer-Czernilofsky, Danielle D. Engle, Pedro A. Perez-Mancera, Sarah E. Coupland, Azzam Taktak, Thomas Bogenrieder, David A. Tuveson, Fiona Campbell, Michael C. Schmid, and Ainhoa Mielgo (Nov. 2016). "Chemoresistance in Pancreatic Cancer Is Driven by Stroma-Derived Insulin-Like Growth Factors". *Cancer Research* 76.23, pp. 6851–6863. DOI: 10.1158/0008-5472.CAN-16-1201.

eprint: https://aacrjournals.org/cancerres/article-pdf/76/23/6851/2743339/6851.pdf.

Ireland, Lucy, Almudena Santos, Fiona Campbell, Carlos Figueiredo, Dean Hammond, Lesley G Ellies, Ulrike Weyer-Czernilofsky, Thomas Bogenrieder, Michael Schmid, and Ainhoa Mielgo (2018). "Blockade of insulin-like growth factors increases efficacy of paclitaxel in metastatic breast cancer". *Oncogene* 37 (15), pp. 2022–2036. DOI: 10.1038/s41388-017-0115-x.

Irey, Emily A., Chelsea M. Lassiter, Nicholas J. Brady, Pavlina Chuntova, Ying Wang, Todd P. Knutson, Christine Henzler, Thomas S. Chaffee, Rachel I. Vogel, Andrew C. Nelson, Michael A. Farrar, and Kathryn L. Schwertfeger (2019). "JAK/STAT inhibition in macrophages promotes therapeutic resistance by inducing expression of protumorigenic factors". *Proceedings of the National Academy of Sciences* 116.25, pp. 12442–12451. DOI: 10.1073/pnas.1816410116. eprint: https://www.pnas.org/doi/pdf/10.1073/pnas.1816410116.

Ishida, Y., Y. Agata, K. Shibahara, and T. Honjo (1992). "Induced expression of PD-1, a novel member of the immunoglobulin gene superfamily, upon programmed cell death." *The EMBO Journal* 11.11, pp. 3887–3895. DOI: https://doi.org/10.1002/j.1460-2075.1992.tb05481.x. eprint: https://www.embopress.org/doi/pdf/10.1002/j.1460-2075.1992.tb05481.x.

Issa, Fadi, Joanna Hester, Ryoichi Goto, Satish N Nadig, Tim E Goodacre, and Kathryn Wood (2010). "Ex Vivo–Expanded Human Regulatory T Cells Prevent the Rejection of Skin Allografts in a Humanized Mouse Model". *Transplantation* 90 (12).

Iwai, Yoshiko, Masayoshi Ishida, Yoshimasa Tanaka, Taku Okazaki, Tasuku Honjo, and Nagahiro Minato (2002). "Involvement of PD-L1 on tumor cells in the escape from host immune system and tumor immunotherapy by PD-L1 blockade". *Proceedings of the National Academy of Sciences* 99.19, pp. 12293–12297. DOI: 10.1073/pnas.192461099. eprint: https://www.pnas.org/doi/pdf/10.1073/pnas.192461099.

Iwasaki, Akiko and Ruslan Medzhitov (2010). "Regulation of Adaptive Immunity by the Innate Immune System". *Science* 327.5963, pp. 291–295. DOI: 10.1126/science.1183021. eprint: https://www.science.org/doi/pdf/10.1126/science.1183021.

Jackson, Hartland W, Virginie Defamie, Paul Waterhouse, and Rama Khokha (2017). "TIMPs: versatile extracellular regulators in cancer". *Nature Reviews Cancer* 17 (1), pp. 38–53. DOI: 10.1038/nrc.2016.115.

Jaime-Sanchez, Paula, Iratxe Uranga-Murillo, Nacho Aguilo, Sofia C Khouili, Maykel A Arias, David Sancho, and Julian Pardo (2020). "Cell death induced by cytotoxic CD8+ T cells is immunogenic and primes caspase-3–dependent spread immunity against endogenous tumor antigens". *Journal for ImmunoTherapy of Cancer* 8.1. DOI: 10.1136/jitc-2020-000528. eprint: https://jitc.bmj.com/content/8/1/e000528.full.pdf.

Jaiswal, Siddhartha, Mark P. Chao, Ravindra Majeti, and Irving L. Weissman (June 2010). "Macrophages as mediators of tumor immunosurveillance". *Trends in Immunology* 31 (6), pp. 212–219. DOI: 10.1016/j.it.2010.04.001.

Jamaspishvili, Tamara, David M Berman, Ashley E Ross, Howard I Scher, Angelo M De Marzo, Jeremy A Squire, and Tamara L Lotan (2018). "Clinical implications of PTEN loss in prostate cancer". *Nature Reviews Urology* 15 (4), pp. 222–234. DOI: 10.1038/nrurol.2018.9.

James, Nicholas D, Matthew R Sydes, Noel W Clarke, Malcolm D Mason, David P Dearnaley, Melissa R Spears, Alastair W S Ritchie, Christopher C Parker, J Martin Russell, Gerhardt Attard, Johann de Bono, William Cross, Rob J Jones,

George Thalmann, Claire Amos, David Matheson, Robin Millman, Mymoona Alzouebi, Sharon Beesley, Alison J Birtle, Susannah Brock, Richard Cathomas, Prabir Chakraborti, Simon Chowdhury, Audrey Cook, Tony Elliott, Joanna Gale, Stephanie Gibbs, John D Graham, John Hetherington, Robert Hughes, Robert Laing, Fiona McKinna, Duncan B McLaren, Joe M O'Sullivan, Omi Parikh, Clive Peedell, Andrew Protheroe, Angus J Robinson, Narayanan Srihari, Rajaguru Srinivasan, John Staffurth, Santhanam Sundar, Shaun Tolan, David Tsang, John Wagstaff, and Mahesh K B Parmar (Mar. 2016). "Addition of docetaxel, zoledronic acid, or both to first-line long-term hormone therapy in prostate cancer (STAMPEDE): survival results from an adaptive, multiarm, multistage, platform randomised controlled trial". *The Lancet* 387 (10024). doi: 10.1016/S0140-6736(15)01037-5, pp. 1163–1177. DOI: 10.1016/S0140-6736(15)01037-5.

James, Nicholas D., Johann S. de Bono, Melissa R. Spears, Noel W. Clarke, Malcolm D. Mason, David P. Dearnaley, Alastair W.S. Ritchie, Claire L. Amos, Clare Gilson, Rob J. Jones, David Matheson, Robin Millman, Gerhardt Attard, Simon Chowdhury, William R. Cross, Silke Gillessen, Christopher C. Parker, J. Martin Russell, Dominik R. Berthold, Chris Brawley, Fawzi Adab, San Aung, Alison J. Birtle, Jo Bowen, Susannah Brock, Prabir Chakraborti, Catherine Ferguson, Joanna Gale, Emma Gray, Mohan Hingorani, Peter J. Hoskin, Jason F. Lester, Zafar I. Malik, Fiona McKinna, Neil McPhail, Julian Money-Kyrle, Joe O'Sullivan, Omi Parikh, Andrew Protheroe, Angus Robinson, Narayanan N. Srihari, Carys Thomas, John Wagstaff, James Wylie, Anjali Zarkar, Mahesh K.B. Parmar, and Matthew R. Sydes (2017). "Abiraterone for Prostate Cancer Not Previously Treated with Hormone Therapy". *New England Journal of Medicine* 377.4, pp. 338–351. DOI: 10.1056/NEJMoa1702900. eprint: https://www.nejm.org/doi/pdf/10.1056/NEJMoa1702900.

Al-janabi, Haider, Katy Moyes, Richard Allen, Matthew Fisher, Mateus Crespo, Bora Gurel, Pasquale Rescigno, Johann de Bono, Harry Nunns, Christopher Bailey, Anna Junker-Jensen, Munitta Muthana, Wayne A Phillips, Helen B Pearson, Mary-Ellen Taplin, Janet E Brown, and Claire E Lewis (2024). "Targeting a STING agonist to perivascular macrophages in prostate tumors delays resistance to androgen deprivation therapy". *Journal for ImmunoTherapy of Cancer* 12.7. DOI: 10.1136/jitc-2024-009368. eprint: https://jitc.bmj.com/content/12/7/e009368.full.pdf.

Janssen, Edith M, Edward E Lemmens, Tom Wolfe, Urs Christen, Matthias G von Herrath, and Stephen P Schoenberger (2003). "CD4+ T cells are required for secondary expansion and memory in CD8+ T lymphocytes". *Nature* 421 (6925), pp. 852–856. DOI: 10.1038/nature01441.

Jansson, Magnus, Dan Hallen, Hannu Koho, Gunilla Andersson, Lotta Berghard, Jessica Heidrich, Elisabeth Nyberg, Mathias Uhlén, Johan Kordel, and Bjorn Nilsson (1997). "Characterization of Ligand Binding of a Soluble Human Insulin-like Growth Factor I Receptor Variant Suggests a Ligand-induced Conformational Change*". *Journal of Biological Chemistry* 272.13, pp. 8189–8197. DOI: https://doi.org/10.1074/jbc.272.13.8189.

Jardieu, P, R Clark, D Mortensen, and K Dorshkind (May 1994). "In vivo administration of insulin-like growth factor-I stimulates primary B lymphopoiesis and enhances lymphocyte recovery after bone marrow transplantation." *The Journal of Immunology* 152.9, pp. 4320–4327. DOI: 10.4049/jimmunol.152.9.4320. eprint: https://journals.aai.org/jimmunol/article-pdf/152/9/4320/1065322/4320.pdf.

Ji, Zhe, Lizhi He, Aviv Regev, and Kevin Struhl (2019). "Inflammatory regulatory network mediated by the joint action of NF-kB, STAT3, and AP-1 factors is involved in many human cancers". *Proceedings of the National Academy of Sciences* 116.19, pp. 9453–9462. DOI: 10.1073/pnas.1821068116. eprint: https://www.pnas.org/doi/pdf/10.1073/pnas.1821068116.

Jian, Jiang, Yanli Pang, H. Hannah Yan, Yongfen Min, Bhagelu R. Achyut, M. Christine Hollander, P. Charles Lin, Xinhua Liang, and Li Yang (Apr. 2017). "Platelet factor 4 is produced by subsets of myeloid cells in premetastatic lung and inhibits tumor metastasis". *Oncotarget* 8 (17), p. 27725. DOI: 10.18632/ONCOTARGET.9486.

Jiang, Chonghua, Hao Zhang, Wantao Wu, Zeyu Wang, Ziyu Dai, Liyang Zhang, Zhixiong Liu, and Quan Cheng (Feb. 2022). "Immune Characteristics of LYN in Tumor Microenvironment of Gliomas". *Frontiers in Cell and Developmental Biology* 9, p. 760929. DOI: 10.3389/FCELL.2021.760929.

Johannesson, Bjarki, Susanne Sattler, Ekaterina Semenova, Saveria Pastore, Teresa M. Kennedy-Lydon, Robert D. Sampson, Michael D. Schneider, Nadia Rosenthal, and Daniel Bilbao (Aug. 2014). "Insulin-like growth factor-1 induces regulatory T cell-mediated suppression of allergic contact dermatitis in mice". *Disease Models and Mechanisms* 7.8, pp. 977–985. DOI: 10.1242/dmm.015362. eprint: https://journals.biologists.com/dmm/article-pdf/7/8/977/1867350/977.pdf.

Johansson, Anna, Juliana Hamzah, Christine J. Payne, and Ruth Ganss (2012). "Tumor-targeted TNFa stabilizes tumor vessels and enhances active immunotherapy". *Proceedings of the National Academy of Sciences* 109.20, pp. 7841–7846. DOI: 10.1073/pnas.1118296109. eprint: https://www.pnas.org/doi/pdf/10.1073/pnas.1118296109.

Johansson, Anna, Stina Rudolfsson, Peter Hammarsten, Sofia Halin, Kristian Pietras, Jonathan Jones, Pär Stattin, Lars Egevad, Torvald Granfors, Pernilla Wikström, and Anders Bergh (2010). "Mast Cells Are Novel Independent Prognostic Markers in Prostate Cancer and Represent a Target for Therapy". *The American Journal of Pathology* 177.2, pp. 1031–1041. DOI: https://doi.org/10.2353/ajpath.2010.100070.

Johnson, ED and GA Cole (Apr. 1975). "Functional heterogeneity of lymphocytic choriomeningitis virus-specfic T lymphocytes. I. Identification of effector amd memory subsets". *The Journal of experimental medicine* 141.4, pp. 866–881. DOI: 10.1084/jem.141.4.866.

Joller, Nicole, Ester Lozano, Patrick R. Burkett, Bonny Patel, Sheng Xiao, Chen Zhu, Junrong Xia, Tze G. Tan, Esen Sefik, Vijay Yajnik, Arlene H. Sharpe, Francisco J. Quintana, Diane Mathis, Christophe Benoist, David A. Hafler, and Vijay K. Kuchroo (Apr. 2014). "Treg Cells Expressing the Coinhibitory Molecule TIGIT Selectively Inhibit Proinflammatory Th1 and Th17 Cell Responses". *Immunity* 40 (4). doi: 10.1016/j.immuni.2014.02.012, pp. 569–581. DOI: 10.1016/j.immuni.2014.02.012.

Jones, John I. and David R. Clemmons (Feb. 1995). "Insulin-Like Growth Factors and Their Binding Proteins: Biological Actions". *Endocrine Reviews* 16.1, pp. 3–34. DOI: 10.1210/edrv-16-1-3. eprint: https://academic.oup.com/edrv/article-pdf/16/1/3/9075290/edrv0003.pdf.

Jones, R. Brad, Lishomwa C. Ndhlovu, Jason D. Barbour, Prameet M. Sheth, Aashish R. Jha, Brian R. Long, Jessica C. Wong, Malathy Satkunarajah, Marc Schweneker, Joan M. Chapman, Gabor Gyenes, Bahareh Vali, Martin D. Hyrcza, Feng Yun Yue, Colin Kovacs, Aref Sassi, Mona Loutfy, Roberta Halpenny, Desmond Persad, Gerald Spotts, Frederick M. Hecht, Tae-Wook Chun, Joseph M. McCune, Rupert Kaul,

James M. Rini, Douglas F. Nixon, and Mario A. Ostrowski (Nov. 2008). "Tim-3 expression defines a novel population of dysfunctional T cells with highly elevated frequencies in progressive HIV-1 infection ". *Journal of Experimental Medicine* 205.12, pp. 2763–2779. DOI: 10.1084/jem.20081398. eprint: https://rupress.org/jem/article-pdf/205/12/2763/1909503/jem_20081398.pdf.

Jones, Robin L., Edward S. Kim, Pilar Nava-Parada, Salma Alam, Faye M. Johnson, Andrew W. Stephens, Ronit Simantov, Srinivasu Poondru, Rich Gedrich, Scott M. Lippman, Stan B. Kaye, and Craig P. Carden (Feb. 2015). "Phase I Study of Intermittent Oral Dosing of the Insulin-like Growth Factor-1 and Insulin Receptors Inhibitor OSI-906 in Patients With Advanced Solid Tumors". *Clinical Cancer Research* 21.4, pp. 693–700. DOI: 10.1158/1078-0432.CCR-14-0265. eprint: https://aacrjournals.org/clincancerres/article-pdf/21/4/693/2029202/693.pdf.

Joshua, A M, V E Zannella, M R Downes, B Bowes, K Hersey, M Koritzinsky, M Schwab, U Hofmann, A Evans, T van der Kwast, J Trachtenberg, A Finelli, N Fleshner, J Sweet, and M Pollak (2014). "A pilot 'window of opportunity' neoadjuvant study of metformin in localised prostate cancer". *Prostate Cancer and Prostatic Diseases* 17 (3), pp. 252–258. DOI: 10.1038/pcan.2014.20.

Kallenbach, Julia, Golnaz Atri Roozbahani, Mehdi Heidari Horestani, and Aria Baniahmad (2022). "Distinct mechanisms mediating therapy-induced cellular senescence in prostate cancer". *Cell and Bioscience* 12 (1), p. 200. DOI: 10.1186/s13578-022-00941-0.

Kammerer-Jacquet, Solene-Florence, Amar Ahmad, Henrik Moller, Holly Sandu, Peter Scardino, Geraldine Soosay, Luis Beltran, Jack Cuzick, and Daniel M Berne (Sept. 2019). "Ki-67 is an independent predictor of prostate cancer death in routine needle biopsy samples: proving utility for routine assessments". *Modern Pathology* 32.9, pp. 1303–1309. DOI: 10.1038/s41379-019-0268-y.

Kaplan, Daniel H., Vijay Shankaran, Anand S. Dighe, Elisabeth Stockert, Michel Aguet, Lloyd J. Old, and Robert D. Schreiber (1998). "Demonstration of an interferon gamma-dependent tumor surveillance system in immunocompetent mice". *Proceedings of the National Academy of Sciences* 95.13, pp. 7556–7561. DOI: 10.1073/pnas.95.13.7556. eprint: https://www.pnas.org/doi/pdf/10.1073/pnas.95.13.7556.

Karantanos, T, P G Corn, and T C Thompson (2013). "Prostate cancer progression after androgen deprivation therapy: mechanisms of castrate resistance and novel therapeutic approaches". *Oncogene* 32 (49), pp. 5501–5511. DOI: 10.1038/onc.2013.206.

Karsch-Bluman, Adi, Ariel Feiglin, Eliran Arbib, Tal Stern, Hila Shoval, Ouri Schwob, Michael Berger, and Ofra Benny (2019). "Tissue necrosis and its role in cancer progression". *Oncogene* 38.11, pp. 1920–1935. DOI: 10.1038/s41388-018-0555-y.

Kearney, Conor J and Seamus J Martin (Mar. 2017). "An Inflammatory Perspective on Necroptosis". *Molecular Cell* 65 (6). doi: 10.1016/j.molcel.2017.02.024, pp. 965–973. DOI: 10.1016/j.molcel.2017.02.024.

Kelly, Aoife, Sezin Gunaltay, Craig P. McEntee, Elinor E. Shuttleworth, Catherine Smedley, Stephanie A. Houston, Thomas M. Fenton, Scott Levison, Elizabeth R. Mann, and Mark A. Travis (Nov. 2018). "Human monocytes and macrophages regulate immune tolerance via integrin avB8–mediated TGFB activation". *Journal of Experimental Medicine* 215 (11), pp. 2725–2736. DOI: 10.1084/JEM.20171491.

Kershaw, Michael H. and Mark J. Smyth (2013). "Making Macrophages Eat Cancer". *Science* 341.6141, pp. 41–42. DOI: 10.1126/science.1241716. eprint: https://www.science.org/doi/pdf/10.1126/science.1241716.

Khan, Arshad, Kangling Zhang, Vipul K Singh, Abhishek Mishra, Priyanka Kachroo, Tian Bing, Jong Hak Won, Arunmani Mani, Ramesha Papanna, Lovepreet K Mann, Eder Ledezma-Campos, Genesis Aguillon-Duran, David H Canaday, Sunil A David, Blanca I Restrepo, Nhung Nguyen Viet, Ha Phan, Edward A Graviss, James M Musser, Deepak Kaushal, Marie Claire Gauduin, and Chinnaswamy Jagannath (2022). "Human M1 macrophages express unique innate immune response genes after mycobacterial infection to defend against tuberculosis". *Communications Biology* 5 (1), p. 480. DOI: 10.1038/s42003-022-03387-9.

Kharitonenkov, Alexei, Zhengjun Chen, Irmi Sures, Hongyang Wang, James Schilling, and Axel Ullrich (Mar. 1997). "A family of proteins that inhibit signalling through tyrosine kinase receptors". *Nature 1997 386:6621* 386 (6621), pp. 181–186. DOI: 10.1038/386181a0.

Kiernan, Kaitlin, Yazan Alwarawrah, Amanda G Nichols, Keiko Danzaki, and Nancie J MacIver (2024). "Insulin and IGF-1 have both overlapping and distinct effects on CD4+ T cell mitochondria, metabolism, and function". *Scientific Reports* 14 (1), p. 4331. DOI: 10.1038/s41598-024-54836-w.

Kilkenny, Carol, William J. Browne, Innes C. Cuthill, Michael Emerson, and Douglas G. Altman (June 2010). "Improving Bioscience Research Reporting: The ARRIVE Guidelines for Reporting Animal Research". *PLOS Biology* 8 (6), e1000412. DOI: 10.1371/JOURNAL.PBIO.1000412.

Kim, Eric, Natalia Miheecheva, Akshaya Ramachandran, Ilia Lyu Yang Galkin, Viktor Svekolkin, Ekaterina Postovalova, Alexander Baggey, Krystle Nomie, Anna Ogloblina, Felix Frenkel, Ravshan Ataullakhanov, James J Hsieh, and Russell Kent Pachynski (2020). "Integrated-omics of MRI-visible and -invisible prostate cancer identifies molecular correlations with clinical outcome". *Journal of Clinical Oncology* 38.15, e17506.

Kim, Hye Jin and Won Jun Lee (2009). "Insulin-Like Growth Factor-I Induces Androgen Receptor Activation in Differentiating C2C12 Skeletal Muscle Cells". *Molecules and Cells* 28.3, pp. 189–194. DOI: https://doi.org/10.1007/S10059-009-0118-8.

Kim, Hyun-Jung, Beate C. Litzenburger, Xiaojiang Cui, David A. Delgado, Brian C. Grabiner, Xin Lin, Michael T. Lewis, Marco M. Gottardis, Tai W. Wong, Ricardo M. Attar, Joan M. Carboni, and Adrian V. Lee (2007a). "Constitutively Active Type I Insulin-Like Growth Factor Receptor Causes Transformation and Xenograft Growth of Immortalized Mammary Epithelial Cells and Is Accompanied by an Epithelial-to-Mesenchymal Transition Mediated by NF-kB and Snail". *Molecular and Cellular Biology* 27.8. PMID: 17296734, pp. 3165–3175. DOI: 10.1128/MCB.01315-06. eprint: https://doi.org/10.1128/MCB.01315-06.

Kim, Kwang Seok, Young Bae Seu, Suk-Hwan Baek, Mi Jin Kim, Keuk Jun Kim, Jung Hye Kim, and Jae-Ryong Kim (2007b). "Induction of Cellular Senescence by Insulin-like Growth Factor Binding Protein-5 through a p53-dependent Mechanism". *Molecular Biology of the Cell* 18.11. PMID: 17804819, pp. 4543–4552. DOI: 10.1091/mbc.e07-03-0280. eprint: https://doi.org/10.1091/mbc.e07-03-0280.

Kim, Won Kyung, Adam W Olson, Jiaqi Mi, Jinhui Wang, Dong-Hoon Lee, Vien Le, Alex Hiroto, Joseph Aldahl, Christian H Nenninger, Alyssa J Buckley, Robert Cardiff, Sungyong You, and Zijie Sun (2022). "Aberrant androgen action in prostatic progenitor cells induces oncogenesis and tumor development through IGF1 and Wnt axes". *Nature Communications* 13 (1), p. 4364. DOI: 10.1038/s41467-022-32119-0.

Kimata, H and M Fujimoto (Aug. 1994). "Growth hormone and insulin-like growth factor I induce immunoglobulin (Ig)E and IgG4 production by human B cells." *Journal of*

Experimental Medicine 180.2, pp. 727–732. DOI: 10.1084/jem.180.2.727. eprint: https://rupress.org/jem/article-pdf/180/2/727/1676079/727.pdf.

King, Jennifer C, Jin Xu, John Wongvipat, Haley Hieronymus, Brett S Carver, David H Leung, Barry S Taylor, Chris Sander, Robert D Cardiff, Suzana S Couto, William L Gerald, and Charles L Sawyers (2009). "Cooperativity of TMPRSS2-ERG with PI3-kinase pathway activation in prostate oncogenesis". *Nature Genetics* 41.5, pp. 524–526. DOI: 10.1038/ng.371.

Kiniwa, Yukiko, Yoshihiro Miyahara, Helen Y. Wang, Weiyi Peng, Guangyong Peng, Thomas M. Wheeler, Timothy C. Thompson, Lloyd J. Old, and Rong-Fu Wang (Dec. 2007). "CD8+ Foxp3+ Regulatory T Cells Mediate Immunosuppression in Prostate Cancer". *Clinical Cancer Research* 13.23, pp. 6947–6958. DOI: 10.1158/1078-0432.CCR-07-0842. eprint: https://aacrjournals.org/clincancerres/article-pdf/13/23/6947/1973284/6947.pdf.

Kirby, M., C. Hirst, and E. D. Crawford (2011). "Characterising the castration-resistant prostate cancer population: a systematic review". *International Journal of Clinical Practice* 65.11, pp. 1180–1192. DOI: https://doi.org/10.1111/j.1742-1241.2011.02799.x. eprint: https://onlinelibrary.wiley.com/doi/pdf/10.1111/j.1742-1241.2011.02799.x.

Kitamura, Takanori, Kohei Kometani, Hiroki Hashida, Akihiro Matsunaga, Hiroyuki Miyoshi, Hisahiro Hosogi, Masahiro Aoki, Masanobu Oshima, Masakazu Hattori, Arimichi Takabayashi, Nagahiro Minato, and Makoto M. Taketo (Mar. 2007). "SMAD4-deficient intestinal tumors recruit CCR1+ myeloid cells that promote invasion". *Nature Genetics 2007 39:4* 39 (4), pp. 467–475. DOI: 10.1038/ng1997.

Kloosterman, Daan J and Leila Akkari (Apr. 2023). "Macrophages at the interface of the co-evolving cancer ecosystem". *Cell* 186 (8). doi: 10.1016/j.cell.2023.02.020, pp. 1627–1651. DOI: 10.1016/j.cell.2023.02.020.

Klug, Felix, Hridayesh Prakash, Peter E. Huber, Tobias Seibel, Noemi Bender, Niels Halama, Christina Pfirschke, Ralf Holger Voss, Carmen Timke, Ludmila Umansky, Kay Klapproth, Knut Schakel, Natalio Garbi, Dirk Jager, Jurgen Weitz, Hubertus Schmitz-Winnenthal, Gunter J. Hammerling, and Philipp Beckhove (Nov. 2013). "Low-Dose Irradiation Programs Macrophage Differentiation to an iNOS+/M1 Phenotype that Orchestrates Effective T Cell Immunotherapy". *Cancer Cell* 24 (5). doi: 10.1016/j.ccr.2013.09.014, pp. 589–602. DOI: 10.1016/j.ccr.2013.09.014.

Knochelmann, Hannah M, Connor J Dwyer, Stefanie R Bailey, Sierra M Amaya, Dirk M Elston, Joni M Mazza-McCrann, and Chrystal M Paulos (2018). "When worlds collide: Th17 and Treg cells in cancer and autoimmunity". *Cellular and Molecular Immunology* 15 (5), pp. 458–469. DOI: 10.1038/s41423-018-0004-4.

Knuppel, Anika, Georgina K. Fensom, Eleanor L. Watts, Marc J. Gunter, Neil Murphy, Keren Papier, Aurora Perez-Cornago, Julie A. Schmidt, Karl Smith Byrne, Ruth C. Travis, and Timothy J. Key (Sept. 2020). "Circulating Insulin-like Growth Factor-I Concentrations and Risk of 30 Cancers: Prospective Analyses in UK Biobank". *Cancer Research* 80.18, pp. 4014–4021. DOI: 10.1158/0008-5472.CAN-20-1281. eprint: https://aacrjournals.org/cancerres/article-pdf/80/18/4014/2798002/4014.pdf.

Knutson, K L and M L Disis (2005). "Tumor antigen-specific T helper cells in cancer immunity and immunotherapy". *Cancer Immunology, Immunotherapy* 54 (8), pp. 721–728. DOI: 10.1007/s00262-004-0653-2.

Kobie, James J., Pranav R. Shah, Li Yang, Jonathan A. Rebhahn, Deborah J. Fowell, and Tim R. Mosmann (Nov. 2006). "T Regulatory and Primed Uncommitted CD4 T Cells

Express CD73, Which Suppresses Effector CD4 T Cells by Converting 5'-Adenosine Monophosphate to Adenosine". *The Journal of Immunology* 177.10, pp. 6780–6786. DOI: 10.4049/jimmunol.177.10.6780. eprint: https://journals.aai.org/jimmunol/article-pdf/177/10/6780/1226810/zim02206006780.pdf.

Kohno, Keizo, Satomi Koya-Miyata, Akira Harashima, Takahiko Tsukuda, Masataka Katakami, Toshio Ariyasu, Shimpei Ushio, and Kanso Iwaki (2021). "Inflammatory M1-like macrophages polarized by NK-4 undergo enhanced phenotypic switching to an anti-inflammatory M2-like phenotype upon co-culture with apoptotic cells". *Journal of Inflammation* 18 (1), p. 2. DOI: 10.1186/s12950-020-00267-z.

Kooijman, R, M Willems, C J De Haas, G T Rijkers, A L Schuurmans, S C Van Buul-Offers, C J Heijnen, and B J Zegers (Nov. 1992). "Expression of type I insulin-like growth factor receptors on human peripheral blood mononuclear cells". *Endocrinology* 131.5, pp. 2244–2250. DOI: 10.1210/endo.131.5.1425423. eprint: https://academic.oup.com/endo/article-pdf/131/5/2244/10632636/endo2244.pdf.

Kooijman, Ron (2006). "Regulation of apoptosis by insulin-like growth factor (IGF)-I". *Cytokine and Growth Factor Reviews* 17.4, pp. 305–323. DOI: https://doi.org/10.1016/j.cytogfr.2006.02.002.

Kooijman, Ron and Astrid Coppens (July 2004). "Insulin-like growth factor-I stimulates IL-10 production in human T cells". *Journal of Leukocyte Biology* 76 (4), pp. 862–867. DOI: 10.1189/JLB.0404248.

Krebs, Danielle L., Manreet K. Chehal, Alexander Sio, Nicholas D. Huntington, Mei Lin Da, Pascal Ziltener, Melissa Inglese, Nicole Kountouri, John J. Priatel, Jessica Jones, David M. Tarlinton, Gary P. Anderson, Margaret L. Hibbs, and Kenneth W. Harder (May 2012). "Lyn-Dependent Signaling Regulates the Innate Immune Response by Controlling Dendritic Cell Activation of NK Cells". *The Journal of Immunology* 188 (10), pp. 5094–5105. DOI: 10.4049/JIMMUNOL.1103395.

Krilaviciute, Agne, Nikolaus Becker, Jale Lakes, Jan Philipp Radtke, Markus Kuczyk, Inga Peters, Nina N. Harke, Jurgen Debus, Stefan A. Koerber, Kathleen Herkommer, Jurgen E. Gschwend, Valentin H. Meissner, Axel Benner, Petra Seibold, Glen Kristiansen, Boris Hadaschik, Christian Arsov, Lars Schimmoller, Frederik Lars Giesel, Gerald Antoch, Marcus Makowski, Frank Wacker, Heinz-Peter Schlemmer, Rudolf Kaaks, and Peter Albers (2023). "Digital Rectal Examination Is Not a Useful Screening Test for Prostate Cancer". *European Urology Oncology* 6.6, pp. 566–573. DOI: https://doi.org/10.1016/j.euo.2023.09.008.

Kroemer, Guido, Claudia Galassi, Laurence Zitvogel, and Lorenzo Galluzzi (2022). "Immunogenic cell stress and death". *Nature Immunology* 23 (4), pp. 487–500. DOI: 10.1038/s41590-022-01132-2.

Kruse, Bastian, Anthony C Buzzai, Naveen Shridhar, Andreas D Braun, Susan Gellert, Kristin Knauth, Joanna Pozniak, Johannes Peters, Paulina Dittmann, Miriam Mengoni, Tetje Cornelia van der Sluis, Simon Hohn, Asier Antoranz, Anna Krone, Yan Fu, Di Yu, Magnus Essand, Robert Geffers, Dimitrios Mougiakakos, Sascha KahlfuB, Hamid Kashkar, Evelyn Gaffal, Francesca M Bosisio, Oliver Bechter, Florian Rambow, Jean-Christophe Marine, Wolfgang Kastenmuller, Andreas J Muller, and Thomas Tuting (2023). "CD4+ T cell-induced inflammatory cell death controls immune-evasive tumours". *Nature* 618 (7967), pp. 1033–1040. DOI: 10.1038/s41586-023-06199-x.

Krystel-Whittemore, Melissa, Kottarappat N. Dileepan, and John G. Wood (2016). "Mast Cell: A Multi-Functional Master Cell". *Frontiers in Immunology* 6. DOI: 10.3389/fimmu.2015.00620.

Ku, Nam-On, Pavel Strnad, Heike Bantel, and M Bishr Omary (2016). "Keratins: Biomarkers and modulators of apoptotic and necrotic cell death in the liver". *Hepatology* 64 (3).

Kuilman, Thomas and Daniel S. Peeper (2009). "Senescence-messaging secretome: SMS-ing cellular stress". *Nature Reviews Cancer* 9.2, pp. 81–94. DOI: 10.1038/nrc2560.

Kumar, Sanjay, Jeffrey Boehm, and John C Lee (2003). "p38 MAP kinases: key signalling molecules as therapeutic targets for inflammatory diseases". *Nature Reviews Drug Discovery* 2 (9), pp. 717–726. DOI: 10.1038/nrd1177.

Kunzli, Marco and David Masopust (2023). "CD4+ T cell memory". *Nature Immunology* 24.6, pp. 903–914. DOI: 10.1038/s41590-023-01510-4.

Kurosaki, Tomohiro, Kohei Kometani, and Wataru Ise (2015). "Memory B cells". *Nature Reviews Immunology* 15 (3), pp. 149–159. DOI: 10.1038/nri3802.

Kurzrock, Razelle, Amita Patnaik, Joseph Aisner, Terri Warren, Stephen Leong, Robert Benjamin, S. Gail Eckhardt, Joseph E. Eid, Gerard Greig, Kai Habben, Cinara D. McCarthy, and Lia Gore (Apr. 2010). "A Phase I Study of Weekly R1507, A Human Monoclonal Antibody Insulin-like Growth Factor-I Receptor Antagonist, in Patients with Advanced Solid Tumors". *Clinical Cancer Research* 16.8, pp. 2458–2465. DOI: 10.1158/1078-0432.CCR-09-3220. eprint: https://aacrjournals.org/clincancerres/article-pdf/16/8/2458/1995310/2458.pdf.

Kusmartsev, Sergei and Dmitry I. Gabrilovich (Apr. 2005). "STAT1 Signaling Regulates Tumor-Associated Macrophage-Mediated T Cell Deletion1". *The Journal of Immunology* 174.8, pp. 4880–4891. DOI: 10.4049/jimmunol.174.8.4880. eprint: https://journals.aai.org/jimmunol/article-pdf/174/8/4880/1200395/4880.pdf.

Kwak, Kihyuck, Munir Akkaya, and Susan K Pierce (2019). "B cell signaling in context". *Nature Immunology* 20 (8), pp. 963–969. DOI: 10.1038/s41590-019-0427-9.

Kwon, Eugene D, Charles G Drake, Howard I Scher, Karim Fizazi, Alberto Bossi, Alfons J M van den Eertwegh, Michael Krainer, Nadine Houede, Ricardo Santos, Hakim Mahammedi, Siobhan Ng, Michele Maio, Fabio A Franke, Santhanam Sundar, Neeraj Agarwal, Andries M Bergman, Tudor E Ciuleanu, Ernesto Korbenfeld, Lisa Sengeløv, Steinbjorn Hansen, Christopher Logothetis, Tomasz M Beer, M Brent McHenry, Paul Gagnier, David Liu, and Winald R Gerritsen (June 2014). "Ipilimumab versus placebo after radiotherapy in patients with metastatic castration-resistant prostate cancer that had progressed after docetaxel chemotherapy (CA184-043): a multicentre, randomised, double-blind, phase 3 trial". *The Lancet Oncology* 15 (7). doi: 10.1016/S1470-2045(14)70189-5, pp. 700–712. DOI: 10.1016/S1470-2045(14)70189-5.

Kwon, J T W, R J Bryant, and E E Parkes (2021). "The tumor microenvironment and immune responses in prostate cancer patients". *Endocrine-Related Cancer* 28.8, T95–T107. DOI: 10.1530/ERC-21-0149.

Lake, David, Sonia A.L. Corrêa, and Jürgen Müller (June 2016). "Negative feedback regulation of the ERK1/2 MAPK pathway". *Cellular and Molecular Life Sciences* 73 (23), p. 4397. DOI: 10.1007/S00018-016-2297-8.

Lam, Nora, YoonSeung Lee, and Donna L Farber (2024). "A guide to adaptive immune memory". *Nature Reviews Immunology*. DOI: 10.1038/s41577-024-01040-6.

Lamb, Alastair D., Charlie E. Massie, and David E. Neal (2014). "The transcriptional programme of the androgen receptor (AR) in prostate cancer". *BJU International* 113.3,

pp. 358–366. DOI: https://doi.org/10.1111/bju.12415. eprint: https://bjui-journals.onlinelibrary.wiley.com/doi/pdf/10.1111/bju.12415.

Landreth, Kenneth S., Ramaswamy Narayanan, and Kenneth Dorshkind (1992). "Insulin-like Growth Factor-I Regulates Pro-B Cell Differentiation". *Blood* 80.5, pp. 1207–1212. DOI: https://doi.org/10.1182/blood.V80.5.1207.1207.

Lane, J. Athene, Jenny L. Donovan, Michael Davis, Eleanor Walsh, Daniel Dedman, Liz Down, Emma L. Turner, Malcolm D. Mason, Chris Metcalfe, Tim J. Peters, Richard M. Martin, David E. Neal, and Freddie C. Hamdy (Sept. 2014). "Active monitoring, radical prostatectomy, or radiotherapy for localised prostate cancer: Study design and diagnostic and baseline results of the ProtecT randomised phase 3 trial". *The Lancet Oncology* 15 (10), pp. 1109–1118. DOI: 10.1016/S1470-2045(14)70361-4.

Larionova, Irina, Gulnara Tuguzbaeva, Anastasia Ponomaryova, Marina Stakheyeva, Nadezhda Cherdyntseva, Valentin Pavlov, Evgeniy Choinzonov, and Julia Kzhyshkowska (Oct. 2020). "Tumor-Associated Macrophages in Human Breast, Colorectal, Lung, Ovarian and Prostate Cancers". *Frontiers in Oncology* 10, p. 1. DOI: 10.3389/FONC.2020.566511.

Laron, Z (2001). "Insulin-like growth factor 1 (IGF-1): a growth hormone". *Molecular Pathology* 54.5, pp. 311–316. DOI: 10.1136/mp.54.5.311. eprint: https://mp.bmj.com/content/54/5/311.full.pdf.

Laron, Zvi and Haim Werner (2023). "Congenital IGF-1 deficiency protects from cancer: lessons from Laron syndrome". *Endocrine-Related Cancer* 30.9, e220394. DOI: 10.1530/ERC-22-0394.

Latchman, Yvette, Clive R Wood, Tatyana Chernova, Divya Chaudhary, Madhuri Borde, Irene Chernova, Yoshiko Iwai, Andrew J Long, Julia A Brown, Raquel Nunes, Edward A Greenfield, Karen Bourque, Vassiliki A Boussiotis, Laura L Carter, Beatriz M Carreno, Nelly Malenkovich, Hiroyuki Nishimura, Taku Okazaki, Tasuku Honjo, Arlene H Sharpe, and Gordon J Freeman (2001). "PD-L2 is a second ligand for PD-1 and inhibits T cell activation". *Nature Immunology* 2 (3), pp. 261–268. DOI: 10.1038/85330.

LaTulippe, Eva, Jaya Satagopan, Alex Smith, Howard Scher, Peter Scardino, Victor Reuter, and William L Gerald (Aug. 2002). "Comprehensive Gene Expression Analysis of Prostate Cancer Reveals Distinct Transcriptional Programs Associated with Metastatic Disease". *Cancer Research* 62 (15), pp. 4499–4506.

Laumont, Celine M, Allyson C Banville, Mara Gilardi, Daniel P Hollern, and Brad H Nelson (2022). "Tumour-infiltrating B cells: immunological mechanisms, clinical impact and therapeutic opportunities". *Nature Reviews Cancer* 22 (7), pp. 414–430. DOI: 10.1038/s41568-022-00466-1.

Le, Kang, Jing Sun, Javid Ghaemmaghami, Mitchell R. Smith, W. K. Eddie Ip, Tycel Phillips, and Mamta Gupta (2023). "Blockade of CCR1 induces a phenotypic shift in macrophages and triggers a favorable antilymphoma activity". *Blood Advances* 7.15, pp. 3952–3967. DOI: https://doi.org/10.1182/bloodadvances.2022008722.

Leach, Dana R., Matthew F. Krummel, and James P. Allison (1996). "Enhancement of Antitumor Immunity by CTLA-4 Blockade". *Science* 271.5256, pp. 1734–1736. DOI: 10.1126/science.271.5256.1734. eprint: https://www.science.org/doi/pdf/10.1126/science.271.5256.1734.

Lee, Ji-Sun, Michael W Lero, Jose Mercado-Matos, Sha Zhu, Minjeong Jo, Claire E Tocheny, Jennifer S Morgan, and Leslie M Shaw (Dec. 2022). "The insulin and IGF signaling pathway sustains breast cancer stem cells by IRS2/PI3K-mediated regulation of MYC". *Cell Reports* 41 (10). doi: 10.1016/j.celrep.2022.111759. DOI: 10.1016/j.celrep.2022.111759.

Leiphrakpam, Premila D., Ekta Agarwal, Michelle Mathiesen, Katie L. Haferbier, Michael G. Brattain, and Sanjib Chowdhury (Jan. 2014). "In vivo analysis of insulin-like growth factor type 1 receptor humanized monoclonal antibody MK-0646 and small molecule kinase inhibitor OSI-906 in colorectal cancer". *Oncology Reports* 31 (1), pp. 87–94. DOI: 10.3892/OR.2013.2819/HTML.

LeRoith, Derek and Charles T. Roberts (2003). "The insulin-like growth factor system and cancer". *Cancer Letters* 195.2, pp. 127–137. DOI: https://doi.org/10.1016/S0304-3835(03)00159-9.

Lessmann, Eva, Gordon Grochowy, Lars Weingarten, Torsten Giesemann, Klaus Aktories, Michael Leitges, Gerald Krystal, and Michael Huber (Nov. 2006). "Insulin and insulin-like growth factor-1 promote mast cell survival via activation of the phosphatidylinositol-3-kinase pathway". *Experimental Hematology* 34 (11). doi: 10.1016/j.exphem.2006.05.022, pp. 1532–1541. DOI: 10.1016/j.exphem.2006.05.022.

Leung, Elaine Lai-Han, Run-Ze Li, Xing-Xing Fan, Lily Yan Wang, Yan Wang, Zebo Jiang, Jumin Huang, Hu-Dan Pan, Yue Fan, Hongmei Xu, Feng Wang, Haopeng Rui, Piu Wong, Hermi Sumatoh, Michael Fehlings, Alessandra Nardin, Paul Gavine, Longen Zhou, Yabing Cao, and Liang Liu (2023). "Longitudinal high-dimensional analysis identifies immune features associating with response to anti-PD-1 immunotherapy". *Nature Communications* 14 (1), p. 5115. DOI: 10.1038/s41467-023-40631-0.

Li, Guanghao, Xiaoxuan Wang, Yongheng Liu, Huikai Li, Han Mu, Yanting Zhang, and Qiang Li (June 2022a). "Multi-omics analysis reveals the panoramic picture of necroptosis-related regulators in pan-cancer". *Aging* 14 (12), pp. 5034–5058. DOI: 10.18632/AGING.204124.

Li, Hanjie, Anne M van der Leun, Ido Yofe, Yaniv Lubling, Dikla Gelbard-Solodkin, Alexander C J van Akkooi, Marlous van den Braber, Elisa A Rozeman, John B A G Haanen, Christian U Blank, Hugo M Horlings, Eyal David, Yael Baran, Akhiad Bercovich, Aviezer Lifshitz, Ton N Schumacher, Amos Tanay, and Ido Amit (Feb. 2019). "Dysfunctional CD8 T Cells Form a Proliferative, Dynamically Regulated Compartment within Human Melanoma". *Cell* 176 (4). doi: 10.1016/j.cell.2018.11.043, 775–789.e18. DOI: 10.1016/j.cell.2018.11.043.

Li, Hanxiao, P Anton van der Merwe, and Shivan Sivakumar (2022b). "Biomarkers of response to PD-1 pathway blockade". *British Journal of Cancer* 126 (12), pp. 1663–1675. DOI: 10.1038/s41416-022-01743-4.

Li, Heming, Izhar Singh Batth, Xiujuan Qu, Ling Xu, Na Song, Ruoyu Wang, and Yunpeng Liu (2017). "IGF-IR signaling in epithelial to mesenchymal transition and targeting IGF-IR therapy: overview and new insights". *Molecular Cancer* 16.1, p. 6. DOI: 10.1186/s12943-016-0576-5.

Li, Heming, Ling Xu, Ce Li, Lei Zhao, Yanju Ma, Huachuan Zheng, Zhi Li, Ye Zhang, Ruoyu Wang, Yunpeng Liu, and Xiujuan Qu (2014). "Ubiquitin ligase Cbl-b represses IGF-I-induced epithelial mesenchymal transition via ZEB2 and microRNA-200c regulation in gastric cancer cells". *Molecular Cancer* 13 (1), p. 136. DOI: 10.1186/1476-4598-13-136.

Li, Rongshi, Alan Pourpak, and Stephan W Morris (Aug. 2009). "Inhibition of the Insulin-like Growth Factor-1 Receptor (IGF1R) Tyrosine Kinase as a Novel Cancer Therapy Approach". *Journal of Medicinal Chemistry* 52 (16). doi: 10.1021/jm9002395, pp. 4981–5004. DOI: 10.1021/jm9002395.

Li, Ruo Qi, Lei Yan, Ling Zhang, Yanli Zhao, and Jing Lian (2024). "CD74 as a prognostic and M1 macrophage infiltration marker in a comprehensive pan-cancer analysis". *Scientific Reports* 14 (1), p. 8125. DOI: 10.1038/s41598-024-58899-7.

Li, Yan-Ruide, Kuangyi Zhou, Matthew Wilson, Adam Kramer, Yichen Zhu, Niels Dawson, and Lili Yang (Mar. 2023a). "Mucosal-associated invariant T cells for cancer immunotherapy". *Molecular Therapy* 31 (3). doi: 10.1016/j.ymthe.2022.11.019, pp. 631–646. DOI: 10.1016/j.ymthe.2022.11.019.

Li, Si-Yuan, Yong-Lin Guo, Jia-Wen Tian, He-Jing Zhang, Rui-Fang Li, Ping Gong, and Zi-Li Yu (2023b). "Anti-Tumor Strategies by Harnessing the Phagocytosis of Macrophages". *Cancers* 15.10. DOI: 10.3390/cancers15102717.

Liang, Bitao, Craig Workman, Janine Lee, Claude Chew, Benjamin M. Dale, Lucrezia Colonna, Marcella Flores, Nianyu Li, Edina Schweighoffer, Steven Greenberg, Victor Tybulewicz, Dario Vignali, and Raphael Clynes (May 2008). "Regulatory T Cells Inhibit Dendritic Cells by Lymphocyte Activation Gene-3 Engagement of MHC Class II". *The Journal of Immunology* 180.9, pp. 5916–5926. DOI: 10.4049/jimmunol.180.9.5916. eprint: https://journals.aai.org/jimmunol/article-pdf/180/9/5916/1255250/zim00908005916.pdf.

Liao, Yang, Gordon K. Smyth, and Wei Shi (Nov. 2013). "featureCounts: an efficient general purpose program for assigning sequence reads to genomic features". *Bioinformatics* 30.7, pp. 923–930. DOI: 10.1093/bioinformatics/btt656. eprint: https://academic.oup.com/bioinformatics/article-pdf/30/7/923/48921621/bioinformatics_30_7_923.pdf.

Lin, Shiyu, Qi Zhang, Xiaoru Shao, Tao Zhang, Changyue Xue, Sirong Shi, Dan Zhao, and Yunfeng Lin (2017). "IGF-1 promotes angiogenesis in endothelial cells/adipose-derived stem cells co-culture system with activation of PI3K/Akt signal pathway". *Cell Proliferation* 50.6, e12390. DOI: https://doi.org/10.1111/cpr.12390. eprint: https://onlinelibrary.wiley.com/doi/pdf/10.1111/cpr.12390.

Lin, Weiwei, Rui Niu, Seong-Min Park, Yan Zou, Sung Soo Kim, Xue Xia, Songge Xing, Qingshan Yang, Xinhong Sun, Zheng Yuan, Shuchang Zhou, Dongya Zhang, Hyung Joon Kwon, Saewhan Park, Chan Il Kim, Harim Koo, Yang Liu, Haigang Wu, Meng Zheng, Heon Yoo, Bingyang Shi, Jong Bae Park, and Jinlong Yin (2023). "IGFBP5 is an ROR1 ligand promoting glioblastoma invasion via ROR1/HER2-CREB signaling axis". *Nature Communications* 14 (1), p. 1578. DOI: 10.1038/s41467-023-37306-1.

Lindholm, Paul F, Neela Sivapurapu, Borko Jovanovic, and Andre Kajdacsy-Balla (2015). "Monocyte-Induced Prostate Cancer Cell Invasion is Mediated by Chemokine ligand 2 and Nuclear Factor-kB Activity". *Journal of clinical and cellular immunology* 6 (2). DOI: 10.4172/2155-9899.1000308.

Lito, Piro, Christine A. Pratilas, Eric W. Joseph, Madhavi Tadi, Ensar Halilovic, Matthew Zubrowski, Alan Huang, Wai Lin Wong, Margaret K. Callahan, Taha Merghoub, Jedd D. Wolchok, Elisa de Stanchina, Sarat Chandarlapaty, Poulikos I. Poulikakos, James A. Fagin, and Neal Rosen (Nov. 2012). "Relief of profound feedback inhibition of mitogenic signaling by RAF inhibitors attenuates their activity in BRAFV600E melanomas". *Cancer cell* 22 (5), pp. 668–682. DOI: 10.1016/J.CCR.2012.10.009.

Liu, Dan and Peter J. Hornsby (Apr. 2007). "Senescent Human Fibroblasts Increase the Early Growth of Xenograft Tumors via Matrix Metalloproteinase Secretion". *Cancer Research* 67.7, pp. 3117–3126. DOI: 10.1158/0008-5472.CAN-06-3452. eprint: https://aacrjournals.org/cancerres/article-pdf/67/7/3117/2579994/3117.pdf.

Liu, Fengchao, Susu Ye, Liu Zhao, and Qinghui Niu (2024). "The role of IGF/IGF-1R signaling in the regulation of cancer stem cells". *Clinical and Translational Oncology*. DOI: 10.1007/s12094-024-03561-x.

Liu, Guoqiang, Minggang Zhu, Mingrui Zhang, and Feng Pan (2023a). "Emerging Role of IGF-1 in Prostate Cancer: A Promising Biomarker and Therapeutic Target". *Cancers* 15.4. DOI: 10.3390/cancers15041287.

Liu, Ting, Lingyun Zhang, Donghyun Joo, and Shao-Cong Sun (2017). "NF-kB signaling in inflammation". *Signal Transduction and Targeted Therapy* 2 (1), p. 17023. DOI: 10.1038/sigtrans.2017.23.

Liu, Weiyong, Yunkai Zhu, Lei Ye, Yajuan Zhu, and Yuhao Wang (July 2021a). "Comparison of tumor angiogenesis in subcutaneous and orthotopic LNCaP mouse models using contrast-enhanced ultrasound imaging". *Translational Cancer Research* 10 (7), pp. 3268–3277. DOI: 10.21037/TCR-21-372.

Liu, Xia, Lingyun Li, Fusheng Si, Lan Huang, Yangjing Zhao, Chenchen Zhang, Daniel F Hoft, and Guangyong Peng (2021b). "NK and NKT cells have distinct properties and functions in cancer". *Oncogene* 40 (27), pp. 4521–4537. DOI: 10.1038/s41388-021-01880-9.

Liu, Xiangdang, Thomas Turbyville, Anne Fritz, and Luke Whitesell (Dec. 1998). "Inhibition of Insulin-like Growth Factor I Receptor Expression in Neuroblastoma Cells Induces the Regression of Established Tumors in Mice". *Cancer Research* 58 (23), pp. 5432–5438.

Liu, Xindong, Yun Wang, Huiping Lu, Jing Li, Xiaowei Yan, Minglu Xiao, Jing Hao, Andrei Alekseev, Hiep Khong, Tenghui Chen, Rui Huang, Jin Wu, Qiwen Zhao, Qi Wu, Senlin Xu, Xiaohu Wang, Wei Jin, Shicang Yu, Yan Wang, Lai Wei, Aibo Wang, Bo Zhong, Ling Ni, Xiaolong Liu, Roza Nurieva, Lilin Ye, Qiang Tian, Xiu-Wu Bian, and Chen Dong (2019a). "Genome-wide analysis identifies NR4A1 as a key mediator of T cell dysfunction". *Nature* 567 (7749), pp. 525–529. DOI: 10.1038/s41586-019-0979-8.

Liu, Yingnan, Shixuan Shen, Ziwei Yan, Lirong Yan, Hanxi Ding, Ang Wang, Qian Xu, Liping Sun, and Yuan Yuan (2023b). "Expression characteristics and their functional role of IGFBP gene family in pan-cancer". *BMC Cancer* 23 (1), p. 371. DOI: 10.1186/s12885-023-10832-3.

Liu, Zhen-Ling, Huan-Huan Chen, Li-Li Zheng, Li-Ping Sun, and Lei Shi (2023c). "Angiogenic signaling pathways and anti-angiogenic therapy for cancer". *Signal Transduction and Targeted Therapy* 8 (1), p. 198. DOI: 10.1038/s41392-023-01460-1.

Liu, Zheng Gang and Delong Jiao (Jan. 2019b). "Necroptosis, tumor necrosis and tumorigenesis". *Cell Stress* 4 (1), p. 1. DOI: 10.15698/CST2020.01.208.

Livingstone, Callum (2013). "IGF2 and cancer". *Endocrine-Related Cancer* 20.6, R321–R339. DOI: 10.1530/ERC-13-0231.

Llopiz, Diana, Marta Ruiz, Stefany Infante, Lorea Villanueva, Leyre Silva, Sandra Hervas-Stubbs, Diego Alignani, Elizabeth Guruceaga, Juan J. Lasarte, Pablo Sarobe, Diana Llopiz, Marta Ruiz, Stefany Infante, Lorea Villanueva, Leyre Silva, Sandra Hervas-Stubbs, Diego Alignani, Elizabeth Guruceaga, Juan J. Lasarte, and Pablo Sarobe (Dec. 2016). "IL-10 expression defines an immunosuppressive dendritic cell population induced by antitumor therapeutic vaccination". *Oncotarget* 8 (2), pp. 2659–2671. DOI: 10.18632/ONCOTARGET.13736.

Lloyd, Catherine M., Anthony R.J. Phillips, Garth J.S. Cooper, and P. Rod Dunbar (2008). "Three-colour fluorescence immunohistochemistry reveals the diversity of cells staining for macrophage markers in murine spleen and liver". *Journal of Immunological Methods* 334.1, pp. 70–81. DOI: https://doi.org/10.1016/j.jim.2008.02.005.

Longo, Joseph, Robert J Hamilton, Mehdi Masoomian, Najia Khurram, Emily Branchard, Peter J Mullen, Mohamad Elbaz, Karen Hersey, Dianne Chadwick, Sangeet Ghai, David W Andrews, Eric X Chen, Theodorus H van der Kwast, Neil E Fleshner, and Linda Z Penn (2020). "A pilot window-of-opportunity study of preoperative fluvastatin in localized prostate cancer". *Prostate Cancer and Prostatic Diseases* 23 (4), pp. 630–637. DOI: 10.1038/s41391-020-0221-7.

Lopez-Bujanda, Zoila A, Michael C Haffner, Matthew G Chaimowitz, Nivedita Chowdhury, Nicholas J Venturini, Radhika A Patel, Aleksandar Obradovic, Corey S Hansen, Joanna Jacków, Janielle P Maynard, Karen S Sfanos, Cory Abate-Shen, Charles J Bieberich, Paula J Hurley, Mark J Selby, Alan J Korman, Angela M Christiano, Angelo M De Marzo, and Charles G Drake (2021). "Castration-mediated IL-8 promotes myeloid infiltration and prostate cancer progression". *Nature Cancer* 2.8, pp. 803–818. DOI: 10.1038/s43018-021-00227-3.

Loty, Sabine, Nadine Forest, Habib Boulekbache, and Jean-Michel Sautier (1995). "Cytochalasin D induces changes in cell shape and promotes in vitro chondrogenesis: A morphological study". *Biology of the Cell* 93.2-3, pp. 149–161. DOI: https://doi.org/10.1016/0248-4900(96)81303-7.

Love, Michael I., Wolfgang Huber, and Simon Anders (Dec. 2014). "Moderated estimation of fold change and dispersion for RNA-seq data with DESeq2". *Genome Biology* 15 (12), pp. 1–21. DOI: 10.1186/S13059-014-0550-8/FIGURES/9.

Lovf, Marthe, Sen Zhao, Ulrika Axcrona, Bjarne Johannessen, Anne Cathrine Bakken, Kristina Totland Carm, Andreas M. Hoff, Ola Myklebost, Leonardo A. Meza-Zepeda, A. Kathrine Lie, Karol Axcrona, Ragnhild A. Lothe, and Rolf I. Skotheim (2019). "Multifocal Primary Prostate Cancer Exhibits High Degree of Genomic Heterogeneity". *European Urology* 75.3, pp. 498–505. DOI: https://doi.org/10.1016/j.eururo.2018.08.009.

Lu, Geming, Ruihua Zhang, Shuo Geng, Liang Peng, Padmini Jayaraman, Chun Chen, Feifong Xu, Jianjun Yang, Qin Li, Hao Zheng, Kimberly Shen, Juan Wang, Xiyu Liu, Weidong Wang, Zihan Zheng, Chen-Feng Qi, Chuanping Si, John Cijiang He, Kebin Liu, Sergio A Lira, Andrew G Sikora, Liwu Li, and Huabao Xiong (2015). "Myeloid cell-derived inducible nitric oxide synthase suppresses M1 macrophage polarization". *Nature Communications* 6 (1), p. 6676. DOI: 10.1038/ncomms7676.

Lu, Xin, James W Horner, Erin Paul, Xiaoying Shang, Patricia Troncoso, Pingna Deng, Shan Jiang, Qing Chang, Denise J Spring, Padmanee Sharma, John A Zebala, Dean Y Maeda, Y Alan Wang, and Ronald A DePinho (2017). "Effective combinatorial immunotherapy for castration-resistant prostate cancer". *Nature* 543 (7647), pp. 728–732. DOI: 10.1038/nature21676.

Lu, Yi, Zhong Cai, Guozhi Xiao, Yulin Liu, Evan T. Keller, Zhi Yao, and Jian Zhang (2007). "CCR2 expression correlates with prostate cancer progression". *Journal of Cellular Biochemistry* 101.3, pp. 676–685. DOI: https://doi.org/10.1002/jcb.21220. eprint: https://onlinelibrary.wiley.com/doi/pdf/10.1002/jcb.21220.

Luo, Xiaoying, Xiaoke Jiang, Jun Li, Yangqiu Bai, Zhen Li, Peiru Wei, Suofeng Sun, Yuan Liang, Shuangyin Han, Xiuling Li, and Bingyong Zhang (2019). "Insulin-like growth factor-1 attenuates oxidative stress-induced hepatocyte premature senescence in liver fibrogenesis via regulating nuclear p53-progerin interaction". *Cell Death and Disease* 10 (6), p. 451. DOI: 10.1038/s41419-019-1670-6.

Lv, Juan, Chao Liu, Fukun K. Chen, Zhiping P. Feng, Li Jia, Pengjie J. Liu, Zhixian X. Yang, Fei Hou, and Zhiyong Y. Deng (Aug. 2021). "M2-like tumour-associated

macrophage-secreted IGF promotes thyroid cancer stemness and metastasis by activating the PI3K/AKT/mTOR pathway". *Molecular Medicine Reports* 24 (2), pp. 1–10. DOI: 10.3892/MMR.2021.12249/HTML.

Ma, Ying, Rosa F. Hwang, Craig D. Logsdon, and Stephen E. Ullrich (June 2013). "Dynamic Mast Cell–Stromal Cell Interactions Promote Growth of Pancreatic Cancer". *Cancer Research* 73.13, pp. 3927–3937. DOI: 10.1158/0008-5472.CAN-12-4479. eprint: https://aacrjournals.org/cancerres/article-pdf/73/13/3927/2684959/3927.pdf.

Macaulay, Valentine M., Simon Lord, Syed Hussain, Jose Pablo Maroto, Robert Hugh Jones, Miguel Angel Climent, Natalie Cook, Chia Chi Lin, Shian Shiang Wang, Diletta Bianchini, Mark Bailey, Laura Schlieker, Thomas Bogenrieder, and Johann de Bono (Aug. 2023). "A Phase Ib/II study of IGF-neutralising antibody xentuzumab with enzalutamide in metastatic castration-resistant prostate cancer". *British Journal of Cancer* 129 (6), pp. 965–973. DOI: 10.1038/s41416-023-02380-1.

Macaulay, Valentine M., Mark R. Middleton, S. Gail Eckhardt, Charles M. Rudin, Rosalyn A. Juergens, Richard Gedrich, Sven Gogov, Sean McCarthy, Srinivasu Poondru, Andrew W. Stephens, and Shirish M. Gadgeel (2016). "Phase I Dose-Escalation Study of Linsitinib (OSI-906) and Erlotinib in Patients with Advanced Solid Tumors". *Clinical Cancer Research* 22.12, pp. 2897–2907. DOI: 10.1158/1078-0432.CCR-15-2218. eprint: https://aacrjournals.org/clincancerres/article-pdf/22/12/2897/2963198/2897.pdf.

Maeda, Hiroyuki, Hiroyuki Yonou, Keiichi Yano, Genichiro Ishii, Seiichi Saito, and Atsushi Ochiai (2009). "Prostate-specific antigen enhances bioavailability of insulin-like growth factor by degrading insulin-like growth factor binding protein 5". *Biochemical and Biophysical Research Communications* 381.3, pp. 311–316. DOI: https://doi.org/10.1016/j.bbrc.2009.01.096.

Magi-Galluzzi, Cristina, Toyonori Tsusuki, Paul Elson, Kelly Simmerman, Chris LaFargue, Raquel Esgueva, Eric Klein, Mark A. Rubin, and Ming Zhou (2011). "TMPRSS2–ERG gene fusion prevalence and class are significantly different in prostate cancer of caucasian, african-american and japanese patients". *The Prostate* 71.5, pp. 489–497. DOI: https://doi.org/10.1002/pros.21265. eprint: https://onlinelibrary.wiley.com/doi/pdf/10.1002/pros.21265.

Mahajan, Sahil, Ankita Saini, Vemika Chandra, Ravikanth Nanduri, Rashi Kalra, Ella Bhagyaraj, Neeraj Khatri, and Pawan Gupta (July 2015). "Nuclear Receptor Nr4a2 Promotes Alternative Polarization of Macrophages and Confers Protection in Sepsis". *Journal of Biological Chemistry* 290 (30). doi: 10.1074/jbc.M115.638064, pp. 18304–18314. DOI: 10.1074/jbc.M115.638064.

Maile, Laura A., Jane Badley-Clarke, and David R. Clemmons (2003). "The Association between Integrin-associated Protein and SHPS-1 Regulates Insulin-like Growth Factor-I Receptor Signaling in Vascular Smooth Muscle Cells". *Molecular Biology of the Cell* 14.9. PMID: 12972543, pp. 3519–3528. DOI: 10.1091/mbc.e03-04-0239. eprint: https://doi.org/10.1091/mbc.e03-04-0239.

Majeti, Ravindra, Mark P. Chao, Ash A. Alizadeh, Wendy W. Pang, Siddhartha Jaiswal, Kenneth D. Gibbs, Nico van Rooijen, and Irving L. Weissman (July 2009). "CD47 Is an Adverse Prognostic Factor and Therapeutic Antibody Target on Human Acute Myeloid Leukemia Stem Cells". *Cell* 138 (2), pp. 286–299. DOI: 10.1016/j.cell.2009.05.045.

Majorini, Maria Teresa, Mario Paolo Colombo, and Daniele Lecis (Apr. 2022). "Few, but Efficient: The Role of Mast Cells in Breast Cancer and Other Solid Tumors". *Cancer*

Research 82.8, pp. 1439–1447. DOI: 10.1158/0008-5472.CAN-21-3424. eprint: https://aacrjournals.org/cancerres/article-pdf/82/8/1439/3112745/1439.pdf.

Mamane, Y, E Petroulakis, O LeBacquer, and N Sonenberg (2006). "mTOR, translation initiation and cancer". *Oncogene* 25 (48), pp. 6416–6422. DOI: 10.1038/sj.onc.1209888.

Mancarella, Caterina, Irene Casanova-Salas, Ana Calatrava, Maria Garcia-Flores, Cecilia Garofalo, Andrea Grilli, Jose Rubio-Briones, Katia Scotlandi, and JoseAntonio Lopez-Guerrero (2017). "Insulin-like growth factor 1 receptor affects the survival of primary prostate cancer patients depending on TMPRSS2-ERG status". *BMC Cancer* 17.1, p. 367. DOI: 10.1186/s12885-017-3356-8.

Mancarella, Caterina, Irene Casanova-Salas, Ana Calatrava, Selena Ventura, Cecilia Garofalo, Jose Rubio-Briones, Vera Magistroni, Maria Cristina Manara, Jose Antonio Lopez-Guerrero, and Katia Scotlandi (Mar. 2015). "ERG deregulation induces IGF-1R expression in prostate cancer cells and affects sensitivity to anti-IGF-1R agents". *Oncotarget* 6 (18), pp. 16611–16622. DOI: 10.18632/ONCOTARGET.3425.

Mangelsdorf, David J., Carl Thummel, Miguel Beato, Peter Herrlich, Günther Schütz, Kazuhiko Umesono, Bruce Blumberg, Philippe Kastner, Manuel Mark, Pierre Chambon, and Ronald M. Evans (1995). "The nuclear receptor superfamily: The second decade". *Cell* 83.6, pp. 835–839. DOI: https://doi.org/10.1016/0092-8674(95)90199-X.

Manning, Brendan D and Lewis C Cantley (June 2007). "AKT/PKB Signaling: Navigating Downstream". *Cell* 129 (7), pp. 1261–1274. DOI: 10.1016/j.cell.2007.06.009.

Mantovani, Alberto, Paola Allavena, Federica Marchesi, and Cecilia Garlanda (2022). "Macrophages as tools and targets in cancer therapy". *Nature Reviews Drug Discovery* 21 (11), pp. 799–820. DOI: 10.1038/s41573-022-00520-5.

Mantovani, Alberto, Federica Marchesi, Alberto Malesci, Luigi Laghi, and Paola Allavena (2017). "Tumour-associated macrophages as treatment targets in oncology". *Nature Reviews Clinical Oncology* 14 (7), pp. 399–416. DOI: 10.1038/nrclinonc.2016.217.

Mantovani, Alberto, Antonio Sica, Silvano Sozzani, Paola Allavena, Annunciata Vecchi, and Massimo Locati (Dec. 2004). "The chemokine system in diverse forms of macrophage activation and polarization". *Trends in Immunology* 25 (12), pp. 677–686. DOI: 10.1016/j.it.2004.09.015.

Mantovani, Alberto, Silvano Sozzani, Massimo Locati, Paola Allavena, and Antonio Sica (2002). "Macrophage polarization: tumor-associated macrophages as a paradigm for polarized M2 mononuclear phagocytes". *Trends in Immunology* 23.11, pp. 549–555. DOI: https://doi.org/10.1016/S1471-4906(02)02302-5.

Maolake, Aerken, Kouji Izumi, Kazuyoshi Shigehara, Ariunbold Natsagdorj, Hiroaki Iwamoto, Suguru Kadomoto, Yuta Takezawa, Kazuaki Machioka, Kazutaka Narimoto, Mikio Namiki, Wen Jye Lin, Guzailinuer Wufuer, and Atsushi Mizokami (Feb. 2017). "Tumor-associated macrophages promote prostate cancer migration through activation of the CCL22–CCR4 axis". *Oncotarget* 8 (6), p. 9739. DOI: 10.18632/ONCOTARGET.14185.

Maor, Sharon B., Shirley Abramovitch, Mike R. Erdos, Lawrence C. Brody, and Haim Werner (2000). "BRCA1 Suppresses Insulin-like Growth Factor-I Receptor Promoter Activity: Potential Interaction between BRCA1 and Sp1". *Molecular Genetics and Metabolism* 69.2, pp. 130–136. DOI: https://doi.org/10.1006/mgme.1999.2958.

Marron, Thomas U, Matthew D Galsky, Bachir Taouli, Maria Isabel Fiel, Stephen Ward, Edward Kim, David Yankelevitz, Deborah Doroshow, Emma Guttman-Yassky, Benjamin Ungar, Saurabh Mehandru, Benjamin J Golas, Daniel Labow, John Sfakianos, Sujit S Nair, Dimple Chakravarty, Michael Buckstein, Xiaoyu Song, Effi Kenigsberg, Sacha Gnjatic, Brian D Brown, Joseph Sparano, Ashutosh Tewari, Myron Schwartz,

Nina Bhardwaj, and Miriam Merad (2022). "Neoadjuvant clinical trials provide a window of opportunity for cancer drug discovery". *Nature Medicine* 28 (4), pp. 626–629. DOI: 10.1038/s41591-022-01681-x.

Marshall, Catherine Handy, Wei Fu, Hao Wang, Alexander S Baras, Tamara L Lotan, and Emmanuel S Antonarakis (2019). "Prevalence of DNA repair gene mutations in localized prostate cancer according to clinical and pathologic features: association of Gleason score and tumor stage". *Prostate Cancer and Prostatic Diseases* 22 (1), pp. 59–65. DOI: 10.1038/s41391-018-0086-1.

Marshall, Jean S (2004). "Mast-cell responses to pathogens". *Nature Reviews Immunology* 4 (10), pp. 787–799. DOI: 10.1038/nri1460.

Martin, Marcel (May 2011). "Cutadapt removes adapter sequences from high-throughput sequencing reads". *EMBnet.journal* 17 (1), pp. 10–12. DOI: 10.14806/EJ.17.1.200.

Martin, Richard M., Jenny L. Donovan, Emma L. Turner, Chris Metcalfe, Grace J. Young, Eleanor I. Walsh, J. Athene Lane, Sian Noble, Steven E. Oliver, Simon Evans, Jonathan A. C. Sterne, Peter Holding, Yoav Ben-Shlomo, Peter Brindle, Naomi J. Williams, Elizabeth M. Hill, Siaw Yein Ng, Jessica Toole, Marta K. Tazewell, Laura J. Hughes, Charlotte F. Davies, Joanna C. Thorn, Elizabeth Down, George Davey Smith, David E. Neal, Freddie C. Hamdy, and CAP Trial Group (Mar. 2018). "Effect of a Low-Intensity PSA-Based Screening Intervention on Prostate Cancer Mortality: The CAP Randomized Clinical Trial". *JAMA* 319.9, pp. 883–895. DOI: 10.1001/jama.2018.0154. eprint: https://jamanetwork.com/journals/jama/articlepdf/2673968/jama_martin_2018_oi_180003_1692284700.42629.pdf.

Martin-Orozco, Natalia, Pawel Muranski, Yeonseok Chung, Xuexian O. Yang, Tomohide Yamazaki, Sijie Lu, Patrick Hwu, Nicholas P. Restifo, Willem W. Overwijk, and Chen Dong (2009). "T Helper 17 Cells Promote Cytotoxic T Cell Activation in Tumor Immunity". *Immunity* 31.5, pp. 787–798. DOI: https://doi.org/10.1016/j.immuni.2009.09.014.

Martinez-Lostao, Luis, Alberto Anel, and Julian Pardo (Nov. 2015). "How Do Cytotoxic Lymphocytes Kill Cancer Cells?" *Clinical Cancer Research* 21.22, pp. 5047–5056. DOI: 10.1158/1078-0432.CCR-15-0685. eprint: https://aacrjournals.org/clincancerres/article-pdf/21/22/5047/2298293/5047.pdf.

Mateo, Joaquin, George Seed, Claudia Bertan, Pasquale Rescigno, David Dolling, Ines Figueiredo, Susana Miranda, Daniel Nava Rodrigues, Bora Gurel, Matthew Clarke, Mark Atkin, Rob Chandler, Carlo Messina, Semini Sumanasuriya, Diletta Bianchini, Maialen Barrero, Antonella Petermolo, Zafeiris Zafeiriou, Mariane Fontes, Raquel Perez-Lopez, Nina Tunariu, Ben Fulton, Robert Jones, Ursula McGovern, Christy Ralph, Mohini Varughese, Omi Parikh, Suneil Jain, Tony Elliott, Shahneen Sandhu, Nuria Porta, Emma Hall, Wei Yuan, Suzanne Carreira, and Johann S. de Bono (Apr. 2020). "Genomics of lethal prostate cancer at diagnosis and castration resistance". *The Journal of Clinical Investigation* 130.4, pp. 1743–1751. DOI: 10.1172/JCI132031.

Matsushita, Makoto, Kazutoshi Fujita, Koji Hatano, Marco A. De Velasco, Hirotsugu Uemura, and Norio Nonomura (2022). "Connecting the Dots Between the Gut–IGF-1–Prostate Axis: A Role of IGF-1 in Prostate Carcinogenesis". *Frontiers in Endocrinology* 13. DOI: 10.3389/fendo.2022.852382.

Mawson, Amanda, Angela Lai, Jason S. Carroll, C. Marcelo Sergio, Christopher J. Mitchell, and Boris Sarcevic (2005). "Estrogen and insulin/IGF-1 cooperatively stimulate cell cycle progression in MCF-7 breast cancer cells through differential regulation of c-Myc and

cyclin D1". *Molecular and Cellular Endocrinology* 229.1, pp. 161–173. DOI: https://doi.org/10.1016/j.mce.2004.08.002.

Mazet, Julie M, Jagdish N Mahale, Orion Tong, Robert A Watson, Ana Victoria Lechuga-Vieco, Gabriela Pirgova, Vivian W C Lau, Moustafa Attar, Lada A Koneva, Stephen N Sansom, Benjamin P Fairfax, and Audrey Gerard (2023). "IFN gamma signaling in cytotoxic T cells restricts anti-tumor responses by inhibiting the maintenance and diversity of intra-tumoral stem-like T cells". *Nature Communications* 14 (1), p. 321. DOI: 10.1038/s41467-023-35948-9.

Mazzaschi, Giulia, Denise Madeddu, Angela Falco, Giovanni Bocchialini, Matteo Goldoni, Francesco Sogni, Giovanna Armani, Costanza Annamaria Lagrasta, Bruno Lorusso, Chiara Mangiaracina, Rocchina Vilella, Caterina Frati, Roberta Alfieri, Luca Ampollini, Michele Veneziani, Enrico Maria Silini, Andrea Ardizzoni, Konrad Urbanek, Franco Aversa, Federico Quaini, and Marcello Tiseo (Jan. 2018). "Low PD-1 Expression in Cytotoxic CD8+ Tumor-Infiltrating Lymphocytes Confers an Immune-Privileged Tissue Microenvironment in NSCLC with a Prognostic and Predictive Value". *Clinical Cancer Research* 24.2, pp. 407–419. DOI: 10.1158/1078-0432.CCR-17-2156. eprint: https://aacrjournals.org/clincancerres/article-pdf/24/2/407/2048443/407.pdf.

McHugh, Deaglan J, Jay Chudow, Mia DeNunzio, Susan F Slovin, Daniel C Danila, Michael J Morris, Howard I Scher, and Dana E Rathkopf (June 2020). "A Phase I Trial of IGF-1R Inhibitor Cixutumumab and mTOR Inhibitor Temsirolimus in Metastatic Castration-resistant Prostate Cancer". *Clinical Genitourinary Cancer* 18 (3). doi: 10.1016/j.clgc.2019.10.013, 171–178.e2. DOI: 10.1016/j.clgc.2019.10.013.

McLane, Laura M., Mohamed S. Abdel-Hakeem, and E. John Wherry (2019). "CD8 T Cell Exhaustion During Chronic Viral Infection and Cancer". *Annual Review of Immunology* 37.Volume 37, 2019, pp. 457–495. DOI: https://doi.org/10.1146/annurev-immunol-041015-055318.

McLeod, Jamie J.A., Bianca Baker, and John J. Ryan (2015). "Mast cell production and response to IL-4 and IL-13". *Cytokine* 75.1. IL 4/IL 13 family, pp. 57–61. DOI: https://doi.org/10.1016/j.cyto.2015.05.019.

Mehta, Hemal H., Qinglei Gao, Colette Galet, Vladislava Paharkova, Junxiang Wan, Jonathan Said, Joanne J. Sohn, Gregory Lawson, Pinchas Cohen, Laura J. Cobb, and Kuk-Wha Lee (July 2011). "IGFBP-3 Is a Metastasis Suppression Gene in Prostate Cancer". *Cancer Research* 71.15, pp. 5154–5163. DOI: 10.1158/0008-5472.CAN-10-4513. eprint: https://aacrjournals.org/cancerres/article-pdf/71/15/5154/2652299/5154.pdf.

Mellman, Ira, Daniel S. Chen, Thomas Powles, and Shannon J. Turley (2023). "The cancer-immunity cycle: Indication, genotype, and immunotype". *Immunity* 56.10, pp. 2188–2205. DOI: https://doi.org/10.1016/j.immuni.2023.09.011.

Melo Garcia, Luciana and Frederic Barabe (2021). "Harnessing Macrophages through the Blockage of CD47: Implications for Acute Myeloid Leukemia". *Cancers* 13.24. DOI: 10.3390/cancers13246258.

Meurette, Olivier and Patrick Mehlen (2018). "Notch Signaling in the Tumor Microenvironment". *Cancer Cell* 34.4, pp. 536–548. DOI: https://doi.org/10.1016/j.ccell.2018.07.009.

Meyer-Siegler, Katherine L., Kenneth A. Iczkowski, Lin Leng, Richard Bucala, and Pedro L. Vera (Dec. 2006). "Inhibition of Macrophage Migration Inhibitory Factor or Its Receptor (CD74) Attenuates Growth and Invasion of DU-145 Prostate Cancer Cells1". *The Journal of Immunology* 177.12, pp. 8730–8739. DOI: 10.4049/jimmunol.177.12.8730.

eprint: https://journals.aai.org/jimmunol/article-pdf/177/12/8730/1220526/zim02406008730.pdf.

Meyts, Pierre De and Jonathan Whittaker (2002). "Structural biology of insulin and IGF1 receptors: implications for drug design". *Nature Reviews Drug Discovery* 1, pp. 769–783. DOI: 10.1038/nrd917.

Miller, Gary J and James M Cygan (Nov. 1994). "Morphology of Prostate Cancer: The Effects of Multifocality on Histological Grade, Tumor Volume and Capsule Penetration". *Journal of Urology* 152 (5 Part 2). doi: 10.1016/S0022-5347(17)32368-6, pp. 1709–1713. DOI: 10.1016/S0022-5347(17)32368-6.

Mills, Charles D., Kristi Kincaid, Jennifer M. Alt, Michelle J. Heilman, and Annette M. Hill (June 2000). "M-1/M-2 Macrophages and the Th1/Th2 Paradigm". *The Journal of Immunology* 164.12, pp. 6166–6173. DOI: 10.4049/jimmunol.164.12.6166. eprint: https://journals.aai.org/jimmunol/article-pdf/164/12/6166/1114770/6166.pdf.

Mills, Ian G (2014). "Maintaining and reprogramming genomic androgen receptor activity in prostate cancer". *Nature Reviews Cancer* 14 (3), pp. 187–198. DOI: 10.1038/nrc3678.

Mills, Jack V, Eliot Osher, Guillaume Rieunier, Ian G Mills, and Valentine M Macaulay (2021). "IGF-1R nuclear import and recruitment to chromatin involves both alpha and beta subunits". *Discover Oncology* 12 (1), p. 13. DOI: 10.1007/s12672-021-00407-8.

Mireuta, Matei, Elena Birman, Melinda Barmash, and Michael Pollak (Mar. 2014). "Quantification of Binding of IGF-1 to BI 836845, a Candidate Therapeutic Antibody Against IGF-1 and IGF-2, and Effects of This Antibody on IGF-1:IGFBP-3 Complexes In Vitro and in Male C57BL/6 Mice". *Endocrinology* 155.3, pp. 703–715. DOI: 10.1210/en.2013-1791. eprint: https://academic.oup.com/endo/article-pdf/155/3/703/10824847/endo0703.pdf.

Mitchem, Jonathan B., Donal J. Brennan, Brett L. Knolhoff, Brian A. Belt, Yu Zhu, Dominic E. Sanford, Larisa Belaygorod, Danielle Carpenter, Lynne Collins, David Piwnica-Worms, Stephen Hewitt, Girish Mallya Udupi, William M. Gallagher, Craig Wegner, Brian L. West, Andrea Wang-Gillam, Peter Goedegebuure, David C. Linehan, and David G. DeNardo (Jan. 2013). "Targeting Tumor-Infiltrating Macrophages Decreases Tumor-Initiating Cells, Relieves Immunosuppression, and Improves Chemotherapeutic Responses". *Cancer Research* 73.3, pp. 1128–1141. DOI: 10.1158/0008-5472.CAN-12-2731. eprint: https://aacrjournals.org/cancerres/article-pdf/73/3/1128/2692408/1128.pdf.

Mitri, Diletta Di, Michela Mirenda, Jelena Vasilevska, Arianna Calcinotto, Nicolas Delaleu, Ajinkya Revandkar, Veronica Gil, Gunther Boysen, Marco Losa, Simone Mosole, Emiliano Pasquini, Rocco D'Antuono, Michela Masetti, Elena Zagato, Giovanna Chiorino, Paola Ostano, Andrea Rinaldi, Letizia Gnetti, Mariona Graupera, Ana Raquel Martins Figueiredo Fonseca, Ricardo Pereira Mestre, David Waugh, Simon Barry, Johann De Bono, and Andrea Alimonti (Aug. 2019). "Re-education of Tumor-Associated Macrophages by CXCR2 Blockade Drives Senescence and Tumor Inhibition in Advanced Prostate Cancer". *Cell Reports* 28, pp. 2156–2168.

Mitri, Diletta Di, Alberto Toso, Jing Jing Chen, Manuela Sarti, Sandra Pinton, Tanja Rezzonico Jost, Rocco D'Antuono, Erica Montani, Ramon Garcia-Escudero, Ilaria Guccini, Sabela Da Silva-Alvarez, Manuel Collado, Mario Eisenberger, Zhe Zhang, Carlo Catapano, Fabio Grassi, and Andrea Alimonti (Aug. 2014). "Tumour-infiltrating Gr-1+ myeloid cells antagonize senescence in cancer". *Nature* 515, pp. 134–137. DOI: 10.1038/nature13638.

Mittal, Deepak, Matthew M Gubin, Robert D Schreiber, and Mark J Smyth (2014). "New insights into cancer immunoediting and its three component phases—elimination, equilibrium and escape". *Current Opinion in Immunology* 27. Lymphocyte development * Tumour immunology, pp. 16–25. DOI: https://doi.org/10.1016/j.coi.2014.01.004.

Miyake, Hideaki, Michael Pollak, and Martin E Gleave (June 2000). "Castration-induced Up-Regulation of Insulin-like Growth Factor Binding Protein-5 Potentiates Insulin-like Growth Factor-I Activity and Accelerates Progression to Androgen Independence in Prostate Cancer Models". *Cancer Research* 60 (11), pp. 3058–3064.

Miyake, Makito, Shunta Hori, Yosuke Morizawa, Yoshihiro Tatsumi, Yasushi Nakai, Satoshi Anai, Kazumasa Torimoto, Katsuya Aoki, Nobumichi Tanaka, Keiji Shimada, Noboru Konishi, Michihiro Toritsuka, Toshifumi Kishimoto, Charles J. Rosser, and Kiyohide Fujimoto (2016). "CXCL1-Mediated Interaction of Cancer Cells with Tumor-Associated Macrophages and Cancer-Associated Fibroblasts Promotes Tumor Progression in Human Bladder Cancer". *Neoplasia* 18.10, pp. 636–646. DOI: https://doi.org/10.1016/j.neo.2016.08.002.

Molon, Barbara, Stefano Ugel, Federica Del Pozzo, Cristiana Soldani, Serena Zilio, Debora Avella, Antonella De Palma, PierLuigi Mauri, Ana Monegal, Maria Rescigno, Benedetta Savino, Piergiuseppe Colombo, Nives Jonjic, Sanja Pecanic, Loretta Lazzarato, Roberta Fruttero, Alberto Gasco, Vincenzo Bronte, and Antonella Viola (Sept. 2011). "Chemokine nitration prevents intratumoral infiltration of antigen-specific T cells". *Journal of Experimental Medicine* 208.10, pp. 1949–1962. DOI: 10.1084/jem.20101956. eprint: https://rupress.org/jem/article-pdf/208/10/1949/1738588/jem_20101956.pdf.

Monnier, Marine, Lea Paolini, Emeline Vinatier, Alberto Mantovani, Yves Delneste, and Pascale Jeannin (2022). "Antitumor strategies targeting macrophages: the importance of considering the differences in differentiation/polarization processes between human and mouse macrophages". *Journal for ImmunoTherapy of Cancer* 10.10. DOI: 10.1136/jitc-2022-005560. eprint: https://jitc.bmj.com/content/10/10/e005560.full.pdf.

Moody, Gordon, Pedro J Beltran, Petia Mitchell, Elaina Cajulis, Young-Ah Chung, David Hwang, Richard Kendall, Robert Radinsky, Pinchas Cohen, and Frank J Calzone (2014). "IGF1R blockade with ganitumab results in systemic effects on the GH–IGF axis in mice". *Journal of Endocrinology* 221.1, pp. 145–155. DOI: 10.1530/JOE-13-0306.

Morrissey, Meghan A., Nadja Kern, and Ronald D. Vale (June 2020). "CD47 Ligation Repositions the Inhibitory Receptor SIRPA to Suppress Integrin Activation and Phagocytosis". *Immunity* 53.2, 290–302.e6. DOI: 10.1016/j.immuni.2020.07.008.

Moschos, Stergios J. and Christos S. Mantzoros (Nov. 2002). "The Role of the IGF System in Cancer: From Basic to Clinical Studies and Clinical Applications". *Oncology* 63.4, pp. 317–332. DOI: 10.1159/000066230. eprint: https://karger.com/ocl/article-pdf/63/4/317/3279901/000066230.pdf.

Mosser, David M and Justin P Edwards (2008). "Exploring the full spectrum of macrophage activation". *Nature Reviews Immunology* 8 (12), pp. 958–969. DOI: 10.1038/nri2448.

Movahedi, Kiavash, Damya Laoui, Conny Gysemans, Martijn Baeten, Geert Stangé, Jan Van den Bossche, Matthias Mack, Daniel Pipeleers, Peter In't Veld, Patrick De Baetselier, and Jo A. Van Ginderachter (July 2010). "Different Tumor Microenvironments Contain Functionally Distinct Subsets of Macrophages Derived from Ly6C(high) Monocytes". *Cancer Research* 70.14, pp. 5728–5739. DOI: 10.1158/0008-5472.CAN-09-4672. eprint: https://aacrjournals.org/cancerres/article-pdf/70/14/5728/2638750/5728.pdf.

Muenchen, Heather J, Din-Lii Lin, Michael A Walsh, Evan T Keller, and Kenneth J Pienta (May 2000). "Tumor Necrosis Factor-a-induced Apoptosis in Prostate Cancer Cells through Inhibition of Nuclear Factor-kB by an IkBa "Super-Repressor"". *Clinical Cancer Research* 6 (5), pp. 1969–1977.

Muhammad, Shan, Tao Fan, Yang Hai, Yibo Gao, and Jie He (2023). "Reigniting hope in cancer treatment: the promise and pitfalls of IL-2 and IL-2R targeting strategies". *Molecular Cancer* 22 (1), p. 121. DOI: 10.1186/s12943-023-01826-7.

Murdoch, Craig, Athina Giannoudis, and Claire E. Lewis (Oct. 2004). "Mechanisms regulating the recruitment of macrophages into hypoxic areas of tumors and other ischemic tissues". *Blood* 104.8, pp. 2224–2234. DOI: 10.1182/blood-2004-03-1109. eprint: https://ashpublications.org/blood/article-pdf/104/8/2224/1702495/zh802004002224.pdf.

Murray, Peter J and Thomas A Wynn (2011). "Protective and pathogenic functions of macrophage subsets". *Nature Reviews Immunology* 11 (11), pp. 723–737. DOI: 10.1038/nri3073.

Nackiewicz, Dominika, Meixia Dan, Madeleine Speck, Samuel Z Chow, Yi-Chun Chen, J Andrew Pospisilik, C Bruce Verchere, and Jan A Ehses (Jan. 2020). "Islet Macrophages Shift to a Reparative State following Pancreatic Beta-Cell Death and Are a Major Source of Islet Insulin-like Growth Factor-1". *iScience* 23 (1). doi: 10.1016/j.isci.2019.100775. DOI: 10.1016/j.isci.2019.100775.

Nadler, Robert B., Peter A. Humphrey, Deborah S. Smith, William J. Catalona, and Timothy L. Ratliff (1995). "Effect of Inflammation and Benign Prostatic Hyperplasia on Elevated Serum Prostate Specific Antigen Levels". *Journal of Urology* 154.2, pp. 407–413. DOI: 10.1016/S0022-5347(01)67064-2.

Nagaya, Naoya, Geun Taek Lee, Shigeo Horie, and Isaac Yi Kim (2020). "CXC Chemokine/Receptor Axis Profile and Metastasis in Prostate Cancer". *Frontiers in Molecular Biosciences* 7. DOI: 10.3389/fmolb.2020.579874.

Naji, Leen, Harkanwal Randhawa, Zahra Sohani, Brittany Dennis, Deanna Lautenbach, Owen Kavanagh, Monica Bawor, Laura Banfield, and Jason Profetto (2018). "Digital Rectal Examination for Prostate Cancer Screening in Primary Care: A Systematic Review and Meta-Analysis". *The Annals of Family Medicine* 16.2, pp. 149–154. DOI: 10.1370/afm.2205. eprint: https://www.annfammed.org/content/16/2/149.full.pdf.

Nandakumar, Ashwin (2022). *Investigating high circulating IGF-1 as a risk factor for development of prostate cancer*. eng. MacAulay, Valentine.

Nederlof, Rianne, Sophia Reidel, André Spychala, Stefanie Gödecke, André Heinen, Tobias Lautwein, Patrick Petzsch, Karl Köhrer, and Axel Gödecke (2022). "Insulin-Like Growth Factor 1 Attenuates the Pro-Inflammatory Phenotype of Neutrophils in Myocardial Infarction". *Frontiers in Immunology* 13. DOI: 10.3389/fimmu.2022.908023.

Newman, Aaron M, Chloe B Steen, Chih Long Liu, Andrew J Gentles, Aadel A Chaudhuri, Florian Scherer, Michael S Khodadoust, Mohammad S Esfahani, Bogdan A Luca, David Steiner, Maximilian Diehn, and Ash A Alizadeh (2019). "Determining cell type abundance and expression from bulk tissues with digital cytometry". *Nature Biotechnology* 37 (7), pp. 773–782. DOI: 10.1038/s41587-019-0114-2.

Nguyen, Chi Huu, Angela Schlerka, Alexander M. Grandits, Elisabeth Koller, Emiel van der Kouwe, George S. Vassiliou, Philipp B. Staber, Gerwin Heller, and Rotraud Wieser (Oct. 2020). "IL2RA Promotes Aggressiveness and Stem Cell–Related Properties of Acute Myeloid Leukemia". *Cancer Research* 80.20, pp. 4527–4539. DOI:

10.1158/0008-5472.CAN-20-0531. eprint: https://aacrjournals.org/cancerres/article-pdf/80/20/4527/2871941/4527.pdf.

Ni, Fang, Rui Sun, Binqing Fu, Fuyan Wang, Chuang Guo, Zhigang Tian, and Haiming Wei (2013). "IGF-1 promotes the development and cytotoxic activity of human NK cells". *Nature Communications* 4 (1), p. 1479. DOI: 10.1038/ncomms2484.

Nickerson, Tara, Francis Chang, Donald Lorimer, Steven P Smeekens, Charles L Sawyers, and Michael Pollak (Aug. 2001). "In Vivo Progression of LAPC-9 and LNCaP Prostate Cancer Models to Androgen Independence Is Associated with Increased Expression of Insulin-like Growth Factor I (IGF-I) and IGF-I Receptor (IGF-IR)1". *Cancer Research* 61 (16), pp. 6276–6280.

Nolz, Jeffrey C, Gabriel R Starbeck-Miller, and John T Harty (2011). "Naive, Effector and Memory CD8 T-cell Trafficking: Parallels and Distinctions". *Immunotherapy* 3.10. PMID: 21995573, pp. 1223–1233. DOI: 10.2217/imt.11.100. eprint: https://doi.org/10.2217/imt.11.100.

Nonomura, Norio, Hitoshi Takayama, Masashi Nakayama, Yasutomo Nakai, Atsunari Kawashima, Masatoshi Mukai, Akira Nagahara, Katsuyuki Aozasa, and Akira Tsujimura (2011). "Infiltration of tumour-associated macrophages in prostate biopsy specimens is predictive of disease progression after hormonal therapy for prostate cancer". *BJU International* 107.12, pp. 1918–1922. DOI: https://doi.org/10.1111/j.1464-410X.2010.09804.x.

Nordlohne, Johannes, Ilona Hulsmann, Svenja Schwafertz, Jasmin Zgrajek, Manuel Grundmann, Sibylle von Vietinghoff, Frank Eitner, and Michael S Becker (2021). "A flow cytometry approach reveals heterogeneity in conventional subsets of murine renal mononuclear phagocytes". *Scientific Reports* 11 (1), p. 13251. DOI: 10.1038/s41598-021-92784-x.

Noto, Christine N., Stella G. Hoft, and Richard J. DiPaolo (2021). "Mast Cells as Important Regulators in Autoimmunity and Cancer Development". *Frontiers in Cell and Developmental Biology* 9. DOI: 10.3389/fcell.2021.752350.

O'Donnell, Jake S., Michele W.L. Teng, and Mark J. Smyth (Dec. 2018). "Cancer immunoediting and resistance to T cell-based immunotherapy". *Nature Reviews Clinical Oncology* 16, pp. 151–167. DOI: 10.1038/s41571-018-0142-8.

Obr, Alison E, Sushil Kumar, Yun-Juan Chang, Joseph J Bulatowicz, Betsy J Barnes, Raymond B Birge, Deborah A Lazzarino, Emily Gallagher, Derek LeRoith, and Teresa L Wood (2018). "Insulin-like growth factor receptor signaling in breast tumor epithelium protects cells from endoplasmic reticulum stress and regulates the tumor microenvironment". *Breast Cancer Research* 20 (1), p. 138. DOI: 10.1186/s13058-018-1063-2.

Obr, Alison E., Joseph J. Bulatowicz, Yun-Juan Chang, Virginia Ciliento, Alexander Lemenze, Krystopher Maingrette, Quan Shang, Emily J. Gallagher, Derek LeRoith, and Teresa L. Wood (2022). "Breast tumor IGF1R regulates cell adhesion and metastasis: alignment of mouse single cell and human breast cancer transcriptomics". *Frontiers in Oncology* 12. DOI: 10.3389/fonc.2022.990398.

Odagiu, Livia, Salix Boulet, Dave Maurice De Sousa, Jean-Francois Daudelin, Sandrine Nicolas, and Nathalie Labrecque (2020). "Early programming of CD8+ T cell response by the orphan nuclear receptor NR4A3". *Proceedings of the National Academy of Sciences* 117.39, pp. 24392–24402. DOI: 10.1073/pnas.2007224117. eprint: https://www.pnas.org/doi/pdf/10.1073/pnas.2007224117.

Oft, Martin (Mar. 2014). "IL-10: Master Switch from Tumor-Promoting Inflammation to Antitumor Immunity". *Cancer Immunology Research* 2.3, pp. 194–199. DOI: 10.1158/2326-6066.CIR-13-0214. eprint: https://aacrjournals.org/cancerimmunolres/article-pdf/2/3/194/2344778/194.pdf.

Ogawara, Yoko, Shohei Kishishita, Toshiyuki Obata, Yuko Isazawa, Toshiaki Suzuki, Keiji Tanaka, Norihisa Masuyama, and Yukiko Gotoh (June 2002). "Akt Enhances Mdm2-mediated Ubiquitination and Degradation of p53". *Journal of Biological Chemistry* 277 (24). doi: 10.1074/jbc.M109745200, pp. 21843–21850. DOI: 10.1074/jbc.M109745200.

Oh, Jonathan C., Weiguo Wu, Guillermo Tortolero-Luna, Russell Broaddus, David M. Gershenson, Thomas W. Burke, Rosemarie Schmandt, and Karen H. Lu (May 2004). "Increased Plasma Levels of Insulin-Like Growth Factor 2 and Insulin-Like Growth Factor Binding Protein 3 Are Associated with Endometrial Cancer Risk". *Cancer Epidemiology, Biomarkers and Prevention* 13.5, pp. 748–752. DOI: 10.1158/1055-9965.748.13.5. eprint: https://aacrjournals.org/cebp/article-pdf/13/5/748/2261761/748-752.pdf.

Ohlsson, Claes, Nikolai Kley, Haim Werner, and Derek LeRoith (Mar. 1998). "p53 Regulates Insulin-Like Growth Factor-I (IGF-I) Receptor Expression and IGF-I-Induced Tyrosine Phosphorylation in an Osteosarcoma Cell Line: Interaction between p53 and Sp1". *Endocrinology* 139.3, pp. 1101–1107. DOI: 10.1210/endo.139.3.5832. eprint: https://academic.oup.com/endo/article-pdf/139/3/1101/10352980/endo1101.pdf.

Oldenborg, Per-Arne, Hattie D. Gresham, and Frederik P. Lindberg (Apr. 2001). "Cd47-Signal Regulatory Protein a (Sirpa) Regulates Fcy and Complement Receptor–Mediated Phagocytosis". *Journal of Experimental Medicine* 193.7, pp. 855–862. DOI: 10.1084/jem.193.7.855. eprint: https://rupress.org/jem/article-pdf/193/7/855/1701911/010027.pdf.

Oldenborg, Per-Arne, Alex Zheleznyak, Yi-Fu Fang, Carl F. Lagenaur, Hattie D. Gresham, and Frederik P. Lindberg (2000). "Role of CD47 as a Marker of Self on Red Blood Cells". *Science* 288.5473, pp. 2051–2054. DOI: 10.1126/science.288.5473.2051. eprint: https://www.science.org/doi/pdf/10.1126/science.288.5473.2051.

Olivo-Marston, Susan E., Stephen D. Hursting, Jackie Lavigne, Susan N. Perkins, Rami S. Maarouf, Shoshana Yakar, and Curtis C. Harris (2009). "Genetic reduction of circulating insulin-like growth factor-1 inhibits azoxymethane-induced colon tumorigenesis in mice". *Molecular Carcinogenesis* 48.12, pp. 1071–1076. DOI: https://doi.org/10.1002/mc.20577. eprint: https://onlinelibrary.wiley.com/doi/pdf/10.1002/mc.20577.

Orange, Samuel T., Jack Leslie, Mark Ross, Derek A. Mann, and Henning Wackerhage (2023). "The exercise IL-6 enigma in cancer". *Trends in Endocrinology and Metabolism* 34.11, pp. 749–763. DOI: https://doi.org/10.1016/j.tem.2023.08.001.

Orio, Francesco, Beatrice Terouanne, Virginie Georget, Serge Lumbroso, Christophe Avances, Christian Siatka, and Charles Sultan (2002). "Potential action of IGF-1 and EGF on androgen receptor nuclear transfer and transactivation in normal and cancer human prostate cell lines". *Molecular and Cellular Endocrinology* 198.1, pp. 105–114. DOI: https://doi.org/10.1016/S0303-7207(02)00374-X.

Osher, Eliot and Valentine M. Macaulay (2019). "Therapeutic Targeting of the IGF Axis". *Cells* 8.8. DOI: 10.3390/cells8080895.

Osorio, Juan C., Patrick Smith, David A. Knorr, and Jeffrey V. Ravetch (2023). "The antitumor activities of anti-CD47 antibodies require Fc-FcyR interactions". *Cancer Cell* 41.12, 2051–2065.e6. DOI: https://doi.org/10.1016/j.ccell.2023.10.007.

Osuka, Satoru, Dan Zhu, Zhaobin Zhang, Chaoxi Li, Christian T. Stackhouse, Oltea Sampetrean, Jeffrey J. Olson, G. Yancey Gillespie, Hideyuki Saya, Christopher D. Willey, and Erwin G. Van Meir (Mar. 2021). "N-cadherin upregulation mediates adaptive radioresistance in glioblastoma". *The Journal of Clinical Investigation* 131.6. DOI: 10.1172/JCI136098.

Ouyang, Wenjun and Anne O'Garra (Apr. 2019). "IL-10 Family Cytokines IL-10 and IL-22: from Basic Science to Clinical Translation". *Immunity* 50 (4). doi: 10.1016/j.immuni.2019.03.020, pp. 871–891. DOI: 10.1016/j.immuni.2019.03.020.

Owen, David L., Louisa E. Sjaastad, and Michael A. Farrar (Oct. 2019). "Regulatory T Cell Development in the Thymus". *The Journal of Immunology* 203.8, pp. 2031–2041. DOI: 10.4049/jimmunol.1900662. eprint: https://journals.aai.org/jimmunol/article-pdf/203/8/2031/1451688/ji1900662.pdf.

Oza, Amit, Stanley Kaye, Jan Van Tornout, Cristiana Sessa, Martin Gore, R. Wendel Naumann, Hal Hirte, Nicoletta Colombo, Jihong Chen, Seema Gorla, Srinivasu Poondru, Margaret Singh, Joyce Steinberg, Geoff Yuen, and Susana Banerjee (2018). "Phase 2 study evaluating intermittent and continuous linsitinib and weekly paclitaxel in patients with recurrent platinum resistant ovarian epithelial cancer". *Gynecologic Oncology* 149.2, pp. 275–282. DOI: https://doi.org/10.1016/j.ygyno.2018.01.019.

Pacey, Simon, Javier Garcia Corbacho, Nimish Shah, Ola Bratt, Anne Warren, Richard D. Baird, Vincent Gnanapragasam, Sara Stearn, Susan Ingle, Leanne K Bell, William Dott, Wendi Qian, Wanfeng Zhao, Barry Davies, Elizabeth A. Harrington, Elisabeth Maria Oelmann, Mirela Hategan, and Sanjeev Kumar (2017). "CANCAP02: A study into the pharmacodynamic biomarker effects of vistusertib (AZD2014), an mTORC1/2 inhibitor, given prior to radical prostatectomy (RP)". *Journal of Clinical Oncology* 35.6, p. 97. DOI: 10.1200/JCO.2017.35.6_suppl.97.

Pacey, Simon, Mark David Linch, Howard Kynaston, Anne Warren, Alex Freeman, Ruth Tysoe, Greg Shaw, Krishna Narahari, Satish Kumar, Henno Martin, Bihani Kularatne, Vincent Gnanapragasam, Barry Davies, Josephine Khan, Ola Bratt, Harveer Dev, Charles Massie, and Nimish Shah (Feb. 2019). "A study into the pharmacodynamic biomarker effects of olaparib (PARP Inhibitor) and degarelix (GnRH antagonist) given prior to radical prostatectomy (RP) CANCAP03". *Journal of Clinical Oncology* 37 (7), p. 35. DOI: 10.1200/JCO.2019.37.7_suppl.35.

Pacey, Simon, Nimish Shah, Barry Davies, Ola Bratt, Anne Warren, Richard D. Baird, Vincent Gnanapragasam, Susan Ingle, Sara Stearn, Andrea Machin, Wendi Qian, Wanfeng Zhao, Elizabeth Harrington, Elisabeth Maria Oelmann, Mirela Hategan, Sanjeev Srinivas Kumar, and Javier Garcia Corbacho (2018). "A pharmacodynamic biomarker study of vistusertib (AZD2014), an mTORC1/2 inhibitor, given prior to radical prostatectomy (CANCAP02)". *Journal of Clinical Oncology* 36.15, p. 5081. DOI: 10.1200/JCO.2018.36.15_suppl.5081.

Pachynski, Russell K., Eric H. Kim, Natalia Miheecheva, Nikita Kotlov, Akshaya Ramachandran, Ekaterina Postovalova, Ilia Galkin, Viktor Svekolkin, Yang Lyu, Qiong Zou, Dengfeng Cao, Joseph Gaut, Joseph E. Ippolito, Alexander Bagaev, Maria Bruttan, Olga Gancharova, Krystle Nomie, Maria Tsiper, Gerald L. Andriole, Ravshan Ataullakhanov, and James J. Hsieh (June 2021). "Single-cell Spatial Proteomic Revelations on the Multiparametric MRI Heterogeneity of Clinically Significant Prostate Cancer". *Clinical Cancer Research* 27.12, pp. 3478–3490. DOI:

10.1158/1078-0432.CCR-20-4217. eprint: https://aacrjournals.org/clincancerres/article-pdf/27/12/3478/3089916/3478.pdf.

Pai, Chien Chun Steven, John T. Huang, Xiaoqing Lu, Donald M. Simons, Chanhyuk Park, Anthony Chang, Whitney Tamaki, Eric Liu, Kole T. Roybal, Jane Seagal, Mingyi Chen, Katsunobu Hagihara, Xiao X. Wei, Michel DuPage, Serena S. Kwek, David Y. Oh, Adil Daud, Katy K. Tsai, Clint Wu, Li Zhang, Marcella Fasso, Ravi Sachidanandam, Anitha Jayaprakash, Ingrid Lin, Amy Jo Casbon, Gillian A. Kinsbury, and Lawrence Fong (Feb. 2019). "Clonal Deletion of Tumor-Specific T Cells by Interferon-gamma Confers Therapeutic Resistance to Combination Immune Checkpoint Blockade". *Immunity* 50 (2), 477–492.e8. DOI: 10.1016/j.immuni.2019.01.006.

Palmieri, Erika M, Marieli Gonzalez-Cotto, Walter A Baseler, Luke C Davies, Bart Ghesquière, Nunziata Maio, Christopher M Rice, Tracey A Rouault, Teresa Cassel, Richard M Higashi, Andrew N Lane, Teresa W.-M. Fan, David A Wink, and Daniel W McVicar (2020). "Nitric oxide orchestrates metabolic rewiring in M1 macrophages by targeting aconitase 2 and pyruvate dehydrogenase". *Nature Communications* 11 (1), p. 698. DOI: 10.1038/s41467-020-14433-7.

Pandey, Veethika, Alicia Fleming-Martinez, Ligia Bastea, Heike R Doeppler, Jillian Eisenhauer, Tam Le, Brandy Edenfield, and Peter Storz (July 2021). "CXCL10/CXCR3 signaling contributes to an inflammatory microenvironment and its blockade enhances progression of murine pancreatic precancerous lesions". *eLife* 10. Ed. by Matthew G Vander Heiden, Tadatsugu Taniguchi, and Mara Sherman, e60646. DOI: 10.7554/eLife.60646.

Pandini, Giuseppe, Rossana Mineo, Francesco Frasca, Jr. Roberts Charles T., Marco Marcelli, Riccardo Vigneri, and Antonino Belfiore (Mar. 2005). "Androgens Up-regulate the Insulin-like Growth Factor-I Receptor in Prostate Cancer Cells". *Cancer Research* 65.5, pp. 1849–1857. DOI: 10.1158/0008-5472.CAN-04-1837. eprint: https://aacrjournals.org/cancerres/article-pdf/65/5/1849/2541447/1849-1857.pdf.

Park, Josiah Voth, Raghav Chandra, Ling Cai, Debolina Ganguly, Huiyu Li, Jason E. Toombs, Luc Girard, Rolf A. Brekken, and John D. Minna (Oct. 2022). "Tumor Cells Modulate Macrophage Phenotype in a Novel In Vitro Co-Culture Model of the NSCLC Tumor Microenvironment". *Journal of Thoracic Oncology* 17 (10), pp. 1178–1191. DOI: 10.1016/j.jtho.2022.06.011.

Park, Keunchil, Daniel Shao Weng Tan, Wu Chou Su, Byoung Chul Cho, Sang We Kim, Ki Hyeong Lee, Chin Chou Wang, Takashi Seto, Dennis Chin Lun Huang, Helen Hayoun Jung, Ming Chi Hsu, Thomas Bogenrieder, and Chia Chi Lin (Sept. 2021). "Phase 1b Open-Label Trial of Afatinib Plus Xentuzumab (BI 836845) in Patients With EGFR Mutation-Positive NSCLC After Progression on EGFR Tyrosine Kinase Inhibitors". *JTO Clinical and Research Reports* 2 (9). DOI: 10.1016/j.jtocrr.2021.100206.

Park, SunYoung, Terri A. DiMaio, Elizabeth A. Scheef, Christine M. Sorenson, and Nader Sheibani (2010). "PECAM-1 regulates proangiogenic properties of endothelial cells through modulation of cell-cell and cell-matrix interactions". *American Journal of Physiology-Cell Physiology* 299.6. PMID: 20810911, pp. C1468–C1484. DOI: 10.1152/ajpcell.00246.2010. eprint: https://doi.org/10.1152/ajpcell.00246.2010.

Parker, Chris C., Nicholas D. James, Christopher D. Brawley, Noel W. Clarke, Adnan Ali, Claire L. Amos, Gerhardt Attard, Simon Chowdhury, Adrian Cook, William Cross, David P. Dearnaley, Hassan Douis, Duncan C. Gilbert, Clare Gilson, Silke Gillessen, Alex Hoyle, Rob J. Jones, Ruth E. Langley, Zafar I. Malik, Malcolm D. Mason,

David Matheson, Robin Millman, Mary Rauchenberger, Hannah Rush, J Martin Russell, Hannah Sweeney, Amit Bahl, Alison Birtle, Lisa Capaldi, Omar Din, Daniel Ford, Joanna Gale, Ann Henry, Peter Hoskin, Mohammed Kagzi, Anna Lydon, Joe M. O'Sullivan, Sangeeta A. Paisey, Omi Parikh, Delia Pudney, Vijay Ramani, Peter Robson, Narayanan Nair Srihari, Jacob Tanguay, Mahesh K. B. Parmar, Matthew R. Sydes, and for the STAMPEDE Trial Collaborative Group (June 2022). "Radiotherapy to the prostate for men with metastatic prostate cancer in the UK and Switzerland: Long-term results from the STAMPEDE randomised controlled trial". *PLOS Medicine* 19.6, pp. 1–20. DOI: 10.1371/journal.pmed.1003998.

Patro, Rob, Geet Duggal, Michael I. Love, Rafael A. Irizarry, and Carl Kingsford (Mar. 2017). "Salmon provides fast and bias-aware quantification of transcript expression". *Nature Methods 2017 14:4* 14 (4), pp. 417–419. DOI: 10.1038/nmeth.4197.

Patsoukis, Nikolaos, Julia Brown, Victoria Petkova, Fang Liu, Lequn Li, and Vassiliki A. Boussiotis (2012). "Selective Effects of PD-1 on Akt and Ras Pathways Regulate Molecular Components of the Cell Cycle and Inhibit T Cell Proliferation". *Science Signaling* 5.230, ra46–ra46. DOI: 10.1126/scisignal.2002796. eprint: https://www.science.org/doi/pdf/10.1126/scisignal.2002796.

Patterson, Michael T., Adam L. Burrack, Yingzheng Xu, Grant H. Hickok, Zoe C. Schmiechen, Samuel Becker, Eduardo Cruz-Hinojoza, Patricia R. Schrank, Ainsley E. Kennedy, Maria M. Firulyova, Ebony A. Miller, Konstantin Zaitsev, Jesse W. Williams, and Ingunn M. Stromnes (2023). "Tumor-specific CD4 T cells instruct monocyte fate in pancreatic ductal adenocarcinoma". *Cell Reports* 42.7, p. 112732. DOI: https://doi.org/10.1016/j.celrep.2023.112732.

Pearl, Laurence H and David Barford (2002). "Regulation of protein kinases in insulin, growth factor and Wnt signalling". *Current Opinion in Structural Biology* 12.6, pp. 761–767. DOI: https://doi.org/10.1016/S0959-440X(02)00386-X.

Pearson, Helen B., Jason Li, Valerie S. Meniel, Christina M. Fennell, Paul Waring, Karen G. Montgomery, Richard J. Rebello, Arthi A. Macpherson, Sarah Koushyar, Luc Furic, Carleen Cullinane, Richard W. Clarkson, Matthew J. Smalley, Kaylene J. Simpson, Toby J. Phesse, Peter R. Shepherd, Patrick O. Humbert, Owen J. Sansom, and Wayne A. Phillips (May 2018). "Identification of Pik3ca Mutation as a Genetic Driver of Prostate Cancer That Cooperates with Pten Loss to Accelerate Progression and Castration-Resistant Growth". *Cancer Discovery* 8.6, pp. 764–779. DOI: 10.1158/2159-8290.CD-17-0867. eprint: https://aacrjournals.org/cancerdiscovery/article-pdf/8/6/764/2952135/764.pdf.

Pellegrino, Marsha, Valerio Secli, Silvia D'Amico, Lucia Lisa Petrilli, Matteo Caforio, Valentina Folgiero, Nicola Tumino, Paola Vacca, Maria Vinci, Doriana Fruci, and Emmanuel de Billy (2024). "Manipulating the tumor immune microenvironment to improve cancer immunotherapy: IGF1R, a promising target". *Frontiers in Immunology* 15. DOI: 10.3389/fimmu.2024.1356321.

Pepper, Marion and Marc K Jenkins (2011). "Origins of CD4+ effector and central memory T cells". *Nature Immunology* 12 (6), pp. 467–471. DOI: 10.1038/ni.2038.

Perner, Sven, Juan-Miguel Mosquera, Francesca Demichelis, Matthias D Hofer, Pamela L Paris, Jeff Simko, Colin Collins, Tarek A Bismar, Arul M Chinnaiyan, Angelo M De Marzo, and Mark A Rubin (2007). "TMPRSS2-ERG Fusion Prostate Cancer: An Early Molecular Event Associated With Invasion". *The American Journal of Surgical Pathology* 31 (6).

Pernicova, Zuzana, Eva Slabakova, Gvantsa Kharaishvili, Jan Bouchal, Milan Kral, Zuzana Kunicka, Miroslav Machala, Alois Kozubik, and Karel Souccek (2011). "Androgen Depletion Induces Senescence in Prostate Cancer Cells through Down-regulation of Skp2". *Neoplasia* 13.6, 526–IN13. DOI: https://doi.org/10.1593/neo.11182.

Peters, P J, J Borst, V Oorschot, M Fukuda, O Krähenbühl, J Tschopp, J W Slot, and H J Geuze (May 1991). "Cytotoxic T lymphocyte granules are secretory lysosomes, containing both perforin and granzymes". *Journal of Experimental Medicine* 173.5, pp. 1099–1109. DOI: 10.1084/jem.173.5.1099. eprint: https://rupress.org/jem/article-pdf/173/5/1099/1672060/1099.pdf.

Petley, Emma V, Hui-Fern Koay, Melissa A Henderson, Kevin Sek, Kirsten L Todd, Simon P Keam, Junyun Lai, Imran G House, Jasmine Li, Magnus Zethoven, Amanda X Y Chen, Amanda J Oliver, Jessica Michie, Andrew J Freeman, Lauren Giuffrida, Jack D Chan, Angela Pizzolla, Jeffrey Y W Mak, Timothy R McCulloch, Fernando Souza-Fonseca-Guimaraes, Conor J Kearney, Rosemary Millen, Robert G Ramsay, Nicholas D Huntington, James McCluskey, Jane Oliaro, David P Fairlie, Paul J Neeson, Dale I Godfrey, Paul A Beavis, and Phillip K Darcy (2021). "MAIT cells regulate NK cell-mediated tumor immunity". *Nature Communications* 12 (1), p. 4746. DOI: 10.1038/s41467-021-25009-4.

Pierorazio, Phillip M., Patrick C. Walsh, Alan W. Partin, and Jonathan I. Epstein (2013). "Prognostic Gleason grade grouping: data based on the modified Gleason scoring system". *BJU International* 111.5, pp. 753–760. DOI: https://doi.org/10.1111/j.1464-410X.2012.11611.x. eprint: https://bjui-journals.onlinelibrary.wiley.com/doi/pdf/10.1111/j.1464-410X.2012.11611.x.

Pineiro-Hermida, Sergio, Icíar P Lopez, Elvira Alfaro-Arnedo, Raquel Torrens, Maria Iniguez, Lydia Alvarez-Erviti, Carlos Ruiz-Martínez, and Jose G Pichel (2017). "IGF1R deficiency attenuates acute inflammatory response in a bleomycin-induced lung injury mouse model". *Scientific Reports* 7, p. 4290. DOI: 10.1038/s41598-017-04561-4.

Pittoni, Paola and Mario Paolo Colombo (Feb. 2012). "The Dark Side of Mast Cell–Targeted Therapy in Prostate Cancer". *Cancer Research* 72.4, pp. 831–835. DOI: 10.1158/0008-5472.CAN-11-3110. eprint: https://aacrjournals.org/cancerres/article-pdf/72/4/831/2678208/831.pdf.

Pittoni, Paola, Claudio Tripodo, Silvia Piconese, Giorgio Mauri, Mariella Parenza, Alice Rigoni, Sabina Sangaletti, and Mario P. Colombo (Sept. 2011). "Mast Cell Targeting Hampers Prostate Adenocarcinoma Development but Promotes the Occurrence of Highly Malignant Neuroendocrine Cancers". *Cancer Research* 71.18, pp. 5987–5997. DOI: 10.1158/0008-5472.CAN-11-1637. eprint: https://aacrjournals.org/cancerres/article-pdf/71/18/5987/2657220/5987.pdf.

Pollak, Michael (2012). "The insulin and insulin-like growth factor receptor family in neoplasia: an update". *Nature Reviews Cancer* 12 (3), pp. 159–169. DOI: 10.1038/nrc3215.

Pollak, Michael N, Eva S Schernhammer, and Susan E Hankinson (2004). "Insulin-like growth factors and neoplasia". *Nature Reviews Cancer* 4 (7), pp. 505–518. DOI: 10.1038/nrc1387.

Powles, Thomas, Kobe C Yuen, Silke Gillessen, Edward E Kadel, Dana Rathkopf, Nobuaki Matsubara, Charles G Drake, Karim Fizazi, Josep M Piulats, Piotr J Wysocki, Gary L Buchschacher, Boris Alekseev, Begoña Mellado, Bogusława Karaszewska, Jennifer F Doss, Grozdana Rasuo, Asim Datye, Sanjeev Mariathasan, Patrick Williams, and Christopher J Sweeney (2022). "Atezolizumab with enzalutamide versus enzalutamide

alone in metastatic castration-resistant prostate cancer: a randomized phase 3 trial". *Nature Medicine* 28 (1), pp. 144–153. DOI: 10.1038/s41591-021-01600-6.

Prager, Isabel, Clarissa Liesche, Hanna van Ooijen, Doris Urlaub, Quentin Verron, Niklas Sandstrom, Frank Fasbender, Maren Claus, Roland Eils, Joel Beaudouin, Bjorn Onfelt, and Carsten Watzl (July 2019). "NK cells switch from granzyme B to death receptor–mediated cytotoxicity during serial killing". *Journal of Experimental Medicine* 216.9, pp. 2113–2127. DOI: 10.1084/jem.20181454. eprint: https://rupress.org/jem/article-pdf/216/9/2113/1841650/jem_20181454.pdf.

Price, Alison J., Naomi E. Allen, Paul N. Appleby, Francesca L. Crowe, Ruth C. Travis, Sarah J. Tipper, Kim Overvad, Henning Gronbaek, Anne Tjonneland, Nina Fons Johnsen, Sabina Rinaldi, Rudolf Kaaks, Annie Lukanova, Heiner Boeing, Krasimira Aleksandrova, Antonia Trichopoulou, Dimitrios Trichopoulos, George Andarakis, Domenico Palli, Vittorio Krogh, Rosario Tumino, Carlotta Sacerdote, H. Bas Bueno-de-Mesquita, Marcial V. Arguelles, Maria-Jose Sanchez, Maria-Dolores Chirlaque, Aurelio Barricarte, Nerea Larranaga, Carlos A. Gonzalez, Par Stattin, Mattias Johansson, Kay-Tee Khaw, Nick Wareham, Marc Gunter, Elio Riboli, and Timothy Key (Sept. 2012). "Insulin-like Growth Factor-I Concentration and Risk of Prostate Cancer: Results from the European Prospective Investigation into Cancer and Nutrition". *Cancer Epidemiology, Biomarkers and Prevention* 21.9, pp. 1531–1541. DOI: 10.1158/1055-9965.EPI-12-0481-T. eprint: https://aacrjournals.org/cebp/article-pdf/21/9/1531/2275205/1531.pdf.

Pritchard, Colin C., Joaquin Mateo, Michael F. Walsh, Navonil De Sarkar, Wassim Abida, Himisha Beltran, Andrea Garofalo, Roman Gulati, Suzanne Carreira, Rosalind Eeles, Olivier Elemento, Mark A. Rubin, Dan Robinson, Robert Lonigro, Maha Hussain, Arul Chinnaiyan, Jake Vinson, Julie Filipenko, Levi Garraway, Mary-Ellen Taplin, Saud AlDubayan, G. Celine Han, Mallory Beightol, Colm Morrissey, Belinda Nghiem, Heather H. Cheng, Bruce Montgomery, Tom Walsh, Silvia Casadei, Michael Berger, Liying Zhang, Ahmet Zehir, Joseph Vijai, Howard I. Scher, Charles Sawyers, Nikolaus Schultz, Philip W. Kantoff, David Solit, Mark Robson, Eliezer M. Van Allen, Kenneth Offit, Johann de Bono, and Peter S. Nelson (2016). "Inherited DNA-Repair Gene Mutations in Men with Metastatic Prostate Cancer". *New England Journal of Medicine* 375.5, pp. 443–453. DOI: 10.1056/NEJMoa1603144. eprint: https://www.nejm.org/doi/pdf/10.1056/NEJMoa1603144.

Prokhnevska, Nataliya, Maria A. Cardenas, Rajesh M. Valanparambil, Ewelina Sobierajska, Benjamin G. Barwick, Caroline Jansen, Adriana Reyes Moon, Petra Gregorova, Luke delBalzo, Rachel Greenwald, Mehmet Asim Bilen, Mehrdad Alemozaffar, Shreyas Joshi, Cara Cimmino, Christian Larsen, Viraj Master, Martin Sanda, and Haydn Kissick (2023). "CD8+ T cell activation in cancer comprises an initial activation phase in lymph nodes followed by effector differentiation within the tumor". *Immunity* 56.1, 107–124.e5. DOI: https://doi.org/10.1016/j.immuni.2022.12.002.

Prostate cancer statistics, World Cancer Research Fund International (Mar. 2022).

Puzanov, Igor, Colin R. Lindsay, Laura Goff, Jeff Sosman, Jill Gilbert, Jordan Berlin, Srinivasu Poondru, Ronit Simantov, Rich Gedrich, Andrew Stephens, Emily Chan, and T.R. Jeffry Evans (Feb. 2015). "A Phase I Study of Continuous Oral Dosing of OSI-906, a Dual Inhibitor of Insulin-Like Growth Factor-1 and Insulin Receptors, in Patients with Advanced Solid Tumors". *Clinical Cancer Research* 21.4, pp. 701–711. DOI: 10.1158/1078-0432.CCR-14-0303. eprint: https://aacrjournals.org/clincancerres/article-pdf/21/4/701/2028887/701.pdf.

Qin, Rui, Weihong Ren, Guoqi Ya, Bei Wang, Jiao He, Shaoxin Ren, Lu Jiang, and Shuo Zhao (2023). "Role of chemokines in the crosstalk between tumor and tumor-associated macrophages". *Clinical and Experimental Medicine* 23 (5), pp. 1359–1373. DOI: 10.1007/s10238-022-00888-z.

Qiu, Xintao, Nadia Boufaied, Tarek Hallal, Avery Feit, Anna de Polo, Adrienne M Luoma, Walaa Alahmadi, Janie Larocque, Giorgia Zadra, Yingtian Xie, Shengqing Gu, Qin Tang, Yi Zhang, Sudeepa Syamala, Ji-Heui Seo, Connor Bell, Edward O'Connor, Yang Liu, Edward M Schaeffer, R Jeffrey Karnes, Sheila Weinmann, Elai Davicioni, Colm Morrissey, Paloma Cejas, Leigh Ellis, Massimo Loda, Kai W Wucherpfennig, Mark M Pomerantz, Daniel E Spratt, Eva Corey, Matthew L Freedman, X Shirley Liu, Myles Brown, Henry W Long, and David P Labbe (2022). "MYC drives aggressive prostate cancer by disrupting transcriptional pause release at androgen receptor targets". *Nature Communications* 13 (1), p. 2559. DOI: 10.1038/s41467-022-30257-z.

Qu, Hu, Zihao Zou, Zhaojun Pan, Tianwei Zhang, Nan Deng, Guoxi Chen, and Zhongyang Wang (2016). "IL-7/IL-7 receptor axis stimulates prostate cancer cell invasion and migration via AKT/NF-kB pathway". *International Immunopharmacology* 40, pp. 203–210. DOI: https://doi.org/10.1016/j.intimp.2016.08.017.

Quah, Benjamin J.C. and Christopher R. Parish (2010). "The use of carboxyfluorescein diacetate succinimidyl ester (CFSE) to monitor lymphocyte proliferation". *Journal of Visualized Experiments* (44). DOI: 10.3791/2259.

Quail, Daniela F., Robert L. Bowman, Leila Akkari, Marsha L. Quick, Alberto J. Schuhmacher, Jason T. Huse, Eric C. Holland, James C. Sutton, and Johanna A. Joyce (2016). "The tumor microenvironment underlies acquired resistance to CSF-1R inhibition in gliomas". *Science* 352.6288, aad3018. DOI: 10.1126/science.aad3018. eprint: https://www.science.org/doi/pdf/10.1126/science.aad3018.

Quaranta, Valeria, Carolyn Rainer, Sebastian R. Nielsen, Meirion L. Raymant, Muhammad S. Ahmed, Dannielle D. Engle, Arthur Taylor, Trish Murray, Fiona Campbell, Daniel H. Palmer, David A. Tuveson, Ainhoa Mielgo, and Michael C. Schmid (July 2018). "Macrophage-Derived Granulin Drives Resistance to Immune Checkpoint Inhibition in Metastatic Pancreatic Cancer". *Cancer Research* 78.15, pp. 4253–4269. DOI: 10.1158/0008-5472.CAN-17-3876. eprint: https://aacrjournals.org/cancerres/article-pdf/78/15/4253/2604271/4253.pdf.

Rahmoon, Mai Atef, Rana Ahmed Youness, Asmaa Ibrahim Gomaa, Mohamed Tarif Hamza, Imam Waked, Hend Mohamed El Tayebi, and Ahmed Ihab Abdelaziz (2017). "MiR-615-5p depresses natural killer cells cytotoxicity through repressing IGF-1R in hepatocellular carcinoma patients". *Growth Factors* 35.2-3. PMID: 28747084, pp. 76–87. DOI: 10.1080/08977194.2017.1354859. eprint: https://doi.org/10.1080/08977194.2017.1354859.

Rajaram, Sujatha, David J. Baylink, and Subburaman Mohan (Dec. 1997). "Insulin-Like Growth Factor-Binding Proteins in Serum and Other Biological Fluids: Regulation and Functions". *Endocrine Reviews* 18.6, pp. 801–831. DOI: 10.1210/edrv.18.6.0321. eprint: https://academic.oup.com/edrv/article-pdf/18/6/801/8859664/edrv0801.pdf.

Ramamurthy, Vidya P., Senthilmurugan Ramalingam, Lalji Gediya, Andrew K. Kwegyir-Afful, Vincent C.O. Njar, Vidya P. Ramamurthy, Senthilmurugan Ramalingam, Lalji Gediya, Andrew K. Kwegyir-Afful, and Vincent C.O. Njar (Dec. 2014). "Simultaneous targeting of androgen receptor (AR) and

MAPK-interacting kinases (MNKs) by novel retinamides inhibits growth of human prostate cancer cell lines". *Oncotarget* 6 (5), pp. 3195–3210. DOI: 10.18632/ONCOTARGET.3084.

Ramirez-Castillejo, Carmen, Francisco Sanchez-Sanchez, Celia Andreu-Agulló, Sacri R Ferron, J Daniel Aroca-Aguilar, Pilar Sanchez, Helena Mira, Julio Escribano, and Isabel Farinas (2006). "Pigment epithelium–derived factor is a niche signal for neural stem cell renewal". *Nature Neuroscience* 9.3, pp. 331–339. DOI: 10.1038/nn1657.

Rao, Srinivasa R., Nasullah K. Alham, Elysia Upton, Stacey McIntyre, Richard J. Bryant, Lucia Cerundolo, Emma Bowes, Stephanie Jones, Molly Browne, Ian Mills, Alastair Lamb, Ian Tomlinson, David Wedge, Lisa Browning, Korsuk Sirinukunwattana, Claire Palles, Freddie C. Hamdy, Jens Rittscher, and Clare Verrill (2020). "Detailed Molecular and Immune Marker Profiling of Archival Prostate Cancer Samples Reveals an Inverse Association between TMPRSS2:ERG Fusion Status and Immune Cell Infiltration". *The Journal of Molecular Diagnostics* 22.5, pp. 652–669. DOI: https://doi.org/10.1016/j.jmoldx.2020.02.012.

Rath, Meera, Ingrid Muller, Pascale Kropf, Ellen I. Closs, and Markus Munder (2014). "Metabolism via Arginase or Nitric Oxide Synthase: Two Competing Arginine Pathways in Macrophages". *Frontiers in Immunology* 5. DOI: 10.3389/fimmu.2014.00532.

Ray, Sumantra, Sue Fitzpatrick, Rajna Golubic, Susan Fisher, and Sarah Gibbings (Feb. 2016). *Oxford Handbook of Clinical and Healthcare Research*. Oxford University Press. DOI: 10.1093/med/9780199608478.001.0001.

Rebello, Richard J, Christoph Oing, Karen E Knudsen, Stacy Loeb, David C Johnson, Robert E Reiter, Silke Gillessen, Theodorus Van der Kwast, and Robert G Bristow (2021). "Prostate cancer". *Nature Reviews Disease Primers* 7 (1), p. 9. DOI: 10.1038/s41572-020-00243-0.

Rechler, Matthew M and David R Clemmons (1998). "Regulatory Actions of Insulin-like Growth Factor-binding Proteins". *Trends in Endocrinology and Metabolism* 9.5, pp. 176–183. DOI: 10.1016/S1043-2760(98)00047-2.

Reinhardt, R Lee, Alexander Khoruts, Rebecca Merica, Traci Zell, and Marc K Jenkins (2001). "Visualizing the generation of memory CD4 T cells in the whole body". *Nature* 410 (6824), pp. 101–105. DOI: 10.1038/35065111.

Reis, Ana Filipa Palma dos, Toby Milne-Clark, Amit Dipak Amin, Liliya Nazlamova, Simon Pacey, and Harveer Dev (Jan. 2024). "Abstract A021: Pre and post treatment transcriptomic analysis provide new insights on the mechanisms underlying the efficacy of PARPi and Androgen blockage in prostate cancer". *Cancer Research* 84.1. DOI: 10.1158/1538-7445.DNAREPAIR24-A021.

Reis, Edimara S, Dimitrios C Mastellos, Daniel Ricklin, Alberto Mantovani, and John D Lambris (2018). "Complement in cancer: untangling an intricate relationship". *Nature Reviews Immunology* 18 (1), pp. 5–18. DOI: 10.1038/nri.2017.97.

Ren, Meng, Xia Zhong, Chun-yan Ma, Ying Sun, Qing-bo Guan, Bin Cui, Jun Guo, Hai Wang, Ling Gao, and Jia-jun Zhao (2009). "Insulin-like growth factor-1 promotes cell cycle progression via upregulation of cyclin D1 expression through the phosphatidylinositol 3-kinase/nuclear factor-kB signaling pathway in FRTL thyroid cells". *Acta Pharmacologica Sinica* 30 (1), pp. 113–119. DOI: 10.1038/aps.2008.8.

Ren, X, F Ye, Z Jiang, Y Chu, S Xiong, and Y Wang (2007). "Involvement of cellular death in TRAIL/DR5-dependent suppression induced by CD4+CD25+ regulatory T cells". *Cell Death and Differentiation* 14 (12), pp. 2076–2084. DOI: 10.1038/sj.cdd.4402220.

Resnicoff, Mariana, Domenico Coppola, Christian Sell, Raphael Rubin, Soldano Ferrone, and Renato Baserga (1994). "Growth inhibition of human melanoma cells in nude mice by

antisense strategies to the type 1 insulin-like growth factor receptor". *Cancer research* 54 (18), pp. 4848–4850.

Ribas, Antoni and Jedd D. Wolchok (2018). "Cancer immunotherapy using checkpoint blockade". *Science* 359.6382, pp. 1350–1355. DOI: 10.1126/science.aar4060. eprint: https://www.science.org/doi/pdf/10.1126/science.aar4060.

Ricklin, Daniel, George Hajishengallis, Kun Yang, and John D Lambris (2010). "Complement: a key system for immune surveillance and homeostasis". *Nature Immunology* 11 (9), pp. 785–797. DOI: 10.1038/ni.1923.

Riedemann, J and V M Macaulay (2006). "IGF1R signalling and its inhibition". *Endocrine-Related Cancer Endocr Relat Cancer* 13, pp. 33–43. DOI: 10.1677/erc.1.01280.

Rieger, Leonie, Sandra O'Shea, Grant Godsmark, Joanna Stanicka, Geraldine Kelly, and Rosemary O'Connor (2020). "IGF-1 receptor activity in the Golgi of migratory cancer cells depends on adhesion-dependent phosphorylation of Tyr1250 and Tyr1251". *Science Signaling* 13.633, eaba3176. DOI: 10.1126/scisignal.aba3176. eprint: https://www.science.org/doi/pdf/10.1126/scisignal.aba3176.

Rieunier, Guillaume, Xiaoning Wu, Letitia E. Harris, Jack V. Mills, Ashwin Nandakumar, Laura Colling, Elena Seraia, Stephanie B. Hatch, Daniel V. Ebner, Lisa K. Folkes, Ulrike Weyer-Czernilofsky, Thomas Bogenrieder, Anderson J. Ryan, and Valentine M. Macaulay (Apr. 2021). "Targeting igf perturbs global replication through ribonucleotide reductase dysfunction". *Cancer Research* 81 (8), pp. 2128–2141. DOI: 10.1158/0008-5472.CAN-20-2860/654512/AM/TARGETING-IGF-PERTURBS-GLOBAL-REPLICATION-THROUGH.

Rieunier, Guillaume, Xiaoning Wu, Valentine M. Macaulay, Adrian V. Lee, Ulrike Weyer-Czernilofsky, and Thomas Bogenrieder (June 2019). "Bad to the Bone: The Role of the Insulin-Like Growth Factor Axis in Osseous Metastasis". *Clinical Cancer Research* 25.12, pp. 3479–3485. DOI: 10.1158/1078-0432.CCR-18-2697. eprint: https://aacrjournals.org/clincancerres/article-pdf/25/12/3479/2051329/3479.pdf.

Rinaldi, Sabina, Rebecca Cleveland, Teresa Norat, Carine Biessy, Sabine Rohrmann, Jakob Linseisen, Heiner Boeing, Tobias Pischon, Salvatore Panico, Claudia Agnoli, Domenico Palli, Rosario Tumino, Paolo Vineis, Petra H.M. Peeters, Carla H. van Gils, Bas H. Bueno-de-Mesquita, Alina Vrieling, Naomi E. Allen, Andrew Roddam, Sheila Bingham, Kay-Tee Khaw, Jonas Manjer, Signe Borgquist, Vanessa Dumeaux, Inger Torhild Gram, Eiliv Lund, Antonia Trichopoulou, Georgios Makrygiannis, Vassiliki Benetou, Esther Molina, Ignacio Donate Suárez, Aurelio Barricarte Gurrea, Carlos A. Gonzalez, Maria-Jose Tormo, Jone M. Altzibar, Anja Olsen, Anne Tjonneland, Henning Grønbæk, Kim Overvad, Françoise Clavel-Chapelon, Marie-Christine Boutron-Ruault, Sophie Morois, Nadia Slimani, Paolo Boffetta, Mazda Jenab, Elio Riboli, and Rudolf Kaaks (2010). "Serum levels of IGF-I, IGFBP-3 and colorectal cancer risk: results from the EPIC cohort, plus a meta-analysis of prospective studies". *International Journal of Cancer* 126.7, pp. 1702–1715. DOI: https://doi.org/10.1002/ijc.24927. eprint: https://onlinelibrary.wiley.com/doi/pdf/10.1002/ijc.24927.

Roberts, Allison W, Bettina L Lee, Jacques Deguine, Shinu John, Mark J Shlomchik, and Gregory M Barton (Nov. 2017). "Tissue-Resident Macrophages Are Locally Programmed for Silent Clearance of Apoptotic Cells". *Immunity* 47 (5). doi: 10.1016/j.immuni.2017.10.006, 913–927.e6. DOI: 10.1016/j.immuni.2017.10.006.

Robinson, Dan, Eliezer M. Van Allen, Yi-Mi Wu, Nikolaus Schultz, Robert J. Lonigro, Juan-Miguel Mosquera, Bruce Montgomery, Mary-Ellen Taplin, Colin C. Pritchard, Gerhardt Attard, Himisha Beltran, Wassim Abida, Robert K. Bradley, Jake Vinson, Xuhong Cao, Pankaj Vats, Lakshmi P. Kunju, Maha Hussain, Felix Y. Feng, Scott A. Tomlins, Kathleen A. Cooney, David C. Smith, Christine Brennan, Javed Siddiqui, Rohit Mehra, Yu Chen, Dana E. Rathkopf, Michael J. Morris, Stephen B. Solomon, Jeremy C. Durack, Victor E. Reuter, Anuradha Gopalan, Jianjiong Gao, Massimo Loda, Rosina T. Lis, Michaela Bowden, Stephen P. Balk, Glenn Gaviola, Carrie Sougnez, Manaswi Gupta, Evan Y. Yu, Elahe A. Mostaghel, Heather H. Cheng, Hyojeong Mulcahy, Lawrence D. True, Stephen R. Plymate, Heidi Dvinge, Roberta Ferraldeschi, Penny Flohr, Susana Miranda, Zafeiris Zafeiriou, Nina Tunariu, Joaquin Mateo, Raquel Perez-Lopez, Francesca Demichelis, Brian D. Robinson, Marc Schiffman, David M. Nanus, Scott T. Tagawa, Alexandros Sigaras, Kenneth W. Eng, Olivier Elemento, Andrea Sboner, Elisabeth I. Heath, Howard I. Scher, Kenneth J. Pienta, Philip Kantoff, Johann S. de Bono, Mark A. Rubin, Peter S. Nelson, Levi A. Garraway, Charles L. Sawyers, and Arul M. Chinnaiyan (May 2015). "Integrative Clinical Genomics of Advanced Prostate Cancer". *Cell* 161 (5). doi: 10.1016/j.cell.2015.05.001, pp. 1215–1228. DOI: 10.1016/j.cell.2015.05.001.

Rochester, Mark A, Johann Riedemann, Giles O Hellawell, Simon F Brewster, and Valentine M Macaulay (2005). "Silencing of the IGF1R gene enhances sensitivity to DNA-damaging agents in both PTEN wild-type and mutant human prostate cancer". *Cancer Gene Therapy* 12 (1), pp. 90–100. DOI: 10.1038/sj.cgt.7700775.

Roddam, Andrew W, Naomi E Allen, Paul Appleby, Timothy J Key, Luigi Ferrucci, H Ballentine Carter, E Jeffrey Metter, Chu Chen, Noel S Weiss, Annette Fitzpatrick, Ann W Hsing, James V Lacey, Kathy Helzlsouer, Sabina Rinaldi, Elio Riboli, Rudolf Kaaks, Joop A.M.J.L. Janssen, Mark F Wildhagen, Fritz H Schroder, Elizabeth A Platz, Michael Pollak, Edward Giovannucci, Catherine Schaefer, Charles P Quesenberry, Joseph H Vogelman, Gianluca Severi, Dallas R English, Graham G Giles, Par Stattin, Goran Hallmans, Mattias Johansson, June M Chan, Peter Gann, Steven E Oliver, Jeff M Holly, Jenny Donovan, François Meyer, Isabelle Bairati, and Galan (Oct. 2008). "Insulin-like Growth Factors, Their Binding Proteins, and Prostate Cancer Risk: Analysis of Individual Patient Data from 12 Prospective Studies". *Annals of Internal Medicine* 149 (7). doi: 10.7326/0003-4819-149-7-200810070-00006, pp. 461–471. DOI: 10.7326/0003-4819-149-7-200810070-00006.

Roditi, Laura De Vargas, Andrea Jacobs, Jan H Rueschoff, Pete Bankhead, Stéphane Chevrier, Hartland W Jackson, Thomas Hermanns, Christian D Fankhauser, Cedric Poyet, Felix Chun, Niels J Rupp, Alexandra Tschaebunin, Bernd Bodenmiller, and Peter J Wild (Apr. 2022). "Single-cell proteomics defines the cellular heterogeneity of localized prostate cancer". *Cell Reports Medicine* 3.4. DOI: 10.1016/j.xcrm.2022.100604.

Rodriguez, Paulo C., David G. Quiceno, Jovanny Zabaleta, Blair Ortiz, Arnold H. Zea, Maria B. Piazuelo, Alberto Delgado, Pelayo Correa, Jason Brayer, Eduardo M. Sotomayor, Scott Antonia, Juan B. Ochoa, and Augusto C. Ochoa (Aug. 2004). "Arginase I Production in the Tumor Microenvironment by Mature Myeloid Cells Inhibits T-Cell Receptor Expression and Antigen-Specific T-Cell Responses". *Cancer Research* 64.16, pp. 5839–5849. DOI: 10.1158/0008-5472.CAN-04-0465. eprint: https://aacrjournals.org/cancerres/article-pdf/64/16/5839/2516899/zch01604005839.pdf.

Rodriguez-Garcia, Alba, Rachel C. Lynn, Mathilde Poussin, Monika A. Eiva, Lauren C. Shaw, Roddy S. O'Connor, Nicholas G. Minutolo, Victoria Casado-Medrano, Gonzalo Lopez, Takami Matsuyama, and Daniel J. Powell (2021). "CAR-T cell-mediated depletion of immunosuppressive tumor-associated macrophages promotes endogenous antitumor immunity and augments adoptive immunotherapy". *Nature Communications* 12.1, p. 877. DOI: 10.1038/s41467-021-20893-2.

Rojas, A, G Liu, I Coleman, P S Nelson, M Zhang, R Dash, P B Fisher, S R Plymate, and J D Wu (2011). "IL-6 promotes prostate tumorigenesis and progression through autocrine cross-activation of IGF-IR". *Oncogene* 30 (20), pp. 2345–2355. DOI: 10.1038/onc.2010.605.

Rolny, Charlotte, Massimiliano Mazzone, Sonia Tugues, Damya Laoui, Irja Johansson, Cathy Coulon, Mario Leonardo Squadrito, Inmaculada Segura, Xiujuan Li, Ellen Knevels, Sandra Costa, Stefan Vinckier, Tom Dresselaer, Peter Akerud, Maria De Mol, Henriikka Salomaki, Mia Phillipson, Sabine Wyns, Erik Larsson, Ian Buysschaert, Johan Botling, Uwe Himmelreich, Jo A Van Ginderachter, Michele De Palma, Mieke Dewerchin, Lena Claesson-Welsh, and Peter Carmeliet (Jan. 2011). "HRG Inhibits Tumor Growth and Metastasis by Inducing Macrophage Polarization and Vessel Normalization through Downregulation of PlGF". *Cancer Cell* 19 (1). doi: 10.1016/j.ccr.2010.11.009, pp. 31–44. DOI: 10.1016/j.ccr.2010.11.009.

Rowshanravan, Behzad, Neil Halliday, and David M. Sansom (Jan. 2018). "CTLA-4: a moving target in immunotherapy". *Blood* 131.1, pp. 58–67. DOI: 10.1182/blood-2017-06-741033. eprint: https://ashpublications.org/blood/article-pdf/131/1/58/1367947/blood741033.pdf.

Ruf, Benjamin, Tim F. Greten, and Firouzeh Korangy (Apr. 2023). "Innate lymphoid cells and innate-like T cells in cancer - at the crossroads of innate and adaptive immunity". *Nature Reviews Cancer* 23 (6), pp. 351–371. DOI: 10.1038/s41568-023-00562-w.

Ruscetti, Marcus, John P Morris IV, Riccardo Mezzadra, James Russell, Josef Leibold, Paul B Romesser, Janelle Simon, Amanda Kulick, Yu-jui Ho, Myles Fennell, Jinyang Li, Robert J Norgard, John E Wilkinson, Direna Alonso-Curbelo, Ramya Sridharan, Daniel A Heller, Elisa de Stanchina, Ben Z Stanger, Charles J Sherr, and Scott W Lowe (Apr. 2020). "Senescence-Induced Vascular Remodeling Creates Therapeutic Vulnerabilities in Pancreas Cancer". *Cell* 181 (2). doi: 10.1016/j.cell.2020.03.008, 424–441.e21. DOI: 10.1016/j.cell.2020.03.008.

Ruytinx, Pieter, Paul Proost, Jo Van Damme, and Sofie Struyf (2018). "Chemokine-Induced Macrophage Polarization in Inflammatory Conditions". *Frontiers in Immunology* 9. DOI: 10.3389/fimmu.2018.01930.

Ryan, Charles J., Andrea H. Harzstark, Jonathan Rosenberg, Amy Lin, Christina Claros, Ira D. Goldfine, John F. Kerner, and Eric J. Small (2008). "A pilot dose-escalation study of the effects of nordihydroguareacetic acid on hormone and prostate specific antigen levels in patients with relapsed prostate cancer". *BJU International* 101.4, pp. 436–439. DOI: https://doi.org/10.1111/j.1464-410X.2007.07330.x.

S, Sakaguchi, Sakaguchi N, Asano M, Itoh M, and Toda M (Aug. 1995). "Immunologic self-tolerance maintained by activated T cells expressing IL-2 receptor alpha-chains (CD25). Breakdown of a single mechanism of self-tolerance causes various autoimmune diseases". *Journal of immunology (Baltimore, Md. : 1950)* 155 (3), pp. 1151–1164. DOI: 10.4049/jimmunol.155.3.1151.

Sabatini, David M (2006). "mTOR and cancer: insights into a complex relationship". *Nature Reviews Cancer* 6 (9), pp. 729–734. DOI: 10.1038/nrc1974.

Sachdev, D, X Zhang, I Matise, M Gaillard-Kelly, and D Yee (2010). "The type I insulin-like growth factor receptor regulates cancer metastasis independently of primary tumor growth by promoting invasion and survival". *Oncogene* 29 (2), pp. 251–262. DOI: 10.1038/onc.2009.316.

Sachdev, Deepali, Julie S Hartell, Adrian V Lee, Xihong Zhang, and Douglas Yee (Feb. 2004). "A Dominant Negative Type I Insulin-like Growth Factor Receptor Inhibits Metastasis of Human Cancer Cells". *Journal of Biological Chemistry* 279 (6). doi: 10.1074/jbc.M305403200, pp. 5017–5024. DOI: 10.1074/jbc.M305403200.

Sachdev, Deepali, Rajeeva Singh, Yoko Fujita-Yamaguchi, and Douglas Yee (Feb. 2006). "Down-regulation of Insulin Receptor by Antibodies against the Type I Insulin-Like Growth Factor Receptor: Implications for Anti–Insulin-Like Growth Factor Therapy in Breast Cancer". *Cancer Research* 66.4, pp. 2391–2402. DOI: 10.1158/0008-5472.CAN-05-3126. eprint: https://aacrjournals.org/cancerres/article-pdf/66/4/2391/2560127/2391.pdf.

Sachdev, Deepali and Douglas Yee (Jan. 2007). "Disrupting insulin-like growth factor signaling as a potential cancer therapy". *Molecular Cancer Therapeutics* 6.1, pp. 1–12. DOI: 10.1158/1535-7163.MCT-06-0080. eprint: https://aacrjournals.org/mct/article-pdf/6/1/1/1874182/1.pdf.

Sack, Laura Magill, Teresa Davoli, Mamie Z Li, Yuyang Li, Qikai Xu, Kamila Naxerova, Eric C Wooten, Ronald J Bernardi, Timothy D Martin, Ting Chen, Yumei Leng, Anthony C Liang, Kathleen A Scorsone, Thomas F Westbrook, Kwok-Kin Wong, and Stephen J Elledge (Apr. 2018). "Profound Tissue Specificity in Proliferation Control Underlies Cancer Drivers and Aneuploidy Patterns". *Cell* 173 (2). doi: 10.1016/j.cell.2018.02.037, 499–514.e23. DOI: 10.1016/j.cell.2018.02.037.

Saha, Ramendra N., Malabendu Jana, and Kalipada Pahan (Nov. 2007). "MAPK p38 Regulates Transcriptional Activity of NF-kB in Primary Human Astrocytes via Acetylation of p651". *The Journal of Immunology* 179.10, pp. 7101–7109. DOI: 10.4049/jimmunol.179.10.7101. eprint: https://journals.aai.org/jimmunol/article-pdf/179/10/7101/1246745/zim02207007101.pdf.

Sakaguchi, Shimon (2005). "Naturally arising Foxp3-expressing CD25+CD4+ regulatory T cells in immunological tolerance to self and non-self". *Nature Immunology* 6 (4), pp. 345–352. DOI: 10.1038/ni1178.

Sakuishi, Kaori, Lionel Apetoh, Jenna M. Sullivan, Bruce R. Blazar, Vijay K. Kuchroo, and Ana C. Anderson (May 2011). "Targeting Tim-3 and PD-1 pathways to reverse T cell exhaustion and restore anti-tumor immunity". *Journal of Experimental Medicine* 208.6, pp. 1331–1331. DOI: 10.1084/jem.201006432011512c. eprint: https://rupress.org/jem/article-pdf/208/6/1331/1903612/jem_201006432011512c.pdf.

Salami, Simpa S., Jeremy B. Kaplan, Srinivas Nallandhighal, Mandeep Takhar, Jeffrey J. Tosoian, Matthew Lee, Junhee Yoon, Daniel H. Hovelson, Komal R. Plouffe, Samuel D. Kaffenberger, Edward M. Schaeffer, R. Jeffrey Karnes, Tamara L. Lotan, Todd M. Morgan, Arvin K. George, Jeffrey S. Montgomery, Matthew S. Davenport, Sungyong You, Scott A. Tomlins, Nicole E. Curci, Hyung L. Kim, Daniel E. Spratt, Aaron M. Udager, and Ganesh S. Palapattu (2019). "Biologic Significance of Magnetic Resonance Imaging Invisibility in Localized Prostate Cancer". *JCO Precision Oncology* 3, pp. 1–12. DOI: 10.1200/PO.19.00054. eprint: https://doi.org/10.1200/PO.19.00054.

Sallusto, Federica, Jens Geginat, and Antonio Lanzavecchia (2004). "Central Memory and Effector Memory T Cell Subsets: Function, Generation, and Maintenance". *Annual Review of Immunology* 22.Volume 22, 2004, pp. 745–763. DOI: https://doi.org/10.1146/annurev.immunol.22.012703.104702.

Sallusto, Federica, Danielle Lenig, Reinhold Forster, Martin Lipp, and Antonio Lanzavecchia (1999). "Two subsets of memory T lymphocytes with distinct homing potentials and effector functions". *Nature* 401 (6754), pp. 708–712. DOI: 10.1038/44385.

Salminen, Antero, Kai Kaarniranta, and Anu Kauppinen (2021). "Insulin/IGF-1 signaling promotes immunosuppression via the STAT3 pathway: impact on the aging process and age-related diseases". *Inflammation Research* 70 (10), pp. 1043–1061. DOI: 10.1007/s00011-021-01498-3.

Salmon, Helene, Juliana Idoyaga, Adeeb Rahman, Marylene Leboeuf, Romain Remark, Stefan Jordan, Maria Casanova-Acebes, Makhzuna Khudoynazarova, Judith Agudo, Navpreet Tung, Svetoslav Chakarov, Christina Rivera, Brandon Hogstad, Marcus Bosenberg, Daigo Hashimoto, Sacha Gnjatic, Nina Bhardwaj, Anna Karolina Palucka, Brian D. Brown, Joshua Brody, Florent Ginhoux, and Miriam Merad (Apr. 2016). "Expansion and Activation of CD103⁺ Dendritic Cell Progenitors at the Tumor Site Enhances Tumor Responses to Therapeutic PD-L1 and BRAF Inhibition". *Immunity* 44 (4). doi: 10.1016/j.immuni.2016.03.012, pp. 924–938. DOI: 10.1016/j.immuni.2016.03.012.

Samani, Amir Abbas, Shoshana Yakar, Derek LeRoith, and Pnina Brodt (Feb. 2007). "The Role of the IGF System in Cancer Growth and Metastasis: Overview and Recent Insights". *Endocrine Reviews* 28.1, pp. 20–47. DOI: 10.1210/er.2006-0001. eprint: https://academic.oup.com/edrv/article-pdf/28/1/20/10335462/edrv0020.pdf.

Sancak, Yasemin, Carson C. Thoreen, Timothy R. Peterson, Robert A. Lindquist, Seong A. Kang, Eric Spooner, Steven A. Carr, and David M. Sabatini (2007). "PRAS40 Is an Insulin-Regulated Inhibitor of the mTORC1 Protein Kinase". *Molecular Cell* 25.6, pp. 903–915. DOI: https://doi.org/10.1016/j.molcel.2007.03.003.

Saraiva, Margarida, Paulo Vieira, and Anne O'Garra (Oct. 2019). "Biology and therapeutic potential of interleukin-10". *Journal of Experimental Medicine* 217.1, e20190418. DOI: 10.1084/jem.20190418. eprint: https://rupress.org/jem/article-pdf/217/1/e20190418/1769091/jem_20190418.pdf.

Sarbassov, Dos D., David A. Guertin, Siraj M. Ali, and David M. Sabatini (2005). "Phosphorylation and Regulation of Akt/PKB by the Rictor-mTOR Complex". *Science* 307.5712, pp. 1098–1101. DOI: 10.1126/science.1106148. eprint: https://www.science.org/doi/pdf/10.1126/science.1106148.

Sarfstein, Rive, Metsada Pasmanik-Chor, Adva Yeheskel, Liat Edry, Noam Shomron, Naama Warman, Efrat Wertheimer, Sharon Maor, Lea Shochat, and Haim Werner (Jan. 2012). "Insulin-like Growth Factor-I Receptor (IGF-IR) Translocates to Nucleus and Autoregulates IGF-IR Gene Expression in Breast Cancer Cells". *Journal of Biological Chemistry* 287 (4). doi: 10.1074/jbc.M111.281782, pp. 2766–2776. DOI: 10.1074/jbc.M111.281782.

Sasidharan Nair, Varun, Salman M Toor, Rowaida Z Taha, Ayman A Ahmed, Mohamed A Kurer, Khaled Murshed, Madiha E Soofi, Khalid Ouararhni, Nehad M. Alajez, Mohamed Abu Nada, and Eyad Elkord (2020). "Transcriptomic Profiling of Tumor-Infiltrating CD4+TIM-3+ T Cells Reveals Their Suppressive, Exhausted, and Metastatic Characteristics in Colorectal Cancer Patients". *Vaccines* 8.1. DOI: 10.3390/vaccines8010071.

Saul, Dominik, Robyn Laura Kosinsky, Elizabeth J Atkinson, Madison L Doolittle, Xu Zhang, Nathan K LeBrasseur, Robert J Pignolo, Paul D Robbins, Laura J Niedernhofer, Yuji Ikeno, Diana Jurk, Joao F Passos, LaTonya J Hickson, Ailing Xue, David G Monroe, Tamara Tchkonia, James L Kirkland, Joshua N Farr, and Sundeep Khosla (2022). "A new gene set identifies senescent cells and predicts senescence-associated pathways across tissues". *Nature Communications* 13 (1), p. 4827. DOI: 10.1038/s41467-022-32552-1.

Sayed, Shorouk El, Izabel Patik, Naresh S Redhu, Jonathan N Glickman, Konstantinos Karagiannis, El Sayed Y El Naenaeey, Gamal A Elmowalid, Ashraf M Abd El Wahab, Scott B Snapper, and Bruce H Horwitz (2022). "CCR2 promotes monocyte recruitment and intestinal inflammation in mice lacking the interleukin-10 receptor". *Scientific Reports* 12.1, p. 452. DOI: 10.1038/s41598-021-04098-7.

Sayeed, Aejaz, Carmine Fedele, Marco Trerotola, Kirat K. Ganguly, and Lucia R. Languino (Oct. 2013). "IGF-IR Promotes Prostate Cancer Growth by Stabilizing a5B1 Integrin Protein Levels". *PLOS ONE* 8.10, pp. 1–9. DOI: 10.1371/journal.pone.0076513.

Scapini, Patrizia, Shalini Pereira, Hong Zhang, and Clifford A. Lowell (Mar. 2009). "Multiple Roles of Lyn Kinase in Myeloid Cell Signaling and Function". *Immunological reviews* 228 (1), p. 23. DOI: 10.1111/J.1600-065X.2008.00758.X.

Schally, Andrew V., Norman L. Block, and Ferenc G. Rick (2017). "Discovery of LHRH and development of LHRH analogs for prostate cancer treatment". *The Prostate* 77.9, pp. 1036–1054. DOI: https://doi.org/10.1002/pros.23360. eprint: https://onlinelibrary.wiley.com/doi/pdf/10.1002/pros.23360.

Scher, Howard I., Karim Fizazi, Fred Saad, Mary-Ellen Taplin, Cora N. Sternberg, Kurt Miller, Ronald de Wit, Peter Mulders, Kim N. Chi, Neal D. Shore, Andrew J. Armstrong, Thomas W. Flaig, Aude Fléchon, Paul Mainwaring, Mark Fleming, John D. Hainsworth, Mohammad Hirmand, Bryan Selby, Lynn Seely, and Johann S. de Bono (2012). "Increased Survival with Enzalutamide in Prostate Cancer after Chemotherapy". *New England Journal of Medicine* 367.13, pp. 1187–1197. DOI: 10.1056/NEJMoa1207506. eprint: https://www.nejm.org/doi/pdf/10.1056/NEJMoa1207506.

Scher, Howard I., Ryon P. Graf, Nicole A. Schreiber, Anuradha Jayaram, Eric Winquist, Brigit McLaughlin, David Lu, Martin Fleisher, Sarah Orr, Lori Lowes, Amanda Anderson, Yipeng Wang, Ryan Dittamore, Alison L. Allan, Gerhardt Attard, and Glenn Heller (Sept. 2018). "Assessment of the Validity of Nuclear-Localized Androgen Receptor Splice Variant 7 in Circulating Tumor Cells as a Predictive Biomarker for Castration-Resistant Prostate Cancer". *JAMA Oncology* 4.9, pp. 1179–1186. DOI: 10.1001/jamaoncol.2018.1621. eprint: https://jamanetwork.com/journals/jamaoncology/articlepdf/2686031/jamaoncology_scher_2018_oi_180031.pdf.

Scheuerer, Barbara, Martin Ernst, Iris Dürrbaum-Landmann, Jens Fleischer, Evelin Grage-Griebenow, Ernst Brandt, Hans Dieter Flad, and Frank Petersen (Feb. 2000). "The CXC-chemokine platelet factor 4 promotes monocyte survival and induces monocyte differentiation into macrophages". *Blood* 95 (4), pp. 1158–1166. DOI: 10.1182/BLOOD.V95.4.1158.004K31_1158_1166.

Schluns, Kimberly S, William C Kieper, Stephen C Jameson, and Leo Lefrancois (2000). "Interleukin-7 mediates the homeostasis of naive and memory CD8 T cells in vivo". *Nature Immunology* 1 (5), pp. 426–432. DOI: 10.1038/80868.

Schmid, Peter, Javier Cortes, Ana Joaquim, Noelia Martinez Janez, Serafin Morales, Tamara Diaz-Redondo, Sibel Blau, Patrick Neven, Julie Lemieux, Jose Angel Garcia-Saenz, Lowell Hart, Tsvetan Biyukov, Navid Baktash, Dan Massey, Howard A. Burris, and

Hope S. Rugo (Dec. 2023). "XENERA-1: a randomised double-blind Phase II trial of xentuzumab in combination with everolimus and exemestane versus everolimus and exemestane in patients with hormone receptor-positive/HER2-negative metastatic breast cancer and non-visceral disease". *Breast Cancer Research* 25 (1), pp. 1–10. DOI: 10.1186/S13058-023-01649-W/TABLES/2.

Schmidt, Julie A., Naomi E. Allen, Martin Almquist, Silvia Franceschi, Sabina Rinaldi, Sarah J. Tipper, Konstantinos K. Tsilidis, Elisabete Weiderpass, Kim Overvad, Anne Tjonneland, Marie-Christine Boutron-Ruault, Laure Dossus, Sylvie Mesrine, Rudolf Kaaks, Annekatrin Lukanova, Heiner Boeing, Pagona Lagiou, Dimitrios Trichopoulos, Antonia Trichopoulou, Domenico Palli, Vittorio Krogh, Salvatore Panico, Rosario Tumino, Roberto Zanetti, H. Bas Bueno-de-Mesquita, Petra H. Peeters, Eiliv Lund, Virginia Menendez, Antonio Agudo, Maria-Jose Sanchez, Maria-Dolores Chirlaque, Eva Ardanaz, Nerea Larranaga, Joakim Hennings, Maria Sandstrom, Kay-Tee Khaw, Nick Wareham, Isabelle Romieu, Marc J. Gunter, Elio Riboli, Timothy J. Key, and Ruth C. Travis (June 2014). "Insulin-like Growth Factor-I and Risk of Differentiated Thyroid Carcinoma in the European Prospective Investigation into Cancer and Nutrition". *Cancer Epidemiology, Biomarkers and Prevention* 23.6, pp. 976–985. DOI: 10.1158/1055-9965.EPI-13-1210-T. eprint: https://aacrjournals.org/cebp/article-pdf/23/6/976/2278750/976.pdf.

Schmitt, Clemens A, Boshi Wang, and Marco Demaria (2022). "Senescence and cancer - role and therapeutic opportunities". *Nature Reviews Clinical Oncology* 19 (10), pp. 619–636. DOI: 10.1038/s41571-022-00668-4.

Schneider, Helga, Jos Downey, Andrew Smith, Bernd H. Zinselmeyer, Catherine Rush, James M. Brewer, Bin Wei, Nancy Hogg, Paul Garside, and Christopher E. Rudd (2006). "Reversal of the TCR Stop Signal by CTLA-4". *Science* 313.5795, pp. 1972–1975. DOI: 10.1126/science.1131078. eprint: https://www.science.org/doi/pdf/10.1126/science.1131078.

Schoots, Ivo G., Monique J. Roobol, Daan Nieboer, Chris H. Bangma, Ewout W. Steyerberg, and M.G. Myriam Hunink (2015). "Magnetic Resonance Imaging–targeted Biopsy May Enhance the Diagnostic Accuracy of Significant Prostate Cancer Detection Compared to Standard Transrectal Ultrasound-guided Biopsy: A Systematic Review and Meta-analysis". *European Urology* 68.3, pp. 438–450. DOI: https://doi.org/10.1016/j.eururo.2014.11.037.

Schreiber, Robert D., Lloyd J. Old, and Mark J. Smyth (2011). "Cancer Immunoediting: Integrating Immunity's Roles in Cancer Suppression and Promotion". *Science* 331.6024, pp. 1565–1570. DOI: 10.1126/science.1203486. eprint: https://www.science.org/doi/pdf/10.1126/science.1203486.

Schroder, Fritz H., Arto Boeken Kruger, John Rietbergen, Ries Kranse, Paul van der Maas, Petra Beemsterboer, and Robert Hoedemaeker (Dec. 1998). "Evaluation of the Digital Rectal Examination as a Screening Test for Prostate Cancer". *JNCI: Journal of the National Cancer Institute* 90.23, pp. 1817–1823. DOI: 10.1093/jnci/90.23.1817. eprint: https://academic.oup.com/jnci/article-pdf/90/23/1817/7685166/90-23-1817.pdf.

Sedarsky, Jason, Michael Degon, Shiv Srivastava, and Albert Dobi (2018). "Ethnicity and ERG frequency in prostate cancer". *Nature Reviews Urology* 15 (2), pp. 125–131. DOI: 10.1038/nrurol.2017.140.

Segawa, Naoki, Misa Nakamura, Yasushi Nakamura, Ichiro Mori, Yoji Katsuoka, and Kennichi Kakudo (Aug. 2001). "Phosphorylation of Mitogen-activated Protein Kinase is

Inhibited by Calcitonin in DU145 Prostate Cancer Cells1". *Cancer Research* 61 (16), pp. 6060–6063.

Seger, Rony and Edwin G. Krebs (1995). "The MAPK signaling cascade". *The FASEB Journal* 9.9, pp. 726–735. DOI: https://doi.org/10.1096/fasebj.9.9.7601337. eprint: https://faseb.onlinelibrary.wiley.com/doi/pdf/10.1096/fasebj.9.9.7601337.

Segura-Villalobos, Deisy, Itzel G. Ramirez-Moreno, Magnolia Martinez-Aguilar, Alfredo Ibarra-Sanchez, J. Omar Munoz-Bello, Isabel Anaya-Rubio, Alejandro Padilla, Marina Macias-Silva, Marcela Lizano, and Claudia Gonzalez-Espinosa (2022). "Mast Cell–Tumor Interactions: Molecular Mechanisms of Recruitment, Intratumoral Communication and Potential Therapeutic Targets for Tumor Growth". *Cells* 11.3. DOI: 10.3390/cells11030349.

Sehat, Bita, Ali Tofigh, Yingbo Lin, Eric Trocme, Ulrika Liljedahl, Jens Lagergren, and Olle Larsson (2010). "SUMOylation Mediates the Nuclear Translocation and Signaling of the IGF-1 Receptor". *Science Signaling* 3.108, ra10–ra10. DOI: 10.1126/scisignal.2000628. eprint: https://www.science.org/doi/pdf/10.1126/scisignal.2000628.

Seifert, Lena, Gregor Werba, Shaun Tiwari, Nancy Ngoc Giao Ly, Sara Alothman, Dalia Alqunaibit, Antonina Avanzi, Rocky Barilla, Donnele Daley, Stephanie H Greco, Alejandro Torres-Hernandez, Matthew Pergamo, Atsuo Ochi, Constantinos P Zambirinis, Mridul Pansari, Mauricio Rendon, Daniel Tippens, Mautin Hundeyin, Vishnu R Mani, Cristina Hajdu, Dannielle Engle, and George Miller (2016). "The necrosome promotes pancreatic oncogenesis via CXCL1 and Mincle-induced immune suppression". *Nature* 532 (7598), pp. 245–249. DOI: 10.1038/nature17403.

Seligson, David B, Hong Yu, Sheila Tze, Jonathan Said, Allan J Pantuck, Pinchas Cohen, and Kuk-Wha Lee (2013). "IGFBP-3 Nuclear Localization Predicts Human Prostate Cancer Recurrence". *Hormones and Cancer* 4 (1), pp. 12–23. DOI: 10.1007/s12672-012-0124-8.

Seol, Min A, Jin-Hee Kim, Keunhee Oh, Gwanghun Kim, Myung Won Seo, Young-Kyoung Shin, Ji Hyun Sim, Hyun Mu Shin, Bo Yeon Seo, Dong-Sup Lee, Ja-Lok Ku, Ilkyu Han, Insoo Kang, Serk In Park, and Hang-Rae Kim (2019). "Interleukin-7 Contributes to the Invasiveness of Prostate Cancer Cells by Promoting Epithelial–Mesenchymal Transition". *Scientific Reports* 9 (1), p. 6917. DOI: 10.1038/s41598-019-43294-4.

Sfanos, Karen Sandell, Tullia C. Bruno, Charles H. Maris, Lauren Xu, Christopher J. Thoburn, Angelo M. DeMarzo, Alan K. Meeker, William B. Isaacs, and Charles G. Drake (June 2008). "Phenotypic Analysis of Prostate-Infiltrating Lymphocytes Reveals TH17 and Treg Skewing". *Clinical Cancer Research* 14.11, pp. 3254–3261. DOI: 10.1158/1078-0432.CCR-07-5164. eprint: https://aacrjournals.org/clincancerres/article-pdf/14/11/3254/1977587/3254.pdf.

Shaffer, Paul L., Arif Jivan, D. Eric Dollins, Frank Claessens, and Daniel T. Gewirth (2004). "Structural basis of androgen receptor binding to selective androgen response elements". *Proceedings of the National Academy of Sciences* 101.14, pp. 4758–4763. DOI: 10.1073/pnas.0401123101. eprint: https://www.pnas.org/doi/pdf/10.1073/pnas.0401123101.

Shang, Yongfeng, Molly Myers, and Myles Brown (2002). "Formation of the Androgen Receptor Transcription Complex". *Molecular Cell* 9.3, pp. 601–610. DOI: https://doi.org/10.1016/S1097-2765(02)00471-9.

Shapiro, Melanie R., Leeana D. Peters, Matthew E. Brown, Cecilia Cabello-Kindelan, Amanda L. Posgai, Allison L. Bayer, and Todd M. Brusko (Oct. 2023). "Insulin-like

Growth Factor-1 Synergizes with IL-2 to Induce Homeostatic Proliferation of Regulatory T Cells". *The Journal of Immunology* 211 (7), pp. 1108–1122. DOI: 10.4049/JIMMUNOL.2200651.

Shariat, Shahrokh F., Dolores J. Lamb, Michael W. Kattan, Cuong Nguyen, JaHong Kim, Josie Beck, Thomas M. Wheeler, and Kevin M. Slawin (2002). "Association of Preoperative Plasma Levels of Insulin-Like Growth Factor I and Insulin-Like Growth Factor Binding Proteins-2 and -3 With Prostate Cancer Invasion, Progression, and Metastasis". *Journal of Clinical Oncology* 20.3. PMID: 11821468, pp. 833–841. DOI: 10.1200/JCO.2002.20.3.833. eprint: https://doi.org/10.1200/JCO.2002.20.3.833.

Sharma, Padmanee, Michael Krainer, Fred Saad, Daniel Castellano, Jens Bedke, Mariusz Kwiatkowski, Akash Patnaik, Giuseppe Procopio, Pawel Wiechno, Samith Thomas Kochuparambil, Christian Thomas, Jose Angel Arranz Arija, Steven L McCune, Steinbjorn Hansen, Gedske Daugaard, Neha P Amin, Yumeng Wang, Justin M David, and Russell Kent Pachynski (Feb. 2023). "Nivolumab plus ipilimumab for the treatment of post-chemotherapy metastatic castration-resistant prostate cancer (mCRPC)- Additional results from the randomized phase 2 CheckMate 650 trial." *Journal of Clinical Oncology* 41, p. 22. DOI: 10.1200/JCO.2023.41.6_suppl.22.

Sharma, Padmanee, Siwen Hu-Lieskovan, Jennifer A Wargo, and Antoni Ribas (Feb. 2017). "Primary, Adaptive, and Acquired Resistance to Cancer Immunotherapy". *Cell* 168 (4). doi: 10.1016/j.cell.2017.01.017, pp. 707–723. DOI: 10.1016/j.cell.2017.01.017.

Sharma, Padmanee, Russell K Pachynski, Vivek Narayan, Aude Fléchon, Gwenaelle Gravis, Matthew D Galsky, Hakim Mahammedi, Akash Patnaik, Sumit K Subudhi, Marika Ciprotti, Burcin Simsek, Abdel Saci, Yanhua Hu, G Celine Han, and Karim Fizazi (Oct. 2020). "Nivolumab Plus Ipilimumab for Metastatic Castration-Resistant Prostate Cancer: Preliminary Analysis of Patients in the CheckMate 650 Trial". *Cancer Cell* 38 (4), pp. 489–499. DOI: 10.1016/j.ccell.2020.08.007.

Sharon, Shilhav Meisel, Yair Pozniak, Tamar Geiger, Haim Werner, Shilhav Meisel Sharon, Yair Pozniak, Tamar Geiger, and Haim Werner (June 2016). "TMPRSS2-ERG fusion protein regulates insulin-like growth factor-1 receptor (IGF1R) gene expression in prostate cancer: involvement of transcription factor Sp1". *Oncotarget* 7 (32), pp. 51375–51392. DOI: 10.18632/ONCOTARGET.9837.

Sharp, Adam, Ilsa Coleman, Wei Yuan, Cynthia Sprenger, David Dolling, Daniel Nava Rodrigues, Joshua W. Russo, Ines Figueiredo, Claudia Bertan, George Seed, Ruth Riisnaes, Takuma Uo, Antje Neeb, Jonathan Welti, Colm Morrissey, Suzanne Carreira, Jun Luo, Peter S. Nelson, Steven P. Balk, Lawrence D. True, Johann S. de Bono, and Stephen R. Plymate (Jan. 2019). "Androgen receptor splice variant-7 expression emerges with castration resistance in prostate cancer". *The Journal of Clinical Investigation* 129.1, pp. 192–208. DOI: 10.1172/JCI122819.

Shaw, Aubie K., Michael W. Pickup, Anna Chytil, Mary Aakre, Philip Owens, Harold L. Moses, and Sergey V. Novitskiy (Jan. 2015). "TGFB Signaling in Myeloid Cells Regulates Mammary Carcinoma Cell Invasion through Fibroblast Interactions". *PLOS ONE* 10.1, pp. 1–13. DOI: 10.1371/journal.pone.0117908.

Shaw, Greg L., Hayley Whitaker, Marie Corcoran, Mark J. Dunning, Hayley Luxton, Jonathan Kay, Charlie E. Massie, Jodi L. Miller, Alastair D. Lamb, Helen Ross-Adams, Roslin Russell, Adam W. Nelson, Matthew D. Eldridge, Andrew G. Lynch, Antonio Ramos-Montoya, Ian G. Mills, Angela E. Taylor, Wiebke Arlt, Nimish Shah, Anne Y. Warren, and David E. Neal (2016). "The Early Effects of Rapid Androgen

Deprivation on Human Prostate Cancer". *European Urology* 70.2, pp. 214–218. DOI: https://doi.org/10.1016/j.eururo.2015.10.042.

Shen, Michael M. and Cory Abate-Shen (2010). "Molecular genetics of prostate cancer: new prospects for old challenges". *Genes and Development* 24.18, pp. 1967–2000. DOI: 10.1101/gad.1965810.

Shi, Yi, David J. Riese, and Jianzhong Shen (2020). "The Role of the CXCL12/CXCR4/CXCR7 Chemokine Axis in Cancer". *Frontiers in Pharmacology* 11. DOI: 10.3389/fphar.2020.574667.

Shiao, Stephen L., Brian Ruffell, David G. DeNardo, Bruce A. Faddegon, Catherine C. Park, and Lisa M. Coussens (May 2015). "TH2-Polarized CD4+ T Cells and Macrophages Limit Efficacy of Radiotherapy". *Cancer Immunology Research* 3.5, pp. 518–525. DOI: 10.1158/2326-6066.CIR-14-0232. eprint: https://aacrjournals.org/cancerimmunolres/article-pdf/3/5/518/2347689/518.pdf.

Shin, Incheol, F Michael Yakes, Federico Rojo, Nah-Young Shin, Andrei V Bakin, Jose Baselga, and Carlos L Arteaga (2002). "PKB/Akt mediates cell-cycle progression by phosphorylation of p27Kip1 at threonine 157 and modulation of its cellular localization". *Nature Medicine* 8 (10), pp. 1145–1152. DOI: 10.1038/nm759.

Shinoda, Kenta, Koji Tokoyoda, Asami Hanazawa, Koji Hayashizaki, Sandra Zehentmeier, Hiroyuki Hosokawa, Chiaki Iwamura, Haruhiko Koseki, Damon J. Tumes, Andreas Radbruch, and Toshinori Nakayama (2012). "Type II membrane protein CD69 regulates the formation of resting T-helper memory". *Proceedings of the National Academy of Sciences* 109.19, pp. 7409–7414. DOI: 10.1073/pnas.1118539109. eprint: https://www.pnas.org/doi/pdf/10.1073/pnas.1118539109.

Shoji, Kazuyasu, Kazumasa Ohashi, Kaori Sampei, Masato Oikawa, and Kensaku Mizuno (2012). "Cytochalasin D acts as an inhibitor of the actin–cofilin interaction". *Biochemical and Biophysical Research Communications* 424.1, pp. 52–57. DOI: https://doi.org/10.1016/j.bbrc.2012.06.063.

Shu, Yuxin, Menghao Qin, Yue Song, Qing Tang, Yahong Huang, Pingping Shen, and Yan Lu (2020). "M2 polarization of tumor-associated macrophages is dependent on integrin B3 via peroxisome proliferator-activated receptor-y up-regulation in breast cancer". *Immunology* 160.4, pp. 345–356. DOI: https://doi.org/10.1111/imm.13196. eprint: https://onlinelibrary.wiley.com/doi/pdf/10.1111/imm.13196.

Shulman, David S., Priscilla Merriam, Edwin Choy, Lillian M. Guenther, Kerri L. Cavanaugh, Pei-Chi Kao, Andrew Posner, Ketki Bhushan, Grace Fairchild, Emma Barker, Kelly Klega, Kimberly Stegmaier, Brian D. Crompton, Wendy B. London, and Steven G. DuBois (2023). "Phase 2 trial of palbociclib and ganitumab in patients with relapsed Ewing sarcoma". *Cancer Medicine* 12.14, pp. 15207–15216. DOI: https://doi.org/10.1002/cam4.6208. eprint: https://onlinelibrary.wiley.com/doi/pdf/10.1002/cam4.6208.

Sica, Antonio and Alberto Mantovani (Mar. 2012). "Macrophage plasticity and polarization: in vivo veritas". *The Journal of Clinical Investigation* 122.3, pp. 787–795. DOI: 10.1172/JCI59643.

Siefert, Joseph C., Bianca Cioni, Mauro J. Muraro, Mohammed Alshalalfa, Judith Vivie, Henk G. van der Poel, Ivo G. Schoots, Elise Bekers, Felix Y. Feng, Lodewyk F.A. Wessels, Wilbert Zwart, and Andries M. Bergman (Oct. 2021). "The Prognostic Potential of Human Prostate Cancer-Associated Macrophage Subtypes as Revealed by Single-Cell Transcriptomics". *Molecular cancer research : MCR* 19 (10), pp. 1778–1791. DOI: 10.1158/1541-7786.MCR-20-0740.

Simanshu, Dhirendra K, Dwight V Nissley, and Frank McCormick (June 2017). "RAS Proteins and Their Regulators in Human Disease". *Cell* 170 (1). doi: 10.1016/j.cell.2017.06.009, pp. 17–33. DOI: 10.1016/j.cell.2017.06.009.

Simental, J A, M Sar, M V Lane, F S French, and E M Wilson (1991). "Transcriptional activation and nuclear targeting signals of the human androgen receptor". *Journal of Biological Chemistry* 266.1, pp. 510–518. DOI: https://doi.org/10.1016/S0021-9258(18)52466-2.

Simpson, Aaron, Wilfride Petnga, Valentine M Macaulay, Ulrike Weyer-Czernilofsky, and Thomas Bogenrieder (2017). "Insulin-Like Growth Factor (IGF) Pathway Targeting in Cancer: Role of the IGF Axis and Opportunities for Future Combination Studies". *Targeted Oncology* 12 (5), pp. 571–597. DOI: 10.1007/s11523-017-0514-5.

Simpson, Aaron D, Ying Wei Jenetta Soo, Guillaume Rieunier, Tamara Aleksic, Olaf Ansorge, Chris Jones, and Valentine M Macaulay (2020). "Type 1 IGF receptor associates with adverse outcome and cellular radioresistance in paediatric high-grade glioma". *British Journal of Cancer* 122 (5), pp. 624–629. DOI: 10.1038/s41416-019-0677-1.

Smith, Christopher M, Nicholas S Wilson, Jason Waithman, Jose A Villadangos, Francis R Carbone, William R Heath, and Gabrielle T Belz (2004). "Cognate CD4+ T cell licensing of dendritic cells in CD8+ T cell immunity". *Nature Immunology* 5 (11), pp. 1143–1148. DOI: 10.1038/ni1129.

Smith, Matthew R., Fred Saad, Simon Chowdhury, Stéphane Oudard, Boris A. Hadaschik, Julie N. Graff, David Olmos, Paul N. Mainwaring, Ji Youl Lee, Hiroji Uemura, Angela Lopez-Gitlitz, Géralyn C. Trudel, Byron M. Espina, Youyi Shu, Youn C. Park, Wayne R. Rackoff, Margaret K. Yu, and Eric J. Small (2018a). "Apalutamide Treatment and Metastasis-free Survival in Prostate Cancer". *New England Journal of Medicine* 378.15, pp. 1408–1418. DOI: 10.1056/NEJMoa1715546. eprint: https://www.nejm.org/doi/pdf/10.1056/NEJMoa1715546.

Smith, Terry J and Joseph A M J L Janssen (Sept. 2018b). "Insulin-like Growth Factor-I Receptor and Thyroid-Associated Ophthalmopathy". *Endocrine Reviews* 40.1, pp. 236–267. DOI: 10.1210/er.2018-00066. eprint: https://academic.oup.com/edrv/article-pdf/40/1/236/27509513/er.2018-00066.pdf.

Smith, Terry J., George J. Kahaly, Daniel G. Ezra, James C. Fleming, Roger A. Dailey, Rosa A. Tang, Gerald J. Harris, Alessandro Antonelli, Mario Salvi, Robert A. Goldberg, James W. Gigantelli, Steven M. Couch, Erin M. Shriver, Brent R. Hayek, Eric M. Hink, Richard M. Woodward, Kathleen Gabriel, Guido Magni, and Raymond S. Douglas (2017). "Teprotumumab for Thyroid-Associated Ophthalmopathy". *New England Journal of Medicine* 376.18, pp. 1748–1761. DOI: 10.1056/NEJMoa1614949. eprint: https://www.nejm.org/doi/pdf/10.1056/NEJMoa1614949.

Snyder, Annelise G., Nicholas W. Hubbard, Michelle N. Messmer, Sigal B. Kofman, Cassidy E. Hagan, Susana L. Orozco, Kristy Chiang, Brian P. Daniels, David Baker, and Andrew Oberst (June 2019). "Intratumoral activation of the necroptotic pathway components RIPK1 and RIPK3 potentiates antitumor immunity". *Science Immunology* 4 (36), p. 2004. DOI: 10.1126/SCIIMMUNOL.AAW2004/SUPPL_FILE/AAW2004_SM.PDF.

Somri-Gannam, Lina, Shilhav Meisel-Sharon, Shay Hantisteanu, Gabriel Groisman, Ofer Limonad, Mordechai Hallak, and Ilan Bruchim (2020). "IGF1R Axis Inhibition Restores Dendritic Cell Antitumor Response in Ovarian Cancer". *Translational Oncology* 13.8, p. 100790. DOI: https://doi.org/10.1016/j.tranon.2020.100790.

Song, Chunjiao and Huan Chen (2018). "Predictive significance of TMRPSS2-ERG fusion in prostate cancer: a meta-analysis". *Cancer Cell International* 18 (1), p. 177. DOI: 10.1186/s12935-018-0672-2.

Song, Dandan, Yan Lian, and Lin Zhang (2023). "The potential of activator protein 1 (AP-1) in cancer targeted therapy". *Frontiers in Immunology* 14. DOI: 10.3389/fimmu.2023.1224892.

Song, Hanbing, Hannah N W Weinstein, Paul Allegakoen, Marc H Wadsworth, Jamie Xie, Heiko Yang, Ethan A Castro, Kevin L Lu, Bradley A Stohr, Felix Y Feng, Peter R Carroll, Bruce Wang, Matthew R Cooperberg, Alex K Shalek, and Franklin W Huang (2022). "Single-cell analysis of human primary prostate cancer reveals the heterogeneity of tumor-associated epithelial cell states". *Nature Communications* 13 (1), p. 141. DOI: 10.1038/s41467-021-27322-4.

Spadaro, Olga, Christina D. Camell, Lidia Bosurgi, Kim Y. Nguyen, Yun-Hee Youm, Carla V. Rothlin, and Vishwa Deep Dixit (2017). "IGF1 Shapes Macrophage Activation in Response to Immunometabolic Challenge". *Cell Reports* 19.2, pp. 225–234. DOI: https://doi.org/10.1016/j.celrep.2017.03.046.

Spratt, Daniel E, Zachary S Zumsteg, Felix Y Feng, and Scott A Tomlins (2016). "Translational and clinical implications of the genetic landscape of prostate cancer". *Nature Reviews Clinical Oncology* 13 (10), pp. 597–610. DOI: 10.1038/nrclinonc.2016.76.

Stabile, Armando, Francesco Giganti, Andrew B Rosenkrantz, Samir S Taneja, Geert Villeirs, Inderbir S Gill, Clare Allen, Mark Emberton, Caroline M Moore, and Veeru Kasivisvanathan (2020). "Multiparametric MRI for prostate cancer diagnosis: current status and future directions". *Nature Reviews Urology* 17 (1), pp. 41–61. DOI: 10.1038/s41585-019-0212-4.

Stambolic, Vuk, Akira Suzuki, Jose Luis de la Pompa, Greg M Brothers, Christine Mirtsos, Takehiko Sasaki, Jurgen Ruland, Josef M Penninger, David P Siderovski, and Tak W Mak (Oct. 1998). "Negative Regulation of PKB/Akt-Dependent Cell Survival by the Tumor Suppressor PTEN". *Cell* 95 (1), pp. 29–39. DOI: 10.1016/S0092-8674(00)81780-8.

Stemberger, Christian, Katharina M Huster, Martina Koffler, Florian Anderl, Matthias Schiemann, Hermann Wagner, and Dirk H Busch (Dec. 2007). "A Single Naive CD8+ T Cell Precursor Can Develop into Diverse Effector and Memory Subsets". *Immunity* 27 (6). doi: 10.1016/j.immuni.2007.10.012, pp. 985–997. DOI: 10.1016/j.immuni.2007.10.012.

Sternberg, Cora N., Karim Fizazi, Fred Saad, Neal D. Shore, Ugo De Giorgi, David F. Penson, Ubirajara Ferreira, Eleni Efstathiou, Katarzyna Madziarska, Michael P. Kolinsky, Daniel I. G. Cubero, Bettina Noerby, Fabian Zohren, Xun Lin, Katharina Modelska, Jennifer Sugg, Joyce Steinberg, and Maha Hussain (2020). "Enzalutamide and Survival in Nonmetastatic, Castration-Resistant Prostate Cancer". *New England Journal of Medicine* 382.23, pp. 2197–2206. DOI: 10.1056/NEJMoa2003892. eprint: https://www.nejm.org/doi/pdf/10.1056/NEJMoa2003892.

Steuerman, Rachel, Orit Shevah, and Zvi Laron (Apr. 2011). "Congenital IGF1 deficiency tends to confer protection against post-natal development of malignancies". *European Journal of Endocrinology* 164.4, pp. 485–489. DOI: 10.1530/EJE-10-0859. eprint: https://academic.oup.com/ejendo/article-pdf/164/4/485/45552442/485.pdf.

Stinchcombe, Jane C and Gillian M Griffiths (2003). "The role of the secretory immunological synapse in killing by CD8+ CTL". *Seminars in Immunology* 15.6. The Immunological Synapse, pp. 301–305. DOI: https://doi.org/10.1016/j.smim.2003.09.003.

Stockmann, Christian, Andrew Doedens, Alexander Weidemann, Na Zhang, Norihiko Takeda, Joshua I Greenberg, David A Cheresh, and Randall S Johnson (2008). "Deletion of vascular endothelial growth factor in myeloid cells accelerates tumorigenesis". *Nature* 456 (7223), pp. 814–818. DOI: 10.1038/nature07445.

Stokoe, David, Susan G Macdonald, Karen Cadwallader, Marc Symons, and John F Hancock (1994). "Activation of Raf as a Result of Recruitment to the Plasma Membrane". *Science* 264 (5164), pp. 1463–1467. DOI: 10.1126/science.7811320.

Stopsack, Konrad H., Subhiksha Nandakumar, Andreas G. Wibmer, Samuel Haywood, Emily S. Weg, Ethan S. Barnett, Chloe J. Kim, Emily A. Carbone, Samantha E. Vasselman, Bastien Nguyen, Melanie A. Hullings, Howard I. Scher, Michael J. Morris, David B. Solit, Nikolaus Schultz, Philip W. Kantoff, and Wassim Abida (July 2020). "Oncogenic Genomic Alterations, Clinical Phenotypes, and Outcomes in Metastatic Castration-Sensitive Prostate Cancer". *Clinical Cancer Research* 26.13, pp. 3230–3238. DOI: 10.1158/1078-0432.CCR-20-0168. eprint: https://aacrjournals.org/clincancerres/article-pdf/26/13/3230/2061313/3230.pdf.

Stout, Robert D., Chuancang Jiang, Bharati Matta, Illya Tietzel, Stephanie K. Watkins, and Jill Suttles (July 2005). "Macrophages Sequentially Change Their Functional Phenotype in Response to Changes in Microenvironmental Influences". *The Journal of Immunology* 175.1, pp. 342–349. DOI: 10.4049/jimmunol.175.1.342. eprint: https://journals.aai.org/jimmunol/article-pdf/175/1/342/1202266/342.pdf.

Stribbling, Stephen M., Callum Beach, and Anderson J. Ryan (2024). "Orthotopic and metastatic tumour models in preclinical cancer research". *Pharmacology and Therapeutics* 257, p. 108631. DOI: https://doi.org/10.1016/j.pharmthera.2024.108631.

Su, Wenjing, Hyun Ho Han, Yan Wang, Boyu Zhang, Bing Zhou, Yuanming Cheng, Alekya Rumandla, Sreeharsha Gurrapu, Goutam Chakraborty, Jie Su, Guangli Yang, Xin Liang, Guocan Wang, Neal Rosen, Howard I Scher, Ouathek Ouerfelli, and Filippo G Giancotti (Aug. 2019). "The Polycomb Repressor Complex 1 Drives Double-Negative Prostate Cancer Metastasis by Coordinating Stemness and Immune Suppression". *Cancer Cell* 36 (2). doi: 10.1016/j.ccell.2019.06.009, 139–155.e10. DOI: 10.1016/j.ccell.2019.06.009.

Al-Sudani, Hussein, Ying Ni, Philip Jones, Huseyin Karakilic, Lei Cui, Lisa D S Johnson, Peter G Rose, Alexander Olawaiye, Robert P Edwards, Robert A Uger, Gloria H Y Lin, and Haider Mahdi (2023). "Targeting CD47-SIRPa axis shows potent preclinical anti-tumor activity as monotherapy and synergizes with PARP inhibition". *npj Precision Oncology* 7, p. 69.

Sun, Jingjing, Zhiyuan Lu, Yun Deng, Wei Wang, Qianting He, Wangxiang Yan, and Anxun Wang (2018). "Up-regulation of INSR/IGF1R by C-myc promotes TSCC tumorigenesis and metastasis through the NF-kB pathway". *Biochimica et Biophysica Acta (BBA) - Molecular Basis of Disease* 1864.5, Part A, pp. 1873–1882. DOI: https://doi.org/10.1016/j.bbadis.2018.03.004.

Suzuki, Hiroyoshi, Diha Freije, Deborah R Nusskern, Kenji Okami, Paul Cairns, David Sidransky, William B Isaacs, and G Steven Bova (Jan. 1998). "Interfocal Heterogeneity of PTEN or MMAC1 Gene Alterations in Multiple Metastatic Prostate Cancer Tissues". *Cancer Research* 58 (2), pp. 204–209.

Syeda, Madiha Zahra, Tu Hong, Chunming Huang, Wenhua Huang, and Qingchun Mu (2024). "B cell memory: from generation to reactivation: a multipronged defense wall against pathogens". *Cell Death Discovery* 10 (1), p. 117. DOI: 10.1038/s41420-024-01889-5.

Szabo, Peter A, Hanna Mendes Levitin, Michelle Miron, Mark E Snyder, Takashi Senda, Jinzhou Yuan, Yim Ling Cheng, Erin C Bush, Pranay Dogra, Puspa Thapa, Donna L Farber, and Peter A Sims (2019). "Single-cell transcriptomics of human T cells reveals tissue and activation signatures in health and disease". *Nature Communications* 10 (1), p. 4706. DOI: 10.1038/s41467-019-12464-3.

Tadokoro, Carlos E., Guy Shakhar, Shiqian Shen, Yi Ding, Andreia C. Lino, Antonio Maraver, Juan J. Lafaille, and Michael L. Dustin (Mar. 2006). "Regulatory T cells inhibit stable contacts between CD4+ T cells and dendritic cells in vivo ". *Journal of Experimental Medicine* 203.3, pp. 505–511. DOI: 10.1084/jem.20050783. eprint: https://rupress.org/jem/article-pdf/203/3/505/1720046/505.pdf.

Tahimic, Candice G. T., Yongmei Wang, and Daniel D. Bikle (2013). "Anabolic effects of IGF-1 signaling on the skeleton". *Frontiers in Endocrinology* 4. DOI: 10.3389/fendo.2013.00006.

Takahashi, Kazuki, Katarzyna A. Podyma-Inoue, Maki Saito, Shintaro Sakakitani, Akinari Sugauchi, Keita Iida, Sadahiro Iwabuchi, Daizo Koinuma, Kyoko Kurioka, Toru Konishi, Susumu Tanaka, Atsushi Kaida, Masahiko Miura, Shinichi Hashimoto, Mariko Okada, Toshihiro Uchihashi, Kohei Miyazono, and Tetsuro Watabe (2022). "TGF-B generates a population of cancer cells residing in G1 phase with high motility and metastatic potential via KRTAP2-3". *Cell Reports* 40.13, p. 111411. DOI: https://doi.org/10.1016/j.celrep.2022.111411.

Takahashi, Toshiyuki, Keiichi Fukuda, Jing Pan, Hiroaki Kodama, Motoaki Sano, Shinji Makino, Takahiro Kato, Tomohiro Manabe, and Satoshi Ogawa (1999). "Characterization of Insulin-Like Growth Factor-1–Induced Activation of the JAK/STAT Pathway in Rat Cardiomyocytes". *Circulation Research* 85.10, pp. 884–891. DOI: 10.1161/01.RES.85.10.884. eprint: https://www.ahajournals.org/doi/pdf/10.1161/01.RES.85.10.884.

Tan, M H Eileen, Jun Li, H Eric Xu, Karsten Melcher, and Eu-leong Yong (2015). "Androgen receptor: structure, role in prostate cancer and drug discovery". *Acta Pharmacologica Sinica* 36 (1), pp. 3–23. DOI: 10.1038/aps.2014.18.

Tang, Qizhi, Jason Y Adams, Aaron J Tooley, Mingying Bi, Brian T Fife, Pau Serra, Pere Santamaria, Richard M Locksley, Matthew F Krummel, and Jeffrey A Bluestone (2006). "Visualizing regulatory T cell control of autoimmune responses in nonobese diabetic mice". *Nature Immunology* 7 (1), pp. 83–92. DOI: 10.1038/ni1289.

Tape, Christopher J., Stephanie Ling, Maria Dimitriadi, Kelly M. McMahon, Jonathan D. Worboys, Hui Sun Leong, Ida C. Norrie, Crispin J. Miller, George Poulogiannis, Douglas A. Lauffenburger, and Claus Jorgensen (May 2016). "Oncogenic KRAS Regulates Tumor Cell Signaling via Stromal Reciprocation". *Cell* 165 (4). doi: 10.1016/j.cell.2016.03.029, pp. 910–920. DOI: 10.1016/j.cell.2016.03.029.

Tay, Christopher, Atsushi Tanaka, and Shimon Sakaguchi (2023). "Tumor-infiltrating regulatory T cells as targets of cancer immunotherapy". *Cancer Cell* 41.3, pp. 450–465. DOI: https://doi.org/10.1016/j.ccell.2023.02.014.

Tay, Rong En, Emma K Richardson, and Han Chong Toh (2021). "Revisiting the role of CD4+ T cells in cancer immunotherapy - new insights into old paradigms". *Cancer Gene Therapy* 28 (1), pp. 5–17. DOI: 10.1038/s41417-020-0183-x.

Taylor, Avigail, Valentine M Macaulay, Anand K Maurya, Matthieu J Miossec, and Francesca M Buffa (2023). *GeneFEAST: the pivotal, gene-centric step in functional enrichment analysis interpretation.*

Taylor, Barry S, Nikolaus Schultz, Haley Hieronymus, Anuradha Gopalan, Yonghong Xiao, Brett S Carver, Vivek K Arora, Poorvi Kaushik, Ethan Cerami, Boris Reva, Yevgeniy Antipin, Nicholas Mitsiades, Thomas Landers, Igor Dolgalev, John E Major, Manda Wilson, Nicholas D Socci, Alex E Lash, Adriana Heguy, James A Eastham, Howard I Scher, Victor E Reuter, Peter T Scardino, Chris Sander, Charles L Sawyers, and William L Gerald (July 2010). "Integrative Genomic Profiling of Human Prostate Cancer". *Cancer Cell* 18 (1). doi: 10.1016/j.ccr.2010.05.026, pp. 11–22. DOI: 10.1016/j.ccr.2010.05.026.

Taylor, Renea A, Michael Fraser, Richard J Rebello, Paul C Boutros, Declan G Murphy, Robert G Bristow, and Gail P Risbridger (2019). "The influence of BRCA2 mutation on localized prostate cancer". *Nature Reviews Urology* 16 (5), pp. 281–290. DOI: 10.1038/s41585-019-0164-8.

Teng, Linda K. H., Brooke A. Pereira, Shivakumar Keerthikumar, Cheng Huang, Birunthi Niranjan, Sophie N. Lee, Michelle Richards, Ralf B. Schittenhelm, Luc Furic, David L. Goode, Mitchell G. Lawrence, Renea A. Taylor, Stuart J. Ellem, Gail P. Risbridger, and Natalie L. Lister (2021). "Mast Cell-Derived SAMD14 Is a Novel Regulator of the Human Prostate Tumor Microenvironment". *Cancers* 13.6. DOI: 10.3390/cancers13061237.

Testi, R, J H Phillips, and L L Lanier (Mar. 1989). "Leu 23 induction as an early marker of functional CD3/T cell antigen receptor triggering. Requirement for receptor cross-linking, prolonged elevation of intracellular [Ca++] and stimulation of protein kinase C." *The Journal of Immunology* 142.6, pp. 1854–1860. DOI: 10.4049/jimmunol.142.6.1854. eprint: https://journals.aai.org/jimmunol/article-pdf/142/6/1854/1046065/1854.pdf.

Theruvath, Johanna, Marie Menard, Benjamin A.H. Smith, Miles H. Linde, Garry L. Coles, Guillermo Nicolas Dalton, Wei Wu, Louise Kiru, Alberto Delaidelli, Elena Sotillo, John L. Silberstein, Anna C. Geraghty, Allison Banuelos, Molly Thomas Radosevich, Shaurya Dhingra, Sabine Heitzeneder, Aidan Tousley, John Lattin, Peng Xu, Jing Huang, Nicole Nasholm, Andy He, Tracy C. Kuo, Emma R.B. Sangalang, Jaume Pons, Amira Barkal, Rachel E. Brewer, Kristopher D. Marjon, Jose G. Vilches-Moure, Payton L. Marshall, Ricardo Fernandes, Michelle Monje, Jennifer R. Cochran, Poul H. Sorensen, Heike E. Daldrup-Link, Irving L. Weissman, Julien Sage, Ravindra Majeti, Carolyn R. Bertozzi, William A. Weiss, Crystal L. Mackall, and Robbie G. Majzner (Jan. 2022). "Anti-GD2 synergizes with CD47 blockade to mediate tumor eradication". *Nature Medicine 2022 28:2* 28 (2), pp. 333–344. DOI: 10.1038/s41591-021-01625-x.

Thiese, Matthew S. (2014). "Observational and interventional study design types; an overview". *Biochemia Medica* 24 (2), p. 199. DOI: 10.11613/BM.2014.022.

Thompson, Ian M., Donna K. Pauler, Phyllis J. Goodman, Catherine M. Tangen, M. Scott Lucia, Howard L. Parnes, Lori M. Minasian, Leslie G. Ford, Scott M. Lippman, E. David Crawford, John J. Crowley, and Charles A. Coltman (2004). "Prevalence of Prostate Cancer among Men with a Prostate-Specific Antigen Level <4.0 ng per Milliliter". *New England Journal of Medicine* 350.22, pp. 2239–2246. DOI: 10.1056/NEJMoa031918. eprint: https://www.nejm.org/doi/pdf/10.1056/NEJMoa031918.

Tian, Lei, Bo Xu, Kun-Yu Teng, Mihae Song, Zheng Zhu, Yuqing Chen, Jing Wang, Jianying Zhang, Mingye Feng, Balveen Kaur, Lorna Rodriguez, Michael A. Caligiuri, and Jianhua Yu (Jan. 2022). "Targeting Fc Receptor-Mediated Effects and the "Don't Eat Me" Signal with an Oncolytic Virus Expressing an Anti-CD47 Antibody to Treat Metastatic

Ovarian Cancer". *Clinical Cancer Research* 28.1, pp. 201–214. DOI: 10.1158/1078-0432.CCR-21-1248. eprint: https://aacrjournals.org/clincancerres/article-pdf/28/1/201/3015502/201.pdf.

Timms, John F., Kristen Carlberg, Haihua Gu, Haiyan Chen, Shubhangi Kamatkar, Monica J. S. Nadler, Larry R. Rohrschneider, and Benjamin G. Neel (1998). "Identification of Major Binding Proteins and Substrates for the SH2-Containing Protein Tyrosine Phosphatase SHP-1 in Macrophages". *Molecular and Cellular Biology* 18.7. PMID: 9632768, pp. 3838–3850. DOI: 10.1128/MCB.18.7.3838. eprint: https://doi.org/10.1128/MCB.18.7.3838.

Togashi, Yosuke, Kohei Shitara, and Hiroyoshi Nishikawa (2019). "Regulatory T cells in cancer immunosuppression — implications for anticancer therapy". *Nature Reviews Clinical Oncology* 16 (6), pp. 356–371. DOI: 10.1038/s41571-019-0175-7.

Tomlins, Scott A, Bharathi Laxman, Saravana M Dhanasekaran, Beth E Helgeson, Xuhong Cao, David S Morris, Anjana Menon, Xiaojun Jing, Qi Cao, Bo Han, Jindan Yu, Lei Wang, James E Montie, Mark A Rubin, Kenneth J Pienta, Diane Roulston, Rajal B Shah, Sooryanarayana Varambally, Rohit Mehra, and Arul M Chinnaiyan (2007). "Distinct classes of chromosomal rearrangements create oncogenic ETS gene fusions in prostate cancer". *Nature* 448 (7153), pp. 595–599. DOI: 10.1038/nature06024.

Tomlins, Scott A., Anders Bjartell, Arul M. Chinnaiyan, Guido Jenster, Robert K. Nam, Mark A. Rubin, and Jack A. Schalken (2009). "ETS Gene Fusions in Prostate Cancer: From Discovery to Daily Clinical Practice". *European Urology* 56.2, pp. 275–286. DOI: https://doi.org/10.1016/j.eururo.2009.04.036.

Tomlins, Scott A., Bharathi Laxman, Sooryanarayana Varambally, Xuhong Cao, Jindan Yu, Beth E. Helgeson, Qi Cao, John R. Prensner, Mark A. Rubin, Rajal B. Shah, Rohit Mehra, and Arul M. Chinnaiyan (2008). "Role of the TMPRSS2-ERG Gene Fusion in Prostate Cancer". *Neoplasia* 10.2, 177–IN9. DOI: https://doi.org/10.1593/neo.07822.

Tomlins, Scott A., Rohit Mehra, Daniel R. Rhodes, Lisa R. Smith, Diane Roulston, Beth E. Helgeson, Xuhong Cao, John T. Wei, Mark A. Rubin, Rajal B. Shah, and Arul M. Chinnaiyan (Apr. 2006). "TMPRSS2:ETV4 Gene Fusions Define a Third Molecular Subtype of Prostate Cancer". *Cancer Research* 66.7, pp. 3396–3400. DOI: 10.1158/0008-5472.CAN-06-0168. eprint: https://aacrjournals.org/cancerres/article-pdf/66/7/3396/2560001/3396.pdf.

Tomlins, Scott A., Daniel R. Rhodes, Sven Perner, Saravana M. Dhanasekaran, Rohit Mehra, Xiao-Wei Sun, Sooryanarayana Varambally, Xuhong Cao, Joelle Tchinda, Rainer Kuefer, Charles Lee, James E. Montie, Rajal B. Shah, Kenneth J. Pienta, Mark A. Rubin, and Arul M. Chinnaiyan (2005). "Recurrent Fusion of TMPRSS2 and ETS Transcription Factor Genes in Prostate Cancer". *Science* 310.5748, pp. 644–648. DOI: 10.1126/science.1117679. eprint: https://www.science.org/doi/pdf/10.1126/science.1117679.

Tonkin, Joanne, Lieve Temmerman, Robert D Sampson, Enrique Gallego-Colon, Laura Barberi, Daniel Bilbao, Michael D Schneider, Antonio Musaro, and Nadia Rosenthal (July 2015). "Monocyte/Macrophage-derived IGF-1 Orchestrates Murine Skeletal Muscle Regeneration and Modulates Autocrine Polarization". *Molecular Therapy* 23 (7). doi: 10.1038/mt.2015.66, pp. 1189–1200. DOI: 10.1038/mt.2015.66.

Tosoian, Jeffrey J., Mufaddal Mamawala, Jonathan I. Epstein, Patricia Landis, Katarzyna J. Macura, Demetrios N. Simopoulos, H. Ballentine Carter, and Michael A. Gorin (2020). "Active Surveillance of Grade Group 1 Prostate Cancer:

Long-term Outcomes from a Large Prospective Cohort". *European Urology* 77.6, pp. 675–682. DOI: https://doi.org/10.1016/j.eururo.2019.12.017.

Travis, Ruth C., Paul N. Appleby, Richard M. Martin, Jeff M.P. Holly, Demetrius Albanes, Amanda Black, H. Bas Bueno-de-Mesquita, June M. Chan, Chu Chen, Maria-Dolores Chirlaque, Michael B. Cook, Melanie Deschasaux, Jenny L. Donovan, Luigi Ferrucci, Pilar Galan, Graham G. Giles, Edward L. Giovannucci, Marc J. Gunter, Laurel A. Habel, Freddie C. Hamdy, Kathy J. Helzlsouer, Serge Hercberg, Robert N. Hoover, Joseph A.M.J.L. Janssen, Rudolf Kaaks, Tatsuhiko Kubo, Loic Le Marchand, E. Jeffrey Metter, Kazuya Mikami, Joan K. Morris, David E. Neal, Marian L. Neuhouser, Kotaro Ozasa, Domenico Palli, Elizabeth A. Platz, Michael N. Pollak, Alison J. Price, Monique J. Roobol, Catherine Schaefer, Jeannette M. Schenk, Gianluca Severi, Meir J. Stampfer, Par Stattin, Akiko Tamakoshi, Catherine M. Tangen, Mathilde Touvier, Nicholas J. Wald, Noel S. Weiss, Regina G. Ziegler, Timothy J. Key, Naomi E. Allen, Nutritional Biomarkers the Endogenous Hormones, and Prostate Cancer Collaborative Group (Apr. 2016). "A Meta-analysis of Individual Participant Data Reveals an Association between Circulating Levels of IGF-I and Prostate Cancer Risk". *Cancer Research* 76.8, pp. 2288–2300. DOI: 10.1158/0008-5472.CAN-15-1551. eprint: https://aacrjournals.org/cancerres/article-pdf/76/8/2288/2870181/2288.pdf.

Triozzi, Pierre L. and Wayne Aldrich (2010). "Effects of Interleukin-1 Receptor Antagonist and Chemotherapy on Host–Tumor Interactions in Established Melanoma". *Anticancer Research* 30.2, pp. 345–354. eprint: https://ar.iiarjournals.org/content/30/2/345.full.pdf.

Trojan, J, B K Blossey, T R Johnson, S D Rudin, M Tykocinski, J Ilan, and J Ilan (1992). "Loss of tumorigenicity of rat glioblastoma directed by episome-based antisense cDNA transcription of insulin-like growth factor I." *Proceedings of the National Academy of Sciences* 89.11, pp. 4874–4878. DOI: 10.1073/pnas.89.11.4874. eprint: https://www.pnas.org/doi/pdf/10.1073/pnas.89.11.4874.

Trojan, Jerzy, Thomas R. Johnson, Susan D. Rudin, Judith Ilan, Mark L. Tykocinski, and Joseph Ilan (1993). "Treatment and Prevention of Rat Glioblastoma by Immunogenic C6 Cells Expressing Antisense Insulin-Like Growth Factor I RNA". *Science* 259.5091, pp. 94–97. DOI: 10.1126/science.8418502. eprint: https://www.science.org/doi/pdf/10.1126/science.8418502.

Trompetter, Marleen, Frank Smedts, Jan Van der Wijk, Coen Schoots, Hans-Jurien de Jong, Anton Hopman, and Jean de la Rosette (2008). "Keratin Profiling in the Developing Human Prostate. A Different Approach to Understanding Epithelial Lineage". *Anticancer Research* 28.1A, pp. 237–243. eprint: https://ar.iiarjournals.org/content/28/1A/237.full.pdf.

Tu, Megan M., Hany A. Abdel-Hafiz, Robert T. Jones, Annie Jean, Katelyn J. Hoff, Jason E. Duex, Ana Chauca-Diaz, James C. Costello, Garrett M. Dancik, Beth A. Jirón Tamburini, Bogdan Czerniak, Jonathan Kaye, and Dan Theodorescu (2020). "Inhibition of the CCL2 receptor, CCR2, enhances tumor response to immune checkpoint therapy". *Communications Biology* 3.1, p. 720. DOI: 10.1038/s42003-020-01441-y.

Tu, Mengyu, Lukas Klein, Elisa Espinet, Theodoros Georgomanolis, Florian Wegwitz, Xiaojuan Li, Laura Urbach, Adi Danieli-Mackay, Stefan Küffer, Kamil Bojarczuk, Athanasia Mizi, Ufuk Günesdogan, Björn Chapuy, Zuguang Gu, Albrecht Neesse, Uday Kishore, Philipp Ströbel, Elisabeth Hessmann, Stephan A Hahn, Andreas Trumpp,

Argyris Papantonis, Volker Ellenrieder, and Shiv K Singh (2021). "TNF-a-producing macrophages determine subtype identity and prognosis via AP1 enhancer reprogramming in pancreatic cancer". *Nature Cancer* 2 (11), pp. 1185–1203. DOI: 10.1038/s43018-021-00258-w.

Tumeh, Paul C, Christina L Harview, Jennifer H Yearley, I Peter Shintaku, Emma J M Taylor, Lidia Robert, Bartosz Chmielowski, Marko Spasic, Gina Henry, Voicu Ciobanu, Alisha N West, Manuel Carmona, Christine Kivork, Elizabeth Seja, Grace Cherry, Antonio J Gutierrez, Tristan R Grogan, Christine Mateus, Gorana Tomasic, John A Glaspy, Ryan O Emerson, Harlan Robins, Robert H Pierce, David A Elashoff, Caroline Robert, and Antoni Ribas (2014). "PD-1 blockade induces responses by inhibiting adaptive immune resistance". *Nature* 515 (7528), pp. 568–571. DOI: 10.1038/nature13954.

Tuong, Zewen Kelvin, Kevin W Loudon, Brendan Berry, Nathan Richoz, Julia Jones, Xiao Tan, Quan Nguyen, Anne George, Satoshi Hori, Sarah Field, Andy G Lynch, Katarzyna Kania, Paul Coupland, Anne Babbage, Richard Grenfell, Tristan Barrett, Anne Y Warren, Vincent Gnanapragasam, Charlie Massie, and Menna R Clatworthy (Dec. 2021). "Resolving the immune landscape of human prostate at a single-cell level in health and cancer". *Cell Reports* 37 (12). doi: 10.1016/j.celrep.2021.110132. DOI: 10.1016/j.celrep.2021.110132.

Turney, Benjamin W, Martin Kerr, Meenali M Chitnis, Kunal Lodhia, Yong Wang, Johann Riedemann, Mark Rochester, Andrew S Protheroe, Simon F Brewster, and Valentine M Macaulay (June 2012). "Depletion of the type 1 IGF receptor delays repair of radiation-induced DNA double strand breaks". *Radiotherapy and Oncology* 103 (3). doi: 10.1016/j.radonc.2012.03.009, pp. 402–409. DOI: 10.1016/j.radonc.2012.03.009.

Ullrich, A., A. Gray, A.W. Tam, T. Yang-Feng, M. Tsubokawa, C. Collins, W. Henzel, T. Le Bon, S. Kathuria, and E. Chen (1986). "Insulin-like growth factor I receptor primary structure: comparison with insulin receptor suggests structural determinants that define functional specificity". *The EMBO Journal* 5.10, pp. 2503–2512. DOI: https://doi.org/10.1002/j.1460-2075.1986.tb04528.x.

Unger, C, N Kramer, D Unterleuthner, M Scherzer, A Burian, A Rudisch, M Stadler, M Schlederer, D Lenhardt, A Riedl, S Walter, A Wernitznig, L Kenner, M Hengstschläger, J Schüler, W Sommergruber, and H Dolznig (2017). "Stromal-derived IGF2 promotes colon cancer progression via paracrine and autocrine mechanisms". *Oncogene* 36 (38), pp. 5341–5355. DOI: 10.1038/onc.2017.116.

Ushach, Irina and Albert Zlotnik (June 2016). "Biological role of granulocyte macrophage colony-stimulating factor (GM-CSF) and macrophage colony-stimulating factor (M-CSF) on cells of the myeloid lineage". *Journal of Leukocyte Biology* 100.3, pp. 481–489. DOI: 10.1189/jlb.3RU0316-144R. eprint: https://academic.oup.com/jleukbio/article-pdf/100/3/481/48716581/jlb0481.pdf.

Valeta-Magara, Amanda, Abhilash Gadi, Viviana Volta, Beth Walters, Rezina Arju, Shah Giashuddin, Hua Zhong, and Robert J. Schneider (July 2019). "Inflammatory Breast Cancer Promotes Development of M2 Tumor-Associated Macrophages and Cancer Mesenchymal Cells through a Complex Chemokine Network". *Cancer Research* 79.13, pp. 3360–3371. DOI: 10.1158/0008-5472.CAN-17-2158. eprint: https://aacrjournals.org/cancerres/article-pdf/79/13/3360/2779611/3360.pdf.

Van Gassen, Sofie, Britt Callebaut, Mary J. Van Helden, Bart N. Lambrecht, Piet Demeester, Tom Dhaene, and Yvan Saeys (2015). "FlowSOM: Using self-organizing maps for visualization and interpretation of cytometry data". *Cytometry Part A* 87.7, pp. 636–645.

DOI: https://doi.org/10.1002/cyto.a.22625. eprint: https://onlinelibrary.wiley.com/doi/pdf/10.1002/cyto.a.22625.

Vaniotis, George, Serge Moffett, Traian Sulea, Ni Wang, S. Mehdy Elahi, Etienne Lessard, Jason Baardsnes, Stephanie Perrino, Yves Durocher, Jan Frystyk, Bernard Massie, and Pnina Brodt (Nov. 2018). "Enhanced anti-metastatic bioactivity of an IGF-TRAP re-engineered to improve physicochemical properties". *Scientific Reports* 8 (1), pp. 1–13. DOI: 10.1038/s41598-018-35407-2.

Van Leenders, Geert J. L. H., Tilly W. Aalders, Christina A. Hulsbergen-van de Kaa, Dirk J. Ruiter, and Jack A. Schalken (2001). "Expression of basal cell keratins in human prostate cancer metastases and cell lines". *The Journal of Pathology* 195.5, pp. 563–570. DOI: https://doi.org/10.1002/path.993. eprint: https://pathsocjournals.onlinelibrary.wiley.com/doi/pdf/10.1002/path.993.

Varricchi, Gilda, Maria Rosaria Galdiero, Stefania Loffredo, Giancarlo Marone, Raffaella Iannone, Gianni Marone, and Francescopaolo Granata (2017). "Are Mast Cells MASTers in Cancer?" *Frontiers in Immunology* 8. DOI: 10.3389/fimmu.2017.00424.

Veglia, Filippo, Emilio Sanseviero, and Dmitry I Gabrilovich (2021). "Myeloid-derived suppressor cells in the era of increasing myeloid cell diversity". *Nature Reviews Immunology* 21 (8), pp. 485–498. DOI: 10.1038/s41577-020-00490-y.

Vellky, Jordan E. and William A. Ricke (2020). "Development and prevalence of castration-resistant prostate cancer subtypes". *Neoplasia* 22.11, pp. 566–575. DOI: https://doi.org/10.1016/j.neo.2020.09.002.

Verhagen, Anja P. M., Tilly W. Aalders, Frans C. S. Ramaekers, Frans M. J. Debruyne, and Jack A. Schalken (1988). "Differential expression of keratins in the basal and luminal compartments of rat prostatic epithelium during degeneration and regeneration". *The Prostate* 13.1, pp. 25–38. DOI: https://doi.org/10.1002/pros.2990130104. eprint: https://onlinelibrary.wiley.com/doi/pdf/10.1002/pros.2990130104.

Vidal, Samuel J., Veronica Rodriguez-Bravo, S. Aidan Quinn, Ruth Rodriguez-Barrueco, Amaia Lujambio, Estrelania Williams, Xiaochen Sun, Janis de la Iglesia-Vicente, Albert Lee, Ben Readhead, Xintong Chen, Matthew Galsky, Berta Esteve, Daniel P. Petrylak, Joel T. Dudley, Raul Rabadan, Jose M. Silva, Yujin Hoshida, Scott W. Lowe, Carlos Cordon-Cardo, and Josep Domingo-Domenech (Feb. 2015). "A Targetable GATA2-IGF2 Axis Confers Aggressiveness in Lethal Prostate Cancer". *Cancer Cell* 27 (2). doi: 10.1016/j.ccell.2014.11.013, pp. 223–239. DOI: 10.1016/j.ccell.2014.11.013.

Vidyarthi, Aurobind, Nargis Khan, Tapan Agnihotri, Shikha Negi, Deepjyoti K. Das, Mohammad Aqdas, Deepyan Chatterjee, Oscar R. Colegio, Manoj K. Tewari, and Javed N. Agrewala (2018). "TLR-3 Stimulation Skews M2 Macrophages to M1 Through IFN-aB Signaling and Restricts Tumor Progression". *Frontiers in Immunology* 9. DOI: 10.3389/fimmu.2018.01650.

Vignali, Dario A A, Lauren W Collison, and Creg J Workman (2008). "How regulatory T cells work". *Nature Reviews Immunology* 8 (7), pp. 523–532. DOI: 10.1038/nri2343.

Vijayan, Vijith, Pooja Pradhan, Laura Braud, Heiko R. Fuchs, Faikah Gueler, Roberto Motterlini, Roberta Foresti, and Stephan Immenschuh (2019). "Human and murine macrophages exhibit differential metabolic responses to lipopolysaccharide - A divergent role for glycolysis". *Redox Biology* 22, p. 101147. DOI: https://doi.org/10.1016/j.redox.2019.101147.

Visakorpi, Tapio, Eija Hyytinen, Pasi Koivisto, Minna Tanner, Riitta Keinänen, Christian Palmberg, Aarno Palotie, Teuvo Tammela, Jorma Isola, and Olli-P. Kallioniemi

(1995). "In vivo amplification of the androgen receptor gene and progression of human prostate cancer". *Nature Genetics* 9 (4), pp. 401–406. DOI: 10.1038/ng0495-401.

Vitkin, Natasha, Sarah Nersesian, David Robert Siemens, and Madhuri Koti (2019). "The Tumor Immune Contexture of Prostate Cancer". *Frontiers in Immunology* 10. DOI: 10.3389/fimmu.2019.00603.

Von Roemeling, Christina A., Yifan Wang, Yaqing Qie, Hengfeng Yuan, Hai Zhao, Xiujie Liu, Zhaogang Yang, Mingming Yang, Weiye Deng, Katelyn A. Bruno, Charles K. Chan, Andrew S. Lee, Stephen S. Rosenfeld, Kyuson Yun, Aaron J. Johnson, Duane A. Mitchell, Wen Jiang, and Betty Y.S. Kim (Mar. 2020). "Therapeutic modulation of phagocytosis in glioblastoma can activate both innate and adaptive antitumour immunity". *Nature Communications* 11, pp. 1–12.

Voskoboinik, Ilia, James C Whisstock, and Joseph A Trapani (2015). "Perforin and granzymes: function, dysfunction and human pathology". *Nature Reviews Immunology* 15 (6), pp. 388–400. DOI: 10.1038/nri3839.

Waldman, Alex D., Jill M. Fritz, and Michael J. Lenardo (2020). "A guide to cancer immunotherapy: from T cell basic science to clinical practice". *Nature Reviews Immunology* 20.11, pp. 651–668. DOI: 10.1038/s41577-020-0306-5.

Wallach, David, Tae-Bong Kang, Christopher P. Dillon, and Douglas R. Green (2016). "Programmed necrosis in inflammation: Toward identification of the effector molecules". *Science* 352.6281. DOI: 10.1126/science.aaf2154. eprint: https://www.science.org/doi/pdf/10.1126/science.aaf2154.

Walsh, Patrick T and Rosemary O'Connor (Apr. 2000). "The insulin-like growth factor-I receptor is regulated by CD28 and protects activated T cells from apoptosis". *European Journal of Immunology* 30 (4), pp. 1010–1018. DOI: https://doi.org/10.1002/(SICI)1521-4141(200004)30:4<1010::AID-IMMU1010>3.0.CO;2-C.

Waltering, Kati K., Alfonso Urbanucci, and Tapio Visakorpi (2012). "Androgen receptor (AR) aberrations in castration-resistant prostate cancer". *Molecular and Cellular Endocrinology* 360.1. Novel Endocrine Aspects of Prostatic Cancer, pp. 38–43. DOI: https://doi.org/10.1016/j.mce.2011.12.019.

Walunas, Theresa L., Deborah J. Lenschow, Christina Y. Bakker, Peter S. Linsley, Gordon J. Freeman, Jonathan M. Green, Craig B. Thompson, and Jeffrey A. Bluestone (June 1994). "CTLA-4 can function as a negative regulator of T cell activation". *Immunity* 1.5, pp. 405–413. DOI: 10.1016/1074-7613(94)90071-X.

Wan, X, B Harkavy, N Shen, P Grohar, and L J Helman (2007). "Rapamycin induces feedback activation of Akt signaling through an IGF-1R-dependent mechanism". *Oncogene* 26 (13), pp. 1932–1940. DOI: 10.1038/sj.onc.1209990.

Wang, Changqi, Xiao Yu, Qi Cao, Ya Wang, Guoping Zheng, Thian Kui Tan, Hong Zhao, Ye Zhao, Yiping Wang, and David C H Harris (2013). "Characterization of murine macrophages from bone marrow, spleen and peritoneum". *BMC Immunology* 14 (1), p. 6. DOI: 10.1186/1471-2172-14-6.

Wang, Fang, Liqiong Yang, Mintao Xiao, Zhuo Zhang, Jing Shen, Songyot Anuchapreeda, Singkome Tima, Sawitree Chiampanichayakul, and Zhangang Xiao (2022a). "PD-L1 regulates cell proliferation and apoptosis in acute myeloid leukemia by activating PI3K-AKT signaling pathway". *Scientific Reports* 12 (1), p. 11444. DOI: 10.1038/s41598-022-15020-0.

Wang, Ya-fang, Lei Yu, Zong-long Hu, Yan-fen Fang, Yan-yan Shen, Min-fang Song, and Yi Chen (2022b). "Regulation of CCL2 by EZH2 affects tumor-associated macrophages

polarization and infiltration in breast cancer". *Cell Death and Disease* 13 (8), p. 748. DOI: 10.1038/s41419-022-05169-x.

Wang, Jianghua, Yi Cai, Chengxi Ren, and Michael Ittmann (Sept. 2006). "Expression of Variant TMPRSS2-ERG Fusion Messenger RNAs Is Associated with Aggressive Prostate Cancer". *Cancer Research* 66.17, pp. 8347–8351. DOI: 10.1158/0008-5472.CAN-06-1966. eprint: https://aacrjournals.org/cancerres/article-pdf/66/17/8347/2553989/8347.pdf.

Wang, Neng, Weiping Liu, Yifeng Zheng, Shengqi Wang, Bowen Yang, Min Li, Juxian Song, Fengxue Zhang, Xiaotong Zhang, Qi Wang, and Zhiyu Wang (2018). "CXCL1 derived from tumor-associated macrophages promotes breast cancer metastasis via activating NF-kB/SOX4 signaling". *Cell Death and Disease* 9 (9), p. 880. DOI: 10.1038/s41419-018-0876-3.

Wang, Ni, Roni F. Rayes, Seyyed Mehdy Elahi, Yifan Lu, Mark A. Hancock, Bernard Massie, Gerald E. Rowe, Hafida Aomari, Sazzad Hossain, Yves Durocher, Maxime Pinard, Sébastien Tabariès, Peter M. Siegel, and Pnina Brodt (Apr. 2015). "The IGF-Trap: Novel Inhibitor of Carcinoma Growth and Metastasis". *Molecular Cancer Therapeutics* 14.4, pp. 982–993. DOI: 10.1158/1535-7163.MCT-14-0751. eprint: https://aacrjournals.org/mct/article-pdf/14/4/982/2238511/982.pdf.

Wang, Panpan, Victor CY. Mak, and Lydia WT. Cheung (2023). "Drugging IGF-1R in cancer: New insights and emerging opportunities". *Genes and Diseases* 10.1, pp. 199–211. DOI: https://doi.org/10.1016/j.gendis.2022.03.002.

Wang, Shu Qing, Xiang Yu Yang, Shu Xiang Cui, Zu Hua Gao, and Xian Jun Qu (2019). "Heterozygous knockout insulin-like growth factor-1 receptor (IGF-1R) regulates mitochondrial functions and prevents colitis and colorectal cancer". *Free Radical Biology and Medicine* 134, pp. 87–98. DOI: https://doi.org/10.1016/j.freeradbiomed.2018.12.035.

Wang, Shujing, Jingrui Wang, Zhiqiang Chen, Jiamin Luo, Wei Guo, Lingling Sun, and Lizhu Lin (2024). "Targeting M2-like tumor-associated macrophages is a potential therapeutic approach to overcome antitumor drug resistance". *npj Precision Oncology* 8 (1), p. 31. DOI: 10.1038/s41698-024-00522-z.

Waraky, Ahmed, Yingbo Lin, Dudi Warsito, Felix Haglund, Eiman Aleem, and Olle Larsson (Nov. 2017). "Nuclear insulin-like growth factor 1 receptor phosphorylates proliferating cell nuclear antigen and rescues stalled replication forks after DNA damage". *Journal of Biological Chemistry* 292 (44). doi: 10.1074/jbc.M117.781492, pp. 18227–18239. DOI: 10.1074/jbc.M117.781492.

Watanabe, Satoshi, Katsuya Deguchi, Rongxiu Zheng, Hidemasa Tamai, Li-xin Wang, Peter A. Cohen, and Suyu Shu (Sept. 2008). "Tumor-Induced CD11b+Gr-1+ Myeloid Cells Suppress T Cell Sensitization in Tumor-Draining Lymph Nodes". *The Journal of Immunology* 181.5, pp. 3291–3300. DOI: 10.4049/jimmunol.181.5.3291. eprint: https://journals.aai.org/jimmunol/article-pdf/181/5/3291/1267705/zim01708003291.pdf.

Waters, Jennifer A., Ixchel Urbano, Mikella Robinson, and Carrie D. House (2022). "Insulin-like growth factor binding protein 5: Diverse roles in cancer". *Frontiers in Oncology* 12. DOI: 10.3389/fonc.2022.1052457.

Watson, Philip A, Vivek K Arora, and Charles L Sawyers (2015). "Emerging mechanisms of resistance to androgen receptor inhibitors in prostate cancer". *Nature Reviews Cancer* 15 (12), pp. 701–711. DOI: 10.1038/nrc4016.

Watson, Philip A., Katharine Ellwood-Yen, Jennifer C. King, John Wongvipat, Michelle M. LeBeau, and Charles L. Sawyers (Dec. 2005). "Context-Dependent Hormone-Refractory Progression Revealed through Characterization of a Novel Murine Prostate Cancer Cell Line". *Cancer Research* 65.24, pp. 11565–11571. DOI: 10.1158/0008-5472.CAN-05-3441. eprint: https://aacrjournals.org/cancerres/article-pdf/65/24/11565/2542698/11565-11571.pdf.

Watts, Eleanor L., Georgina K. Fensom, Karl Smith Byrne, Aurora Perez-Cornago, Naomi E. Allen, Anika Knuppel, Marc J. Gunter, Michael V. Holmes, Richard M. Martin, Neil Murphy, Konstantinos K. Tsilidis, Bu B. Yeap, Timothy J. Key, and Ruth C. Travis (2021). "Circulating insulin-like growth factor-I, total and free testosterone concentrations and prostate cancer risk in 200,000 men in UK Biobank". *International Journal of Cancer* 148.9, pp. 2274–2288. DOI: https://doi.org/10.1002/ijc.33416. eprint: https://onlinelibrary.wiley.com/doi/pdf/10.1002/ijc.33416.

Webb, Siobhan L., Andrew J. Sanders, Malcolm D. Mason, and Wen G. Jiang (Oct. 2012). "The influence of matriptase-2 on prostate cancer in vitro: A possible role for B-catenin". *Oncology Reports* 28 (4), pp. 1491–1497. DOI: 10.3892/OR.2012.1945/HTML.

Weichhart, Thomas, Markus Hengstschläger, and Monika Linke (2015). "Regulation of innate immune cell function by mTOR". *Nature Reviews Immunology* 15 (10), pp. 599–614. DOI: 10.1038/nri3901.

Welcker, Markus, Jeffrey Singer, Keith R Loeb, Jonathan Grim, Andrew Bloecher, Mark Gurien-West, Bruce E Clurman, and James M Roberts (Aug. 2003). "Multisite Phosphorylation by Cdk2 and GSK3 Controls Cyclin E Degradation". *Molecular Cell* 12 (2). doi: 10.1016/S1097-2765(03)00287-9, pp. 381–392. DOI: 10.1016/S1097-2765(03)00287-9.

Wendel, Hans-Guido, Elisa de Stanchina, Jordan S Fridman, Abba Malina, Sagarika Ray, Scott Kogan, Carlos Cordon-Cardo, Jerry Pelletier, and Scott W Lowe (2004). "Survival signalling by Akt and eIF4E in oncogenesis and cancer therapy". *Nature* 428 (6980), pp. 332–337. DOI: 10.1038/nature02369.

Werner, H (2012). "Tumor suppressors govern insulin-like growth factor signaling pathways: implications in metabolism and cancer". *Oncogene* 31 (22), pp. 2703–2714. DOI: 10.1038/onc.2011.447.

Werner, Haim (2023). "The IGF1 Signaling Pathway: From Basic Concepts to Therapeutic Opportunities". *International Journal of Molecular Sciences* 24.19. DOI: 10.3390/ijms241914882.

Werner, Haim, Shilhav Meisel-Sharon, and Ilan Bruchim (2018). "Oncogenic fusion proteins adopt the insulin-like growth factor signaling pathway". *Molecular Cancer* 17 (1), p. 28. DOI: 10.1186/s12943-018-0807-z.

Werner, Haim, Charles T Roberts, Frank J Rauscher, and Derek LeRoith (1996). "Regulation of insulin-like growth factor I receptor gene expression by the wilms' tumor supressor WT1". *Journal of Molecular Neuroscience* 7 (2), pp. 111–123. DOI: 10.1007/BF02736791.

Werner, Haim, Rive Sarfstein, Derek LeRoith, and Ilan Bruchim (2016). "Insulin-like Growth Factor 1 Signaling Axis Meets p53 Genome Protection Pathways". *Frontiers in Oncology* 6. DOI: 10.3389/fonc.2016.00159.

Westaby, Daniel, Maria de Los Dolores Fenor de La Maza, Alec Paschalis, Juan M. Jimenez-Vacas, Jon Welti, Johann de Bono, and Adam Sharp (2022). "A New Old Target: Androgen Receptor Signaling and Advanced Prostate Cancer". *Annual Review*

of Pharmacology and Toxicology 62.Volume 62, 2022, pp. 131–153. DOI: https://doi.org/10.1146/annurev-pharmtox-052220-015912.

Weston, Claire R and Roger J Davis (2002). "The JNK signal transduction pathway". *Current Opinion in Genetics and Development* 12.1, pp. 14–21. DOI: https://doi.org/10.1016/S0959-437X(01)00258-1.

Weyer-Czernilofsky, Ulrike, Marco H. Hofmann, Katrin Friedbichler, Rosa Baumgartinger, Paul J. Adam, Flavio Solca, Norbert Kraut, Holly M. Nguyen, Eva Corey, Gang Liu, Cynthia C. Sprenger, Stephen R. Plymate, and Thomas Bogenrieder (Apr. 2020). "Antitumor Activity of the IGF-1/IGF-2–Neutralizing Antibody Xentuzumab (BI 836845) in Combination with Enzalutamide in Prostate Cancer Models". *Molecular Cancer Therapeutics* 19.4, pp. 1059–1069. DOI: 10.1158/1535-7163.MCT-19-0378. eprint: https://aacrjournals.org/mct/article-pdf/19/4/1059/1849108/1059.pdf.

Wherry, E John (2011). "T cell exhaustion". *Nature Immunology* 12 (6), pp. 492–499. DOI: 10.1038/ni.2035.

Wiedemann, Aurelie, David Depoil, Mustapha Faroudi, and Salvatore Valitutti (2006). "Cytotoxic T lymphocytes kill multiple targets simultaneously via spatiotemporal uncoupling of lytic and stimulatory synapses". *Proceedings of the National Academy of Sciences* 103.29, pp. 10985–10990. DOI: 10.1073/pnas.0600651103. eprint: https://www.pnas.org/doi/pdf/10.1073/pnas.0600651103.

Wightman, S C, A Uppal, S P Pitroda, S Ganai, B Burnette, M Stack, G Oshima, S Khan, X Huang, M C Posner, R R Weichselbaum, and N N Khodarev (2015). "Oncogenic CXCL10 signalling drives metastasis development and poor clinical outcome". *British Journal of Cancer* 113 (2), pp. 327–335. DOI: 10.1038/bjc.2015.193.

Willenborg, Sebastian, Tina Lucas, Geert van Loo, Johanna A. Knipper, Thomas Krieg, Ingo Haase, Bent Brachvogel, Matthias Hammerschmidt, Andras Nagy, Napoleone Ferrara, Manolis Pasparakis, and Sabine A. Eming (July 2012). "CCR2 recruits an inflammatory macrophage subpopulation critical for angiogenesis in tissue repair". *Blood* 120.3, pp. 613–625. DOI: 10.1182/blood-2012-01-403386. eprint: https://ashpublications.org/blood/article-pdf/120/3/613/1362211/zh802912000613.pdf.

Willingham, Stephen B., Jens-Peter Volkmer, Andrew J. Gentles, Debashis Sahoo, Piero Dalerba, Siddhartha S. Mitra, Jian Wang, Humberto Contreras-Trujillo, Robin Martin, Justin D. Cohen, Patricia Lovelace, Ferenc A. Scheeren, Mark P. Chao, Kipp Weiskopf, Chad Tang, Anne Kathrin Volkmer, Tejaswitha J. Naik, Theresa A. Storm, Adriane R. Mosley, Badreddin Edris, Seraina M. Schmid, Chris K. Sun, Mei-Sze Chua, Oihana Murillo, Pradeep Rajendran, Adriel C. Cha, Robert K. Chin, Dongkyoon Kim, Maddalena Adorno, Tal Raveh, Diane Tseng, Siddhartha Jaiswal, Per Oyvind Enger, Gary K. Steinberg, Gordon Li, Samuel K. So, Ravindra Majeti, Griffith R. Harsh, Matt van de Rijn, Nelson N. H. Teng, John B. Sunwoo, Ash A. Alizadeh, Michael F. Clarke, and Irving L. Weissman (2012). "The CD47-signal regulatory protein alpha (SIRPa) interaction is a therapeutic target for human solid tumors". *Proceedings of the National Academy of Sciences* 109.17, pp. 6662–6667. DOI: 10.1073/pnas.1121623109. eprint: https://www.pnas.org/doi/pdf/10.1073/pnas.1121623109.

Wing, Kajsa, Yasushi Onishi, Paz Prieto-Martin, Tomoyuki Yamaguchi, Makoto Miyara, Zoltan Fehervari, Takashi Nomura, and Shimon Sakaguchi (2008). "CTLA-4 Control over Foxp3+ Regulatory T Cell Function". *Science* 322.5899, pp. 271–275. DOI: 10.1126/science.1160062. eprint: https://www.science.org/doi/pdf/10.1126/science.1160062.

Wolf, Yochai, Ana C Anderson, and Vijay K Kuchroo (2020). "TIM3 comes of age as an inhibitory receptor". *Nature Reviews Immunology* 20 (3), pp. 173–185. DOI: 10.1038/s41577-019-0224-6.

Wolters, Thalijn Liliana Catharina, Mihai Gheorghe Netea, Adrianus Rudolfus Marinus Maria Hermus, Johannes Willem Adriaan Smit, and Romana Teodora Netea-Maier (2017). "IGF1 potentiates the pro-inflammatory response in human peripheral blood mononuclear cells via MAPK". *Journal of Molecular Endocrinology* 59.2, pp. 129–139. DOI: 10.1530/JME-17-0062.

Wu, Dong-Dong, David M Irwin, and Ya-Ping Zhang (2008). "Molecular evolution of the keratin associated protein gene family in mammals, role in the evolution of mammalian hair". *BMC Evolutionary Biology* 8 (1), p. 241. DOI: 10.1186/1471-2148-8-241.

Wu, Gen Sheng (2004). "The functional Interactions Between the MAPK and p53 Signaling Pathways". *Cancer Biology and Therapy* 3.2. PMID: 14764989, pp. 156–161. DOI: 10.4161/cbt.3.2.614. eprint: https://doi.org/10.4161/cbt.3.2.614.

Wu, Jennifer D., Kathy Haugk, Libby Woodke, Peter Nelson, Ilsa Coleman, and Stephen R. Plymate (2006). "Interaction of IGF signaling and the androgen receptor in prostate cancer progression". *Journal of Cellular Biochemistry* 99.2, pp. 392–401. DOI: https://doi.org/10.1002/jcb.20929. eprint: https://onlinelibrary.wiley.com/doi/pdf/10.1002/jcb.20929.

Wu, Shiqi, Meixi Li, Fangfang Chen, Yan Zeng, and Chen Xu (June 2024). "Inhibition of B2-adrenergic receptor regulates necroptosis in prostate cancer cell". *Heliyon* 10 (11). doi: 10.1016/j.heliyon.2024.e31865. DOI: 10.1016/j.heliyon.2024.e31865.

Wu, Xiaoning, Elena Seraia, Stephanie B. Hatch, Xiao Wan, Daniel V. Ebner, Francesca Aroldi, Yanyan Jiang, Anderson J. Ryan, Thomas Bogenrieder, Ulrike Weyer-Czernilofsky, Guillaume Rieunier, and Valentine M. Macaulay (Nov. 2021). "CHK1 inhibition exacerbates replication stress induced by IGF blockade". *Oncogene* 41 (4), pp. 476–488. DOI: 10.1038/s41388-021-02080-1.

Wu, Yiping, Shoshana Yakar, Ling Zhao, Lothar Hennighausen, and Derek LeRoith (Feb. 2002). "Circulating Insulin-like Growth Factor-I Levels Regulate Colon Cancer Growth and Metastasis". *Cancer Research* 62 (4), pp. 1030–1035.

Wu, Yong, Weidong Zhao, Jingbo Zhao, Jiangping Pan, Qiaqia Wu, Yuanfei Zhang, William A. Bauman, and Christopher P. Cardozo (June 2007). "Identification of Androgen Response Elements in the Insulin-Like Growth Factor I Upstream Promoter". *Endocrinology* 148.6, pp. 2984–2993. DOI: 10.1210/en.2006-1653. eprint: https://academic.oup.com/endo/article-pdf/148/6/2984/10726277/endo2984.pdf.

Xia, Jie, Lixing Zhang, Xilei Peng, Juchuanli Tu, Siqin Li, Xueyan He, Fengkai Li, Jiankun Qiang, Haonan Dong, Qiaodan Deng, Cuicui Liu, Jiahui Xu, Rui Zhang, Quentin Liu, Guohong Hu, Chong Liu, Yi-Zhou Jiang, Zhi-Ming Shao, Ceshi Chen, and Suling Liu (July 2024). "IL1R2 Blockade Alleviates Immunosuppression and Potentiates Anti-PD-1 Efficacy in Triple-Negative Breast Cancer". *Cancer Research* 84.14, pp. 2282–2296. DOI: 10.1158/0008-5472.CAN-23-3429. eprint: https://aacrjournals.org/cancerres/article-pdf/84/14/2282/3474537/can-23-3429.pdf.

Xia, Tingting, Meng Zhang, Wei Lei, Ruilin Yang, Shengping Fu, Zhenhai Fan, Ying Yang, and Tao Zhang (2023). "Advances in the role of STAT3 in macrophage polarization". *Frontiers in Immunology* 14. DOI: 10.3389/fimmu.2023.1160719.

Xiong, Huizhong, Stephanie Mittman, Ryan Rodriguez, Marina Moskalenko, Patricia Pacheco-Sanchez, Yagai Yang, Dorothee Nickles, and Rafael Cubas (Apr. 2019).

"Anti–PD-L1 Treatment Results in Functional Remodeling of the Macrophage Compartment". *Cancer Research* 79.7, pp. 1493–1506. DOI: 10.1158/0008-5472.CAN-18-3208. eprint: https://aacrjournals.org/cancerres/article-pdf/79/7/1493/2789237/1493.pdf.

Xiong, Lei, Fei Kou, Ying Yang, and Jiarui Wu (Sept. 2007). "A novel role for IGF-1R in p53-mediated apoptosis through translational modulation of the p53-Mdm2 feedback loop ". *Journal of Cell Biology* 178.6, pp. 995–1007. DOI: 10.1083/jcb.200703044. eprint: https://rupress.org/jcb/article-pdf/178/6/995/1549001/jcb_200703044.pdf.

Xu, Wen Wen, Bin Li, Xin Yuan Guan, Sookja K Chung, Yang Wang, Yim Ling Yip, Simon Y K Law, Kin Tak Chan, Nikki P Y Lee, Kwok Wah Chan, Li Yan Xu, En Min Li, Sai Wah Tsao, Qing-Yu He, and Annie L M Cheung (2017). "Cancer cell-secreted IGF2 instigates fibroblasts and bone marrow-derived vascular progenitor cells to promote cancer progression". *Nature Communications* 8 (1), p. 14399. DOI: 10.1038/ncomms14399.

Xue, Wen, Lars Zender, Cornelius Miething, Ross A Dickins, Eva Hernando, Valery Krizhanovsky, Carlos Cordon-Cardo, and Scott W Lowe (2007). "Senescence and tumour clearance is triggered by p53 restoration in murine liver carcinomas". *Nature* 445 (7128), pp. 656–660. DOI: 10.1038/nature05529.

Yadav, Ajay, Anjana Kalita, Shivani Dhillon, and Kakoli Banerjee (Sept. 2005). "JAK/STAT3 Pathway Is Involved in Survival of Neurons in Response to Insulin-like Growth Factor and Negatively Regulated by Suppressor of Cytokine Signaling-3". *Journal of Biological Chemistry* 280 (36), pp. 31830–31840. DOI: 10.1074/jbc.M501316200.

Yadav, Upendra, Pradeep Kumar, and Vandana Rai (2021). "Interleukin-10 (IL-10) gene polymorphisms and prostate cancer susceptibility: Evidence from a meta-analysis". *Gene Reports* 25, p. 101377. DOI: https://doi.org/10.1016/j.genrep.2021.101377.

Yaddanapudi, Kavitha, Kalyani Putty, Beatriz E. Rendon, Gwyneth J. Lamont, Jonathan D. Faughn, Abhay Satoskar, Amanda Lasnik, John W. Eaton, and Robert A. Mitchell (Mar. 2013). "Control of Tumor-Associated Macrophage Alternative Activation by Macrophage Migration Inhibitory Factor". *The Journal of Immunology* 190.6, pp. 2984–2993. DOI: 10.4049/jimmunol.1201650. eprint: https://journals.aai.org/jimmunol/article-pdf/190/6/2984/1372188/1201650.pdf.

Yamada-Hunter, Sean A, Johanna Theruvath, Brianna J McIntosh, Katherine A Freitas, Frank Lin, Molly T Radosevich, Amaury Leruste, Shaurya Dhingra, Naiara Martinez-Velez, Peng Xu, Jing Huang, Alberto Delaidelli, Moksha H Desai, Zinaida Good, Roel Polak, Audre May, Louai Labanieh, Jeremy Bjelajac, Tara Murty, Zach Ehlinger, Christopher W Mount, Yiyun Chen, Sabine Heitzeneder, Kristopher D Marjon, Allison Banuelos, Omair Khan, Savannah L Wasserman, Jay Y Spiegel, Sebastian Fernandez-Pol, Calvin J Kuo, Poul H Sorensen, Michelle Monje, Robbie G Majzner, Irving L Weissman, Bita Sahaf, Elena Sotillo, Jennifer R Cochran, and Crystal L Mackall (2024). "Engineered CD47 protects T cells for enhanced antitumour immunity". *Nature* 630, pp. 457–465. DOI: 10.1038/s41586-024-07443-8.

Yamamoto, Takuya, Miki Ebisuya, Fumito Ashida, Kazuo Okamoto, Shin Yonehara, and Eisuke Nishida (2006). "Continuous ERK Activation Downregulates Antiproliferative Genes throughout G1 Phase to Allow Cell-Cycle Progression". *Current Biology* 16.12, pp. 1171–1182. DOI: https://doi.org/10.1016/j.cub.2006.04.044.

Yamashita, Iwao, Taeko Nagata, Tomio Tada, and Toshinori Nakayama (Sept. 1993). "CD69 cell surface expression identifies developing thymocytes which audition for T cell antigen receptor-mediated positive selection". *International Immunology* 5.9, pp. 1139–1150. DOI:

10.1093/intimm/5.9.1139. eprint: https://academic.oup.com/intimm/article-pdf/5/9/1139/2090179/5-9-1139.pdf.

Yan, Hangyi H., Jian Jiang, Yanli Pang, B. R. Achyut, Michael Lizardo, Xinhua Liang, Kent Hunter, Chand Khanna, Christine Hollander, and Li Yang (Dec. 2015). "CCL9 induced by TGF-B signaling in myeloid cells enhances tumor cell survival in the premetastatic organ". *Cancer research* 75 (24), p. 5283. DOI: 10.1158/0008-5472.CAN-15-2282-T.

Yan, Xiaocai, Elizabeth Managlia, You-Yang Zhao, Xiao-Di Tan, and Isabelle G De Plaen (2022). "Macrophage-derived IGF-1 protects the neonatal intestine against necrotizing enterocolitis by promoting microvascular development". *Communications Biology* 5 (1), p. 320. DOI: 10.1038/s42003-022-03252-9.

Yang, Hui, Qiannan Zhang, Miao Xu, Lei Wang, Xuewei Chen, Yongquan Feng, Yongning Li, Xin Zhang, Wenming Cui, and Xudong Jia (2020a). "CCL2-CCR2 axis recruits tumor associated macrophages to induce immune evasion through PD-1 signaling in esophageal carcinogenesis". *Molecular Cancer* 19 (1), p. 41. DOI: 10.1186/s12943-020-01165-x.

Yang, Yinhui, Yang Bai, Yundong He, Yu Zhao, Jiaxiang Chen, Linlin Ma, Yunqian Pan, Michael Hinten, Jun Zhang, R. Jeffrey Karnes, Manish Kohli, Jennifer J. Westendorf, Benyi Li, Runzhi Zhu, Haojie Huang, and Wanhai Xu (Feb. 2018a). "PTEN Loss Promotes Intratumoral Androgen Synthesis and Tumor Microenvironment Remodeling via Aberrant Activation of RUNX2 in Castration-Resistant Prostate Cancer". *Clinical Cancer Research* 24.4, pp. 834–846. DOI: 10.1158/1078-0432.CCR-17-2006. eprint: https://aacrjournals.org/clincancerres/article-pdf/24/4/834/2048777/834.pdf.

Yang, Zhi-Zhang, Hyo Jin Kim, Shahrzad Jalali, Hongyan Wu, Tammy Price-Troska, and Stephen M. Ansell (Nov. 2018b). "Tigit Expression Defines a Subset of Activated Treg Cells with Prognostic Relevance in Follicular Lymphoma". *Blood* 132.Supplement 1, pp. 1590–1590. DOI: 10.1182/blood-2018-99-115328.

Yang, Zhi-Zhang, Hyo Jin Kim, Hongyan Wu, Shahrzad Jalali, Xinyi Tang, Jordan E. Krull, Wei Ding, Anne J. Novak, and Stephen M. Ansell (Oct. 2020b). "TIGIT Expression Is Associated with T-cell Suppression and Exhaustion and Predicts Clinical Outcome and Anti–PD-1 Response in Follicular Lymphoma". *Clinical Cancer Research* 26.19, pp. 5217–5231. DOI: 10.1158/1078-0432.CCR-20-0558. eprint: https://aacrjournals.org/clincancerres/article-pdf/26/19/5217/2061353/5217.pdf.

Yatim, Nader, Helene Jusforgues-Saklani, Susana Orozco, Oliver Schulz, Rosa Barreira da Silva, Caetano Reis e Sousa, Douglas R. Green, Andrew Oberst, and Matthew L. Albert (2015). "RIPK1 and NF-kB signaling in dying cells determines cross-priming of CD8+ T cells". *Science* 350.6258, pp. 328–334. DOI: 10.1126/science.aad0395. eprint: https://www.science.org/doi/pdf/10.1126/science.aad0395.

Yee, Patricia P. and Wei Li (2021). "Tumor necrosis: A synergistic consequence of metabolic stress and inflammation". *BioEssays* 43.7, p. 2100029. DOI: https://doi.org/10.1002/bies.202100029. eprint: https://onlinelibrary.wiley.com/doi/pdf/10.1002/bies.202100029.

Yeh, Elizabeth, Melissa Cunningham, Hugh Arnold, Dawn Chasse, Teresa Monteith, Giovanni Ivaldi, William C Hahn, P Todd Stukenberg, Shirish Shenolikar, Takafumi Uchida, Christopher M Counter, Joseph R Nevins, Anthony R Means, and Rosalie Sears (2004). "A signalling pathway controlling c-Myc degradation that impacts oncogenic transformation of human cells". *Nature Cell Biology* 6 (4), pp. 308–318. DOI: 10.1038/ncb1110.

Yi, Ming, Dechao Jiao, Hanxiao Xu, Qian Liu, Weiheng Zhao, Xinwei Han, and Kongming Wu (2018). "Biomarkers for predicting efficacy of PD-1/PD-L1 inhibitors". *Molecular Cancer* 17 (1), p. 129. DOI: 10.1186/s12943-018-0864-3.

Yi, Ming, Tianye Li, Mengke Niu, Qi Mei, Bin Zhao, Qian Chu, Zhijun Dai, and Kongming Wu (2023). "Exploiting innate immunity for cancer immunotherapy". *Molecular Cancer* 22 (1), p. 187. DOI: 10.1186/s12943-023-01885-w.

Yu, Guangchuang, Li-Gen Wang, Yanyan Han, and Qing-Yu He (2012). "clusterProfiler: an R Package for Comparing Biological Themes Among Gene Clusters". *OMICS: A Journal of Integrative Biology* 16.5. PMID: 22455463, pp. 284–287. DOI: 10.1089/omi.2011.0118. eprint: https://doi.org/10.1089/omi.2011.0118.

Yu, Hua, Drew Pardoll, and Richard Jove (2009a). "STATs in cancer inflammation and immunity: a leading role for STAT3". *Nature Reviews Cancer* 9 (11), pp. 798–809. DOI: 10.1038/nrc2734.

Yu, Xin, Kristin Harden, Lino C Gonzalez, Michelle Francesco, Eugene Chiang, Bryan Irving, Irene Tom, Sinisa Ivelja, Canio J Refino, Hilary Clark, Dan Eaton, and Jane L Grogan (2009b). "The surface protein TIGIT suppresses T cell activation by promoting the generation of mature immunoregulatory dendritic cells". *Nature Immunology* 10 (1), pp. 48–57. DOI: 10.1038/ni.1674.

Yuen, J S P, M E Cockman, M Sullivan, A Protheroe, G D H Turner, I S Roberts, C W Pugh, H Werner, and V M Macaulay (2007). "The VHL tumor suppressor inhibits expression of the IGF1R and its loss induces IGF1R upregulation in human clear cell renal carcinoma". *Oncogene* 26 (45), pp. 6499–6508. DOI: 10.1038/sj.onc.1210474.

Zaidi, M. Raza and Glenn Merlino (Oct. 2011). "The Two Faces of Interferon-gamma in Cancer". *Clinical Cancer Research* 17.19, pp. 6118–6124. DOI: 10.1158/1078-0432.CCR-11-0482. eprint: https://aacrjournals.org/clincancerres/article-pdf/17/19/6118/2000033/6118.pdf.

Zajac, Allan J., Joseph N. Blattman, Kaja Murali-Krishna, David J.D. Sourdive, M. Suresh, John D. Altman, and Rafi Ahmed (Dec. 1998). "Viral Immune Evasion Due to Persistence of Activated T Cells Without Effector Function ". *Journal of Experimental Medicine* 188.12, pp. 2205–2213. DOI: 10.1084/jem.188.12.2205. eprint: https://rupress.org/jem/article-pdf/188/12/2205/1688908/98-1509.pdf.

Zardan, A., K. M. Nip, D. Thaper, P. Toren, S. Vahid, E. Beraldi, L. Fazli, F. Lamoureux, K. M. Gust, M. E. Cox, J. L. Bishop, and A. Zoubeidi (Aug. 2014). "Lyn tyrosine kinase regulates androgen receptor expression and activity in castrate-resistant prostate cancer". *Oncogenesis 2014 3:8* 3 (8), e115–e115. DOI: 10.1038/oncsis.2014.30.

Zarek, Paul E., Ching-Tai Huang, Eric R. Lutz, Jeanne Kowalski, Maureen R. Horton, Joel Linden, Charles G. Drake, and Jonathan D. Powell (Jan. 2008). "A2A receptor signaling promotes peripheral tolerance by inducing T-cell anergy and the generation of adaptive regulatory T cells". *Blood* 111.1, pp. 251–259. DOI: 10.1182/blood-2007-03-081646. eprint: https://ashpublications.org/blood/article-pdf/111/1/251/1220304/zh800108000251.pdf.

Zhang, Fan, Hongsheng Wang, Xianfeng Wang, Guanmin Jiang, Hao Liu, Ge Zhang, Hao Wang, Rui Fang, Xianzhang Bu, Shaohui Cai, Jun Du, Fan Zhang, Hongsheng Wang, Xianfeng Wang, Guanmin Jiang, Hao Liu, Ge Zhang, Hao Wang, Rui Fang, Xianzhang Bu, Shaohui Cai, and Jun Du (July 2016a). "TGF-B induces M2-like macrophage polarization via SNAIL-mediated suppression of a pro-inflammatory phenotype". *Oncotarget* 7 (32), pp. 52294–52306. DOI: 10.18632/ONCOTARGET.10561.

Zhang, Hao, Lin Liu, Jinbo Liu, Pengyuan Dang, Shengyun Hu, Weitang Yuan, Zhenqiang Sun, Yang Liu, and Chengzeng Wang (2023a). "Roles of tumor-associated macrophages in anti-PD-1/PD-L1 immunotherapy for solid cancers". *Molecular Cancer* 22 (1), p. 58. DOI: 10.1186/s12943-023-01725-x.

Zhang, Michael, Gregor Hutter, Suzana A. Kahn, Tej D. Azad, Sharareh Gholamin, Chelsea Y. Xu, Jie Liu, Achal S. Achrol, Chase Richard, Pia Sommerkamp, Matthew Kenneth Schoen, Melissa N. McCracken, Ravi Majeti, Irving Weissman, Siddhartha S. Mitra, and Samuel H. Cheshier (Apr. 2016b). "Anti-CD47 Treatment Stimulates Phagocytosis of Glioblastoma by M1 and M2 Polarized Macrophages and Promotes M1 Polarized Macrophages In Vivo". *PLOS ONE* 11.4, pp. 1–21. DOI: 10.1371/journal.pone.0153550.

Zhang, Qindong and Mouldy Sioud (2023b). "Tumor-Associated Macrophage Subsets: Shaping Polarization and Targeting". *International Journal of Molecular Sciences* 24.8. DOI: 10.3390/ijms24087493.

Zhang, Siyuan and Dihua Yu (Sept. 2010). "PI(3)king apart PTEN's role in cancer". *Clinical Cancer Research* 16 (17), pp. 4325–4330. DOI: 10.1158/1078-0432.CCR-09-2990/83877/AM/PI-3-KING-APART-PTEN-S-ROLE-IN-CANCERPTEN.

Zhang, Tiehong, Hongchang Shen, Wei Dong, Xiao Qu, Qi Liu, and Jiajun Du (2014). "Antitumor effects and molecular mechanisms of figitumumab, a humanized monoclonal antibody to IGF-1 receptor, in esophageal carcinoma". *Scientific Reports* 4.1, p. 6855. DOI: 10.1038/srep06855.

Zhang, Wei and Hui Tu Liu (2002). "MAPK signal pathways in the regulation of cell proliferation in mammalian cells". *Cell Research* 12.1, pp. 9–18. DOI: 10.1038/sj.cr.7290105.

Zhang, Wen-Bo, Zu-Xiang Chen, Zhen Liu, Xin-Yu Qian, Yan-Zhi Ge, Hai-Yan Zhang, Wen-Ting Xu, Le-Tian Shan, and Dong-Bao Zhao (2024). "PBMC-mediated modulation of macrophage polarization in RAW264.7 cells through STAT1/STAT6 signaling cascades". *International Immunopharmacology* 138, p. 112651. DOI: https://doi.org/10.1016/j.intimp.2024.112651.

Zhang, Wenting, Wei Fan, Satyanarayana Rachagani, Zhengyuan Zhou, Subodh M Lele, Surinder K Batra, and Jered C Garrison (2019). "Comparative Study of Subcutaneous and Orthotopic Mouse Models of Prostate Cancer: Vascular Perfusion, Vasculature Density, Hypoxic Burden and BB2r-Targeting Efficacy". *Scientific Reports* 9 (1), p. 11117. DOI: 10.1038/s41598-019-47308-z.

Zhang, Yan, Qing Wang, Li Chen, and Hsin Sheng Yang (Mar. 2015). "Inhibition of p70S6K1 activation by Pdcd4 overcomes the resistance to an IGF-1R/IR inhibitor in colon carcinoma cells". *Molecular Cancer Therapeutics* 14 (3), pp. 799–809. DOI: 10.1158/1535-7163.MCT-14-0648/85514/AM/INHIBITION-OF-P70S6K1-ACTIVATION-BY-PDCD4.

Zhang, Yinqi, Chengqi Gao, Fei Cao, Ying Wu, Shuanggang Chen, Xue Han, Jingqin Mo, Zhiyu Qiu, Weijun Fan, Penghui Zhou, and Lujun Shen (2021). "Pan-Cancer Analysis of IGF-1 and IGF-1R as Potential Prognostic Biomarkers and Immunotherapy Targets". *Frontiers in Oncology* 11. DOI: 10.3389/fonc.2021.755341.

Zhang, Yuan-Yuan, Ling-Qun Kong, Xiao-Dong Zhu, Hao Cai, Cheng-Hao Wang, Wen-Kai Shi, Man-Qing Cao, Xiao-Long Li, Kang-Shuai Li, Shi-Zhe Zhang, Zong-Tao Chai, Jian-Yang Ao, Bo-Gen Ye, and Hui-Chuan Sun (2018). "CD31 regulates metastasis by inducing epithelial–mesenchymal transition in hepatocellular carcinoma via the ITGB1-FAK-Akt signaling pathway". *Cancer Letters* 429, pp. 29–40. DOI: https://doi.org/10.1016/j.canlet.2018.05.004.

Zhao, Huiyong, Sheng Wei, Dachen Zhou, Yongfan Liu, Zicheng Guo, Chuibao Fang, Xiaoxi Pang, Fei Li, Hui Hou, and Xiao Cui (2023). "Blocking the CXCL1-CXCR2 axis enhances the effects of doxorubicin in HCC by remodelling the tumour microenvironment via the NF-kB/IL-1B/CXCL1 signalling pathway". *Cell Death Discovery* 9 (1), p. 120. DOI: 10.1038/s41420-023-01424-y.

Zhao, Zhiming, Ningyue Zhang, Anqi Li, Bin Zhou, Yali Chen, Shaomu Chen, Moli Huang, Fengying Wu, and Liang Zhang (2020). "Insulin-like growth factor-1 receptor induces immunosuppression in lung cancer by upregulating B7–H4 expression through the MEK/ERK signaling pathway". *Cancer Letters* 485, pp. 14–26. DOI: https://doi.org/10.1016/j.canlet.2020.04.013.

Zheng, Xianan, Guohua Lu, Yinan Yao, and Wei Gu (2019). "An Autocrine IL-6/IGF-1R Loop Mediates EMT and Promotes Tumor Growth in Non-small Cell Lung Cancer". *Int J Biol Sci* 15, pp. 1882–1891. DOI: 10.7150/ijbs.31999.

Zhou, Binhua P, Jiong Deng, Weiya Xia, Jihong Xu, Yan M Li, Mehmet Gunduz, and Mien-Chie Hung (2004). "Dual regulation of Snail by GSK-3B-mediated phosphorylation in control of epithelial–mesenchymal transition". *Nature Cell Biology* 6 (10), pp. 931–940. DOI: 10.1038/ncb1173.

Zhou, Juan, Jinjing Wang, Yunyun Zeng, Xi Zhang, Qiaoting Hu, Jihua Zheng, Bei Chen, Bo Xie, Wei-Min Zhang, Juan Zhou, Jinjing Wang, Yunyun Zeng, Xi Zhang, Qiaoting Hu, Jihua Zheng, Bei Chen, Bo Xie, and Wei-Min Zhang (Nov. 2015). "Implication of epithelial-mesenchymal transition in IGF1R-induced resistance to EGFR-TKIs in advanced non-small cell lung cancer". *Oncotarget* 6 (42), pp. 44332–44345. DOI: 10.18632/ONCOTARGET.6293.

Zhou, Liang, Mark M W Chong, and Dan R Littman (May 2009). "Plasticity of CD4+ T Cell Lineage Differentiation". *Immunity* 30 (5). doi: 10.1016/j.immuni.2009.05.001, pp. 646–655. DOI: 10.1016/j.immuni.2009.05.001.

Zhou, Ming (2018). "High-grade prostatic intraepithelial neoplasia, PIN-like carcinoma, ductal carcinoma, and intraductal carcinoma of the prostate". *Modern Pathology* 31, pp. 71–79. DOI: https://doi.org/10.1038/modpathol.2017.138.

Zhou, Yingyu, Tomohiro Takano, Xuyang Li, Yimei Wang, Rong Wang, Zhangliang Zhu, Masaru Tanokura, Takuya Miyakawa, and Satoshi Hachimura (2022). "B-elemene regulates M1-M2 macrophage balance through the ERK/JNK/P38 MAPK signaling pathway". *Communications Biology* 5 (1), p. 519. DOI: 10.1038/s42003-022-03369-x.

Zhou, Yue, Zhilei Zhang, Ning Wang, Jizheng Chen, Xu Zhang, Min Guo, Li John Zhong, and Qian Wang (2018). "Suppressor of cytokine signalling-2 limits IGF1R-mediated regulation of epithelial–mesenchymal transition in lung adenocarcinoma". *Cell Death and Disease* 9 (4), p. 429. DOI: 10.1038/s41419-018-0457-5.

Zhu, Meng-Lei and Natasha Kyprianou (2008a). "Androgen receptor and growth factor signaling cross-talk in prostate cancer cells". *Endocrine-Related Cancer* 15.4, pp. 841–849. DOI: 10.1677/ERC-08-0084.

Zhu, Weidong, Ichiro Shiojima, Yuzuru Ito, Zhi Li, Hiroyuki Ikeda, Masashi Yoshida, Atsuhiko T Naito, Jun-ichiro Nishi, Hiroo Ueno, Akihiro Umezawa, Tohru Minamino, Toshio Nagai, Akira Kikuchi, Makoto Asashima, and Issei Komuro (2008b). "IGFBP-4 is an inhibitor of canonical Wnt signalling required for cardiogenesis". *Nature* 454 (7202), pp. 345–349. DOI: 10.1038/nature07027.

Zhu, Yu, Brett L. Knolhoff, Melissa A. Meyer, Timothy M. Nywening, Brian L. West, Jingqin Luo, Andrea Wang-Gillam, S. Peter Goedegebuure, David C. Linehan, and David G. DeNardo (Sept. 2014). "CSF1/CSF1R Blockade Reprograms Tumor-Infiltrating

Macrophages and Improves Response to T-cell Checkpoint Immunotherapy in Pancreatic Cancer Models". *Cancer Research* 74.18, pp. 5057–5069. DOI: 10.1158/0008-5472.CAN-13-3723. eprint: https://aacrjournals.org/cancerres/article-pdf/74/18/5057/2704627/5057.pdf.

Zong, Cong S, Joseph Chan, David E Levy, Curt Horvath, Henry B Sadowski, and Lu-Hai Wang (May 2000). "Mechanism of STAT3 Activation by Insulin-like Growth Factor I Receptor". *Journal of Biological Chemistry* 275 (20), pp. 15099–15105. DOI: 10.1074/jbc.M000089200.

Zuo, Yong, Jiawei Bai, Huiyuan Bai, Siyu Tian, Hongtao Sun, Zhenhua Shi, Peng Yu, Guofen Gao, Yuan Li, and Yan-Zhong Chang (2024). "Transmembrane serine protease 6, a novel target for inhibition of neuronal tumor growth". *Cell Death and Disease* 15 (1), p. 49. DOI: 10.1038/s41419-024-06442-x.